AVIAN MUSCLE DEVELOPMENT AND GROWTH MECHANISMS: ASSOCIATION WITH MUSCLE MYOPATHIES AND MEAT QUALITY VOLUME II

EDITED BY: Massimiliano Petracci and Sandra G. Velleman

PUBLISHED IN: Frontiers in Physiology

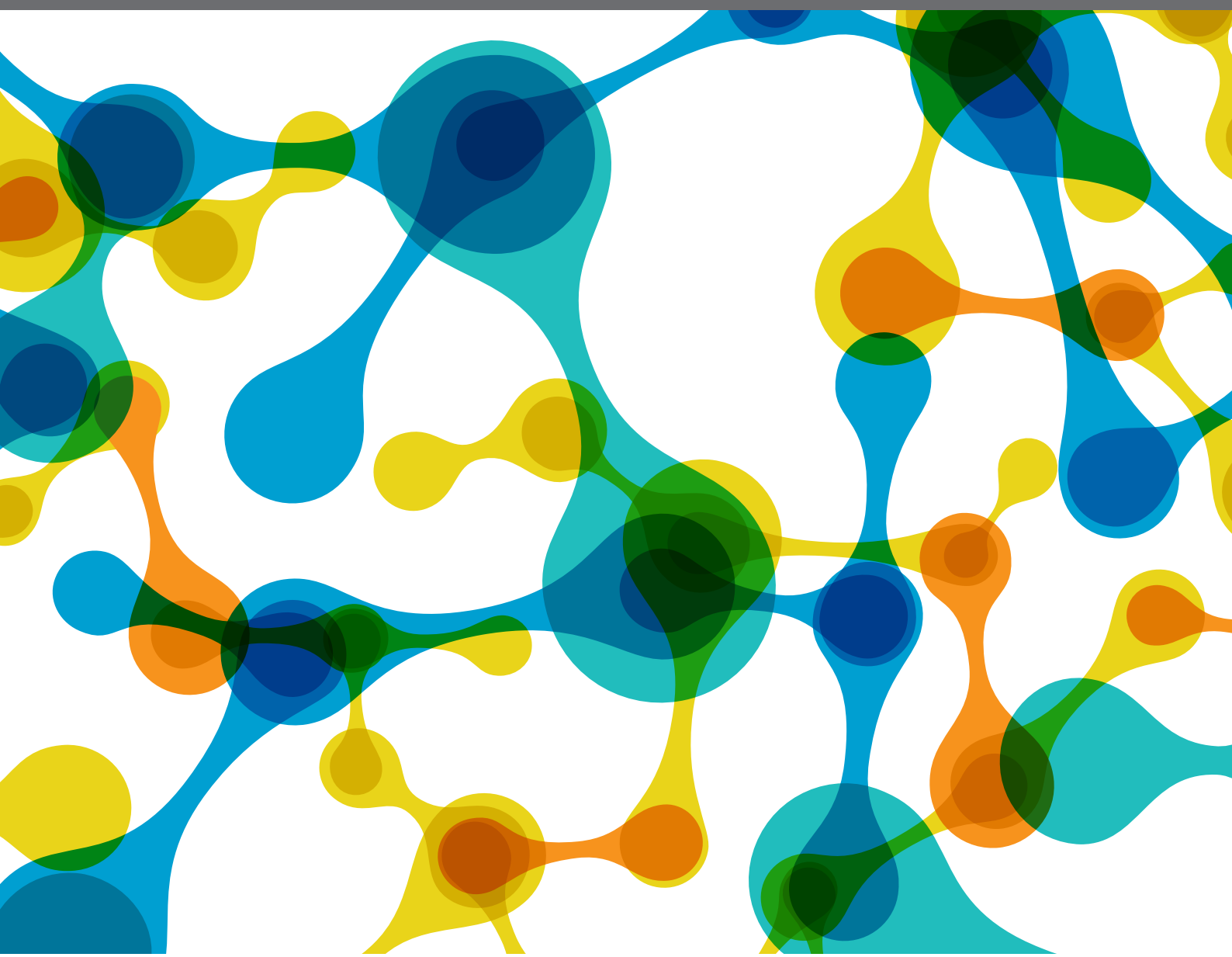

frontiers Research Topics

frontiers

ISSN 1664-8714
ISBN 978-2-88971-759-0
DOI 10.3389/978-2-88971-759-0

About Frontiers

Frontiers is more than just an open-access publisher of scholarly articles: it is a pioneering approach to the world of academia, radically improving the way scholarly research is managed. The grand vision of Frontiers is a world where all people have an equal opportunity to seek, share and generate knowledge. Frontiers provides immediate and permanent online open access to all its publications, but this alone is not enough to realize our grand goals.

Frontiers Journal Series

The Frontiers Journal Series is a multi-tier and interdisciplinary set of open-access, online journals, promising a paradigm shift from the current review, selection and dissemination processes in academic publishing. All Frontiers journals are driven by researchers for researchers; therefore, they constitute a service to the scholarly community. At the same time, the Frontiers Journal Series operates on a revolutionary invention, the tiered publishing system, initially addressing specific communities of scholars, and gradually climbing up to broader public understanding, thus serving the interests of the lay society, too.

Dedication to Quality

Each Frontiers article is a landmark of the highest quality, thanks to genuinely collaborative interactions between authors and review editors, who include some of the world's best academicians. Research must be certified by peers before entering a stream of knowledge that may eventually reach the public - and shape society; therefore, Frontiers only applies the most rigorous and unbiased reviews.
Frontiers revolutionizes research publishing by freely delivering the most outstanding research, evaluated with no bias from both the academic and social point of view. By applying the most advanced information technologies, Frontiers is catapulting scholarly publishing into a new generation.

What are Frontiers Research Topics?

Frontiers Research Topics are very popular trademarks of the Frontiers Journals Series: they are collections of at least ten articles, all centered on a particular subject. With their unique mix of varied contributions from Original Research to Review Articles, Frontiers Research Topics unify the most influential researchers, the latest key findings and historical advances in a hot research area! Find out more on how to host your own Frontiers Research Topic or contribute to one as an author by contacting the Frontiers Editorial Office: frontiersin.org/about/contact

AVIAN MUSCLE DEVELOPMENT AND GROWTH MECHANISMS: ASSOCIATION WITH MUSCLE MYOPATHIES AND MEAT QUALITY VOLUME II

Topic Editors:
Massimiliano Petracci, University of Bologna, Italy
Sandra G. Velleman, The Ohio State University, United States

Citation: Petracci, M., Velleman, S. G., eds. (2021). Avian Muscle Development and Growth Mechanisms: Association With Muscle Myopathies and Meat Quality Volume II. Lausanne: Frontiers Media SA. doi: 10.3389/978-2-88971-759-0

Table of Contents

frontiers in Physiology

EDITORIAL
published: 14 October 2021
doi: 10.3389/fphys.2021.765515

Editorial: Avian Muscle Development and Growth Mechanisms: Association With Muscle Myopathies and Meat Quality Volume II

Massimiliano Petracci[1]* *and Sandra G. Velleman*[2]

[1] Department of Agricultural and Food Sciences, Alma Mater Studiorum – University of Bologna, Bologna, Italy, [2] Department of Animal Sciences, The Ohio State University, Wooster, OH, United States

Keywords: meat, myopathies, poultry, spaghetti meat, white striping, wooden breast

Editorial on the Research Topic

Avian Muscle Development and Growth Mechanisms: Association With Muscle Myopathies and Meat Quality Volume II

Given the significant interest in Volume I, it was decided to launch Volume II of the Research Topic "*Avian Muscle Development and Growth Mechanisms: Association With Muscle Myopathies and Meat Quality*." The broiler industry is still facing an unsustainable occurrence of growth-related muscular abnormalities that mainly affect fast-growing genotypes selected for high growth rate and breast yield. From their onset, research interest in these issues continues as proven by the temporal trend of published papers during the past decade (**Figure 1**). Even if meat affected by white striping, wooden breast, and spaghetti meat abnormalities is not harmful for human nutrition, these conditions impair quality traits of both raw and processed meat products causing severe economic losses in the poultry industry worldwide (Petracci et al., 2019; Velleman, 2019). Since the Research Topic of "*Avian Muscle Development and Growth Mechanisms: Association With Muscle Myopathies and Meat Quality*" is quite diverse, contributions in this second volume reflect the broad scope of areas of investigation related to muscle growth and development with 11 original research papers and one mini-review from prominent scientists in the sector. We hope that this collection will instigate novel questions in the minds of our readers and will be helpful in facilitating the development of the field.

The majority of papers included in this Research Topic further investigated possible mechanisms directly and indirectly involved in the development of growth-related broiler breast abnormalities. Recently, an extensive review paper confirmed that myopathic disorders affecting pectoral muscles of fast-growing broilers have a complex etiology, and several biological pathways, as well as response mechanisms, are involved in their progression (Soglia et al., 2021). Aside from distinctive phenotypes of white striping, wooden breast, and spaghetti meat, these conditions share common histological features. Hence, it seems that common causative mechanisms are responsible for the physiological and structural perturbations commonly detected in muscles showing these conditions and might underpin their appearance (Soglia et al., 2021). The narrative mini-review by Baldi et al. provides a critical evaluation of the state of research on the spaghetti meat condition which is one of the more recent muscular abnormalities affecting the breast muscles of fast-growing broilers. Due to its recentness, the causative mechanisms are still partially unknown and less investigated than wooden breast and white striping abnormalities (**Figure 1**). This mini-review highlights knowledge gaps and unexplored areas including a critical view on current uncertainties and future directions. To deepen the knowledge on the genetic mechanisms involved in white

OPEN ACCESS

Edited and reviewed by:
Colin Guy Scanes,
University of Arkansas, United States

***Correspondence:**
Massimiliano Petracci
m.petracci@unibo.it

Specialty section:
This article was submitted to Avian Physiology, a section of the journal Frontiers in Physiology

Received: *27 August 2021*
Accepted: *16 September 2021*
Published: *14 October 2021*

Citation:
Petracci M and Velleman SG (2021) Editorial: Avian Muscle Development and Growth Mechanisms: Association With Muscle Myopathies and Meat Quality Volume II. Front. Physiol. 12:765515. doi: 10.3389/fphys.2021.765515

striping, Marciano et al. evaluated by quantitative PCR a selected group of 15 functional candidate genes in breast muscles of normal and white striping-affected broilers. Among them, six genes (CA2, CSRP3, PLIN1, CALM2, DNASE1L3, and MYLK2) associated with myogenic and calcium signaling were differentially expressed. These findings confirmed that dysregulation of the muscle and calcium signaling pathways plays a role in the development at least of white striping in broilers. Malila et al. evaluated transcriptional profiles associated with the wooden breast condition in broilers slaughtered at two commercial slaughter ages. The analysis of up and downregulated transcripts in wooden breast samples in comparison with normal counterparts showed that an abnormal remodeling of an extracellular matrix focal adhesion mediated the signaling pathway. In addition, remarkable perturbations in the glucose and lipid metabolic and signaling pathways are of utmost importance in broilers at 6 weeks of age, while failure of muscle regeneration was more evident in birds slaughtered at 7 weeks of age. On the other hand, Xing et al. investigated the potential physiological alterations and the possible related mechanisms in the chicken liver in order to explain its possible involvement in wooden breast occurrence. The primary findings revealed that wooden breast-affected birds exhibited clear clinical signs of liver injury associated with reduced antioxidant capacity, mitochondrial dysfunction, hepatocyte apoptosis, and a higher inflammatory response, which possibly contribute to the aggravation of liver injury in WB myopathic birds.

The paper of Ran et al. focused on DNA methylation which is a crucial epigenetic mechanism associated with skeletal muscle development during the embryonic period and exerts a key role during the early post-hatch period in broiler chickens. It was revealed that the many differentially methylated genes were strongly involved in several aspects related to embryonic muscle development. The CFL2 gene has been specifically screened for effects on satellite cells *in vitro* and demonstrated a remarkable function as a negative regulator of muscle satellite cell proliferation by leading to an induction of apoptosis. On the same topic, Orlowski et al. investigated the implications of selection for high breast-yield during the period of hyperplastic growth in order to ascertain if the number of muscle fibers is changed. For this study, two chicken lines after five generations of divergent selection for breast yield were used and sampled at different stages (late embryonic development, post-hatching, and commercial slaughter age). The high breast-yield line showed a greater rate of muscle fiber formation, while at market age, greater breast development was merely due to a larger fiber diameter as no differences were detected between the lines for fiber number. The paper of Xu et al. explored how

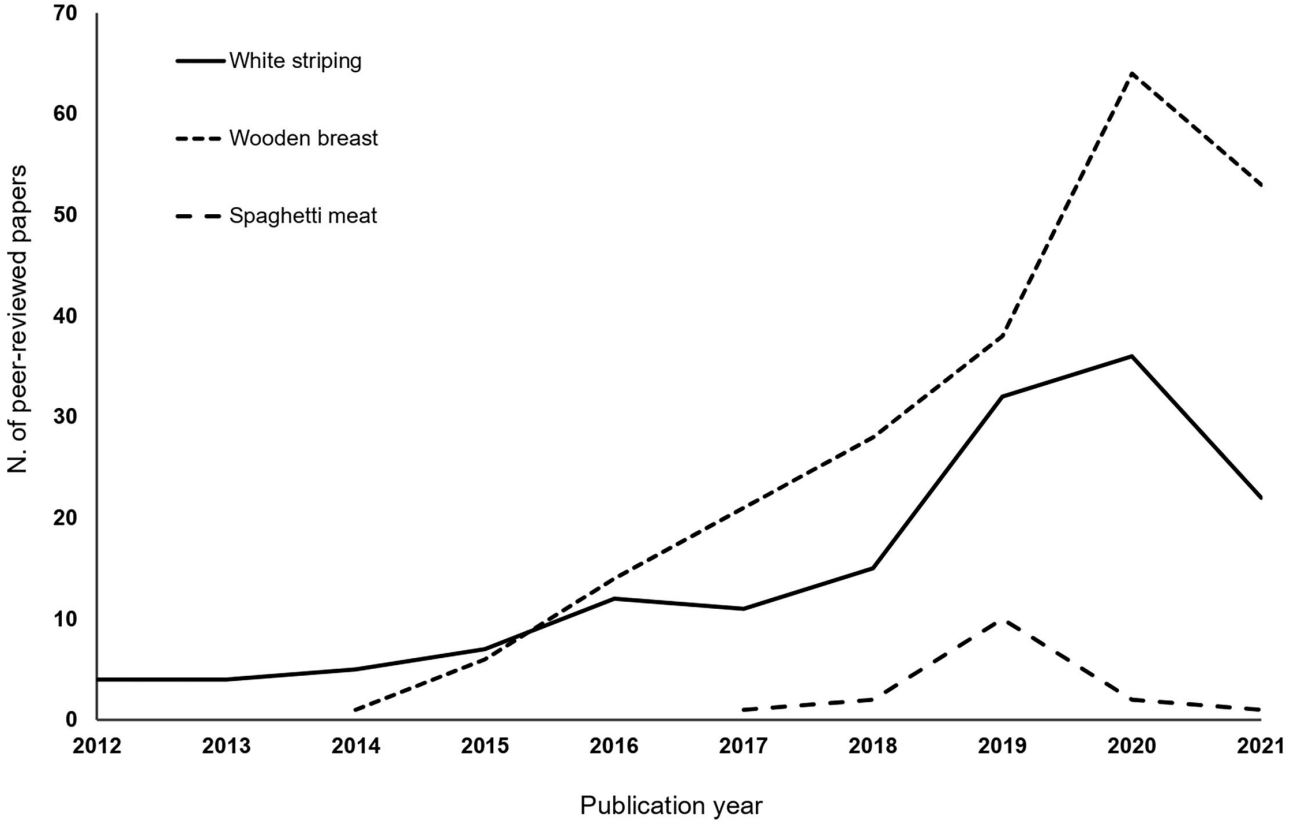

FIGURE 1 | Number of publications produced per year containing concerning white striping, wooden breast, and spaghetti meat myopathies affecting broilers' pectoralis major muscles. Data obtained from Scopus on August 27, 2021.

temperature and growth selection can influence intracellular lipid accumulation and adipogenic gene expression in turkey pectoralis major muscle satellite cells. It was found that heat stress impairs the adipogenic potential of turkeys even at 7 days of age and increased the intracellular lipid content in pectoralis major muscle satellite cells during proliferation, while cold temperature exposure showed a reverse effect.

The research paper of Zhang et al. is conversely devoted to evaluating the progression of protein expression profiles in breast muscle of a native Chinese chicken breed in the final stage of growth prior to slaughter (90, 120, and 150 days) by using a proteomic approach (namely tandem mass tag). Overall, the main findings revealed that differentially expressed proteins among different ages were especially associated with carbohydrate metabolism, adrenergic signaling in cardiac myocytes, focal adhesion, oocyte meiosis, and phagosomes. These last couple of studies can help to unravel the molecular mechanisms of economically important traits in chickens.

The papers of Liu et al. and Métayer-Coustard et al. focused on the biological control glycogen content in muscle which can affect body homeostasis, live performance, and final meat quality. Liu et al. investigated the poorly explored role of FOS-like 2 AP-1 transcription factor subunit (FOSL2) in the regulation of muscle glycogen content in poultry. It was revealed that the FOSL2 gene could regulate the amount of glycogen stored in skeletal muscles through their influence on a downstream gene (CEBPB), and small differences were detected when effects of breed and gender were assessed. Métayer-Coustard et al. used chicken lines divergently selected on ultimate pH as a model to generate new knowledge on molecular mechanisms linked to energy metabolism and protein synthesis during the early post-hatch period. The primary findings revealed that muscle metabolic differences in chicken lines divergently selected are already well evident at hatch, and lower muscle glycogen storage potential is associated with higher protein synthesis rates, muscle growth, and proportion of white striping cases in the pectoralis major muscle. Further studies are needed to understand if changes observed at hatching could be due to differences in nutrient use or availability during embryonic development.

Two papers in our Research Topic focused on biomarkers for the early prediction of growth-related abnormalities in live birds with an emphasis on wooden breast. Currently, wooden breast–affected birds are phenotypically detected especially at the breeder level through manual palpation of the pectoralis major muscle. Kong B. et al. examined blood plasma proteins and metabolites in chickens at 4 and 8 weeks of age to identify early-age biomarkers for the wooden breast abnormality using untargeted metabolomics based on gas chromatography coupled with time-of-flight mass spectrometry. Among the 32 examined metabolites, raffinose, and 3-hydroxybutyric acid were reported to have the highest fold-changes in chickens showing the wooden breast condition, and their concentrations were also shown by targeted biochemical assays. In addition, Kong F. et al. assessed enzyme activity in serum and breast tissue and compression force of raw breast filets in broilers at 4 and 6 weeks of age. The main findings evidenced that creatine kinase activity in both serum and breast tissue was much higher in wooden breast–affected birds even if only in birds of 6 weeks of age. Furthermore, a linear relationship between creatine kinase levels and compression force was found. Overall, both studies have been able to identify candidate biomarkers for the prediction of the wooden breast condition and to assist genetic selection in fast-growing broiler breeding.

There is also the need for objective methods to detect and grade abnormal breasts after deboning in commercial chicken processing plants. Currently, wooden breast meat is usually sorted out by visual evaluation and manual hand-palpation. Siddique et al. assessed bioelectrical impedance analysis combined with advanced data analytics techniques such as supervised learning algorithms as an objective tool to identify wooden breast filets. Machine learning is already effectively used in the food industry (i.e., quality control, processing optimization) and this first study evidenced that supervised learning algorithms can also assist to accurately sort breasts filets into myopathy categories.

The last paper by Kuttappan et al. explored possible nutritional intervention strategies to reduce the incidence of wooden breast. Their selected approach was to test dietary supplementation of feed additives with potential antioxidant effectors such as ethoxyquin, combination of chelated trace minerals (Zn, Cu, and Mn), and organic selenium in three independent experiments. Overall, it was proven that the dietary use of antioxidants and chelated trace minerals was able to reduce oxidative stress in the tissue and reduce the severity of wooden breast.

AUTHOR CONTRIBUTIONS

MP wrote the first draft. SGV added notes and revised the manuscript. All authors contributed to the article and approved the submitted version.

ACKNOWLEDGMENTS

We are grateful for the contributions to this Research Topic made by Frontiers editorial staff members. We also thank the reviewers who provided valuable input for each manuscript.

REFERENCES

Petracci, M., Soglia, F., Madruga, M., Carvalho, L., Ida, E., and Estévez, M. (2019). Wooden-breast, white striping, and spaghetti meat: causes, consequences and consumer perception of emerging broiler meat abnormalities. *Compr. Rev. Food Sci. Food Saf.* 18, 565–583. doi: 10.1111/1541-4337.12431

Soglia, F., Petracci, M., Davoli, R., and Zappaterra, M. (2021). A critical review of the mechanisms involved in the occurrence of growth-related abnormalities affecting broiler chickens breast muscle. *Poultry Sci.* 100:101180. doi: 10.1016/j.psj.2021.101180

Velleman, S. G. (2019). Recent developments in breast muscle myopathies associated with growth in poultry. *Annu. Rev.*

Anim. Biosci. 7, 1–20. doi: 10.1146/annurev-animal-020518-115311

Conflict of Interest: The authors declare that the research was conducted in the absence of any commercial or financial relationships that could be construed as a potential conflict of interest.

Publisher's Note: All claims expressed in this article are solely those of the authors and do not necessarily represent those of their affiliated organizations, or those of the publisher, the editors and the reviewers. Any product that may be evaluated in this article, or claim that may be made by its manufacturer, is not guaranteed or endorsed by the publisher.

frontiers in Physiology

ORIGINAL RESEARCH
published: 04 March 2021
doi: 10.3389/fphys.2021.643580

Early Growth and Protein-Energy Metabolism in Chicken Lines Divergently Selected on Ultimate pH

Sonia Métayer-Coustard[1], Sophie Tesseraud[1], Christophe Praud[1], David Royer[1], Thierry Bordeau[1], Edouard Coudert[1], Estelle Cailleau-Audouin[1], Estelle Godet[1], Joël Delaveau[2], Elisabeth Le Bihan-Duval[1] and Cécile Berri[1]*

[1]*INRAE, Université de Tours, BOA, Nouzilly, France,* [2]*INRAE, PEAT, Nouzilly, France*

In chickens, a divergent selection on the *Pectoralis major* pHu allowed the creation of the pHu+ and pHu− lines, which represent a unique model for studying the biological control of carbohydrate storage in muscle. The present study aimed to describe the early mechanisms involved in the establishment of pHu+ and pHu− phenotypes. At hatching, pHu+ chicks were slightly heavier but exhibited lower plasma glucose and triglyceride and higher uric acid. After 5 days, pHu+ chicks exhibited higher breast meat yield compared to pHu− while their body weight was no different. At both ages, *in vivo* muscle glycogen content was lower in pHu+ than in pHu− muscles. The lower ability of pHu+ chicks to store carbohydrate in their muscle was associated with the increased expression of *SLC2A1* and *SLC2A3* genes coding glucose transporters 1 and 3, and of *CS* and *LDHα* coding key enzymes of oxidative and glycolytic pathways, respectively. Reduced muscle glycogen content at hatching of the pHu+ was concomitant with higher activation by phosphorylation of S6 kinase 1/ribosomal protein S6 pathway, known to activate protein synthesis in chicken muscle. In conclusion, differences observed in muscle at slaughter age in the pHu+ and pHu− lines are already present at hatching. They are associated with several changes related to both carbohydrate and protein metabolism, which are likely to affect their ability to use eggs or exogenous nutrients for muscle growth or energy storage.

Keywords: chicks, metabolism, muscle, protein synthesis, glycogen, carbohydrate metabolism

OPEN ACCESS

Edited by:
Sandra G. Velleman, The Ohio State University, United States

Reviewed by:
Paul Siegel, Virginia Tech, United States
Eddy Decuypere, KU Leuven Kulak, Belgium

****Correspondence:***
Sonia Métayer-Coustard
sonia.metayer-coustard@inrae.fr

Specialty section:
This article was submitted to Avian Physiology, a section of the journal Frontiers in Physiology

Received: *18 December 2020*
Accepted: *26 January 2021*
Published: *04 March 2021*

Citation:
Métayer-Coustard S, Tesseraud S, Praud C, Royer D, Bordeau T, Coudert E, Cailleau-Audouin E, Godet E, Delaveau J, Le Bihan-Duval E and Berri C (2021) Early Growth and Protein-Energy Metabolism in Chicken Lines Divergently Selected on Ultimate pH. Front. Physiol. 12:643580. doi: 10.3389/fphys.2021.643580

INTRODUCTION

To answer the growing demand for poultry meat, breeding companies have focused their efforts on improving live performances (i.e., growth rate and feed efficiency) and breast meat yield (Rauw et al., 1998; Havenstein et al., 2003a,b). The selection of meat-type chicken lines for increased growth and muscle development has been accompanied by significant anatomical, physiological, and metabolic changes. As a result, limitations appear in terms of physiology affecting both animal robustness and product quality. In these meat-type chicken lines, a decrease in muscle energy reserves, evaluated through *in vivo* glycogen content, is observed (Berri et al., 2001, 2007). In chicken, there is a strong genetic link (with a correlation of −0.97) between the muscle glycogen reserves available *in vivo* and the ultimate pH (pHu) of

the meat (Le Bihan Duval et al., 2008). Changes in pHu affect most of the meat quality traits such as color, water-holding capacity, texture, and processing ability (Le Bihan-Duval et al., 2008; Petracci et al., 2015). Recent studies also highlighted high pHu as a predisposing factor favoring the emergence of white striping (WS) and wooden breast (WB) defects in heavy broiler lines (Kuttappan et al., 2009; Petracci et al., 2013; Abasht et al., 2016; Alnahhas et al., 2016). Several studies have shown that chicken breast meat pHu is a highly heritable trait that can therefore be modified by genetic selection (Le Bihan Duval et al., 2001, 2008). On this basis, a divergent selection on breast meat pHu was initiated from a common fast-growing grand-parental population in order to increase (in the high pHu line, pHu+) or decrease (in the low pHu line, pHu−) the genetic value for pHu. After six generations of divergent selection, the two divergent lines exhibited a difference of around 0.5 pH unit, that was associated with significant differences in muscle glycogen and sensory and technological meat quality (Alnahhas et al., 2014, 2015). It also appeared that while body weight at 6 weeks was similar between the two lines, pHu+ birds exhibited higher thigh and breast muscle yield than pHu− birds. As already described for heavy broiler lines, the incidence of WS was higher in pHu+, the line presenting higher pHu and lower muscle glycogen reserves (Alnahhas et al., 2016). On the other hand, neither the pHu− nor the pHu+ line is affected by the WB syndrome. The etiology of WS and WB is poorly understood, but a new hypothesis suggests a potential dysregulation of lipid and glucose metabolism in these muscle disorders (Lake and Abasht, 2020). Regarding metabolism, the depletion of glycogen reserves that characterizes the pHu+ line is associated with a partial reorientation of muscle metabolism towards oxidative stress, protein catabolism, and lipid beta-oxidation rather than glycolysis, as well as an over-activation of processes related to muscle remodeling (Beauclercq et al., 2016, 2017). Conversely, carbohydrate metabolites are over-represented in the serum and muscle of the pHu− birds, consistent with their high level of muscle glycogen content. The purpose of the present study was to determine the extent to which the phenotypic differences between lines were programmed early, by considering chicks at the time of hatching or after a few days of nutrition. To improve our understanding of the molecular mechanisms involved in the establishment of line-related phenotypic differences, several molecular actors related to energy metabolism and protein synthesis were explored *in vivo* and *in vitro*.

MATERIALS AND METHODS

Animals and Muscle Tissue Collection

All investigators were certified by the French government to carry out animal experiments. All procedures were approved by the French Agricultural Agency and the Scientific Research Agency (under referenced authorization N° 201,503,111,710,750). This study was conducted in accordance with the guidelines for Care and Use of Agricultural Animals in Agricultural Research and Teaching. The study used fast-growing chicks belonging to the eighth generation of selection for high (pHu+) or low (pHu−) *Pectoralis major* muscle pHu. Thirty chicks (males and females) from both lines were hatched and sacrificed by cervical dislocation (D0 that corresponds to the time when chicks were taken out from the hatchery). A second batch of thirty chicks per line (males and females) were reared for 5 days under conventional conditions at PEAT INRAE Poultry Experimental Facility (2018, https://doi.org/10.15454/1.5572326250887292E12), as described by Alnahhas et al. (2014). Males and females of both divergent lines were reared as a single population. They were fed and watered *ad libitum* until 8 h before sacrifice by cervical dislocation at D5. A third batch of birds from both lines (425 in total) was also reared until slaughter age (42 days) following classical rearing conditions (Alnahhas et al., 2014).

Blood samples were collected at day 0 (D0) and day 5 (D5) on heparin (135 USP U Lithium Heparin, VENOSAFE, Dominique Dutscher, Brumath, France), stored on ice, centrifuged at 3000 *g* for 10 min at 4°C, and plasma aliquoted and frozen at −80°C until analysis. Tissues were sampled from hatched chicks (D0; liver, *Pectoralis major*, and pipping muscles) and 5-day-old chicks (D5; liver and *Pectoralis major*) of both lines. The pipping muscle is a cervical muscle, which is solicited for shell breaking and regresses after hatching (Pulikanti et al., 2010). At each age of sampling (D0 and D5), both muscle types and the liver of eight females and eight males per line were sampled, weighed, and frozen in liquid nitrogen before storage at −80°C until further molecular and biochemical analyses. At D0 and D5, *Pectoralis major* muscles from six male chicks of each line were snap-frozen in isopentane cooled in liquid nitrogen before storage at −80°C until further histochemical study. Fresh muscle samples were finally kept for 24 h for pHu measurement.

Cell Culture

The primary cell culture studies were conducted as previously described (Praud et al., 2017) in which procedures were validated to study muscle biology in the chicken model. Briefly, the *Pectoralis major* muscles were sliced with a scalpel and washed with sterile PBS for 15 min. After 1 min of gentle centrifugation (20 *g*) and supernatant discarding, myogenic cells derived from satellite cells were extracted by enzymatic dissociation with 0.14% pronase (Sigma Aldrich, Lyon, France) for 10 min at room temperature. After centrifugation (20 *g*, 30 s, at room temperature), the supernatant was kept while the pellet was treated three times more with pronase. All supernatants were gathered and centrifuged at 200 *g* for 10 min at room temperature. Pelleted cells were then suspended in a DMEM-HAMF12 culture medium containing 3 g/L glucose (Sigma Aldrich, Lyon, France) and supplemented with 10% of fetal calf serum (Sigma Aldrich, Lyon, France), 2% ultroser G (PALL biosepra, Cergy, France) containing penicillin and streptomycin 1%, and antifungal fungizone (Sigma-Aldrich, Lyon, France).

The cells were seeded in six-well plates at 30,000 cells/cm ^{2} in a complete DMEM-HAMF12 proliferation medium (DMEM-HamF12 with 10% fetal calf serum, 2% of ultroser G, and

0.365 g/L glutamine) for cell stimulation experiments. After 48 h of proliferation, the cell culture medium was replaced by a DMEM-HAMF12 differentiation medium, containing the same antibiotics and antifungal as the proliferation medium, but supplemented with 2% horse serum and 0.5% fetal calf serum. After 48 h of differentiation, the cells were washed once with PBS and weaned in DMEM-HAMF12 serum-free medium for 4 h. Then, cells were incubated in a DMEM-HAMF12 medium supplemented or not with insulin (100 nM) for 0, 15, or 45 min to measure the response of protein synthesis pathways to insulin. This stimulation was stopped by washing with cold PBS and cells were recovered by scraping with 200 µl of lysis buffer (composition). The cell extracts were then lysed for 30 min at 4°C before centrifugation (12,000 *g*, 30 min, 4°C) and supernatants were sampled and stored at −80°C until further SDS-PAGE and Western blot analyses.

Immunocytochemistry

Immunocytochemistry procedures were done on cells cultured in plates and fixed using cold methanol, as previously described by Praud et al. (2017). After blocking with goat serum 10% (Sigma), the cells were incubated with primary antibodies against sarcomeric myosin (MF20, 1/50) for 1 h. The MF20 antibody developed by Donald A. Fischman was obtained from the Developmental Studies Hybridoma Bank, created by the NICHD of the NIH and maintained at The University of Iowa, Department of Biology, Iowa City, IA 52242. The immunolocalization was performed using a biotinylated goat anti-mouse antibody (anti IgG H+L, Southern Biotech) and with streptavidin-Cy2 (Southern Biotech). All nuclei were labeled using DAPI 0.05 µg/ml (Sigma). Fluorescence imaging on cells was done using a Zeiss Axiovert 200 Microscope (Carl Zeiss S.A.S) and a Zeiss Camera AxioCam MRm (Carl Zeiss S.A.S) controlled by the Axiovision software (Axiovision Rel. 4.6.3; Carl Zeiss Imaging Solutions, GmbH, 2007).

Histochemical Traits

Ten-micrometer-thick *Pectoralis major* muscle cross-sections were used to perform periodic acid-Schiff (PAS) staining. They were fixed in Carnoy's fixative and incubated for 5 min in periodic acid 1% and 90 min in Schiff's reagent (Sigma-Aldrich, Saint-Quentin Fallavier, France) before washing with distilled water, dehydration, and mounting in Canada balsam (Sigma Aldrich, Saint-Quentin Fallavier, France).

Plasma Metabolite Measurements

Glycemia, uric acid, and triglyceride were measured using commercial kits (RTUTM Glucose, Enrique Uric Acid PAP 150, Enzyme Triglycerides PAP 150, Biomérieux, Craponne, France). The free amino acids (Free AA) were measured after extraction with 10% (v/v) of sulfosalicylic acid using 2% of ninhydrin reagent (Sigma Aldrich, Lyon, France). L-serine was used as a standard (Dupont et al., 2008). All enzymatic colorimetric assays were performed in 96-well plates using a TECAN infinite M200 spectrophotometer according to the supplier's recommendations (Artiss and Entwistle, 1981; Fossati and Prencipe, 1982).

Liver and Muscle Glycogen Content

About 500 mg of frozen *Pectoralis major*, pipping muscle, and liver sampled within 10 min post-mortem was powdered and used to estimate the glycogen content. Tissue *in vivo* glycogen content was estimated through the measurement of the glycolytic potential that reflects the glycogen that is in the tissue prior to slaughter as it considers the main intermediates of glycogen degradation (glucose-6-phosphate, free glucose, and lactate; Monin and Sellier, 1985). Glycogen was measured through enzymatic procedures according to Dalrymple and Hamm (1973). The glycolytic potential (GP) was calculated according to the equation: GP = 2[glycogen + glucose + glucose-6-phosphate] + lactate, and was expressed as µmoles of lactate equivalent per gram of tissue.

Ultimate pH Measurement in *Pectoralis major* Muscle

For D0 and D5 samples, after storage (24 h at 4°C), 1 g of *Pectoralis major* muscle was crushed with an Ultra-Turrax T25 (Janke and Kunkelika-labortechnick) in 9 ml of a solution of KCl-iodoacetate (sodium iodoacetate 5 mM, KCl 150 mM). The pH of this solution was then measured using a portable pH meter (model 506; Crison Instruments SA, Alella, Bercelona, Spain) with a glass electrode.

At day 42, pHu was recorded in the right *Pectoralis major* muscles sampled on chickens originating from 213 birds from the pHu+ line and 212 birds from the pHu− line. At this age, the pHu was measured 24 h post-mortem using a portable pH meter (model 506, Crison Instruments SA, Alella, Barcelona, Spain) by direct insertion of its glass electrode into the muscles.

WS Incidence

The prevalence and severity of WS were assessed on the right *Pectoralis major* muscle using the scoring grid of Kuttappan et al. (2012). Muscles were classified as normal (WS0) in the absence of WS, moderate (WS1) when the thickness of the white stripes was less than 1 mm, or severely affected (WS2) when the thickness of the stripes was equal to or greater than 1 mm.

Western Blotting and Cell Signaling

Tissue lysates were prepared for cell signaling analyses as previously described in Duchêne et al. (2008). Lysates were first centrifuged at 1000 *g* for 30 min at 10°C and supernatants were then centrifuged at 31,000 *g* for 45 min at 10°C. Solubilized lysates (containing 40 µg of protein) were subjected to SDS-PAGE and Western blotting with the appropriate antibody. Antibodies raised against phospho-S6K1 [T389], phospho-S6 [S235/S236], and S6 ribosomal protein, were obtained from Cell Signaling Technology (Beverly, MA, United States). Anti-S6K1, and anti-vinculin antibodies were obtained from Santa Cruz Biotechnology (Santa Cruz, CA, United States), Upstate (Millipore, Paris, France), and Sigma Chemical Company (St. Louis, MO, United States).

After washing, membranes were incubated with a DyLight® 680-conjugated antibody. Alexa Fluor 680-conjugated secondary

antibodies were obtained from Molecular Probes (Invitrogen, Carlsbad, CA, United States). Bands were visualized with Infrared Fluorescence using the Odyssey® Imaging System (LI-COR Inc. Biotechnology, Lincoln, NE) and quantified with the Odyssey imaging system software (Application software, version 1.2).

RNA Isolation and RT-qPCR

Total RNA was extracted from 100 mg of tissue samples using RNA Now (Biogentec, Seabrook, TX, United States) according to the manufacturer's recommendations. After RNase-Free DNase treatment (Ambion, Clinisciences, Montrouge, France), RNA was reverse-transcribed using Super Script II RNase H Reverse Transcriptase (Invitrogen, Carlsbad, CA, United States) with Random Primers (Promega, Charbonnieres-les-Bains, France). The sequences of forward and reverse primers used to amplify chicken *SLC2A1* (**NM_205209.1**), *SLC2A3* (**NC_006088.5**), *SLC2A8* (**NM_204375.1**), *SLC2A12* (**XM_419733.4**), β-hydroxyacyl-CoA dehydrogenase (*HAD*; **NM_001277897.1**), citrate synthase (*CS*; **XM_015300289.1**), lactate dehydrogenase (*LDH*; **XM_015864180**), and housekeeping *18S rRNA* (**AF173612.1**) genes were specifically designed or reproduced from the literature (Dupont et al., 2008; Joubert et al., 2010; Coudert et al., 2015, 2018); these are presented in **Table 1**. Each cDNA sample was amplified in triplicate by real-time PCR using Sybr Green I Master kit (Roche, Mannheim, Germany) on a LightCycler® 480 II apparatus (Roche, Meylan, France). Gene expression levels were estimated based on PCR efficiency and threshold cycle (Ct) deviation of an unknown sample vs. a control, as previously described (Pfaffl, 2001). The expression of the studied genes was normalized with the *18S rRNA* housekeeping gene that was confirmed to be invariable.

TABLE 1 | Sequences of the forward and reverse primers used to quantify gene expression by real-time PCR.

Genes[1]	Forward	Reverse
18S	TCC AGC TAG GAA TAA TGG AAT AGG A	CCG GCC GTC CCT CTT AAT
CS	AGG GAT TTC ATC TGG AAC ACA CT	CAC CGT GTA GTA CTT CAT CTC CT
HAD	ATC CTT GCA AAT CAC GCA GTT	AAT GGA GGC CAC CAA ATC G
LDH	TTA ACT TGG TCC AAC GCA ACG TCA AT	TCC ACT GGG TTT GAG ACA ATC AG
SLC2A1	ACA ACA CCG GCG TCA TCA A	TTG ACA TCA GCA TGG AGT TAC G
SLC2A3	TGC TCA TCT TCT TCA TAT TCA CAT	ACT TCT TTG TCA GGT TCT ATG C
SLC2A8	CTG GAG GAA TAC TGG GAG GC	CAC CAC CAT CAA CTG GAC AA
SLC2A12	AGA GAG TGG GGA GGT TCC C	TCA GGA CGA GCC AAG ACA

[1]*18S, 18S ribosomal RNA (used as housekeeping gene); CS, citrate synthase; HAD, β-hydroxyacyl-CoA dehydrogenase; LDH, lactate dehydrogenase; SLC2A1, solute carrier family 2 member 1; SLC2A3, solute carrier family 2 member 3; SLC2A8, solute carrier family 2 member 8; SLC2A12, solute carrier family 2 member 12.*

Statistics

Values are presented as mean ± SEM. Results were analyzed firstly by three-way ANOVA (including sex, line, and age effect) after having checked the normality of the residual distribution and the homoscedasticity. When there was no sex effect, the results were analyzed by one- or two-way ANOVA, to test the line effect or line × age effect, respectively. The accepted type I error was set at 5%. Comparisons of means for each significant effect were performed using Fisher's least significant difference test. When the residuals were not normally distributed and variances were not homogeneous between groups, data were analyzed with the non-parametric Kruskal-Wallis test and a multiple comparison test. Differences were considered to be significant when p values were below 0.05.

RESULTS

Body Weight and Composition

There was no sex effect on the parameters of body weight and composition (data not shown). The pHu+ chicks exhibited a slightly higher (+3.9%, $p = 0.01$) average body weight at hatching (D0) than pHu− chicks, but their liver and *Pectoralis major* muscle weights and yields were similar (**Table 2**). The difference in body weight between the two lines was no longer significant 5 days post-hatching, while the *Pectoralis major* muscle weight and yield of pHu+ chicks became 10% ($p = 0.005$) and 8% ($p = 0.0006$) higher than those of pHu− chicks, respectively (**Table 2**).

Plasma Metabolites

Plasma glucose and triglyceride concentrations were higher in pHu− hatched chicks while uric acid concentrations were higher in pHu+ ones (**Figure 1**). There was no effect of the line on free AA and no sex effect on all the characters measured at the plasma level (data not shown). Free AA concentration was no different between D0 and D5. Uric acid concentrations significantly decreased from D0 to D5 in pHu+ birds (−37%, $p < 0.0001$) while they remained constant in pHu− birds (**Figure 1**). Uric acid concentrations were in turn similar between the two lines at D5. On the other hand, triglyceride concentrations decreased in both lines between the time of hatching and D5 at the rate of −35 and −46% ($p < 0.0001$) in pHu+ and pHu−, respectively (**Figure 1**). As for uric acid concentrations, no differences were observed for triglycerides between the two lines at D5, as was also the case for plasma glucose.

Muscle and Liver Characteristics

There was no difference between the lines in the lactate and glycogen contents in the liver of hatched and 5-day-old chicks (**Table 3**). At hatching, glycogen content was higher in pHu− muscles, with differences being more pronounced in the pipping than in the *Pectoralis major* muscle (**Table 3**). Higher values of glycogen were also observed 5 days post-hatch in the *Pectoralis major* muscle of pHu− compared to pHu+ chicks. In the pipping

TABLE 2 | Body composition of chicks of the pHu+ and pHu− lines at hatching (D0) and 5 days post-hatching (D5).

Age	Lines	Body weight (g)	PM[1] weight (g)	Liver weight (g)	PM yield[2]	Liver yield[2]
D0	pHu+	42.4 ± 0.46	0.52 ± 0.02	0.98 ± 0.02	1.21 ± 0.03	2.30 ± 0.05
	pHu−	40.8 ± 0.41	0.48 ± 0.01	0.94 ± 0.02	1.27 ± 0.03	2.26 ± 0.05
	Line effect[3]	$P = 0.01$	NS	NS	NS	NS
D5	pHu+	99.0 ± 1.40	4.39 ± 0.09	3.27 ± 0.09	4.43 ± 0.07	3.29 ± 0.06
	pHu−	96.0 ± 1.97	3.92 ± 0.13	3.05 ± 0.12	4.07 ± 0.08	3.17 ± 0.08
	Line effect[3]	NS	0.005	NS	0.0006	NS

Data are presented as mean ± SEM (n = 30 per line).
[1]PM = Pectoralis major muscle.
[2]% of body weight.
[3]NS = not significant.

muscle, which is highly solicited during the hatching process, the lactate content measured around 10 min post-mortem was also higher in pHu− than in pHu+ hatch chicks. Higher values of lactate were also observed in the *Pectoralis major* muscle of pHu− compared to pHu+ chicks 5 days post-hatching (**Table 3**). Regardless of the line, both lactate and glycogen contents increased between D0 and D5 in the *Pectoralis major* muscle ($p < 0.0001$; tested by two-way ANOVA, including age and line as the main effects). Differences in *Pectoralis major* muscle fiber glycogen content between the lines were clearly observable by microscopy after PAS staining at both ages (**Figure 2**). Despite the differences in *in vivo* glycogen content observed at hatching between the pHu + and pHu− lines, their pHu (measured 24 h post-mortem) was no different (**Figure 3**). By contrast, a difference in pHu of 0.45 units was observed 5 days after hatching between pHu+ and pHu− chicks.

At slaughter age (42 days), the pHu of the *Pectoralis major* muscle was very different between lines: 6.12 vs. 5.54 ($p < 0.001$) in the pHu+ and pHu− lines, respectively. Similarly, the incidence and severity of the WS defect was very different between pHu+ and pHu− lines ($p < 0.001$). Thus, the proportion of unaffected pectoral muscles (WS0) was 61.3% in the pHu− while it was only 38.5% in the pHu+ line. Conversely, the proportions of moderately (WS1) or severely (WS2) affected muscles were higher in the pHu+ (41.8 and 19.7%, respectively) than in the pHu− line (31.1 and 7.6%, respectively). Whether for pHu or the WS defect, we did not observe any effect of sex on these traits (data not shown).

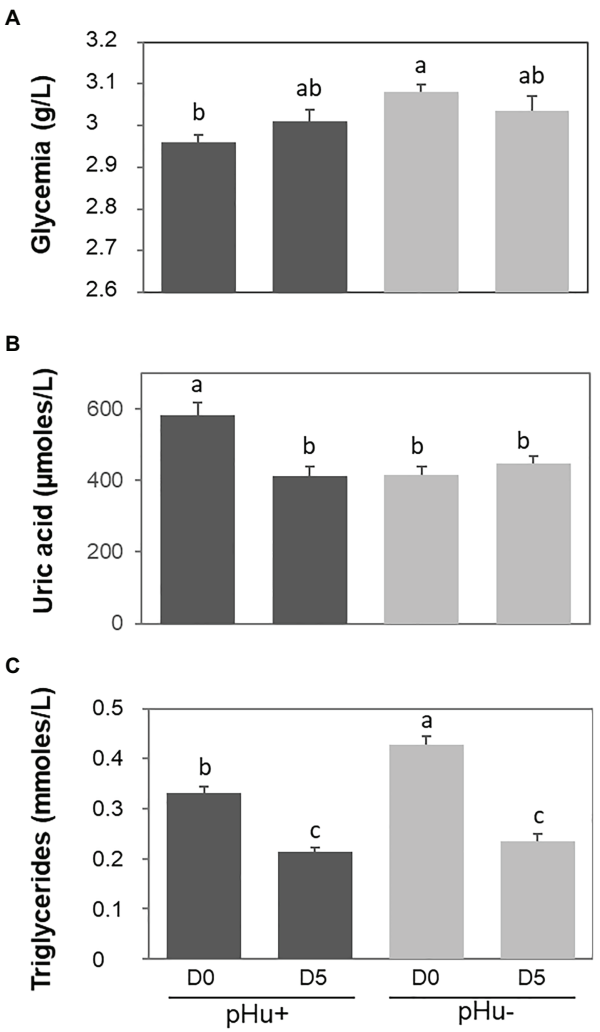

FIGURE 1 | Plasma concentration in glucose (glycemia, **A**), uric acid **(B)**, and triglyceride **(C)** measured at hatching (D0) and 5 days post-hatching (D5) in the pHu+ and pHu− lines. Data are presented as mean ± SEM; $n = 15$ per line and per age. Different letters indicate significant differences between muscle groups ($p \leq 0.05$).

Gene Expression in *Pectoralis major* Muscles

The mRNA expression levels of genes coding the main isoforms of the glucose transporter (GLUT), i.e., *SLC2A1*, *SLC2A3*, *SLC2A8*, and *SLC2A12*, were measured in the *Pectoralis major* of the two lines at hatching and 5 days later (**Table 4**). There was no sex effect on the expression of these genes (data not shown). There was an age × line interaction for the *SLC2A12* expression. The *SLC2A12* expression increased between hatching and D5 while that of *SLC2A1*, *SLC2A3*, and *SLC2A8* decreased. Among these genes, only the expressions of *SLC2A1* and *SLC2A3* were upregulated in pHu+ compared to pHu− muscles, whether at D0 or D5.

The mRNA expression of genes coding key enzymes of glycolytic and oxidative metabolisms, i.e., citrate synthase (CS), 3-hydroxyacyl-CoA-dehydrogenase (HAD), and lactate dehydrogenase (LDHα), were also measured in the *Pectoralis major* muscle of the two lines (**Table 4**). There were no

TABLE 3 | Lactate and glycogen contents in the muscle and liver of the pHu+ and pHu− lines at hatching (D0) and 5 days post-hatching.

Age	Tissue	Metabolites[1]	pHu+	pHu−	Line effect[2]
D0	Liver	Lactate	13.66 ± 0.15	13.79 ± 0.11	NS
		Glycogen content	116.97 ± 4.76	105.60 ± 6.77	NS
	PM muscle[3]	Lactate	24.48 ± 1.24	25.90 ± 1.37	NS
		Glycogen content	108.50 ± 4.71	122.87 ± 4.61	0.04
	Pipping muscle	Lactate	23.40 ± 0.85	31.71 ± 1.96	0.001
		Glycogen content	111.40 ± 3.81	142.49 ± 6.68	0.0008
D5	Liver	Lactate	14.51 ± 0.20	14.89 ± 0.25	NS
		Glycogen content	90.83 ± 3.45	95.74 ± 3.66	NS
	PM muscle	Lactate	37.88 ± 1.11	42.47 ± 1.45	0.02
		Glycogen content	119.80 ± 2.94	149.78 ± 4.14	<0.0001

Data are presented as mean ± SEM (n = 8 males and n = 8 females per line).

[1]Lactate expressed as µmol/g; glycolytic potential expressed as µmol equivalent lactate/g.

[2]NS = not significant.

[3]PM muscle = Pectoralis major muscle.

age × line interactions in any of them. The CS expression almost halved between hatching and day 5, while LDHα expression strongly increased (up to 10 times). The HAD expression remained quite stable during this period. The CS and LDHα expressions were greater in the pHu+ muscle. The calculation of the ratio LDH/CS (glycolysis with pyruvate reduction/aerobic potential of the Krebs cycle) has been proposed by Hochachka et al. (1983) to classify muscles according to their glycolytic capacity. LDH/CS ratio, and therefore glycolytic capacity, significantly increased between D0 and D5 but no differences were observed between the pHu+ and pHu− lines.

Myogenic Differentiation in pHu+ and pHu− Chicks

The immunolocalization and quantification of the sarcomeric myosin (MF20) were assessed *in vitro* to compare the differentiation ability of myogenic cells from pHu+ and pHu− lines. Immunolocalization of MF20 was done on primary cell cultures prepared from pHu+ or from pHu− *Pectoralis major* muscles at D0 and D5. Myoblasts derived from pHu+ showed a better ability to differentiate (**Figures 4A,C**) compared to pHu−-derived myoblasts (**Figures 4B,D**). This was confirmed by Western blot, which revealed a higher expression of the MF20 protein in pHu+ compared to pHu− cell lysates, regardless of sampling age (**Figure 4E**).

S6K1 and S6 Activation

The ribosomal proteins S6 kinase 1 (S6K1) and ribosomal protein S6 (S6) are key regulators of muscle cell growth and protein synthesis. Their activation by phosphorylation, on threonine 389 for S6K1 and on serine 235/236 for S6, was measured in *Pectoralis major* muscles at hatching (D0) both *in vivo* and *in vitro*. The phosphorylation *in vivo* of both S6K1 and S6 was three times higher in the *Pectoralis major* muscles of the pHu+ line than those of the pHu− line at hatching (**Figure 5A**). No sex effect was observed upon activation of the S6K1/ribosomal protein S6 pathway. Greater phosphorylation of S6K1 and S6 was also observed *in vitro* in a primary cell culture prepared from pHu+ than from pHu− *Pectoralis major* muscles, whether under basal conditions or following insulin stimulation (muscles sampled at hatching, **Figure 5B**). Similarly, the S6K1/ribosomal protein S6 pathway was more activated in myotubes originating from pHu+ *Pectoralis major* muscles in chicks at D5, than in those from the pHu− line (data not shown).

DISCUSSION

In chickens, a near-perfect genetic correlation (of −0.97) was established between the *in vivo* glycogen content of breast muscle and pHu, which is a key factor of meat quality (Le Bihan-Duval et al., 2008). In this species, selection for increased growth rate and/or breast muscle mass has been associated with reduced *in vivo* glycogen storage and in turn with higher pHu (Berri et al., 2001, 2007); according to recent studies, this could be a condition associated with a greater occurrence of degenerative disorders such as WS and WB defects (Kuttappan et al., 2009; Petracci et al., 2013; Abasht et al., 2016; Alnahhas et al., 2016, 2017). The understanding of the biological determinism of glycogen content is thus a key point for the control of muscle integrity and meat quality in chickens. While several studies have studied these processes at slaughter age in relation to the control of meat quality and muscle integrity, none have focused on the earlier stages of chicken development. The two broiler lines divergently selected for breast muscle pHu constitute a unique resource population to explore the molecular pathways involved in the control of muscle glycogen storage. To add to the studies carried out at slaughter age (Beauclercq et al., 2016, 2017), this study aims to investigate both *in vivo* and *in vitro* whether phenotypic divergence is established earlier during development, by considering pHu+ and pHu− chicks at hatching, before any exogenous nutrient intake, and after 5 days on a starting diet composed mainly of carbohydrates.

According to our results, pHu+ chicks are heavier at hatching than pHu− chicks. In chickens, the hatching weight is

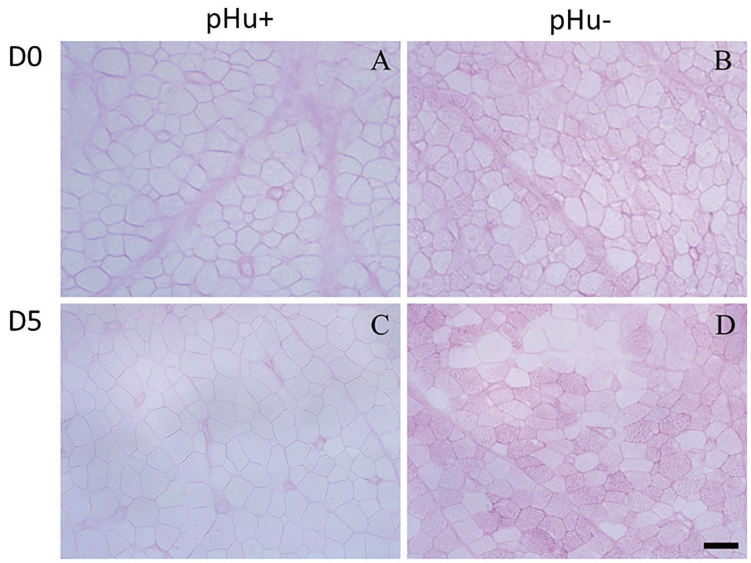

FIGURE 2 | Periodic acid-Schiff staining of *Pectoralis major* muscle cross-sections from pHu+ (**A,C)** vs. pHu− **(B,D)** at hatching (D0, **A,B**) and 5 days post-hatching (D5, **C,D**). Scale bar = 13 μm **(A,B)** and 25 μm **(C,D)**.

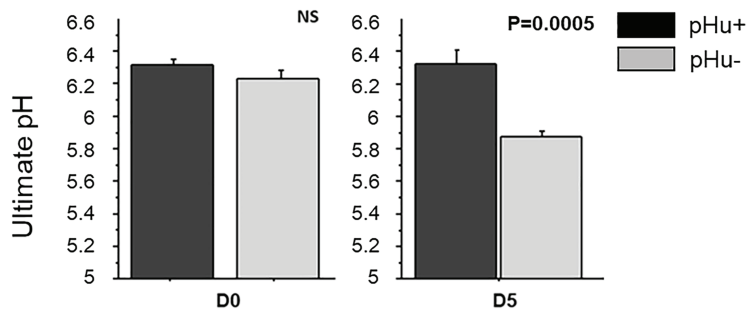

FIGURE 3 | Ultimate pH in *Pectoralis major* muscles at hatching (D0) and at 5 days post-hatching (D5) in the pHu+ and pHu− lines. Data are presented as mean ± SEM; n = 6 per line and per age at D0 and D5.

highly related to egg weight (Halbersleben and Mussehl, 1922; Iqbal et al., 2017). Although we did not measure this trait in the studied generation (G8), we have since acquired data that show a significantly higher egg weight in the pHu+ compared to the pHu− line; e.g., in the 9th generation, the pHu+ egg weight was 57.9 ± 0.3 g compared to 54.7 ± 0.2 g for the pHu− line ($p < 0.0001$). We also clearly showed that differences in muscle glycogen exist as soon as hatching occurs, with pHu− chicks exhibiting higher glycogen reserves in both the *Pectoralis major* muscle, targeted by the selection on the ultimate pH of the meat, and the pipping muscle, which is highly solicited at hatching for shell breaking. This result is consistent with previous observations, which showed that the selection on breast meat pHu was affected in the same way but to a lower extent of glycogen storage in thigh *Sartorius* muscle (Alnahhas et al., 2014). By contrast, selection on muscle pHu did not alter liver glycogen, suggesting a specific effect of selection on skeletal muscle energy stores. In the egg, less than 1% of the total available nutrients are carbohydrates and only 0.3% are free glucose. Thus, glucose homeostasis during late embryonic development depends on the amount of glucose generated by gluconeogenesis from amino acids originating from the degradation of proteins (including muscle proteins) and which are stored as glycogen in the liver. The glycerol issued from the triglyceride hepatic metabolism is the main substrate for liver and muscle glycogen synthesis at the end of incubation (Sunny and Bequette, 2011). Between embryonic days 15 and 19, liver metabolism is activated mainly to ensure the transfer of glucose and fatty acids to muscles solicited for hatching, such as the pipping muscle whose contents in glucose, glycogen, and proteins increase during this period (Pulikanti et al., 2010). During the late-hatching stage, carbohydrates rather than lipids are preferentially metabolized, and as a consequence, glycogen is

TABLE 4 | Relative mRNA abundance of genes[1] coding *SLC2A1*, *SLC2A3*, *SLC2A8*, *SLC2A12*, *CS*, *LDHa*, and *HAD* in the *Pectoralis major* muscles of chicks of the pHu+ and pHu− lines measured at hatching (D0) and 5 days post-hatching (D5).

Age	D0		D5		Effect[2]		
Lines	pHu+	pHu−	pHu+	pHu−	Age	Line	Age × line
SLC2A1	1.04 ± 0.08	0.91 ± 0.05	0.87 ± 0.06	0.66 ± 0.04	<0.0001	0.0005	NS
SLC2A3	1.17 ± 0.08	1.03 ± 0.04	0.82 ± 0.04	0.69 ± 0.02	<0.0001	0.01	NS
SLC2A8	1.18 ± 0.08	1.30 ± 0.07	0.55 ± 0.03	0.47 ± 0.03	<0.0001	NS	NS
SLC2A12	0.36 ± 0.03[a]	0.42 ± 0.02[a]	1.14 ± 0.07[b]	1.00 ± 0.06[b]	<0.0001	NS	0.03
CS	1.26 ± 0.08	1.14 ± 0.05	0.75 ± 0.03	0.61 ± 0.02	<0.0001	0.0008	NS
HAD	0.92 ± 0.07	0.82 ± 0.05	0.90 ± 0.05	0.76 ± 0.03	0.08	NS	NS
LDHa	0.15 ± 0.02	0.11 ± 0.01	1.78 ± 0.1	1.54 ± 0.09	<0.0001	0.02	NS
LDHa/CS	0.08 ± 0.01	0.09 ± 0.01	2.68 ± 0.09	2.81 ± 0.14	<0.0001	NS	NS

Data are presented as mean ± SEM (n = 8 males and n = 8 females per line). 18S was used for normalization.

[1]CS, citrate synthase; HAD, β-hydroxyacyl-CoA dehydrogenase; LDH, lactate dehydrogenase; SLC2A1, solute carrier family 2 member 1; SLC2A3, solute carrier family 2 member 3; SLC2A8, solute carrier family 2 member 8; SLC2A12, solute carrier family 2 member 12.

[2]NS = not significant.

[a,b]Within a row, mean values without a common letter differ between groups ($p \leq 0.05$).

highly consumed. This induces a high rate of muscle protein degradation and of amino acid production for gluconeogenesis (Chen et al., 2009; Noy and Uni, 2010). This intensive use of proteins for an energy purpose at the end of embryogenesis specially affects *Pectoralis major* muscle development, whose yield relative to the weight of the embryo decreases between embryonic day 11 and hatching (Guernec et al., 2003). Accordingly, an increase in the expression of atrophy-related genes involved in muscle protein degradation such as atrogin-1 and MuRF1 is observed in *Pectoralis major* muscles between embryonic day 18 and hatching, which likely contributes to the decreased rate of breast muscle development (Everaert et al., 2013). Our study revealed higher blood uric acid contents in the hatched pHu+ chicks, which likely indicates a higher rate of muscle protein catabolism and amino acid utilization to produce energy in a context of muscle glycogen depletion, compared to pHu− chicks. Moreover, even though pHu+ chicks were heavier at hatching than pHu− ones, the two lines exhibited similar *Pectoralis muscle* weights and yields. At hatching, pHu− chicks exhibited higher glycemia, which was already observed at 6 weeks of age (Beauclercq et al., 2015), and higher blood triglyceride contents than pHu+ chicks, indicating that metabolic differences exist between the two lines independently of any exogenous nutrient supply. Higher blood glucose and triglyceride contents in pHu− may reflect a better use of yolk lipid as source of energy during embryogenesis, in agreement with the greater occurrence of highly resorbed yolk observed at hatching in this line compared to the pHu+ one (data not shown).

Obviously, differences in glucose homeostasis exist between the lines before hatching, when lipids are the principal source of nutrients for the embryo. However, the higher glycemia of the pHu− chicks may also reflect lower glucose uptake by muscle cells compared to pHu+ chicks. Similar to mammals, the striated skeletal muscle in birds is a major glucose-utilizing tissue. Glucose is an essential metabolic substrate that is transported into cells by several glucose transporters belonging to the GLUT family. As for mammals, glucose transport in chickens involves several glucose transporters that play a crucial role in cellular glucose uptake and glucose homeostasis. Among them, GLUT1, 3, 8, and 12 are expressed in chicken muscles (Kono et al., 2005; Coudert et al., 2015, 2018; Shimamoto et al., 2016), with the levels of mRNA expressions of GLUT1, 3, and 8 (but not GLUT12) being particularly high during the post-hatching period in the glycolytic *Pectoralis major* muscle compared to more oxidative muscles (Shimamoto et al., 2016). Moreover, although GLUT4 is the major glucose transporter in mammalian muscles, it is not expressed in chickens and the insulin-sensitive glucose transporter GLUT12 could partially play the role of GLUT4 in this species (Coudert et al., 2015, 2018). In our study, both *SLC2A1* and *SLC2A3* genes, coding, respectively, for GLUT1 and 3, were significantly more expressed in the pHu+ *Pectoralis major* muscles compared to those of pHu− chicks, both at hatching and at day 5. The mRNA expressions of *SLC2A1* have been shown to gradually decrease during late embryogenesis (from day 12 to 18) before increasing again between hatching and 5 days post-hatching in chicken *Pectoralis major* muscles (Coudert et al., 2018), when breast muscle growth rate and therefore energy requirement is maximal. The higher expressions of *SLC2A1* and *SLC2A3* in the *Pectoralis major* of pHu+ chicks through the enhancement of glucose uptake from blood into muscle could therefore contribute to the lower glycemia of pHu+ at hatching. Upon hatching, pHu+ muscles also exhibited lower glycogen stores compared to pHu− muscles. It could be hypothesized that despite a possibly higher glucose uptake in pHu+ muscles, the consumption of glucose for ATP production is also more intense than in pHu−. These results, obtained in the early stages of development in chicks, may be of more general interest, especially concerning the later appearance of degenerative muscle disorders in fast-growing chickens, which, according to several authors, would imply dysregulation of carbohydrate metabolism (for review, see Lake and Abasht, 2020).

A greater glucose uptake capacity has already been associated with greater metabolic demand when comparing

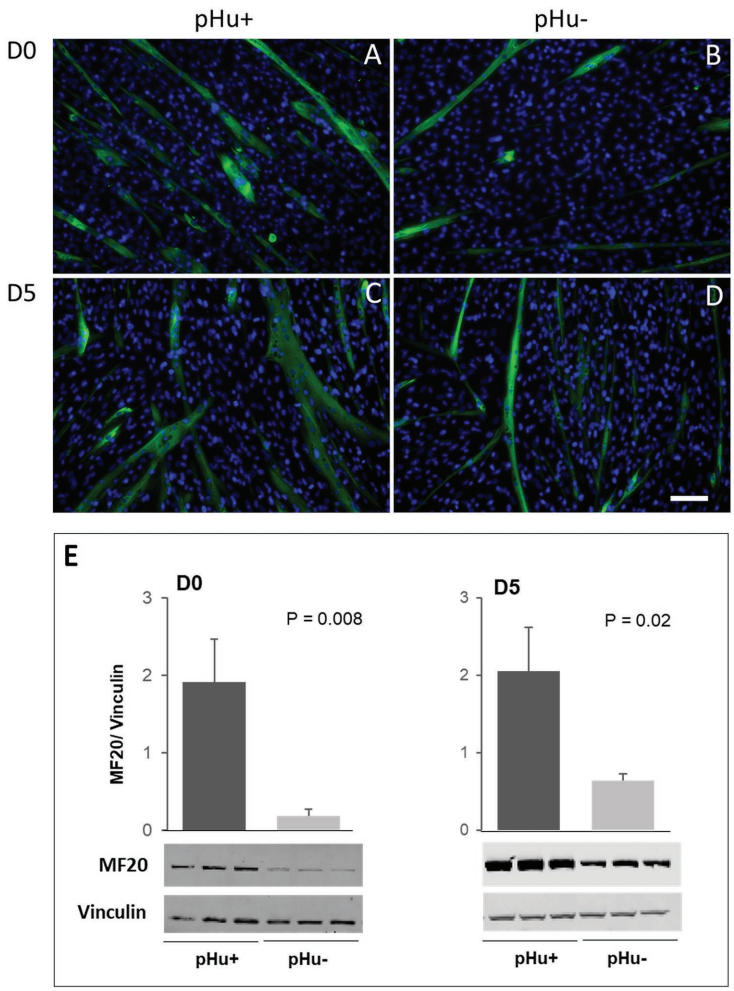

FIGURE 4 | Immunolocalization **(A–D)** and quantification **(E)** of sarcomeric myosin (MF20) on satellite cells derived from *Pectoralis major* muscles sampled at hatching (D0) and 5 days post-hatching (D5) in the pHu+ and pHu− lines. Scale bar = 70 μm. Data are expressed as mean ± SEM. Different letters indicate significant differences between muscle groups ($p \leq 0.05$). The anti-vinculin antibody was used as a loading control.

muscles from chicken lines selected for high or low body weights (Zhang et al., 2013). It is likely that the pHu+ muscles exhibited a higher metabolic demand than pHu− muscles, since they are characterized by a greater activation of the S6K1/ribosomal protein S6 signaling pathway that is involved in the stimulation of growth and protein synthesis. The higher propensity of pHu+ chicks for muscle protein synthesis at hatching was observed both *in vitro*, with greater phosphorylation of S6K1 and ribosomal protein S6 in primary muscle cells with or without insulin stimulation, and *in vivo* in the *Pectoralis major* muscle sampled at hatching. This higher protein synthesis in the pHu+ muscles of hatched chicks is likely to be accompanied by higher muscle protein degradation to provide amino acid for energy production during the late-hatching stage. Moreover, higher proteolysis and AA catabolism has already been observed in the breast muscles of pHu+ compared to pHu− chickens at slaughter age (Beauclercq et al., 2016). Altogether, our findings suggest that breast muscle deposition could require a more intense protein turnover in pHu+ around hatching, likely leading to a higher energy requirement compared to pHu−, since both protein degradation and synthesis are energetically costly processes. This is consistent with the higher expression of genes coding LDH and CS, which are indicative of the glycolytic and oxidative capacities, respectively, and lower glycogen contents in the *Pectoralis major* muscles of pHu+ compared to pHu− lines.

Between hatching and 5 days post-hatching, blood triglycerides decreased in the two lines, likely in response to dietary carbohydrate instead of the lipids and AA mainly provided *in ovo* (Moran, 2007; Cherian, 2015). After 5 days, there was no further line effect on uric acid, triglyceride, or glycemia. However, at day 5, the pHu+ chicks exhibited higher *Pectoralis major* muscle weights and yields compared to pHu− chicks. As shown by the strong increase in LDH/CS ratio, there is a shift from oxidative to glycolytic metabolism

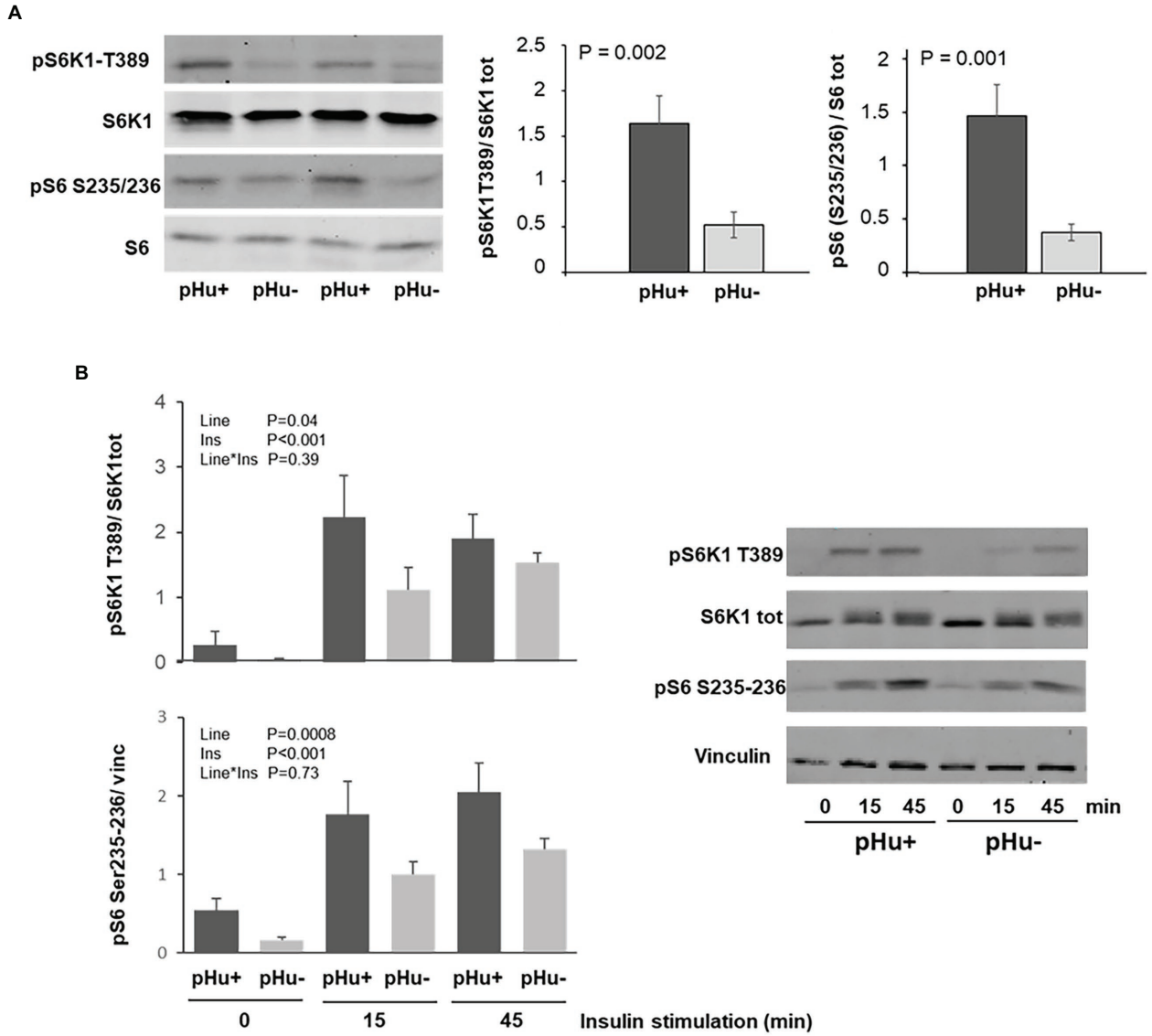

FIGURE 5 | Regulation of the S6K1 pathway in the *Pectoralis major* muscles sampled in the pHu+ and pHu− at hatch (D0; **A**) and in the cell culture of satellite cells from *Pectoralis major* muscles sampled at hatching (D0) following insulin stimulation (100 nM for 0, 15, or 45 min; **B**). Membranes were incubated with polyclonal antibodies against phospho-S6K1 [T389] (pS6K1 T389), S6K1, phospho-S6 [S235/236] (pS6 S235/236), and ribosomal protein S6. Vinculin was used as loading control. Data are expressed as mean ± SEM.

between hatching and day 5 in the breast muscles of both lines (Hochachka et al., 1983). Both lines exhibited similar LDH/CS ratios, suggesting that they have similar metabolic profiles at this age despite the higher metabolic activity and lower glycogen content observed in pHu+ muscles.

The pHu+ muscles of 5-day-old chicks were also characterized by a greater expression of both *SLC2A1* and *SLC2A3* genes coding for glucose transporters 1 and 3, respectively. This could indicate that between hatching and day 5, the glucose transport is greater in pHu+ muscles both to face the lack of carbohydrate availability and to support the higher breast muscle growth rate observed post-hatching in this line compared to the pHu− one.

In vitro experiments clearly showed the higher capability of myoblasts derived from pHu+ muscles to differentiate in myotubes compared to those derived from pHu− ones, which is concomitant with the higher activation of the S6K1/S6 pathway in muscle cells derived from the pHu+ line, a pathway known to stimulate protein synthesis in chickens as in other species (Tesseraud et al., 2006; Nakashima et al., 2020). As mentioned above, the better ability of pHu+ muscles to activate the cascading phosphorylation of the S6K1/S6 pathway was also shown *in vivo* at hatching. Therefore, both *in vitro* and *in vivo* results indicated the greater propensity of pHu+ chicks for growth and muscle protein synthesis compared to pHu− ones. As discussed earlier, a higher protein synthesis rate of

pHu+ chicks accompanied by higher muscle catabolism for energy supply during the late incubation phase may explain why pectoral muscle deposition was similar between pHu+ and pHu− lines at hatching. By contrast, during early post-hatching growth when chicks received carbohydrates and proteins as main sources of nutrients, a higher protein synthesis rate of pHu+ clearly led to higher muscle deposition compared to pHu−, while differences in glycogen content increased between the two lines. Breast muscle glycogen content was around 20% lower in pHu+ than in pHu− 5 days post-hatching, while it was less than 12% lower at hatching. According to the present study and our previous observations, the differences observed 5 days post-hatching remained until slaughter age (i.e., 6 weeks), when pHu+ chickens exhibited higher breast and thigh muscle yields and lower muscle glycogen, and thus higher pHu, compared to pHu− chickens (Alnahhas et al., 2014, 2015; present study). Such a competition between muscle protein and energy deposition had already been suggested in other fast-growing strains of chickens. Indeed, the selection for growth and breast meat yield in chickens led to decreased muscle glycogen content, affecting meat pHu and related quality traits, such as color and water-holding capacity (Berri et al., 2001, 2007).

In conclusion, this study had provided new information regarding the early development of phenotypic differences in two divergent chicken lines on the ultimate pH of breast meat, as well as the mechanisms involved. It revealed that muscle metabolic differences, in particular the glycogen content, induced by the selection at slaughter age, are already present at hatching and amplified by the exogenous supply of nutrients during the early post-hatching stage. Interestingly, reduced muscle glycogen content at hatching appeared to be associated with enhanced glucose transport and a higher propensity of muscle cells for protein synthesis, leading to greater breast muscle growth after hatching. However, the question of whether the higher protein turnover associated with the low carbohydrate reserves that characterize the pHu+ line from hatching onwards may contribute to their greater propensity to develop WS-type defects at slaughter age requires further study. All metabolic differences observed at hatching between the two lines are likely to be related to differences in nutrient use or availability *in ovo*, which deserves further investigation to decipher how embryos from the two lines interact with the main sources of nutrients during incubation, i.e., the yolk sac and amniotic fluid, and to determine if part of the effects of selection on the ultimate pH of breast meat are due to changes in their composition.

DATA AVAILABILITY STATEMENT

The raw data supporting the conclusions of this article will be made available by the authors, without undue reservation.

ETHICS STATEMENT

The animal study was reviewed and approved by the French Agricultural Agency and the Scientific Research Agency.

AUTHOR CONTRIBUTIONS

Conceived and designed the experiments: SM-C, CB, and EB-D. Performed the experiments: DR, TB, EC, EC-A, EG, CP, JD, and SM-C. Analyzed the data: SM-C, CP, and EC-A. Wrote the paper: SM-C under the supervision of CB, ST, and EB-D. All authors contributed to the article and approved the submitted version.

FUNDING

This work was supported by INRAE.

ACKNOWLEDGMENTS

We thank the staff of PEAT INRAE Poultry Experimental Facility (2018, https://doi.org/10.15454/1.5572326250887292E12) for producing and rearing animals, the technicians of the BOA unit (INRAE, Université de Tours, UMR BOA, F-37380 Nouzilly, France) for measurements on birds, sample collection, and laboratory analyses.

REFERENCES

Abasht, B., Mutryn, M. F., Michalek, R. D., and Lee, W. R. (2016). Oxidative stress and metabolic perturbations in wooden breast disorder in chickens. *PLoS One* 11:e0153750. doi: 10.1371/journal.pone.0153750

Alnahhas, N., Berri, C., Boulay, M., Baéza, E., Jégo, Y., Baumard, Y., et al. (2014). Selecting broiler chickens for ultimate pH of breast muscle: analysis of divergent selection experiment and phenotypic consequences on meat quality, growth, and body composition traits. *J. Anim. Sci.* 92, 3816–3824. doi: 10.2527/jas.2014-7597

Alnahhas, N., Berri, C., Chabault, M., Chartrin, P., Boulay, M., Bourin, M. C., et al. (2016). Genetic parameters of white striping in relation to body weight, carcass composition, and meat quality traits in two broiler lines divergently selected for the ultimate pH of the pectoralis major muscle. *BMC Genet.* 17:61. doi: 10.1186/s12863-016-0369-2

Alnahhas, N., Berri, C., Chabault-Dhuit, M., Bourin, M., Arnould, C., and Le Bihan-Duval, E. (2017). Combined effect of divergent selection for breast muscle ultimate pH and dietary amino acids on chicken performance, physical activity and meat quality. *Animal* 11, 335–344. doi: 10.1017/S1751731116001580

Alnahhas, N., Le Bihan-Duval, E., Baéza, E., Chabault, M., Chartrin, P., Bordeau, T., et al. (2015). Impact of divergent selection for ultimate pH of pectoralis major muscle on biochemical, histological, and sensorial attributes of broiler meat. *J. Anim. Sci.* 93, 4524–4531. doi: 10.2527/jas.2015-9100

Artiss, J. D., and Entwistle, W. M. (1981). The application of a sensitive uricase-peroxidase coupled reaction to a centrifugal fast analyser for the determination of uric acid. *Clin. Chim. Acta* 116, 301–309. doi: 10.1016/0009-8981(81)90049-8

Beauclercq, S., Baéza, E., Bordeau, T., Chartrin, P., Godet, E., le Bihan-Duval, E., et al. (2015). "Consequences of a selection on breast meat ultimate pH on

muscle fiber typology and metabolism in broiler" in *Actes des 11èmes Journées de la Recherche Avicole et Palmipèdes à Foie Gras, Tours, France*. 1117–1121.

Beauclercq, S., Hennequet-Antier, C., Praud, C., Godet, E., Collin, A., Tesseraud, S., et al. (2017). Muscle transcriptome analysis reveals molecular pathways and biomarkers involved in extreme ultimate pH and meat defect occurrence in chicken. *Sci. Rep.* 7:6447. doi: 10.1038/s41598-017-06511-6

Beauclercq, S., Nadal-Desbarats, L., Hennequet-Antier, C., Collin, A., Tesseraud, S., Bourin, M., et al. (2016). Serum and muscle metabolomics for the prediction of ultimate pH, a key factor for chicken-meat quality. *J. Proteome Res.* 15, 1168–1178. doi: 10.1021/acs.jproteome.5b01050

Berri, C., Le Bihan-Duval, E., Debut, M., Santé-Lhoutellier, V., Baéza, E., Gigaud, V., et al. (2007). Consequence of muscle hypertrophy on characteristics of *Pectoralis major* muscle and breast meat quality of broiler chickens. *J. Anim. Sci.* 85, 2005–2011. doi: 10.2527/jas.2006-398

Berri, C., Wacrenier, N., Millet, N., and Le Bihan-Duval, E. (2001). Effect of selection for improved body composition on muscle and meat characteristics of broilers from experimental and commercial lines. *Poult. Sci.* 80, 833–838. doi: 10.1093/ps/80.7.833

Chen, W., Wang, R., Wan, H. F., Xiong, X. L., Peng, P., and Peng, J. (2009). Influence of in ovo injection of glutamine and carbohydrates on digestive organs and pectoralis muscle mass in the duck. *Br. Poult. Sci.* 50, 436–442. doi: 10.1080/00071660903114341

Cherian, G. (2015). Nutrition and metabolism in poultry: role of lipids in early diet. *J. Anim. Sci. Biotechnol.* 6:28. doi: 10.1186/s40104-015-0029-9

Coudert, E., Praud, C., Dupont, J., Crochet, S., Cailleau-Audouin, E., Bordeau, T., et al. (2018). Expression of glucose transporters SLC2A1, SLC2A8, and SLC2A12 in different chicken muscles during ontogenesis. *J. Anim. Sci.* 96, 498–509. doi: 10.1093/jas/skx084

Coudert, E., Pascal, G., Dupont, J., Simon, J., Cailleau-Audouin, E., Crochet, S., et al. (2015). Phylogenesis and biological characterization of a new glucose transporter in the chicken (*Gallus gallus*), GLUT12. *PLoS One* 10:e0139517. doi: 10.1371/journal.pone.0139517

Dalrymple, R. H., and Hamm, R. (1973). A method for the extraction of glycogen and metabolites from a single muscle sample. *Fd. Technol.* 8, 439–444.

Duchêne, S., Métayer, S., Audouin, E., Bigot, K., Dupont, J., and Tesseraud, S. (2008). Refeeding and insulin activate the AKT/p70S6 kinase pathway without affecting IRS1 tyrosine phosphorylation in chicken muscle. *Domest. Anim. Endocrinol.* 34, 1–13. doi: 10.1016/j.domaniend.2006.09.002

Dupont, J., Tesseraud, S., Derouet, M., Collin, A., Rideau, N., Crochet, S., et al. (2008). Insulin immuno-neutralization in chicken: effects on insulin signaling and gene expression in liver and muscle. *J. Endocrinol.* 197, 531–542. doi: 10.1677/JOE-08-0055

Everaert, N., Métayer-Coustard, S., Willemsen, H., Han, H., Song, Z., Ansari, Z., et al. (2013). The effect of albumen removal before incubation (embryonic protein under-nutrition) on the post-hatch performance, regulators of protein translation activation and proteolysis in neonatal broilers. *Br. J. Nutr.* 110, 265–274. doi: 10.1017/S000711451200503X

Fossati, P., and Prencipe, L. (1982). Serum triglycerides determined colorimetrically with an enzyme that produces hydrogen peroxide. *Clin. Chem.* 28, 2077–2080. doi: 10.1093/clinchem/28.10.2077

Guernec, A., Berri, C., Chevalier, B., Wacrenier-Cere, N., Le Bihan-Duval, E., and Duclos, M. J. (2003). Muscle development, insulin-like growth factor-I and myostatin mRNA levels in chickens selected for increased breast muscle yield. *Growth Hormon. IGF Res.* 13, 8–18. doi: 10.1016/s1096-6374(02)00136-3

Halbersleben, D. L., and Mussehl, F. E. (1922). Relation of egg weight to chick weight at hatching. *Poult. Sci.* 1, 143–144. doi: 10.3382/ps.0010143

Havenstein, G. B., Ferket, P. R., and Qureshi, M. A. (2003a). Carcass composition and yield of 1957 versus 2001 broilers when fed representative 1957 and 2001 broiler diets. *Poult. Sci.* 82, 1509–1518. doi: 10.1093/ps/82.10.1509

Havenstein, G. B., Ferket, P. R., and Qureshi, M. A. (2003b). Growth, livability, and feed conversion of 1957 versus 2001 broilers when fed representative 1957 and 2001 broiler diets. *Poult. Sci.* 82, 1500–1508. doi: 10.1093/ps/82.10.1500

Hochachka, P. W., Stanley, C., Merkt, J., and Sumar-Kalinowski, J. (1983). Metabolic meaning of elevated levels of oxidative enzymes in high altitude adapted animals: an interpretive hypothesis. *Respir. Physiol.* 52, 303–313. doi: 10.1016/0034-5687(83)90087-7

Iqbal, J., Mukhtar, N., Ur Rehman, Z., Khan, S. H., Ahmad, T., Anjum, M. S., et al. (2017). Effects of egg weight on the egg quality, chick quality, and broiler performance at the later stages of production (week 60) in broiler breeders. *J. Appl. Poult. Res.* 26, 183–191. doi: 10.3382/japr/pfw061

Joubert, R., Métayer Coustard, S., Swennen, Q., Sibut, V., Crochet, S., Cailleau-Audouin, E., et al. (2010). The beta-adrenergic system is involved in the regulation of the expression of avian uncoupling protein in the chicken. *Domest. Anim. Endocrinol.* 38, 115–125. doi: 10.1016/j.domaniend.2009.08.002

Kono, T., Nishida, M., Nishiki, Y., Seki, Y., Sato, K., and Akiba,Y. (2005). Characterisation of glucose transporter (GLUT) gene expression in broiler chickens. *Br. Poult. Sci.* 46, 510–515. doi: 10.1080/00071660500181289

Kuttappan, V. A., Brewer, V. B., Clark, F. D., McKee, S. R., Meullenet, J. F., Emmert, J. L., et al. (2009). Effect of white striping on the histological and meat quality characteristics of broiler fillets. *Poult. Sci.* 88 (E-Suppl. 1), 136–137.

Kuttappan, V. A., Lee, Y. S., Erf, G. F., Meullenet, J. -F. C., McKee, S. R., and Owens, C. M. (2012). Consumer acceptance of visual appearance of broiler breast meat with varying degrees of white striping. *Poult. Sci.* 91, 1240–1247. doi: 10.3382/ps.2011-01947

Lake, J. A., and Abasht, B. (2020). Glucolipotoxicity: a proposed etiology for wooden breast and related myopathies in commercial broiler chickens. *Front. Physiol.* 11:169. doi: 10.3389/fphys.2020.00169

Le Bihan-Duval, E., Berri, C., Baeza, E., Millet, N., and Beaumont, C. (2001). Estimation of the genetic parameters of meat characteristics and of their genetic correlations with growth and body composition in an experimental broiler line. *Poult. Sci.* 80, 839–843. doi: 10.1093/ps/80.7.839

Le Bihan-Duval, E., Debut, M., Berri, C., Sellier, N., Santé-Lhoutellier, V., Jégo, Y., et al. (2008). Chicken meat quality: genetic variability and relationship with growth and muscle characteristics. *BMC Genet.* 9:53. doi: 10.1186/1471-2156-9-53

Monin, G., and Sellier, P. (1985). Pork of low technological quality with a normal rate of muscle pH fall in the immediate post-mortem period: The case of the Hampshire breed. *Meat Sci.* 13, 49–63. doi: 10.1016/S0309-1740(85)80004-8

Moran, E. T. Jr. (2007). Nutrition of the developing embryo and hatchling. *Poult. Sci.* 86, 1043–1049. doi: 10.1093/ps/86.5.1043

Nakashima, K., Ishida, A., Shimamoto, S., Ijiri, D., and Ohtsuka, A. (2020). Insulin stimulation of protein synthesis and mTOR signaling in chick myotube cultures. *J. Poult. Sci.* 57, 205–209. doi: 10.2141/jpsa.0190082

Noy, Y., and Uni, Z. (2010). Early nutritional strategies. *Worlds Poult. Sci. J.* 66, 639–646. doi: 10.1017/S0043933910000620

Petracci, M., Mudalal, S., Bonfiglio, A., and Cavani, C. (2013). Occurrence of white striping under commercial conditions and its impact on breast meat quality in broiler chickens. *Poult. Sci.* 92, 1670–1675. doi: 10.3382/ps.2012-03001

Petracci, M., Mudalal, S., Soglia, F., and Cavani, C. (2015). Meat quality in fast-growing broiler chickens. *Worlds Poult. Sci. J.* 71, 363–374. doi: 10.1017/S0043933915000367

Pfaffl, M. W. (2001). A new mathematical model for relative quantification in real-time RT-PCR. *Nucleic Acids Res.* 29:e45. doi: 10.1093/nar/29.9.e45

Praud, C., Al Ahmadieh, S., Voldoire, E., Le Vern, Y., Godet, E., Couroussé, N., et al. (2017). Beta-carotene preferentially regulates chicken myoblast proliferation withdrawal and differentiation commitment via BCO1 activity and retinoic acid production. *Exp. Cell Res.* 358, 140–146. doi: 10.1016/j.yexcr.2017.06.011

Pulikanti, R., Peebles, E. D., Keirs, R. W., Bennett, L. W., Keralapurath, M. M., and Gerard, P. D. (2010). Pipping muscle and liver metabolic profile changes and relationships in broiler embryos on days 15 and 19 of incubation. *Poult. Sci.* 89, 860–865. doi: 10.3382/ps.2009-00531

Rauw, W. M., Kanis, E., Noordhuizen-Stassen, E. N., and Grommers, F. J. (1998). Undesirable side effects of selection for high production efficiency in farm animals: a review. *Livest. Prod. Sci.* 56, 15–33. doi: 10.1016/S0301-6226(98)00147-X

Shimamoto, S., Ijiri, D., Kawaguchi, M., Nakashima, K., and Ohtsuka, A. (2016). Gene expression pattern of glucose transporters in the skeletal muscles of newly hatched chicks. *Biosci. Biotechnol. Biochem.* 80, 1382–1385. doi: 10.1080/09168451.2016.1162088

Sunny, N. E., and Bequette, B. J. (2011). Glycerol is a major substrate for glucose, glycogen, and nonessential amino acid synthesis in late-term chicken embryos. *J. Anim. Sci.* 89, 3945–3953. doi: 10.2527/jas.2011-3985

Tesseraud, S., Abbas, M., Duchene, S., Bigot, K., Vaudin, P., and Dupont, J. (2006). Mechanisms involved in the nutritional regulation of mRNA translation: features of the avian model. *Nutr. Res. Rev.* 19, 104–116. doi: 10.1079/NRR2006120

Zhang, W., Sumners, L. H., Siegel, P. B., Cline, M. A., and Gilbert, E. R. (2013). Quantity of glucose transporter and appetite-associated factor mRNA in various tissues after insulin injection in chickens selected for low or high body weight. *Physiol. Genomics* 45, 1084–1094. doi: 10.1152/physiolgenomics.00102.2013

Conflict of Interest: The authors declare that the research was conducted in the absence of any commercial or financial relationships that could be construed as a potential conflict of interest.

frontiers in Physiology

ORIGINAL RESEARCH
published: 18 March 2021
doi: 10.3389/fphys.2021.658711

Comprehensive Proteomic Characterization of the Pectoralis Major at Three Chronological Ages in Beijing-You Chicken

*Jian Zhang[1], Jing Cao[1], Ailian Geng[1], Haihong Wang[1], Qin Chu[1], Linbing Yang[2], Zhixun Yan[1], Xiaoyue Zhang[1], Yao Zhang[1], Jie Dai[2] and Huagui Liu[1]**

[1] Institute of Animal Husbandry and Veterinary Medicine, Beijing Academy of Agriculture and Forestry Sciences, Beijing, China, [2] Shanghai Bioprofile Technology Co., Ltd., Shanghai, China

Chronological age is one of the important factors influencing muscle development and meat quality in chickens. To evaluate the protein expression profiles during skeletal muscle development, we performed a tandem mass tag (TMT)-based quantitative proteomic strategy in pectoralis major (breast muscle) of Beijing-You chicken (BYC) at the chronological age of 90, 120, and 150 days. Each chronological age contained 3 pooling samples or 15 birds (five birds per pooling sample). A total of 1,413 proteins were identified in chicken breast muscle with FDR $< 1\%$ and 197 of them were differentially expressed (fold change ≥ 1.2 or ≤ 0.83 and $p < 0.05$). There were 110 up- and 71 down-regulated proteins in 120 d vs 90 d group, 13 up- and 10 down-regulated proteins in 150 d vs 120 d group. The proteomic profiles of BYC at 120 d were very similar to those at 150 d and highly different from those at 90 d, suggesting that 120 d might be an important chronological age for BYC. Kyoto Encyclopedia of Genes and Genomes (KEGG) analyses indicated that these differentially expressed proteins were mainly involved in the pathway of glycolysis/gluconeogenesis, adrenergic signaling in cardiomyocytes, focal adhesion, oocyte meiosis and phagosome. Furthermore, some DEPs were quantified using parallel reaction monitoring (PRM) to validate the results from TMT analysis. In summary, these results provided some candidate protein-coding genes for further functional validation and contribute to a comprehensive understanding of muscle development and age-dependent meat quality regulation by proteins in chickens.

Keywords: Beijing-You chicken, pectoralis major, chronological age, TMT-based quantitative proteomic analysis, parallel reaction monitoring

OPEN ACCESS

Edited by:
Sandra G. Velleman, The Ohio State University, United States

Reviewed by:
Francesca Soglia, University of Bologna, Italy
Yuwares Malila, National Center for Genetic Engineering and Biotechnology (BIOTEC), Thailand

***Correspondence:**
Huagui Liu
yj_baafs@126.com

Specialty section:
This article was submitted to Avian Physiology, a section of the journal Frontiers in Physiology

Received: *26 January 2021*
Accepted: *22 February 2021*
Published: *18 March 2021*

Citation:
Zhang J, Cao J, Geng A, Wang H, Chu Q, Yang L, Yan Z, Zhang X, Zhang Y, Dai J and Liu H (2021) Comprehensive Proteomic Characterization of the Pectoralis Major at Three Chronological Ages in Beijing-You Chicken. Front. Physiol. 12:658711. doi: 10.3389/fphys.2021.658711

INTRODUCTION

Muscle development and meat quality are traits that are comprehensively affected by age, gender, nutrition, and species (López et al., 2011; Díaz et al., 2012; Umaya, 2014; Tasoniero et al., 2018). Among these parameters, the animal's chronological age is one of the most important factors that can strongly influence these traits (Peterson et al., 1959; Brant and Hanson, 1962;

Mehaffey et al., 2006; Tougan et al., 2013). Moreover, the intramuscular fat (IMF) content also plays an important role in the flavor of chicken meat (Chizzolini et al., 1999; Ros-Freixedes et al., 2014; Li et al., 2019); in previous studies, the IMF content in chicken breast meat increased with age from 56 to 140 d, accompanied by enhanced flavor and taste of the meat (Liu et al., 2016; Cui et al., 2018).

The emerging quantitative proteomic technology allows the systematic study of static or perturbation-induced changes in proteome-wide expression profiles (Pan and Aebersold, 2007) and the discovery of different meat quality biomarkers (Paredi et al., 2012; Wu et al., 2015). Recently, several studies have been carried out to elucidate muscle development and meat quality traits in chickens through proteomics-based methods. For instance, Doherty et al. (2004) characterized the proteome of layer chicken breast muscle at specified time points from 1 to 27 d after hatching and 51 proteins were identified. In addition, Teltathum and Mekchay (2009) applied two-dimensional gel electrophoresis and matrix-assisted laser desorption ionization time-of-flight mass spectrometry to analyze proteomic changes in Thai indigenous chicken during the growth period. Five protein spots were characterized, and significant differences in energy metabolism and stress proteins were suggested to exist between age groups. In another work, Cai et al. (2018) characterized the whole muscle proteome and indicated that eight proteins were differentially expressed between normal and woody breast meat samples using two-dimensional gel electrophoresis. However, most of these studies were limited to gel-based proteomic approaches. In addition, early studies mainly focused on commercial broilers and layers, but an understanding of the molecular mechanisms underlying muscle development and meat quality due to Chinese indigenous chickens remains lacking.

The Beijing-You chicken (BYC), a famous Chinese native chicken breed, is more acceptable in China because of its taste, rich fragrance, and tenderness (Zhao et al., 2011). Liu et al. (2016) identified differentially expressed proteins in breast muscles of BYC at day 1 (hatching), 56 (fast growth age), 98 (marketing age), and 140 (first egg age). However, the criteria of identifying the marketing age of yellow chicken in China are varied due mainly to the customers' preference, and the proteins profiles may exhibit great differences coming from the different chronological ages. Thus, we aim to assess the protein expression profiles for these different chronological ages of day 90 (fast growth age), 120 (extremely high quality marketing age), and 150 (first egg age for the bird population) of BYC. In this study, the tandem mass tag (TMT)-LC-MS/MS (Thompson et al., 2003) proteomic strategy was applied to systematically investigate the protein expression profiles, and related biomarkers contributing to breast muscle development and meat quality during these different chronological ages. In addition, some candidate proteins were validated by the targeted parallel reaction monitoring (PRM) method (Rauniyar, 2015; Ronsein et al., 2015). This study could improve our knowledge of the temporal expression profile during development and provide opportunities for exploring biological mechanisms and characterizing biomarkers underlying muscle development and meat quality.

MATERIALS AND METHODS

Ethics Statement

All of the animal experiments were conducted in accordance with the guidelines for experimental animals established by the Ministry of Science and Technology (Beijing, China). Animal experiments were approved by the Science Research Department (in charge of animal welfare issues) of the Institute of Animal Husbandry and Veterinary Medicine, Beijing Academy of Agriculture and Forestry Sciences (Beijing, China) and the approval number was BAAFS-IAHVM20191009.

Animals and Tissue Sampling

Ninety one-day-old female BYC birds were obtained from the Institute of Animal Husbandry and Veterinary Medicine, Beijing Academy of Agriculture and Forestry Sciences and the individual birds had the same genetic background. All the birds entered the experiment at the same time and were randomly distributed into three replicate groups; each group comprised 30 BYC birds. Birds were raised in an environmentally controlled room with three floor pens under the recommended environmental and nutritional conditions for BYC. Feed and water were provided ad libitum during the experiment.

For each chronological age (90, 120, or 150 d), five birds of similar weight from each replication were weighed individually to obtain the live weight before the birds were electrically stunned and killed by exsanguination, and each chronological age contained 15 birds. Breast muscle from both sides was used. After 10 cube samples (200 mg per cube) of each left filet were snap-frozen in liquid nitrogen and stored at −80°C until the TMT and PRM test, the remaining meat samples from the left side were used to obtain the IMF content. The right filets were collected as well and were weighed and stored at 4°C for measurement of meat quality characteristics.

Meat Quality Characteristics

Drip loss was measured as described previously (Berri et al., 2008). The Warner-Bratzler shear force (WBSF) analysis was performed as described previously (Geesink et al., 1995). Shear force determinations were conducted on a TMS-PRO (FTC Co., United States) equipped with a WBSF head at a crosshead speed of 200 mm/min. The shear force on the breast meat sample was represented as the arithmetic mean value of six cuts. The filet samples, which were individually vacuum sealed in cook bags, were stored at 4°C for 24 h and then cooked in a water bath at 85°C until the internal temperature of cooked samples reached 80°C. The internal temperature of meat samples and water bath were monitored with thermometer (Reed SD-947, Reed Instruments, Canada). Cooked samples were chilled to room temperature, drained of liquid and patted dry. The samples were further cut into strips with the size of 1.0 cm (width) × 0.5 cm (thickness) × 2.5 cm (length). The strips parallel to the muscle fiber were prepared from the medial portion of the filet and sheared vertically. The IMF content of breast muscle was determined by extraction with petroleum ether in a Soxhlet

apparatus (Zerehdaran et al., 2004) and expressed as a percentage of the dry weight of the muscle.

Protein Extraction

An appropriate amount (100 mg) of chicken breast muscle from each sample was ground with liquid nitrogen. Then, 1.5 mL of lysis buffer (4% SDS, 100 mM DTT, 150 mM Tris-HCl, pH 8.0) was added to the ground meat for protein extraction. Samples were disrupted, ultrasonicated, and then boiled for 3 min. Then, after centrifugation (16,000 × *g*, 15 min, 4°C), the supernatant was collected, and the protein content was quantified using a BCA Protein Assay Kit (Bio-Rad, United States). In order to minimize the difference due to subject-to-subject variation and better identifies characteristics of the population, the pooling strategy was carried out in this study (Kendziorski et al., 2005). In brief, every five samples from each stage were pooled using equal amounts of protein, followed by diluting nine pools (three pools per age) to the same concentration with Tris-buffered saline (TBS) before protein digestion. Each pool was tested twice.

Protein Digestion

A total of 300 μg of protein from each diluting pool sample, which was made up of five individual samples, was taken for protein digestion according to the FASP procedure (Wiśniewski et al., 2009). Briefly, the detergent (i.e., SDS), DTT and other low-molecular-weight components were removed using 200 μL of urea (UA) buffer (8 M UA, 150 mM Tris-HCl, pH 8.0) by repeated ultrafiltration (Microcon units, 30 kDa) facilitated by centrifugation. Then, iodoacetamide in UA buffer (final concentration 50 mM) was added to block reduced cysteine residues, followed by incubation of the samples for 20 min in darkness. The filter was washed with 100 μL of UA buffer three times and then with 100 μL of 40 mM NH_4HCO_3 twice. Finally, the protein suspension was digested with 4 μg of LysC/trypsin (Promega) in 40 μL of 40 mM NH_4HCO_3 overnight at 37°C for 18 h, followed by termination of the digestion procedure with an appropriate amount of formic acid (FA). The resulting peptides were collected by centrifugation. Then, the peptides were desalted using a C18 cartridge (Sigma-Aldrich) and resolved with OD280 peptide quantification.

TMT Labeling and Peptide Fractionation

Peptides (100 μg) were labeled with TMT reagents according to the manufacturer's instructions (Thermo Fisher Scientific). Briefly, after the sample was dissolved in 100 μL of 50 mM triethyl ammonium bicarbonate (TEAB) solution at pH 8.5, the TMT reagent was dissolved in 41 μL of anhydrous acetonitrile. The peptide mixture was incubated at room temperature for 1 h. Then, 8 μL of 5% hydroxylamine was added into the sample, and the mixture incubated for 15 min to quench the reaction. The multiplex labeled samples were pooled together in equal amounts, followed by lyophilization. The High-pH Reversed-Phase Peptide Fractionation Kit (Thermo Fisher Scientific) was used for fractionation of dried TMT-labeled peptides. Eventually, the sample was collected and pooled into 15 fractions. The peptides of each fraction were dried and reconstituted with 0.1% FA for LC-MS analysis.

LC-MS/MS Analysis

The fractionated peptides were subjected to LC-MS/MS analysis and analyzed on a Q Exactive Plus mass spectrometer coupled to an Easy nLC 1200 (Thermo Fisher Scientific). Peptides from each fraction were loaded onto a C18 reversed-phase column (15 cm long, 75 μm ID, 3 μm) in buffer A (0.1% FA) and separated with a linear gradient of buffer B (85% acetonitrile and 0.1% FA) at a flow rate of 300 nL/min over 75 min. The gradient was as follows: 0–5 min, linear gradient from 2 to 5% buffer B; 5–50 min, linear gradient from 5 to 23% buffer B; 50–60 min, linear gradient from 23 to 40% buffer B; 60–65 min, linear gradient from 40 to 100% buffer B; 65–75 min, buffer B maintained at 100%. MS data were acquired using a data-dependent top-20 method, dynamically choosing the most abundant precursor ions from the survey scan (300–1,800 m/z) for MS/MS acquisition. Determination of the target value was based on predictive automatic gain control (pAGC). The AGC target value was 3.0×10^6 and the maximum injection time was 50 ms for full MS, and the target AGC value was 1.0×10^5 and the maximum injection time was 100 ms for MS2. The dynamic exclusion duration was 30 s. Survey scans were acquired at a resolution of 70,000 at m/z 200, and the resolution for MS/MS was set to 17,500 at m/z 200. The normalized collision energy was 30. The instrument was run with peptide recognition mode enabled. The mass spectrometry proteomics data have been deposited to the ProteomeXchange Consortium via the PRIDE (Perez-Riverol et al., 2019) partner repository with the dataset identifier PXD023871.

Database Search

The resulting LC-MS/MS raw files were imported into MaxQuant software (version 1.6.1.0) for data interpretation and protein identification against the database UniProt-gallus gallus-35124-20190830.fasta (released in August 2019 and including 35,124 sequences), which was sourced from the protein database at https://www.uniprot.org/uniprot/?query=taxonomy:9031. An initial search was performed with a precursor mass window of 6 ppm. The search followed an enzymatic cleavage rule of trypsin/P and allowed two maximal missed cleavage sites and a mass tolerance of 20 ppm for fragment ions. The modification set was as follows: fixed modification: carbamidomethyl (C), TMT6plex (K), and TMT6plex (*N*-term); variable modification: oxidation (M) and acetyl (protein *N*-term). A minimum of six amino acids was required for peptides, and ≥1 unique peptide was required per protein. For peptide and protein identification, the false discovery rate (FDR) was set to 1%. Normalized TMT reporter ion intensity was used for peptide and protein quantification. The relative quantitative protein analysis of samples was conducted using the MaxQuant algorithms[1].

Data Statistics and Bioinformatics Analysis

Analyses of bioinformatics data were carried out with Perseus software, Microsoft Excel and R statistical computing software. Significant DEPs were screened with a fold change (FC) ratio

[1]http://www.maxquant.org

cutoff of > 1.20 or <0.83 and *P*-values < 0.05 among two pairwise comparison groups (120 d vs 90 d and 150 d vs 120 d). Expression data were grouped together by hierarchical clustering according to the protein level. To annotate the sequences, information was extracted from UniProtKB/Swiss-Prot, Kyoto Encyclopedia of Genes and Genomes (KEGG), and Gene Ontology (GO). GO and KEGG enrichment analyses were carried out with Fisher's exact test, and FDR correction for multiple testing was also performed. GO terms were grouped into three categories: biological process (BP), molecular function (MF), and cellular component (CC). Enriched GO and KEGG pathways were nominally statistically significant at the $P < 0.05$ level. Construction of protein–protein interaction (PPI) networks was also conducted by using the STRING database with Cytoscape software.

Targeted Protein Quantification by LC-PRM/MS Analysis

To further validate the protein expression level gain through TMT quantification, additional quantification through LC-PRM/MS analysis was performed. PRM analysis was performed on a Q Exactive HF-X mass spectrometer (Thermo Fisher Scientific). Methods optimized for charge state and retention times for the most significantly regulated peptides were generated experimentally using 1 to 3 unique peptides of high intensity and confidence for each target protein. Briefly, the TMT protocol was used for peptide preparation. Then, tryptic peptides were loaded on C18 stage tips for desalting prior to reversed-phase chromatography on an Easy nLC-1200 system (Thermo Fisher Scientific) with a constant flow rate of 300 nL/min and the following liquid gradient: from 0 to 5 min, mobile phase B (0.1% FA in 85% acetonitrile) was increased from 2 to 5%; from 5 to 45 min, mobile phase B was increased from 5 to 23%; from 45 to 50 min, mobile phase B was increased from 23 to 40%; from 50 to 52 min, mobile phase B was increased from 40 to 100%; and from 52 to 60 min, mobile phase B was held at 100%. The mass spectrometer was operated in positive ion mode with the following parameters: The full MS1 scan was acquired with a resolution of 60,000 (at m/z 200), an AGC target value of 3.0×10^6, and a maximum ion injection time of 250 ms. Full MS scans were followed by 20 PRM scans at a resolution of 30,000 (at m/z 200) with an AGC value of 1.0×10^6 and a maximum injection time of 200 ms. The targeted peptides were isolated with a 1.6Th window and fragmented at a normalized collision energy of 28 in a higher-energy collisional dissociation (HCD) cell. The raw data were analyzed using Skyline 4.1 (MacCoss Lab, University of Washington) to obtain the signal intensities of individual peptide sequences.

For the PRM-MS data, each sample's average base peak intensity was extracted from the full scan acquisition using RawMeat (version 2.1, VAST Scientific[2]). The normalization factor for sample *N* was calculated as f_N = the average base peak intensity of sample *N*/the median of the average base peak intensities of all samples. The area under the curve (AUC) for each transition from sample *N* was multiplied by this factor. After normalization, the AUC of each transition was summed to obtain AUCs at the peptide level. The relative protein abundance was defined as the intensity of a certain peptide.

[2]www.vastscientific.com

Statistical Analysis

The parameters are shown as averages and standard errors. Data on carcass and meat characteristics were obtained and compared in a completely randomized design by using the General Linear Model procedure of SAS (version 9.2, SAS Institute Inc., Cary, NC, United States). Differences among ages were separated by Duncan's multiple range tests. Significant differences were based on $P < 0.05$.

RESULTS

Growth Characteristics and Meat Quality

The breast muscle samples for the three chronological ages were tested to characterize the following traits: live weight, IMF content, WBSF value and drip loss (**Table 1**). The live weight at 90 d (945 g) was lower ($P < 0.05$) than those at 120 and 150 d (1,205 and 1,295 g), which did not differ from each other ($P > 0.05$). As expected, the WBSF value and IMF content showed a significant increasing trend with the age of the chickens ($P < 0.05$). The WBSF value and IMF content at 90 d (18.52 N, 2.44%) were significantly lower ($P < 0.05$) than those at 120 d (29.15 N, 4.68%) and 150 d (30.60 N, 5.66%), which exhibited no significant difference ($P > 0.05$). Moreover, the drip loss exhibited the lowest value at 120 d ($P < 0.05$). These results indicated that there was a rapid increase in live weight during the stage from 90 to 120 d, and there was a larger amount of IMF deposition at this stage than there was from 120 to 150 d. This finding suggested that bird development reaches a relatively moderate level after a rapid increase in growth rate and IMF accumulation, suggesting that the stage from 90 to 120 d might be an important chronological stage for BYC.

Protein Identification and Quantification

A total of 10,661 peptides and 1,413 proteins were identified with an FDR <1%. Details of all the accurately identified proteins are shown in **Supplementary Table S1**. Among all the identified proteins, 57.89% had a molecular weight of approximately 10-50 kDa, and 15% were more than 100 kDa in weight (**Figure 1A**). Approximately 49.02% of the peptides were 6–10 amino acids in length (**Figure 1B**). In addition, more than 82% of the

TABLE 1 | Characteristics of breast meat of Beijing-You chickens at different ages (mean ± SD, *n* = 15).

Item	90 d	120 d	150 d
Live Weight (g)	945 ± 87^b	1205 ± 136^a	1295 ± 136^a
Drip Loss (%)	3.90 ± 1.08^a	2.83 ± 0.78^b	3.61 ± 1.11^a
IMF (%)	2.44 ± 2.25^b	4.68 ± 2.88^a	5.66 ± 2.72^a
WBSF(N)	18.52 ± 4.84^b	29.15 ± 8.46^a	30.62 ± 6.90^a

[a,b]Means within the same row followed by a different superscript are significantly different (P ≤ 0.05).

IMF, intramuscular fat; WBSF, Warner-Bratzler shear force.

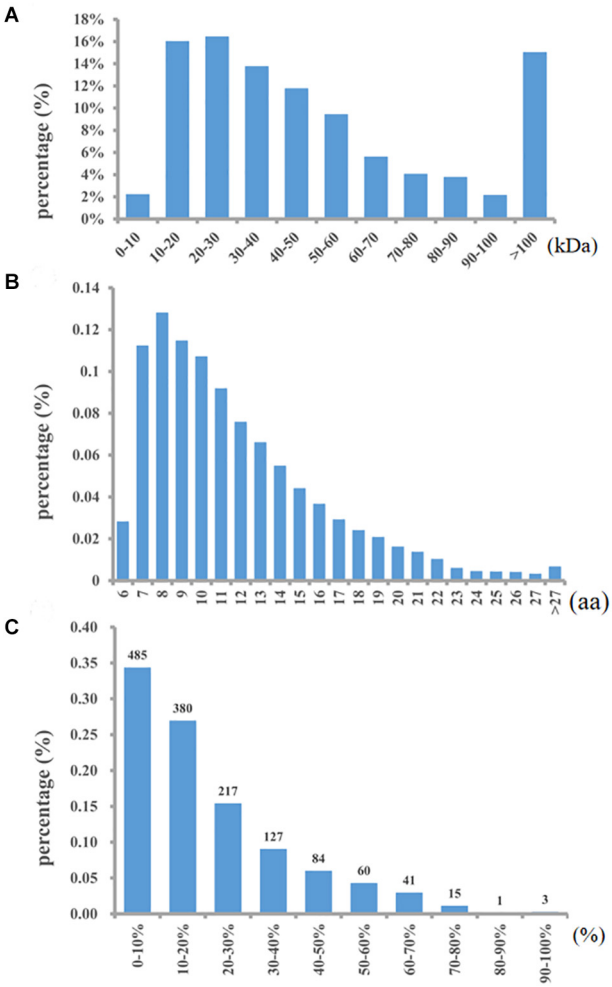

FIGURE 1 | Distributions of all identified proteins. Mass **(A)**, length **(B)**, and coverage **(C)**.

proteins included at least two unique peptides. The proteins were identified with low sequence coverage; approximately 76.57% of proteins had less than 30% sequence coverage (**Figure 1C**).

DEPs of Comparison Groups

To assess dynamic changes in proteins at different chronological ages, a total of 197 DEPs (after deredundancy analysis) were identified (FC $>$ 1.2 or $<$0.83 and $P < 0.05$) from the two pairwise comparison groups (120 d vs 90 d and 150 d vs 120 d) (**Supplementary Table S2**). In the 120 d vs 90 d comparison group, 181 proteins (110 upregulated and 71 downregulated) were significantly changed. Moreover, 23 DEPs (13 upregulated and 10 downregulated) were significantly changed in the 150 d vs 120 d comparison group (**Supplementary Table S2**). The number of DEPs in the 120 d vs 90 d comparison group was larger than that in the 150 d vs 120 d comparison group, indicating that there were much more changes in the protein profiles from 90 to 120 d than from 120 to 150 d. Two volcano plots were generated to visualize the data for the two pairwise comparison groups (120 d vs 90 d and 150 d vs 120 d) (**Figures 2A,B**).

Hierarchical cluster analysis was performed to better visualize the differences in protein abundance among pairwise comparison groups, and the results were visualized as a heat map. As illustrated in **Supplementary Figure S1**, DEPs at three different chronological ages (90, 120, and 150 d) were identified. Samples from chickens of these ages displayed different color distributions; however, the three biological replicates of each sample group exhibited similar color layouts. These results confirmed that there were characteristic differences in the proteome among samples of different chronological ages. When the Euclidean distance was increased, the samples from 120 to 150 d were aggregated into a cluster and separated from the 90 d samples, which corroborated the difference in phenotypic traits. All of these results indicated that these differentially abundant proteins were the source of the variation in response to increasing chronological age.

Functional Analysis of DEPs From 90 to 120 d

To gain insights into the functions of DEPs in the 120 d vs 90 d comparison group, GO and KEGG enrichment analyses were carried out to identify the meaningful biological functions of the DEPs. GO annotation of 181 DEPs identified 1,671, 296, and 379 categories in the BP, CC, and MF categories, respectively (**Supplementary Table S3**), of which 334, 105, and 99 categories were significant ($P < 0.05$) by Fisher's exact test. In these pairwise comparisons, the DEPs in the BP group were mainly distributed in muscle system process, glycosyl compound metabolic process, cofactor metabolic process, generation of precursor metabolites and energy organophosphate metabolic process. The DEPs in CC group were mainly enriched in the terms cytoplasm, extracellular exosome, extracellular membrane-bounded organelle, vesicle and myosin complex. Additionally, the DEPs in the MF group were mainly distributed in cytoskeletal protein binding, heme-copper terminal oxidase activity, oxidoreductase activity, ligase activity and peptide transporter activity. The top 10 categories in BP, CC, and MF are shown in **Figure 3A**. The glycolysis/gluconeogenesis, oocyte meiosis, tight junction, and adrenergic signaling in cardiomyocyte pathways were significantly enriched by KEGG pathway enrichment analysis in the 120 d vs 90 d comparison group (**Figure 4A** and **Supplementary Table S4**), and more than half of these pathways are involved in energy metabolism and muscle development.

Protein–protein interaction network analysis was performed to show the interaction networks of some important DEPs in the comparison groups. The PPI network analysis focused on several key pathways of energy metabolism and muscle development from 90 to 120 d (**Figure 5A**). The results showed that L-lactate dehydrogenase A chain (LDHA), beta-enolase (ENO3), and fructose-bisphosphate aldolase (ALDOC) were enriched in the glycolysis/gluconeogenesis pathway, while myosin regulatory light chain 2 (MYLPF) and myosin heavy chain (P13538) were derived from the tight junction pathway and tropomyosin alpha-1 chain (TPM1) was derived from the adrenergic signaling in

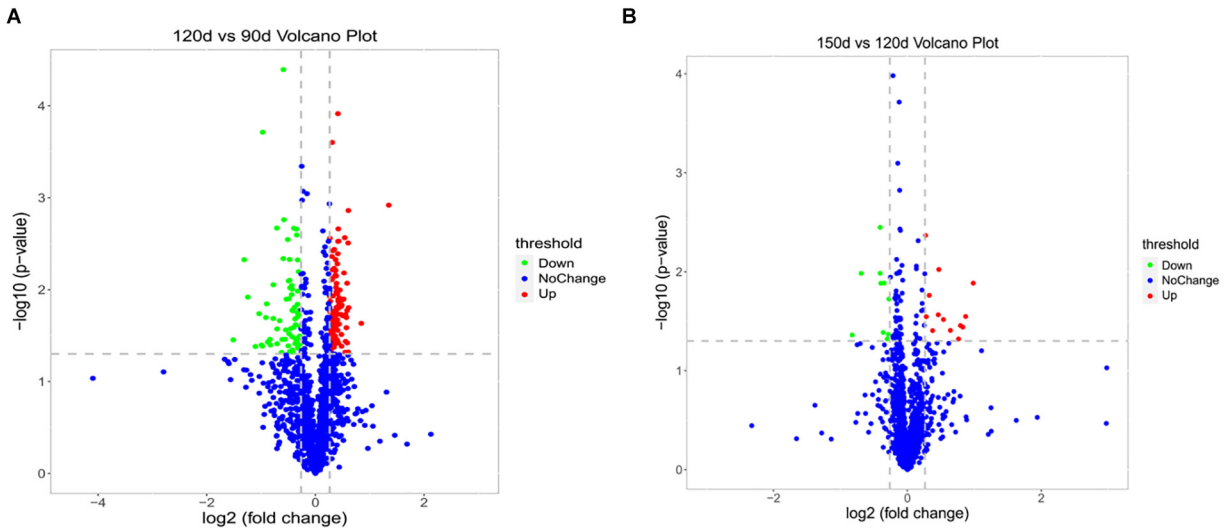

FIGURE 2 | Volcano plots of the univariate statistical analysis results. 120 d vs 90 d **(A)** and 150 d vs 120 d **(B)**. The red dots indicate significantly upregulated proteins ($P < 0.05$ and FC > 1.2), and the green dots indicate significantly downregulated proteins ($P < 0.05$ and FC < 0.83). The blue dots represent proteins with non-significant ($P > 0.05$ or $0.83 <$ FC < 1.2) differences in expression.

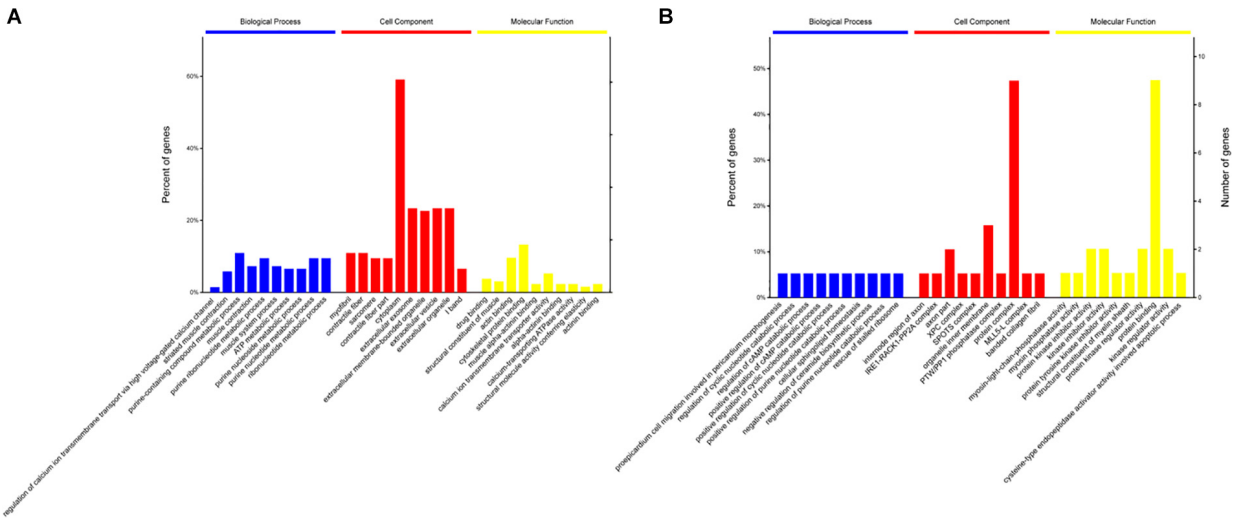

FIGURE 3 | Go enrichment analysis of differentially expressed proteins in 120 d vs 90 d **(A)** and 150 d vs 90 d **(B)**.

cardiomyocytes pathway. Striking increases were observed for LDHA, ENO3, ALDOC, MYLPF, P13538 and TPM1 from 90 to 120 d (**Supplementary Table S4**), which was closely associated with muscle growth through the glycolysis/gluconeogenesis, tight junction and adrenergic signaling in cardiomyocytes pathways.

Functional Analysis of DEPs From 120 to 150 d

For the 150 d vs 120 d comparison group, GO annotation of 23 DEPs identified 758, 170, and 117 categories in the BP, CC and MF categories, respectively (**Supplementary Table S3**), of which 189, 66, and 46 categories were significant ($P < 0.05$) by Fisher's exact test. In this pairwise comparison, the DEPs in the BP group were mainly distributed in positive regulation of mitochondrial depolarization, embryonic morphogenesis, myoblast proliferation, negative regulation of response to oxidative stress and generation of precursor metabolites and energy. Regarding the CC group, the DEPs were mainly located in the IRE1-RACK1-PP2A complex, axon part, organelle inner membrane, fibrillar collagen trimer, and extrinsic component of mitochondrial inner membrane. Additionally, the DEPs in the MF group were mainly distributed in kinase regulator activity, enzyme binding, cysteine-type endopeptidase regulator activity involved in apoptotic process, enzyme inhibitor activity and channel inhibitor activity. The top 10 categories in BP, CC,

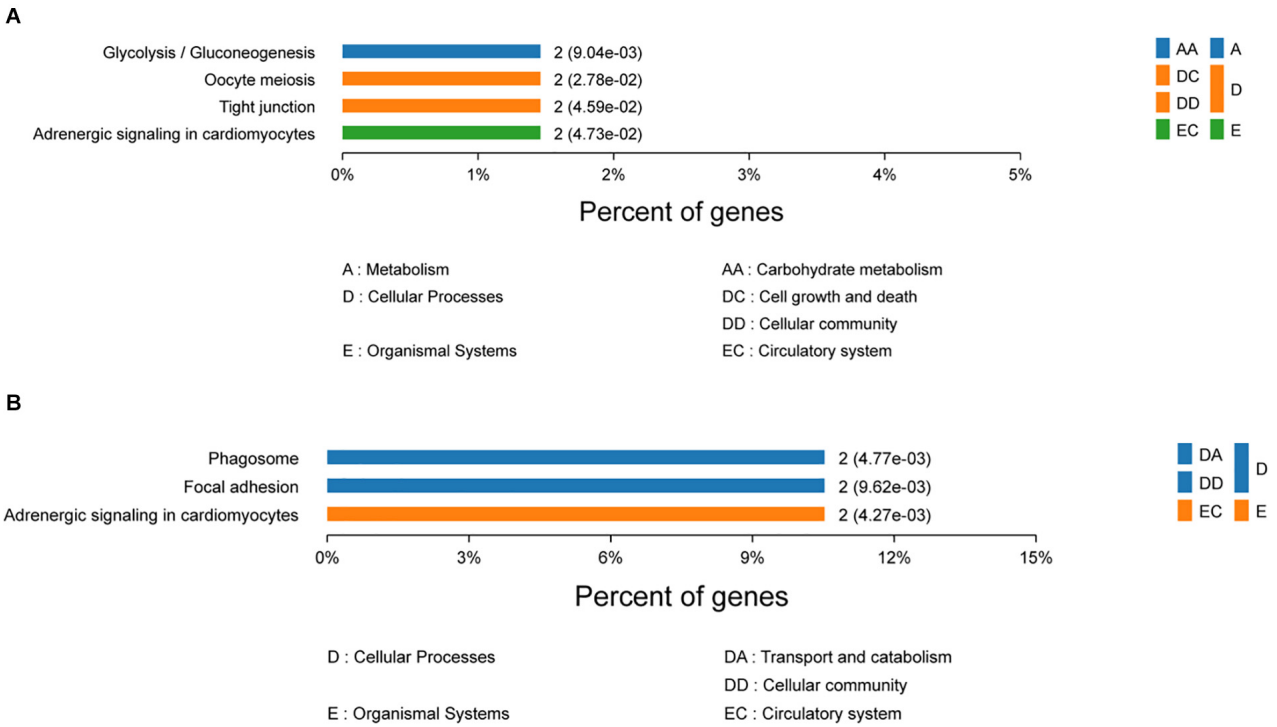

FIGURE 4 | KEGG pathway enrichment analysis of differentially expressed proteins in 120 d vs 90 d **(A)** and 150 d vs 120 d **(B)**.

and MF are shown in **Figure 3B**. The adrenergic signaling in cardiomyocytes, phagosome and focal adhesion pathways were significantly enriched by KEGG pathway enrichment analysis in the 150 d vs 120 d comparison group (**Figure 4B**, **Supplementary Table S4**).

For the PPI network in this stage (**Figure 5B**), the serine/threonine-protein phosphatase PP1-beta catalytic subunit (PPP1CB), cartilage oligomeric matrix protein (COMP), ras-related protein Rab-5C (RAB5C), protein ATP1B4 (ATP1B4), and receptor of activated protein C kinase 1 (RACK1) proteins were involved in some important pathways, including adrenergic signaling in cardiomyocytes, focal adhesion, phagosome, the insulin signaling pathway, insulin resistance, vascular smooth muscle contraction, oocyte meiosis, and extracellular matrix (ECM)–receptor interaction.

Protein Validation by PRM

To assess the validity of the TMT data, PRM was used to examine the relative levels of ten important functional proteins at different chronological ages. As shown in **Table 2**, the protein expression levels obtained by TMT were confirmed by quantifying the expression levels of some proteins through PRM-MS analysis. Five proteins (LDHA, ENO3, MYBPC2, Q91348, and UCH-L1) related to muscle development, two proteins (CACNA2D1 and FKBP12.6) related to muscle contraction, and three proteins (COL1A2, GSTAL2, and HSP70) related to meat quality were selected for PRM analysis. The PRM results had good correlation with the TMT data (**Table 2**). The Pearson correlation coefficient between the TMT and PRM results was $R^2 = 0.897$, indicating that these quantitative results were strongly convincing.

DISCUSSION

Proteomic analysis was known as a powerful technique for studying the protein expression patterns, and has been widely carried out in identifying proteome changes of skeletal muscle at different development stages in chickens (Doherty et al., 2004; Teltathum and Mekchay, 2009; Liu et al., 2016; Ouyang et al., 2017). For example, Ouyang et al. (2017) characterized the proteome of breast muscle during embryonic development. Protein expression profiles were also investigated in the breast muscle of BYC at ages 1, 56, 98, and 140 days and Thai indigenous chickens at 0, 3, 6, and 18 weeks of age (Teltathum and Mekchay, 2009; Liu et al., 2016). In this study, we performed a TMT-LC-MS/MS-based proteomic analysis of breast muscle of BYC at 90, 120, and 150 days of age, and a total of 197 DEPs (after deredundancy analysis) were identified (FC $>$ 1.2 or $<$0.83 and $P < 0.05$) from the two pairwise comparison groups (120 d vs 90 d and 150 d vs 120 d). These DEPs were mainly associated with glycolysis/gluconeogenesis, ECM–receptor interaction, focal adhesion, calcium signaling pathway, cysteine and methionine metabolism, pyruvate metabolism, oocyte meiosis, oxytocin signaling pathway and cardiac muscle contraction. The results of this study could strengthen our knowledge of the proteins temporal expression profile and make a complementary to previous findings. Some discussion on the key proteins of each

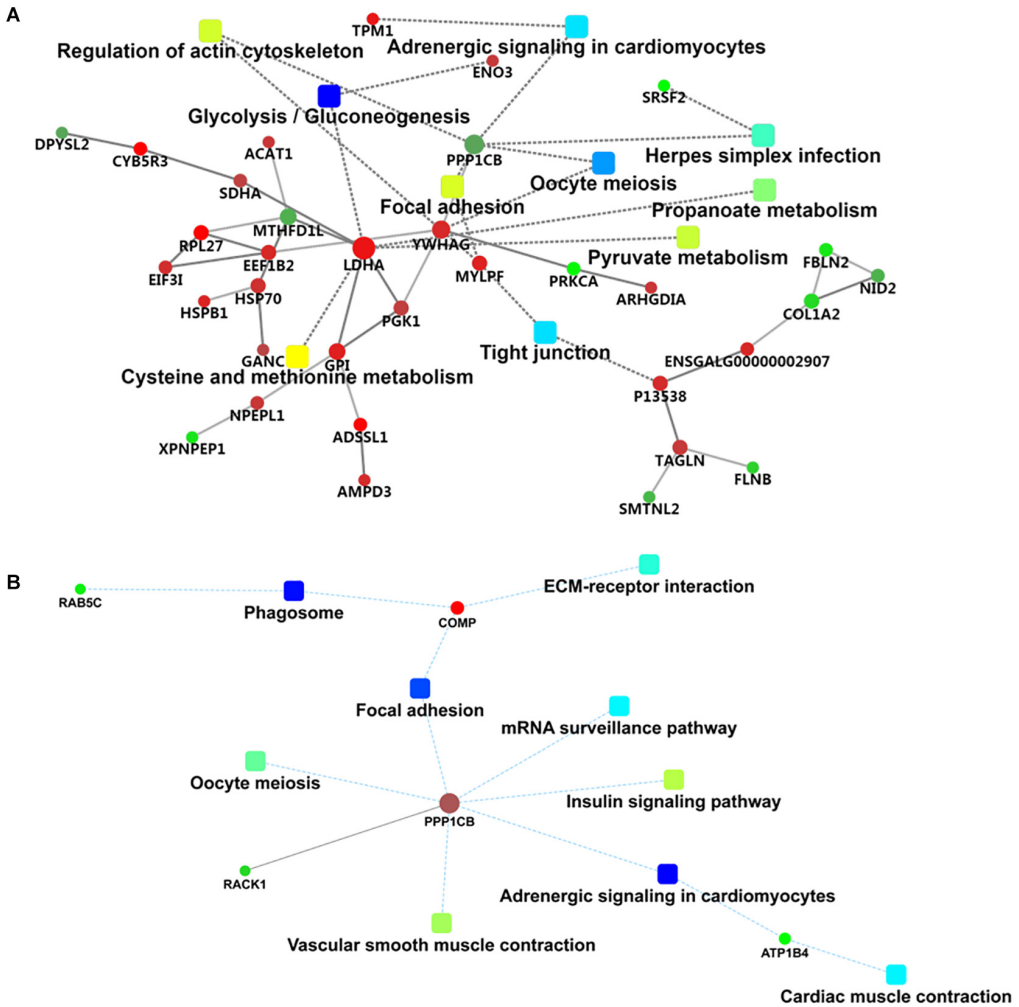

FIGURE 5 | Interaction network of differentially expressed proteins in 120 d vs 90 d **(A)** and 150 d vs 120 d **(B)**.

chronological age, and their association with meat quality were provided as below.

Muscle Development

Fontanesi et al. (2012) reported that LDHA associated with average daily gain in Italian Large White pigs. Qiu et al. (2010) mapped LDHA gene close to myogenic differentiation 1 (MyoD1), which is involved in the regulation of energy metabolism and protein transport processes, and suggested that LDHA gene could have great effect on muscle development. Wu et al. (2008) performed the genomic structure, polymorphism, expression of ENO3 and showed that ENO3 might affect not only skeletal muscle growth during muscle development but also meat flavor and carcass quality. All these studies demonstrated that glycolysis/gluconeogenesis, cardiac muscle contraction and dilated cardiomyopathy (DCM) might be the related pathways involved in muscle development (Liu et al., 2016). In the present study, we found the L-lactate dehydrogenase A chain (LDHA), and Beta-enolase (ENO3) were lower expressed in 90 d than those in 120 and 150 d, which did not differ from each other (**Supplementary Table S2**). In addition, Our data showed that the weight of 90 d (945 g) was lower ($P < 0.05$) than 120 d and 150 d (1,205 and 1,295 g), which did not differ from each other ($P > 0.05$). The results showed that the grow speed of breast muscle from 90 to 120 d is about threefold mort than the stage from 120 to 150 d (**Table 1**). These results suggested that the proteins, such as LDHA and ENO3, might have important effect on breast muscle development in BYC.

IMF and Collagen Deposition

The deposition of IMF had extremely closely relationship with the developmental stages (Chartrin et al., 2007; Liu et al., 2016). Previous studies demonstrated that ECM–receptor interaction might form a network with pathways related to lipid metabolism to influence the deposition of IMF (Cui et al., 2012; Zhang et al., 2019). Zhang et al. (2019) identified 2,039 DEGs through a pairwise comparison of preadipocytes at different stages of differentiation and reported that pathways related to

TABLE 2 | Comparison of the quantification results between TMT and PRM analyses of the 10 candidate proteins.

Accession	Gene Name	Protein	Group Ratio (TMT)[a]			Group Comparison (PRM)[b]		
			120 d/90 d	150 d/120 d	150 d/90 d	120 d/90 d	150 d/120 d	150 d/90 d
P00340	LDHA	L-lactate dehydrogenase A chain	1.41	1.05	1.48	1.40	1.05	1.47
P07322	ENO3	Beta-enolase	1.24	0.97	1.20	1.17	1.21	1.41
A0A3Q3ATJ1	CACNA2D1	VWFA domain-containing protein	1.20	0.94	1.12	1.55	0.89	1.39
A1IMF0	UCH-L1	Ubiquitin carboxyl-terminal hydrolase	1.44	0.95	1.36	1.77	0.86	1.52
P16419	MYBPC2	Myosin-binding protein C, fast-type	1.24	0.96	1.20	1.35	0.96	1.28
Q8QGU2	FKBP12.6	Peptidylprolyl isomerase	0.77	0.88	0.68	0.83	0.90	0.75
P02467	COL1A2	Collagen alpha-2(I) chain	0.58	1.73	1.01	0.38	2.35	0.90
Q91348	Q91348	6-Phosphofructo-2-kinase/fructose-2,6-bisphosphatase	1.04	1.24	1.29	1.03	1.50	1.54
A0A0A0MQ61	GSTAL2	Uncharacterized protein	1.46	1.25	1.82	1.28	1.37	1.76
Q7SX63	HSP70	Heat shock protein 70	1.28	0.99	1.27	1.24	1.01	1.26

[a] *Fold changes in protein abundance from the comparisons among 90, 120, and 150 d by tandem mass tag (TMT).*
[b] *Fold changes in protein abundance from the comparisons among 90, 120, and 150 d by parallel reaction monitoring (PRM).*

ECM–receptor interaction, focal adhesion pathway and PPAR signaling pathway were significantly enriched for IMF-derived preadipocyte differentiation. Li et al. (2019) performed RNA-Seq analysis of breast muscle from Gushi chicken at two physiological stages and showed that differentially expressed mRNAs and IncRNAs were mainly involved in ECM–receptor interaction, glycerophospholipid metabolism. Collagen is an abundant connective tissue protein and is contributing factor to variation in meat tenderness and texture (Uitto and Larjava, 1991). Collagen cross-linking increased with age was the major contributor to meat generally tougher from older birds (Fletcher, 2002; Rajkumar et al., 2016).

In the present study, we found that the expression of type I collagen alpha 2 (COL1A2) was lower in 120 d than those in 90 and 150 d, which did not differ from each other (**Supplementary Table S2**). Furthermore, pathway enrichment analysis show the proteins, including serine/threonine-protein phosphatase PP1-beta catalytic subunit (PPP1CB) and COMP (A0A3Q2UFV6) were also involved in the ECM–receptor interaction and focal adhesion (**Supplementary Table S4**). Among these proteins, PPP1CB, a novel adipogenic activator, has been reported to played an important function in regulating meat quality, which mainly associated with focal adhesion, cAMP signaling pathway, cGMP-PKG signaling pathway, adrenergic signaling in cardiomyocytes and oxytocin signaling pathway. Moreover, PPP1CB was significantly lower at 120 d compared to 90 and 150 d, which exhibiting the same pattern as the COL1A2. This result was consistent with the data published by Cho et al. (2015), who indicated that PPP1CB is essential for adipocyte differentiation, which supplied that PPP1CB might play a prominent role in regulating meat quality traits, such as juiciness and tenderness due to adipogenic process. COL1A2 was suggested through transcriptome sequencing to affect the growth of Jinghai yellow chickens recently (Wu et al., 2020). In addition, our result showed that IMF and WBSF exhibited an increasing trend with the increase in physiological stages ($P < 0.05$). The IFM and WBSF of 90 d (2.44%, 18.52 N) was lower ($P < 0.05$) than 120 d (4.68%, 29.15 N) and 150 d (5.66% and 30.60 N), respectively, which did not differ from each other ($P > 0.05$) (**Table 1**). These results were consistent with the results of previous studies suggesting that proteins involved in collagen and lipid metabolism were associated with tenderness and accumulation of IMF during chicken development (Li et al., 2010, 2019; Zhang et al., 2019). Hence, we speculated that the proteins, such as COL1A2, PPP1CB, and COMP having an important relationship to the ECM-receptor and focal adhesion pathway, played a critical role in the lipid metabolism and the meat tenderness due to fat and collagen accumulated with aging. These data were complementary to the findings reported by Liu et al. (2016) who identified pathways involved in muscle development that were dominant during the rapid muscle growth period (from 56 to 98 d) and suggested apolipoprotein A-1 (APOA1) and Heat shock protein beta 1 (HSPB1) as molecular markers for IMF deposition in chickens.

Water-Holding Capacity

ATP2A1 encodes sarco/endoplasmic reticulum Ca^{2+}-ATPase (SERCA), which is a pump that transports calcium ions from the cytoplasm into the sarcoplasmic reticulum (SR) (Periasamy and Kalyanasundaram, 2007). SERCA and the calcium release channel were demonstrated to be the most important regulators of the intracellular Ca^{2+} concentration (Xing et al., 2017), which included the mRNA and protein expression of SERCA1 and αRYR in the pectoralis major muscles of broilers from the normal and pale, soft and exudative (PSE) groups, and the expression was found to be significantly decreased in the PSE group compared to the normal group. In this study, we found ATPase Ca^{2+} transporting gene 1 (ATP2A1), calcium-transporting ATPase (ATP2B4), ryanodine receptor gene 3 (RYR3), tropomyosin alpha-1 chain (TPM1), and calcium channel and voltage-dependent alpha-2/delta subunit 1 (CACNA2D1) were lower expressed in 90 d than those in 120 d (**Supplementary Table S2**), which was accompanied by the decrease in the drip loss (from 3.90 to 2.83%) (**Table 1**). Moreover, pathway analysis showed that these proteins were involved in the calcium signaling pathway, the oxytocin signaling pathway, cardiac muscle contraction,

and adrenergic signaling in cardiomyocytes. These results were consistent with the results of previous studies, supporting the views that proteins involved in calcium channel moderation and muscle contraction were associated with water-holding capacity (WHC) (Paião et al., 2013; Yalcin et al., 2019). Notably, heat shock protein 70 (HSP70) was more abundant at 120 d than at 90 d (**Supplementary Table S2**). Similar results have been reported in previous studies (Di Luca et al., 2011, 2013), which found that the upregulated expression of HSP70 could prevent protein denaturation and lead to reduced drip loss. One possible explanation could be that these proteins play an essential role in the maintenance of cellular integrity in response to stress (Wu et al., 2015). In addition, it is of interest to point out that there were no significant differences in proteins expression of ATP2A1, ATP2B4, RYR3, TPM1, CACNA2D1, and HSP70 between 120 and 150 d; however, significant differences of drip loss (from 2.83 to 3.61%) were noted between the stages. Taken together, our data collected in the present study provided the evidence that drip loss in pectoralis major muscles might be influenced by various proteins, and the relative affection of these proteins may be changing with the different physiological stages.

Sexual Maturation

Notably, RACK1, a multifaceted scaffolding protein, was less abundant at 150 d than at 120 d (**Supplementary Table S2**), and this protein functions as a hub for spatiotemporal orchestration of signaling events across diverse pathways (Adams et al., 2011). Kadrmas et al. (2007) found RACK1-specific enrichment in the ovary and demonstrated that RACK1 is essential at multiple steps of Drosophila development, particularly in oogenesis. These results suggested that RACK1 might play a key role in sexual maturation in local BYC as well, which reached sexual maturity at the age of 150 d.

In conclusion, the present study examined the differences in protein expression levels in chicken breast muscle for three different chronological ages through TMT-LC-MS/MS-based quantitative proteomic analysis. The temporal expression patterns of some age-dependent proteins were determined and eluciated the dynamic changes in the chicken breast muscle proteomes with aging as well. Overall, the present work could strengthen our view of the temporal expression profile during development and identify novel biomarkers for genetic breeding of chickens.

DATA AVAILABILITY STATEMENT

The datasets presented in this study can be found in online repositories. The names of the repository/repositories and accession number(s) can be found below: ProteomeXchange Consortium via the PRIDE partner repository and PXD023871.

ETHICS STATEMENT

The animal study was reviewed and approved by Science Research Department of the Institute of Animal Husbandry and Veterinary Medicine, Beijing Academy of Agriculture and Forestry Sciences (Beijing, China).

AUTHOR CONTRIBUTIONS

JZ: performed the experiments, analyzed the data, and wrote the manuscript. JC and AG: collected the samples. HW and QC: project administration. ZY, XZ, and YZ: performed the experiments. LY and JD: analyzed the data. HL: designed the study and reviewed the manuscript. All authors have read and approved the final manuscript.

FUNDING

This research was financially supported by the Beijing Municipal Science and Technology Project (D171100007817005 and D171100007817003), Public Institution Research and Service Project of Beijing Academy of Agriculture and Forestry Sciences (XMS201903), and the Earmarked Fund for Modern Agro-Industry Technology Research System (CARS41-Z01).

ACKNOWLEDGMENTS

We would like to express their profound gratitude to Hou for his technical assistance.

SUPPLEMENTARY MATERIAL

The Supplementary Material for this article can be found online at: https://www.frontiersin.org/articles/10.3389/fphys.2021.658711/full#supplementary-material

Supplementary Figure 1 | Heatmap analysis of all differentially expressed proteins in three different chronological ages of breast muscle.

Supplementary Table 1 | The identified 10,661 peptides and 1,413 proteins list in chicken breast muscle by TMT.

Supplementary Table 2 | Differentially expressed proteins for 120 d vs 90 d, 150 d vs 120 d, and 150 d vs 90 d.

Supplementary Table 3 | Gene Ontology (GO) analysis of 1,413 proteins in chicken breast muscle.

Supplementary Table 4 | KEGG pathway enrichment analysis in chicken breast muscle.

REFERENCES

Adams, D. R., Ron, D., and Kiely, P. A. (2011). RACK1, a multifaceted scaffolding protein: structure and function. *Cell Commun. signal.* 9, 22–46. doi: 10.1186/1478-811X-9-22

Berri, C., Besnard, J., and Relandeau, C. (2008). Increasing dietary lysine increases final pH and decreases drip loss of broiler breast meat. *Poult. Sci.* 87, 480–484. doi: 10.3382/ps.2007-00226

Brant, A. W., and Hanson, H. L. (1962). Age, sex and genetic effects on poultry flavor. *XIIth World's Poultry Congr. Proc.* 12, 409–413.

Cai, K., Shao, W., Chen, X., Campbell, Y. L., Nair, M. N., Suman, S. P., et al. (2018). Meat quality traits and proteome profile of woody broiler breast (pectoralis major) meat. *Poult. Sci.* 97, 337–346. doi: 10.3382/ps/pex284

Chartrin, P., Bernadet, M. D., Guy, G., Mourot, J., Hocquette, J. F., Rideau, N., et al. (2007). Do age and feeding levels have comparable effects on fat deposition in breast muscle of mule ducks? *Animal* 1, 113–123. doi: 10.1017/S1751731107658029

Chizzolini, R., Zanardi, E., Dorigoni, V., and Ghidini, S. (1999). Calorific value and cholesterol content of normal and low-fat meat and meat products. *Trends Food Sci. Tech.* 10, 119–128. doi: 10.1016/S0924-2244(99)00034-5

Cho, Y.-L., Min, J.-K., Roh, K. M., Kim, W. K., Han, B. S., Bae, K.-H., et al. (2015). Phosphoprotein phosphatase 1CB (PPP1CB), a novel adipogenic activator, promotes 3T3-L1 adipogenesis. *Biochem. Biophys. Res. Commun.* 467, 211–217. doi: 10.1016/j.bbrc.2015.10.004

Cui, H., Liu, R., Zhao, G., Zheng, M., Chen, J., and Wen, J. (2012). Identification of differentially expressed genes and pathways for intramuscular fat deposition in pectoralis major tissues of fast-and slow-growing chickens. *BMC Genomics* 13:213. doi: 10.1186/1471-2164-13-213

Cui, H., Zheng, M., Zhao, G., Liu, R., and Wen, J. (2018). Identification of differentially expressed genes and pathways for intramuscular fat metabolism between breast and thigh tissues of chickens. *BMC Genomics* 19:55. doi: 10.1186/s12864-017-4292-3

Di Luca, A., Elia, G., Hamill, R., and Mullen, A. M. (2013). 2D DIGE proteomic analysis of early post mortem muscle exudate highlights the importance of the stress response for improved water-holding capacity of fresh pork meat. *Proteomics* 13, 1528–1544. doi: 10.1002/pmic.201200145

Di Luca, A., Mullen, A. M., Elia, G., Davey, G., and Hamill, R. M. (2011). Centrifugal drip is an accessible source for protein indicators of pork ageing and water-holding capacity. *Meat Sci.* 88, 261–270. doi: 10.1016/j.meatsci.2010.12.033

Díaz, O., Rodríguez, L., Torres, A., and Cobos, A. (2012). Fatty acid composition of the meat from Mos breed and commercial strain capons slaughtered at different ages. *Grasas Y Aceites* 63, 296–302. doi: 10.3989/gya.011312

Doherty, M. K., McLean, L., Hayter, J. R., Pratt, J. M., Robertson, D. H. L., Ei-Shafei, A., et al. (2004). The proteome of chicken skeletal muscle: changes in soluble protein expression during growth in a layer strain. *Proteomics* 4, 2082–2093. doi: 10.1002/pmic.200300716

Fletcher, D. L. (2002). Poultry meat quality. *World's Poult. Sci. J.* 58, 131–145. doi: 10.1079/WPS20020013

Fontanesi, L., Buttazzoni, L., Scotti, E., and Russo, V. (2012). Confirmation of the association between a single nucleotide polymorphism in the porcine LDHA gene and average daily gain and correlated traits in Italian Large White pigs. *Anim. Genet.* 43, 649–650. doi: 10.1111/j.1365-2052.2012.02355.x

Geesink, G. H., Koolmees, P. A., van Laack, H. L., and Smulders, F. J. (1995). Determinants of tenderisation in beef *Longissimus* dorsi and *triceps brachii* muscles. *Meat Sci.* 41, 7–17. doi: 10.1016/0309-1740(94)00066-G

Kadrmas, J. L., Smith, M. A., Pronovost, S. M., and Beckerle, M. C. (2007). Characterization of RACK1 function in *drosophila* development. *Dev. Dyn.* 236, 2207–2215. doi: 10.1002/dvdy.21217

Kendziorski, C., Irizarry, R., Chen, K.-S., Haag, J., and Gould, M. (2005). On the utility of pooling biological samples in microarray experiments. *Proc. Natl. Acad. Sci. U.S.A.* 102, 4252–4257. doi: 10.1073/pnas.0500607102

Li, Y., Chen, Y., Jin, W., Fu, S., Li, D., Zhang, Y., et al. (2019). Analyses of microRNA and mRNA expression profiles reveal the crucial interaction networks and pathways for regulation of chicken breast muscle development. *Front. Genet.* 10:197. doi: 10.3389/fgene.2019.00197

Li, Y., Xu, Z., Li, H., Xiong, Y., and Zuo, B. (2010). Differential transcriptional analysis between red and white skeletal muscle of Chinese Meishan pigs. *Int. J. Biol. Sci.* 6, 350–360. doi: 10.7150/ijbs.6.350

Liu, J., Fu, R., Liu, R., Zhao, G., Zheng, M., Cui, H., et al. (2016). Protein profiles for muscle development and intramuscular fat accumulation at different post-hatching ages in chickens. *PLoS One* 11:e0159722. doi: 10.1371/journal.pone.0159722

López, K. P., Schilling, M. W., and Corzo, A. (2011). Broiler genetic strain and sex effects on meat characteristics. *Poult. Sci.* 90, 1105–1111. doi: 10.3382/ps.2010-01154

Mehaffey, J. M., Pradhan, S. P., Meullenet, J. F., Emmert, J. L., McKee, S. R., and Owens, C. M. (2006). Meat quality evaluation of minimally aged broiler breast fillets from five commercial genetic strains. *Poult. Sci.* 85, 902–908. doi: 10.1093/ps/85.5.902

Ouyang, H., Wang, Z., Chen, X., Yu, J., Li, Z., and Nie, Q. (2017). Proteomic analysis of chicken skeletal muscle during embryonic development. *Front. Physiol.* 8:281. doi: 10.3389/fphys.2017.00281

Paião, F. G., Ferracin, L. M., Pedrão, M., Kato, T., and Shimokomaki, M. (2013). Skeletal muscle calcium channel ryanodine and the development of pale, soft, and exudative meat in poultry. *Genet. Mol. Res.* 12, 3017–3027. doi: 10.4238/2013.August.20.3

Pan, S., and Aebersold, R. (2007). Quantitative proteomics by stable isotope labeling and mass spectrometry. *Methods Mol. Biol* 367, 209–218. doi: 10.1385/1-59745-275-0:209

Paredi, G., Raboni, S., Bendixen, E., de Almeida, A. M., and Mozzarelli, A. (2012). "Muscle to meat" molecular events and technological transformations: the proteomics insight. *J. Proteomics* 75, 4275–4289. doi: 10.1016/j.jprot.2012.04.011

Perez-Riverol, Y., Csordas, A., Bai, J., Bernal-Llinares, M., Hewapathirana, S., Kundu, D. J., et al. (2019). The PRIDE database and related tools and resources in 2019: improving support for quantification data. *Nucleic Acids Res.* 47(D1), D442–D450. doi: 10.1093/nar/gky1106

Periasamy, M., and Kalyanasundaram, A. (2007). SERCA Pump Isoforms: their role in calcium transport and disease. *Muscle Nerve* 35, 430–442. doi: 10.1002/mus.20745

Peterson, D. W., Simone, M., Lilyblade, A. L., and Martin, R. (1959). Some factors affecting intensity of flavor and toughness of chicken muscle. *Food Technol.* 13, 204–207.

Qiu, H., Xu, X., Fan, B., Rothschild, M. F., Martin, Y., and Liu, B. (2010). Investigation of LDHA and COPB1 as candidate genes for muscle development in the MYOD1 region of pig chromosome 2. *Mol. Biol. Rep.* 37, 629–636. doi: 10.1007/s11033-009-9882-y

Rajkumar, U., Muthukumar, M., Haunshi, S., Niranjan, M., Raju, M. V. L. N., Rama Rao, S. V., et al. (2016). Comparative evaluation of carcass traits and meat quality in native Aseel chickens and commercial broilers. *Br. Poult. Sci.* 57, 339–347. doi: 10.1080/00071668.2016.1162282

Rauniyar, N. (2015). Parallel reaction monitoring: a targeted experiment performed using high resolution and high mass accuracy mass spectrometry. *Int. J. Mol. Sci.* 16, 28566–28581. doi: 10.3390/ijms161226120

Ronsein, G. E., Pamir, N., von Haller, P. D., Kim, D. S., Oda, M. N., Jarvik, G. P., et al. (2015). Parallel reaction monitoring (PRM) and selected reaction monitoring (SRM) exhibit comparable linearity, dynamic range and precision for targeted quantitative HDL proteomics. *J. Proteomics* 113, 388–399. doi: 10.1016/j.jprot.2014.10.017

Ros-Freixedes, R., Reixach, J., Bosch, L., Tor, M., and Estany, J. (2014). Genetic correlations of intramuscular fat content and fatty acid composition among muscles and with subcutaneous fat in Duroc pigs. *J. Anim. Sci.* 92, 5417–5425. doi: 10.2527/jas.2014-8202

Tasoniero, G., Cullere, M., Baldan, G., and Zotte, A. D. (2018). Productive performances and carcase quality of male and female Italian Padovana and Polverara slow-growing chicken breeds. *Ital. J. Anim. Sci.* 17, 530–539. doi: 10.1080/1828051X.2017.1364611

Teltathum, T., and Mekchay, S. (2009). Proteome changes in Thai indigenous chicken muscle during growth period. *Int. J. Biol. Sci.* 5, 679–685. doi: 10.7150/ijbs.5.679

Thompson, A., Schäfer, J., Kuhn, K., Kienle, S., Schwarz, J., Schmidt, G., et al. (2003). Tandem mass tags: a novel quantification strategy for comparative analysis of complex protein mixtures by MS/MS. *Anal. Chem.* 75, 1895–1904. doi: 10.1021/ac0262560

Tougan, P. U., Dahouda, M., Salifou, C. F. A., Ahounou, G. S., Kossou, D. N. F., Amenou, C., et al. (2013). Nutritional quality of meat from local poultry population of Gallus gallus species of Benin. *J. Anim. Plant Sci.* 19, 2908–2922.

Uitto, V. J., and Larjava, H. (1991). Extracellular matrix molecules and their receptors: an overview with special emphasis on periodontal tissues. *Crit. Rev. Oral Biol. Med.* 2, 323–354. doi: 10.1177/10454411910020030301

Umaya, S. R. (2014). The uniqueness of immunocompetence and meat quality of native chickens: a specialized review. *World J. Pharm. Pharm. Sci.* 3, 2576–2588.

Wiśniewski, J. R., Zougman, A., and Mann, M. (2009). Combination of FASP and StageTip-Based fractionation allows indepth analysis of the hippocampal membrane proteome. *J. Proteome Res.* 8, 5674–5678. doi: 10.1021/pr900748n

Wu, J., Zhou, D., Deng, C., Wu, X., Long, L., and Xiong, Y. (2008). Characterization of porcine ENO3: genomic and cDNA structure, polymorphism and expression. *Genet. Sel. Evol.* 40, 563–579. doi: 10.1186/1297-9686-40-5-563

Wu, P., Zhang, X., Zhang, G., Chen, F., He, M., Zhang, T., et al. (2020). Transcriptome for the breast muscle of Jinghai yellow chicken at early growth stages. *PeerJ* 8:e8950. doi: 10.7717/peerj.8950

Wu, W., Fu, Y., Therkildsen, M., Li, X. M., and Dai, R. T. (2015). Molecular understanding of meat quality through application of proteomics. *Food Rev. Int.* 31, 13–28. doi: 10.1080/87559129.2014.961073

Xing, T., Zhao, X., Wang, P., Chen, H., Xu, X., and Zhou, G. (2017). Different oxidative status and expression of calcium channel components in stress-induced dysfunctional chicken muscle. *J. Anim. Sci.* 95, 1565–1573. doi: 10.2527/jas.2016.0868

Yalcin, S., Şahin, K., Tuzcu, M., Bilgen, G., Özkan, S., Izzetoğlu, G. T., et al. (2019). Muscle structure and gene expression in pectoralis major muscle in response to deep pectoral myopathy induction in fast- and slow-growing commercial broilers. *Br. Poul. Sci.* 60, 195–201. doi: 10.1080/00071668.2018.1430351

Zerehdaran, S., Vereijken, A. L. J., van Arendonk, J. A. M., and van der Waaijt, E. H. (2004). Estimation of genetic parameters for fat deposition and carcass traits in broilers. *Poult. Sci.* 83, 521–525. doi: 10.1093/ps/83.4.521

Zhang, M., Li, F., Ma, X. F., Li, W. T., Jiang, R. R., Han, R. L., et al. (2019). Identification of differentially expressed genes and pathways between intramuscular and abdominal fat-derived preadipocyte differentiation of chickens *in vitro*. *BMC Genomics* 20:743. doi: 10.1186/s12864-019-6116-0

Zhao, G. P., Cui, H. X., Liu, R. R., Zheng, M. Q., Chen, J. L., and Wen, J. (2011). Comparison of breast muscle meat quality in 2 broiler breeds. *Poult. Sci.* 90, 2355–2359. doi: 10.3382/ps.2011-01432

Conflict of Interest: LY and JD were employed at Shanghai Bioprofile Technology Co., Ltd., Shanghai, China.

The remaining authors declare that the research was conducted in the absence of any commercial or financial relationships that could be construed as a potential conflict of interest.

frontiers in Physiology

ORIGINAL RESEARCH
published: 06 April 2021
doi: 10.3389/fphys.2021.663409

Nutritional Intervention Strategies Using Dietary Antioxidants and Organic Trace Minerals to Reduce the Incidence of Wooden Breast and Other Carcass Quality Defects in Broiler Birds

Vivek A. Kuttappan, Megharaja Manangi, Matthew Bekker, Juxing Chen and Mercedes Vazquez-Anon*

Novus International, Inc., St. Charles, MO, United States

OPEN ACCESS

Edited by:
Sandra G. Velleman,
The Ohio State University,
United States

Reviewed by:
Casey M. Owens,
University of Arkansas, United States
Nabeel Alnahhas,
Laval University, Canada

****Correspondence:***
Vivek A. Kuttappan
Vivek.Kuttappan@novusint.com

Specialty section:
This article was submitted to Avian Physiology, a section of the journal Frontiers in Physiology

Received: *02 February 2021*
Accepted: *11 March 2021*
Published: *06 April 2021*

Citation:
Kuttappan VA, Manangi M, Bekker M, Chen J and Vazquez-Anon M (2021) Nutritional Intervention Strategies Using Dietary Antioxidants and Organic Trace Minerals to Reduce the Incidence of Wooden Breast and Other Carcass Quality Defects in Broiler Birds. Front. Physiol. 12:663409. doi: 10.3389/fphys.2021.663409

Wooden breast (WB) is a degenerative myopathy seen in modern broiler birds resulting in quality downgrade of breast fillets. Affected filets show increased toughness both before as well as after cooking and have decreased water holding capacity and marinade pick up compared to normal fillets. Although the exact etiology is unknown, the circulatory insufficiency and increased oxidative stress in the breast muscles of modern broiler birds could be resulting in damage and degeneration of muscle fibers leading to myopathies. Three independent experiments were conducted to evaluate the effect of various dietary interventions on the incidence of WB when birds are exposed to oxidative stress associated with feeding oxidized fat and mild heat stress. Feed additives such as dietary antioxidant [Ethoxyquin (ETX)], mineral methionine hydroxy analog chelate (MMHAC) of Zn, Cu, and Mn, and organic selenium (Org Se) were tested at recommended levels. In experiment 1, ETX reduced ($P < 0.05$) the incidence of severe WB induced by oxidized fat diet. The magnitude of improvement in percentage of normal (no WB) filets and reduction in muscle lipid peroxidation was greater ($P < 0.05$) when ETX and MMHAC were fed together as shown by experiment 2. In birds exposed to mild heat stress (Experiment 3), feeding MMHAC by itself reduced ($P < 0.05$) tissue damage by reducing incidence of tibial head lesions, skin scratches, breast blisters, in addition to increasing the incidence of normal (no WB) fillets. When MMHAC was combined with ETX and Org Se, further improvement ($P < 0.05$) in normal (no WB) filets was observed. In summary, under different oxidative stress conditions, dietary intervention programs that contain ETX, MMHA-Zn, -Cu, and -Mn and Org Se can improve performance and increase carcass integrity, reducing problems, such as WB, either independently or with additive effect. This effect is most likely attained by simultaneously improving the exogenous and endogenous antioxidant status, reducing oxidative stress, and improving tissue healing process of the bird.

Keywords: myopathy, wooden breast, skin scratches, tibial head lesions, nutrition, minerals, antioxidants

INTRODUCTION

Wooden breast (WB) is a breast myopathy affecting modern broiler birds resulting in downgrading of breast filets causing economic loss to the poultry industry. WB is defined as the occurrence of toughness in raw breast filets and the severity varies from toughness only at the cranial region to a generalized toughness affecting the whole filet (Sihvo et al., 2014; Tijare et al., 2016). On average, the incidence of the condition reported in different publications is around 20% although, the reports may be confounded by the classification criteria and the absolute incidence across industry could vary tremendously (Petracci et al., 2019). Histologically, WB is characterized by multifocal and multiphasic degeneration and regeneration of muscle fibers, variability in shape, size, and diameter of the muscle fibers, increased deposition of fibrous tissue and lipid, infiltration of macrophages and lymphocytes, edema, vasculitis, and perivascular infiltrations in veins (Sihvo et al., 2014, 2017; Papah et al., 2017; Soglia et al., 2017; Petracci et al., 2019). These tissue changes are reported to have resulted in reduced protein as well as lipid content (Soglia et al., 2016a,b; Wold et al., 2017; Cai et al., 2018), and increased moisture (Soglia et al., 2016a,b; Wold et al., 2017; Cai et al., 2018) as well as collagen (Soglia et al., 2016a,b) contents in severe WB filets (Petracci et al., 2019). Various studies showed that severe WB results in increased toughness, drip loss, reduced marinade absorption and retention, also increased moisture loss in cooking of meat products (Mudalal et al., 2015; Chatterjee et al., 2016; Soglia et al., 2016b; Tijare et al., 2016; Dalle Zotte et al., 2017; Kuttappan et al., 2017a; Aguirre et al., 2018; Bowker et al., 2018; Brambila et al., 2018). Interestingly, the meat batters and meat balls produced from WB meat had inferior protein gelation and product texture compared to products from normal filets (Xing et al., 2017a; Chen et al., 2018). Based on its impact on the quality of fillets, the estimated economic loss due to WB condition could be $200 million to $1 billion per year for the United States poultry industry (Kuttappan et al., 2016; Huang and Ahn, 2018).

Despite the large number of studies conducted in WB over the past decade, the exact etiology of the condition is not clear yet. Various studies reported that the condition is associated with birds having faster growth rate or heavier filets (Mudalal et al., 2015; Kuttappan et al., 2017a), although the incidence of this condition can occur on birds of any size or growth rate. Furthermore, Soglia et al. (2016a) reported that severe WB is characterized by an increased oxidative stress in muscle tissue measured using thiobarbituric acid reactive substances (TBARS) and protein carbonyl levels. Several studies conducted using "omics" approach have revealed that incidence of WB is associated with signs of vascular disturbances, hypoxia, increased oxidative stress and altered metabolic pathways (Mutryn et al., 2015; Abasht et al., 2016; Kuttappan et al., 2017b; Papah et al., 2018). Arguably, one of the more popular hypothesis on the etiology of WB or similar myopathies is that broilers with higher rate of hypertrophic muscle growth results in increased metabolic and circulatory demand leading to increased risk of accumulation of metabolic waste products (such as oxygen free radicals) in muscle tissues resulting in increased oxidative stress (Petracci et al., 2019). The accumulated free radicals are highly reactive and can damage DNA, RNA, proteins, and lipids present in the muscle cells (Surai, 2015) causing inflammation and metabolic disturbances, eventually causing degeneration of muscle fibers. Once the damage caused by increased oxidative stress is beyond the regenerative capacity of the muscle cells, the result is an accumulation of fibrous tissue and fat leading to myopathies such as WB (Petracci et al., 2019).

Various intervention strategies are already being considered to reduce the incidence of WB in the industry. These strategies can be broadly classified into growth-rate-related and antioxidant-based approaches. Growth-rate-related approaches focus on manipulating or slowing down the birds during the entire or a part of the growth period and thus reduce myopathies, utilizing the knowledge of positive correlation between growth rate and incidence of myopathies (Kuttappan et al., 2016). Dietary restriction, reduced nutrient density, and lysine reduction during growth phase have been studied with variable success in different studies (Kuttappan et al., 2013a; Cruz et al., 2016; Bodle et al., 2018; Livingston et al., 2018; Meloche et al., 2018a,b,c,d). However, if not applied properly, these approaches have a risk of compromising the performance in addition to reduction in myopathies. On the other hand, the antioxidant-based approaches such as the use of dietary arginine, vitamin C, selenium, and trace minerals (Sirri et al., 2016; Bodle et al., 2018; Cemin et al., 2018) have been evaluated to reduce myopathies. Similar to the growth-rate-related approach, the benefits from the antioxidant-based approach are also variable and sometimes confounded by its effect on growth rate, slaughter weight and/or breast yield which makes it difficult to draw any meaningful conclusions. It is well known that factors such as oxidized fat in the diet and heat stress, which are very relevant to commercial poultry production in certain world areas, can also lead to increased oxidative stress in tissues (Jensen et al., 1997; Willcox et al., 2004; Slimen et al., 2014; Delles et al., 2015; Surai, 2015; Akbarian et al., 2016; Wang et al., 2018), and eventually could result in increased myopathies. In fact, dietary antioxidants, vitamins, and bioavailable trace minerals such as zinc, copper, manganese, and selenium have been proven to reduce oxidative stress in animal tissue (Dibner et al., 1996; Avanzo et al., 2001; Xiang et al., 2002; Surai, 2015). So, the main objective of the present study was to evaluate the effect of various dietary antioxidant based (synthetic antioxidants) or endogenous antioxidant support (through highly bioavailable trace minerals such as zinc, copper, manganese, and selenium) approaches on the incidence of WB in broilers under oxidative challenge (oxidized fat or heat stress) and identify an appropriate strategy which may reduce WB without compromising performance in broiler birds.

MATERIALS AND METHODS

Experiment 1

The study was conducted at Novus International, Inc., Green Acres Experimental Farm, Montgomery, MO, United States and all the procedures were approved by the Animal Use Committee.

Total of 792 1-day-old male broilers were allocated to four diet treatments, with 18 pen replicates per treatment with 11 males per pen, in a randomized complete block design. All the treatment groups received the same corn-soybean meal-based basal diet (**Table 1**) with Zn, Cu, and Mn in the form of sulfates at 110-20-120 ppm, respectively, with respective treatment feed

TABLE 1 | Basal diet for different phases for Experiment 1 and 2.

Ingredient (%)	Starter	Grower	Finisher 1	Finisher 2	Withdrawal
Corn	54.22	57.94	66.52	68.4	68.76
Soybean meal	38.78	34.52	26.06	24.3	24.15
Dicalcium phosphate	1.9	1.72	1.53	1.44	1.38
Limestone	0.95	0.89	0.84	0.82	0.78
Salt	0.31	0.24	0.33	0.24	0.25
Sodium bicarbonate	0.3	0.42	0.29	0.47	0.47
[1]MHA®84%	0.3	0.26	0.27	0.22	0.18
[2]Mineral premix	0.2	0.2	0.2	0.2	0.2
L-LYSINE HCL 78%	0.14	0.11	0.21	0.18	0.13
Choline Cl-60%	0.05	0.07	0.09	0.09	0.09
[3]Coban 90	0.05	0.05	0.05	0.05	0.05
Threonine	0.1	0.05	0.08	0.06	0.03
[4]Vitamin premix	0.05	0.05	0.05	0.05	0.05
[5]Sand	0.15	0.15	0.15	0.15	0.15
[6]Soybean oil	2.5	3.33	3.33	3.33	3.33
Total	100	100	100	100	100
Calculated nutrient content					
ME (Kcal/Kg)	3030	3120	3201	3226	3230
CP (%)	23.62	21.83	18.67	17.91	17.78
dLys (%)	1.28	1.15	1.02	0.95	0.91
dMet (%)	0.59	0.54	0.51	0.46	0.43
dSAA (%)	0.95	0.87	0.80	0.74	0.71
dThr (%)	0.87	0.77	0.68	0.64	0.61
dCys (%)	0.36	0.33	0.29	0.28	0.28
dArg (%)	1.44	1.32	1.09	1.04	1.04
Calcium (%)	0.96	0.88	0.79	0.75	0.72
Phosphorus (%)	0.48	0.44	0.39	0.37	0.36

Proximate analysis was done for all the diets and confirmed the nutrient value matched the table values.

[1]DL-Methionine Hydroxy Analog Calcium, Novus International, Inc., St Charles, MO, United States. For experiment 2, ∼0.06% was reduced in the basal diet for all phase to account the amount coming from mineral premix.

[2]Trace mineral premix

- Experiment 1: Added at this rate yields 120 mg manganese (sulfate), 110 mg zinc (sulfate), 35 mg iron (sulfate), 20 mg copper (sulfate), iodate (calcium iodate) 1.25 mg per kg of diet. The premix contained calcium carbonate as carrier and less than 1% mineral oil.
- Experiment 2: For treatments OxF and OxF + ETX, premix added at this rate had 120 mg manganese (sulfate), 110 mg zinc (sulfate), 35 mg iron (sulfate), 20 mg copper (sulfate), iodate (calcium iodate), and 575.4 mg MHA per kg of diet. For treatments OxF + MMHAC and OxF + MMHAC + ETX, premix added at this rate had 40 mg manganese (MINTREX®), 40 mg zinc (MINTREX®), 35 mg iron (sulfate), 25 mg copper (MINTREX®), and iodate (calcium iodate) per kg of diet.

[3]Active drug ingredient monensin sodium (Elanco Animal Health, Greenfield, IN, United States). For the prevention of coccidiosis caused by Eimeria necatrix, Eimeria tenella, Eimeria acervulina, Eimeria brunetti, Eimeria mivati, and Eimeria maxima.

[4]Vitamin premix: for Experiment 1 and 2, added at this rate yields 11574 IU vitamin A, 4125 ICU vitamin D, 125 IU vitamin E, 3.1 mg vitamin K, 0.019 mg B12, 10.0 mg riboflavin, 68.8 mg niacin, 18.8 mg pantothenic acid, 1.87 mg folic acid, 4.4 mg pyroxidine, 3.13 mg thiamine, 0.188 mg biotin per kg diet.

[5]Sand was used as a filler

- Experiment 1: ETX-Ethoxyquin [SANTOQUIN® M6 at 188 ppm (Ethoxyquin-125 ppm)]. SANTOQUIN® M6 has 66.6% ethoxyquin and was added at 0.0188% in the FrF + ETX and OxF + ETX diets replacing the same amount of sand.
- Experiment 2: ETX- Ethoxyquin [SANTOQUIN® M6 at 188 ppm (Ethoxyquin-125 ppm)]. SANTOQUIN® M6 has 66.6% ethoxyquin and was added at 0.0188% in the OxF + ETX, OxF + MMHAC + ETX diets replacing the same amount of sand.

[6]Soybean oil was used as source of fat.

- Experiment 1: Oxidized soy oil to contain 225 meq peroxide/kg so that the final starter diet to have ∼5–5.5 mEq/kg diet, and the grower and finisher diets to have ∼7–7.5 meq peroxide/kg for OxF and OxF + ETX, while FrF and FrF + ETX received fresh soybean oil.
- Experiment 2: All diets received oxidized soy oil to contain 225 meq peroxide/kg so that the final starter diet to have ∼5–5.5 mEq/kg diet, and the grower and finisher diets to have ∼7–7.5 meq peroxide/kg.

additives in different phases–Starter (0–11 days), Grower (11–25 days), Finisher-1 (25–39 days), Finisher-2 (39–46 days), and withdrawal (46–58 days). Oxidized vegetable fat/oil used for the diet was prepared by bubbling air through the fat at 92°C for 24 h (method Cd 12-57; AOCS., 1997) to contain peroxide value of 225 mEq/kg so that the final starter diet would have ∼5–5.5 mEq/kg diet, and the grower and finisher diets will have ∼7–7.5 mEq/kg. Antioxidant used for respective treatments in the diets was SANTOQUIN® M6 [with 66.6% ethoxyquin (ETX)] added at 188 ppm in the treatments diets to get a final concentration of 125 ppm ETX in diet. All diets were conditioned and pelleted at 85°C for 30 s and fed as crumbles during starter phase and as pellets for the remainder of grow out. Four treatments in the study were: 1. Fresh fat without antioxidants (FrF), 2. Fresh fat with antioxidant (FrF + ETX) 3. Oxidized fat without antioxidant (OxF) and 4. Oxidized fat with antioxidant (OxF + ETX). Other than the differences in treatments, all diets satisfied the nutritional requirements described by Aviagen breed recommendations. On 59 days, two birds per pen were randomly selected to collect blood and muscle tissue for plasma enzymes and TBARS measurement, respectively. All the remaining birds were processed according to standard commercial style system as described by Kuttappan et al. (2013a). At 10 h before processing, all birds were withheld feed while having *ad libitum* access to water. At the first stage of processing, birds were electrically stunned, the left carotid artery and jugular vein were manually severed, bled out, carcasses were soft scalded, defeathered, and eviscerated. The carcasses were then pre-chilled at 12°C for 15 min followed by further chilling for 90 min at 1°C in immersion chilling tanks. The carcasses were then removed from the chilling tanks and stored at 4°C overnight until deboned. Live weight, carcass weight, filet weight, and abdominal fat were recorded. Filets were scored for different degrees of WB according to the procedure by Tijare et al. (2016) and Kuttappan et al. (2016). Briefly, degree of hardness of whole raw breast filets was evaluated (WB) and categorized as: 0 = filets that were flexible throughout (normal); 1 = filets that were hard mainly in the cranial region but flexible otherwise (mild); 2 = filets that were hard throughout but flexible in mid to caudal region (moderate); 3 = filets that were extremely hard and rigid throughout from cranial region to caudal tip (severe).

Experiment 2

The study was conducted at Novus International, Inc., Green Acres Experimental Farm, Montgomery, MO, United States and all the procedures were approved by the Animal Use Committee. The experimental design consisted of four treatments, 18 pen replicates per treatment with 15 males per pen. Total of 1080 day old male broilers were allocated to one of the four diet treatments in a randomized complete block design with Starter (0–12 days), Grower (12–26 days), and Finisher (26–40days) periods. Feed and bird weights were taken on 0, 12, 26, and 41 days. All birds in the study received a corn-soy-based basal diet (**Table 1**) with oxidized vegetable fat/oil along with the respective treatments. Four treatment groups were: (1) Treatment containing inorganic trace minerals without any feed additives (OxF), (2) Oxidized fat with antioxidant (OxF + ETX), (3) Oxidized fat with inorganic trace minerals replaced by reduced levels of mineral methionine hydroxy analog chelate (MMHAC) trace minerals (OxF + MMHAC), (4) Oxidized fat with both antioxidant and MMHAC trace minerals (OxF + ETX + MMHAC). Antioxidant used in the study was SANTOQUIN® M6 (Novus International, Inc.) at the levels mentioned in experiment 1. Zn, Cu, and Mn in the form of inorganic trace minerals (sulfates) at 110-20-120 ppm and MMHAC (MINTREX®, Novus International, Inc.) at 40-25-40 ppm, respectively, for respective treatments were used. All diets, satisfied the nutritional requirements described by Aviagen breed recommendations, were conditioned and pelleted at 85°C for 30 s and fed as crumbles during starter phase and as pellets for the rest of the grow out. Body weight, feed intake, and mortality were recorded until 41 days and cumulative feed conversion corrected for mortality (cFCR) as well as performance index (cPERFIDX) were calculated as described by Anjos et al. (2012). On day 41, two randomly selected male birds were removed from each pen and processed using a standard commercial style system. From the same birds, blood and muscle samples were collected for serum lactate dehydrogenase (LDH) and muscle TBARS measurement as described below. Filets were scored for different degrees of WB according to the procedure by Tijare et al. (2016) and Kuttappan et al. (2016).

Experiment 3

The study was conducted at Bangkok Animal Research Center Co., Ltd. in Thailand and all the procedures were approved by Internal Ethics Committee. A total of 234 1-day-old male broilers were assigned to 3 dietary treatments with 6 replicates and 13 birds per replicate. All diets satisfied the nutritional requirements described by Aviagen breed recommendations. Corn and soybean meal basal diet formed the basis of the ration (**Table 2**). The treatments in the study were: (1) CON-ITM with sulfate of zinc (110 ppm), copper (6 ppm), and manganese (120 ppm) with inorganic selenium (0.3 ppm); (2) MMHAC (MINTREX®, Novus International, Inc.) with MMHAC sources of zinc (50 ppm), copper (10 ppm), manganese (60 ppm) with inorganic selenium (0.3 ppm); (3) MMHAC + Org Se + ETX with MMHAC sources of zinc (50 ppm), copper (10 ppm), manganese (60 ppm) with organic selenium (Org Se) (ZORIEN® SeY, Novus International, Inc., added at 0.3 ppm) and ETX at 125 ppm of final concentration. Diets were mixed by a double ribbon horizontal mixer. Mash feeds were processed at 82°C conditioning temperature and fed in crumble form for the first 14 days, and in pellet form thereafter until finishing the 35 days test period. The diets were identical and nutritionally equivalent across all parameters outside of the minerals and antioxidant. All birds were grown up to age of 35 days and the heat in the shed was increased to 30°C in the growing period from 21–35 days which would mimic the mild heat stress situation common in South East Asia and many other poultry rearing regions. On 35 days, randomly selected birds (n = 24/treatment) were processed using a standard commercial type processing system and live weight, carcass weight, filet weight, and abdominal fat were recorded. Filets were scored for different degrees of WB according to Tijare et al. (2016) and Kuttappan et al. (2016). Tibial strength and severity (Score 0-normal to Score 3-severe) of tibial head

TABLE 2 | Basal diet for different phases for Experiment 3.

Ingredient (%)	Starter	Grower	Finisher
Corn	55.38	57.70	61.83
Soybean meal	36.32	33.29	28.63
Soybean oil	3.18	4.37	5.31
Monodicalcium phosphate	2.15	1.91	1.70
Limestone	1.02	0.96	0.85
Salt	0.20	0.23	0.24
[1]Pelex® Dry	0.30	0.30	0.30
[2]BS Premix	0.20	0.20	0.20
[3]MHA®84%	0.39	0.33	0.30
L-Lysine HCl	0.30	0.23	0.21
L-Threonine	0.18	0.13	0.10
Sodium bicarbonate	0.25	0.22	0.21
Choline Chloride 60%	0.08	0.07	0.08
[4]Salinomycin 12% (Sacox)	0.05	0.05	0.05
Total	100.00	100.00	100.00
Calculated nutrient content			
ME (Kcal/Kg)	3,000	3,100	3,200
CP (%)	23.0	21.5	19.5
dLys (%)	1.28	1.15	1.02
dMet (%)	0.64	0.57	0.53
dCys (%)	0.31	0.30	0.27
dThr (%)	0.86	0.77	0.68
dArg (%)	1.32	1.23	1.10
Calcium (%)	0.96	0.87	0.78
Total phosphorus (%)	0.84	0.77	0.71
Phosphorus (%)	0.48	0.44	0.39

Proximate analysis was done for all the diets and confirmed the nutrient value matched the table values.

[1]Pelex® is an advanced-generation, synthetic resin that is effective at low inclusion levels as a livestock feed/pellet binder.

[2]Trace mineral premix: All treatments received 20 mg iron, and 1.2 mg iodine. In addition to that, CON–ITM received 110 mg zinc sulfate, 6 mg copper sulfate, 120 mg manganese sulfate, and 0.3 mg sodium selenite; MMHAC received 50, 10, and 60 mg of MINTREX® Zn, MINTREX® Cu, and MINTREX® Mn, respectively, and 0.3 mg sodium selenite; MMHAC + Org Se + ETX received 50, 10, and 60 mg of MINTREX® Zn, MINTREX® Cu, and MINTREX® Mn, respectively, 0.3 mg ZORIEN® SeY (A special strain of Saccharomyces cerevisiae enriched with selenium in an organic highly bioavailable form) and 125 mg of ethoxyquin (SANTOQUIN® M6 at 188 ppm) per kg of diet.

[3]DL-Methionine Hydroxy Analog Calcium, Novus International, Inc., St Charles, MO, United States.

[4]Salinomycin sodium concentrations ranging from 40 to 60 g/ton (0.0044–0.0066%) for the prevention of coccidiosis in broiler, roaster and replacement chickens caused by Eimeria tenella, Eimeria necatrix, Eimeria acervulina, Eimeria maxima, Eimeria brunetti, and Eimeria mivati.

necrosis lesions (Wideman et al., 2014) were recorded. Presence or absence of breast and skin scratches were also scored.

Measurement of Serum/Plasma Markers and Muscle TBARS

Plasma LDH and creatine kinase (CK) activity were measured using LDH activity assay kit and CK activity assay kit from Sigma (St. Louis, MO, United States) as described in the manuals. Serum TBARS was measured using TBARS assay kit (Ann Arbor, MI, United States) from Cayman Chemical as described in the manual.

Statistical Analysis

Performance, tibial strength, and processing weight as well as yield data were analyzed using a one-way or two-way ANOVA, according to the experimental design, using the SAS GLM procedure and means were separated at $P < 0.05$ using Fisher's protected LSD test. Incidence of different degrees of myopathies and tibial head necrosis were analyzed using a Chi-square test or the SAS GLIMMIX procedure with significant differences ($P < 0.05$) tested assuming a binomial response distribution, with a logit link function.

RESULTS AND DISCUSSION

Increased oxidative stress due to circulatory insufficiency and hypoxia in muscle tissue of modern broilers have been reported to be associated with the incidence of WB (Kuttappan et al., 2016; Soglia et al., 2016b; Papah et al., 2018; Sihvo et al., 2018). In fact, tissue levels of free radicals, which contribute to the oxidative stress, can be influenced by various endogenous (ischemia, inflammatory response, mitochondrial metabolism and other cytosolic sources) and exogenous (oxidized fat in diet, heat stress, ionization, radiation) factors (Jensen et al., 1997; Willcox et al., 2004; Slimen et al., 2014; Delles et al., 2015; Surai, 2015; Akbarian et al., 2016; Wang et al., 2018). Furthermore, dietary oxidized fat caused increased rancidity in meat products with concomitant increase in drip loss and reduced shelf life (Jensen et al., 1997; Delles et al., 2015). Based on this information, experiment 1 was conducted to confirm the association between oxidized fat as a source of oxidative stress on the incidence of WB and evaluate the effect of proven nutritional antioxidant intervention. As expected, oxidized fat had an impact ($P < 0.05$) on the performance of birds (**Table 3**) in accordance with previous reports (Dibner et al., 1996; Ao et al., 2017). A factorial analysis of live body weight for the effect of fat type showed that birds fed with oxidized fat (4.65 ± 0.04 kg) had lower ($P < 0.05$) live weight than birds fed with fresh fat (4.82 ± 0.04 kg). Previous studies have shown that presence of oxidized fat in the diet can destroy other nutrients in the diet matrix such as protein and fat-soluble vitamins (Sheehy et al., 1994; Zdunczyk et al., 2002) and increase oxidative stress related damages in tissue (Dibner et al., 1996) leading to reduced performance in broiler birds (Ao et al., 2017). However, there were no effects ($P > 0.05$) of oxidized fat on other carcass weight and yield parameters (**Table 3**) in the present study. The incidence of severe degree of WB (score 3) tended to be higher ($P = 0.064$; pairwise comparison) in OxF (29%) compared to FrF birds (18%). Furthermore, higher levels of plasma LDH were seen in birds fed with oxidized fat (2596.31 + 375.60 U/L) compared to fresh fat (1149.23 + 375.60 U/L) group based on factorial analysis. LDH is an enzyme present in most of the living animal cells, which is involved in metabolism of lactate (an end product of anaerobic glycolysis) and is used as an indicator of cell/tissue damage in human (Zhao et al., 2020). Previously,
Kuttappan et al. (2013b) reported that increased serum levels of LDH in case of white striping myopathy, which is similar to WB, suggestive of increased muscle damage. In fact,

TABLE 3 | Carcass weight and yield data from Experiment 1.

	Live weight, kg	Dressing %	Filet (kg)	Breast yield (%)	% Fat
FrF	4.788^{A}	77.08	1.164	24.32	1.45
FrF + ETX	4.855^{A}	77.34	1.183	24.35	1.43
OxF	4.588^{B}	77.23	1.138	24.85	1.45
OxF + ETX	4.719^{AB}	76.92	1.155	24.51	1.44
SEM	0.0523	0.1470	0.0158	0.176	0.029
	P-values from factorial analysis				
Fat Type	**0.002**	0.35	0.10	0.05	0.81
AO	0.06	0.85	0.26	0.40	0.70
Fat type*AO	0.54	0.06	0.96	0.29	0.99

^{A,B}Different superscript in each column differ significantly ($P < 0.05$).
n = 162 birds/treatment.
FrF, Fresh fat; FrF + ETX, Fresh fat and ethoxyquin; OxF, Oxidized fat; OxF + ETX, Oxidized fat and ethoxyquin.
*Fat type*AO means interaction between Fat type and AO.*
Bold P-values means significant ($P < 0.05$) effect.

TABLE 4 | Plasma and tissue parameters from Experiment 1.

	Plasma enzymes (units per L)		TBARS (umol per g)	
	LDH	CK	Breast muscle§	Liver
FrF	1209.52^{B}	124.37	0.026^{AB}	0.209^{A}
FrF + ETX	1088.95^{B}	125.67	0.022^{B}	0.197^{AB}
OxF	3436.56^{A}	119.50	0.030^{A}	0.182^{B}
OxF + ETX	1756.06^{B}	124.71	0.025^{AB}	0.182^{B}
SEM	530.26	2.21	0.0019	0.0088
	P-values from factorial analysis			
Fat type	**0.0096**	0.19	0.08	**0.0224**
AO	0.10	0.15	**0.0191**	0.51
Fat type*AO	0.15	0.38	0.73	0.49

^{A,B}Different superscript in each column differ significantly ($P < 0.05$).
n = 162 birds/treatment.
FrF, Fresh fat; FrF + ETX, Fresh fat and ethoxyquin; OxF, Oxidized fat; OxF + ETX, Oxidized fat and ethoxyquin.
*Fat type*AO means interaction between Fat type and AO.*
Bold P-values means significant ($P < 0.05$) effect.

Meloche et al., 2018a,c) reported positive association between severe WB and elevated plasma LDH. There was no difference in plasma CK levels in the present study. Meloche et al. (2018a) reported the lack of association with plasma CK and incidence of WB which could be due to non-specificity of CK to indicate muscle damage. This data confirmed that inclusion of oxidized fat in the diet is an effective exogenous way to induce muscle damage in birds. Interestingly, incidence of WB Score 3 was decreased ($P < 0.05$) in OxF + ETX (15%) group when compared to OxF (29%) group (**Figure 1**). A decrease ($P < 0.05$) in breast muscle TBARS was seen in ETX fed group (0.023 umol/g) when compared to non-ETX fed group (0.028 umol/g) based on factorial analysis. Soglia et al. (2016a) had reported that increased TBARS and protein carbonyls levels in muscle tissue are associated with incidence of WB in broiler birds. It is also important to point out a factorial comparison between ETX and non-ETX groups revealing a directional decrease in plasma LDH (1422.51 vs. 2323.04 U/L; $P = 0.098$) and improvement in live weight (4.787 vs. 4.688 kg/bird; $P = 0.063$) in ETX group. Nonetheless, Dibner et al. (1996) reported that inclusion of ETX in the feed had shown benefits in improving performance in broiler birds fed with oxidized fat. In short, these results confirm that dietary oxidized fat cause muscle damage as indicated by elevated LDH levels (**Table 4**), and ETX is effective in reducing muscle oxidative stress as shown by breast muscle TBARS levels (**Table 4**). Inclusion of ETX to diet with bad quality or oxidized fat significantly reduced the incidence of severe WB (**Figure 1**).

In Experiment 2, multiple nutritional interventions which can support the reduction of oxidative stress level in tissue were tested in the presence of oxidized fat in diet. The study

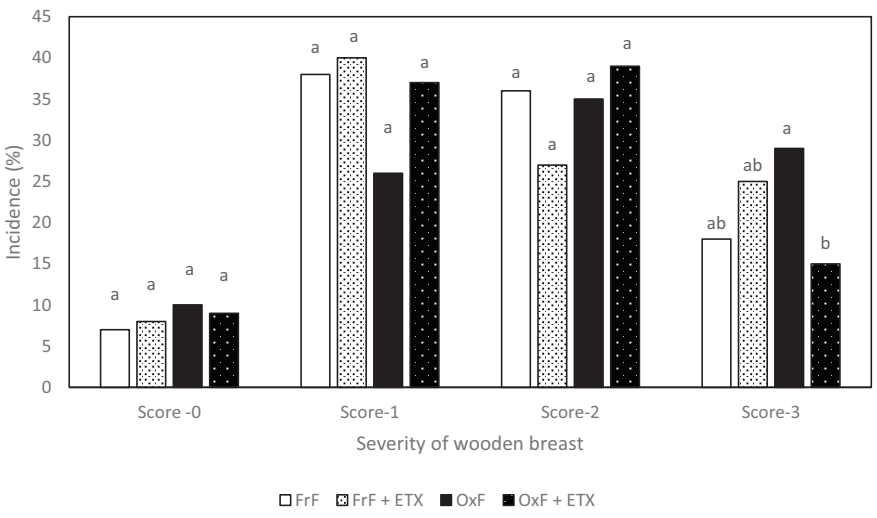

FIGURE 1 | Incidence of different degrees of wooden breast in birds from Experiment 1. ^{a,b}Different superscript under each score differ significantly ($P < 0.05$). *n* = 162 birds/treatment. FrF, Fresh fat; FrF + ETX, Fresh fat and ethoxyquin; OxF, Oxidized fat; OxF + ETX, Oxidized fat and ethoxyquin.

TABLE 5 | Performance data and tissue parameters from birds from Experiment 2.

	Performance* (*n* = 18 pens/treatment; 15 birds/pen)				Tissue parameters (36 birds/treatment)	
	BW (kg)	cFCR (kg:kg)	cFI (kg)	cPerfidx	Serum LDH (milliunits/mL)	Breast muscle TBARS (mmol/g)
OxF	3.807	1.564^{A}	5.891	504.580^{B}	1690.44	0.038^{AB}
OxF + ETX	3.906	1.537^{B}	5.941	529.600^{A}	1397.47	0.033^{BC}
OxF + MMHAC	3.868	1.540^{B}	5.897	519.985^{AB}	1305.15	0.043^{A}
OxF + MMHAC + ETX	3.861	1.539^{B}	5.879	521.465^{A}	1560.95	0.027^{C}
SEM	0.0287	0.0044	0.0445	5.8773	161.95	0.002
P-value	0.11	**<0.0001**	0.77	**0.0257**	0.34	**0.0001**

^{A,B}Different superscript in each column differ significantly ($P < 0.05$).

**Pens were used as experimental units for performance parameters.*

OxF, Oxidized fat; OxF + ETX, Oxidized fat and ethoxyquin; OxF + MMHAC, Oxidized fat and Zn, Cu, Mn–MMHAC; OxF + MMHAC + ETX, Oxidized fat, Zn, Cu, Mn–MMHAC, and ethoxyquin. Bold numbers means $P < 0.05$.

compared the effect of ETX and organic source of Zn, Cu, and Mn individually or in combination, on the effect of tissue oxidative stress level and incidence of WB. Results from the study showed that the individual or combined addition of ETX with MMHAC resulted in improved ($P < 0.05$) cFCR when compared to OxF (**Table 5**). Both, OxF + ETX, and OxF + MMHAC + ETX were able to improve ($P < 0.05$) the cPERFIDX when compared to OxF (**Table 5**). OxF + MMHAC + ETX resulted in an additive effect with an improvement ($P < 0.05$) in incidence of normal filets when compared to OxF (**Figure 2**). Interestingly, OxF + MMHAC + ETX showed the lowest ($P < 0.05$) level of breast muscle TBARS among the treatments in the study. Superoxide radicals, contributing to increased oxidative stress and higher TBARS levels in tissues, are primarily produced in mitochondria by the electron transport chain and in the cytoplasm by enzymes such as xanthine oxidase, cytochrome P450-monooxygenases, NADPH oxidase (Wang et al., 2018). Once produced in mitochondria, superoxides can move to cytoplasm where they can move back and forth to the extracellular space (Wang et al., 2018). These superoxides can then be reactive with other molecules to form reactive oxygen species which can cause damage to DNA, RNA, proteins, and lipids in the cell (Surai, 2015). The antioxidant system present in the body plays an important role to convert the superoxide to harmless substances. Primarily, superoxides are converted to hydrogen peroxide by a group of enzymes called superoxide dismutases (SOD). Surai (2015) reported there are mainly three types of SODs found in mammals and chickens. Mn-SOD (mitochondria), Zn, Cu-SOD (cytoplasm), and Cu-SOD (extracellular space) which need the respective trace minerals as cofactors for proper functioning (Surai, 2015; Wang et al., 2018). According to Surai (2015), the activity of these SOD in tissues can be enhanced by adequate bioavailable levels of Zn, Cu, and Mn in diet. In fact, MMHAC trace minerals have been well studied for their improved bioavailability compared to ITMs (Yan and Waldroup, 2006; Wang et al., 2007). Furthermore, the enhanced tissue activity of SOD can increase conversion of oxygen free radicals to hydrogen peroxide which in turn is acted upon by catalase and glutathione peroxidase to water (Surai, 2015; Wang et al., 2018), thereby reducing the damage from oxidative stress. A combination of ETX and MMHAC–Zn, Cu, Mn in experiment 2 could be reducing the effect of both exogenous (dietary oxidized fat) and endogenous (superoxides in mitochondria, cytoplasm, and extracellular space) factors to cause oxidative stress and thereby provided a greater magnitude of reduction in tissue oxidative stress and severity of WB along with improving performance in broiler birds. In addition, Richards et al. (2010) reported that Zn, Cu, and Mn play an important role in the development of connective tissue and tissue repair. Plausibly, this benefit could also be contributing to the advantage of MMHAC reducing severity of muscle damage leading to WB. However, the treatments only showed numerical reduction in serum LDH levels in this study suggesting of a tendency to reduce muscle damage (**Table 5**).

In Experiment 3, various nutritional intervention strategies to reduce oxidative stress in tissue were combined and tested in a commercial relevant situation where birds were fed a corn-soy based diet with no oxidized fat but exposed to mild heat stress during the grow out period to mimic environmental

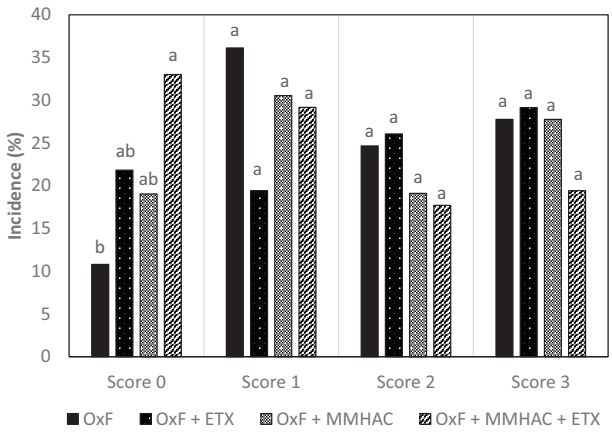

FIGURE 2 | Incidence of different degrees of myopathies in birds from Experiment 2 at 42 days. ^{a,b}Different superscript under each score differ significantly ($P < 0.05$). n = 36 birds/treatment. OxF, Oxidized fat; OxF + ETX, Oxidized fat and ethoxyquin; OxF + MMHAC, Oxidized fat and Zn, Cu, Mn–MMHAC; OxF + MMHAC + ETX, Oxidized fat, Zn, Cu, Mn–MMHAC, and ethoxyquin.

TABLE 6 | Live weight, carcass weight as well as yield and tibial breaking strength of birds from Experiment 3.

	Live weight, kg	Dressing %	Filet (g)	Breast yield (%)	% Fat	Tibial strength (kg/cm^2)
CON-ITM	2.563	76.90	550	27.90	2.27	0.34^{B}
MMHAC	2.611	77.15	577	28.66	2.16	0.37^{AB}
MMHAC + Org Se + ETX	2.586	76.79	563	28.36	2.15	0.41^{A}
SEM	0.02	0.27	8.2	0.26	0.08	0.02
P-value	0.54	0.06	0.96	0.29	0.99	**<0.01**

^{A,B}Different superscript in each column differ significantly ($P < 0.05$). $n = 24$ birds/treatment.

- CON-ITM with sulfate of zinc (110 ppm), copper (6 ppm), and manganese (120 ppm) with inorganic selenium (0.3 ppm).
- MMHAC with MMHAC sources of zinc (50 ppm), copper (10 ppm), manganese (60 ppm) with inorganic selenium (0.3 ppm).
- MMHAC + Org Se + ETX with MMHAC sources of zinc (50 ppm), copper (10 ppm), manganese (60 ppm) with organic selenium (ZORIEN® SeY, Novus International, Inc., added at 0.3 ppm) and AO at 125 ppm of final concentration. Bold numbers means $P < 0.05$.

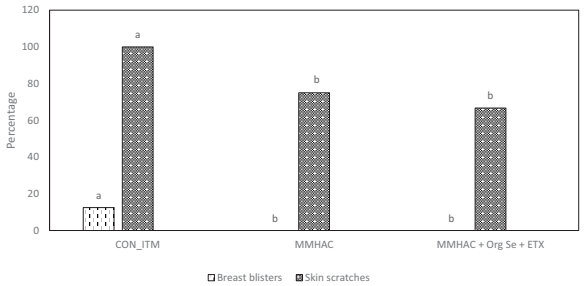

FIGURE 4 | Incidence of breast blisters and skin scratches in birds from Experiment 3. ^{a,b}Different superscript under each score differ significantly ($P < 0.05$). $n = 24$ birds/treatment. CON-ITM with sulfate of zinc (110 ppm), copper (6 ppm), and manganese (120 ppm) with inorganic selenium (0.3 ppm). MMHAC with MMHAC sources of zinc (50 ppm), copper (10 ppm), manganese (60 ppm) with inorganic selenium (0.3 ppm). MMHAC + Org Se + ETX with MMHAC sources of zinc (50 ppm), copper (10 ppm), manganese (60 ppm) with organic selenium (ZORIEN® SeY, Novus International, Inc., added at 0.3 ppm) and AO at 125 ppm of final concentration.

conditions that could lead to oxidative stress (Slimen et al., 2014; Akbarian et al., 2016; Lu et al., 2017). The harmful effects of heat stress in birds could be attributed through disruption of mitochondrial function, increased oxidative stress and lipid peroxidation, decreased vitamin levels and altered enzyme activity leading to reduced production performance (Horváth and Babinszky, 2018). In this study, there were no differences ($P > 0.05$) between the treatment groups with respect to live weight, or carcass weight and yield (**Table 6**). However, MMHAC treatment resulted an increase ($P < 0.05$) in the incidence of normal filets (Score 0) with respect to CON-ITM (**Figure 3A**). Previously, Sirri et al. (2016) reported that use of MMHAC resulted in numerical improvement in incidence of WB score 0 (MMHAC 88% vs. ITM 84%) and the lack of significant difference could be due to overall lower incidence of WB in that study. In fact, the results from Experiment 1 showed the effect of these intervention strategies will be more prominent when there is higher challenge. In addition, it was observed in Experiment 2 that combining MMHAC + ETX provided a higher magnitude of benefit in reducing oxidative stress in muscle and increasing percentage of normal (no WB) fillets. One step further in Experiment 3, adding Org Se and ETX to MMHAC resulted in a higher magnitude of increase ($P < 0.05$) in normal filets and a reduction ($P < 0.05$) in Score 2 WB when compared to

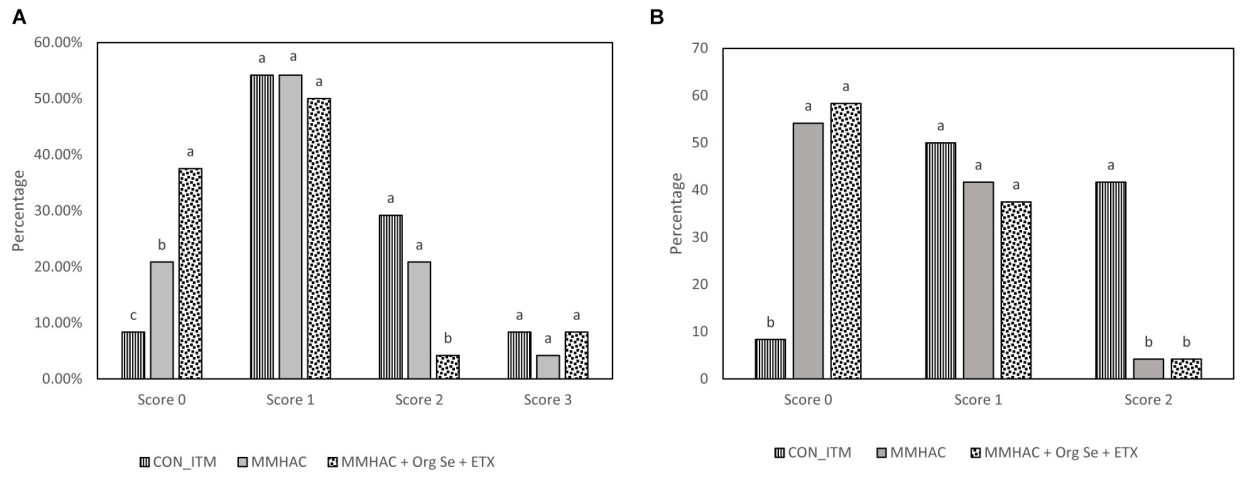

FIGURE 3 | Incidence of different degrees of WB **(A)** and tibial head lesions **(B)** in birds from Experiment 3. $^{a-c}$Different superscript under each score differ significantly ($P < 0.05$). $n = 24$ birds/treatment. CON-ITM with sulfate of zinc (110 ppm), copper (6 ppm), and manganese (120 ppm) with inorganic selenium (0.3 ppm). MMHAC with MMHAC sources of zinc (50 ppm), copper (10 ppm), manganese (60 ppm) with inorganic selenium (0.3 ppm). MMHAC + Org Se + ETX with MMHAC sources of zinc (50 ppm), copper (10 ppm), manganese (60 ppm) with organic selenium (ZORIEN® SeY, Novus International, Inc., added at 0.3 ppm) and AO at 125 ppm of final concentration.

both CON-ITM and MMHAC groups (**Figure 3A**). Selenium is a cofactor for glutathione peroxidase which converts hydrogen peroxide to water (Slimen et al., 2014; Surai, 2015). Kumbhar et al. (2018) reported that dietary combination of Se and Vitamin E (rather than used individually) was effective in increasing the catalase, SOD, as well as glutathione peroxidase activities thereby reducing malondialdehyde level or oxidative stress in breast muscle tissue from birds under heat stress. Horváth and Babinszky (2018) reported that high levels of vitamin A, E, C, and Zn as well as Se can support enzyme activity, reduce oxidative stress, and improve production performance in birds under heat stress. Interestingly, the antioxidant benefits from vitamins and microminerals were greater when combined in diets for birds under heat stress (Horváth and Babinszky, 2018). When different dietary interventions to reduce oxidative stress are combined, the benefits could be expressed at different points and sources of oxidative stress such as, at dietary fat sources, during cellular level conversion of superoxides to hydrogen peroxide and then to water in mitochondria, cytoplasm as well as extracellular space. The multi-step cellular oxidative stress process could be the reason why the magnitude of response is higher when combined than when supplemented individually. In addition, inclusion of MMHAC–Zn, Cu, Mn with or without Org Se and ETX resulted in an increase ($P < 0.05$) in normal tibial bones and a decrease ($P < 0.05$) in tibia with severe bacterial necrosis lesions (**Figure 3B**). According to Wideman and Prisby (2013), bacterial necrosis of bone can occur through the translocation of bacteria from gut or respiratory tract to the bone along with microdamages happening in the bone tissue, resulting in colonization of bacteria in bone marrow. Results from the present study also showed that the inclusion of MMHAC–Zn, Cu, Mn in the diet resulted in numerical improvement although MMHAC + Org Se + ETX showed significant ($P < 0.05$) improvement in tibial strength (**Table 6**), thus preventing the occurrence of microdamage leading to bacterial necrosis. Dibner et al. (2007) had reported that feeding a combination of MMHAC Zn, Cu, and Mn in broiler birds can enhance the cortical thickness and improve the breaking strength in tibia which agrees with the present study. Furthermore, Sirri et al. (2016) showed similar results where the use of Zn, Cu, Mn–MMHAC showed lower femoral and tibial lesions when compared to ITMs. Interestingly, inclusion of MMHAC and antioxidants in the diet also resulted in decreased breast blisters and skin scratches (**Figure 4**). In addition to the benefits of Zn, Cu, and Mn in the integrity of connective tissue and tissue repair (Richards et al., 2010; Chen et al., 2017), zinc plays an important role in the wound healing process and feathering in birds (El-Hack et al., 2017). Thus, the benefits of MMHAC on reducing carcass skin lesions could be due to greater skin and feather integrity and/or faster recovery and wound healing (Chen et al., 2017) from scratches and blisters (because of the enhanced tissue repair).

CONCLUSIONS

The factors that increase the incidence of WB are not clearly known, however circulatory insufficiency and increased oxidative stress in the breast muscles is reported to be associated with WB. The results from the first experiment showed that presence of oxidized fat in the diet can reduce performance in birds and increase muscle damage. Interestingly, inclusion of ETX to diet with oxidized fat reduced the incidence of severe WB in broilers. Based on the muscle TBARS levels, ETX was effective in reducing oxidative stress in muscle tissue. In experiment 2, combination of MMHAC (Zn, Cu, and Mn) chelated trace minerals with ETX reduced oxidative stress in muscle tissue and increased the percentage of normal (without WB) filets in birds fed diet with oxidized fat. In the third experiment under mild heat stress, feeding MMHAC alone reduced incidence of tibial head lesions, skin scratches, breast blisters, and increased the incidence of normal fillets. When MMHAC was combined with ETX and Org Se, further increase in the incidence of normal filets were observed. The combination of ETX, chelated trace minerals in the form of MMHAC, and Org Se resulted in the reduction of oxidative stress in the tissue plausibly through activation of endogenous antioxidant enzymes and reducing dietary sources of oxidative stress. Nonetheless, MMHAC could provide additional benefits in improving the connective tissue integrity and enhanced tissue repair in muscle, skin, and bone. Further studies are needed to understand the mode of action of these dietary interventions in reducing carcass quality defects such as myopathies.

DATA AVAILABILITY STATEMENT

The original contributions presented in the study are included in the article/supplementary material, further inquiries can be directed to the corresponding author/s.

ETHICS STATEMENT

The animal study was reviewed and approved by Animal Use Committee, Novus International, Inc., Green Acres Experimental Farm, Montgomery, Missouri Internal Ethics Committee, at Bangkok Animal Research Center Co., Ltd., Thailand.

AUTHOR CONTRIBUTIONS

VK, MM, and MB carried out the project and data analysis, while JC supported with the tissue analysis. VK put together the information, interpreted the results, and prepared the manuscript under the supervision of MV-A. All authors contributed to experimental design, discussed the results, and reviewed the manuscript.

ACKNOWLEDGMENTS

Support provided by Aviagen, Inc., and lead researcher Ms. Takawan Sooksridang as well as the research team at Bangkok Animal Research Center (BARC) during various stages of experimental design and processing of birds.

REFERENCES

Abasht, B., Mutryn, M. F., Michalek, R. D., and Lee, W. R. (2016). Oxidative stress and metabolic perturbations in wooden breast disorder in chickens. *PLoS One* 11:e0153750. doi: 10.1371/journal.pone.0153750

Aguirre, M. E., Owens, C. M., Miller, R. K., and Alvarado, C. Z. (2018). Descriptive sensory and instrumental texture profile analysis of woody breast in marinated chicken. *Poult. Sci.* 97, 1456–1461. doi: 10.3382/ps/pex428

Akbarian, A., Michiels, J., Degroote, J., Majdeddin, M., Golian, A., and De Smet, S. (2016). Association between heat stress and oxidative stress in poultry; mitochondrial dysfunction and dietary interventions with phytochemicals. *J. Anim. Sci. Biotechnol.* 7:37.

Anjos, F., Vazquez-Anon, M., Yan, F., Dibner, J., and Dierenfeld, E. (2012). Influence of diets containing raw or heat processed cowpea on the performance and gut health of broiler chickens. *Uganda J. Agri. Sci.* 13, 83–93.

Ao, T., Macalintal, L. M., Paul, M. A., Pescatore, A. J., Delles, R. M., Cantor, A. H., et al. (2017). Effects of dietary supplementation of organic minerals on the performance of broiler chicks fed oxidised soybean oil. *J. Appl. Anim. Nutr.* 5, 1–5.

AOCS. (1997). *Official Methods and Recommended Practices of the AOCS*. Urbana, IL: AOCS.

Avanzo, J. L., de Mendonça, C. X. Jr., Pugine, S. M., and de Cerqueira Cesar, M. (2001). Effect of vitamin E and selenium on resistance to oxidative stress in chicken superficial pectoralis muscle. *Comp. Biochem. Physiol. C Toxicol. Pharmacol.* 129, 163–173. doi: 10.1016/s1532-0456(01)00197-1

Bodle, B. C., Alvarado, C., Shirley, R. B., Mercier, Y., and Lee, J. T. (2018). Evaluation of different dietary alterations in their ability to mitigate the incidence and severity of woody breast and white striping in commercial male broilers. *Poult. Sci.* 97, 3298–3310. doi: 10.3382/ps/pey166

Bowker, B. C., Maxwell, A., Zhuang, D. H., and Adhikari, K. (2018). Marination and cooking performance of portioned broiler breast fillets with the wooden breast condition. *Poult. Sci.* 97, 2966–2970. doi: 10.3382/ps/pey144

Brambila, G. S., Bowker, B. C., Chatterjee, D., and Zhuang, H. (2018). Descriptive texture analyses of broiler breast fillets with the wooden breast condition stored at 4°C and −20°C. *Poult. Sci.* 97, 1762–1767. doi: 10.3382/ps/pew327

Cai, K., Shao, W., Chen, X., Campbell, Y. L., Nair, M. N., Suman, S. P., et al. (2018). Meat quality traits and proteome profile of woody broiler breast (pectoralis major) meat. *Poult. Sci.* 97, 337–346. doi: 10.3382/ps/pex284

Cemin, H. S., Vieira, S. L., Stefanello, C., Kindlein, L., Ferreira, T. Z., and Fireman, A. K. (2018). Broiler responses to increasing selenium supplementation using Zn-L-selenomethionine with special attention to breast myopathies. *Poult. Sci.* 97, 1832–1840. doi: 10.3382/ps/pey001

Chatterjee, D., Zhuang, H., Bowker, B. C., Rincon, A. M., and Sanchez-Brambila, G. (2016). Instrumental texture characteristics of broiler pectoralis major with the wooden breast condition. *Poult. Sci.* 95, 2449–2454. doi: 10.3382/ps/pew204

Chen, H., Wang, H., Qi, J., Wang, M., Xu, X., and Zhou, G. (2018). Chicken breast quality – normal, pale, soft and exudative (PSE) and woody – influences the functional properties of meat batters. *Int. J. Food Sci. Tech.* 53, 654–664. doi: 10.1111/ijfs.13640

Chen, J., Tellez, G., Escobar, J., and Vazquez-Anon, M. (2017). Impact of trace minerals on wound healing of footpad dermatitis in broilers. *Sci. Rep.* 7:1894.

Cruz, R. F. A., Vieira, S. L., Kindlein, L., Kipper, M., Cemin, H. S., and Rauber, S. M. (2016). Occurrence of white striping and wooden breast in broilers fed grower and finisher diets with increasing lysine levels. *Poult. Sci.* 96, 501–510. doi: 10.3382/ps/pew310

Dalle Zotte, A., Tasoniero, G., Puolanne, A., Remignon, H., Cecchinato, M., Catelli, E., et al. (2017). Effect of 'wooden breast' appearance on poultry meat quality, histological traits, and lesions characterization. *Czech. J. Anim. Sci.* 62, 51–57. doi: 10.17221/54/2016-cjas

Delles, R. M., Xiong, Y. L., True, A. D., Ao, T., and Dawson, K. A. (2015). Augmentation of water-holding and textural properties of breast meat from oxidatively stressed broilers through dietary antioxidant regimens. *Br. Poult. Sci.* 56, 304–314. doi: 10.1080/00071668.2015.1032889

Dibner, J. J., Atwell, C. A., Kitchell, M. L., Shermer, W. D., and Ivey, F. J. (1996). Feeding of oxidized fats to broilers and swine: effects on enterocyte turnover, hepatocyte proliferation and the gut associated lymphoid tissue. *Anim. Feed Sci. Tech.* 62, 1–13. doi: 10.1016/s0377-8401(96)01000-0

Dibner, J. J., Richards, J. D., Kitchell, M. L., and Quiroz, M. A. (2007). Metabolic challenges and early bone development. *J. Appl. Poult. Res.* 16, 126–137. doi: 10.1093/japr/16.1.126

El-Hack, M. E. A., Alagawany, M., Arif, M., Chaudhry, M. T., Emam, M., and Patra, A. (2017). Organic or inorganic zinc in poultry nutrition: a review. *World's Poult. Sci. J.* 73, 904–915. doi: 10.1017/s0043933917000769

Horváth, M., and Babinszky, L. (2018). Impact of selected antioxidant vitamins (vitamin A, E and C) and micro minerals (Zn, Se) on the antioxidant status and performance under high environmental temperature in poultry. A review. *Acta Agric. Scandinavica Sec. A Anim. Sci.* 68, 152–160. doi: 10.1080/09064702.2019.1611913

Huang, X., and Ahn, D. U. (2018). The incidence of muscle abnormalities in broiler breast meat – a review. *Korean J. Food Sci. Anim. Resour.* 38, 835–850. doi: 10.5851/kosfa.2018.e2

Jensen, C., Engberg, R., Jacobsen, K., Skibsted, L. H., and Bertelsen, G. (1997). Influence of the oxidative quality of dietary oil on broiler meat storage stability. *Meat Sci.* 47, 211–222. doi: 10.1016/s0309-1740(97)00052-1

Kumbhar, S., Khan, A. Z., Parveen, F., Nizamani, Z. A., Siyal, F. A., Abd El-Hack, M. E., et al. (2018). Impacts of selenium and vitamin E supplementation on mRNA of heat shock proteins, selenoproteins and antioxidants in broilers exposed to high temperature. *AMB Expr.* 8:112.

Kuttappan, V. A., Hargis, B. M., and Owens, C. M. (2016). White striping and woody breast myopathies in the modern poultry industry: a review. *Poult. Sci.* 95, 2724–2733. doi: 10.3382/ps/pew216

Kuttappan, V. A., Brewer, V. B., Mauromoustakos, A., McKee, S. R., Emmert, J. L., Meullenet, J. F., et al. (2013a). Estimation of factors associated with the occurrence of white striping in broiler breast fillets. *Poult. Sci.* 92, 811–819. doi: 10.3382/ps.2012-02506

Kuttappan, V. A., Huff, G. R., Huff, W. E., Hargis, B. M., Apple, J. K., Coon, C., et al. (2013b). Comparison of hematologic and serologic profiles of broiler birds with normal and severe degrees of whitestriping in breast fillets. *Poult. Sci.* 92, 339–345. doi: 10.3382/ps.2012-02647

Kuttappan, V. A., Owens, C. M., Coon, C., Hargis, B. M., and Vazquez-Añon, M. (2017a). Incidence of broiler breast myopathies at 2 different ages and its impact on selected raw meat quality parameters. *Poult. Sci.* 96, 3005–3009. doi: 10.3382/ps/pex072

Kuttappan, V. A., Bottje, W., Ramnathan, R., Hartson, S. D., Coon, C., Kong, B., et al. (2017b). Proteomic analysis reveals changes in carbohydrate and protein metabolism associated with broiler breast myopathy. *Poult. Sci.* 96, 2992–2999. doi: 10.3382/ps/pex069

Livingston, M. L., Landon, C., Barnes, H. J., and Brake, J. (2018). White striping and wooden breast myopathies of broiler breast muscle is affected by time-limited feeding, genetic background, and egg storage. *Poult. Sci.* 98, 217–226. doi: 10.3382/ps/pey333

Lu, Z., He, X., Ma, B., Zhang, L., Li, J., Jiang, Y., et al. (2017). Chronic heat stress impairs the quality of breast-muscle meat in broilers by affecting redox status and energy-substance metabolism. *J. Agric. Food Chem.* 2017, 11251–11258. doi: 10.1021/acs.jafc.7b04428

Meloche, K. J., Dozier, W. A. III, Brandebourg, T. D., and Starkey, J. D. (2018d). Skeletal muscle growth characteristics and myogenic stem cell activity in broiler chickens affected by wooden breast. *Poult. Sci.* 97, 4401–4414. doi: 10.3382/ps/pey287

Meloche, K. J., Fancher, B. I., Emmerson, D. A., Bilgili, S. F., and Dozier, W. A. III (2018a). Effects of quantitative nutrient allocation on myopathies of the pectoralis major muscles in broiler chickens at 32, 43, and 50 days of age. *Poult. Sci.* 97, 1786–1793. doi: 10.3382/ps/pex453

Meloche, K. J., Fancher, B. I., Emmerson, D. A., Bilgili, S. F., and Dozier, W. A. (2018b). Effects of reduced digestible lysine density on myopathies of the pectoralis major muscles in broiler chickens at 48 and 62 days of age. *Poult. Sci.* 97, 3311–3324. doi: 10.3382/ps/pey171

Meloche, K. J., Fancher, B. I., Emmerson, D. A., Bilgili, S. F., and Dozier, W. A. III (2018c). Effects of reduced dietary energy and amino acid density on pectoralis major myopathies in broiler chickens at 36 and 49 days of age. *Poult. Sci.* 97, 1794–1807. doi: 10.3382/ps/pex454

Mudalal, S., Lorenzi, M., Soglia, F., Cavani, C., and Petracci, M. (2015). Implications of white striping and wooden breast abnormalities on quality traits of raw and marinated chicken meat. *Animal* 9, 728–734. doi: 10.1017/s175173111400295x

Mutryn, M. F., Brannick, E. M., Fu, W., Lee, W. R., and Abasht, B. (2015). Characterization of a novel chicken muscle disorder through differential gene expression and pathway analysis using RNA-sequencing. *BMC Genom.* 16:399. doi: 10.1186/s12864-015-1623-0

Papah, M. B., Brannick, E. M., Schmidt, C. J., and Abasht, B. (2018). Gene expression profiling of the early pathogenesis of wooden breast disease in commercial broiler chickens using RNA-sequencing. *Plos One* 13:e0207346. doi: 10.1371/journal.pone.0207346

Papah, M. B., Brannick, E. M., Schmidt, C. J., and Abasht, B. (2017). Evidence and role of phlebitis and lipid infiltration in the onset and pathogenesis of wooden breast disease in modern broiler chickens. *Avian Pathol.* 46, 623–643. doi: 10.1080/03079457.2017.1339346

Petracci, M., Soglia, F., Madruga, M., Carvalho, L., Ida, E., and Est'evez, M. (2019). Wooden-breast, white striping, and spaghetti meat: causes, consequences and consumer perception of emerging broiler meat abnormalities. *Compr. Rev. Food Sci. Food Saf.* 18, 565–583. doi: 10.1111/1541-4337.12431

Richards, J. D., Zhao, J., Harrell, R. J., Atwell, C. A., and Dibner, J. J. (2010). Trace mineral nutrition in poultry and swine. *Asian-Australas. J. Anim. Sci.* 23, 1527–1534.

Sheehy, P. J. A., Morrissey, P. A., and Flynn, A. (1994). Consumption of thermally-oxidised sunflower oil by chicks reduces α-tocopherol status and increases susceptibility of tissues to lipid oxidation. *Br. J. Nutr.* 71, 53–65. doi: 10.1079/bjn19940110

Sihvo, H. K., Airas, N., Lind'en, J., and Puolanne, E. (2018). Pectoral vessel density and early ultrastructural changes in broiler chicken wooden breast myopathy. *J. Comp. Pathol.* 161, 1–10. doi: 10.1016/j.jcpa.2018.04.002

Sihvo, H. K., Immonen, K., and Puolanne, E. (2014). Myodegeneration with fibrosis and regeneration in the pectoralis major muscle of broilers. *Vet. Pathol.* 51, 619–623. doi: 10.1177/0300985813497488

Sihvo, H. K., Lind'en, J., Airas, N., Immonen, K., Valaja, J., and Puolanne, E. (2017). Wooden breast myodegeneration of pectoralis major muscle over the growth period in broilers. *Vet. Pathol.* 54, 119–128. doi: 10.1177/0300985816658099

Sirri, F., Maiorano, G., Tavaniello, S., Chen, J., Petracci, M., and Meluzzi, A. (2016). Effect of different levels of dietary zinc, manganese, and copper from organic or inorganic sources on performance, bacterial chondronecrosis, intramuscular collagen characteristics, and occurrence of meat quality defects of broiler chickens. *Poult. Sci.* 95, 1813–1824. doi: 10.3382/ps/pew064

Slimen, I. B., Najar, T., Ghram, A., Dabbebi, H., Ben Mrad, M., and Abdrabbah, M. (2014). Reactive oxygen species, heat stress and oxidative-induced mitochondrial damage. A review. *Int. J. Hyperthermia.* 30, 513–523. doi: 10.3109/02656736.2014.971446

Soglia, F., Gao, J., Mazzoni, M., Puolanne, E., Cavani, C., Petracci, M., et al. (2017). Superficial and deep changes of histology, texture and particle size distribution in broiler wooden breast muscle during refrigerated storage. *Poult. Sci.* 96, 3465–3472. doi: 10.3382/ps/pex115

Soglia, F., Laghi, L., Canonico, L., Cavani, C., and Petracci, M. (2016a). Functional property issues in broiler breast meat related to emerging muscle abnormalities. *Food Res. Int.* 89, 1071–1076. doi: 10.1016/j.foodres.2016.04.042

Soglia, F., Mudalal, S., Babini, E., Di Nunzio, M., Mazzoni, M., Sirri, F., et al. (2016b). Histology, composition, and quality traits of chicken pectoralis major muscle affected by wooden breast abnormality. *Poult. Sci.* 95, 651–659. doi: 10.3382/ps/pev353

Surai, F. (2015). Antioxidant systems in poultry biology: Superoxide Dismutase. *Anim. Nutri.* 1:8.

Tijare, V. V., Yang, F. L., Kuttappan, V. A., Alvarado, C. Z., Coon, C. N., and Owens, C. M. (2016). Meat quality of broiler breast fillets with white striping and woody breast muscle myopathies. *Poult. Sci.* 95, 2167–2173. doi: 10.3382/ps/pew129

Wang, Y., Branicky, R., Noë, A., and Hekimi, S. (2018). Superoxide dismutases: dual roles in controlling ROS damage and regulating ROS signaling. *J. Cell. Biol.* 217, 1915–1928. doi: 10.1083/jcb.201708007

Wang, Z., Cerrate, S., Coto, C., Yan, F., and Waldroup, P. W. (2007). Evaluation of MINTREX® copper as a source of copper in broiler diets. *Int. J. Poult. Sci.* 5, 308–313. doi: 10.3923/ijps.2007.308.313

Willcox, J. K., Ash, S. L., and Catignani, G. L. (2004). Antioxidants and prevention of chronic disease. *Crit. Rev. Food Sci. Nutr.* 44, 275–295.

Wold, J. P., Veiseth-Kent, E., Høst, V., and Løvland, A. (2017). Rapid on-line detection and grading of wooden breast myopathy in chicken fillets by near-infrared spectroscopy. *PloS One* 12:e0173384. doi: 10.1371/journal.pone.0173384

Xiang, R. P., Sun, W. D., Wang, J. Y., and Wang, X. L. (2002). Effect of vitamin C on pulmonary hypertension and muscularisation of pulmonary arterioles in broilers. *Br. Poult. Sci.* 43, 705–712. doi: 10.1080/00071660210006025064

Xing, T., Zhao, X., Han, M., Cai, L., Deng, S., Zhou, G., et al. (2017a). A comparative study of functional properties of normal and wooden breast broiler chicken meat with NaCl addition. *Poult. Sci.* 96, 3473–3481. doi: 10.3382/ps/pex116

Wideman, R. F. Jr., Al-Rubaye, A., Reynolds, D., Yoho, D., Lester, H., Spencer, C. et al. (2014). Bacterial chondronecrosis with osteomyelitis in broilers: Influence of sires and straight-run versus sex-separate rearing. *Poult. Sci.* 93:1675–1687. doi: 10.3382/ps.2014-03912

Wideman, R. F., and Prisby, R. D. (2013). Bone circulatory disturbances in the development of spontaneous bacterial chondronecrosis with osteomyelitis: a translational model for the pathogenesis of femoral head necrosis. *Front. Endocrin.* 3:183. doi: 10.3389/fendo.2012.00183

Yan, F., and Waldroup, P. W. (2006). Evaluation of MINTREX® manganese as a source of manganese for young broilers. *Int. J. Poult. Sci.* 5, 708–713. doi: 10.3923/ijps.2006.708.713

Zdunczyk, Z., Jankowski, J., and Koncicki, A. (2002). Growth performance and physiological state of turkeys fed diets with higher content of lipid oxidation products, selenium, vitamin E and vitamin A. *World's Poult. Sci. J.* 58, 357–364. doi: 10.1079/wps20020028

Zhao, D., Kogut, M. H., Genovese, K. J., Hsu, C. Y., Lee, J. T., and Farnell, Y. Z. (2020). Altered expression of lactate dehydrogenase and monocarboxylate transporter involved in lactate metabolism in broiler wooden breast. *Poult. Sci.* 99, 11–20. doi: 10.3382/ps/pez572

Conflict of Interest: All the authors are employed by Novus International, Inc. and declare that the research was conducted in the absence of any commercial or financial relationships that could be construed as a potential conflict of interest.

frontiers in Physiology

ORIGINAL RESEARCH
published: 14 April 2021
doi: 10.3389/fphys.2021.659777

Hepatic Oxidative Stress, Apoptosis, and Inflammation in Broiler Chickens With Wooden Breast Myopathy

*Tong Xing, Xiaona Pan, Lin Zhang and Feng Gao**

Key Laboratory of Animal Origin Food Production and Safety Guarantee of Jiangsu Province, Joint International Research Laboratory of Animal Health and Food Safety, Jiangsu Collaborative Innovation Center of Meat Production and Processing, Quality and Safety Control, National Experimental Teaching Demonstration Center of Animal Science, College of Animal Science and Technology, Nanjing Agricultural University, Nanjing, China

Wooden breast (WB) syndrome has emerged as a global myopathy in modern commercial broiler chickens, mainly affecting the pectoralis major muscle. Recent evidence suggests that WB myopathy is a systemic disease, which might be accompanied by other physiological disparities and metabolic changes. This study was conducted to systemically investigate the potential physiological changes in liver tissues as well as the possible mechanisms involved to enhance the understanding of the etiology. A total of 93 market-age Arbor Acres male broiler chickens were sampled and categorized into control (CON) and WB groups based on the evaluation of myopathic lesions. Liver samples were collected (n = 10 in each group) for histopathological evaluation and biochemical analyses. Results indicated that WB birds exhibited significantly higher plasma aspartate amino transferase, alkaline phosphatase, and gamma glutamyl transpeptidase activities. Histopathological changes in hydropic/fatty degeneration, inflammatory cell infiltration, intrahepatic hemorrhages, elevated myeloperoxidase activity, and overproduction of nitric oxide were observed in WB liver compared with CON, suggesting the occurrence of liver injury in birds affected by WB myopathy. The WB group showed increased levels of reactive oxygen species, oxidative products, as well as enhanced antioxidant capacities in the liver. These changes were associated with impaired mitochondria morphology and mitochondrial dysfunction. WB myopathy also induced mitochondria-mediated hepatic apoptosis by upregulating levels of caspases 3 and 9, altering the expressions of apoptotic B-cell lymphoma-2 family regulators, as well as increasing the release of cytochrome c. The activation of nuclear factor kappa-light-chain-enhancer of activated B cell signaling enhanced the mRNA expression of downstream inflammatory mediators, contributing to the production of inflammatory cytokines in WB liver. Combined, these findings suggest that hepatic disorders may be conjoined with WB myopathy in broiler chickens and indicating systemic physiological disparities, and other metabolic changes accompanying this myopathy need further assessment.

Keywords: wooden breast, broiler chicken, liver, oxidative stress, apoptosis, inflammation

OPEN ACCESS

Edited by:
Massimiliano Petracci, University of Bologna, Italy

Reviewed by:
Maurizio Mazzoni, University of Bologna, Italy
Alessandra Piccirillo, University of Padua, Italy

****Correspondence:***
Feng Gao
gaofeng0629@sina.com

Specialty section:
This article was submitted to Avian Physiology, a section of the journal Frontiers in Physiology

Received: *28 January 2021*
Accepted: *10 March 2021*
Published: *14 April 2021*

Citation:
Xing T, Pan X, Zhang L and Gao F (2021) Hepatic Oxidative Stress, Apoptosis, and Inflammation in Broiler Chickens With Wooden Breast Myopathy. Front. Physiol. 12:659777. doi: 10.3389/fphys.2021.659777

INTRODUCTION

Over the past few decades, the demand for poultry meat has increased notably. Consequently, genetic selection of modern commercial broiler chickens has been pushed toward fast growth and enhanced breast muscle yield (Petracci et al., 2015). Despite achieving extraordinary improvements, this selection pressure accompanied with the modern intense breeding programs have caused the increasing incidence of spontaneous breast muscle abnormalities. These emerging myopathies have drawn worldwide attention due to their high occurrence and negative impacts on meat quality (Petracci et al., 2019). One abnormality, wooden breast (WB) myopathy, is macroscopically characterized by hardened areas, pale ridge-like bulges, as well as occasional appearance of clear viscous fluid, small hemorrhages, and white striping in the pectoralis major (PM) muscle (Sihvo et al., 2014). Due to the unappealing appearance, WB fillets are usually downgraded and used only for highly processed products. Although still usable, WB myopathy seriously impairs the quality and nutritional value of breast meat (Mudalal et al., 2015; Soglia et al., 2016), thereby causing substantial economic losses to the poultry industry.

Extensive studies have been carried out to investigate the histological lesions, physiological properties, and molecular changes involved in the development of WB myopathy. The findings imply that the underlying mechanisms of this growth-related muscular abnormality are complicated and multifaceted processes, which might be related with the abnormal accumulation of endomysial and perimysial connective tissue and the consequent fibrosis, hypoxia, oxidative stress, and inflammatory response as well as metabolic shift (Sihvo et al., 2014; Mutryn et al., 2015; Soglia et al., 2017; Liu et al., 2020). Recently, accumulating evidence suggests that the etiology of WB myopathy is not limited to the PM muscle, but is also associated with perturbations in blood circulation and other organs. Greene et al. (2019) demonstrated that the circulatory oxygen homeostasis was dysregulated in WB myopathic broiler chickens as indicated by the altered pressure of blood gases and hemoglobin levels. Our recent study revealed that the inflammatory cytokines including interleukin (IL)-1β, IL-8, and tumor necrosis factor (TNF)-α were enhanced in the serum of WB affected birds (Xing et al., 2021). Furthermore, lung histopathology of WB myopathic birds exhibited occasional localized multifocal lymphoplasmacytic phlebitis and more foci of chondro-osseous metaplasia compared with the unaffected birds (Lake et al., 2020). WB myopathy increased stress hormone corticosterone levels in plasma and altered expression patterns of stress response-related genes in the liver (Kang et al., 2020). Assessment of potential systemic physiological disparities accompanying WB myopathy might contribute to a profound understanding of its etiology.

The liver is a primary metabolic organ, which has important physiological functions such as biosynthesis, clearance, detoxification, and host defense. Liver damage has become a common disease, which can be caused by various risk factors of xenobiotics, malnutrition, and other chronic diseases (Malhi and Gores, 2008). In patients with Duchenne muscular dystrophy (DMD), liver atrophy was shown to occur concomitantly with skeletal muscle wasting (Moriuchi et al., 1991). Liver abnormalities in mdx dystrophic mice, including decreased glycogen levels and hyperglycemia, have been observed (David et al., 2014). Furthermore, patients with muscular dystrophies showed an increased susceptibility to acute liver failure upon therapeutic paracetamol administration (Pearce and Grant, 2010). It appears that there is a strong link between hepatic disorders and muscular diseases. Interestingly, PM muscle, and liver transcriptome through the ingenuity pathway analysis identified critical transcriptional response network associations in WB myopathic birds (Phillips et al., 2020), suggesting the systemic pathology involved in the progression of this myopathy.

To date, limited data exist on the hepatic changes associated with WB myopathy. The current study was designed to systemically compare the histological and biochemical characteristics and the underlying mechanism causing these differences, if any, in the liver between normal and WB myopathic broiler chickens.

MATERIALS AND METHODS

Experimental Broiler Chickens and Tissue Collection

All experimental procedures and bird managements were approved by the Institutional Animal Care and Use Committee of Nanjing Agricultural University. Broiler chickens used in the current study were all Arbor Acres males raised in three layered cages and received commercially formulated feed and husbandry. Birds were provided *ad libitum* access to feed and water. Birds were vaccinated against Newcastle disease virus, infectious bronchitis virus, and infectious bursal disease virus through neck injection at 11 days of age, using commercially available vaccines. At 42 days of age, a total of 300 live birds were clinically examined for WB myopathy involving visual observations for posture and wing contact as well as bilateral manual palpation for hardness of the pectoralis major (PM) in a cranio-caudal direction by two trained personnel (Papah et al., 2017). This resulted in 63 suspected WB-affected and 30 WB-unaffected broilers. These broilers were electrically stunned (50 V, alternating current, 400 Hz for 5 s each) and exsanguinated via the carotid arteries and jugular veins. Immediately after execution, birds were necropsied, and samples of PM muscle and liver tissues were collected and labeled. Liver tissues from the caudal region of the left lobe were taken and fixed in 4% paraformaldehyde or 2.5% glutaraldehyde for histological evaluation or ultrastructural observation. The remaining liver tissues were frozen in liquid nitrogen and stored at −80°C for biochemical analysis.

Wooden Breast Myopathy Scoring and Sample Selection

During necropsy, the dissected PM muscle was further evaluated using a more accurate WB myopathy scoring system based

on gross lesions and palpable firmness as described by Livingston et al. (2019). Briefly, the ordinal scale ranged from 0 to 3 points, where a score of (0) was used when there was no presence of macroscopic myopathic lesion (normal), (1) was used when the fillets were hard primarily in the cranial region but otherwise pliable (mild), (2) was used when the fillets were hard throughout but flexible in the mid to caudal region (moderate), and (3) was used when the fillets were extremely hard and rigid throughout from cranial region to caudal tip (severe). We found 30 normal, 31 mild, 20 moderate, and 12 severe WB myopathy affected PM muscles among the 93 selected birds. After scoring, 10 liver tissues from birds with normal PM muscle (CON) and 10 samples from birds affected by moderate-to-severe WB myopathy (WB) were randomly selected to evaluate the subsequent biochemical parameters.

Histopathological Evaluation

For histological analysis, liver tissues were fixed in 4% paraformaldehyde for more than 24 h at room temperature, dehydrated in a graded series of ethanol, trimmed, and embedded in paraffin blocks. Liver sections were cut into 8-μm thickness and mounted on polylysine-coated slides. Subsequently, the slides were rehydrated by a series of incubations in xylene and ethanol solutions and then subjected to hematoxylin and eosin (H&E) and Masson trichrome staining according to the procedures described by Huang et al. (2010) and Xing et al. (2017a). Images were acquired under identical conditions and at the same magnification using a light microscope (Axio Scope.A1, Carl Zeiss, Oberbochen, Germany). Liver tissue was examined for histopathologic changes including the presence of inflammation, intrahepatic hemorrhages, or fibrosis. Assessment of all slides was performed as a blind study to prevent bias in the examination of tissues.

Determination of Serum Enzymes Activity

Serum enzymatic activities of alanine amino transferase (ALT), aspartate amino transferase (AST), alkaline phosphatase (AKP), and gamma glutamyl transferase (γ-GT) were determined by using the corresponding kits (Nanjing Jiancheng Bioengineering Institute, Nanjing, China) following the manufacturer's instructions.

Determination of Myeloperoxidase Activity and Nitric Oxide Level

Myeloperoxidase (MPO) activity and nitric oxide (NO) level were assessed spectrophotometrically with commercial kits purchased from Nanjing Jiancheng Bioengineering Institute (Nanjing, China), per the manufacturer's instructions. The protein concentration of the liver was determined using a BCA protein assay kit (Pierce Chemical Co., Rockford, IL, United States). The activity of MPO was expressed as units per gram of wet tissue, and the level of NO was expressed as micromoles per gram of protein.

Analysis of Hepatic Oxidative Products and Antioxidant Ability

Liver tissues were homogenized in 0.9% NaCl buffer and centrifuged at 2,000 × *g* for 10 min at 4°C. The supernatants were collected for the determination of oxidative products and antioxidant ability. Protein concentration was determined using a BCA protein assay kit. The measurements of malondialdehyde (MDA), lipid peroxidation (LPO), and protein carbonyl were performed using corresponding commercial kits obtained from Nanjing Jiancheng Bioengineering Institute (Nanjing, China). The content of the 8-hydroxydeoxyguanosine (8-OHdG) was determined using an ELISA kit obtained from Aogene Bioengineering Institute (Nanjing, China). Results of MDA and protein carbonyl were expressed as micromoles per milligram protein. The content of LPO and 8-OHdG were expressed as moles per milligram protein and nanogram per milligram protein, respectively. The activities of total antioxidant capacity (T-AOC), catalase (CAT), superoxide dismutase (SOD), glutathione peroxidase (GSH-Px), and glutathione S-transferase (GSH-ST) were measured using the corresponding kits (Nanjing Jiancheng Bioengineering Institute, Nanjing, China). The results were all expressed as units per milligram protein.

Ultrastructural Observation

Liver tissue specimens were fixed in 2.5% glutaraldehyde solution and washed with 0.1 M PBS, followed by postfixing with 1% osmium tetroxide. After washing with PBS, the tissues were hierarchically dehydrated with gradually increasing concentrations of ethanol (30–70%) and then embedded in Spurr's resin. Samples were embedded in Epon812 and sectioned using an ultra-microtome (RMC Power Tome XL, Leica, Wetzlar, Germany). Ultrathin sections (30 nm) were collected and stained with 3% uranyl acetate and lead citrate. Ultrastructural changes were examined using a transmission electron microscope (TEM, Hi-tachi H-7650, Tokyo, Japan).

Determination of Reactive Oxygen Species

Intracellular reactive oxygen species (ROS) in liver was measured using a fluorescent probe, 2,7-dichlorofluorescein diacetate (DCFH-DA, Nanjing Jiancheng Bioengineering Institute, Nanjing, China) as previously described (Xing et al., 2017b). The fluorescence intensity was detected at an excitation wavelength of 500 nm and emission wavelength of 525 nm, respectively, using a fluorescence Microplate Reader (Spectramax M2; Molecular Devices, Sunnyvale, CA, United States).

Mitochondria Isolation and Mitochondrial Function Assay

The liver mitochondria were extracted as described by Frolova et al. (2019) with some modifications. Briefly, fresh liver tissues were rinsed using phosphate buffer solution (PBS) and minced into mash. Minced tissues were homogenized in chilled isolation buffer (20 mM Tris-HCl, 250 mM sucrose, and 1 mM EDTA, pH 7.4) and then centrifuged at 1,000 × *g* for 15 min at 4°C. The supernatants were collected and

centrifuged at 12,000 × *g* for 15 min at 4°C, where mature heavy mitochondria were precipitated. Subsequently, the mitochondria pellets were washed thrice using the isolation buffer. Finally, all mitochondrial fractions were suspended in ice-cold isolation buffer and diluted to a protein concentration of 1 mg/ml. Protein concentration was determined using the BCA protein assay kit. Aliquots of the mitochondrial suspension were stored at −80°C for further use.

Mitochondria membrane potential ($\Delta\psi m$) assay was performed using a JC-1 kit (Solarbio Science & Technology, Co., Ltd, Beijing, China), per the manufacturer's instructions. Briefly, mitochondrial suspension (20 μl) with a total protein content of 20 μg was mixed with 180 μl of JC-1 dyeing working solution for 10 min, and the fluorescence intensity was measured using a microplate reader. The wavelengths for the detection of the monomeric and aggregated forms of JC-1 were 514/529 and 585/590 nm (excitation/emission).

The mitochondrial swelling was assessed according to Zhang et al. (2015). The obtained liver mitochondria suspension (20 μl) was incubated with 170 μl of swelling assay buffer containing 150 mM KCl, mM HEPES, 2 mM K_2HPO_4, 5 mM glutamate, and 5 mM malate to get a 20-μg total protein content. The mitochondrial swelling was triggered by the addition of 10 μl of calcium solution (1 mM). The absorbance was continuously determined at 540 nm for 18 min with an interval of 45 s using a microplate reader. Low mitochondria swelling exhibits high absorbance, and mitochondria with high swelling has low absorbance.

Apoptotic Nuclei Analysis

The detection of nuclei exhibiting apoptosis was performed using a terminal deoxynucleotidyl transferase (TdT)-mediated dUTP nick-end labeling (TUNEL) kit according to the manufacturer's instructions (Vazyme Biotech Co., Ltd., Nanjing, China) with minor modifications. Briefly, the paraffin-embedded liver tissues were sectioned at 5 μm, rehydrated by a series of incubations in xylene and ethanol solutions, and permeabilized using proteinase K (20 μg/ml) at 37°C for 25 min. After rinsing in PBS, the sections were incubated with mixed reagents consisting of TdT and dUTP at 37°C for 1 h. The sections were counterstained with 4',6-diamidino-2-phenylindole (DAPI, Beyotime Biotechnology, Shanghai, China) to label the nuclei. Finally, the TUNEL-positive cells were visualized using a fluorescence microscope (Axio Scope.A1, Carl Zeiss, Oberbochen, Germany). For apoptotic nuclei evaluation, four fields of 137,600 square micrometers per section were randomly selected and analyzed using the Image-Pro Plus software, version 6.0 (Media Cybernetics, Inc., Rockville, MD, United State). The hepatic apoptotic index was calculated as percentage of the total number of nuclei.

RNA Extraction, cDNA Synthesis, and Quantitative Real-Time PCR

Total RNA was isolated from the liver tissues of broiler chickens using RNAiso Plus reagent (Takara Biotechnology Co., Ltd, Dalian, China) following the manufacturer's instructions. Total RNA concentration was quantified by measuring the absorbance at 260 nm with a NanoDrop ND-100 spectrophotometer (NanoDrop Technologies, Rockland, DE, United State), and the purity was assessed by determining the ratios of optical density (OD) value at 260 and 280 nm. cDNA was reverse transcribed using a commercial cDNA Synthesis Kit (PrimeScript^{TM} RT Master Mix, Takara) and diluted 20 times with DEPC water before use. Quantitative real-time PCR was performed on an Applied Biosystems 7500 instrument (Foster City, CA, United State) using SYBR Premix EX Taq (Takara, United State). The PCR reaction conditions consisted of denaturation at 95°C for 10 min, followed by 40 cycles of 95°C for 15 s, annealing at 60°C for 1 min, and extension at 60°C for 20 s. Primer sets used for quantitative RT-PCR analysis are listed in **Supplementary Table 1**. All gene expressions are calculated as the relative fold changes compared with CON, and glyceraldehyde-3-phosphate dehydrogenase (GAPDH) was used as the internal reference to normalize the expression of target genes. Relative mRNA expression was calculated according to the $2^{-\Delta\Delta CT}$ method.

Total Protein Extraction and Western Blot Analysis

Frozen liver tissues were homogenized in RIPA lysis buffer (Beyotime Biotechnology, Jiangsu, China) containing 1 mM PMSF. The homogenate was centrifuged at 12,000 × *g* for 20 min at 4°C, and the supernatant was collected. The BCA assay was used to determine protein concentration. Equal amounts of total protein (40 μg) were resolved on 10% SDS-PAGE using a BioRad Electrophoresis System (Richmond, CA, United State) and transferred to a nitrocellulose membrane (Millipore, Merck, Germany). The membranes were blocked with 5% skim milk for 1 h at room temperature and then incubated in primary antibodies against kappa-light-chain-enhancer of activated B cells (NF-κB), inducible nitric oxide synthase (iNOS), cyclooxygenase-2 (COX-2), cytochrome c (Cytc), GAPDH (Servicebio Biological Technology, Wuhan, China), B-cell lymphoma (Bcl)-2 (Boster Biological Technology, Wuhan, China), and caspase3 (Absin Bioscience Inc., Shanghai, China) overnight at 4°C followed by incubation with the corresponding horseradish peroxidase-conjugated secondary antibodies (Bioworld, Nanjing, China) for 1 h. Finally, the membranes were visualized using ECL reagents (Pierce, IL, United States) and scanned using ImageQuant LAS4000 (GE, CT, United State). The density of each band was quantified by using Quantity One software (Bio-rad) and normalized to its respective housekeeping protein (GAPDH). All protein contents are calculated as the relative fold changes compared with CON.

Statistical Analysis

Data were analyzed by one-way analysis of variance (ANOVA) using SAS 9.12 (2003; SAS Inst. Inc., Cary, NC), and the differences between individuals were compared using Student's t-tests. Data were reported as means ± SE. Significance was considered when $P \leq 0.05$, and a trend was indicated when $0.05 < P < 0.1$.

RESULTS

Enzymatic Activities in the Serum of Wooden Breast Myopathic Birds

Measuring levels of serum ALT, AST, AKP, and other enzymes provides a clinical sign of liver injury and ascertains the severity of liver disease. As exhibited in **Table 1**, the activities of AST, AKP, and γ-GT were elevated by 73.3 ± 15.3% ($P < 0.01$), 63.7 ± 10.6% ($P < 0.01$), and 46.1 ± 3.0% ($P < 0.01$), respectively, in the serum of WB affected broiler chickens compared with CON. No significant difference in ALT activity was observed between the two groups ($P > 0.05$).

Histopathological Observation and Biochemical Parameters in the Liver of Wooden Breast Myopathic Birds

We stained the liver tissues using H&E and Masson staining to reveal the damage caused by WB myopathy (**Figure 1A**). Histology of the liver tissues from the CON group showed normal structures with regular morphology. On the contrary, the liver tissue of WB broiler chickens showed widespread lesions with hydropic/fatty degeneration (indicated by black arrows), infiltration of inflammatory cells (indicated by *), and severe intrahepatic hemorrhages (indicated by white arrows). In addition, occasional collagen deposition or fibrosis (indicated by black triangle) were simultaneously observed in the liver of WB birds. Both MPO activity and NO production were significantly elevated in WB compared with CON ($P < 0.05$; **Figures 1B,C**).

Hepatic Oxidative Products and Antioxidant Ability of Wooden Breast Myopathic Birds

As exhibited in **Table 2,** WB myopathy induced oxidative stress and led to damage in the cellular biomacromolecules in the liver tissues as indicated by the considerable elevated ($P < 0.05$) contents of MDA, LPO, protein carbonyl, and 8-OHdG. Additionally, the liver samples from WB broiler chickens exhibited significantly higher ($P < 0.05$) activities of T-AOC,

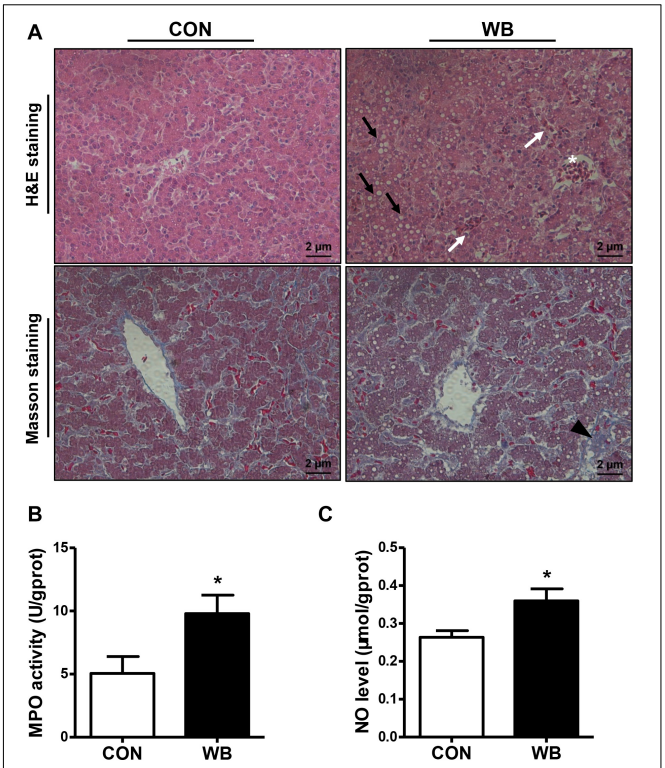

FIGURE 1 | Histopathological observation and biochemical parameters in liver tissues of broiler chickens with normal (CON) and wooden breast (WB) pectoralis major muscle. **(A)** Representative images of hematoxylin and eosin (H&E) and Masson staining of liver, indicating the widespread lesions with hydropic/fatty degeneration (black arrowhead), inflammatory cell infiltration (*), and intrahepatic hemorrhages (white arrowhead) as well as occasional fibrosis (black triangle) in WB. **(B)** Myeloperoxidase (MPO) activity and (**C**) nitric oxide (NO) level. Data are expressed as the mean ± SE (n = 10). *$P < 0.05$.

TABLE 1 | Enzymatic activities in serum of broiler chickens with normal (CON) and wooden breast (WB) pectoralis major muscle (n = 10).

Items[1]	Category		SEM	*P* value
	CON	WB		
ALT activity (U/L)	1.74	1.76	0.12	ns
AST activity (U/L)	21.07[b]	36.52[a]	2.44	***
AKP activity (U/L)	455.45[b]	745.77[a]	39.25	***
γ-GT activity (U/L)	24.50[b]	35.81[a]	0.62	***

[a,b]Mean values within the same row followed by different superscript letters indicating significance (P < 0.05).
****Significant difference at P < 0.001.*
ns, indicates no significant difference.
[1]SEM, standard error of mean; ALT, alanine amino transferase; AST, aspartate amino transferase; AKP, alkaline phosphatase; γ-GT, gamma glutamyl transpeptidase.

TABLE 2 | Oxidative products and antioxidant ability in liver tissues of broiler chickens with normal (CON) and wooden breast (WB) pectoralis major muscle (n = 10).

Items[1]	Category		SEM	*P* value
	CON	WB		
MDA (nmol/mg protein)	0.99[b]	1.16[a]	0.06	*
LPO (mol/mg protein)	0.33[b]	0.42[a]	0.03	*
Protein carbonyl (nmol/mg protein)	1.44[b]	1.70[a]	0.08	*
8-OHdG (ng/g protein)	0.41[b]	0.51[a]	0.06	*
T-AOC (U/mg protein)	3.67[b]	4.45[a]	0.15	**
CAT (U/mg protein)	32.60[b]	47.01[a]	2.56	**
SOD (U/mg protein)	186.13[b]	211.32[a]	6.98	*
GSH-Px (U/mg protein)	25.81[b]	31.21[a]	1.55	*
GSH-ST (U/mg protein)	14.86[b]	23.53[a]	1.40	***

[a,b]Mean values within the same row followed by different superscript letters indicating significance (P < 0.05).
**P < 0.05.*
***Significant difference at P < 0.01.*
****significant difference at P < 0.001.*
[1]SEM, standard error of mean; MDA, malondialdehyde; LPO, lipid peroxidation; 8-OHdG, 8-hydroxydeoxyguanosine; T-AOC, total antioxidant capacity; CAT, catalase; SOD, superoxide dismutase; GSH-Px, glutathione peroxidase; GSH-ST, glutathione S-transferase.

CAT, SOD, GSH-Px, and GSH-ST than those from the CON birds. These results implied a disturbed redox status in the liver tissue of WB myopathic birds.

Wooden Breast Myopathy Induced Liver Mitochondria Morphology Changes and Mitochondrial Dysfunction

The ultrastructure of the mitochondria of liver tissues from the CON group was well developed with intact membrane integrity and rich cristae density, whereas the collapse of cristae and membrane swelling was observed in the liver tissues of the WB group (**Figure 2A**). The production of ROS was significantly increased in WB when compared with CON ($P < 0.01$; **Figure 2B**). We further detected $\Delta\psi$m and mitochondrial swelling to evaluate mitochondrial function changes. Results indicated that $\Delta\psi$m presented a significant decrease in the WB group compared with the CON group ($P < 0.05$). Consistently, the mitochondria in the WB birds had significantly decreased OD values at 540 nm triggered by calcium compared with those of the CON birds ($P < 0.01$), showing that the mitochondria in the liver tissue of birds affected by WB myopathy were prone to swelling.

Wooden Breast Myopathy Induced Apoptosis in Chicken Liver

Apoptotic hepatocytes were detected using TUNEL staining as exhibited in **Figure 3A**. WB myopathy significantly increased apoptotic index of hepatocyte when compared with the CON group ($P < 0.01$; **Figure 3B**). The mRNA expressions of pro-apoptotic factors including Bcl-2-associated X protein (*Bax*, $P < 0.05$), Bcl-2 antagonist or killer 1 (*Bak1*, $P < 0.01$), and *Cyt c* ($P < 0.01$) were upregulated, whereas the antiapoptotic regulators of *B cell lymphoma (Bcl)-2* ($P < 0.05$) and *Bcl-xl* ($P < 0.1$) were downregulated in the WB group compared with the CON group (**Figure 3C**). In addition, the transcription of caspase 9 and caspase 3 were significantly enhanced in WB compared with CON ($P < 0.01$). Consistently, WB myopathy increased the protein contents of Cytc and caspase 3, but decreased the Bcl-2 protein content in comparison with the CON group ($P < 0.05$; **Figures 3D,E**).

Wooden Breast Myopathy Induced Inflammatory Responses in Chicken Liver

The protein contents of NF-κB, iNOS, and COX-2 were significantly increased in the liver of WB birds compared with the CON birds ($P < 0.05$, **Figures 4A,B**). Similarly, WB myopathy enhanced the transcription of *NF-κB*, *iNOS*, *COX-2*, and prostaglandin E synthetases (*PTGEs*) in chicken liver in comparison with the CON group ($P < 0.05$, **Figure 4C**). Furthermore, WB broiler chickens exhibited significantly increased mRNA expressions of pro-inflammatory cytokines including IL-1β, IL-6, IL-8, and TNF-α in the liver compared

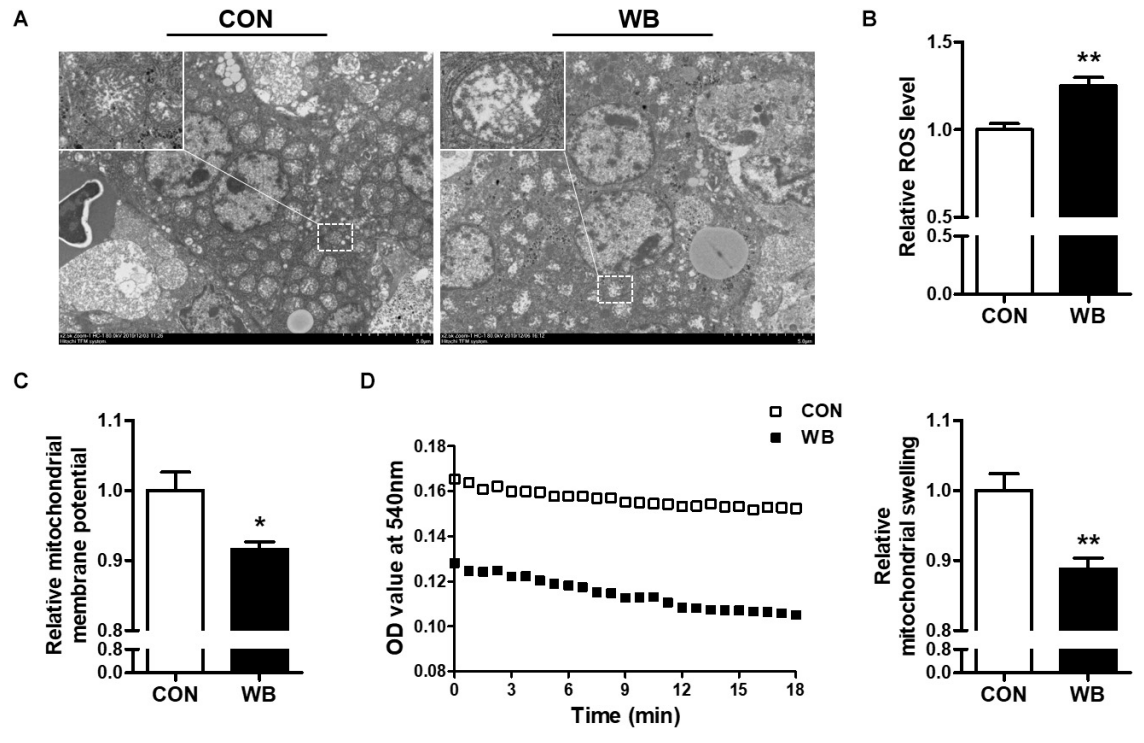

FIGURE 2 | Mitochondria morphology and mitochondrial function changes in the liver tissues of broiler chickens with normal (CON) and wooden breast (WB) pectoralis major muscle. **(A)** Representative transmission electron microscope images of liver. **(B)** Relative reactive oxygen species (ROS) level. **(C)** Relative mitochondrial membrane potential. **(D)** Relative mitochondrial swelling. Data are expressed as the mean ± SE ($n = 10$). $^{**}P < 0.01$ and $^{*}P < 0.05$.

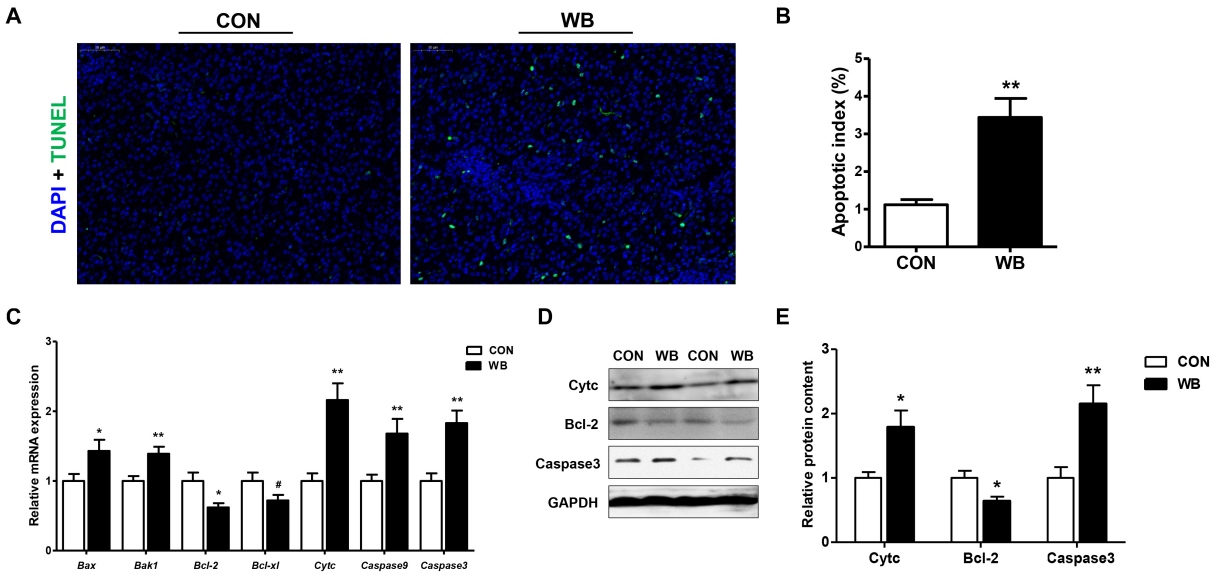

FIGURE 3 | Apoptotic status and apoptosis-related mediators in the liver tissues of broiler chickens with normal (CON) and wooden breast (WB) pectoralis major muscle. **(A)** Representative images of terminal deoxynucleotidyl transferase-mediated dUTP nick-end labeling (TUNEL) staining of liver. **(B)** Relative percentage of hepatocyte apoptosis. **(C)** Relative mRNA expression of Bcl-2-associated X protein (Bax), Bcl-2 antagonist or killer 1 (Bak1), B cell lymphoma (Bcl)-2, Bcl-xl, cytochrome c (Cytc), caspase 9, and caspase3. **(D)** Representative Western blotting images of Cytc, Bcl-2, and caspase 3. **(E)** Relative protein content of Cytc, Bcl-2, and caspase 3. Data are expressed as the mean ± SE (n = 10). $^{**}P < 0.01$, $^{*}P < 0.05$, and $^{\#}0.05 < P < 0.1$.

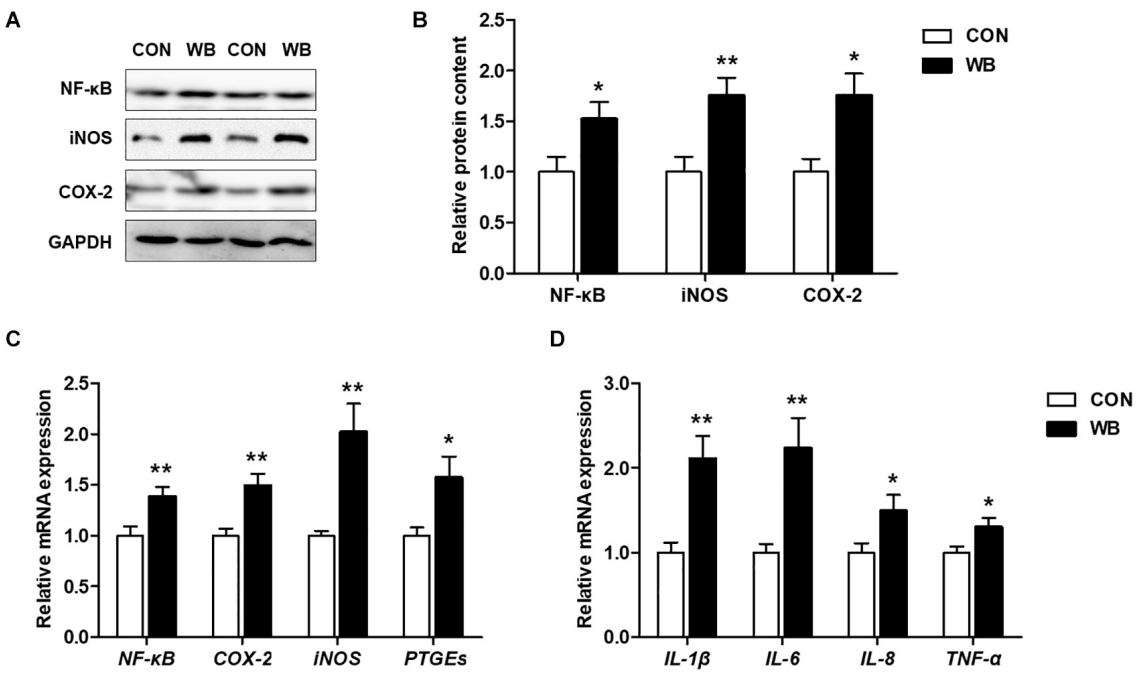

FIGURE 4 | Inflammatory mediators and proinflammatory cytokines in the liver tissues of broiler chickens with normal (CON) and wooden breast (WB) pectoralis major muscle. **(A)** Representative Western blotting images of nuclear factor kappa-light-chain-enhancer of activated B cells (NF-κB), inducible nitric oxide synthase (iNOS), and cyclooxygenase-2 (COX-2). **(B)** Relative protein content of NF-κB, iNOS, and COX-2. **(C)** Relative mRNA expression of NF-κB, iNOS, COX-2, and prostaglandin E synthetases (PTGEs). **(D)** Relative mRNA expression of pro-inflammatory cytokines including interleukin (IL)-1β, IL-6, IL-8, and tumor necrosis factor (TNF)-α. Data are expressed as the mean ± SE (n = 10). $^{**}P < 0.01$ and $^{*}P < 0.05$.

with the CON birds ($P < 0.05$, **Figure 4D**). These results suggested that WB myopathy induced inflammatory responses in the liver by activating inflammatory mediators and enhancing production of proinflammatory cytokines.

DISCUSSION

WB myopathy has been identified as an emerging muscular disease in modern broiler chickens over the past decade. Chronic WB myopathy-affected muscles exhibit histological lesions of polyphasic myodegeneration, myofiber necrosis, small regenerating myofibers, inflammatory cell infiltration, as well as deposition of lipid and connective tissue (Sihvo et al., 2014). Growing evidence suggests that the excessive development of breast muscle leads to the hypertrophy of myofiber, thereby reducing perimysial and endomysial space available for capillaries and compromising blood supply (Velleman, 2019), which possibly trigger an intricate pathogenesis including oxidative stress, impaired calcium homeostasis, inflammatory responses, and metabolic shifts (Petracci et al., 2019). Meanwhile, the aberrant accumulation of interstitial fibrotic tissues and a consequent increase in the spaces between muscle fibers might be associated with a lower capillary density and a greater intercapillary distance, which could further deteriorate the microvascular architecture and aggravate this situation (Soglia et al., 2017). Besides breast muscle abnormalities, broilers afflicted with WB myopathy also exhibit secondary pathophysiological perturbations in blood circulation and in other organ systems (Lake et al., 2020; Phillips et al., 2020).

The liver is defined as the primary internal organ for poultry exerting a variety of metabolic and homeostatic functions including digestion, metabolism, biosynthesis, excretion, and detoxification. The disruption of hepatic function has been implicated to reduce growth performance and threaten the health of birds, causing economic losses to the poultry industry (Zaefarian et al., 2019). In addition, mammalian studies indicate that liver disease might be implicated as a conjoint pathological mechanism underlying several metabolic disorders including neuromuscular disease (Pearce and Grant, 2010; David et al., 2014). Recent studies have likewise assessed the alterations of transcriptome and stress response genes in both liver and muscle of WB myopathic birds and revealed that the etiology of this myopathy is not limited to muscle, but is a systemic pathology (Kang et al., 2020; Phillips et al., 2020). Therefore, this study was conducted to investigate the histological and biochemical status and to depict the possible mechanistic changes involved in the liver of myopathic birds for better understanding of the molecular basis of the underlying pathological process and thereby promoting the healthy production of broiler chickens.

Injury to the liver tissue can lead to the release of various hepatic enzymes into the bloodstream. Increases in plasma levels of aminotransferases, AKP, and γ-GT are widely used as diagnostic markers of hepatic damage (Li et al., 2019). Herein, we reported that serum AST, AKP, and γ-GT activities were significantly elevated in WB birds, suggesting that liver injury occurs in this myopathy. Similarly, broilers affected by other myopathies such as white striping (WS) and dorsal cranial myopathy exhibited increased levels of ALT and AST in the serum (Kuttappan et al., 2013; Sesterhenn et al., 2017). However, Kuttappan et al. (2013) observed the unchanged γ-GT and decreased AKP activity in the serum of WS-affected birds compared with the normal. We ascribed this inconsistency to the different stages of myopathy progression. Since WS and WB are both growth-associated myopathies sharing similar histological lesions (Sihvo et al., 2014), the myopathic aberrations of PM muscle might start with the onset of WS and progress into WB during the whole growth period (Griffin et al., 2018). Consistent with the elevations of indicators of hepatic damage in the plasma, we observed widespread lesions with hydropic/fatty degeneration, infiltration of inflammatory cells, occasional fibrosis, and severe intrahepatic hemorrhages in liver sections of WB myopathic birds. The increase in MPO activity and the overproduction of NO further implied the infiltration of neutrophil and mononuclear cells, and confirmed the induction of the inflammatory process in the liver tissue (Aktan, 2004; Loria et al., 2008).

Oxidative stress occurs when the balance of pro-oxidants and endogenous antioxidants in a living system is disturbed, which can lead to the overproduction of free radicals (Sies et al., 2017). Previous studies suggested the presence of altered redox homeostasis and oxidative stress as possible biological processes linked with the pathogenesis of WB disease (Abasht et al., 2016; Papah et al., 2018). In addition, the excessive formation of ROS was directly observed in WS and WB-affected PM muscle (Salles et al., 2019; Pan et al., 2020). Intracellular macromolecules are vulnerable to free radicals, and the resultant lipid peroxidation, modification of proteins, and nucleic acid breaks may further contribute to structural collapse and dysfunction. Herein, we observed an aberrant ROS accumulation and augmented levels of MDA, LPO, protein carbonyl, and 8-OHdG, indicating that oxidative stress occurs in the liver of WB-affected birds. Oxidative stress or disturbed redox state has been implicated as a crucial mediator contributing to hepatic damage and the progression of pathological liver disorders (Zhu et al., 2012). Aflatoxin B1 administration induced oxidative stress in the liver of broilers, which contributed to hepatic dysfunction characterized by pallor discoloration, enlargement, and necrosis (Li et al., 2019). Intraperitoneal injection of hydrogen peroxide triggered hepatic oxidative stress by increasing ROS level and contents of oxidative products, thereby exerting a negative impact on the histomorphology and redox status in the liver, as well as the resultant decline in growth performance of broilers (Chen et al., 2018). Furthermore, oxidative markers could serve as prognostic indicators of liver damage and chronic hepatic diseases such as non-alcoholic steatohepatitis and liver fibro-proliferative disease (Cichoż-Lach and Michalak, 2014). To counteract oxidative stress, organisms generally stimulate multiple layers of antioxidant defense system to reduce the formation of excessive free radicals. As expected, we observed significantly enhanced activities of T-AOC, CAT, SOD, GSH-Px, and GSH-ST in the liver of the WB group compared with the CON group. Accordingly, the antioxidant enzyme defensive system was activated in the PM muscle of WB myopathic

broilers (Pan et al., 2020). The inhibited activities of GSH-Px and GSH-ST were also observed in the PM muscle of severe WS-affected birds (Salles et al., 2019), suggesting that the activation of antioxidant armamentarium depends on the stage and severity of injury or disease. The mitochondria not only constitute primary sources of ROS but also are vulnerable to oxidative attack due to the high content of phospholipid and protein in their membranes (Cadenas and Davies, 2000). In the current study, the ultrastructural examination indicated the damaged mitochondrial structure in WB liver. In addition, the WB liver mitochondria exhibited loss of $\Delta\psi m$ and were prone to go through swelling, indicating an impaired function. In the meantime, mitochondria dysfunction may interact with cellular redox environment, contributing to ROS overproduction and the impaired antioxidant defense system (Balaban et al., 2005). Collectively, these results demonstrated the occurrence of oxidative stress in the liver of WB myopathic birds as evidenced by the disturbed redox homeostasis and mitochondria damage, which possibly contribute to hepatic pathological changes.

Oxidative stress triggered by various insults or pathological states is closely associated with the induction of programmed cell apoptosis (Ryter et al., 2007). The present study revealed a significantly increased number of hepatocytes undergoing apoptosis in WB demonstrated by the TUNEL assay. The apoptosis process is executed through the caspase family, among which, caspase3 plays a vital role in mediating both intrinsic and extrinsic signaling pathways. The present results indicated the mRNA expression of *caspase 3* and *9* as well as the protein content of caspase 3 that was upregulated in the WB liver compared with the CON. Similarly, the occurrence of apoptosis is involved in liver injury, alcoholic and non-alcoholic steatohepatitis, and chronic liver disease (Aizawa et al., 2020). The mitochondrial and endoplasmic reticulum-mediated intrinsic apoptosis is usually triggered by a variety of stimuli such as calcium overload, ROS overproduction, and unfolded protein response. In addition, loss of $\Delta\psi m$ is an important hallmark in apoptosis and occurs in the early phase of mitochondria-mediated apoptosis (Kinnally et al., 2011). Based on the elevated ROS accumulation and mitochondrial dysfunction in WB liver, we speculated that the activation of apoptosis was mitochondria mediated caspase dependent. The mitochondrial pathway is regulated by pro- and antiapoptotic Bcl-2 family members. The imbalance of these regulators causes the permeation of the mitochondrial outer membrane and promotes the release of pro-apoptotic protein, thereby activating the caspase cascade (Xing et al., 2019). Therefore, the increased levels of Bax and Bak1, decreased levels of Bcl-2 and Bcl-xl, as well as the release of Cytc confirmed the activated mitochondrial pathway were involved in liver apoptosis of WB myopathic birds.

Hepatocytes undergoing injury can promote the release of cytokines and recruit inflammatory cells, such as neutrophils and macrophages to clean up debris and stimulate regeneration (Malhi and Gores, 2008). In this study, we observed the upregulated mRNA expression of proinflammatory cytokines including *IL-1*β, *IL-6*, *TNF*-α, and *IL-8* in the liver of WB compared with CON. TNF-α acts as a potent activator of both proinflammatory and proapoptotic pathways, exerting important roles in the pathogenesis of liver injury (Schwabe and Brenner, 2006). IL-1β might contribute to the pathogenesis of liver damage as IL-1β knockout mice showed attenuated hepatocellular damage, steatosis, and fibrosis in atherogenic diet-induced steatohepatitis (Kamari et al., 2011). Therefore, these dysregulated cytokines could further lead to immune disorder and contribute to the aggravation of liver damage. This result also supports our recent finding of the systemic inflammatory response in WB myopathic broilers as implied by the elevation of circulating cytokines (Xing et al., 2021). Besides the secretion of cytokines, inflammatory cells can also produce excessive oxygen free radicals to attack host cells, leading to hepatocyte damage (Zhu et al., 2012). NF-κB is a central regulator in mediating liver inflammatory responses by controlling the expression of cytokines; the activation of NF-κB signaling has been implicated in various liver diseases (Luedde and Schwabe, 2011). In accordance with these studies, the expression of NF-κB was enhanced, and the expressions of its downstream targets including iNOS, COX-2, and PTGEs were upregulated in WB compared with those in CON. Meanwhile, these increased inflammatory mediators could further contribute to the exacerbation of inflammatory progression and cytokine production (Aktan, 2004; Subbaramaiah et al., 2012).

CONCLUSION

In summary, this study provides evidence of liver damage in birds affected by WB myopathy primarily by impaired liver morphology as well as elevated serum AST, AKP, and γ-GT activities. Oxidative stress in WB liver triggered by the excessive ROS accumulation might be associated with disturbance of redox status and mitochondrial dysfunction. Additionally, the present study confirms the mitochondria-mediated hepatocyte apoptosis and NF-κB signaling-regulated inflammatory response, which possibly contribute to the aggravation of liver injury of WB myopathic birds. In general, our results strongly suggest that hepatic disorders might be strongly correlated with WB myopathy and provide evidence to explain the possible mechanisms involved in these perturbations. Further studies are needed to assess systemic physiological disparities and other metabolic changes accompanying this myopathy for further recognition of its etiology.

DATA AVAILABILITY STATEMENT

The original contributions presented in the study are included in the article/**Supplementary Material**, further inquiries can be directed to the corresponding author.

ETHICS STATEMENT

The animal study was reviewed and approved by Institutional Animal Care and Use Committee of Nanjing Agricultural University.

AUTHOR CONTRIBUTIONS

TX and FG conceived and designed the study. TX, XP, and LZ performed the experiments and conducted the data analysis. TX drafted the manuscript. All authors contributed to the article and approved the submitted version.

FUNDING

This study was supported by the China Postdoctoral Science Foundation Grant (2018M640492 and 2019T120432), the Jiangsu Postdoctoral Science Foundation (2019K013), the Natural Science Foundation of Jiangsu Province in China (BK20190516), the National Natural Science Foundation of China (31872374 and 32072780), the National Key Research and Development Program of China (2018YFD0500405), and the Earmarked Fund for Jiangsu Agricultural Industry Technology System (JATS[2020]407).

ACKNOWLEDGMENTS

We thank Mrs. Jeanene M. de Avila (Department of Animal Sciences, and School of Molecular Bioscience, Washington State University, United State) for revising and editing this manuscript to provide grammatical coherence.

SUPPLEMENTARY MATERIAL

The Supplementary Material for this article can be found online at: https://www.frontiersin.org/articles/10.3389/fphys.2021.659777/full#supplementary-material

REFERENCES

Abasht, B., Mutryn, M. F., Michalek, R. D., and Lee, W. R. (2016). Oxidative stress and metabolic perturbations in wooden breast disorder in chickens. *PLoS One* 11:e0153750. doi: 10.1371/journal.pone.0153750

Aizawa, S., Brar, G., and Tsukamoto, H. (2020). Cell death and liver disease. *Gut Liver* 14, 20–29. doi: 10.5009/gnl18486

Aktan, F. (2004). iNOS-mediated nitric oxide production and its regulation. *Life Sci.* 75, 639–653. doi: 10.1016/j.lfs.2003.10.042

Balaban, R. S., Nemoto, S., and Finkel, T. (2005). Mitochondria, oxidants, and aging. *Cell* 120, 483–495. doi: 10.1016/j.cell.2005.02.001

Cadenas, E., and Davies, K. J. (2000). Mitochondrial free radical generation, oxidative stress, and aging. *Free Radical Bio. Med.* 29, 222–230. doi: 10.1016/S0891-5849(00)00317-8

Chen, X., Gu, R., Zhang, L., Li, J., Jiang, Y., Zhou, G., et al. (2018). Induction of nuclear factor-κB signal-mediated apoptosis and autophagy by reactive oxygen species is associated with hydrogen peroxide-impaired growth performance of broilers. *Animal* 12, 2561–2570. doi: 10.1017/S1751731118000903

Cichoż-Lach, H., and Michalak, A. (2014). Oxidative stress as a crucial factor in liver diseases. *World J. Gastroenterol.* 20, 8082–8091. doi: 10.3748/wjg.v20.i25.8082

David, I., Lau, X., Flores, M., Trieu, J., Gehrig, S. M., Chee, A., et al. (2014). Dysfunctional muscle and liver glycogen metabolism in mdx dystrophic mice. *PLoS One* 9:e91514. doi: 10.1371/journal.pone.0091514

Frolova, M. S., Marchenkov, V. V., and Vekshin, N. L. (2019). Disruption of flavin homeostasis in isolated rat liver mitochondria. *Biochem. Bioph. Res. Commun.* 516, 1211–1215. doi: 10.1016/j.bbrc.2019.07.021

Greene, E., Flees, J., Dadgar, S., Mallmann, B., Orlowski, S., Dhamad, A., et al. (2019). Quantum blue reduces the severity of woody breast myopathy via modulation of oxygen homeostasis-related genes in broiler chickens. *Front. Physiol.* 10:1251. doi: 10.3389/fphys.2019.01251

Griffin, J. R., Moraes, L., Wick, M., and Lilburn, M. S. (2018). Onset of white striping and progression into wooden breast as defined by myopathic changes underlying Pectoralis major growth. Estimation of growth parameters as predictors for stage of myopathy progression. *Avian Pathol.* 47, 2–13. doi: 10.1080/03079457.2017.1356908

Huang, Y., Yan, X., Zhu, M. J., Mccormick, R. J., Ford, S. P., Nathanielsz, P. W., et al. (2010). Enhanced transforming growth factor-β signaling and fibrogenesis in ovine fetal skeletal muscle of obese dams at late gestation. *Am. J. Physiol. Endoc. Metab.* 298, E1254–E1260. doi: 10.1152/ajpendo.00015.2010

Kamari, Y., Shaish, A., Vax, E., Shemesh, S., Kandel-Kfir, M., Arbel, Y., et al. (2011). Lack of interleukin-1α or interleukin-1β inhibits transformation of steatosis to steatohepatitis and liver fibrosis in hypercholesterolemic mice. *J. Hepatol.* 55, 1086–1094. doi: 10.1016/j.jhep.2011.01.048

Kang, S. W., Kidd, M. T., Kadhim, H. J., Shouse, S., and Kong, B. C. (2020). Characterization of stress response involved in chicken myopathy. *Gen. Comp. Endocr.* 295:113526. doi: 10.1016/j.ygcen.2020.113526

Kinnally, K. W., Peixoto, P. M., Ryu, S.-Y., and Dejean, L. M. (2011). Is mPTP the gatekeeper for necrosis, apoptosis, or both? *BBA Mol. Cell Res.* 1813, 616–622. doi: 10.1016/j.bbamcr.2010.09.013

Kuttappan, V. A., Huff, G. R., Huff, W. E., Hargis, B. M., Apple, J. K., Coon, C., et al. (2013). Comparison of hematologic and serologic profiles of broiler birds with normal and severe degrees of white striping in breast fillets. *Poult. Sci.* 92, 339–345. doi: 10.3382/ps.2012-02647

Lake, J. A., Brannick, E. M., Papah, M. B., Lousenberg, C., and Abasht, B. (2020). Blood gas disturbances and disproportionate body weight distribution in broilers with wooden breast. *Front. Physiol.* 11:304. doi: 10.3389/fphys.2020.00304

Li, S., Muhammad, I., Yu, H., Sun, X., and Zhang, X. (2019). Detection of Aflatoxin adducts as potential markers and the role of curcumin in alleviating AFB1-induced liver damage in chickens. *Ecotox. Environ. Saf.* 176, 137–145. doi: 10.1016/j.ecoenv.2019.03.089

Liu, J., Puolanne, E., Schwartzkopf, M., and Arner, A. (2020). Altered sarcomeric structure and function in woody breast myopathy of avian pectoralis major muscle. *Front. Physiol.* 11:287. doi: 10.3389/fphys.2020.00287

Livingston, M. L., Landon, C., Barnes, H. J., and Brake, J. (2019). White striping and wooden breast myopathies of broiler breast muscle is affected by time-limited feeding, genetic background, and egg storage. *Poult. Sci.* 98, 217–226. doi: 10.3382/ps/pey333

Loria, V., Dato, I., Graziani, F., and Biasucci, L. M. (2008). Myeloperoxidase: a new biomarker of inflammation in ischemic heart disease and acute coronary syndromes. *Mediators Inflamm.* 2008:135625. doi: 10.1155/2008/135625

Luedde, T., and Schwabe, R. F. (2011). NF-κB in the liver—linking injury, fibrosis and hepatocellular carcinoma. *Nat. Rev. Gastro. Hepat.* 8, 108–118. doi: 10.1038/nrgastro.2010.213

Malhi, H., and Gores, G. J. (2008). Cellular and molecular mechanisms of liver injury. *Gastroenterology* 134, 1641–1654. doi: 10.1053/j.gastro.2008.03.002

Moriuchi, T., Fujii, Y., Kagawa, N., and Hizawa, K. (1991). Autopsy study on the weight of the heart, liver, kidney and brain in Duchenne muscular dystrophy. *Tokushima J. Exp. Med.* 38, 5–13.

Mudalal, S., Lorenzi, M., Soglia, F., Cavani, C., and Petracci, M. (2015). Implications of white striping and wooden breast abnormalities on quality traits of raw and marinated chicken meat. *Animal* 9, 728–734. doi: 10.1017/S175173111400295X

Mutryn, M. F., Brannick, E. M., Fu, W., Lee, W. R., and Abasht, B. (2015). Characterization of a novel chicken muscle disorder through differential gene expression and pathway analysis using RNA-sequencing. *BMC Genomics* 16:399. doi: 10.1186/s12864-015-1623-0

Pan, X., Zhang, L., Xing, T., Li, J., and Gao, F. (2020). The impaired redox status and activated Nrf2/ARE pathway in wooden breast myopathy in broiler chickens. *Asian. Austral. J. Anim.* 34, 652–661. doi: 10.5713/ajas.19.0953

Papah, M. B., Brannick, E. M., Schmidt, C. J., and Abasht, B. (2017). Evidence and role of phlebitis and lipid infiltration in the onset and pathogenesis of Wooden Breast Disease in modern broiler chickens. *Avian Pathol.* 46, 623–643. doi: 10.1080/03079457.2017.1339346

Papah, M. B., Brannick, E. M., Schmidt, C. J., and Abasht, B. (2018). Gene expression profiling of the early pathogenesis of wooden breast disease in commercial broiler chickens using RNA-sequencing. *PLoS One* 13:e0207346. doi: 10.1371/journal.pone.0207346

Pearce, B., and Grant, I. S. (2010). Acute liver failure following therapeutic paracetamol administration in patients with muscular dystrophies. *Anaesthesia* 63, 89–91. doi: 10.1111/j.1365-2044.2007.05340.x

Petracci, M., Mudalal, S., Soglia, F., and Cavani, C. (2015). Meat quality in fast-growing broiler chickens. *World. Poultry Sci. J.* 71, 363–374. doi: 10.1017/S0043933915000367

Petracci, M., Soglia, F., Madruga, M., Carvalho, L., Ida, E., and Estévez, M. (2019). Wooden−breast, white striping, and spaghetti meat: causes, consequences and consumer perception of emerging broiler meat abnormalities. *Compr. Rev. Food Sci. Foog* 18, 565–583. doi: 10.1111/1541-4337.12431

Phillips, C. A., Reading, B. J., Livingston, M., Livingston, K. A., and Ashwell, C. M. (2020). Evaluation via supervised machine learning of the broiler pectoralis major and liver transcriptome in association with the muscle myopathy wooden breast. *Front. Physiol.* 11:101. doi: 10.3389/fphys.2020.00101

Ryter, S. W., Kim, H. P., Hoetzel, A., Park, J. W., Nakahira, K., Wang, X., et al. (2007). Mechanisms of cell death in oxidative stress. *Antioxid. Redox Sign.* 9, 49–89. doi: 10.1089/ars.2007.9.49

Salles, G. B. C., Boiago, M. M., Silva, A. D., Morsch, V. M., Gris, A., Mendes, R. E., et al. (2019). Lipid peroxidation and protein oxidation in broiler breast fillets with white striping myopathy. *J. Food Biochem.* 43:e12792. doi: 10.1111/jfbc.12792

Schwabe, R. F., and Brenner, D. A. (2006). Mechanisms of liver injury. I. TNF-α-induced liver injury: role of IKK, JNK, and ROS pathways. *Am. J. Physiol. Gastr. Liver Physiol.* 290, G583–G589. doi: 10.1152/ajpgi.00422.2005

Sesterhenn, R., Siqueira, F., Hamerski, A., Driemeier, D., Valle, S., Vieira, S., et al. (2017). Histomorphometric study of the anterior latissimus dorsi muscle and evaluation of enzymatic markers of broilers affected with dorsal cranial myopathy. *Poult. Sci.* 96, 4217–4223. doi: 10.3382/ps/pex252

Sies, H., Berndt, C., and Jones, D. P. (2017). Oxidative stress. *Annu. Rev. Biochem.* 86, 715–748. doi: 10.1146/annurev-biochem-061516-045037

Sihvo, H. K., Immonen, K., and Puolanne, E. (2014). Myodegeneration with fibrosis and regeneration in the pectoralis major muscle of broilers. *Vet. Pathol.* 51, 619–623. doi: 10.1177/0300985813497488

Soglia, F., Gao, J., Mazzoni, M., Puolanne, E., Cavani, C., Petracci, M., et al. (2017). Superficial and deep changes of histology, texture and particle size distribution in broiler wooden breast muscle during refrigerated storage. *Poult. Sci.* 96, 3465–3472. doi: 10.3382/ps/pex115

Soglia, F., Mudalal, S., Babini, E., Di Nunzio, M., Mazzoni, M., Sirri, F., et al. (2016). Histology, composition, and quality traits of chicken Pectoralis major muscle affected by wooden breast abnormality. *Poult. Sci.* 95, 651–659. doi: 10.3382/ps/pev353

Subbaramaiah, K., Morris, P. G., Zhou, X. K., Morrow, M., Du, B., Giri, D., et al. (2012). Increased levels of COX-2 and prostaglandin E2 contribute to elevated aromatase expression in inflamed breast tissue of obese women. *Cancer Discov.* 2, 356–365. doi: 10.1158/2159-8290.CD-11-0241

Velleman, S. G. (2019). Recent developments in breast muscle myopathies associated with growth in poultry. *Annu. Rev. Anim. Biosci.* 7, 289–308. doi: 10.1146/annurev-animal-020518-115311

Xing, T., Gao, F., Tume, R. K., Zhou, G., and Xu, X. (2019). Stress effects on meat quality: a mechanistic perspective. *Compr. Rev. Food Sci. Food* 18, 380–401. doi: 10.1111/1541-4337.12417

Xing, T., Luo, D., Zhao, X., Xu, X., and Gao, F. (2021). Enhanced cytokine expression and upregulation of inflammatory signaling pathways in broiler chickens affected by wooden breast myopathy. *J. Sci. Food Agr.* 101, 279–286. doi: 10.1002/jsfa.10641

Xing, T., Wang, C., Zhao, X., Dai, C., Zhou, G., and Xu, X. (2017a). Proteome analysis using isobaric tags for relative and absolute analysis quantitation (iTRAQ) reveals alterations in stress-induced dysfunctional chicken muscle. *J. Agr. Food Chem.* 65, 2913–2922. doi: 10.1021/acs.jafc.6b05835

Xing, T., Zhao, X., Wang, P., Chen, H., Xu, X., and Zhou, G. (2017b). Different oxidative status and expression of calcium channel components in stress-induced dysfunctional chicken muscle. *J. Anim. Sci.* 95, 1565–1573. doi: 10.2527/jas.2016.0868

Zaefarian, F., Abdollahi, M. R., Cowieson, A., and Ravindran, V. (2019). Avian liver: the forgotten organ. *Animals* 9:63. doi: 10.3390/ani9020063

Zhang, J., Hu, Z. P., Lu, C., Yang, M. X., Zhang, L. L., and Wang, T. (2015). Dietary curcumin supplementation protects against heat-stress-impaired growth performance of broilers possibly through a mitochondrial pathway. *J. Anim. Sci.* 93, 1656–1665. doi: 10.2527/jas.2014-8244

Zhu, R., Wang, Y., Zhang, L., and Guo, Q. (2012). Oxidative stress and liver disease. *Hepatol. Res.* 42, 741–749. doi: 10.1111/j.1872-034X.2012.00996.x

Conflict of Interest: The authors declare that the research was conducted in the absence of any commercial or financial relationships that could be construed as a potential conflict of interest.

frontiers in Physiology

MINI REVIEW
published: 31 May 2021
doi: 10.3389/fphys.2021.684497

Spaghetti Meat Abnormality in Broilers: Current Understanding and Future Research Directions

*Giulia Baldi, Francesca Soglia and Massimiliano Petracci**

Department of Agricultural and Food Sciences, University of Bologna, Cesena, Italy

Spaghetti meat (SM) is a recent muscular abnormality that affects the *Pectoralis major* muscle of fast-growing broilers. As the appellative suggests, this condition phenotypically manifests as a loss of integrity of the breast muscle, which appears soft, mushy, and sparsely tight, resembling spaghetti pasta. The incidence of SM can reach up to 20% and its occurrence exerts detrimental effects on meat composition, nutritional value, and technological properties, accounting for an overall decreased meat value and important economic losses related to the necessity to downgrade affected meats. However, due to its recentness, the causative mechanisms are still partially unknown and less investigated compared to other muscular abnormalities (i.e., White Striping and Wooden Breast), for which cellular stress and hypoxia caused by muscle hypertrophy are believed to be the main triggering factors. Within this scenario, the present review aims at providing a clear and concise summary of the available knowledge concerning SM abnormality and concurrently presenting the existing research gaps, as well as the potential future developments in the field.

Keywords: broilers, spaghetti meat, spaghetti breast, growth-related abnormalities, histology, meat quality, causative mechanisms

OPEN ACCESS

Edited by:
Mahmoud M. Alagawany, Zagazig University, Egypt

Reviewed by:
Eero Puolanne, University of Helsinki, Finland
Servet Yalcin, Ege University, Turkey

***Correspondence:**
Massimiliano Petracci
m.petracci@unibo.it

Specialty section:
This article was submitted to Avian Physiology, a section of the journal Frontiers in Physiology

Received: *23 March 2021*
Accepted: *26 April 2021*
Published: *31 May 2021*

Citation:
Baldi G, Soglia F and Petracci M (2021) Spaghetti Meat Abnormality in Broilers: Current Understanding and Future Research Directions. Front. Physiol. 12:684497. doi: 10.3389/fphys.2021.684497

INTRODUCTION

About 10 years ago, the appearance of a novel cluster of muscular abnormalities affecting the *Pectoralis major* muscle of fast-growing broilers has alarmed the poultry industry. From there on, a growing body of literature has been focused on the etiology behind their appearance, implications on meat quality, as well as the attempts to mitigate their occurrence and narrow down the negative perception related to animal welfare (Griffin et al., 2018; Petracci et al., 2019; Baldi et al., 2020a). Within the industry vernacular, these myopathies are commonly called White Striping (WS), Wooden Breast (WB), and Spaghetti Meat (SM), each of which owning peculiar and distinctive traits from which their names originated. The first is indeed characterized by the occurrence of white lines running parallel to the muscle fibers on the surface of *P. major* muscle (Kuttappan et al., 2013b); the second manifests as a severe hardening of the pectoral muscle (Sihvo et al., 2014), while the third displays as a loss of integrity of the muscle fiber bundles composing the breast muscle itself, which appears mushy and sparsely tight (Baldi et al., 2018). Due to their alarming incidence rates and outstanding impact on meat quality, a large number of studies has been published on WS and WB abnormalities over the years, focusing on the understanding of their etiology, the molecular pathways potentially responsible for their occurrence as well as their implications on eating, nutritional, and technological properties of meat (Petracci et al., 2019). On the contrary, the information regarding SM is today still limited and only few studies have been published since

its appearance (**Table 1**). Thus, the present review aims at providing a clear and succinct summary of the available knowledge concerning SM condition and presenting the current research challenges as well as the potential future developments in the field.

UP-TO-DATE KNOWLEDGE

Morphological Characteristics and Incidence Levels

Spaghetti Meat defect was first recounted in 2015 with the name of "Mushy Breast" and described as a myopathy causing the loss of muscle integrity of the *P. major* muscle of fast-growing chickens (Bilgili, 2015). Later on, this condition has been commonly recognized with the name of "Spaghetti Meat" or "Spaghetti Breast" since, as the appellative suggests, it phenotypically manifests with the detachment of the fiber bundles composing the pectoral muscle, which appears soft, mushy, and sparsely thigh, resembling spaghetti pasta. Since the severity of SM defect might be variable, Sirri et al. (2016) proposed a classification criterion based on a three-score scale. Indeed, depending on the severity score, the occurrence of SM can be detected either palpably, due to the soft and stringy structure perceived by pinching the muscle on its surface, or visually, due to the expanded superficial lacerations (**Figure 1**). As will be further explained (see section "Implications on meat quality and practical solutions"), meats severely affected by SM are usually downgraded and incorporated into the formulation of further processed products, while moderate cases can be marketed for fresh retailing. Generally, SM condition mostly manifests in the ventro-cranial portion of the fillet, but there is growing evidence that also the caudal section and, occasionally, leg muscles might be affected as well. Recently, a sporadic occurrence of SM defect has been also signaled on the pectoral muscles of commercial turkeys, even though no information is yet available concerning possible similarities with the same condition reported for broilers (Zampiga et al., 2020).

Data concerning the incidence rates of SM condition are limited and sometimes contradictory, likely due to both the variation of classification criteria among the abattoirs and the complication related to the concurrent presence of other myopathies within the same muscle, since SM can be comorbid with WB and, more likely, with WS (Baldi et al., 2018; Bailey et al., 2020). However, an Italian survey carried out on 16,000 breasts reported that around 21% of samples were affected by SM (Baldi et al., 2020a), while a Brazilian study evaluated about 10% of SM fillets on a total of 5,580 breasts (Montagna et al., 2019). While it has been widely recognized that the incidence rates of WS and WB significantly upsurge with higher growth rate, breast yield as well as body weight and age at slaughter of birds (Kuttappan et al., 2013a, 2016; Papah et al., 2018), this trend has not been fully confirmed for SM. However, Pascual et al. (2020) intriguingly found significantly higher rates of SM in females rather than males (25.0% vs. 3.1%, respectively), contrarily to what observed for WS and WB, whose incidence levels were found to be greater in males regardless the slaughter weight (Lorenzi et al., 2014; Trocino et al., 2015). To the best of our knowledge, the reasons for the higher incidence of SM condition in female individuals are still unknown, albeit a recent study highlighted an increased expression of genes related to connective tissue proliferation in male broilers, making them more prone than females to develop WB condition (Brothers et al., 2019). However, a possible role of a different hormonal response (e.g., insulin growth factor, somatotropic hormone, myostatin, etc.) regulating metabolism, protein synthesis, patterns of intramuscular fat deposition, and intracellular signaling during the development of myopathic conditions might be also speculated.

Histological Traits

Microscopic investigations performed on SM muscles highlighted several histologic features commonly reported also for WS and WB, such as nuclei internalization, inflammatory cells infiltration, necrosis, fiber lysis, and concurrent presence of small regenerative fibers combined with abnormal ones showing larger diameter (Baldi et al., 2018). On the other hand, the distinctive microscopic feature of SM condition is the progressive rarefaction of the endomysial and perimysial connective tissue, that likely leads to the detachment of the muscle fibers from each others (Baldi et al., 2018). Moreover, histological observations highlighted the presence of small and thin fibers, interspersed by immature/newly deposited connective tissue (Baldi et al., 2018; Sanden et al., 2021). The presence of these fibers, distinguished by a remarkably reduced cross-sectional area, suggests the ongoing of regenerative processes taking place in the muscle, as a natural response mechanism to cell necrosis (Mazzoni et al., 2020). However, a different phase of cell regeneration can be hypothesized when comparing SM and WS samples' immunoreactivity to vimentin, suggesting a different progression of the regenerative processes (Soglia et al., 2020). A recent study also investigated the distribution of collagen type III and its precursor (i.e., procollagen type III) in SM samples since, being involved in fibrillogenesis, their possible altered deposition might have a key role in the occurrence of muscular abnormalities. In this regard, the findings highlighted an altered immunoreactivity to procollagen type III in SM samples, suggesting a compromised collagen turnover and synthesis (Mazzoni et al., 2020).

Implications on Meat Composition

The degenerative processes and repair mechanisms taking place in the muscles affected by growth-related abnormalities (e.g., inflammatory processes, necrosis, fibrosis, lipidosis, etc.) inevitably alter the proximate composition of meat and, as a direct consequence, negatively affect its nutritional value (Petracci et al., 2019). In detail, as reported by Baldi et al. (2018, 2019), the occurrence of SM is associated with a remarkable relatively reduction of protein content (-10%, when compared to unaffected muscles) coupled with a concurrent increase in fat and moisture levels (+21.8 and + 3.0%, respectively). The same authors reported a lower content of EPA and DHA in meat affected by SM, likely accountable for a different expression of the genes encoding for Δ5 and Δ6 desaturases, as previously hypothesized by Soglia et al. (2016a). As concern mineral profile, a study carried out by Tasoniero et al. (2020) reported greater calcium and sodium levels in SM samples if compared to unaffected ones, speculating a possible connection

TABLE 1 | Chronological sequence of available published studies concerning spaghetti meat condition and relative addressed topics.

References	Implications of genetic and environmental factors on incidence levels	Detection tools	Meat processing solutions	Examined traits				
				Histology	Proximate composition	Protein and/or amino acid profile	Collagen	Technological quality
Sirri et al., 2016	●							
Baldi et al., 2018			●	●	●	●		●
Córdova-Noboa et al., 2018	●							
Zampiga et al., 2018	●							
Baldi et al., 2019			●		●	●	●	●
Montagna et al., 2019	●							
Soglia et al., 2019a			●			●		●
Mazzoni et al., 2020				●			●	
Bailey et al., 2020	●							
Campo et al., 2020		●						●
Morey et al., 2020		●						
Pascual et al., 2020	●							
Soglia et al., 2020						●	●	
Tasoniero et al., 2020					●	●	●	●
Yu et al., 2020								●
Pascual et al., 2021					●			●
Sanden et al., 2021				●			●	

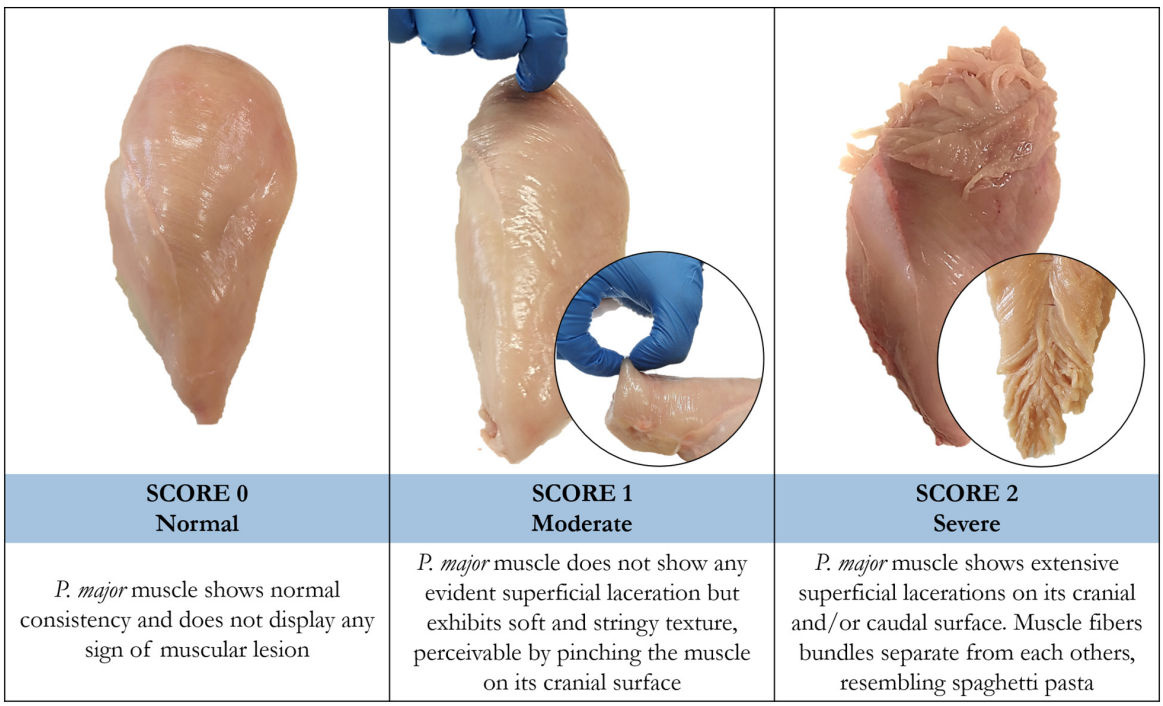

FIGURE 1 | Representative images of chicken breast fillets with normal (score 0), moderate (score 1) and severe (score 2) degrees of Spaghetti Meat.

between cation homeostasis disturbances and the appearance of pathological mechanisms leading to cell injury development. Intriguingly, the analysis of the available literature highlighted that SM samples possess analogous amounts of total and soluble collagen of unaffected breasts (Baldi et al., 2018; Campo et al., 2020; Tasoniero et al., 2020). On the other hand, Baldi et al. (2019) found lower hydroxylysylpyridinoline contents in muscles affected by SM, suggesting a feeble collagen cross-linking (i.e.,

presence of immature collagen) and corroborating what found from previous histological observations (see section "Histological traits"). Accordingly, following investigations through polarized FTIR-spectroscopy, Sanden et al. (2021) reported that SM muscles possess thin, loose and immature collagen fiber bundles, which are also poorly packed. The same authors also mentioned that SM shows a higher amount of glycosaminoglycans in perimysial connective tissue, corroborating the hypothesis put forward by Papah et al. (2018) of a shift in glucose flux toward the synthesis of molecules composing the extracellular matrix in myopathic muscles.

Implications on Meat Quality and Practical Solutions

Albeit only few studies have been published concerning the implications of SM condition on meat quality (see **Table 1**), its occurrence seems to affect meat technological properties and functionality to a lesser extent if compared to WS and WB (Baldi et al., 2019; Pascual et al., 2021). Overall, the occurrence of SM is associated with higher meat yellowness and ultimate pH values (Baldi et al., 2018; Soglia et al., 2019a; Tasoniero et al., 2020). While Yu et al. (2020) did not find any difference in water holding capacity assessed on fresh, frozen, and cooked SM samples, Pascual et al. (2021) reported greater drip and cooking losses in SM samples compared to normal ones. The latter result corroborates the outcomes obtained through time-domain nuclear magnetic resonance analysis, which evidenced increased amounts of bound and extra-myofibrillar water fractions in SM fillets (Soglia et al., 2019a). As suggested by the longer relaxation times, the abovementioned water fractions are concurrently less tightly bound to the muscle tissue, highlighting an altered water distribution and mobility within SM muscles and, thus, an impaired ability to hold constitutional water (Baldi et al., 2019). This hypothesis is further supported by the results obtained by Tasoniero et al. (2020), who found a remarkable reduction of myofibrillar protein solubility, salted-induced water uptake, final yield as well as emulsion stability in SM fillets if compared to unaffected ones. Intriguingly, SM breasts did not display any upsurge in protein carbonylation levels (Baldi et al., 2018; Soglia et al., 2019a), suggesting that the reduced water holding capacity is not imputable to the ongoing of oxidative processes occurring at the expenses of muscular proteins. Thus, overall, this phenomenon can be explained by further mechanisms which essentially share the same underpinning factor. Precisely, the complete re-organization of muscle architecture following myodegeneration and necrosis leads to a reduction in the number of functional myofibrils and, therefore, to a lower potential of the muscle to bind water (Soglia et al., 2016a; Tasoniero et al., 2017). Indeed, the impaired water holding capacity of SM samples might be the direct consequence of their reduced protein solubility, probably due to the ongoing of protein degradation processes as evidenced by both the higher myofibrillar fragmentation index of SM muscles if compared to unaffected ones (Baldi et al., 2018; Tasoniero et al., 2020) and the greater concentration of free amino acids deriving from the breakdown of muscular proteins (Soglia et al., 2019a). In support of this, electrophoretic analysis evidenced an increased number of high molecular-weight bands in SM samples, presumably originating from the degenerative processes associated with the occurrence of muscular abnormalities (Baldi et al., 2018).

As concern texture, compression forces obtained for raw meat did not evidence any difference between SM samples and their unaffected counterparts (Baldi et al., 2019). However, after the cooking process, SM fillets showed a softer texture following compression, Meullenet-Owens Razor Shear as well as Allo–Kramer tests (Baldi et al., 2019; Pascual et al., 2021), probably as a result of their reduced collagen cross-linking degree. In addition, a number of studies have been carried out to investigate whether SM lesions display intra-fillet variations, revealing that the occurrence of this condition mainly alters meat composition and quality traits of the superficial layer of the muscle, while the deep one is almost unaffected (Baldi et al., 2019; Tasoniero et al., 2020; Yu et al., 2020). However, to the best of our knowledge, any published study specifically speculates about those divergences. Nevertheless, intensive selection practices carried out over years permitted to accomplish a remarkable development of the breast muscle, so much so that the impressive thickness of its cranial section might compress the pectoral artery, reducing muscular oxygenation (Soglia et al., 2021). Thus, a feasible hypothesis for the abovementioned intra-fillet variations may rely on a different blood flow between the surface of the muscle, phenotypically exhibiting the defect, and its deep counterpart. The first, being thicker and likely less oxygenated compared to the latter, might be more prone to develop inflammatory processes due to the weakened blood supply and impaired displacement of metabolic end-products, thus resulting in the advancing of hypoxic conditions which are believed to be the triggering factor for the manifestation of growth-related abnormalities (Abasht et al., 2016; Malila et al., 2019; Greene et al., 2020). Indeed, as observed at least for WS and WB, the severity of the histological lesions gradually weakens when moving from the antero-ventral to the antero-dorsal section of *P. major* muscle (Soglia et al., 2016b; Clark and Velleman, 2017; Baldi et al., 2020b).

The abovementioned detrimental effects of SM condition on meat quality may account for economic losses related to decreased yields during processing. Generally speaking, meats severely affected by SM are usually downgraded and incorporated into the formulation of further processed products, while moderate cases can be marketed for fresh retailing (Petracci et al., 2019). However, the growing consumers' demand for thin-sliced chicken breast meat has made the occurrence of SM particularly challenging for the processing industry since, being SM often detectable only after the slicing process, the amount of downgraded/discarded meat could be even exacerbated. Thus, being the in-line detection of abnormal meat a relevant matter especially for the meat packing plants, Morey et al. (2020) recently proposed the feasibility of bioelectrical impedance analysis to identify SM breasts, while Campo et al. (2020) suggested the analysis of color reflectance as a possible tool to detect those breasts affected by any degree of WS and SM in the processing line. Aside from this, it is noteworthy to mention that SM myopathy cannot be noticed in the living animal, contrarily to WB condition whose presence can be detected by palpating the

breast of the live bird and lifting up its wings to assess the ability to achieve back-to-back wing contact (Hosotani et al., 2020). This might represent a useful tool for breeder companies to exclude birds showing WB defect from the pedigree lines, even though this would entail the possible risk to indirectly select individuals showing SM condition. Indeed, evidence suggests that a reduction of WB occurrence in some flocks is sometimes associated with a concurrent increase in SM condition levels.

Thus, given the detrimental impact of SM condition and, more generally, of growth-related abnormalities on chicken meat quality and the economy of poultry meat producers, the pursuit for potential solutions to mitigate these undesirable implications is calling the attention of the scientific community and have been recently summarized in the reviews written by Barbut (2019), Petracci et al. (2019), and Baldi et al. (2020a). Considering the current lack of efficient animals' nutrition and management strategies to reduce SM defect without affecting slaughter performances (Sirri et al., 2016; Córdova-Noboa et al., 2018; Zampiga et al., 2018), to date, the most promising approach seems to develop processing solutions aimed at reducing the implications on the final quality of meat. Within this context, the most practical solution so far is represented by the separation of the superficial and deep sections of the fillets, addressing the first for the manufacture of processed products, while the latter for fresh retailing. Indeed, as reported in the previous paragraph, the occurrence of SM negatively impacts only the surface of the muscle, thus allowing to downgrade a reduced portion of the fillet. As previously suggested for WB (Brambila et al., 2017; Xing et al., 2017; Chen et al., 2018), downgraded meat could be then included in the formulation of ground or finely comminuted meat products, where the addition of functional ingredients (i.e., starches, phosphates, hydrocolloids, etc.) could mask its impaired technological properties (Petracci et al., 2019). Moreover, since it has been reported that freezing – and subsequent thawing – do not result in any further worsening of SM meat quality traits (Soglia et al., 2019a), downgraded fillets can be frozen and afterward included in the formulation of processed products, guaranteeing a greater flexibility for the poultry processing industry.

CURRENT CHALLENGES AND POTENTIAL FUTURE DEVELOPMENTS

Considering the recentness of SM condition, the mechanisms underpinning its appearance are still partially unknown and less investigated compared to WB and WS. However, the same histological alterations shared among WB, WS, and SM fillets suggest a common network of causative mechanisms responsible for their occurrence, in which cellular stress and hypoxia – caused by muscle hypertrophy induced by selection – play a key role (Sihvo et al., 2018; Young and Rasmussen, 2020; Soglia et al., 2021). Considering their common histological traits, one of the most compelling challenges for the scientific community is to determine the reason why growth-related myopathies phenotypically manifest differently. Within this context, Soglia et al. (2020) recently speculated that the distinctive phenotype of WB, WS, and SM meat could be associated, at least partially, to the synthesis of vimentin, a protein considered a marker of muscle fiber regeneration and directly involved in the coordination of fibroblast proliferation (Cheng et al., 2016). In more detail, it has been suggested that the lack of correspondence between the up-regulated gene encoding for vimentin and its encoded protein found in SM muscles might be responsible for an altered distribution of fibroblasts in the perimysial compartment, which would ultimately result in a progressive rarefaction of the connective tissue, a typical trait of SM myopathy (Soglia et al., 2020).

Otherwise, the distinctive phenotype of SM has been also thought to be associated with an excessive build-up of lactic acid in the muscle, leading to the inhibition of protein synthesis regulating collagen development (Anton et al., 2019). On the other hand, contrarily to what previously observed for WS and WB (Radaelli et al., 2017), it must be pointed out that the low heritability levels of SM may indicate the impact of non-genetic factors on the variance of the myopathy traits (Bailey et al., 2020). Indeed, the weak correlation between the incidence of SM condition and animals' growth rate, age, and weight at slaughter might hint at other "contributing factors" related to slaughtering operations (e.g., scalding, de-feathering, chilling, post-mortem deboning time and technology, etc.) which can exploit a role in the manifestation of SM condition or, at least, in the worsening of its severity level. Indeed, a recent technical report highlighted that the incidence of SM was found to be up to 50% higher in carcasses subjected to slow carcass chilling compared to their fast-cooled counterparts (Anton et al., 2019). The authors justified this phenomenon with an excessive accumulation of lactic acid in the muscle when the carcass is still warm. This would stimulate the activity of proteases responsible for the degradation of connective tissue and subsequent excessive softening of the meat (Anton et al., 2019). However, from the analysis of the available literature, no research aimed at establishing the effect of chilling conditions on the occurrence of SM is available yet, thus being a stimulating starting point for future investigations. Another appealing challenge for the poultry processors could be the understanding of the possible role of scalding and plucking procedures in a further worsening of the consistency of those fillets exhibiting a mild level of muscle destructuration. Indeed, given the presence of weakened perimysial connective tissue in SM samples (Baldi et al., 2018), it could be hypothesized that scalding temperatures combined with an aggressive de-feathering could likely worsen an already compromised muscular structure, making the muscle fibers more prone to be torn apart during handling and fileting. In addition, a new emerging quality issue phenotypically resembling SM condition was recently found to affect the *P. minor* muscles of broiler chickens. This defect is named "gaping" and has been examined for the first time in the study of Soglia et al. (2019b), who suggested that its occurrence is especially related to peri-mortem factors as well as slaughtering procedures. Notwithstanding, further studies should be performed to establish whether a relationship exists between the occurrence of gaping defect in the *P. minor* muscles and SM in their corresponding *major* counterparts.

In conclusion, considering the available knowledge and the existing research gaps about SM myopathy, the focus of future investigations might be directed into the unraveling of the role

of peri-mortem procedures in the development of this condition, as well as the underpinning factors that make the incidence of SM higher in female individuals and inversely correlated to the manifestation of WB condition.

AUTHOR CONTRIBUTIONS

GB was the primary writer and performed most of the literature search. FS and MP supported the redaction of all sections. All authors listed have made a substantial, direct and intellectual contribution to the work, and approved it for publication.

FUNDING

This work has been partially supported by the PRIN project "Use of local chicken breeds in alternative production chain: welfare, quality and sustainability" (Prot. 2017S229WC) funded by the Italian Ministery of Research (MIUR).

REFERENCES

Abasht, B., Mutryn, M. F., Michalek, R. D., and Lee, W. R. (2016). Oxidative stress and metabolic perturbations in wooden breast disorder in chickens. *PLoS One* 11:e0153750. doi: 10.1371/journal.pone.0153750

Anton, P., Avendanō, S., Biley, R., Bilgili, S., Canela, L., and Corzo, A. (2019). *Breast muscle myopathies Aviagen*. Available online at: http://en.aviagen.com/assets/Tech_Center/Broiler_Breeder_Tech_Articles/English/Breast-Muscle-Myopathies-2019-EN.pdf%0A (accessed April 20, 2021).

Bailey, R. A., Souza, E., and Avendano, S. (2020). Characterising the influence of genetics on breast muscle myopathies in broiler chickens. *Front. Physiol.* 11:1041. doi: 10.3389/fphys.2020.01041

Baldi, G., Soglia, F., Laghi, L., Tappi, S., Rocculi, P., Tavaniello, S., et al. (2019). Comparison of quality traits among breast meat affected by current muscle abnormalities. *Food Res. Int.* 115, 369–376. doi: 10.1016/j.foodres.2018.11.020

Baldi, G., Soglia, F., Mazzoni, M., Sirri, F., Canonico, L., Babini, E., et al. (2018). Implications of white striping and spaghetti meat abnormalities on meat quality and histological features in broilers. *Animal* 12, 164–173. doi: 10.1017/S1751731117001069

Baldi, G., Soglia, F., and Petracci, M. (2020a). Current status of poultry meat abnormalities. *Meat Muscle Biol.* 4, 1–7. doi: 10.22175/mmb.9503

Baldi, G., Yen, C.-N., Daughtry, M. R., Bodmer, J., Bowker, B., Zhuang, H., et al. (2020b). Exploring the factors contributing to the high ultimate ph of broiler pectoralis major muscles affected by wooden breast condition. *Front. Physiol* 11:343. doi: 10.3389/fphys.2020.00343

Barbut, S. (2019). Recent myopathies in broiler's breast meat fillets. *Worlds. Poult. Sci. J.* 75, 559–582. doi: 10.1017/S0043933919000436

Bilgili, S. (2015). *Broiler chicken myopathies IV. Stringy/mushy breast. in Worthwhile Operational Guidelines and Suggestion*. Available online at: http://poul.auburn.edu/wp-content/uploads/sites/13/2015/11/WOGS-FEB15.pdf (accessed April 20, 2021).

Brambila, G. S., Chatterjee, D., Bowker, B., and Zhuang, H. (2017). Descriptive texture analyses of cooked patties made of chicken breast with the woody breast condition. *Poult. Sci.* 96, 3489–3494. doi: 10.3382/ps/pex118

Brothers, B., Zhuo, Z., Papah, M. B., and Abasht, B. (2019). RNA-seq analysis reveals spatial and sex differences in pectoralis major muscle of broiler chickens contributing to difference in susceptibility to wooden breast disease. *Front. Physiol.* 10:764. doi: 10.3389/fphys.2019.00764

Campo, M. D. M., Mur, L., Guerrero, A., Barahona, M., Resconi, V. C., Magalhaes, D. R., et al. (2020). Differentiating breast myopathies through color and texture analyses in broiler. *Foods* 9:824. doi: 10.3390/foods9060824

Chen, H., Wang, H. H., Qi, J., Wang, M., Xu, X., and Zhou, G. (2018). Chicken breast quality – normal, pale, soft and exudative (PSE) and woody – influences the functional properties of meat batters. *Int. J. Food Sci. Technol.* 53, 654–664. doi: 10.1111/ijfs.13640

Cheng, F., Shen, Y., Mohanasundaram, P., Lindström, M., Ivaska, J., Ny, T., et al. (2016). Vimentin coordinates fibroblast proliferation and keratinocyte differentiation in wound healing via tgf-β-slug signaling. *Proc. Natl. Acad. Sci. U.S.A.* 113, E4320–E4327. doi: 10.1073/pnas.1519197113

Clark, D. L., and Velleman, S. G. (2017). Spatial influence on breast muscle morphological structure, myofiber size, and gene expression associated with the wooden breast myopathy in broilers. *Poult. Sci.* 95, 2930–2945. doi: 10.3382/ps/pew243

Córdova-Noboa, H. A., Oviedo-Rondón, E. O., Sarsour, A. H., Barnes, J., Ferzola, P., Rademacher-Heilshorn, M., et al. (2018). Performance, meat quality, and pectoral myopathies of broilers fed either corn or sorghum based diets supplemented with guanidinoacetic acid. *Poult. Sci.* 97, 2479–2493. doi: 10.3382/ps/pey096

Greene, E., Cauble, R., Dhamad, A. E., Kidd, M. T., Kong, B., Howard, S. M., et al. (2020). Muscle metabolome profiles in woody breast-(un)affected broilers: effects of quantum blue phytase-enriched diet. *Front. Vet. Sci.* 7:458. doi: 10.3389/fvets.2020.00458

Griffin, J. R., Moraes, L., Wick, M., and Lilburn, M. S. (2018). Onset of white striping and progression into wooden breast as defined by myopathic changes underlying Pectoralis major growth. Estimation of growth parameters as predictors for stage of myopathy progression. *Avian Pathol.* 47, 2–13. doi: 10.1080/03079457.2017.1356908

Hosotani, M., Kawasaki, T., Hasegawa, Y., Wakasa, Y., Hoshino, M., Takahashi, N., et al. (2020). Physiological and pathological mitochondrial clearance is related to pectoralis major muscle pathogenesis in broilers with wooden breast syndrome. *Front. Physiol.* 11:579. doi: 10.3389/fphys.2020.00579

Kuttappan, V. A., Brewer, V. B., Mauromoustakos, A., McKee, S. R., Emmert, J. L., Meullenet, J. F., et al. (2013a). Estimation of factors associated with the occurence of white striping in broilr breast fillets. *Poult. Sci.* 92, 811–819. doi: 10.3382/ps.2012-02506

Kuttappan, V. A., Hargis, B. M., and Owens, C. M. (2016). White striping and woody breast myopathies in the modern poultry industry: a review. *Poult. Sci.* 95, 2724–2733. doi: 10.3382/ps/pew216

Kuttappan, V. A., Shivaprasad, H. l, Shaw, D. P., Valentine, B. A., Hargis, B. M., Clark, F. D., et al. (2013b). Pathological changes associated with white striping in broiler breast muscles. *Poult. Sci* 92, 331–338. doi: 10.3382/ps.2012-02646

Lorenzi, M., Mudalal, S., Cavani, C., and Petracci, M. (2014). Incidence of white striping under commercial conditions in medium and heavy broiler chickens in Italy. *J. Appl. Poult. Res.* 23, 754–758. doi: 10.3382/japr.2014-00968

Malila, Y., Thanatsang, K., Arayamethakorn, S., Uengwetwanit, T., Srimarut, Y., Petracci, M., et al. (2019). Absolute expressions of hypoxia-inducible factor-1 alpha (HIF1A) transcript and the associated genes in chicken skeletal muscle with white striping and wooden breast myopathies. *PLoS One* 14:e0220904. doi: 10.1371/journal.pone.0220904

Mazzoni, M., Soglia, F., Petracci, M., Sirri, F., Lattanzio, G., and Clavenzani, P. (2020). Fiber metabolism, procollagen and collagen type III immunoreactivity in broiler pectoralis major affected by muscle abnormalities. *Animals* 10:1081. doi: 10.3390/ani10061081

Montagna, F. S., Garcia, G., Nääs, I. A., Lima, N. D. S., and Caldara, F. R. (2019). Practical Assessment of spaghetti breast in diverse genetic strain broilers reared under different environments. *Rev. Bras. Cienc. Avic* 21:eRBCA-2019-0759. doi: 10.1590/1806-9061-2018-0759

Morey, A., Smith, A. E., Garner, L. J., and Cox, M. K. (2020). Application of bioelectrical impedance analysis to detect broiler breast filets affected with woody breast myopathy. *Front. Physiol.* 11:808. doi: 10.3389/fphys.2020.00808

Papah, M. B., Brannick, E. M., Schmidt, C. J., and Abasht, B. (2018). Gene expression profiling of the early pathogenesis of wooden breast disease in commercial broiler chickens using RNA-sequencing. *PLoS One* 13:e0207346. doi: 10.1371/journal.pone.0207346

Pascual, A., Trocino, A., Birolo, M., Cardazzo, B., Bordignon, F., Ballarin, C., et al. (2020). Dietary supplementation with sodium butyrate: growth, gut response at different ages, and meat quality of female and male broiler chickens. *Ital. J. Anim. Sci.* 19, 1135–1146. doi: 10.1080/1828051X.2020.1824590

Pascual, A., Trocino, A., Susta, L., and Barbut, S. (2021). Comparing three textural measurements of chicken breast fillets affected by severe wooden breast and spaghetti meat. *Ital. J. Anim. Sci.* 20, 465–471. doi: 10.1080/1828051X.2021.1893134

Petracci, M., Soglia, F., Madruga, M., Carvalho, L., Ida, E., and Estévez, M. (2019). Wooden-breast, white striping, and spaghetti meat: causes, consequences and consumer perception of emerging broiler meat abnormalities. *Compr. Rev. Food Sci. Food Saf.* 18, 565–583. doi: 10.1111/1541-4337.12431

Radaelli, G., Piccirillo, A., Birolo, M., Bertotto, D., Gratta, F., Ballarin, C., et al. (2017). Effect of age on the occurrence of muscle fiber degeneration associated with myopathies in broiler chickens submitted to feed restriction. *Poult. Sci.* 96, 309–319. doi: 10.3382/ps/pew270

Sanden, K. W., Bocker, U., Ofstad, R., Pedersen, M. E., Host, V., Afseth, N. K., et al. (2021). Characterization of collagen structure in normal, wooden breast and spaghetti meat chicken fillets by FTIR microspectroscopy and histology. *Foods* 10:548.

Sihvo, H. K., Airas, N., Lindén, J., and Puolanne, E. (2018). Pectoral vessel density and early ultrastructural changes in broiler chicken wooden breast myopathy. *J. Comp. Pathol.* 161, 1–10. doi: 10.1016/j.jcpa.2018.04.002

Sihvo, H. K., Immonen, K., and Puolanne, E. (2014). Myodegeneration with fibrosis and regeneration in the pectoralis major muscle of broilers. *Vet. Pathol.* 51, 619–623. doi: 10.1177/0300985813497488

Sirri, F., Maiorano, G., Tavaniello, S., Chen, J., Petracci, M., and Meluzzi, A. (2016). Effect of different levels of dietary zinc, manganese, and copper from organic or inorganic sources on performance, bacterial chondronecrosis, intramuscular collagen characteristics, and occurrence of meat quality defects of broiler chickens. *Poult. Sci.* 95, 1813–1824. doi: 10.3382/ps/pew064

Soglia, F., Laghi, L., Canonico, L., Cavani, C., and Petracci, M. (2016a). Functional property issues in broiler breast meat related to emerging muscle abnormalities. *Food Res. Int.* 89, 1071–1076. doi: 10.1016/j.foodres.2016.04.042

Soglia, F., Mazzoni, M., Zappaterra, M., Di Nunzio, M., Babini, E., Bordini, M., et al. (2020). Distribution and expression of vimentin and desmin in broiler pectoralis major affected by the growth-related muscular abnormalities. *Front. Physiol* 10:1581. doi: 10.3389/fphys.2019.01581

Soglia, F., Mudalal, S., Babini, E., Di Nunzio, M., Mazzoni, M., Sirri, F., et al. (2016b). Histology, composition, and quality traits of chicken Pectoralis major muscle affected by wooden breast abnormality. *Poult. Sci.* 95, 651–659. doi: 10.3382/ps/pev353

Soglia, F., Petracci, M., Davoli, R., and Zappaterra, M. (2021). A critical review of the mechanisms involved in the occurrence of growth-related abnormalities affecting broiler chickens breast muscle. *Poultry Sci.* 100:101180. doi: 10.1016/j.psj.2021.101180

Soglia, F., Silva, A. K., Lião, L. M., Laghi, L., and Petracci, M. (2019a). Effect of broiler breast abnormality and freezing on meat quality and metabolites assessed by 1 H-NMR spectroscopy. *Poult. Sci.* 98, 7139–7150. doi: 10.3382/ps/pez514

Soglia, F., Silva, A. K., Tappi, S., Lião, L. M., Rocculi, P., Laghi, L., et al. (2019b). Gaping of pectoralis minor muscles: Magnitude and characterization of an emerging quality issue in broilers. *Poult. Sci.* 98, 6194–6204. doi: 10.3382/ps/pez418

Tasoniero, G., Bertram, H. C., Young, J. F., Dalle Zotte, A., and Puolanne, E. (2017). Relationship between hardness and myowater properties in Wooden Breast affected chicken meat: a nuclear magnetic resonance study. *LWT* 86, 20–24. doi: 10.1016/J.LWT.2017.07.032

Tasoniero, G., Zhuang, H., Gamble, G. R., and Bowker, B. C. (2020). Effect of spaghetti meat abnormality on broiler chicken breast meat composition and technological quality. *Poult. Sci.* 99, 1724–1733. doi: 10.1016/j.psj.2019.10.069

Trocino, A., Piccirillo, A., Birolo, M., Radaelli, G., Bertotto, D., Filiou, E., et al. (2015). Effect of genotype, gender and feed restriction on growth, meat quality and the occurrence of white striping and wooden breast in broiler chickens. *Poult. Sci.* 94, 2996–3004. doi: 10.3382/ps/pev296

Xing, T., Zhao, X., Cai, L., Guanghong, Z., and Xu, X. (2017). Effect of salt content on gelation of normal and wooden breast myopathy chicken pectoralis major meat batters. *Int. J. Food Sci. Technol.* 52, 2068–2077. doi: 10.1111/ijfs.13485

Young, J. F., and Rasmussen, M. K. (2020). Differentially expressed marker genes and glycogen levels in pectoralis major of Ross308 broilers with wooden breast syndrome indicates stress, inflammation and hypoxic conditions. *Food Chem. Mol. Sci.* 1:100001. doi: 10.1016/j.fochms.2020.100001

Yu, X., Feng, Y., Bowker, B., and Zhuang, H. (2020). Expressible fluid measurements of broiler breast meat affected by emerging muscle abnormalities. *LWT* 133:110110. doi: 10.1016/j.lwt.2020.110110

Zampiga, M., Laghi, L., Petracci, M., Zhu, C., Meluzzi, A., Dridi, S., et al. (2018). Effect of dietary arginine to lysine ratios on productive performance, meat quality, plasma and muscle metabolomics profile in fast-growing broiler chickens. *J. Anim. Sci. Biotechnol.* 9:79. doi: 10.1186/s40104-018-0294-5

Zampiga, M., Soglia, F., Baldi, G., Petracci, M., Strasburg, G. M., and Sirri, F. (2020). Muscle abnormalities and meat quality consequences in modern turkey hybrids. *Front. Physiol.* 11:554. doi: 10.3389/fphys.2020.00554

Conflict of Interest: The authors declare that the research was conducted in the absence of any commercial or financial relationships that could be construed as a potential conflict of interest.

The reviewer EP declared a past co-authorship, with one of the authors, FS, to the handling editor.

frontiers in Physiology

ORIGINAL RESEARCH
published: 01 June 2021
doi: 10.3389/fphys.2021.667814

Effect of Temperature and Selection for Growth on Intracellular Lipid Accumulation and Adipogenic Gene Expression in Turkey Pectoralis Major Muscle Satellite Cells

*Jiahui Xu[1], Gale M. Strasburg[2], Kent M. Reed[3] and Sandra G. Velleman[1]**

[1] Department of Animal Sciences, The Ohio State University, Wooster, OH, United States, [2] Department of Food Science and Human Nutrition, Michigan State University, East Lansing, MI, United States, [3] Department of Veterinary and Biomedical Sciences, University of Minnesota, St. Paul, MN, United States

OPEN ACCESS

Edited by:
Krystyna Pierzchala-Koziec, University of Agriculture in Krakow, Poland

Reviewed by:
Monika Proszkowiec-Weglarz, United States Department of Agriculture, United States
Paul Siegel, Virginia Tech, United States

***Correspondence:**
Sandra G. Velleman
Velleman.1@osu.edu

Specialty section:
This article was submitted to Avian Physiology, a section of the journal Frontiers in Physiology

Received: *14 February 2021*
Accepted: *05 May 2021*
Published: *01 June 2021*

Citation:
Xu J, Strasburg GM, Reed KM and Velleman SG (2021) Effect of Temperature and Selection for Growth on Intracellular Lipid Accumulation and Adipogenic Gene Expression in Turkey Pectoralis Major Muscle Satellite Cells. Front. Physiol. 12:667814. doi: 10.3389/fphys.2021.667814

As multipotential stem cells, satellite cells (SCs) have the potential to express adipogenic genes resulting in lipid synthesis with thermal stress. The present study determined the effect of temperature on intracellular lipid synthesis and adipogenic gene expression in SCs isolated from the pectoralis major (p. major) muscle of 7-day-old fast-growing modern commercial (NC) turkeys compared to SCs from unselected slower-growing turkeys [Randombred Control Line 2 (RBC2)]. Since proliferating and differentiating SCs have different responses to thermal stress, three incubation strategies were used: (1) SCs proliferated at the control temperature of 38°C and differentiated at 43° or 33°C; (2) SCs proliferated at 43° or 33°C and differentiated at 38°C; or (3) SCs both proliferated and differentiated at 43°, 38°, or 33°C. During proliferation, lipid accumulation increased at 43°C and decreased at 33°C with the NC line showing greater variation than the RBC2 line. During proliferation at 43°C, peroxisome proliferator-activated receptor-γ (*PPARγ*) and neuropeptide-Y (*NPY*) expression was reduced to a greater extent in the NC line than the RBC2 line. At 33°C, expression of *PPARγ*, *NPY*, and CCAAT/enhancer-binding protein-β (*C/EBPβ*) was upregulated, but only in the RBC2 line. During differentiation, both lines showed greater changes in lipid accumulation and in *C/EBPβ* and *NPY* expression if the thermal challenge was initiated during proliferation. These data suggest that adipogenic gene expression is more responsive to thermal challenge in proliferating SCs than in differentiating SCs, and that growth-selection has increased temperature sensitivity of SCs, which may significantly affect breast muscle structure and composition.

Keywords: adipogenic potential, selection for growth, muscle, satellite cell, temperature

INTRODUCTION

Satellite cells (SCs) are a heterogenous stem cell population (Schultz, 1974; Kuang et al., 2007; Biressi and Rando, 2010; Smith et al., 2013; Tierney and Sacco, 2016), functioning in hypertrophic growth of post-hatch muscle (Moss and Leblond, 1971; Cardiasis and Cooper, 1975). As multipotential stem cells (Asakura et al., 2001; Shefer et al., 2004), SCs with appropriate external stimuli have the potential to spontaneously convert to other lineages such as adipocytes (Asakura et al., 2001; Csete et al., 2001; Shefer et al., 2004; Redshaw and Loughna, 2012). Environmental temperature is an external stimulus that has been shown to alter the cellular function and fate of SCs in chickens (Halevy et al., 2001; Harding et al., 2015; Piestun et al., 2017; Patael et al., 2019) and turkeys (Clark et al., 2016, 2017; Xu et al., 2021). Piestun et al. (2017) and Patael et al. (2019) showed when chickens were challenged with chronic heat stress immediately after hatch for 2 weeks, proliferation of SCs was suppressed while fat deposition was increased in the pectoralis major (p. major; breast) muscle. In contrast, continuous cold stress for the same period of time increased chicken p. major muscle satellite cell (pmSC) proliferation without affecting fat content of the breast muscle (Patael et al., 2019). *In vitro* studies with cultured pmSCs from both chickens (Harding et al., 2015) and turkeys (Clark et al., 2017) have demonstrated an increased amount of intracellular lipid with heat stress. The increased lipid content was hypothesized to arise from the conversion of pmSCs to an adipogenic-like lineage under the thermal stress.

Conversion of SCs to an adipogenic-like lineage is regulated by adipogenic regulatory factors like peroxisome proliferator-activated receptor-gamma (*PPARγ*) (Tontonoz et al., 1994; Rosen et al., 1999; Vettor et al., 2009) and some members in the CCAAT/enhancer-binding protein (C/EBP) family (Freytag et al., 1994; Wu et al., 1995; Rosen and Macdougald, 2006) as well as the kruppel like factor (KLF) family (Rosen and Macdougald, 2006; Tahmasebi et al., 2013; Wu and Wang, 2013). The protein *C/EBPβ* is expressed during the initiation stages of adipogenesis leading to an adipogenic differentiation pathway (Ntambi and Young-Cheul, 2000). The expression of *C/EBPβ* promotes the transcription of *PPARγ* during intermediate stages of adipogenic differentiation (Wu et al., 1995; Clarke et al., 1997; Ntambi and Young-Cheul, 2000). The *PPARγ* is required to stimulate adipogenesis of multiple types of cells including myoblasts (Hu et al., 1995; Holst et al., 2003) and pre-adipocytes (Chawla et al., 1994; Bastie et al., 1999). After being challenged with chronic heat stress immediately after hatch, chicks exhibit increased intramuscular fat deposition coupled with increased *C/EBPβ* expression in the breast muscle (Piestun et al., 2017; Patael et al., 2019). Furthermore, both heat and cold stress modulates the adipogenic characteristics of pmSCs in chickens (Harding et al., 2015) and turkeys (Clark et al., 2017) through altering the expression of *C/EBPβ* and *PPARγ*. Taken together, these findings suggest post-hatch thermal stress may affect lipid homeostasis of pmSCs, in part, by modifying the expression of adipogenic transcriptional factors. The family of KLFs are zinc-finger transcriptional factors (Kaczynski et al., 2003) consists of members involved in adipogenesis (Wu and Wang, 2013). Some members like KLF1 (Zhang et al., 2015) and KLF7 (Kawamura et al., 2006; Cho et al., 2007) are mainly expressed in pre-adipocytes, and inhibit adipogenic differentiation. Thus, KLF1 and KLF7 are regarded as pre-adipocyte markers.

The secretory peptide, Neuropeptide-Y (NPY), functions as an extracellular signal regulating adipogenesis by interacting with NPY receptors (Yang et al., 2008; Baker et al., 2009; Shipp et al., 2016). The expression of *NPY* promotes lipid deposition by promoting adipogenesis (Kuo et al., 2007; Baker et al., 2009; Zhang et al., 2015; Shipp et al., 2016) and inhibiting lipolysis (Valet et al., 1990; Park et al., 2014; Zhang et al., 2014; Liu et al., 2017). At the transcriptional level, *NPY* was the gene in turkey pmSCs most downregulated by cold stress during differentiation (Reed et al., 2017). With heat stress, increased expression of *NPY* and its receptors was observed in turkey pmSCs (Clark et al., 2018). Because NPY promotes chicken adipocyte adipogenesis through regulating *PPARγ* and *C/EBPα* expression (Zhang et al., 2015), it may act as an upstream signal regulating adipogenic transcriptional factors during thermal-stress-induced adipogenic response in avian SCs.

Birds are homotherms and maintain their body temperature in a limited range (Yahav, 2000, 2015). For newly hatched poults, it is difficult to control body temperature due to an immature thermal regulatory system (Dunnington and Siegel, 1984; Modrey and Nichelmann, 1992; Shinder et al., 2007). Furthermore, SCs exhibit their peak mitotic activity (Mozdziak et al., 1994; Halevy et al., 2000) and temperature sensitivity (Halevy et al., 2001; Piestun et al., 2017; Patael et al., 2019; Halevy, 2020) during the first week after hatch. Newly hatched birds are frequently exposed to both hot and cold temperatures during handling and transportation from hatcheries to growing facilities. Heat stress during this period increases fat deposition in chicken breast muscle (Zhang et al., 2012; Patael et al., 2019; Halevy, 2020), which parallels the increased intracellular lipid content of cultured pmSCs in heat challenged chickens (Harding et al., 2015) and turkeys (Clark et al., 2017). Thus, early age thermal stress may detrimentally affect breast muscle structure and composition by altering the adipogenic properties of pmSCs.

Faster-growing chickens produce more metabolic heat than shower-growing lines because of a higher metabolic rate (Konarzewski et al., 2000). In addition, faster-growing heavy weight meat-type chickens have reduced capacity for heat dissipation due to their reduced breast muscle capillary density (Hoving-Bolink et al., 2000; Yahav, 2000; Havenstein et al., 2003; Joiner et al., 2014). Thus, when exposed to thermal stress, faster-growing poultry have reduced thermal tolerance (Berrong and Washburn, 1998; Yahav, 2000; Chiang et al., 2008), resulting in prolonged negative effects on breast muscle structure and growth (Joiner et al., 2014; Piestun et al., 2017; Patael et al., 2019). The proliferation rate and differentiation level of pmSCs in growth-selected faster-growing turkeys is more responsive to both heat and cold stress than non-selected slower-growing turkeys (Clark et al., 2016; Xu et al., 2021). In addition, proliferating pmSCs are more sensitive to both heat and cold stress than differentiating pmSCs (Xu et al., 2021).

The objective of the current study was to determine the effects of both heat and cold stress and selection for growth on

intracellular lipid accumulation and adipogenic regulatory gene expression in pmSCs from 7-day-old Nicholas Commercial (NC) turkeys compared to those from Randombred Control Line 2 (RBC2) turkeys. The commercial turkeys used in this study were selected for growth characteristics including high growth rate and heavy breast muscling, whereas the RBC2 turkeys represent commercial turkeys in the mid-1960s (Nestor et al., 1969) and are slower-growing turkeys without heavy breast muscling. The temperature regimens used in the current study included all the possible combinations of heat and cold stress during pmSC proliferation and/or differentiation as reported by Xu et al. (2021). These regimens allowed a complete assessment of the effect of thermal stress on the adipogenic characteristics of the pmSCs from the two genetic lines. Data from the current study will provide insight on how thermal stress and selection for growth characteristics affects the synthesis of lipid by pmSCs during proliferation and differentiation *in vitro*. These findings have potential application in the development of management strategies to control lipid production by pmSCs which has been reported to affect the fiber organization and cellular properties of the breast muscle (Velleman et al., 2014; Patael et al., 2019).

MATERIALS AND METHODS

Pectoralis Major Muscle Satellite Cell Culture

Satellite cells were isolated from the p. major muscle of 7-day-old RBC2 turkeys and 7-day-old NC turkeys based on the method of Velleman et al. (2000). All the cells were passaged to a fourth pass and stored in liquid nitrogen until use.

Three different experimental strategies were used in the present study: (1) pmSCs proliferated at 38°C (control) and differentiated at 43° or 33°C; (2) pmSCs proliferated at 43° or 33°C and differentiated at 38°C; or (3) pmSCs both proliferated and differentiated at 43°, 38°, or 33°C (**Table 1**). Cell culture procedures were based on the method of Velleman (2014). In brief, 15,000 of cells were plated in each well of 24-well plates (Greiner Bio-One, Monroe, NC, United States) in Dulbecco's Modified Eagle's Medium (DMEM) (Sigma-Aldrich, St. Louis, MO, United States) plating medium containing 10% chicken serum (Gemini Bio-Products, West Sacramento, CA, United States), 5% horse serum (Gemini Bio-Products), 1% antibiotics-antimycotics (Gemini Bio-Products), and 0.1% gentamicin (Gemini Bio-Products). For cell attachment, the cells were initially incubated in a 95% air/5% CO2 incubator (Thermo Fisher Scientific, Waltham, MA, United States) at 38°C for 24 h. After attachment, the plating medium was replaced with McCoy's 5A growth medium (Sigma-Aldrich) containing 10% chicken serum (Gemini Bio-Products), 5% horse serum (Gemini Bio-Products), 1% antibiotics-antimycotics (Gemini Bio-Products), and 0.1% gentamicin (Gemini Bio-Products). The growth medium was refreshed every 24 h for 72 h. After 72 h of proliferation, the growth medium was replaced with a DMEM differentiation medium containing 3% horse serum, 1% antibiotics-antimycotics, 0.1% gentamicin, 0.1% gelatin, and 1 mg/mL bovine serum albumin (BSA) (Sigma-Aldrich) for 72 h of differentiation. The differentiation medium was changed every 24 h for 72 h.

TABLE 1 | Incubation strategies during satellite cell proliferation and differentiation.

	Temperature (°C)	
	Proliferation[1]	Differentiation[2]
Regimen 1	38	43
	38	38
	38	33
Regimen 2	43	38
	38	38
	33	38
Regimen 3	43	43
	38	38
	33	33

[1]*From 0 to 72 h of proliferation.*
[2]*From 0 to 72 h of differentiation.*

Intracellular Lipid Content Measurement

AdipoRed fluorochrome (Lonza, Walkersville, MD, United States) was used to quantify intracellular lipid content in pmSCs every 24 h during 72 h of proliferation and every 24 h during 72 h of differentiation according to the manufacturer's procedure. One plate from each treatment group was collected and was assayed at each sampling time. First, the medium was removed from each plate. Second, phosphate buffered saline (PBS) (pH 7.08), which contained 137 mM of NaCl, 2.68 mM of KCl,1.47 mM of KH_2PO_4, and 7.81 mM of Na_2HPO_4, was used to rinse the plate twice. Third, another 1 mL of PBS containing 30 μL of AdipoRed was added to each well. One well with only 1 mL PBS without AdipoRed was used as a negative control. After incubating for 15 min, the AdipoRed levels were quantified based on the fluorescence absorbance at a wavelength of 485 nm in a plate reader (Fluoroskan Ascent FL, ThermoElectron Co., Waltham, MA, United States). The AdipoRed assay was repeated in three independent cultures with four wells per treatment group per cell line.

Gene Expression Analysis

Effect of thermal stress and selection for growth on the expression of adipogenic regulatory factors was determined. Cells were cultured according to the temperature strategies outlined in **Table 1** and was sampled at 72 h of proliferation and at 48 h of differentiation. Extraction of total RNA from each sample was conducted using RNAzol (Molecular Research Center, Cincinnati, OH, United States) based on manufacturer's procedures. The concentration of each RNA sample was quantified with a spectrophotometer (NanoDrop™ ND-1000, Thermo Fisher Scientific). Reverse transcription was performed using Moloney Murine Leukemia Virus Reverse Transcriptase (M-MLV) (Promega, Madison, WI, United States) to produce cDNA from total RNA. Real-Time Quantitative PCR (RT-qPCR) was conducted using DyNAmo Hot Start SYBR Green qPCR kit (Thermo Fisher Scientific) to quantify the expression of

TABLE 2 | Primer sequences for real-time quantitative polymerase chain reaction.

Primer	Sequence	Product size	GenBank accession number
PPARγ [1]	5′-CCA CTG CAG GAA CAG AAC AA-3′ (forward)	249 bp[7]	XM_010718432.1
	5′-CTC CCG TGT CAT GAA TCC TT-3′ (reverse)		
C/EBPβ[2]	5′-GCA CAG CGA CGA GTA CAA G-3′ (forward)	82 bp	XM_003212165.2
	5′-GTT GCG CAT TTT GGC TTT GTC-3′ (reverse)		
NPY[3]	5′-CCC AGA GAC ACT GAT CTC AGA C-3′ (forward)	76 bp	XM_010712774.3
	5′-AGG GTC TTC AAA CCG GGA TCT-3′ (reverse)		
KLF1[4]	5′-CCC CGA CAT GAT GCA CAG GAT-3′ (forward)	157 bp	XM_422416.6
	5′-AGG CAG AGG GTA ATT GGG GC-3′ (reverse)		
KLF7[5]	5′-CCA TTG TGA CAG GTG TTT TTC C-3′ (forward)	152 bp	XM_010713480.2
	5′-TCT TGC AAG GCA GCA CAT TAT-3′ (reverse)		
GAPDH[6]	5′-GAG GGT AGT GAA GGC TGC TG-3′ (forward)	200 bp	U94327.1
	5′-CCA CAA CAC GGT TGC TGT AT-3′ (reverse)		

[1] *PPARγ, Peroxisome proliferator-activated receptor gamma.*
[2] *C/EBPβ, CCAAT/enhancer-binding protein beta.*
[3] *NPY, Neuropeptide Y.*
[4] *KLF1, Kruppel Like Factor 1.*
[5] *KLF7, Kruppel Like Factor 7.*
[6] *GAPDH, Glyceraldehyde-3-phosphate dehydrogenase.*
[7] *bp, number of base pairs.*

C/EBPβ, *KLF1*, *KLF7*, *NPY*, and *PPARγ*. Primers for *KLF1* and *KLF7* were designed using primer-BLAST tool on the website of National Center for Biotechnology Information. The amplification specificity of each primer was validated by sequencing the PCR product. Primers for *C/EBPβ*, *NPY*, *PPARγ*, and glyceraldehyde-3-phosphate dehydrogenase (*GAPDH*) (a normalizer) were previously designed and specificity confirmed (Velleman et al., 2014; Clark et al., 2017, 2018). Information of all the genes and primers is listed in **Table 2**. The RT-qPCR reaction was the following: 94°C for 15 min; amplification for 35 cycles; and final elongation at 72°C for 5 min in a DNA Engine Opticon 2 real-time machine (Bio-Rad, Hercules, CA, United States). Each amplification cycle was as follows: sample cDNA was denatured for 30 s at 94°C; annealed for 30 s at 60°C for *C/EBPβ* and *KLF1* or at 55°C for *GAPDH*, *KLF7*, *NPY*, and *PPARγ*; and elongated for 30 s at 72°C. According to the method of Liu et al. (2006), a standard curve of each gene was generated using serial dilutions of purified PCR products. Arbitrary concentrations from 1 to 100,000 were assigned to each serial dilution. Since the concentration of each amplified cDNA sample was within the concentration range of the corresponding stander curve, the arbitrary molar concentration of each amplified sample was calculated according to the threshold cycle. The arbitrary molar concentration of each cDNA sample was normalized using *GAPDH*. The RT-qPCR for each gene was repeated in three independent cultures with 12 wells per treatment group per cell line.

Statistical Model and Analysis

Data from the AdipoRed assay and RT-qPCR were analyzed as a completely randomized model at each sampling time in SAS (SAS 9.4, SAS Institute Inc., Cary, NC, United States). Main effect of temperature, main effect of cell line, interaction effect between temperature and cell line, and random effect of repeat experiment were included in this model. The statement of Least Square Means in the MIXED procedure was used to determine each mean value and the standard error of the mean (SEM). Differences between each mean were separated with the Pdiff option. Line effect within each treatment group and temperature effect within each cell line was determined with the SLICE option at each sampling time. For the AdipoRed assay, the REG procedure was used to evaluate the linear relationship between sampling times and optical densities of AdipoRed per cell line per treatment group. Difference in the linear relationship was determined with the Contrast statement. $P \leq 0.05$ was considered as statistically significant.

RESULTS

Effect of Thermal Stress and Selection for Growth on Intracellular Lipid Accumulation During Satellite Cell Proliferation

The effect of heat stress (43°C) on intracellular lipid accumulation in pmSCs from the RBC2 and NC turkeys was measured every 24 h during 72 h of proliferation (**Table 3**). Lipid content in both cell lines increased linearly throughout the duration of proliferation at both 38°C (NC slope: 5.11, RBC2 slope: 2.17) and 43°C (NC slope: 30.50, RBC2 slope: 17.85). The NC line had a greater increase (slope) in lipid content as a function of time at 38°C ($P < 0.001$) and 43°C ($P = 0.003$) than the RBC2 line. At 24 h, the NC line showed a significant increase ($P < 0.001$) in lipid content at 43°C than at 38°C. At 48 and 72 h, lipid content of both the RBC2 ($P \leq 0.001$) and NC ($P < 0.001$) lines was greater at 43°C than at 38°C. Lipid content of the RBC2

and NC lines increased 6.35-fold ($P < 0.001$) and 4.73-fold ($P < 0.001$) at 43°C than at 38°C at 72 h of proliferation, respectively. A significant interaction effect between temperature and cell line was observed at 24 h ($P = 0.002$) and 72 h ($P = 0.041$).

The effect of cold stress (33°C) on intracellular lipid accumulation in pmSCs from both lines was measured every 24 h during 72 h of proliferation (**Table 4**). Lipid content in pmSCs from both lines was slightly higher ($P < 0.001$) at 24 and 72 h than at 0 h at 33°C. At 48 and 72 h, both lines had lower lipid content ($P < 0.001$) at 33°C than at 38°C. Lipid content in the RBC2 and NC lines decreased 4.00-fold ($P = 0.003$) and 11.83-fold ($P < 0.001$) at 33°C compared to 38°C at 72 h of proliferation. There was a significant interaction effect between temperature and cell line at 24 h ($P = 0.014$), 48 h ($P = 0.004$), and 72 h ($P < 0.001$).

Effect of Thermal Stress and Selection for Growth on Intracellular Lipid Accumulation During Satellite Cell Differentiation

A heat stress (43°C) was administrated during the 72 h of proliferation and/or during the 72 h of differentiation. Treatment groups were 38°→43°C, 43°→38°C, and 43°→43°C, and these groups were compared to the 38°→38°C control group. Lipid content in pmSCs from both the RBC2 and NC lines was measured at 24, 48, and 72 h of differentiation (**Table 5**). At 24 h, a lower amount of lipid content was measured only in the NC line in the 38°→43°C group (1.52-fold, $P = 0.007$) than the 38°→38°C group, and no significant change in lipid content occurred in the RBC2 line ($P = 0.329$). Lipid content in the RBC2 and NC lines was 2.21-fold ($P < 0.001$) and 2.36-fold ($P < 0.001$) higher in the 43°→38°C group than the 38°→38°C group at 24 h. In the 43°→43°C group at 24 h, lipid content was 1.60-fold ($P = 0.002$) and 1.42-fold ($P < 0.001$) higher in the RBC2 and NC lines than the 38°→38°C group. Line effect was significant in the 38°→38°C ($P = 0.005$), 43°→38°C ($P < 0.001$), and 43°→43°C ($P = 0.002$) groups at 24 h. A significant interaction effect between temperature and cell line was observed at 24 h ($P < 0.001$). At 48 h, no significant difference in lipid content was observed in either line ($P > 0.118$) between the 38°→43°C and 38°→38°C groups. Lipid content was greater in the 43°→38°C group in both lines ($P < 0.001$) than the 38°→38°C group at 48 h. Greater lipid content was observed only in the NC line ($P = 0.002$) in the 43°→43°C group than the 38°→38°C group at 48 h. A significant line effect was observed in the 43°→38°C ($P < 0.001$) and 43°→43°C ($P = 0.017$) groups at 48 h. An interaction effect between temperature and cell line was not significant at 48 h ($P = 0.179$). At 72 h, no significant difference in lipid content was observed in either line in 38°→43°C ($P > 0.643$) and 43°→43°C ($P > 0.154$) groups than the 38°→38°C group. A slightly greater amount of lipid (1.53-fold, $P = 0.003$) was observed only in the RBC2 line in the 43°→38°C group than the 38°→38°C group at 72 h. Line effect was significant in the 38°→38°C ($P = 0.005$) and 38°→43°C ($P = 0.003$) groups at 72 h. No significant interaction effect was observed between temperature and cell line at 72 h ($P = 0.698$). From 24 to 72 h, a linear decrease in lipid content was observed in both lines in the 38°→38°C, 43°→38°C and 43°→43°C groups. In the 38°→38°C group, the NC line had a steeper linear reduction in lipid content than the RBC2 line (NC slope: −9.05, RBC2 slope: −5.56, $P < 0.001$). Lipid content in the NC line showed greater reduction than the RBC2 line in the 43°→38°C group (NC slope: −26.99, RBC2, slope: −14.35, $P < 0.001$). In the 43°→43°C group, both lines had a linear decrease in lipid content from 24 to 72 h (NC slope: −16.89, RBC2 slope: −11.79), and there was no line difference ($P = 0.067$).

A cold stress (33°C) was administrated during the 72 h of proliferation and/or during the 72 h of differentiation. Treatment groups were 38°→33°C, 33°→38°C, and 33°→33°C, and these groups were compared to the 38°→38°C control group. Lipid content in pmSCs from both lines was measured at 24, 48, and 72 h of differentiation (**Table 6**). At 24 h, lipid content was lower only in the RBC2 line in the 38°→33°C group (1.27-fold, $P = 0.035$) than the 38°→38°C group. Lipid content in the RBC2 and NC lines was 2.75-fold ($P < 0.001$) and 5.44-fold ($P < 0.001$) lower in the 33°→38°C group than the 38°→38°C group at 24 h. In the 33°→33°C group, lipid content was 2.80-fold ($P = 0.002$) and 6.13-fold ($P < 0.001$) lower in RBC2 and NC lines than the 38°→38°C group at 24 h. Line effects were significant in the 38°→38°C ($P < 0.001$) and 38°→33°C ($P < 0.001$) groups at 24 h. An interaction effect between temperature and cell line was significant at 24 h ($P < 0.001$). At 48 h, a greater amount of lipid was measured only in the NC line (1.45-fold, $P < 0.001$) in the 38°→33°C group than the 38°→38°C group. Lipid content in the RBC2 and NC lines was 2.36-fold ($P < 0.001$) and 2.95-fold ($P < 0.001$) lower in the 33°→38°C group than the 38°→38°C group at 48 h. In the 33°→33°C group, lipid content was 2.51-fold ($P = 0.002$) and 3.20-fold ($P < 0.001$) lower in RBC2 and NC lines than the 38°→38°C group at 48 h. A significant line effect occurred in the 38°→38°C ($P < 0.001$) and 38°→33°C ($P < 0.001$) groups at 48 h. There was an interaction effect between temperature and cell line at 48 h ($P < 0.001$). At 72 h, a slightly greater amount of lipid content was observed only in the RBC2 line in the 38°→33°C group (1.47-fold, $P < 0.001$) than the 38°→38°C group. Lipid content in the RBC2 and NC lines was 2.66-fold ($P < 0.001$) and 3.00-fold ($P < 0.001$) lower in the 33°→38°C group than the 38°→38°C group at 72 h. In the 33°→33°C group, lipid content was 3.48-fold ($P = 0.002$) and 3.56-fold ($P < 0.001$) lower in RBC2 and NC lines than the 38°→38°C group at 72 h. A line effect was significant in the 38°→38°C ($P = 0.001$) and 38°→33°C ($P < 0.001$) groups at 72 h. There was an interaction between the effect of temperature and cell line at 72 h ($P < 0.001$). From 24 to 72 h, the amount of lipid content in both lines was very low throughout the duration of the experiment in the 38°→33°C, 33°→38°C, and 33°→33°C groups. A minor linear reduction in lipid content was only observed in the NC line (slope: −5.06) in the 38°→33°C group from 24 to 72 h.

TABLE 3 | Effect of heat stress (43°C) on lipid accumulation during proliferation of satellite cells isolated from the pectoralis major muscle of Randombred Control Line 2 (RBC2) and Nicholas Commercial (NC) turkeys[1].

Line	Temperature (°C)	Sampling time				*P*-value[2]
		0 h	24 h	48 h	72 h	
RBC2	38	$0.06^{a,x} \pm 0.00$	$0.08^{c,yx} \pm 0.00$	$0.09^{c,y} \pm 0.02$	$0.23^{c,z} \pm 0.10$	<0.001
	43	$0.06^{a,y} \pm 0.00$	$0.08^{bc,y} \pm 0.00$	$0.17^{b,y} \pm 0.02$	$1.46^{b,z} \pm 0.10$	<0.001
NC	38	$0.06^{a,y} \pm 0.00$	$0.12^{a,y} \pm 0.00$	$0.12^{bc,y} \pm 0.02$	$0.44^{c,z} \pm 0.10$	<0.001
	43	$0.06^{a,y} \pm 0.00$	$0.10^{b,y} \pm 0.00$	$0.24^{a,y} \pm 0.02$	$2.08^{a,z} \pm 0.10$	<0.001
P-values[3]	L	0.552	<0.001	0.002	<0.001	
	T	0.070	0.082	<0.001	<0.001	
	L × T	0.351	0.002	0.211	0.041	

[1]*Value represents mean of AdipoRed optical density (OD/well) at 485 nm ± Standard error of mean (SEM).*
[2]*Effect of sampling time within each temperature and cell line.*
[3]*Effect of line (L), temperature (T), and line by temperature interaction (L × T) within each sampling time.*
$^{a-c}$*Mean of AdipoRed OD (mean ± SEM) within a column (sampling time) without a common letter are significantly different.*
$^{x-z}$*Mean of AdipoRed OD (mean ± SEM) within a row (temperature and cell line) without a common letter are significantly different.*
P ≤ 0.05 was considered as significantly different.

TABLE 4 | Effect of cold stress (33°C) on lipid accumulation during proliferation of satellite cells isolated from the pectoralis major muscle of Randombred Control Line 2 (RBC2) and Nicholas Commercial (NC) turkeys[1].

Line	Temperature (°C)	Sampling time				*P*-value[2]
		0 h	24 h	48 h	72 h	
RBC2	38	$0.05^{a,x} \pm 0.00$	$0.05^{by,x} \pm 0.00$	$0.08^{b,y} \pm 0.01$	$0.24^{b,z} \pm 0.04$	<0.001
	33	$0.04^{ab,y} \pm 0.00$	$0.07^{a,z} \pm 0.00$	$0.05^{c,y} \pm 0.01$	$0.06^{c,zy} \pm 0.04$	<0.001
NC	38	$0.04^{b,y} \pm 0.00$	$0.06^{a,y} \pm 0.00$	$0.10^{a,y} \pm 0.01$	$0.71^{a,z} \pm 0.04$	<0.001
	33	$0.05^{ab,zy} \pm 0.00$	$0.06^{ab,z} \pm 0.00$	$0.03^{c,y} \pm 0.01$	$0.06^{c,z} \pm 0.04$	0.009
P-values[3]	L	0.136	0.695	0.726	<0.001	
	T	0.822	0.190	<0.001	<0.001	
	L × T	0.110	0.014	0.004	<0.001	

[1]*Value represents mean of AdipoRed optical density (OD/well) at 485 nm ± Standard error of mean (SEM).*
[2]*Effect of sampling time within each temperature and cell line.*
[3]*Effect of line (L), temperature (T), and line by temperature interaction (L × T) within each sampling time.*
$^{a-c}$*Mean of AdipoRed OD (mean ± SEM) within a column (sampling time) without a common letter are significantly different.*
$^{x-z}$*Mean of AdipoRed OD (mean ± SEM) within a row (temperature and cell line) without a common letter are significantly different.*
P ≤ 0.05 was considered as significantly different.

Effect of Thermal Stress and Selection for Growth on Expression of Adipogenic Regulatory Genes

At 72 h of proliferation, *PPARγ* expression was lower ($P < 0.010$) in the NC line than the RBC2 line at 38°C (**Figures 1A,B**). The expression of *PPARγ* at 43°C was decreased 4.06-fold ($P < 0.001$) and 2.32-fold ($P < 0.001$) in the NC and RBC2 lines, respectively, compared to 38°C at 72 h of proliferation (**Figure 1A**). With cold stress (33°C), the expression of *PPARγ* was increased 2.02-fold ($P < 0.001$) and 1.88-fold ($P = 0.021$) in both the RBC2 and NC lines compared to the 38°C at 72 h of proliferation (**Figure 1B**). A significant interaction effect between temperature and cell line was observed at 33°C ($P = 0.015$, **Figure 1B**). At 48 h of differentiation, there was no difference in *PPARγ* expression between the two cell lines in the 38°→38°C group (**Figures 1C,D**). The expression of *PPARγ* was higher only in the RBC2 line (1.22-fold, $P = 0.012$) in the 38°→43°C group than the 38°→38°C group (**Figure 1C**). In the 43°→38°C group, *PPARγ* expression was reduced only in the NC line than the 38°→38°C group (1.41-fold, $P < 0.001$, **Figure 1C**). Both the RBC2 (1.53-fold, $P < 0.001$) and NC (1.86-fold, $P < 0.001$) lines showed a lower expression of *PPARγ* in the 43°→43°C group than the 38°→38°C group (**Figure 1C**). With the cold stress, *PPARγ* expression was upregulated in both the RBC2 (1.69-fold, $P = 0.002$) and NC (1.57-fold, $P = 0.003$) lines in the 38°→33°C group than the 38°→38°C group (**Figure 1D**). Higher expression of *PPARγ* occurred only in the RBC2 line SCs in the 33°→38°C (1.66-fold, $P = 0.002$) and 33°→33°C (2.91-fold, $P < 0.001$) groups than the 38°→38°C group at 48 h of differentiation (**Figure 1D**). Interaction effect between temperature and cell line was significant among the cold treatment groups ($P < 0.001$, **Figure 1D**).

TABLE 5 | Effect of heat stress (43°C) on lipid accumulation during differentiation of satellite cells isolated from the pectoralis major muscle of Randombred Control Line 2 (RBC2) and Nicholas Commercial (NC) line turkeys[1].

Line	Treatment group[2]	Sampling time			*P*-value[3]
		24 h	48 h	72 h	
RBC2	38 → 38	$0.43^{d,z} \pm 0.06$	$0.26^{def,y} \pm 0.03$	$0.17^{c,y} \pm 0.02$	<0.001
	38 → 43	$0.35^{d,z} \pm 0.06$	$0.21^{f,y} \pm 0.03$	$0.18^{c,y} \pm 0.02$	<0.001
	43 → 38	$0.95^{b,z} \pm 0.06$	$0.57^{b,y} \pm 0.03$	$0.26^{ab,x} \pm 0.02$	<0.001
	43 → 43	$0.69^{c,z} \pm 0.06$	$0.33^{d,y} \pm 0.03$	$0.15^{c,y} \pm 0.03$	<0.001
NC	38 → 38	$0.67^{c,z} \pm 0.06$	$0.30^{de,y} \pm 0.03$	$0.26^{ab,y} \pm 0.02$	<0.001
	38 → 43	$0.44^{d,z} \pm 0.06$	$0.24^{ef,y} \pm 0.03$	$0.27^{ab,y} \pm 0.02$	<0.001
	43 → 38	$1.58^{a,z} \pm 0.06$	$0.71^{a,y} \pm 0.03$	$0.32^{a,x} \pm 0.02$	<0.001
	43 → 43	$0.95^{b,z} \pm 0.06$	$0.42^{c,y} \pm 0.03$	$0.20^{bc,x} \pm 0.03$	<0.001
P-values[4]	L	<0.001	<0.001	<0.001	
	T	<0.001	<0.001	<0.001	
	L × T	<0.001	0.179	0.698	

[1] *Value represents mean of AdipoRed optical density (OD/well) at 485 nm ± Standard error of mean (SEM).*
[2] *Group name represents incubation temperature (°C) during proliferation → incubation temperature (°C) during differentiation.*
[3] *Effect of sampling time within each temperature and cell line.*
[4] *Effect of line (L), temperature (T), and line by temperature interaction (L × T) within each sampling time.*
$^{a-f}$ *Mean of AdipoRed OD (mean ± SEM) within a column (sampling time) without a common letter are significantly different.*
$^{x-z}$ *Mean of AdipoRed OD (mean ± SEM) within a row (temperature and cell line) without a common letter are significantly different.*
P ≤ 0.05 was considered as significantly different.

TABLE 6 | Effect of cold stress (33°C) on lipid accumulation during differentiation of satellite cells isolated from the pectoralis major muscle of Randombred Control Line 2 (RBC2) and Nicholas Commercial (NC) line turkeys[1].

Line	Treatment group[2]	Sampling time			*P*-value[3]
		24 h	48 h	72 h	
RBC2	38 → 38	$0.31^{b,z} \pm 0.02$	$0.27^{c,z} \pm 0.02$	$0.30^{c,z} \pm 0.02$	<0.001
	38 → 33	$0.24^{c,z} \pm 0.02$	$0.23^{c,z} \pm 0.02$	$0.25^{c,z} \pm 0.02$	0.649
	33 → 38	$0.11^{d,z} \pm 0.02$	$0.12^{d,z} \pm 0.02$	$0.11^{d,z} \pm 0.02$	0.717
	33 → 33	$0.11^{d,z} \pm 0.02$	$0.11^{d,z} \pm 0.02$	$0.09^{d,y} \pm 0.02$	<0.001
NC	38 → 38	$0.79^{a,z} \pm 0.02$	$0.43^{b,y} \pm 0.02$	$0.39^{b,y} \pm 0.02$	0.007
	38 → 33	$0.78^{a,z} \pm 0.02$	$0.62^{a,y} \pm 0.02$	$0.58^{a,y} \pm 0.02$	<0.001
	33 → 38	$0.15^{d,z} \pm 0.02$	$0.14^{d,z} \pm 0.02$	$0.13^{d,z} \pm 0.02$	0.759
	33 → 33	$0.13^{d,z} \pm 0.02$	$0.13^{d,z} \pm 0.02$	$0.11^{d,y} \pm 0.02$	0.023
P-values[4]	L	<0.001	<0.001	<0.001	
	T	<0.001	<0.001	<0.001	
	L × T	<0.001	<0.001	<0.001	

[1] *Value represents mean of AdipoRed optical density (OD/well) at 485 nm ± Standard error of mean (SEM).*
[2] *Group name represents incubation temperature (°C) during proliferation → incubation temperature (°C) during differentiation.*
[3] *Effect of sampling time within each temperature and cell line.*
[4] *Effect of line (L), temperature (T), and line by temperature interaction (L × T) within each sampling time.*
$^{a-d}$ *Mean of AdipoRed OD (mean ± SEM) within a column (sampling time) without a common letter are significantly different.*
$^{y-z}$ *Mean of AdipoRed OD (mean ± SEM) within a row (temperature and cell line) without a common letter are significantly different.*
P ≤ 0.05 was considered as significantly different.

At 72 h of proliferation, *C/EBPβ* was upregulated ($P < 0.001$) in the NC line than the RBC2 line at 38°C (**Figures 2A,B**). The expression of *C/EBPβ* was reduced 2.23-fold in the NC line ($P = 0.003$) whereas no difference ($P = 0.593$) was observed in the RBC2 line at 43°C compared to the 38°C at 72 h of proliferation (**Figure 2A**). With the cold stress of 33°C, a dramatic increase in *C/EBPβ* expression was observed in the RBC2 line (8.12-fold, $P < 0.001$) compared to the 38°C treatment at 72 h of proliferation, and no significant change ($P = 0.603$) was observed in the NC line (**Figure 2B**). There was a significant interaction effect between temperature and cell line at both 43°C ($P = 0.006$) and 33°C ($P < 0.001$, **Figures 2A,B**). At 48 h of differentiation, the expression of *C/EBPβ* was higher in the NC line ($P = 0.007$) than the RBC2 line in the 38°→38°C group (**Figures 2C,D**). In the 38°→43°C group, *C/EBPβ* expression was upregulated only in the RBC2 line

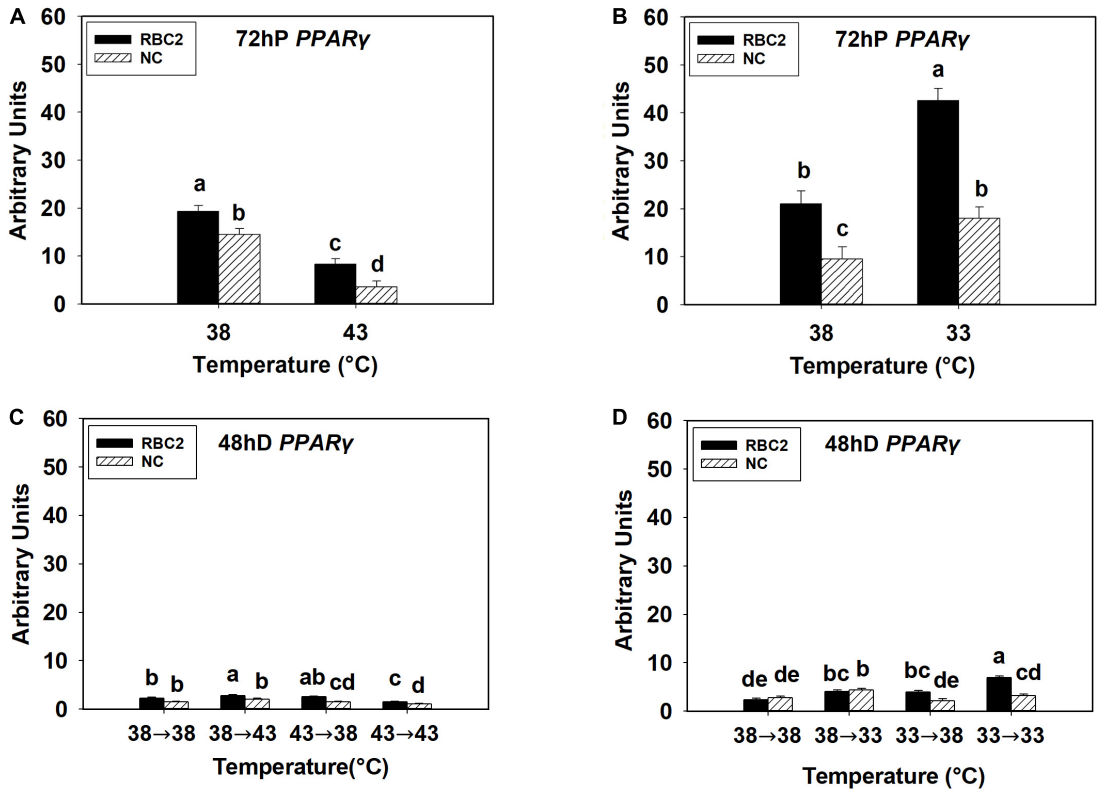

FIGURE 1 | Expression of peroxisome proliferator-activated receptor gamma (*PPARγ*) at 72 h of proliferation (72 hP) and 48 h of differentiation (48 hD) in satellite cells isolated from the pectoralis major (p. major) muscle of 7-day-old Randombred Control Line 2 (RBC2) and 7-day-old Nicholas Commercial (NC) turkeys. **(A)** Satellite cell proliferation at 38° or 43°C for 72 h. **(B)** Satellite cell proliferation at 38° or 33°C for 72 h. **(C)** Satellite cell proliferation for 72 h and differentiation for 48 h, both at 38°C (38°→38°C); proliferation at 38°C for 72 h and differentiation at 43°C for 48 h (38°→43°C); proliferation at 43°C for 72 h and differentiation at 38°C for 48 h (43°→38°C); or proliferation for 72 h and differentiation for 48 h, both at 43°C (43°→43°C). **(D)** Satellite cell proliferation for 72 h and differentiation for 48 h, both at 38°C (38°→38°C); proliferation at 38°C for 72 h and differentiation at 33°C for 48 h (38°→33°C); proliferation at 33°C for 72 h and differentiation at 38°C for 48 h (33°→38°C); or proliferation for 72 h and differentiation for 48 h, both at 33°C (33°→33°C). Each graph bar represents a mean arbitrary unit, and each error bar represents a standard error of the mean. Mean values without a same letter were significantly different ($P \leq 0.05$).

(2.62-fold, $P < 0.001$) than the 38°→38°C group (**Figure 2C**). Both the RBC2 and NC lines showed higher *C/EBPβ* expression in the 43°→38°C (NC: 1.94-fold, $P < 0.001$; RBC2: 2.68-fold, $P < 0.001$) and 43°→43°C (NC: 2.43-fold, $P < 0.001$, RBC2: 4.16-fold, $P < 0.001$) groups than the 38°→38°C group at 48 h of differentiation (**Figure 2C**). With the cold stress, the NC line showed a lower *C/EBPβ* expression in both the 33°→38°C (1.84-fold, $P < 0.001$) and 33°→33°C (3.06-fold, $P < 0.001$) groups than the 38°→38°C group (**Figure 2D**). In the RBC2 line, the expression of *C/EBPβ* was lower only in the 33°→33°C group (2.15-fold, $P = 0.002$) than the 38°→38°C group (**Figure 2D**). Interaction effect between temperature and cell line was significant among the cold treatment groups ($P = 0.042$, **Figure 2D**).

At 72 h of proliferation, *NPY* expression was lower ($P < 0.005$) in the NC line than the RBC2 line at 38°C (**Figures 3A,B**). The expression of *NPY* was downregulated in both the RBC2 (2.53-fold, $P < 0.001$) and NC (1.49-fold, $P = 0.049$) lines at 43°C compared to the 38°C at 72 h of proliferation (**Figure 3A**). At 33°C, the expression of *NPY* was increased 2.67-fold ($P < 0.001$) in the RBC2 line while no significant change ($P = 0.056$) was observed in the NC line compared to the 38°C at 72 h of proliferation (**Figure 3B**). A significant interaction effect between temperature and cell line was observed at both 43°C ($P = 0.003$) and 33°C ($P < 0.001$, **Figures 3A,B**). At 48 h of differentiation, *NPY* expression was higher in the NC line ($P = 0.002$) than the RBC2 line in the 38°→38°C group (**Figures 3C,D**). The expression of *NPY* was higher in the NC line in the 38°→43°C (1.74-fold, $P < 0.001$), 43°→38°C (1.76-fold, $P < 0.001$), and 43°→43°C (2.50-fold, $P < 0.001$) groups than the 38°→38°C group (**Figure 3C**). Greater *NPY* expression was observed in the RBC2 line (3.47-fold, $P < 0.001$) only in the 43°→43°C group than the 38°→38°C group (**Figure 3C**). With the cold stress, *NPY* expression was lower in both the RBC2 ($P < 0.001$) and NC ($P < 0.001$) lines in the 38°→33°C (NC: 3.98-fold, RBC2: 2.77-fold), 33°→38°C (NC: 10.48-fold, RBC2: 3.43-fold), and 33°→33°C (NC: 24.41-fold, RBC2: 3.69-fold) groups than the 38°→38°C group (**Figure 3D**). Interaction effect between temperature and cell line was significant among the cold treatment groups ($P < 0.001$, **Figure 3D**).

The *KLF1* expression was low in all the hot and cold treatment groups in both lines at both 72 h of proliferation and 48 h of

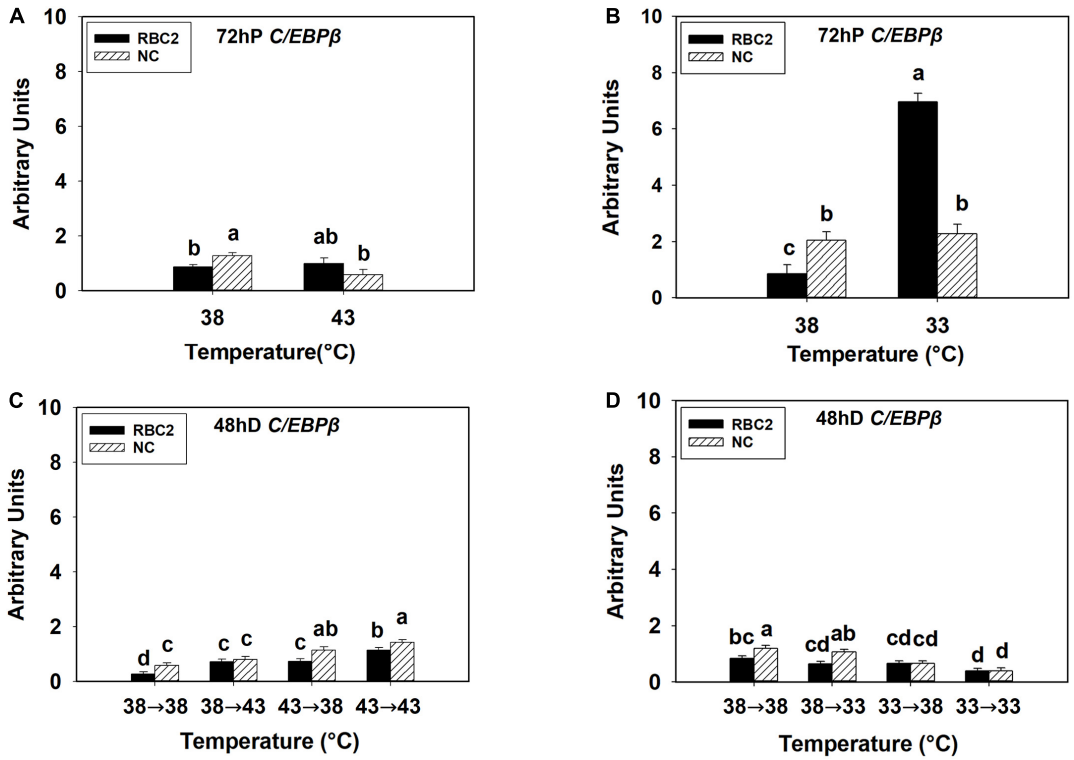

FIGURE 2 | Expression of CCAAT/enhancer-binding protein beta (*C/EBPβ*) at 72 h of proliferation (72 hP) and 48 h of differentiation (48 hD) in satellite cells isolated from the pectoralis major (p. major) muscle of 7-day-old Randombred Control Line 2 (RBC2) and 7-day-old Nicholas Commercial (NC) turkeys. **(A)** Satellite cell proliferation at 38° or 43°C for 72 h. **(B)** Satellite cell proliferation at 38° or 33°C for 72 h. **(C)** Satellite cell proliferation for 72 h and differentiation for 48 h, both at 38°C (38°→38°C); proliferation at 38°C for 72 h and differentiation at 43°C for 48 h (38°→43°C); proliferation at 43°C for 72 h and differentiation at 38°C for 48 h (43°→38°C); or proliferation for 72 h and differentiation for 48 h, both at 43°C (43°→43°C). **(D)** Satellite cell proliferation for 72 h and differentiation for 48 h, both at 38°C (38°→38°C); proliferation at 38°C for 72 h and differentiation at 33°C for 48 h (38°→33°C); proliferation at 33°C for 72 h and differentiation at 38°C for 48 h (33°→38°C); or proliferation for 72 h and differentiation for 48 h, both at 33°C (33°→33°C). Each graph bar represents a mean arbitrary unit, and each error bar represents a standard error of the mean. Mean values without a same letter were significantly different ($P \leq 0.05$).

differentiation (**Figures 4A–D**). At 72 h of proliferation, *KLF1* had greater expression in the RBC2 line ($P < 0.001$) than the NC line at 38°C (**Figures 4A,B**). The expression of *KLF1* was lower only in the RBC2 (1.66-fold, $P < 0.001$) line at 43°C compared to 38°C (**Figure 4A**). There was a significant interaction effect between temperature and cell line at 43°C ($P < 0.001$, **Figure 4A**). At the cold temperature of 33°C, *KLF1* expression was higher in the RBC2 line (1.59-fold, $P < 0.001$) while no significant ($P = 0.659$) difference was observed in the NC line compared to the 38°C at 72 h of proliferation (**Figure 4B**). At 48 h of differentiation, no difference in *KLF1* expression between the two cell lines ($P = 0.473$) was observed in the 38°→38°C group (**Figures 4C,D**). In the 38°→43°C group, reduction in *KLF1* expression occurred only in the RBC2 line (1.44-fold, $P = 0.045$) than the 38°→38°C group (**Figure 4C**). The expression of *KLF1* expression was slightly higher in both lines (NC: 1.59-fold, $P < 0.01$; RBC2: 1.23-fold, $P < 0.01$) in the 43°→43°C group than the 38°→38°C group (**Figure 4C**). With the cold stress, *KLF1* expression was upregulated only in the RBC2 line in the 38°→33°C (1.23-fold, $P = 0.033$) and 33°→38°C (1.24-fold, $P = 0.023$) groups than the 38°→33°C group (**Figure 4D**). In the 33°→33°C group, both the RBC2 (1.59-fold, $P < 0.001$) and NC (1.22-fold, $P = 0.017$) lines had higher expression of *KLF1* than the 38°→33°C group (**Figure 4D**). There was a significant interaction effect between temperature and cell line among the cold treatment groups ($P < 0.001$, **Figure 4D**).

The overall expression of *KLF7* was low in all the hot and cold treatment groups in both lines at both 72 h of proliferation and 48 h of differentiation (**Figures 5A–D**). At 72 h of proliferation, the NC line had higher expression of *KLF7* ($P < 0.001$) than the RBC2 line at 38°C (**Figures 5A,B**). The heat stress had no significant effect on *KLF7* expression ($P = 0.434$) in SCs from both lines at 72 h of proliferation (**Figure 5A**). The cold stress upregulated *KLF7* expression in the RBC2 line (3.5-fold, $P < 0.001$) but not in the NC line ($P = 0.175$) at 72 h of proliferation (**Figure 5B**). A significant interaction effect between temperature and cell line was observed at 33°C ($P < 0.001$, **Figure 5B**). At 48 h of differentiation, no significant difference in *KLF7* expression ($P = 0.087$) was observed between the two cell lines in the 38°→38°C group (**Figures 5C,D**). The expression of *KLF7* was higher only in the RBC2 line in the 38°→43°C (1.44-fold, $P = 0.004$) and 43°→43°C (1.64-fold, $P < 0.001$) groups than the 38°→38°C group (**Figure 5C**). The expression of *KLF7* slightly upregulated in both the RBC2 (1.32-fold, $P = 0.023$)

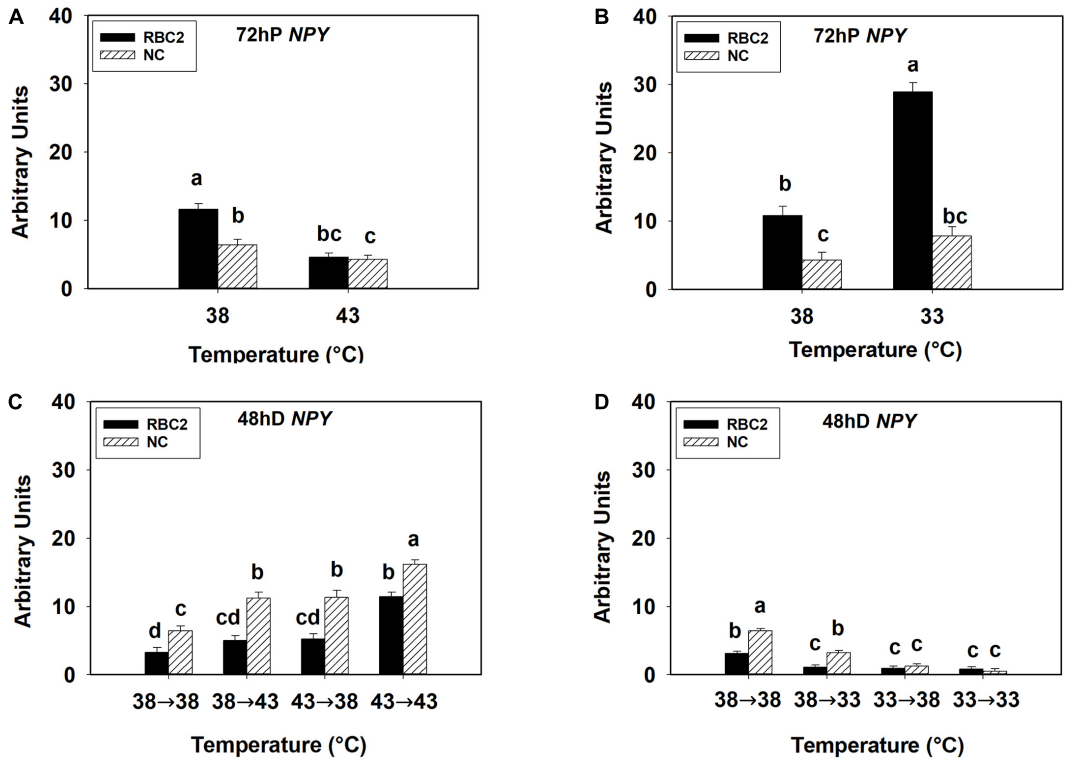

FIGURE 3 | Expression of neuropeptide Y (*NPY*) at 72 h of proliferation (72 hP) and 48 h of differentiation (48 hD) in satellite cells isolated from the pectoralis major (p. major) muscle of 7-day-old Randombred Control Line 2 (RBC2) and 7-day-old Nicholas Commercial (NC) turkeys. **(A)** Satellite cell proliferation at 38° or 43°C for 72 h. **(B)** Satellite cell proliferation at 38° or 33°C for 72 h. **(C)** Satellite cell proliferation for 72 h and differentiation for 48 h, both at 38°C (38°→38°C); proliferation at 38°C for 72 h and differentiation at 43°C for 48 h (38°→43°C); proliferation at 43°C for 72 h and differentiation at 38°C for 48 h (43°→38°C); or proliferation for 72 h and differentiation for 48 h, both at 43°C (43°→43°C). **(D)** Satellite cell proliferation for 72 h and differentiation for 48 h, both at 38°C (38°→38°C); proliferation at 38°C for 72 h and differentiation at 33°C for 48 h (38°→33°C); proliferation at 33°C for 72 h and differentiation at 38°C for 48 h (33°→38°C); or proliferation for 72 h and differentiation for 48 h, both at 33°C (33°→33°C). Each graph bar represents a mean arbitrary unit, and each error bar represents a standard error of the mean. Mean values without a same letter were significantly different ($P \leq 0.05$).

and the NC (1.48-fold, $P = 0.004$) lines in the 43°→38°C group than the 38°→38°C group (**Figure 5C**). With the cold treatment, higher *KLF7* expression occurred only in the NC line in the 38°→33°C (2.92-fold, $P < 0.001$) and 33°→38°C (2.81-fold, $P < 0.001$) groups than the 38°→38°C group (**Figure 5D**). In the 33°→33°C group, *KLF7* expression increased in the NC line (2.45-fold, $P = 0.004$) but decreased in the RBC2 line (2.51-fold, $P = 0.015$) than the 38°→38°C group (**Figure 5D**). Interaction effect between temperature and cell line was significant among the cold treatment groups ($P = 0.001$, **Figure 5D**).

DISCUSSION

Myogenic SCs are partially differentiated stem cells with multiple cellular fates (Asakura et al., 2001; Shefer et al., 2004) that respond to extrinsic stimuli including oxygen concentration (Csete et al., 2001; Redshaw and Loughna, 2012), nutritional status (Powell et al., 2014), and environmental temperature (Harding et al., 2015; Clark et al., 2017) resulting in changes in SC adipogenic characteristics (adipogenic gene expression or lipid synthesis). Post-hatch heat and cold stress has been shown to affect intramuscular fat content in the poultry breast muscle (Zhang et al., 2012; Piestun et al., 2017; Patael et al., 2019). The changes in intramuscular fat deposition may be, in part, attributable to the altered adipogenic potential of SCs (Smith and Johnson, 2014; Piestun et al., 2017; Patael et al., 2019).

During the immediate 7 days after hatch, SCs exhibit peak mitotic activity (Mozdziak et al., 1994; Halevy et al., 2000) and responsiveness to extrinsic temperatures (Halevy et al., 2001; Patael et al., 2019; Xu et al., 2021). Furthermore, selection for growth has increased the proliferation (Merly et al., 1998; Velleman et al., 2000) and thermal sensitivity (Clark et al., 2016; Xu et al., 2021) of pmSCs. Rossi et al. (2010) showed that faster-proliferating SCs have a greater potential to spontaneously express adipogenic characteristics than slower-proliferating populations. Thus, the present study determined the extent to which selection for higher growth rate and increased breast muscle yield at a processing age has altered the adipogenic potential of cultured 7-day-old pmSCs, as well as to identify differential adipogenic gene expression in pmSCs following a hot or cold thermal stress. A previous study by Clark et al. (2017) assessed the effect of both temperature

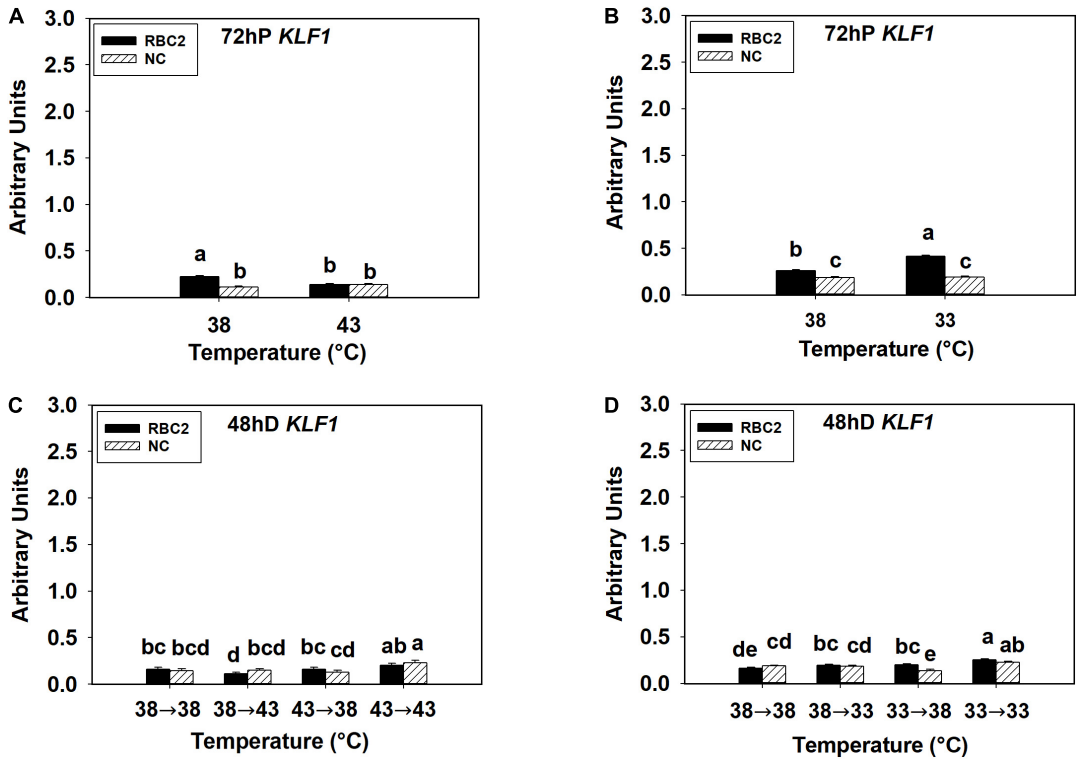

FIGURE 4 | Expression of kruppel like factor 1 (*KLF1*) at 72 h of proliferation (72 hP) and 48 h of differentiation (48 hD) in satellite cells isolated from the pectoralis major (p. major) muscle of 7-day-old Randombred Control Line 2 (RBC2) and 7-day-old Nicholas Commercial (NC) turkeys. **(A)** Satellite cell proliferation at 38° or 43°C for 72 h. **(B)** Satellite cell proliferation at 38° or 33°C for 72 h. **(C)** Satellite cell proliferation for 72 h and differentiation for 48 h, both at 38°C (38°→38°C); proliferation at 38°C for 72 h and differentiation at 43°C for 48 h (38°→43°C); proliferation at 43°C for 72 h and differentiation at 38°C for 48 h (43°→38°C); or proliferation for 72 h and differentiation for 48 h, both at 43°C (43°→43°C). **(D)** Satellite cell proliferation for 72 h and differentiation for 48 h, both at 38°C (38°→38°C); proliferation at 38°C for 72 h and differentiation at 33°C for 48 h (38°→33°C); proliferation at 33°C for 72 h and differentiation at 38°C for 48 h (33°→38°C); or proliferation for 72 h and differentiation for 48 h, both at 33°C (33°→33°C). Each graph bar represents a mean arbitrary unit, and each error bar represents a standard error of the mean. Mean values without a same letter were significantly different ($P \leq 0.05$).

and selection for growth on the adipogenic properties of 7-week-old pmSCs from non-commercial F-line turkeys that were selected from the RBC2 line only for increased 16-week body weight. The current study extends the previous work by comparing 7-day-old pmSCs from a contemporary commercial line with that of the RBC2 line. In addition, the effect of timing of the thermal stress during proliferation and/or differentiation on adipogenic potential of pmSCs was also examined.

Due to an asymmetric division strategy, not all daughter cells are committed to a myogenic pathway during proliferation (Kuang et al., 2007). Thus, proliferation is a critical period in which the cellular fate of SCs is determined by environmental temperature. Xu et al. (2021) showed that both hot and cold temperatures had a greater effect on myogenic differentiation if the thermal stress occurred during proliferation rather than only during differentiation. In the present study, heat-treated pmSCs from both lines had more intracellular lipid during late proliferation than late differentiation. In support of this finding, Clark et al. (2017) reported increased lipid synthesis in 7-week-old turkey pmSCs with hot temperatures during proliferation. Lipid content of both lines was increased to a higher extent during the earlier stages of differentiation (24 and 48 h) if the heat stress was applied during proliferation than only during differentiation. Heat stress-induced increases in intracellular lipid have been shown to result in a concomitant increase in intramuscular fat content and to have a prolonged effect on the structure and composition of the breast muscle (Piestun et al., 2017; Patael et al., 2019; Halevy, 2020).

Under cold temperatures, intracellular lipid decreased in both lines with the NC line showing a greater reduction than the RBC2 line during proliferation. In previous *in vitro* studies, a reduction in lipid content was observed in pmSCs from both chickens (Harding et al., 2015) and turkeys (Clark et al., 2017) with cold stress. This parallels the results from an *in vivo* study of Patael et al. (2019) that showed no significant intramuscular fat content in the p. major muscle of cold-stressed chickens. The decreased lipid content may arise from reduced pmSC proliferation (Clark et al., 2016; Harding et al., 2016; Xu et al., 2021). Furthermore, if the cold stress was applied during proliferation rather than only during differentiation, the reduction in lipid synthesis was greater in both lines. Thus, lipid synthesis in proliferating pmSCs was

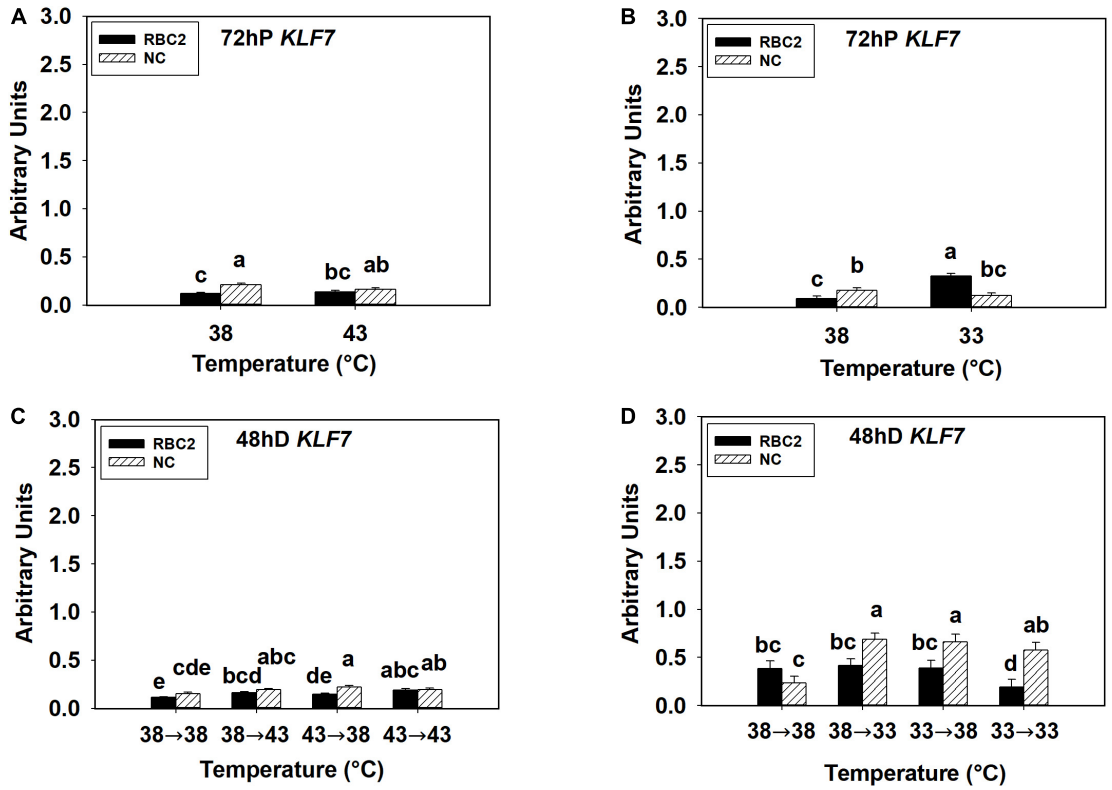

FIGURE 5 | Expression of kruppel like factor 7 (*KLF7*) at 72 h of proliferation (72 hP) and 48 h of differentiation (48 hD) in satellite cells isolated from the pectoralis major (p. major) muscle of 7-day-old Randombred Control Line 2 (RBC2) and 7-day-old Nicholas Commercial (NC) turkeys. **(A)** Satellite cell proliferation at 38° or 43°C for 72 h. **(B)** Satellite cell proliferation at 38° or 33°C for 72 h. **(C)** Satellite cell proliferation for 72 h and differentiation for 48 h, both at 38°C (38°→38°C); proliferation at 38°C for 72 h and differentiation at 43°C for 48 h (38°→43°C); proliferation at 43°C for 72 h and differentiation at 38°C for 48 h (43°→38°C); or proliferation for 72 h and differentiation for 48 h, both at 43°C (43°→43°C). **(D)** Satellite cell proliferation for 72 h and differentiation for 48 h, both at 38°C (38°→38°C); proliferation at 38°C for 72 h and differentiation at 33°C for 48 h (38°→33°C); proliferation at 33°C for 72 h and differentiation at 38°C for 48 h (33°→38°C); or proliferation for 72 h and differentiation for 48 h, both at 33°C (33°→33°C). Each graph bar represents a mean arbitrary unit, and each error bar represents a standard error of the mean. Mean values without a same letter were significantly different ($P \leq 0.05$).

more sensitive to both heat and cold stress than differentiating cells. In addition, the lack of detectable expression of the pre-adipocyte markers *KLF1* and *KLF7* during both proliferation and differentiation suggests a lack of pre-adipocytes in the turkey p. major muscle. This is not unexpected as most fat is deposited in abdominal and subcutaneous adipose depots and not as intramuscular fat in poultry (Cahaner et al., 1986; Crespo and Esteve-Garcia, 2002; Fereidoun et al., 2007). This finding also demonstrates the isolated pmSCs used in this study do not contain pre-adipocytes, and lipid synthesis is directly from the SCs. These data are supported by Shefer et al. (2004) who showed the spontaneous conversion of SCs to an adipogenic lineage. Taken together, these results suggest thermal stress may affect the properties of SCs including the synthesis of lipids, and proliferating SCs are more sensitive to temperature stimuli than differentiating SCs. Since poultry skeletal muscle SCs have their highest mitotic activity during the immediate 7 days after hatch (Mozdziak et al., 1994; Halevy et al., 2000), these data support that extrinsic temperature needs to be maintained at an optimal level to avoid possible harmful effects on breast muscle composition.

Another finding in the present study is that selection for growth for increased breast muscling may have enhanced adipogenic differences between the faster-growing NC pmSCs and the slower-growing RBC2 pmSCs. At 38°C during proliferation, the NC line pmSCs had a greater linear increase in lipid content than the RBC2 line. Similar to the findings of Velleman (2014) and Clark et al. (2017), pmSCs from the growth selected F-line turkeys expressed higher levels of the adipogenic genes *PPARγ* and *C/EBPα* than the RBC2 line during proliferation. The increased adipogenic potential may be partially attributed to the greater proliferation rate of the pmSCs in faster-growing turkeys (Velleman et al., 2000; Clark et al., 2016; Xu et al., 2021). Thus, it is possible that the increased proliferation rates of the growth-selected NC line pmSCs creates a larger SC pool, having a greater potential to express adipogenic properties.

During myogenic differentiation, most SCs are committed to a myogenic pathway, as reflected in the increased myogenic differentiation and enhanced expression of myogenic genes as previously shown (Clark et al., 2016; Xu et al., 2021). This may explain the gradual decrease in lipid synthesis observed in the hot and cold treatment groups in the current

study. Expression of *PPARγ* was significantly reduced during differentiation compared to proliferation in all the treatment groups independent of temperature. However, if the heat stress was continued throughout proliferation and differentiation (43°→43°C), expression of *NPY* and *C/EBPβ* increased in both lines compared to other treatment groups (38°→38°C, 38°→43°C, and 43°→38°C), and the NC line showed the highest increase. Taken together with the results by Xu et al. (2021), the NC line pmSCs tended to generate a larger cell pool than the RBC2 line with heat stress. This suggests that a larger pool of SCs may have a greater adipogenic potential even during myogenic differentiation. Furthermore, these results also suggest an intrinsic difference in adipogenic potential between the NC and RBC2 lines during myogenic differentiation, as the NC line pmSCs expressed more *NPY* and *C/EBPβ* than the RBC2 line in the control group.

In addition to the intrinsic difference in adipogenic potential, selection for growth may have altered the sensitivity of turkey breast muscle to temperature stimuli. Faster-growing poultry lines tend to have larger diameter myofibers from excessive hypertrophic SC-mediated muscle growth in the breast muscle than slower-growing lines (Wilson et al., 1990; Dransfield and Sosnicki, 1999; Velleman et al., 2003; Joiner et al., 2014). As an anaerobic muscle (Smith and Fletcher, 1988), chicken breast muscle has a reduced capillary supply compared to aerobic muscles, and this is exacerbated in faster-growing chickens (Hoving-Bolink et al., 2000; Yahav, 2000; Havenstein et al., 2003; Joiner et al., 2014). The circulatory supply is necessary to remove lactic acid, the byproduct of anaerobic respiration. The presence of excessively large myofibers typically found in growth-selected breast muscles further limits circulatory supply resulting in breast muscle degradation (Wilson et al., 1990; Velleman et al., 2003). Furthermore, because of a higher metabolic activity (Konarzewski et al., 2000), faster-growing chickens also produce more metabolic heat. Since birds are homeotherms and only keep body temperature within a limited interval (Yahav, 2000, 2015), heat cannot be as readily dissipated due to the reduced circulatory support in faster growing poultry. Therefore, faster-growing poultry has an impaired ability to cope with external thermal stress. In the current study, intracellular lipid synthesis in pmSCs from the faster-growing NC turkeys showed greater variations in response to the heat stress during both proliferation and differentiation than the RBC2 line. However, since the lipid content in pmSCs was higher in the NC line than the RBC2 line at 43°C, the intrinsic difference in lipid content between the two cell lines during proliferation was not affected by the heat stress. In contrast, cold stress eliminated this intrinsic difference between the two cell lines during proliferation. The 7-day-old pmSCs from the NC line tend to have increased myogenic differentiation and wider diameter myotubes than the RBC2 line with heat stress (Clark et al., 2016; Xu et al., 2021). Therefore, if faster-growing turkeys are exposed to a heat stress immediately after hatch, giant muscle fibers coupled with increased intramuscular fat content may occur in the breast muscle, resulting in prolonged negative effects on breast muscle structure and composition.

Adipogenic regulatory genes mediate the response to a thermal stress. The expression of both *NPY* and *PPARγ* expression was downregulated in the NC line during proliferation than the RBC2 line at the control temperature, and the expression of *NPY* and *PPARγ* was decreased with heat treatment during proliferation in both lines. A reduction in *PPARγ* and *C/EBPβ* expression in the heat-treated proliferating pmSCs was observed by Clark et al. (2017) as well. In chickens, a high fat diet downregulated *NPY*, *PPARγ*, and *C/EBPα* expression in both abdominal and subcutaneous adipose tissue (Wang et al., 2017). Furthermore, obesity resistance can be stimulated with a diet that is rich in fat and inhibits the expression of *NPY* and *PPARγ* in a rodent model (Cifani et al., 2015). In the current study, the increased intracellular lipid resulting from heat stress may act as an intracellular signal inhibiting *NPY* expression to suppress further lipid synthesis. As a key adipogenic transcription factor, *NPY* promotes lipid synthesis through the *PPARγ* pathway in pre-adipocytes in mice (Tang et al., 2015) and chickens (Zhang et al., 2015; Liu et al., 2017). In turkeys, PPARγ may also be a potential downstream regulator within the NPY-induced adipogenesis pathway in pmSCs, as both *NPY* and *PPARγ* showed a similar expression pattern at 72 h of proliferation in both lines. Alternatively, with cold stress, the expression of *NPY*, *PPARγ*, and *C/EBPβ* was decreased in the RBC2 line during proliferation. This reduction in expression may be stimulated by low intracellular lipid to prevent further loss of intracellular lipids in the RBC2 line. Furthermore, pmSCs from the NC line appear to have a reduced response to the cold-induced lipid loss than the RBC2 line, as neither *NPY* nor *C/EBPβ* showed significant change in the NC line at 33°C compared to the 38°C temperature during proliferation (*PPARγ* expression only showed a slight increase). Thus, when intracellular lipid was decreased with cold stress, pmSCs from the NC line may have difficulty regulating the lipid loss. This may explain why the cold-treated pmSCs from the NC line had a greater reduction in intracellular lipid than the RBC2 line during proliferation.

In summary, the current study showed that thermal stress alters the adipogenic potential of turkey pmSCs at 7-days of age. During pmSC proliferation, hot temperatures increased the intracellular lipid content in pmSCs while cold temperatures had the opposite effect. Proliferating pmSCs were more sensitive to both heat and cold stress in the determination of intracellular lipid content than differentiating pmSCs. The pmSCs from the faster-growing NC turkeys showed a higher lipid synthesis potential and their cellular fate was more sensitive to both heat and cold stress than the slower-growing RBC2 turkeys. The increased intracellular lipid accumulation of the heat-treated pmSCs may eventually promote intramuscular fat deposition *in vivo*, resulting in prolonged effects on turkey breast muscle structure and composition. Future studies will need to focus on defining the signal transduction pathways involved in the regulation of adipogenesis and their response to heat and cold stress.

DATA AVAILABILITY STATEMENT

The raw data supporting the conclusions of this article will be made available by the authors, without undue reservation.

ETHICS STATEMENT

Ethical review and approval was not required for the animal study because the study did not use any birds. Cell lines used in the study were previously isolated. Only satellite cells lines were used.

AUTHOR CONTRIBUTIONS

All authors have made a substantial and intellectual contribution to the work, and approved the submitted article. SV conceived and designed the experiments with GS and KR. JX performed the experiments and statistical analysis, and wrote the manuscript. SV, GS, and KR revised the manuscript.

FUNDING

This project was supported by the Agriculture and Food Research Initiative Competitive Grant No. 2020-67015-30827 from the United States Department of Agriculture to GS, KR, and SV.

REFERENCES

Asakura, A., Rudnicki, M. A., and Komaki, M. (2001). Muscle satellite cells are multipotential stem cells that exhibit myogenic, osteogenic, and adipogenic differentiation. *Differentiation* 68, 245–253. doi: 10.1046/j.1432-0436.2001.680412.x

Baker, S. B., Cohen, M., Kuo, L., Johnson, M., Al-Attar, A., and Zukowska, Z. (2009). The role of the neuropeptide Y-2 receptor in liporemodeling: NPY mediated adipogenesis and adipose graft maintenance. *Plast. Reconstr. Surg.* 123:486. doi: 10.1097/PRS.0b013e3181954c80

Bastie, C., Holst, D., Gaillard, D., Jehl-Pietri, C., and Grimaldi, P. A. (1999). Expression of peroxisome proliferator-activated receptor PPARdelta promotes induction of PPARgamma and adipocyte differentiation in 3T3C2 fibroblasts. *J. Biol. Chem.* 274, 21920–21925. doi: 10.1074/jbc.274.31.21920

Berrong, S. L., and Washburn, K. W. (1998). Effects of genetic variation on total plasma protein, body weight gains, and body temperature responses to heat stress. *Poult. Sci.* 77, 379–385. doi: 10.1093/ps/77.3.379

Biressi, S., and Rando, T. A. (2010). Heterogeneity in the muscle satellite cell population. *Semin. Cell Dev. Biol.* 21, 845–854. doi: 10.1016/j.semcdb.2010.09.003

Cahaner, A., Nitsan, Z., and Nir, I. (1986). Weight and fat content of adipose and nonadipose tissues in broilers selected for or against abdominal adipose tissue. *Poult. Sci.* 65, 215–222. doi: 10.3382/ps.0650215

Cardiasis, A., and Cooper, G. (1975). An analysis of nuclear number in individual muscle fiber during differentiation and growth: A satellite cell-muscle fiber growth unit. *J. Exp. Zool.* 191, 347–358. doi: 10.1002/jez.1401910305

Chawla, A., Schwarz, E. J., Dimaculangan, D. D., and Lazar, M. A. (1994). Peroxisome proliferator-activated receptor (PPAR) gamma: adipose-predominant expression and induction early in adipocyte differentiation. *Endocrinology* 135, 798–800. doi: 10.1210/endo.135.2.8033830

Chiang, W., Booren, A., and Strasburg, G. (2008). The effect of heat stress on thyroid hormone response and meat quality in turkeys of two genetic lines. *Meat Sci.* 80, 615–622. doi: 10.1016/j.meatsci.2008.02.012

Cho, S. Y., Park, P. J., Shin, H. J., Kim, Y. K., Shin, D. W., Shin, E. S., et al. (2007). (-)-Catechin suppresses expression of Kruppel-like factor 7 and increases expression and secretion of adiponectin protein in 3T3-L1 cells. *Am. J. Physiol. Endocrinol. Metabol.* 292, E1166–E1172. doi: 10.1152/ajpendo.00436.2006

Cifani, C., Micioni, Di Bonaventura, M. V., Pucci, M., Giusepponi, M. E., Romano, A., et al. (2015). Regulation of hypothalamic neuropeptides gene expression in diet induced obesity resistant rats: possible targets for obesity prediction? *Front. Neurosci.* 9:187. doi: 10.3389/fnins.2015.00187

Clark, D. L., Coy, C. S., Strasburg, G. M., Reed, K. M., and Velleman, S. G. (2016). Temperature effect on proliferation and differentiation of satellite cells from turkeys with different growth rates1. *Poult. Sci.* 95, 934–947. doi: 10.3382/ps/pev437

Clark, D. L., Mccormick, J. L., and Velleman, S. G. (2018). Effect of incubation temperature on neuropeptide Y and neuropeptide Y receptors in turkey and chicken satellite cells. *Comp. Biochem. Physiol. Part A Mol. Integr. Physiol.* 219-220, 58–66. doi: 10.1016/j.cbpa.2018.02.014

Clark, D. L., Strasburg, G. M., Reed, K. M., and Velleman, S. G. (2017). Influence of temperature and growth selection on turkey pectoralis major muscle satellite cell adipogenic gene expression and lipid accumulation. *Poult. Sci.* 96, 1015–1027. doi: 10.3382/ps/pew374

Clarke, S. L., Robinson, C. E., and Gimble, J. M. (1997). CAAT/enhancer binding proteins directly modulate transcription from the peroxisome proliferator-activated receptor γ2 promoter. *Biochem. Biophys. Res. Commun.* 240, 99–103. doi: 10.1006/bbrc.1997.7627

Crespo, N., and Esteve-Garcia, E. (2002). Dietary polyunsaturated fatty acids decrease fat deposition in separable fat depots but not in the remainder carcass. *Poult. Sci.* 81, 512–518. doi: 10.1093/ps/81.4.512

Csete, M., Walikonis, J., Slawny, N., Wei, Y., Korsnes, S., Doyle, J. C., et al. (2001). Oxygen-mediated regulation of skeletal muscle satellite cell proliferation and adipogenesis in culture. *J. Cell Physiol.* 189, 189–196. doi: 10.1002/jcp.10016

Dransfield, E., and Sosnicki, A. (1999). Relationship between muscle growth and poultry meat quality. *Poult. Sci.* 78, 743–746. doi: 10.1093/ps/78.5.743

Dunnington, E. A., and Siegel, P. B. (1984). Thermoregulation in newly hatched chicks. *Poult. Sci.* 63, 1303–1313. doi: 10.3382/ps.0631303

Fereidoun, H., Bahram, A., Soltanieh, K., Abbass, S., and Pouria, H. (2007). Mean percentage of skin and visible fat in 10 chicken carcass weight. *Int. J. Poult. Sci.* 6, 43–47. doi: 10.3923/ijps.2007.43.47

Freytag, S. O., Paielli, D. L., and Gilbert, J. D. (1994). Ectopic expression of the CCAAT/enhancer-binding protein alpha promotes the adipogenic program in a variety of mouse fibroblastic cells. *Genes Dev.* 8, 1654–1663. doi: 10.1101/gad.8.14.1654

Halevy, O. (2020). Timing is everything—The high sensitivity of avian satellite cells to thermal conditions during embryonic and posthatch periods. *Front. Physiol.* 11:235. doi: 10.3389/fphys.2020.00235

Halevy, O., Geyra, A., Barak, M., Uni, Z., and Sklan, D. (2000). Early posthatch starvation decreases satellite cell proliferation and skeletal muscle growth in chicks. *J. Nutr.* 130, 858–864. doi: 10.1093/jn/130.4.858

Halevy, O., Krispin, A., Leshem, Y., Mcmurtry, J. P., and Yahav, S. (2001). Early-age heat exposure affects skeletal muscle satellite cell proliferation and differentiation in chicks. *Am. J. Physiol. Regul. Integr. Comp. Physiol.* 281, R302–R309. doi: 10.1152/ajpregu.2001.281.1.R302

Harding, R. L., Clark, D. L., Halevy, O., Coy, C. S., Yahav, S., and Velleman, S. G. (2015). The effect of temperature on apoptosis and adipogenesis on skeletal muscle satellite cells derived from different muscle types. *Physiol. Rep.* 3:e12539. doi: 10.14814/phy2.12539

Harding, R. L., Halevy, O., Yahav, S., and Velleman, S. G. (2016). The effect of temperature on proliferation and differentiation of chicken skeletal muscle satellite cells isolated from different muscle types. *Physiol. Rep.* 4:e12770. doi: 10.14814/phy2.12770

Havenstein, G., Ferket, P., and Qureshi, M. (2003). Carcass composition and yield of 1957 versus 2001 broilers when fed representative 1957 and 2001 broiler diets. *Poult. Sci.* 82, 1509–1518. doi: 10.1093/ps/82.10.1509

Holst, D., Luquet, S., Kristiansen, K., and Grimaldi, P. A. (2003). Roles of peroxisome proliferator-activated receptors delta and gamma in myoblast transdifferentiation. *Exp. Cell Res.* 288, 168–176. doi: 10.1016/s0014-4827(03)00179-4

Hoving-Bolink, A. H., Kranen, R. W., Klont, R. E., Gerritsen, C. L., and De Greef, K. H. (2000). Fibre area and capillary supply in broiler breast muscle in relation to productivity and ascites. *Meat Sci.* 56, 397–402. doi: 10.1016/s0309-1740(00)00071-1

Hu, E., Tontonoz, P., and Spiegelman, B. M. (1995). Transdifferentiation of myoblasts by the adipogenic transcription factors PPAR gamma and C/EBP alpha. *PNAS* 92, 9856–9860. doi: 10.1073/pnas.92.21.9856

Joiner, K. S., Hamlin, G. A., Lien, A. R., and Bilgili, S. F. (2014). Evaluation of capillary and myofiber density in the pectoralis major muscles of rapidly growing, high-yield broiler chickens during increased heat stress. *Avian Dis.* 58, 377–382. doi: 10.1637/10733-112513-Reg.1

Kaczynski, J., Cook, T., and Urrutia, R. (2003). Sp1- and Kruppel-like transcription factors. *Genome Biol.* 4:206. doi: 10.1186/gb-2003-4-2-206

Kawamura, Y., Tanaka, Y., Kawamori, R., and Maeda, S. (2006). Overexpression of Kruppel-like factor 7 regulates adipocytokine gene expressions in human adipocytes and inhibits glucose-induced insulin secretion in pancreatic beta-cell line. *Mol. Endocrinol.* 20, 844–856. doi: 10.1210/me.2005-0138

Konarzewski, M., Gavin, A., Mcdevitt, R., and Wallis, I. R. (2000). Metabolic and organ mass responses to selection for high growth rates in the domestic chicken (Gallus domesticus). *Physiol. Biochem. Zool.* 73, 237–248. doi: 10.1086/316729

Kuang, S., Kuroda, K., Le Grand, F., and Rudnicki, M. A. (2007). Asymmetric self-renewal and commitment of satellite stem cells in muscle. *Cell* 129, 999–1010. doi: 10.1016/j.cell.2007.03.044

Kuo, L. E., Kitlinska, J. B., Tilan, J. U., Li, L., Baker, S. B., Johnson, M. D., et al. (2007). Erratum: Corrigenda: Neuropeptide Y acts directly in the periphery on fat tissue and mediates stress-induced obesity and metabolic syndrome. *Nat. Med.* 13, 1120–1120. doi: 10.1038/nm1611

Liu, C., Mcfarland, D. C., Nestor, K. E., and Velleman, S. G. (2006). Differential expression of membrane-associated heparan sulfate proteoglycans in the skeletal muscle of turkeys with different growth rates. *Poult. Sci.* 85, 422–428. doi: 10.1093/ps/85.3.422

Liu, L., Wang, G., Xiao, Y., Shipp, S. L., Siegel, P. B., Cline, M. A., et al. (2017). Peripheral neuropeptide Y differentially influences adipogenesis and lipolysis in chicks from lines selected for low or high body weight. *Comp. Biochem. Physiol. Part A Mol. Integr. Physiol.* 213, 1–10. doi: 10.1016/j.cbpa.2017.08.001

Merly, F., Magras-Resch, C., Rouaud, T., Fontaine-Perus, J., and Gardahaut, M. F. (1998). Comparative analysis of satellite cell properties in heavy- and lightweight strains of turkey. *J. Muscle Res. Cell Motil.* 19, 257–270. doi: 10.1023/a:1005329100247

Modrey, P., and Nichelmann, M. (1992). Development of autonomic and behavioural thermoregulation in turkeys (*Meleagris gallopavo*). *J. Therm. Biol.* 17, 287–292. doi: 10.1016/0306-4565(92)90035-E

Moss, F., and Leblond, C. (1971). Satellite cells as the source of nuclei in muscles of growing rats. *Anat. Rec.* 170, 421–435. doi: 10.1002/ar.1091700405

Mozdziak, P. E., Schultz, E., and Cassens, R. G. (1994). Satellite cell mitotic activity in posthatch turkey skeletal muscle growth. *Poult. Sci.* 73, 547–555. doi: 10.3382/ps.0730547

Nestor, K. E., Mccartney, M. G., and Bachev, N. (1969). Relative contributions of genetics and environment to turkey improvement. *Poult. Sci.* 48, 1944–1949. doi: 10.3382/ps.0481944

Ntambi, J. M., and Young-Cheul, K. (2000). Adipocyte differentiation and gene expression. *J. Nutr.* 130, 3122S–3126S. doi: 10.1093/jn/130.12.3122S

Park, S., Fujishita, C., Komatsu, T., Kim, S. E., Chiba, T., Mori, R., et al. (2014). NPY antagonism reduces adiposity and attenuates age-related imbalance of adipose tissue metabolism. *FASEB J.* 28, 5337–5348. doi: 10.1096/fj.14-258384

Patael, T., Piestun, Y., Soffer, A., Mordechay, S., Yahav, S., Velleman, S. G., et al. (2019). Early posthatch thermal stress causes long-term adverse effects on pectoralis muscle development in broilers. *Poult. Sci.* 98, 3268–3277. doi: 10.3382/ps/pez123

Piestun, Y., Patael, T., Yahav, S., Velleman, S. G., and Halevy, O. (2017). Early posthatch thermal stress affects breast muscle development and satellite cell growth and characteristics in broilers. *Poult. Sci.* 96, 2877–2888. doi: 10.3382/ps/pex065

Powell, D. J., Mcfarland, D. C., Cowieson, A. J., Muir, W. I., and Velleman, S. G. (2014). The effect of nutritional status and muscle fiber type on myogenic satellite cell fate and apoptosis. *Poult. Sci.* 93, 163–173. doi: 10.3382/ps.2013-03450

Redshaw, Z., and Loughna, P. T. (2012). Oxygen concentration modulates the differentiation of muscle stem cells toward myogenic and adipogenic fates. *Differentiation* 84, 193–202. doi: 10.1016/j.diff.2012.06.001

Reed, K. M., Mendoza, K. M., Strasburg, G. M., and Velleman, S. G. (2017). Response of turkey muscle satellite cells to thermal challenge. II. Transcriptome effects in differentiating cells. *Front. Physiol.* 8:948. doi: 10.3389/fphys.2017.00948

Rosen, E. D., and Macdougald, O. A. (2006). Adipocyte differentiation from the inside out. *Nat. Rev. Mol. Cell Biol.* 7, 885–896. doi: 10.1038/nrm2066

Rosen, E. D., Sarraf, P., Troy, A. E., Bradwin, G., Moore, K., Milstone, D. S., et al. (1999). PPARγ is required for the differentiation of adipose tissue in vivo and in vitro. *Mol. Cell* 4, 611–617. doi: 10.1016/s1097-2765(00)80211-7

Rossi, C. A., Pozzobon, M., Ditadi, A., Archacka, K., Gastaldello, A., Sanna, M., et al. (2010). Clonal characterization of rat muscle satellite cells: proliferation, metabolism and differentiation define an intrinsic heterogeneity. *PLoS One* 5:e8523. doi: 10.1371/journal.pone.0008523

Schultz, E. (1974). A quantitative study of the satellite cell population in postnatal mouse lumbrical muscle. *Anat. Rec.* 180, 589–595. doi: 10.1002/ar.1091800405

Shefer, G., Wleklinski-Lee, M., and Yablonka-Reuveni, Z. (2004). Skeletal muscle satellite cells can spontaneously enter an alternative mesenchymal pathway. *J. Cell Sci.* 117, 5393–5404. doi: 10.1242/jcs.01419

Shinder, D., Rusal, M., Tanny, J., Druyan, S., and Yahav, S. (2007). Thermoregulatory responses of chicks (Gallus domesticus) to low ambient temperatures at an early age. *Poult. Sci.* 86, 2200–2209. doi: 10.1093/ps/86.10.2200

Shipp, S. L., Cline, M. A., and Gilbert, E. R. (2016). Promotion of adipogenesis by neuropeptide Y during the later stages of chicken preadipocyte differentiation. *Physiol. Rep.* 4:e13006. doi: 10.14814/phy2.13006

Smith, D., and Fletcher, D. (1988). Chicken breast muscle fiber type and diameter as influenced by age and intramuscular location. *Poult. Sci.* 67, 908–913. doi: 10.3382/ps.0670908

Smith, L. R., Chambers, H. G., and Lieber, R. L. (2013). Reduced satellite cell population may lead to contractures in children with cerebral palsy. *Dev. Med. Child Neurol.* 55, 264–270. doi: 10.1111/dmcn.12027

Smith, S., and Johnson, B. (2014). *Marbling: Management of Cattle to Maximize the Deposition of Intramuscular Adipose Tissue (White Paper).* Colorado: National Cattlement's Beef Association.

Tahmasebi, S., Ghorbani, M., Savage, P., Yan, K., Gocevski, G., Xiao, L., et al. (2013). Sumoylation of Kruppel-like factor 4 inhibits pluripotency induction but promotes adipocyte differentiation. *J. Biol. Chem.* 288, 12791–12804. doi: 10.1074/jbc.M113.465443

Tang, H.-N., Man, X.-F., Liu, Y.-Q., Guo, Y., Tang, A.-G., Liao, E.-Y., et al. (2015). Dose-dependent effects of neuropeptide Y on the regulation of preadipocyte proliferation and adipocyte lipid synthesis via the PPAR γ pathways. *Endocr. J.* 62, 835–846. doi: 10.1507/endocrj.EJ15-0133

Tierney, M. T., and Sacco, A. (2016). Satellite Cell Heterogeneity in Skeletal Muscle Homeostasis. *Trends Cell Biol.* 26, 434–444. doi: 10.1016/j.tcb.2016.02.004

Tontonoz, P., Hu, E., and Spiegelman, B. M. (1994). Stimulation of adipogenesis in fibroblasts by PPARγ2, a lipid-activated transcription factor. *Cell* 79, 1147–1156. doi: 10.1016/0092-8674(94)90006-x

Valet, P., Berlan, M., Beauville, M., Crampes, F., Montastruc, J., and Lafontan, M. (1990). Neuropeptide Y and peptide YY inhibit lipolysis in human and dog fat cells through a pertussis toxin-sensitive G protein. *J. Clin. Investig.* 85, 291–295. doi: 10.1172/jci114425

Velleman, S. G. (2014). Effect of growth selection on adipogenic gene expression during the development of the turkey breast muscle. *Int. J. Poult. Sci.* 13:680. doi: 10.1172/JCI114425

Velleman, S. G., Anderson, J. W., Coy, C. S., and Nestor, K. E. (2003). Effect of selection for growth rate on muscle damage during turkey breast muscle development. *Poult. Sci.* 82, 1069–1074. doi: 10.1093/ps/82.7.1069

Velleman, S. G., Coy, C. S., and Emmerson, D. A. (2014). Effect of the timing of posthatch feed restrictions on the deposition of fat during broiler breast muscle development. *Poult. Sci.* 93, 2622–2627. doi: 10.3382/ps.2014-04206

Velleman, S. G., Liu, X., Nestor, K. E., and Mcfarland, D. C. (2000). Heterogeneity in growth and differentiation characteristics in male and female satellite cells isolated from turkey lines with different growth rates. *Comp. Biochem. Physiol. Part A Mol. Integr. Physiol.* 125, 503–509. doi: 10.1016/s1095-6433(00)00178-1

Vettor, R., Milan, G., Franzin, C., Sanna, M., De Coppi, P., Rizzuto, R., et al. (2009). The origin of intermuscular adipose tissue and its pathophysiological implications. *Am. J. Physiol.* 297, E987–E998. doi: 10.1152/ajpendo.00229.2009

Wang, G., Williams, C. A., Mcconn, B. R., Cline, M. A., and Gilbert, E. R. (2017). A high fat diet enhances the sensitivity of chick adipose tissue to the effects of centrally injected neuropeptide Y on gene expression of adipogenesis-associated factors. *Comp. Biochem. Physiol. Part A Mol. Integr. Physiol.* 211, 49–55. doi: 10.1016/j.cbpa.2017.06.006

Wilson, B. W., Nieberg, P. S., Buhr, R. J., Kelly, B. J., and Shultz, F. T. (1990). Turkey muscle growth and focal myopathy. *Poult. Sci.* 69, 1553–1562. doi: 10.3382/ps.0691553

Wu, Z., and Wang, S. (2013). Role of kruppel-like transcription factors in adipogenesis. *Dev. Biol.* 373, 235–243. doi: 10.1016/j.ydbio.2012.10.031

Wu, Z., Xie, Y., Bucher, N. L., and Farmer, S. R. (1995). Conditional ectopic expression of C/EBP beta in NIH-3T3 cells induces PPAR gamma and stimulates adipogenesis. *Genes Dev.* 9, 2350–2363. doi: 10.1101/gad.9.19.2350

Xu, J., Strasburg, G. M., Reed, K. M., and Velleman, S. G. (2021). Response of turkey pectoralis major muscle satellite cells to hot and cold thermal stress: Effect of growth selection on satellite cell proliferation and differentiation. *Comp. Biochem. Physiol. Part A Mol. Integr. Physiol.* 252:110823. doi: 10.1016/j.cbpa.2020.110823

Yahav, S. (2000). Domestic fowl-strategies to confront environmental conditions. *Poult. Avian Biol. Rev.* 11, 81–95.

Yahav, S. (2015). "Chapter 37 - Regulation of body temperature: strategies and mechanisms," in *Sturkie's Avian Physiology*, 6th Edn. (Cambridge, MA: Academic Press), 869–905. doi: 10.1016/B978-0-12-407160-5.00037-3

Yang, K., Guan, H., Arany, E., Hill, D. J., and Cao, X. (2008). Neuropeptide Y is produced in visceral adipose tissue and promotes proliferation of adipocyte precursor cells via the Y1 receptor. *FASEB J.* 22, 2452–2464. doi: 10.1096/fj.07-100735

Zhang, W., Bai, S., Liu, D., Cline, M. A., and Gilbert, E. R. (2015). Neuropeptide Y promotes adipogenesis in chicken adipose cells in vitro. *Comp. Biochem. Physiol. Part A Mol. Integr. Physiol.* 181, 62–70. doi: 10.1016/j.cbpa.2014.11.012

Zhang, W., Cline, M. A., and Gilbert, E. R. (2014). Hypothalamus-adipose tissue crosstalk: neuropeptide Y and the regulation of energy metabolism. *Nutr. Metab.* 11:27. doi: 10.1186/1743-7075-11-27

Zhang, Z. Y., Jia, G. Q., Zuo, J. J., Zhang, Y., Lei, J., Ren, L., et al. (2012). Effects of constant and cyclic heat stress on muscle metabolism and meat quality of broiler breast fillet and thigh meat. *Poult. Sci.* 91, 2931–2937. doi: 10.3382/ps.2012-02255

Conflict of Interest: The authors declare that the research was conducted in the absence of any commercial or financial relationships that could be construed as a potential conflict of interest.

frontiers in Physiology

ORIGINAL RESEARCH
published: 28 June 2021
doi: 10.3389/fphys.2021.691194

Insights Into Transcriptome Profiles Associated With Wooden Breast Myopathy in Broilers Slaughtered at the Age of 6 or 7 Weeks

Yuwares Malila[1], Tanaporn Uengwetwanit[1], Krittaporn V. Thanatsang[1], Sopacha Arayamethakorn[1], Yanee Srimarut[1], Massimiliano Petracci[2], Francesca Soglia[2], Wanilada Rungrassamee[1] and Wonnop Visessanguan[1]*

[1] National Center for Genetic Engineering and Biotechnology (BIOTEC), Thailand Science Park, Pathum Thani, Thailand, [2] Department of Agricultural and Food Sciences, Alma Mater Studiorum, University of Bologna, Cesena, Italy

OPEN ACCESS

Edited by:
Xiquan Zhang, South China Agricultural University, China

Reviewed by:
Takeshi Kawasaki, Research Office Concerning the Health of Humans and Birds, Japan
Eero Puolanne, University of Helsinki, Finland

***Correspondence:**
Yuwares Malila
yuwares.mal@biotec.or.th

Specialty section:
This article was submitted to Avian Physiology, a section of the journal Frontiers in Physiology

Received: *05 April 2021*
Accepted: *07 June 2021*
Published: *28 June 2021*

Citation:
Malila Y, Uengwetwanit T, Thanatsang KV, Arayamethakorn S, Srimarut Y, Petracci M, Soglia F, Rungrassamee W and Visessanguan W (2021) Insights Into Transcriptome Profiles Associated With Wooden Breast Myopathy in Broilers Slaughtered at the Age of 6 or 7 Weeks. Front. Physiol. 12:691194. doi: 10.3389/fphys.2021.691194

Transcriptomes associated with wooden breast (WB) were characterized in broilers at two different market ages. Breasts (*Pectoralis major*) were collected, 20-min postmortem, from male Ross 308 broilers slaughtered at 6 and 7 weeks of age. The breasts were classified as "non-WB" or "WB" based on palpation hardness scoring (non-WB = no abnormal hardness, WB = consistently hardened). Total RNA was isolated from 16 samples (n = 3 for 6 week non-WB, n = 3 for 6 week WB; n = 5 for 7 week non-WB, n = 5 for 7 week WB). Transcriptome was profiled using a chicken gene expression microarray with one-color hybridization technique, and compared between non-WB and WB samples of the same age. Among 6 week broilers, 910 transcripts were differentially expressed (DE) (false discovery rate, FDR < 0.05). Pathway analysis underlined metabolisms of glucose and lipids along with gap junctions, tight junction, and focal adhesion (FA) signaling as the top enriched pathways. For the 7 week broilers, 1,195 transcripts were identified (FDR < 0.05) with regulation of actin cytoskeleton, mitogen-activated protein kinase (MAPK) signaling, protein processing in endoplasmic reticulum and FA signaling highlighted as the enriched affected pathways. Absolute transcript levels of eight genes (actinin-1 – *ACTN1*, integrin-linked kinase – *ILK*, integrin subunit alpha 8 – *ITGA8*, integrin subunit beta 5 – *ITGB5*, protein tyrosine kinase 2 – *PTK2*, paxillin – *PXN*, talin 1 – *TLN1*, and vinculin – *VCL*) of FA signaling pathway were further elucidated using a droplet digital polymerase chain reaction. The results indicated that, in 6 week broilers, *ITGA8* abundance in WB was greater than that of non-WB samples ($p < 0.05$). Concerning 7 week broilers, greater absolute levels of *ACTN1*, *ILK*, *ITGA8*, and *TLN1*, accompanied with a reduced *ITGB5* were found in WB compared with non-WB ($p < 0.05$). Transcriptional modification of FA signaling underlined the potential of disrupted cell-cell communication that may incite aberrant molecular events in association with development of WB myopathy.

Keywords: broiler chicken, wooden breast, transcriptome profile, droplet digital polymerase chain reaction, focal adhesion

INTRODUCTION

Wooden breast (WB) abnormality, one of the emerging growth-related myopathies affecting chicken pectoral muscle, is characterized by hardened ridges extending from the cranial to the caudal regions of the breast (Sihvo et al., 2014). The abnormal breasts often exhibit pale color, surface hemorrhagic lesions, and clear viscous exudate on the surface (Barbut, 2019). Identified shortly after white striping (WS) abnormality, WB has abruptly raised a wide concern in the broiler industry worldwide (Sihvo et al., 2014; Velleman and Clark, 2015; de Carvalho et al., 2020; Xing et al., 2020) as it exerts remarkable adverse impacts on technological properties, including water holding capacity and texture, of chicken breasts (Chatterjee et al., 2016; Soglia et al., 2016; Tasoniero et al., 2016; Tijare et al., 2016; Cai et al., 2018; Malila et al., 2018; Madruga et al., 2019). Hence, it has caused tremendous economic losses. In United States alone, it was estimated that the growth-related myopathies had costed approximately 70,000 USD losses daily (Zanetti et al., 2018).

The actual etiology and the chronological events underlying development of WB are under extensive investigation. A growing evidence collected from scientific reports have pointed out the association between WB myopathy with artificial selection for rapid growth rate, enlarged muscle mass, and accelerated metabolism (Malila et al., 2018; Barbut, 2019; Petracci et al., 2019). The disproportionate muscles outgrew their supportive systems, particularly vascularization and oxygenation, leading to a series of molecular and ultrastructural disturbances that negatively affected myocellular integrity (Papah et al., 2018; Papah and Abasht, 2019; Maharjan et al., 2020; Abasht et al., 2021). Signs of phlebitis along with muscle damage and regeneration were observed as soon as 14 days of age in broilers (Papah et al., 2017; Radaelli et al., 2017). Damaged muscle fibers were replaced by collagen and adipose tissue and exhibited altered sarcomeric structure and functions (Papah et al., 2017; Velleman et al., 2017; Liu et al., 2020). Metabolic processes, ion homeostasis, as well as oxidative stress response mechanisms can be profoundly disrupted (Mutryn et al., 2015; Abasht et al., 2016; Kang et al., 2020). Soglia et al. (2020) recently demonstrated an increase in vimentin (VIM) and desmin (DES) in WB muscles compared with those of normal counterparts, suggesting the occurrence of intensive regenerative processes within these muscles. Muscle regeneration requires the donation of nuclei from satellite cells, the myogenic stem cells required in post-hatch skeletal muscle growth and regeneration (Velleman, 2015). In agreement with the on-going regenerative process in the presence of WB myopathy, numbers of total nuclei and mitotically active satellite cells were increased in the 43 day broilers compared with those of non-WB (Meloche et al., 2018). However, the mitotic activity of the satellite cell population was significantly altered in WB broiler, suggesting the compromised reparative capacity of the satellite cells in the abnormal birds (Ferreira et al., 2020).

Previous studies demonstrated the effects of age and hypertrophy on increasing the severity of muscle degeneration (Radaelli et al., 2017) and on the losses of satellite cells at both quantitative and functional characteristics, hence impairing muscle regeneration (Daughtry et al., 2017) in broilers. As described by Domingues-Faria et al. (2016), when skeletal muscle undergoes damage, pro-inflammatory cytokines recruit immune cells to the lesion site thus promoting migration and proliferation of satellite cells. Neutrophils take parts in the lysis of damaged cells as well as in phagocytosis to remove cell debris through apoptosis. The pro-inflammatory macrophages are then converted into anti-inflammatory phenotype to initiate differentiation of satellite cells, hence muscle repair. Overall, the repair process requires a well-regulated crosstalk between the muscle cells and the immune cells. In this regard, it is worth mentioning that, although affected by WB at a similar extent, broilers slaughtered at different ages might exhibit different molecular responses. Based on our previous study (Malila et al., 2018), the greater numbers of WB cases were found in the commercial broilers slaughtered at the age of 7 weeks in comparison to those slaughtered at 6 weeks. The increased WB severity was significantly related with the increased proportion of breast mass relative to carcass weight which was observed more in the group of 7-week-old broilers (Malila et al., 2018). Thus, performing further investigations may improve the knowledge relating to key biological processes associated with the development of WB. Here, the transcriptional profiles of non-WB and WB samples collected from commercial broilers at 6 and 7 weeks of age were assessed in order to investigate the progression of the muscular alterations occurring when the slaughter age was postponed.

MATERIALS AND METHODS

Samples and Sample Collection

The breast samples used in this study were collected from carcasses of Ross 308 broilers, males, reared in a commercial farm until the age of 6 weeks (6wk) or 7 weeks (7wk). All birds were slaughtered at a local industrial-scale slaughterhouse. After the scalding step, the carcasses were randomly collected from the processing line, the breasts were dissected, and classified as "non-WB" or "WB" based on the presence of hardened bulge ridges assessed by palpation (Sihvo et al., 2017). The WB samples used in this study could be classified as "severe WB" (>75% of the breast being extremely rigid and with diffuse coverage) (Sihvo et al., 2017; Petracci et al., 2019). A sample was excised from the cranial portion (approximately 1 cm deep from the ventral surface) of the muscle, cut into 1 cm^3 cubes, snap frozen in liquid nitrogen and stored at −80°C until RNA isolation.

Among the samples collected from 6 and 7-week-old birds, three and five samples were identified as WB, respectively. It is worth noting that all WB samples showed macroscopic characteristics of WS. The equal numbers of 6 and 7 week breast samples exhibiting no abnormal hardness were randomly selected to represent the non-WB group in this study. Hence, 16 selected samples were classified into four groups based on age and abnormality, i.e., 6wk; non-WB (n = 3), 6wk; WB (n = 3), 7wk; non-WB (n = 5), and 7wk; WB (n = 5).

Total RNA Isolation

Total RNA was isolated using TRIzol™ Reagent (Invitrogen), subsequently treated with DNase I (Thermo Scientific, Inc.) and re-purified using GeneJET RNA Cleanup and Concentration Micro Kit (Thermo Scientific, Inc.). The samples with an RNA Integrity Number exceeding 7.0 were analyzed by microarray hybridization at Molecular Genomics Pte., Ltd., (Singapore), quantitative real-time polymerase chain reaction (qPCR), and droplet digital PCR (ddPCR).

Microarray Hybridization and Data Analysis

The Agilent SurePrint G3 Custom GE 8 × 60 K chicken gene expression microarray (Agilent Technologies, Inc.) used in this study was designed based on the National Center for Biotechnology Information (NCBI) *Gallus gallus* Annotation Release 103.

One-color microarray hybridization was conducted as described in Malila et al. (2020). Briefly, total RNA was reverse transcribed into cDNA using an oligo(dT) as a primer. The cDNA was *in vitro* transcribed using T7 RNA polymerases to produce cyanine 3-CTP-labeled complementary RNA using a one-color low input quick amp labeling kit (Agilent) following the company's instruction. The purified cRNA (600 ng) was hybridized onto the Agilent SurePrint array at 65°C for 17 h. The array was subsequently scanned using an Agilent High Resolution Microarray Scanner (C Model, Agilent). The TIFF image was exported and analyzed using an Agilent Feature Extraction Software version V10.7.1.1 (Agilent).

Microarray probe quality control was processed using GeneSpring software. The signal values of probes that were not met the quality control were excluded from the analysis (Malila et al., 2020). The filtered raw data were normalized using quantile normalization (Bolstad, 2017) and combat normalization afterward (Müller et al., 2016; Leek et al., 2017) in R version 3.4.3 (R Core Team, 2017). Log_2 transformation was applied to normalized data for statistical analysis. Significant differences in the transcript abundance between non-WB vs WB samples belonging to each slaughter age group (6wk and 7wk) were assessed by *t*-test analyses for independent samples. Positive and negative fold change (FC) values represent increased or decreased expression of a particular gene in the WB samples relative to non-WB of the same slaughter age. The differentially expressed (DE) transcripts were identified using combined criteria of false discovery rate (FDR) ≤ 0.05 and absolute fold change ($|FC|$) ≥ 1.2. All DEGs of each comparison were mapped onto Kyoto Encyclopedia of Genes and Genomes (KEGG) pathway (Kanehisa et al., 2012) to identify possible biological interactions among them.

Confirmation of Differential Gene Expression

Changes in the expression patterns of the selected genes observed in the current microarray study were confirmed using qPCR (Malila et al., 2015). A total of 30 genes were chosen for confirming the microarray data. Primers (**Supplementary Table 1**) were designed using Primer-BLAST[1]. Threshold cycle (Ct) was analyzed using BioRad CFX Manager 2.1 software (BioRad). Hypoxanthine-guanine phosphoribosyltransferase (*HPRT*) was assigned as a reference gene as it showed no differences in expression due to WB development (data not shown). For each gene, relative transcript abundance in WB samples relative to non-WB of the same slaughter age was calculated based on $2^{-\Delta\Delta Ct}$ method (Livak and Schmittgen, 2001) and plot against FC analyzed from microarrays.

Absolute Expression of Genes in Focal Adhesion Signaling Pathway

Absolute expression of eight key genes involved in focal adhesion (FA) signaling pathway was evaluated using an EvaGreen droplet digital polymerase chain reaction (ddPCR) assay of cDNA produced from reverse-transcription reactions. The ddPCR primer sequences are shown in **Supplementary Table 1**. The 20-μL ddPCR mixture contained 1X EvaGreen®supermix (Bio-Rad Laboratories, Inc., Hercules, CA, United States), 0.25 μM of each forward and reverse primer, and cDNA template. The concentration of the template for each gene was specified in **Supplementary Table 1**. The template was replaced by an equal volume of nuclease-free water for no template control. The water-in-oil emulsion droplets were generated using a QX100™ droplet generator (Bio-Rad Laboratories, Inc.) according to the manufacturer's instruction. The droplets were transferred to a 96-well plate, heat sealed and placed into a conventional thermocycler (model T100™, Bio-Rad Laboratories, Inc.). The reaction conditions were 95°C for 5 min; followed by 40 cycles of 95°C for 30 s, 58°C for 1 min, and 4°C for 5 min; and 90°C for 5 min. After the amplification was completed, the plate was transferred to a QX200™ droplet reader (Bio-Rad Laboratories, Inc.) where fluorescent signal intensity of the droplets was measured. The fluorescence amplitude threshold was set under the high amplitude droplet cluster to distinguish positive and negative droplets. The detected droplets were analyzed in copies per 20-μL reaction by QuantaSoft™ software (Bio-Rad Laboratories, Inc.) and divided by the amount of cDNA added to the reaction to obtain the absolute copy numbers per nanogram of template.

The effects of slaughter age and occurrence of WB condition on absolute expression was analyzed based on 2 × 2 factorial analysis of variance. The significant level was set at $\alpha = 0.05$. The statistical analysis was performed using the R package version 3.4.3.

RESULTS

Differential Gene Expression in Chicken Skeletal Muscle Associated With Wooden Breast Abnormality

A total of 2,070 transcripts were differentially expressed between non-WB and WB samples (**Figure 1**). Among the broilers

[1]https://www.ncbi.nlm.nih.gov/tools/primer-blast/

slaughtered at the age of 6 weeks, 509 transcripts were up-regulated, and 401 transcripts were down-regulated in WB in comparison with non-WB samples. As for 7wk, 547 transcripts were up-regulated whereas 648 transcripts were down-regulated upon development of WB myopathy. Top 10 most up-regulated and down-regulated transcripts of the 6wk and 7wk samples are shown in **Tables 1**, **2**, respectively. As illustrated in Venn diagram (**Figure 1**), only 35 out of 2,070 DE transcripts were identified in both 6 and 7 week comparisons with comparable FC (**Table 3**), except for the transcript encoding four and a half LIM domains 5 (*FHL5*) which showed 1.6-fold decrease in 6wk WB but 1.4-fold increase in 7wk WB compared to the expression of their non-WB counterparts. The complete DE transcripts lists are available in **Supplementary Table 2**.

Differential expression from microarray analysis was further confirmed by using a qPCR (**Figure 2**). As for 6 wk samples, 40 DE transcripts were tested. The findings indicated that 35 counterparts, accounting for 87.5% of the total, exhibited similar trends (**Figure 2A**). For the 7wk broilers, 84 out of 88 FC values, accounting for 95.5%, obtained from qPCR showed similar trend with the microarray results (**Figure 2B**).

Functional and Pathway Analysis

Based on pathway analysis (**Figure 3**), alterations of metabolic pathways, cellular processes, particular transport and catabolism through phagosome, as well as cell communication *via* tight junction and FA, were highlighted in both 6wk and 7wk broilers. In 6wk group, metabolisms of purine and pyrimidine together with apoptosis, communication among cells through tight junction, gap junction, and FA were enriched altered pathways. Regulation of actin cytoskeleton signaling, mitogen−activated protein kinase (MAPK) signaling, protein processing in endoplasmic reticulum, FA, phagosome, and lysosome were enriched in the 7wk group.

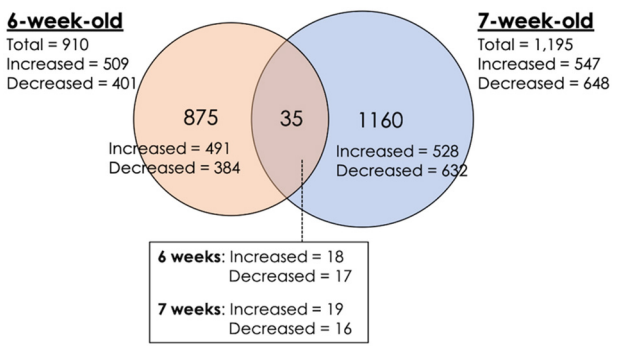

FIGURE 1 | Differential expression of transcripts associated with wooden breast (WB) myopathy in 6-week-old and 7-week-old broilers. Venn diagram depicts number of differentially expressed transcripts obtained from microarray study. Increased expression indicates the greater transcript abundance of the particular genes in WB sample relative to that of non-WB within the same slaughter age, vice versa for decreased expression. The criteria used in identification of differentially expressed transcripts are a combination between false discovery rate ≤ 0.05 and absolute fold change ($|FC|$) ≥ 1.2.

Changes in Absolute Expression of Key Genes in Focal Adhesion Signaling Pathway

Absolute expressions of eight genes in FA signaling were further elucidated using ddPCR (**Figure 4**). For 6 wk, only two genes, including integrin subunit alpha 8 (*ITGA8,* FC = 2.0) and protein tyrosine kinase 2 (*PTK2,* FC = −2.0), were found differentially expressed upon development of WB abnormality ($p < 0.05$). On the other hand, increases in actinin-1 (*ACTN1,* FC = 3.7), integrin-linked kinase (*ILK,* FC = 1.3), *ITGA8* (FC = 2.4), integrin beta subunit 5 (*ITGB5,* FC = 2.3), and talin 1 (*TLN1,* FC = 1.6) were observed in 7wk WB muscles in respect to their non-WB counterparts ($p < 0.05$). In addition, effects of different slaughtered ages on absolute transcript levels in WB muscles were detected for *ACTN1*, *PXN*, and *VCL* whereas such effects in non-WB muscles were observed for *ILK*, and *VCL* ($p < 0.05$).

DISCUSSION

Six-Week-Old Broilers

Metabolic processes of carbohydrates, glycerolipids, cofactors and vitamins, and nucleotides (i.e., purine and pyrimidine) were identified as enriched pathways associated with the development of WB in 6wk broilers (**Table 4** and **Figure 3**). These findings are in agreement with those obtained in previous studies performed on WB muscles (Mutryn et al., 2015; Abasht et al., 2016; Zambonelli et al., 2016). In detail, among the DE transcripts listed in the pathways (**Supplementary Table 3**), aldo-keto reductase (ARK), family 1 member D1 (*AKR1D1*, FC = 6.6) was also listed as the top up-regulated genes in 6wk WB if compared to their unaffected counterparts. Another gene encoding ARK family 1 member 10 (*ARK1B10*) was also increased for 2.6-fold. The ARK superfamily catalyzes oxidation-reduction reactions to detoxify aldehydes and ketones generated during metabolisms or in response to stresses (Huang et al., 2016). Increased expressions of those enzymes could be a consequence of the muscle fibers encountering stressful conditions associated with WB myopathy. In addition, an overexpression of *ARK1B10* was shown to elevate β-catenin, an activator of canonical Wnt signaling, in breast cancer cell lines (Qu et al., 2019). Within this context, the findings of the present study further support the hypothesis formulated by Phillips et al. (2020) in which, in the presence of WB myopathy, satellite cells could lose their capability of proliferation and differentiation due in part to an excessive activation of Wnt signaling pathway that, ultimately, results in the disruption of the muscle repair process.

Grouped in the category of endocrine signaling, alteration of insulin, peroxisome-proliferator-activated receptors (PPAR), and adipocytokine signaling were more pronounced in the 6wk broilers compared to 7wk samples (**Figure 3**). Dysfunction of those signaling pathways caused by, or in association with, excess adipose tissues and insulin resistance leads to negative metabolic effects (Mashek et al., 2007; Contreras et al., 2019). Lake and Abasht (2020) addressed the resemblance between metabolic complications and muscle structural features of WB

myopathy in broilers and that of diabetes in smooth and cardiac muscles of mammals. In this study (**Supplementary Table 3**), expressions of long-chain acyl-CoA ligase 1 (*ACSL1*), encoding the enzyme catalyzing conversion of fatty acid to acyl-CoA, and solute carrier family 27 member 2 (*SLC27A2*), which encodes fatty acid transporter protein (FATP), were reduced in WB at

TABLE 1 | Top 10 most differentially expressed transcripts associated with wooden breast in 6-week-old broilers.

NCBI accession#	Gene	Description	Fold change
NM_001277393.1	*AKR1D1*	Aldo-keto reductase family 1, member D1	6.6
XM_015285521.1	*AKR1D1*	Aldo-keto reductase family 1, member, transcript variant X1	5.7
XM_416766.5	*MAOB*	Monoamine oxidase B	4.8
XM_004936312.2	*SLC25A47*	Solute carrier family 25, member 47, transcript variant X2	4.5
XM_015284744.1	*COL12A1*	Collagen, type XII, alpha 1, transcript variant X5	4.5
XM_015284739.1	*COL12A1*	Collagen, type XII, alpha 1, transcript variant X1	4.4
XM_426381.4	*LOC428824*	SITS-binding protein-like, transcript variant X1	4.4
XM_015287785.1	*SLC25A47*	Solute carrier family 25, member 47, transcript variant X4	4.3
XM_015287786.1	*SLC25A47*	Solute carrier family 25, member 47, transcript variant X5	4.3
XM_015287784.1	*SLC25A47*	Solute carrier family 25, member 47, transcript variant X3	4.2
XR_001469765.1	*LOC419389*	Uncharacterized (miscellaneous RNA)	−5.6
XM_015301040.1	*LOC107055967*	SUN domain-containing protein 3-like	−5.8
XM_015282302.1	*LOC770405*	SUN domain-containing protein 3-like, transcript variant X2	−6.4
XM_015282298.1	*LOC107052644*	SUN domain-containing protein 3-like, transcript variant X2	−6.5
XM_015282297.1	*LOC107052644*	SUN domain-containing protein 3-like, transcript variant X1	−6.6
XM_015282299.1	*LOC107052644*	SUN domain-containing protein 3-like, transcript variant X3	−6.6
XM_015282303.1	*LOC770405*	SUN domain-containing protein 3-like, transcript variant X3	−6.6
XM_015282300.1	*LOC107052644*	SUN domain-containing protein 3-like, transcript variant X4	−6.6
XM_015282301.1	*LOC770405*	SUN domain-containing protein 3-like, transcript variant X1	−6.7
XM_015286039.1	*GFRA4*	GDNF family receptor alpha 4, transcript variant X1	−7.3

Positive fold change, highlighted in red, and negative fold change, highlighted in green, indicate increase and decrease, respectively, in transcript abundance in wooden breast muscle samples collected from commercial broilers at 6 weeks of age.

TABLE 2 | Top 10 most differentially expressed transcripts associated with wooden breast in 7-week-old broilers.

NCBI accession#	Gene	Description	Fold change
XM_015301575.1	*LOC107056542*	Beta-keratin-related protein	16.0
XM_015284051.1	*THBS2*	Thrombospondin 2 transcript variant X1	15.5
XM_015284053.1	*THBS2*	Thrombospondin 2 transcript variant X2	15.0
XM_015289892.1	*FBLN1*	Fibulin 1 transcript variant X1	14.2
NM_001017413.1	*PTX3*	Pentraxin 3	12.2
NM_205478.2	*LECT2*	Leukocyte cell-derived chemotaxin 2	11.6
NM_001024830.2	*CATH2*	Cathelicidin-2	11.4
NM_204992.2	*AvBD2*	Avian beta-defensin 2 transcript variant 1	9.6
XM_015285091.1	*AvBD2*	Avian beta-defensin 2 transcript variant X1	9.1
XM_015285700.1	*SOD3*	Superoxide dismutase 3	8.6
XM_015275012.1	*METTL21C*	Methyltransferase like 21C, transcript variant X1	−3.1
XM_015280910.1	*folr1*	Folate receptor 1, transcript variant X1	−3.3
XM_015282190.1	*MYLK4*	Myosin light chain kinase family, member 4, transcript variant X3	−3.3
XM_015282191.1	*MYLK4*	Myosin light chain kinase family, member 4, transcript variant X4	−3.3
XM_015290780.1	*LOC42447**	Hornerin-like	−3.4
XM_004939079.2	*NKTR*	Natural killer-tumor recognition sequence, transcript variant X8	−3.4
XM_418978.5	*MYLK4*	Myosin light chain kinase family, member 4, transcript variant X1	−3.5
XM_015282188.1	*MYLK4*	Myosin light chain kinase family, member 4, transcript variant X2	−3.5
XR_001464520.1	*LOC101749989*	Uncharacterized (non-coding RNA)	−3.6
XR_001463829.1	*LOC769840*	Uncharacterized (non-coding RNA)	−4.8

**A total of 36 differentially expressed transcripts were annotated as transcript variants of hornerin-like with fold change ranging from −3.4 to −4.1. Positive fold change, highlighted in red, and negative fold change, highlighted in green, indicate increase and decrease, respectively, in transcript abundance in wooden breast muscle samples collected from commercial broilers at 7 weeks of age.*

both ages for 1.7 and 1.9-fold, respectively, compared with those of non-WB samples. These results indicated a decreased β-oxidation likely associated with the accumulation of long-chain and very-long chain fatty acids (Mashek et al., 2007) in WB broilers which were well in agreement with the compromised glucose and lipid metabolisms, impaired energy production and fat deposition observed in the affected muscle (Abasht et al., 2016; Lake et al., 2019; Malila et al., 2019; Papah and Abasht, 2019; Lake and Abasht, 2020). Such impairment was further emphasized by an increased transcript abundance of the gene encoding 5′-AMP-activated protein kinase (AMPK) subunit beta-1 (*PRKAB1*, FC = 1.7), the conserved domain which acts as a positive regulator of AMPK complex (**Supplementary Table 3**).

Apart from metabolism of biochemical molecules, pathway enrichment analysis also reveals the manifestation of apoptosis in 6wk WB-affected broilers (**Table 4**). An impaired programmed cell death in the birds exhibiting growth-related myopathies was previously addressed (Malila et al., 2020; Phillips et al., 2020). In the present study, increased transcriptional levels of cathepsin B (*CTSB*, FC = 2.0), α-tubulin 1C (*TUBA1C*, FC = 1.7) along with a decrease in serine/threonine protein kinase B (*AKT3*, FC = −1.3) were observed in 6 week WB samples. The up-regulation of *CTSB* was previously associated with an enhanced activity of cathepsin B and L in WB breasts measured 12 h postmortem (Hasegawa et al., 2020). In addition, Mizunoe et al. (2020) recently reported that an overexpressed *CTSB* caused dysfunction

TABLE 3 | Differentially expressed transcripts associated with development of wooden breast myopathies identified in skeletal muscles of both 6-week-old and 7-week-old commercial broilers.

NCBI accession#	Gene	Description	FC	
			6 wk	7 wk
XR_001463829.1	*LOC769840*	Uncharacterized transcript variant X2 (non-coding RNA)	−4.6	−4.8
NM_204954.2	*ENTPD2*	Ectonucleoside triphosphate diphosphohydrolase 2,	−2.3	−2.7
XM_004940360.2	*FBXL4*	F-box and leucine-rich repeat protein 4, transcript variant X1	−2.1	−1.8
XR_001466078.1	*FBXL4*	F-box and leucine-rich repeat protein 4, transcript variant X4	−2.1	−1.9
XM_015289766.1	*SLC25A12*	Solute carrier family 25 (aspartate/glutamate carrier), member 12, transcript variant X3	−2.1	−2.5
XM_015289770.1	*SLC25A12*	Solute carrier family 25 (aspartate/glutamate carrier), member 12, transcript variant X8	−2.0	−2.4
NM_206874.2	*RYR3*	Ryanodine receptor 3	−1.9	−2.1
XM_015290749.1	*AGL*	Amylo-alpha-1, 6-glucosidase, 4-alpha-glucanotransferase, transcript variant X4	−1.8	−1.9
XM_015285897.1	*BPGM*	2,3-bisphosphoglycerate mutase, transcript variant X4	−1.7	−2.1
XR_001464938.1	*LOC107052450*	Uncharacterized transcript variant X1 (ncRNA)	−1.6	−1.5
XM_015284614.1	*FHL5*	Four and a half LIM domains 5, transcript variant X3	−1.6	1.4
XM_015289295.1	*LRRFIP1*	Leucine rich repeat (in FLII) interacting protein 1. transcript variant X35	−1.5	−1.5
XR_001464341.1	*HMG20A*	High mobility group 20A, transcript variant X2 (miscellaneous RNA)	−1.5	−2.0
XM_004947576.2	*TTI2*	TELO2 interacting protein 2, transcript variant X2	−1.5	−1.6
XM_421139.5	*rtf1*	RTF1 homolog, Paf1/RNA polymerase II complex component	−1.5	−1.4
XM_015279837.1	*LHX6*	LIM homeobox 6 (LHX6), transcript variant X1	−1.5	−1.6
XR_001461945.1	*LOC107049588*	Uncharacterized (non-coding RNA)	−1.4	−1.8
XM_004936749.2	*MUTYH*	MutY DNA glycosylase, transcript variant X1	1.3	1.7
XM_015295984.1	*DERL2*	Der1-like domain family, member 2	1.4	1.4
XM_015296953.1	*CAMTA1*	Calmodulin binding transcription activator 1, transcript variant X4	1.5	1.4
NM_204110.3	*PDIA3*	Protein disulfide isomerase family A, member 3	1.5	1.5
XM_417530.5	*CAMTA1*	Calmodulin binding transcription activator 1, transcript variant X9	1.6	1.6
XM_015296951.1	*CAMTA1*	Calmodulin binding transcription activator 1, transcript variant X3	1.6	1.5
XM_004947330.2	*CAMTA1*	Calmodulin binding transcription activator 1, transcript variant X5	1.7	1.5
XM_015296950.1	*CAMTA1*	Calmodulin binding transcription activator 1, transcript variant X2	1.7	1.5
XM_015296954.1	*CAMTA1*	Calmodulin binding transcription activator 1, transcript variant X6	1.7	1.5
XM_015296949.1	*CAMTA1*	Calmodulin binding transcription activator 1, transcript variant X1	1.7	1.6
XM_015296459.1	*SLC52A3*	Solute carrier family 52 (riboflavin transporter), member 3, transcript variant X2	1.7	1.7
NM_001199616.1	*SLC35E3*	Solute carrier family 35, member E3	1.8	1.6
XR_213220.2	*P2RX7*	Purinergic receptor P2X, ligand gated ion channel, 7, transcript variant X2 (miscellaneous RNA)	1.8	1.9
NM_001159698.1	*HSPH1*	Heat shock 105 kDa/110 kDa protein 1	1.9	1.9
XM_015277924.1	*HSPH1*	Heat shock 105 kDa/110 kDa protein 1, transcript variant X1	2.0	1.9
XM_015294517.1	*UNKL*	Unkempt family zinc finger-like, transcript variant X8	2.1	1.6
XM_004941810.2	*BATF*	Basic leucine zipper transcription factor, ATF-like, transcript variant X6	2.3	1.7
XM_015276731.1	*RGCC*	Regulator of cell cycle, transcript variant X2	3.7	4.3

FC, fold change; wk, week. Negative FC, highlighted in green, and positive FC, highlighted in red, indicate decrease and increase, respectively, in transcript abundance in wooden breast muscle samples collected from commercial broilers at 6 or 7 weeks of age.

of lipid metabolism in obese white adipose tissue potentially through a chronic state of low-grade inflammation, which was relevant to the condition of WB myopathy. Tubulins, dynamic polymers of microtubules, play important roles in various cellular functions through continual cytoskeletal reorganization in response to developmental and environmental cues (Ambriz et al., 2018). Chemical suppression of microtubules dynamic affected signaling processes that ultimately interfered apoptosis (Mollinedo and Gajate, 2003). It is interesting that Lake et al. (2019) reported an almost 1.7-fold decreased expression of gene encoding α-tubulin 8b in 2-week-old chicks that later (at 7 weeks of age) exhibited WB abnormality in comparison with unaffected broilers (Lake et al., 2019). The opposite directional changes of *TUBA* expression observed in a previous as well as in the current study might be an implication of a difference in the microenvironment at the different stage of WB myopathy (Ambriz et al., 2018). In addition, knockdown of *AKT3* was shown to limit cell proliferation and attenuated mammalian target of rapamycin (mTOR) signaling in the brain of the mouse (Easton et al., 2005), suggesting that the mediated apoptosis in 6wk WB muscle might be attributed to a modified mTOR signaling.

The other enriched altered pathways in the 6wk broilers included gap junction, tight junction and FA (**Table 4**), which are the adhesive structures of cell adhesion molecules in the cell surface that regulate of cell polarity and cell-cell communication (Rao and Wu, 2021). Dysregulation of those cell adhesions together with extracellular matrix (ECM) promotes pathological conditions associated with several diseases in humans (Rao and Wu, 2021). The DE transcripts enlisted in those pathways (**Supplementary Table 3**) include *TUBA1C* (FC = 1.7), Platelet-derived growth factor (PDGF) subunit A (*PDGFA*, FC = −1.4), and subunit B (*PDGFB*, FC = −1.5), serine/threonine-protein phosphatase PP1 catalytic subunit (*LOC100858156*, FC = −1.4), *AKT3* (FC = −1.3) and laminin gamma 1 (*LAMC1*, FC = −1.3). PDGF is considered one of the growth factors regulating cell proliferation, differentiation and angiogenesis through the binding with its receptor located on cell surface (Okonkwo et al., 2020). Up-regulations of its PDGF receptor (PDGFR) at gene level were addressed to be associated with increased fibrosis in WB fillets compared with non-WB counterparts (Papah et al., 2018; Pampouille et al., 2019). Although no differences in transcriptional level of PDGFR were identified in the 6wk WB broilers, we observed, in the affected muscles, a reduction of both *PDGFA* and *PDGFB*, which in mice has been reported to disrupt the wound repair process potentially through the perturbation of angiogenesis as previously observed in diabetic skin wound healing (Beer et al., 1997; Okonkwo et al., 2020). Furthermore, reduced expression of *LAMC1* was previously reported in patients with abnormal coronary atherogenesis (Hebbel et al., 2020), suggesting maladaptive activities of the cells when *LAMC1* expression was low. The importance of *LAMC1* in WB myopathy was recently evidenced in the study of Bordini et al. (2021) as it was defined as one of the hub genes interconnecting the DE gene network in WB and WS affected broilers.

Overall, the intensive perturbations of metabolic processes observed in 6wk broilers, with special reference to glucose and lipid metabolisms, are pronounced in WB broilers along with the convergence of cell-cell communication that regulates various cellular activities, including the processes of muscle repair.

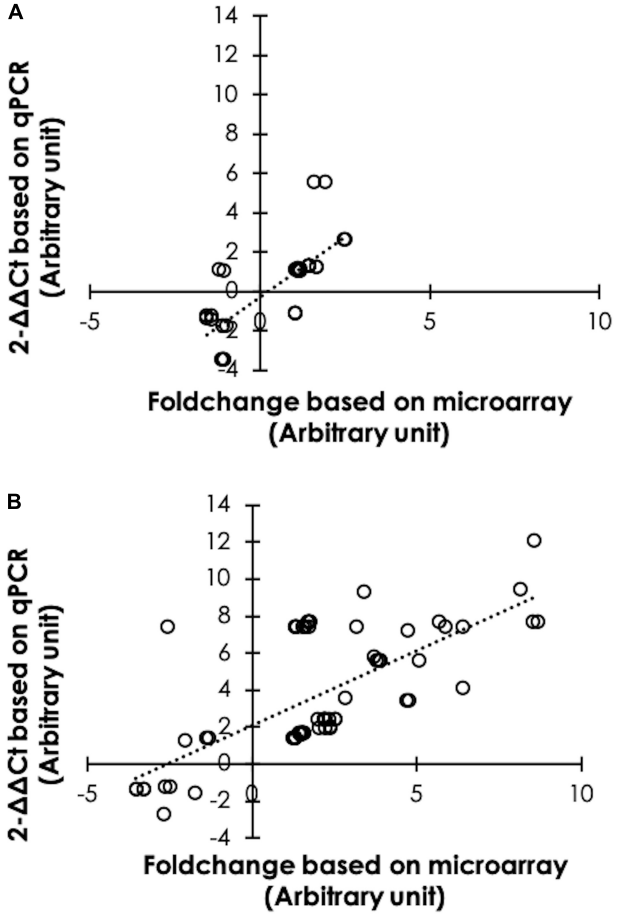

FIGURE 2 | Confirmation of differential expression. Scatter plots illustrate the comparisons between fold changes of 40 differential expressed (DE) transcripts selected from 6-week-old broilers **(A)**, and of 88 DE transcripts from 7-week-old broilers **(B)** obtained from microarray and quantitative real-time polymerase chain reaction (qPCR). The results indicated that 36 (accounted for 87.5%) and 84 (accounted for 95.5%) counterparts show comparable results between microarray and qPCR.

Seven-Week-Old Broilers

Metabolic pathway was one of the top enriched altered pathways observed in 7wk broilers (**Table 4**). Considering the DE transcripts listed in the metabolic pathways (**Supplementary Table 4**), however, the DE transcripts in such pathway were different from those observed in 6 week birds. Indeed, for 7wk samples, a number of those DE transcripts was involved in oxidative phosphorylation, and metabolisms of amino acids (argininosuccinate synthase, *ASS1*, FC = 2.5), amino sugars (glutamine-fructose-6-phosphate transaminase, *GFPT1*, FC = 2.0; sialic acid synthase, *NANS*, FC = 1.7; hexosaminidase, *HEXB*, FC = 2.1), proteoglycans (alpha-1,2-mannosyltransferase, *ALG11*, FC = −2.7; *ALG12*,

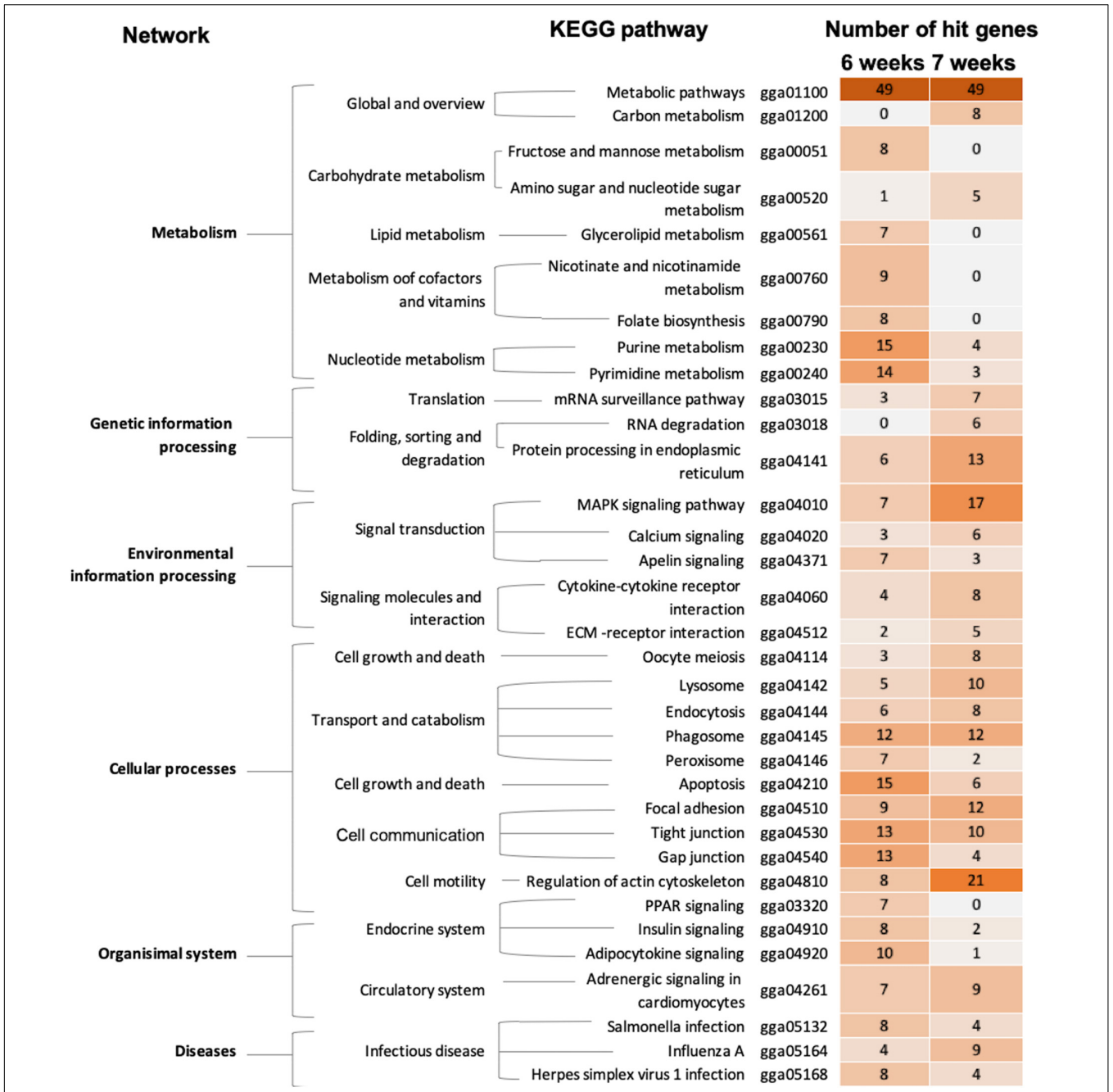

FIGURE 3 | The enriched biological pathways associated with wooden breast (WB) myopathy in 6-week-old and 7-week-old broilers. Heatmap depicts the enriched altered biological pathways, which were further grouped into biological networks, based on KEGG database. The darker color indicated more numbers of differentially expressed genes mapped into the pathway.

FC = 1.9; alpha-1,6-mannosylglycoprotein 6-beta-N-acetylglucosaminyltransferase A, *MGAT5*, FC = 1.3; carbohydrate 4-sulfotransferase 9, *CHST9*, FC = 1.9), and precursor molecules required for biosynthesis and function of lysosomes (acid ceramidase, *ASAH1*, FC = 1.6; adenosine triphosphatase, *ENTPD2*, FC = −2.7). Regarding the biological roles of those DE transcripts, the profound disruption in the molecular events responsible for cell communication, cell transportation, and catalytic processes in the 7wk WB-affected samples is anticipated. The speculation is supported by the presence of phagosome, lysosome, and FA, regulation of actin cytoskeleton, apoptosis, endocytosis and ECM-receptor interaction in the enriched altered pathways (**Table 4** and **Figure 3**). In addition, mitogen-activated protein kinase (MAPK) signaling, protein processing in endoplasmic reticulum, and cytokine-cytokine receptor interaction were among those enriched pathways.

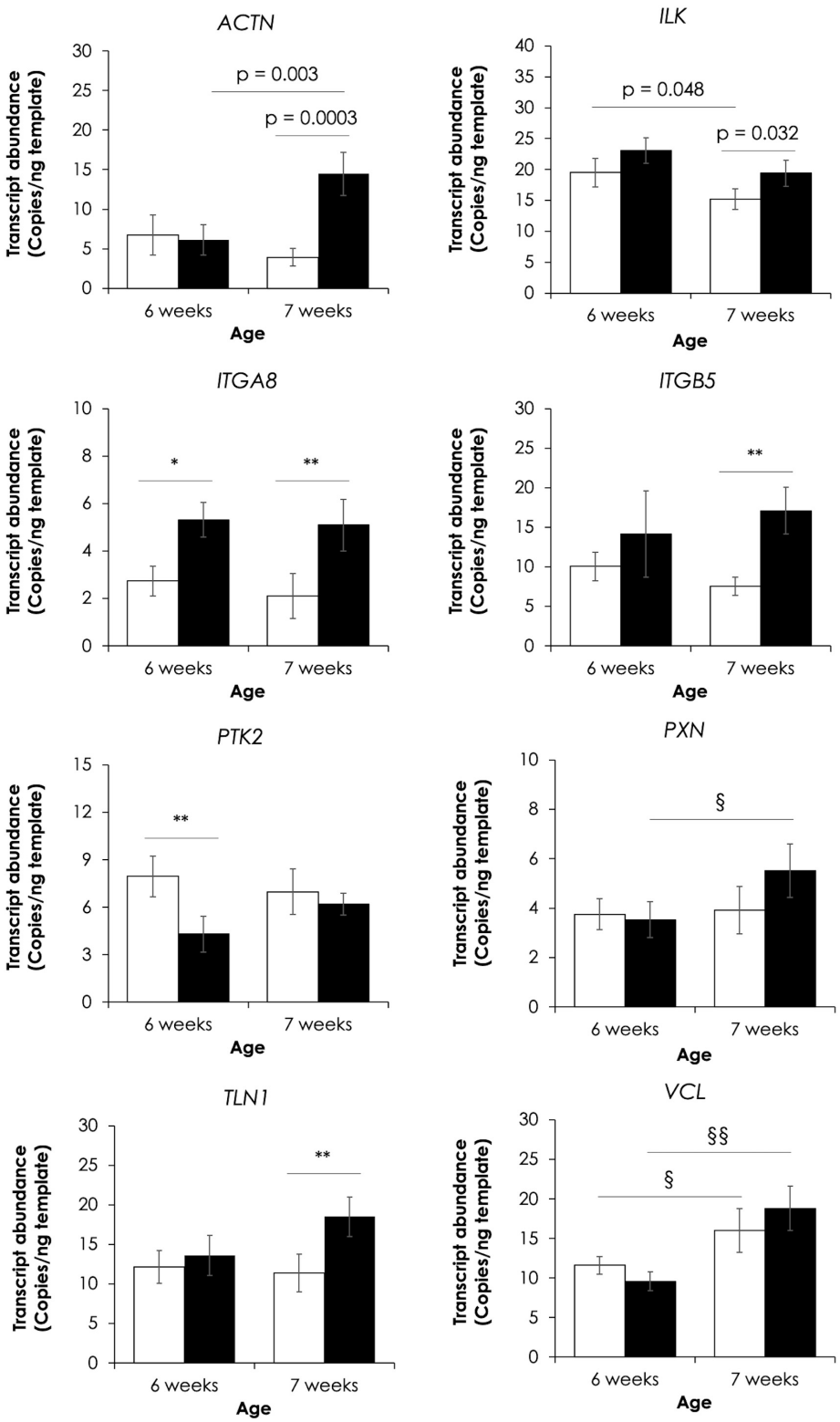

FIGURE 4 | Effects of wooden breast myopathy on absolute expression of eight genes in focal adhesion signaling. The genes include actinin-1 (*ACTN1*), integrin-linked kinase (*ILK*), integrin subunit alpha 8 (*ITGA8*), integrin subunit beta 5 (*ITGB5*), protein tyrosine kinase 2 (*PTK2*), paxillin (*PXN*), talin 1 (*TLN1*), and vinculin (*VCL*). Bars and error bars depict average and standard error in copies per nanogram cDNA template. $^{*}p < 0.05$, $^{**}p < 0.01$ between non-WB and WB samples. $^{\S}p < 0.05$, $^{\S\S}p < 0.01$ between different ages.

The molecular events in the 7wk affected broilers were corresponded with the perturbed processes of muscle regeneration (Domingues-Faria et al., 2016). Expression of C-C motif chemokine ligand 19 (*CCL19*) was increased for 3.7-fold in 7wk WB-affected broilers if compared to their non-WB counterpart, corresponding with the findings of Hughes et al. (2020) in which up-regulated *CCL19* was identified in human skins in response to inflammation. CCL19 binds to C-C chemokine receptor (CCR) type 7 (*CCR7*), playing roles in trafficking of immune cells (Yoshida et al., 1997). Cathepsin S (*CTSS*), another lysosomal protease participating in degradation of ECM and inflammatory processes, was increased for more than 2.4-fold in 7wk WB-affected broilers. Increased expression of *CTSS* was demonstrated in response to the secreted pro-inflammatory cytokines (Fu et al., 2020). Elevated abundances of *CC7* (FC = 2.3), *CCR5* (FC = 2.1), and tumor necrosis factor receptor superfamily member 18 (*TNFRSF18*, FC = 2.4), and neutrophil cytosolic factor 4 (*NCF4*, FC = 2.0) were observed in the affected birds. Overall, these findings supported the recruitment of immune cells to the affected breast muscle.

It is evident that the main components of cytoskeleton were manifested under WB condition. Actin gamma 1 (*ACTG1*, FC = 1.8), beta-keratin related protein (*LOC107056542*, FC = 16.0), α-tubulin 3 (*LOC416695*, FC = 3.0), and α-tubulin 4a (*TUBA4A*, FC = −1.5), the consisting proteins in those structures, were differentially expressed between WB and non-WB samples in the 7 week broilers (**Supplementary Table 2**). Muscle RAS oncogene homolog (*MRAS*), a member of small G proteins responsible for signal transduction and reorganization of actin cytoskeleton (Matsumoto et al., 1997; Kimmelman et al., 2002), was increased for 3.6-fold in the abnormal samples. Decreased transcript abundances of fibroblast growth factor 16 (*FGF16*, FC = −2.7) and son of sevenless (*SOS2*, FC = −1.5), Ras-guanine exchange factor, were detected in the 7wk affected broilers. As observed in the previous study of Sofronescu et al. (2010), activation of *FGF16* at transcriptional level was essential for cardiac growth and postnatal development of human and mice while Guittard et al. (2015) reported limited peripheral T-cell migration, hence impairing immune response when *SOS2* was absent.

Regarding the altered processes of cell communication (**Table 4**), transcript abundance of the gene encoding for one of the epidermal growth factor receptors (EGFR) belonging to the ErbB family of receptor tyrosine kinases, *ERBB2*, was decreased for 1.5-fold in respect to WB myopathy. This receptor is involved in the stabilization of peripheral microtubules in cell adhesion, triggering a rich network of signaling pathways (Yarden and Sliwkowski, 2001). Fibronectin 1 (*FN1*) was up-regulated for 2.7-fold in WB-affected 7wk broilers. Widely distributed in inflammatory lesions, fibronectins, a group of fibroblast surface glycoproteins, generally binds to ECM proteins, were also found to play a major role during wound healing (Grinnell et al., 1981). An extensive localization of FN1 at endomysial and perimysial levels was found in WB coupled with an increased content of this glycoprotein (Praud et al., 2020). In addition, grouped in phagosome, FA (**Table 4**), and ECM receptor interaction (**Supplementary Table 4**), thrombospondin 2 (*THBS2*), disulfide-linked homotrimeric glycoprotein, was highlighted as one of the most highly increased transcripts (FC = 15) in 7wk WB-affected broilers if compared to their non-WB counterparts (**Table 2**). This transient matrix glycoprotein inhibits microvascular endothelial cells proliferation thus resulting in impaired angiogenetic processes and limiting vascularization (Zhang et al., 2020). Intriguingly, these features overlap with the microscopic traits observed in WB affected muscles (Abasht et al., 2021).

A profound impairment of muscle regeneration in 7wk WB-affected broilers was further supported by the expression levels of genes responsible for protein processing within the endoplasmic reticulum (ER, **Table 4** and **Figure 3**). Indeed, increased expressions of genes encoding for several chaperone proteins, including heat shock protein (HSP) 110 kDa (*HSPA4L*, FC = 1.5) and 70 kDa (*HSPA5*, FC = 1.7) were found. In particular, a 1.5-fold increase in protein disulfide-isomerase A3 (*PDAI3*) was found in WB muscles (**Supplementary Table 4**). This multifunctional chaperone is originally located within ER but can escape to cell surface and interacts with integrins. Wang et al. (2020) recently demonstrated that a chemical inhibition of PDIA3 reduces myoblast differentiation in injured skeletal muscle, ultimately impairing muscle regeneration. An activation of ER-associated degradation, the process to

TABLE 4 | Top 10 enriched biological pathways associated with development of wooden breast myopathies in 6-week-old and 7-week-old commercial broilers.

Age	Pathway ID	KEGG pathways	Numbers of hit genes
6 weeks	gga01100	Metabolic pathways	49
	gga04210	Apoptosis	15
	gga00230	Purine metabolism	15
	gga00240	Pyrimidine metabolism	14
	gga04540	Gap junction	13
	gga04530	Tight junction	13
	gga04145	Phagosome	12
	gga04920	Adipocytokine signaling pathway	10
	gga00760	Nicotinate and nicotinamide metabolism	9
	gga04510	Focal adhesion	9
7 weeks	gga01100	Metabolic pathways	49
	gga04810	Regulation of actin cytoskeleton	21
	gga04010	MAPK signaling pathway	17
	gga04141	Protein processing in endoplasmic reticulum	13
	gga04510	Focal adhesion	12
	gga04145	Phagosome	12
	gga04142	Lysosome	10
	gga04530	Tight junction	10
	gga04261	Adrenergic signaling in cardiomyocytes	9
	gga05164	Influenza A	9

eliminate misfolded proteins retained within the ER lumen through the proteasome to restore normal ER function, might be speculated. Under severe stress condition in which ER function was not recovered, the affected cells were entered programmed cell death.

The impaired muscle regeneration in 7wk affected broilers perfectly matches with the altered muscular structure observed associated to WB condition (Velleman, 2020). In this study, a decreased transcript abundance of myopalladin (*MYPN*, FC = −1.4) and myomesin 1 (*MYOM1*, FC = −1.7) together with increased expressions of several genes encoding collagens (*COL1A1*, FC = 2.1, *COL8A1*, FC = 2.0, *COL9A2*, FC = 2.2, *LOC101750377*, FC = 2.1) were found in 7wk affected broilers in comparison with non-WB ones (**Supplementary Table 2**). MYPN tethers nebulin to actinin at Z-line, maintaining sarcomeric integrity (Bang et al., 2001) whereas MYOM1, a major component of myofibrillar M band expressed in almost all striated muscles, stabilizes the three-dimensional structure of the thick filaments by linking together myosin, titin, and light meromyosin (Agarkova and Perriard, 2005). Overall, gene expression is in agreement with the severe disruption of muscular structure coupled with accumulation of collagen observed in WB muscle (Velleman, 2020).

Collectively, differential expression of those genes underlined an extensive molecular alteration among the biological networks playing roles in response to severe muscle damage in the 7wk WB-affected broilers.

Transcriptional Modification of Focal Adhesion Signaling

The main enriched biological pathways associated with the development of WB myopathy in 6wk and 7wk was somewhat different. The molecular disruption in 6wk was more toward metabolic pathways for glucose and lipids whereas an aberrant muscle repair process has a more relevant importance in 7wk samples. Aside from that, the presence of FA signaling was similarly found in both groups, suggesting the relevance of this process in WB development. Here, we further compared absolute transcript abundances of the eight protein components of FA signaling between non-WB and WB samples within each slaughter age using ddPCR (**Figure 4**). The ddPCR technique permits the transcriptional quantification with good precision and sensitivity (Taylor et al., 2017). Therefore, the results could extend the comparative analysis of microarray which normally showed some limitation based on fixed dynamic range of fluorescence (Sharov et al., 2004). Increases or decreases in transcript abundance detected by both microarray and ddPCR studies in 6wk and 7wk were summarized in **Figure 5**.

Focal adhesion, the integrins-mediated contact sites between cell and ECM, acts as the linking points that mediates mechanical and biochemical signaling from the ECM (Turner, 2000; Wozniak et al., 2004; Huveneers and Danen, 2009). The reorganization of actin cytoskeletal structure regulated by FA signal leads to a series of intracellular events in

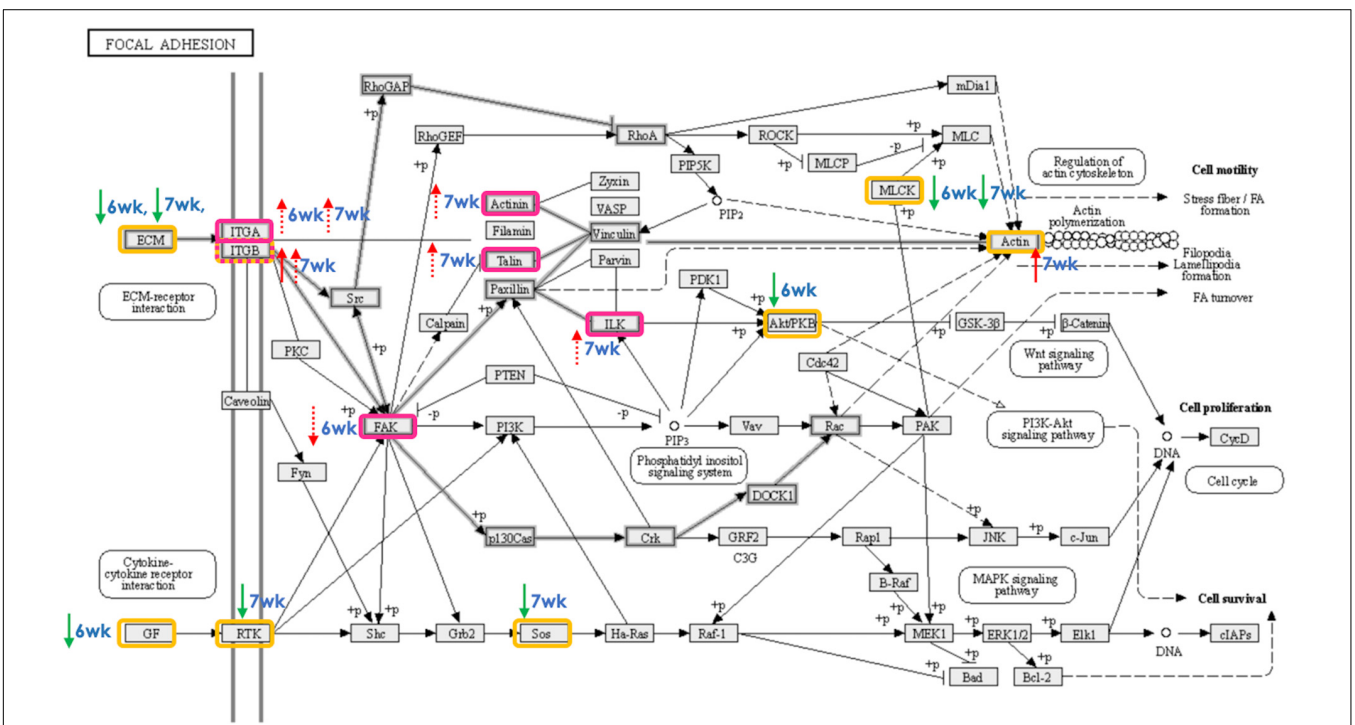

FIGURE 5 | Focal adhesion signaling pathway as affected by development of wooden breast (WB) in 6-week-old and 7-week-old broilers. The proteins highlighted in yellow and pink boxes exhibited differential expression, as detected using microarray and droplet digital polymerase chain reaction, respectively, in skeletal muscle of broilers affected WB myopathy in comparison with their non-defective counterparts. The red and green arrows (solid = microarray, dashed = ddPCR) indicate the increased and decreased expression, respectively, of the gene-encoded protein in WB relative to non-WB of 6-week-old (6wk) or 7-week-old (7wk) broilers.

response to the extracellular initiator. The crosstalk is crucial for controlling several cellular mechanisms, from fundamental development through recovery from any injuries or infection, and, in turn, maintaining tissue homeostasis, thus organism's survival (Zaidel-Bar and Geiger, 2010). A disrupted FA signaling accompanied by defective ECM and insufficient angiogenesis, which results in poor tissue oxygenation (condition consistently observed within the breast muscles of commercial broilers exhibiting growth-related myopathies), was associated with the impaired wound healing that led to an aberrant deposition of ECM molecules (e.g., collagen and decorin) and ultimately resulting in fibrosis (Koivisto et al., 2014).

Corresponded with the current results, up-regulated *ITGA8* was previously reported in broiler breast muscle affected by WS abnormality (Marchesi et al., 2019), and in specimen of 90 patients with hepatic fibrosis (Nishimichi et al., 2021). In addition, the same authors found that *ITGA8* was minimally expressed in healthy liver, underlying its relevance with liver fibrosis. Induced *ITGB5* was found to directly interact with β-catenin, facilitating Wnt/β-catenin activity in hepatocellular carcinoma (Lin et al., 2018). Deletion of *FAK* in mouse liver accelerated liver regeneration through the increased TNFα as well as the activation of apoptosis (Shang et al., 2016). Decreased *PTK2*, gene encoding for FAK, found in 6wk WB broilers may be the result of an adaptive response through FAK-mediated FA to accelerate the removal of damaged cells through apoptosis, and partly mitigate the development of fibrosis within the muscle (Lagares et al., 2012; Velleman, 2020).

Reduced transcript abundances of genes encoding for ECM components (*LAMC1* in 6wk, *FN1* in 7wk), and growth factors (*PDGFA* in 6wk) were identified, based on the current microarray study, in the WB-affected muscles. In contrast, the majority of the genes encoding for FA components tested exhibited increased expression levels. Those genes encode intracellular proteins that mediate integrin binding to actin microfilament, maintain stability of the integrin adhesion, and sense matrix rigidity (Klapholz and Brown, 2017). Most of the transcriptional changes in this pathway were detected in 7wk broilers. The findings suggested an altered crosstalk between immune cell and muscle cells may be hypothesized as a consequence of the chronic inflammatory processes, leading to failure in muscle regeneration (Domingues-Faria et al., 2016).

In conclusion, our findings were congruent with the proposed model of ECM disorders in the pathogenesis of growth-related myopathies in broilers (Bordini et al., 2021). The present study further provides an observation on the alteration of ECM-mediated FA signaling. Such impairment exerted the deleterious effects on immune response and muscle regeneration process at a greater extent in 7wk broilers. Furthermore, molecular perturbation pattern associated with WB development differed between 6wk and 7wk birds. In 6wk broilers, the metabolic processes of glucose and lipid, in particular, were deviated between WB and non-WB group. On the other hand, the importance of impaired muscle regeneration processes was evident in the 7wk affected broilers. Whether the altered FA signaling was a cause or effects of those dysregulated biological pathways remained to be further investigated.

DATA AVAILABILITY STATEMENT

The datasets presented in this study can be found in online repositories. The names of the repository/repositories and accession number(s) can be found below: https://www.ncbi.nlm.nih.gov/, GPL24307; https://www.ncbi.nlm.nih.gov/, GSE107362.

ETHICS STATEMENT

Ethical review and approval was not required for the animal study because all samples used in this study were purchased in the form of whole carcasses from the commercial processing plant without any experimental treatments subjected to the living animals. Thereby, the ethical approval was exempted.

AUTHOR CONTRIBUTIONS

YM, WR, and WV conceived and designed the experiments as well as acquired the funding. YM, TU, YS, SA, and KT performed the experiments and analyzed the data. TU performed bioinformatics. KT performed ddPCR. YM drafted the manuscript with revisions provided by TU, WR, MP, and FS. All authors read and approved the final manuscript.

FUNDING

This research was financially supported by Cluster and Program Management, National Science and Technology Development Agency (Thailand; project number P15-50668), and by Office of the Permanent Secretary, Ministry of Higher Education, Science, Research and Innovation (Thailand; P20-50946 and P21-50165).

ACKNOWLEDGMENTS

The authors would like to acknowledge Juthawut U-chupaj and Premask Chaiwiwattrakul for their assistance during sample collection.

SUPPLEMENTARY MATERIAL

The Supplementary Material for this article can be found online at: https://www.frontiersin.org/articles/10.3389/fphys.2021.691194/full#supplementary-material

REFERENCES

Abasht, B., Mutryn, M. F., Michalek, R. D., and Lee, W. R. (2016). Oxidative stress and metabolic perturbations in wooden breast disorder in chickens. *PLoS One* 11:e0153750. doi: 10.1371/journal.pone.0153750

Abasht, B., Papah, M. B., and Qiu, J. (2021). Evidence of vascular endothelial dysfunction in Wooden Breast disorder in chickens: insights through gene expression analysis, ultra-structural evaluation and supervised machine learning methods. *PLoS One* 16:e0243983. doi: 10.1371/journal.pone.0243983

Agarkova, I., and Perriard, J.-C. (2005). The M-band: an elastic web that crosslinks thick filaments in the center of the sarcomere. *Trends Cell Biol.* 15, 477–485. doi: 10.1016/j.tcb.2005.07.001

Ambriz, X., de Lanerolle, P., and Ambrosio, J. R. (2018). The mechanobiology of the actin cytoskeleton in stem cells during differentiation and interaction with biomaterials. *Stem Cells Int.* 2018:2891957. doi: 10.1155/2018/2891957

Bang, M. L., Mudry, R. E., McElhinny, A. S., Trombitás, K., Geach, A. J., Yamasaki, R., et al. (2001). Myopalladin, a novel 145-kilodalton sarcomeric protein with multiple roles in Z-disc and I-band protein assemblies. *J. Cell. Biol.* 153, 413–427. doi: 10.1083/jcb.153.2.413

Barbut, S. (2019). Recent myopathies in broiler's breast meat fillets. *Worlds Poult. Sci. J.* 75, 559–582. doi: 10.1017/S0043933919000436

Beer, H.-D., Longaker, M. T., and Werner, S. (1997). Reduced expression of PDGF and PDGF receptors during impaired wound healing. *J. Invest. Dermatol.* 109, 132–138. doi: 10.1111/1523-1747.ep12319188

Bolstad, B. (2017). *PreprocessCore: A Collection of Pre-Processing Functions.* R Package Version 1.40.0. Available online at: https://github.com/bmbolstad/preprocessCore (accessed October 23, 2019).

Bordini, M., Zappaterra, M., Soglia, F., Petracci, M., and Davoli, R. (2021). Weighted gene co-expression network analysis identifies molecular pathways and hub genes involved in broiler White Striping and Wooden Breast myopathies. *Sci. Rep.* 11:1776. doi: 10.1038/s41598-021-81303-7

Cai, K., Shao, W., Chen, X., Campbell, Y. L., Nair, M. N., Suman, S. P., et al. (2018). Meat quality traits and proteome profile of woody broiler breast (*pectoralis major*) meat. *Poult. Sci.* 97, 337–346. doi: 10.3382/ps/pex284

Chatterjee, D., Zhuang, H., Bowker, B. C., Sanchez-Brambila, G., and Rincon, A. M. (2016). Instrumental texture characteristics of broiler pectoralis major with the wooden breast condition. *Poult. Sci.* 95, 2449–2454. doi: 10.3382/ps/pew204

Contreras, O., Cruz-Soca, M., Theret, M., Soliman, H., Tung, L. W., Groppa, E., et al. (2019). Cross-talk between TGF-β and PDGFRα signaling pathways regulates the fate of stromal fibro-adipogenic progenitors. *J. Cell Sci.* 132:jcs232157. doi: 10.1242/jcs.232157

Daughtry, M. R., Berio, E., Shen, Z., Suess, E. J. R., Shah, N., Geiger, A. E., et al. (2017). Satellite cell-mediated breast muscle regeneration decreases with broiler size. *Poult. Sci.* 96, 3457–3464. doi: 10.3382/ps/pex068

de Carvalho, L. M., Madruga, M. S., Estévez, M., Badaró, A. T., and Barbin, D. F. (2020). Occurrence of wooden breast and white striping in Brazilian slaughtering plants and use of near-infrared spectroscopy and multivariate analysis to identify affected chicken breasts. *J. Food Sci.* 85, 3102–3112. doi: 10.1111/1750-3841.15465

Domingues-Faria, C., Vasson, M.-P., Goncalves-Mendes, N., Boirie, Y., and Walrand, S. (2016). Skeletal muscle regeneration and impact of aging and nutrition. *Ageing Res. Rev.* 26, 22–36. doi: 10.1016/j.arr.2015.12.004

Easton, R. M., Cho, H., Roovers, K., Shineman, D. W., Mizrahi, M., Forman, M. S., et al. (2005). Role for Akt3/protein kinase Bgamma in attainment of normal brain size. *Mol. Cell Biol.* 25, 1869–1878. doi: 10.1128/MCB.25.5.1869-1878.2005

Ferreira, T. Z., Kindlein, L., Flees, J. J., Shortnacy, L. K., Vieira, S. L., Nascimento, V. P., et al. (2020). Characterization of pectoralis major muscle satellite cell population heterogeneity, macrophage density, and collagen infiltration in broiler chickens affected by wooden breast. *Front. Physiol.* 11:529. doi: 10.3389/fphys.2020.00529

Fu, R., Guo, H., Janga, S., Choi, M., Klinngam, W., Edman, M. C., et al. (2020). Cathepsin S activation contributes to elevated CX3CL1 (fractalkine) levels in tears of a Sjögren's syndrome murine model. *Sci. Rep.* 10:1455. doi: 10.1038/s41598-020-58337-4

Grinnell, F., Billingham, R. E., and Burgess, L. (1981). Distribution of fibronectin during wound healing in vivo. *J. Invest. Dermatol.* 76, 181–189. doi: 10.1111/1523-1747.ep12525694

Guittard, G., Kortum, R. L., Balagopalan, L., Çuburu, N., Nguyen, P., Sommers, C. L., et al. (2015). Absence of both Sos-1 and Sos-2 in peripheral CD4(+) T cells leads to PI3K pathway activation and defects in migration. *Eur. J. Immunol.* 45, 2389–2395. doi: 10.1002/eji.201445226

Hasegawa, Y., Hara, T., Kawasaki, T., Yamada, M., Watanabe, T., and Iwasaki, T. (2020). Effect of wooden breast on postmortem changes in chicken meat. *Food Chem.* 315:126285. doi: 10.1016/j.foodchem.2020.126285

Hebbel, R. P., Wei, P., Milbauer, L., Corban Michel, T., Solovey, A., Kiley, J., et al. (2020). Abnormal endothelial gene expression associated with early coronary atherosclerosis. *J. Am. Heart Assoc.* 9:e016134. doi: 10.1161/JAHA.120.016134

Huang, L., He, R., Luo, W., Zhu, Y.-S., Li, J., Tan, T., et al. (2016). Aldo-keto reductase family 1 member B10 inhibitors: potential drugs for cancer treatment. *Recent Pat. Anticancer Drug Discov.* 11, 184–196. doi: 10.2174/1574892811888160304113346

Hughes, T. K., Wadsworth, M. H., Gierahn, T. M., Do, T., Weiss, D., Andrade, P. R., et al. (2020). Second-strand synthesis-based massively parallel scRNA-Seq reveals cellular states and molecular features of human inflammatory skin pathologies. *Immunity* 53, 878–894.e7. doi: 10.1016/j.immuni.2020.09.015

Huveneers, S., and Danen, E. H. J. (2009). Adhesion signaling – crosstalk between integrins, Src and Rho. *J. Cell Sci.* 122(Pt 8), 1059–1069. doi: 10.1242/jcs.039446

Kanehisa, M., Goto, S., Sato, Y., Furumichi, M., and Tanabe, M. (2012). KEGG for integration and interpretation of large-scale molecular data sets. *Nucleic Acids Res.* 40, D109–D114. doi: 10.1093/nar/gkr988

Kang, S. W., Kidd, M. T., Kadhim, H. J., Shouse, S., Orlowski, S. K., Hiltz, J., et al. (2020). Characterization of stress response involved in chicken myopathy. *Gen. Comp. Endocrinol.* 295:113526. doi: 10.1016/j.ygcen.2020.113526

Kimmelman, A. C., Nuñez Rodriguez, N., and Chan, A. M. (2002). R-Ras3/M-Ras induces neuronal differentiation of PC12 cells through cell-type-specific activation of the mitogen-activated protein kinase cascade. *Mol. Cell. Biol.* 22, 5946–5961. doi: 10.1128/mcb.22.16.5946-5961.2002

Klapholz, B., and Brown, N. H. (2017). Talin – the master of integrin adhesions. *J.Cell Sci.* 130, 2435–2446. doi: 10.1242/jcs.190991

Koivisto, L., Heino, J., Häkkinen, L., and Larjava, H. (2014). Integrins in wound healing. *Adv. Wound Care* 3, 762–783. doi: 10.1089/wound.2013.0436

Lagares, D., Busnadiego, O., García-Fernández, R. A., Kapoor, M., Liu, S., Carter, D. E., et al. (2012). Inhibition of focal adhesion kinase prevents experimental lung fibrosis and myofibroblast formation. *Arthritis Rheum.* 64, 1653–1664. doi: 10.1002/art.33482

Lake, J. A., and Abasht, B. (2020). Glucolipotoxicity: a proposed etiology for wooden breast and related myopathies in commercial broiler chickens. *Front. Physiol.* 11:169. doi: 10.3389/fphys.2020.00169

Lake, J. A., Papah, M. B., and Abasht, B. (2019). Increased expression of lipid metabolism genes in early stages of wooden breast links myopathy of broilers to metabolic syndrome in humans. *Genes* 10:746. doi: 10.3390/genes10100746

Leek, J., McShane, B. B., Gelman, A., Colquhoun, D., Nuijten, M. B., and Goodman, S. N. (2017). Five ways to fix statistics. *Nature* 551, 557–559. doi: 10.1038/d41586-017-07522-z

Lin, Z., He, R., Luo, H., Lu, C., Ning, Z., Wu, Y., et al. (2018). Integrin-β5, a miR-185-targeted gene, promotes hepatocellular carcinoma tumorigenesis by regulating β-catenin stability. *J. Exp. Clin. Cancer Res.* 37:17. doi: 10.1186/s13046-018-0691-9

Liu, J., Puolanne, E., Schwartzkopf, M., and Arner, A. (2020). Altered sarcomeric structure and function in woody breast myopathy of avian pectoralis major muscle. *Front. Physiol.* 11:287. doi: 10.3389/fphys.2020.00287

Livak, K. J., and Schmittgen, T. D. (2001). Analysis of relative gene expression data using real-time quantitative PCR and the 2-ΔΔCt method. *Methods* 25, 402–408. doi: 10.1006/meth.2001.1262

Madruga, M. S., da Rocha, T. C., de Carvalho, L. M., Sousa, A. M. B. L., de Sousa Neto, A. C., Coutinho, D. G., et al. (2019). The impaired quality of chicken affected by the wooden breast myopathy is counteracted in emulsion-type sausages. *J. Food Sci. Technol.* 56, 1380–1388. doi: 10.1007/s13197-019-03612-0

Maharjan, P., Hilton, K., Weil, J., Suesuttajit, N., Beitia, A., Owens, C. M., et al. (2020). Characterizing woody breast myopathy in a meat broiler line by heat production, microbiota, and plasma metabolites. *Front. Vet. Sci.* 6:497. doi: 10.3389/fvets.2019.00497

Malila, Y., Srimarut, Y., U-Chupaj, J., Strasburg, G., and Visessanguan, W. (2015). Monitoring of chicken RNA integrity as a function of prolonged postmortem duration. *Asian Australas J. Anim. Sci.* 28, 1649–1656. doi: 10.5713/ajas.15.0167

Malila, Y., Thanatsang, K., Arayamethakorn, S., Uengwetwanit, T., Srimarut, Y., Petracci, M., et al. (2019). Absolute expressions of hypoxia-inducible factor-1 alpha (*HIF1A*) transcript and the associated genes in chicken skeletal muscle with white striping and wooden breast myopathies. *PLoS One* 14:e0220904. doi: 10.1371/journal.pone.0220904

Malila, Y., U-Chupaj, J., Srimarut, Y., Chaiwiwattrakul, P., Uengwetwanit, T., Arayamethakorn, S., et al. (2018). Monitoring of white striping and wooden breast cases and impacts on quality of breast meat collected from commercial broilers (*Gallus gallus*). *Asian Australas J. Anim. Sci.* 31, 1807–1817. doi: 10.5713/ajas.18.0355

Malila, Y., Uengwetwanit, T., Arayamethakorn, S., Srimarut, Y., Thanatsang, K. V., Soglia, F., et al. (2020). Transcriptional profiles of skeletal muscle associated with increasing severity of white striping in commercial broilers. *Front. Physiol.* 11:580. doi: 10.3389/fphys.2020.00580

Marchesi, J. A. P., Ibelli, A. M. G., Peixoto, J. O., Cantão, M. E., Pandolfi, J. R. C., Marciano, C. M. M., et al. (2019). Whole transcriptome analysis of the pectoralis major muscle reveals molecular mechanisms involved with white striping in broiler chickens. *Poult. Sci.* 98, 590–601. doi: 10.3382/ps/pey429

Mashek, D. G., Li, L. O., and Coleman, R. A. (2007). Long-chain acyl-CoA synthetases and fatty acid channeling. *Future Lipidol.* 2, 465–476. doi: 10.2217/17460875.2.4.465

Matsumoto, K., Asano, T., and Endo, T. (1997). Novel small GTPase M-Ras participates in reorganization of actin cytoskeleton. *Oncogene* 15, 2409–2417. doi: 10.1038/sj.onc.1201416

Meloche, K. J., Dozier, W. A., Brandebourg, T. D., and Starkey, J. D. (2018). Skeletal muscle growth characteristics and myogenic stem cell activity in broiler chickens affected by wooden breast. *Poult. Sci.* 97, 4401–4414. doi: 10.3382/ps/pey287

Mizunoe, Y., Kobayashi, M., Hoshino, S., Tagawa, R., Itagawa, R., Hoshino, A., et al. (2020). Cathepsin B overexpression induces degradation of perilipin 1 to cause lipid metabolism dysfunction in adipocytes. *Sci. Rep.* 10:634. doi: 10.1038/s41598-020-57428-6

Mollinedo, F., and Gajate, C. (2003). Microtubules, microtubule-interfering agents and apoptosis. *Apoptosis* 8, 413–450. doi: 10.1023/A:1025513106330

Müller, C., Schillert, A., Röthemeier, C., Trégouët, D.-A., Proust, C., Binder, H., et al. (2016). Removing batch effects from longitudinal gene expression – quantile normalization plus comBat as best approach for microarray transcriptome data. *PLoS One* 11:e0156594. doi: 10.1371/journal.pone.0156594

Mutryn, M. F., Brannick, E. M., Fu, W., Lee, W. R., and Abasht, B. (2015). Characterization of a novel chicken muscle disorder through differential gene expression and pathway analysis using RNA-sequencing. *BMC Genomics* 16:399. doi: 10.1186/s12864-015-1623-0

Nishimichi, N., Tsujino, K., Kanno, K., Sentani, K., Kobayashi, T., Chayama, K., Sheppard, D., and Yokosaki, Y. (2021). Induced hepatic stellate cell integrin, α8β1, enhances cellular contractility and TGFβ activity in liver fibrosis. *J. Pathol.* 253, 3660–373. doi: 10.1002/path.5618

Okonkwo, U. A., Chen, L., Ma, D., Haywood, V. A., Barakat, M., Urao, N., et al. (2020). Compromised angiogenesis and vascular integrity in impaired diabetic wound healing. *PLoS One* 15:e0231962. doi: 10.1371/journal.pone.0231962

Pampouille, E., Hennequet-Antier, C., Praud, C., Juanchich, A., Brionne, A., Godet, E., et al. (2019). Differential expression and co-expression gene network analyses reveal molecular mechanisms and candidate biomarkers involved in breast muscle myopathies in chicken. *Sci. Rep.* 9:14905. doi: 10.1038/s41598-019-51521-1

Papah, M. B., and Abasht, B. (2019). Dysregulation of lipid metabolism and appearance of slow myofiber-specific isoforms accompany the development of Wooden Breast myopathy in modern broiler chickens. *Sci. Rep.* 9:17170. doi: 10.1038/s41598-019-53728-8

Papah, M. B., Brannick, E. M., Schmidt, C. J., and Abasht, B. (2018). Gene expression profiling of the early pathogenesis of wooden breast disease in commercial broiler chickens using RNA-sequencing. *PLoS One* 13:e0207346. doi: 10.1371/journal.pone.0207346

Papah, M. B., Brannick, E. M., Schmidt, C. J., and Abasht, B. (2017). Evidence and role of phlebitis and lipid infiltration in the onset and pathogenesis of Wooden Breast Disease in modern broiler chickens. *Avian Pathol.* 46, 623–643. doi: 10.1080/03079457.2017.1339346

Petracci, M., Soglia, F., Madruga, M., Carvalho, L., Ida, E., and Estévez, M. (2019). Wooden-breast, white striping, and spaghetti meat: causes, consequences and consumer perception of emerging broiler meat abnormalities. *Compr. Rev. Food Sci. Food Saf.* 18, 565–583. doi: 10.1111/1541-4337.12431

Phillips, C. A., Reading, B. J., Livingston, M., Livingston, K., and Ashwell, C. M. (2020). Evaluation via supervised machine learning of the broiler pectoralis major and liver transcriptome in association with the muscle myopathy wooden breast. *Front. Physiol.* 11:101. doi: 10.3389/fphys.2020.00101

Praud, C., Jimenez, J., Pampouille, E., Couroussé, N., Godet, E., Le Bihan-Duval, E., and Berri, C. (2020). Molecular phenotyping of white striping and wooden breast myopathies in chicken. *Front. Physiol.* 11:633. doi: 10.3389/fphys.2020.00633

Qu, J., Liu, X., Li, J., Gong, K., Duan, L., Luo, W., et al. (2019). [AKR1B10 promotes proliferation of breast cancer cells by activating Wnt/β-catenin pathway]. *Xi bao yu fen zi mian yi xue za zhi.* 35, 1094–1100.

R Core Team (2017). *R: A Language and Environment for Statistical Computing. In R Foundation for Statistical Computing.* Available online at: https://www.R-project.org (accessed October 23, 2019).

Radaelli, G., Piccirillo, A., Birolo, M., Bertotto, D., Gratta, F., Ballarin, C., et al. (2017). Effect of age on the occurrence of muscle fiber degeneration associated with myopathies in broiler chickens submitted to feed restriction. *Poult. Sci.* 96, 309–319. doi: 10.3382/ps/pew270

Rao, R. K., and Wu, Z. (2021). "Cell adhesion and the extracellular matrix," in *Goodman's Medical Cell Biology*, 4th Edn, ed. S. R. Goodman (Cambridge, MA: Academic Press), 203–247. doi: 10.1016/b978-0-12-817927-7.00007-7

Shang, N., Arteaga, M., Chitsike, L., Wang, F., Viswakarma, N., Breslin, P., et al. (2016). FAK deletion accelerates liver regeneration after two-thirds partial hepatectomy. *Sci. Rep.* 6:34316. doi: 10.1038/srep34316

Sharov, V., Kwong, K. Y., Frank, B., Chen, E., Hasseman, J., Gaspard, R., et al. (2004). The limits of log-ratios. *BMC Biotechnol.* 4:3. doi: 10.1186/1472-6750-4-3

Sihvo, H. K., Immonen, K., and Puolanne, E. (2014). Myodegeneration with fibrosis and regeneration in the pectoralis major muscle of broilers. *Vet. Pathol.* 51, 619–623. doi: 10.1177/0300985813497488

Sihvo, H. K., Linden, J., Airas, N., Immonen, K., Valaja, J., and Puolanne, E. (2017). Wooden breast myodegeneration of pectoralis major muscle over the growth period in broilers. *Vet. Pathol.* 54, 119–128. doi: 10.1177/0300985816658099

Sofronescu, A. G., Detillieux, K. A., and Cattini, P. A. (2010). FGF-16 is a target for adrenergic stimulation through NF-κB activation in postnatal cardiac cells and adult mouse heart. *Cardiovasc. Res.* 87, 102–110. doi: 10.1093/cvr/cvq025

Soglia, F., Mazzoni, M., Zappaterra, M., Di Nunzio, M., Babini, E., Bordini, M., et al. (2020). Distribution and expression of vimentin and desmin in broiler pectoralis major affected by the growth-related muscular abnormalities. *Front. Physiol.* 10:1581. doi: 10.3389/fphys.2019.01581

Soglia, F., Mudalal, S., Babini, E., Di Nunzio, M., Mazzoni, M., Sirri, F., et al. (2016). Histology, composition, and quality traits of chicken Pectoralis major muscle affected by wooden breast abnormality. *Poult. Sci.* 95, 651–659. doi: 10.3382/ps/pev353

Tasoniero, G., Cullere, M., Cecchinato, M., Puolanne, E., and Zotte, A. D. (2016). Technological quality, mineral profile, and sensory attributes of broiler chicken breasts affected by white striping and wooden breast myopathies. *Poult. Sci.* 95, 2707–2714. doi: 10.3382/ps/pew215

Taylor, S. C., Laperriere, G., and Germain, H. (2017). Droplet digital PCR versus qPCR for gene expression analysis with low abundant targets: from variable nonsense to publication quality data. *Sci. Rep.* 7:2409. doi: 10.1038/s41598-017-02217-x

Tijare, V. V., Yang, F. L., Kuttappan, V. A., Alvarado, C. Z., Coon, C. N., and Owens, C. M. (2016). Meat quality of broiler breast fillets with white striping and woody breast muscle myopathies. *Poult. Sci.* 95, 2167–2173. doi: 10.3382/ps/pew129

Turner, C. E. (2000). Paxillin and focal adhesion signalling. *Nat. Cell Biol.* 2, E231–E236. doi: 10.1038/35046659

Velleman, S. G. (2015). Relationship of skeletal muscle development and growth to breast muscle myopathies: a review. *Avian Dis.* 59, 525–531. doi: 10.1637/11223-063015-Review.1

Velleman, S. G. (2020). Pectoralis major (Breast) muscle extracellular matrix fibrillar collagen modifications associated with the wooden breast fibrotic myopathy in broilers. *Front. Physiol.* 11:461. doi: 10.3389/fphys.2020.00461

Velleman, S. G., and Clark, D. L. (2015). Histopathologic and myogenic gene expression changes associated with wooden breast in broiler breast muscles. *Avian Dis.* 59, 410–418. doi: 10.1637/11097-042015-Reg.1

Velleman, S. G., Clark, D. L., and Tonniges, J. R. (2017). Fibrillar collagen organization associated with broiler wooden breast fibrotic myopathy. *Avian Dis.* 61, 481–490. doi: 10.1637/11738-080217-Reg.1

Wang, C., Zhu, Y., Wu, D., Wang, Z., Xu, X., Shi, Y., et al. (2020). The role of PDIA3 in myogenesis during muscle regeneration. *Exp. Mol. Med.* 52, 105–117. doi: 10.1038/s12276-019-0368-2

Wozniak, M. A., Modzelewska, K., Kwong, L., and Keely, P. J. (2004). Focal adhesion regulation of cell behavior. *Biochim. Biophys. Acta Mol. Cell Res.* 1692, 103–119. doi: 10.1016/j.bbamcr.2004.04.007

Xing, T., Zhao, X., Zhang, L., Li, J. L., Zhou, G. H., Xu, X. L., et al. (2020). Characteristics and incidence of broiler chicken wooden breast meat under commercial conditions in China. *Poult. Sci.* 99, 620–628. doi: 10.3382/ps/pez560

Yarden, Y., and Sliwkowski, M. X. (2001). Untangling the ErbB signalling network. *Nat. Rev. Mol. Cell Biol.* 2, 127–137. doi: 10.1038/35052073

Yoshida, R., Imai, T., Hieshima, K., Kusuda, J., Baba, M., Kitaura, M., et al. (1997). Molecular cloning of a novel human CC chemokine EBI1-ligand chemokine that is a specific functional ligand for EBI1, CCR7*. *J. Biol. Chem.* 272, 13803–13809. doi: 10.1074/jbc.272.21.13803

Zaidel-Bar, R., and Geiger, B. (2010). The switchable integrin adhesome. *J. Cell Sci.* 123(Pt 9), 1385–1388. doi: 10.1242/jcs.066183

Zambonelli, P., Zappaterra, M., Soglia, F., Petracci, M., Sirri, F., Cavani, C., et al. (2016). Detection of differentially expressed genes in broiler pectoralis major muscle affected by white striping – wooden breast myopathies. *Poult. Sci.* 95, 2771–2785. doi: 10.3382/ps/pew268

Zanetti, M. A., Tedesco, D. C., Schneider, T., Teixeira, S. T. F., Daroit, L., Pilotto, F., et al. (2018). Economic losses associated with wooden breast and white striping in broilers. *Semin. Cienc. Agrar.* 39, 887–892. doi: 10.5433/1679-0359.2018v39n2p887

Zhang, K., Li, M., Yin, L., Fu, G., and Liu, Z. (2020). Role of thrombospondin-1 and thrombospondin-2 in cardiovascular diseases (Review). *Int. J. Mol. Med.* 45, 1275–1293. doi: 10.3892/ijmm.2020.4507

Conflict of Interest: The authors declare that the research was conducted in the absence of any commercial or financial relationships that could be construed as a potential conflict of interest.

frontiers in Physiology

ORIGINAL RESEARCH
published: 02 July 2021
doi: 10.3389/fphys.2021.697121

Comparative Analysis of Skeletal Muscle DNA Methylation and Transcriptome of the Chicken Embryo at Different Developmental Stages

Jinshan Ran[1], Jingjing Li[1], Lingqian Yin[1], Donghao Zhang[1], Chunlin Yu[1,2], Huarui Du[2], Xiaosong Jiang[2], Chaowu Yang[2] and Yiping Liu[1]**

[1] Farm Animal Genetic Resources Exploration and Innovation Key Laboratory of Sichuan Province, Sichuan Agricultural University, Chengdu, China, [2] Animal Breeding and Genetics Key Laboratory of Sichuan Province, Chengdu, China

OPEN ACCESS

Edited by:
Sandra G. Velleman,
The Ohio State University,
United States

Reviewed by:
Kent M. Reed,
University of Minnesota, United States
Gale Strasburg,
Michigan State University,
United States

***Correspondence:**
Yiping Liu
liuyp578@163.com
Chaowu Yang
cwyang@foxmail.com

Specialty section:
This article was submitted to Avian Physiology, a section of the journal Frontiers in Physiology

Received: 18 April 2021
Accepted: 31 May 2021
Published: 02 July 2021

Citation:
Ran J, Li J, Yin L, Zhang D, Yu C, Du H, Jiang X, Yang C and Liu Y (2021) Comparative Analysis of Skeletal Muscle DNA Methylation and Transcriptome of the Chicken Embryo at Different Developmental Stages. Front. Physiol. 12:697121. doi: 10.3389/fphys.2021.697121

DNA methylation is a key epigenetic mechanism involved in embryonic muscle development and plays an important role in early muscle development. In this study, we sought to investigate the effects of genome-wide DNA methylation by combining the expression profiles of the chicken embryonic muscle. Genome-wide DNA methylation maps and transcriptomes of muscle tissues collected from different embryonic development points (E7, E11, E17, and D1) were used for whole-genome bisulfite sequencing (WGBS) and RNA sequencing, respectively. We found that the differentially methylated genes (DMGs) were significantly associated with muscle organ development, regulation of skeletal muscle satellite cell proliferation, and actin filament depolymerization. Furthermore, genes *TBX1*, *MEF2D*, *SPEG*, *CFL2*, and *TWF2* were strongly correlated with the methylation-caused expression switch. Therefore, we chose the *CFL2* gene to explore its function in skeletal muscle satellite cells, and the *in vitro* experiments showed that *CFL2* acts as a negative regulator of chicken skeletal muscle satellite cell proliferation and can induce cell apoptosis. These results provide valuable data for future genome and epigenome studies of chicken skeletal muscle and may help reveal the molecular mechanisms of potential economic traits.

Keywords: DNA methylation, transcriptome, muscle development, chicken, embryonic

INTRODUCTION

Skeletal muscle, as the main component of meat, is one of the most important agricultural animal economic traits. It is developed from myogenic precursor cells called myoblasts. Myoblasts proliferate and then differentiate into myotubes, and finally, myotubes differentiate into muscle fibers (Picard et al., 2002). It is generally believed that the proliferation of muscle fibers in animals, especially birds and mammals, mainly occurs during the embryonic period, and the number of muscle fibers is fixed and remains unchanged after birth (Yin et al., 2014). In birds and mammals, postnatal muscle growth is mainly achieved by skeletal muscle satellite cells fusing with existing fibers to cause muscle hypertrophy. These satellite cells have the potential of stem cells. In newborn

animals, they actively proliferate and supplement the nuclei of existing muscle fibers. In adult animals, their mitosis remains stationary and becomes active only when skeletal muscles are injured or damaged (Moss and Leblond, 1971). A comprehensive understanding of the genetic basis of skeletal muscle performance is essential for animal breeding and human biomedical research related to muscles.

Epigenetics refers to the fact that there is a heritable change in gene expression with no change in the base sequence of DNA. Epigenetic mechanisms include DNA methylation, histone modifications, and microRNAs (Goldberg et al., 2007). Among them, DNA methylation is involved in almost all biological functions, including embryonic development, cell proliferation and differentiation, genomic imprinting, and disease occurrence (Chiappinelli et al., 2015). A crucial role for DNA methylation in muscle development has been reported in humans (Miyata et al., 2015), pig (Yang et al., 2017), rabbits (Huszar, 1972), and chickens (Zhang et al., 2017). DNA methylation in the promoter region and gene body can stably change the gene expression, and this process has important effects on the development and tissue-specific gene expression (Jones, 2012; Yang et al., 2014). Genome-wide methylation and transcriptome association analysis is a commonly used method to study methylation function. Multi-omics association analysis can clarify important signal regulation pathways at multiple levels, and it is also an effective means for large-scale identification of new biological regulatory networks.

In this study, we performed DNA methylome profiling of chicken embryo skeletal muscle in Jiuyuan Black chicken using whole genome bisulfite sequencing (WGBS). A comprehensive analysis of genome-wide DNA methylation and transcriptome was performed to reveal the way DNA methylation can regulate muscle performance by affecting gene expression. We observed that gene expression is negatively correlated with DNA methylation in the promoter regions in chicken. We also screened differentially methylated genes and differentially expressed genes, and explored its role in chicken satellite cells. Our research provides an empirical basis in order to further explore the molecular regulation mechanism of muscle development in the early stage of poultry.

MATERIALS AND METHODS

Ethics Approval

All experimental operations were approved by the Animal Ethics Committee of Sichuan Agricultural University, and the approved number was B20171901-1. Relevant guidelines and regulations were followed while performing all the methods.

Tissue Sampling

The half-sibling fertilized eggs of Jiuyuan black chicken were incubated in the same condition (Temperature 37.8°C, relative humidity 60%, maintain ventilation). The leg muscle and blood were collected at E7, E11, E17, and D1. After sex determination by PCR, only samples identified as male were kept for the next experiments. A total of 12 embryonic chickens were used in the study to form four groups. Each group included three individuals as biological replicates.

DNA and RNA Extraction

The skeletal muscle derived from leg tissues of three embryos in different stages, E7, E11, and E17 (days 7, 11, and 17), and one newborn (D1) was stored in liquid nitrogen immediately after collection and DNA isolated from each aliquot using the QIAamp DNA Mini Kit (QIAGEN, Germany) following the recommended instruction. DNA concentration and quality were evaluated using the Qubit® DNA Assay Kit in Qubit® 2.0 Flurometer (Life Technologies, Carlsbad, CA, United States). Total RNA was isolated using the TRIzol (TAKARA, Dalian, China) reagent according to the manufacturer's instruction. RNA was reverse transcribed by the TAKARA PrimeScriptTM RT reagent kit (TAKARA) according to the manufacturer's instruction. The integrity of RNA was measured using agarose gel electrophoresis, and the purity was evaluated by NanoDrop 2000 spectrophotometer. Only qualified RNA samples were considered acceptable for sequencing.

Genome-Wide DNA Methylation Profiling

Genome-wide DNA methylation profiling of *Gallus gallus* skeletal muscle from four developmental stages was established using an Illumina Hiseq 2500 platform, and 150 bp paired-end reads were generated according to the manufacturer's standard procedure. In brief, genomic DNA was fragmented by sonication to 200–300 bp with Covaris S220, followed by end repair and adenylation. Then, these DNA fragments were treated with bisulfite using the EZ DNA Methylation Kit (Zymo Research, Irvine, CA, United States), before PCR amplification using KAPA HiFi HotStart Uracil + ReadyMix (2X). The resulting DNA products were used for library preparation and subsequent sequencing, and more than 140 million raw reads were produced in each sample. Raw image intensities were scanned by the iScan SQ scanner (iScan System, Illumina, United States) and processed by the Genome Studio software (Illumina, United States). The methylated rate of cytosine (Mc) was calculated as β value in designed windows bins (bin size is 10 kb), and the β value varied from 0 (completely unmethylated) to 1 (completely methylated). Overall, more than 4,100 Mb cytosine sites were measured in all of the samples. The β value was corrected according to Lister et al. (2013) studies to mitigate false positives from bisulfite non-conversion rate.

Differential Methylation Analysis

Differentially methylated regions (DMRs) were identified by a moderated dispersion shrinkage method of the DSS software (Park and Wu, 2016), which combines spatial correlation, read depth of the Cytosine sites, and variance among biological replicates to precisely detect DMRs in improving statistical tests. Genomic feature of DMRs was defined based on gene coordinates on the *Gallus gallus* genome annotation file,[1] and the intervals between upstream 1,000 bp from transcription start site (TSS) to downstream from 200 bp were considered as

[1] ftp://ftp.ensembl.org/pub/release-101/gtf/gallus_gallus/

promoter regions. The DMRs with a greater absolute value of statistical scores between two groups have a more probability of methylation difference.

RNA-Seq Data Preparation and Sequencing

Total RNA was extracted from the collected leg tissues as described above (with three replicates per group) by using the TRIzol reagent (Catalog No.15596-026, Invitrogen, Carlsbad, CA, United States) in accordance with the protocol. A total amount of 3 μg of RNA per sample was used as input material for the RNA sample preparations. RNA integrity was assessed using the RNA Nano 6000 Assay Kit of the Bioanalyzer 2100 system (Agilent Technologies, Santa Clara, CA, United States) with the qualified standard RIN value of >7. After rRNA depletion, second-strand cDNA synthesis, RNase H digestion, and adding adaptor in the 3′ end, the cDNA library for sequencing was constructed by PCR amplification. Then, the cDNA library qualification was detected and sequencing was performed on an Illumina Hiseq platform, and 150 bp paired-end (PE150) reads were generated.

Transcriptome Assembly

The clean data were mapped to the *Gallus gallus* genome[2] using the read aligner HISAT2 (version 2.0.4). Next, the transcriptome was assembled by the StringTie (version 1.3.1) on the basis of the reads mapped to the chicken genome. Annotated gtf files for each samples were produced and their raw counts information for each gene was extracted by using the python script prepDE.py (Pertea et al., 2016).

Differential Expression Analysis

The raw count data from the StringTie output was normalized through the median of ratios method in the DESeq2 (Love et al., 2014) package in R, to exclude the bias from sequencing depth and RNA composition. Normalized counts were used for differential expression analysis and the genes in comparison with an adjusted p-value < 0.05 were assigned as differentially expressed (DE).

Time-Series Expression Profile Analysis

The genes that were DE in at least one adjacent time point comparison (E7 vs. E11, E11 vs. E17, and E17 vs. D1) were used to perform the expression pattern analysis by STEM (version 1.3.11). The expression levels of transcripts were normalized [$\log_2$ (E7/E7), $\log_2$ (E11/E7), $\log_2$ (E17/E7), and $\log_2$ (D1/E7)] before being co-expressionally clustered. There are many designed modal profiles in the STEM software.[3] After inputting these gene expression data, genes were assigned to the model profiles that most closely represented their expression patterns as determined by the correlation coefficient ($r > 0.7$). The profiles with $p < 0.05$ were identified as significant temporal expression profiles, which obviously responded to the embryonic development and muscle tissue processing.

Gene Functional Enrichment Analysis

Biological process in gene ontology (GO) terms was conducted via the GO Biological Process 2018 data source in Enrichr (Kuleshov et al., 2016), which calculates the combined score by taking the log of the p-value from the Fisher exact test and multiplying that by the z-score of the deviation from the expected rank.

Protein Interaction Network of Integrated Genes

We used the STRING database (v11.0) (Damian et al., 2017) to construct and screen for a protein-protein interaction (PPI) network that contained differentially methylated and expressed genes with obvious functional enrichment related to muscle development. We only retained edges of the network that meet the following parameters: confidence score >0.8 and combined score >0.8. Cytoscape (v3.6.0)[4] was used to visualize interactions for the gene-gene pair input, including their strength of interaction reflected by the thickness of the line.

Cell Culture

Following the procedures described in previous studies, SMSCs were isolated and cultured from the pectoralis major of 3-day-old Jiuyuan black chicken. The pectoral muscle was collected and shredded to release cells with 0.1% collagenase I (Sigma Chemical Co., St. Louis, MO, United States) and 0.25% trypsin (Gibco, Grand Island, NY, United States). The satellite cells were isolated from the cell suspension by filtration and differential adhesion. Then, the 10% growth medium [GM: Dulbecco's modified Eagle medium (DMEM) (Gibco), +10% fetal bovine serum (Gibco), +0.2% penicillin/streptomycin (Invitrogen, Carlsbad, CA, United States)] was added to culture the isolated satellite cells. When the cell density reached 70–80% in the growth medium, the cells were cultured in the differentiation medium [DM: DMEM + 2% horse serum (Gibco)] instead, which is used to induce differentiation. The cells were cultured in a constant temperature and humidity cell incubator (Thermo Scientific, San Jose, CA, United States) (5% CO2 humid atmosphere, 37°C), and the medium was changed daily.

Cell Counting Kit-8 (CK-8) and 5-Ethynyl-2-Deoxyuridine (EdU) Assay

SMSCs were seeded in 96-well plates and transfected with siRNA, negative control. A Cell Counting Kit-8 kit (Multisciences, Hangzhou, China) was used to detect cell proliferative activity according to the manufacturer's instructions. Then, 10 μl of CCK-8 Reagent was added to each well cells at 12, 24, 36, and 48 h after cell transfection, and the cells were cultured in a constant temperature incubator (37°C, 5% CO2) for 2 h. The optical density (OD) of each sample at 450 nm was measured by a Thermo Scientific™ Varioskan LUX. For the EdU assay, the

[2] ftp://ftp.ensembl.org/pub/release-101/fasta/gallus_gallus/dna/Gallus_gallus.GRCg6a.dna.toplevel.fa.gz

[3] https://www.cs.cmu.edu/~{}jernst/stem/#

[4] http://www.cytoscape.org/

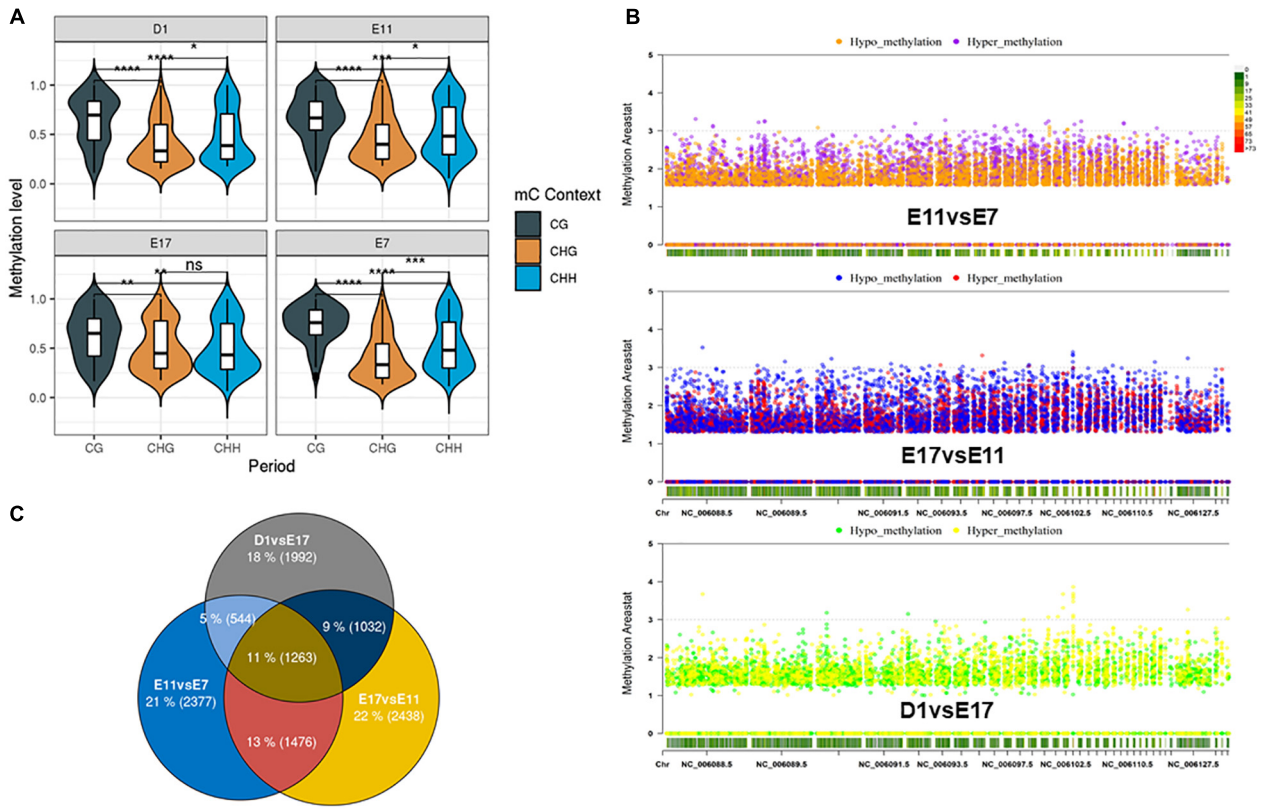

FIGURE 1 | DNA methylation profiles of leg muscle samples in four stages of chicken embryo. **(A)** Genome wide DNA methylation in three contexts of cytosine, *, **, ***, and **** mean *p*-value < 0.05, 0.01, 0.001, and 0.0001, respectively. D1: First day after birth; E7, E11, and E17 represent the 7th, 11th, and 17th day of embryonic stage, respectively. **(B)** Hypo- and hypermethylated regions across chromosomes in the comparison between two periods. **(C)** Amount and overlap of DMRs among the three compared groups.

proliferation state of muscle cells was performed with the Cell-Light^{TM} EdU kit according to the manufacturer's instructions. The quantities of EdU-positive cells were calculated using a fluorescence microscope (Olympus, Tokyo, Japan).

Cell Apoptosis Assay

Cells were stained with the annexin V-fluorescein isothiocyanate (FITC)/propidium iodide (PI) kit (Multisciences). The detailed procedures refer to the manufacturer's instruction and previous research (Li et al., 2018). Cell apoptosis was analyzed by using flow cytometry (Becton Dickinson).

Real-Time Quantitative PCR (qRT-PCR) and Western Blot Analysis

qRT-PCR analysis was performed in 10 μl reaction volumes containing 1 μl of cDNA, 0.5 μl of forward and reverse primers, 5 μl of TB Green^{TM} premix (Takara), and 3 μl of DNase/RNase Free deionized water (Tiangen, Beijing, China). The relative expressions of related genes were calculated by the $2^{-\Delta\Delta Ct}$ method, and three biological replicates were performed on each sample. The proteins were extracted on ice using commercial protein extraction kits (BestBio Biotech Co., Ltd., Shanghai, China) and adjusted to the same concentration, then placed at 95°C to denature for 5 min. The total volume of each well was 20 μl, including 16 μl of protein sample and 4 μl of reducing loading buffer (4:1). The steps and details of the Western blot analysis experiment are described in depth by Liu et al. (2019). The antibodies were diluted according to the manufacturer's instructions as follows: anti-Bcl2 (Santa Cruz Biotechnology, Santa Cruz, CA, United States), anti-Caspase 3 (Biorbyt, Cambridge, United Kingdom), anti-CDK2 (ABclonal Technology, Wuhan, China), anti-PCNA (ABclonal), and anti-CLF2 (ABclonal, Wuhan, China). The last, anti-β-actin (ZenBio, Chengdu, China; 1:2,000), was used as a loading control.

RESULTS

Genome-Wide DNA Methylation Patterns in Four Developmental Stages

Our objective was to determine DNA methylation and transcriptomic dynamics through the embryonic process that controls skeletal myogenesis in chicken tissues. From the genome wide DNA methylation landscape, cytosine with CG context accounted for the largest proportion in all developmental periods; more than 93% of methylated cytosines were adjacent

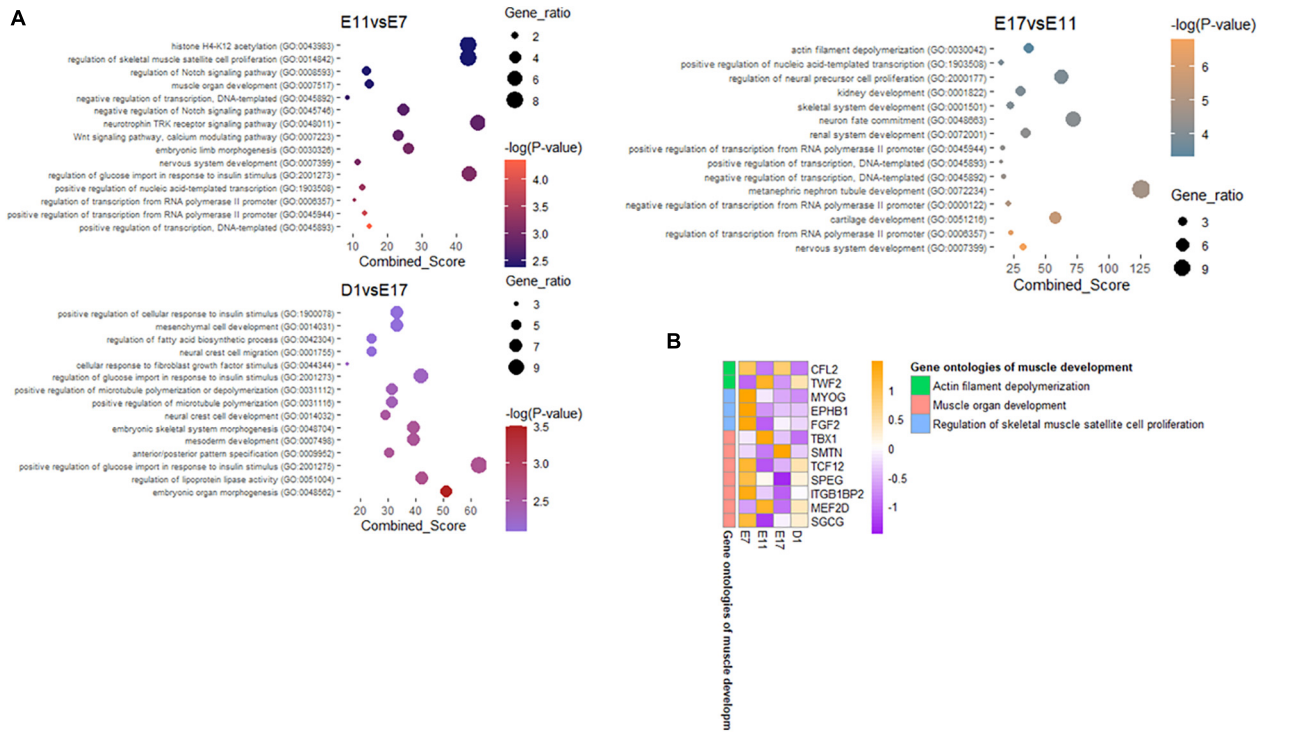

FIGURE 2 | Functional enrichment of DMRs. **(A)** Gene ontology terms of differentially methylated genes in E11 vs. E7, E17 vs. E11, and D1 vs. E17 comparisons, respectively. Combined score is computed by taking the log of the *p*-value from the Fisher exact test and multiplying that by the *z*-score of the deviation from the expected rank. **(B)** The methylation levels of the promoter regions of the genes related to muscle development.

to the guanines (**Supplementary Figure 1**). We found that the average methylation level of the three contexts is almost the same in the functional regions of the genome at the four developmental periods. In the CG context, the lowest methylation levels occurred in the promoter and utr 5 regions, while CHG and CHH contexts have the highest methylation levels in these two regions (**Supplementary Figure 2**). The methylation levels of cytosines in three different contexts also had preferences that CG context showed higher DNA methylation levels among the four groups; while methylation levels in CHG and CHH contexts were slightly lower (**Figure 1A**). In addition, the difference in the methylation levels between CG, CHH, and CHG contexts was extremely significant during E7, while during E17, there was no significant difference in the methylation levels between CHH and CHG contexts. Methylation profiles on the chicken genome were divided into specified and non-overlapped regions by the DSS software [13], the differentially methylated values were corrected by the Areastat score. The amount of DMRs were proportional with the size of the chromosomes, and there were more hypomethylated regions in E11 and E17 periods compared to E7 and D1 (**Figure 1B**). Based on the DMRs categorized by genomic elements, most of the DMRs were distributed on intronic regions and they were less than 200 bp on average (**Supplementary Figures 3**, **4**). After assigning the annotation information to the DMRs, 5,660, 6,209, and 4,831 differentially methylated genes were obtained in E11 vs. E7, E17 vs. E11, and D1 vs. E17 groups, respectively (**Figure 1C**).

To further understand the potential functions of genes that have differentially methylated regions compared to the nearing periods, gene ontology (GO) terms enrichment was conducted using DMRs contained genes (**Figure 2A**). There were muscle organ development (GO: 0007517) and regulation of skeletal muscle satellite cell proliferation (GO: 0014842) enriched by differentially methylated genes in E11 vs. E7 groups, and actin filament depolymerization (GO: 0030042) was an enriched GO term in E17 vs. E11 comparison. We focused on the genes that participate in the muscle development related GO terms and found their methylation levels in the promoter regions, which showed opposite trends with their expressional mode (**Figure 2B**). Most of the genes that were included in the biological process we described above had a lower promoter methylation level, indicating that their activated transcription potential may trigger the active muscle development in the middle and late stages of the egg embryo.

Continuous Expressional Activation of Muscle Development Genes Linked With Promoter Methylation

To identify the expression patterns during embryonic development, a Short Time-series Expression Miner (STEM) was conducted to cluster transcripts based on expressional trends during the time course. We applied all differentially expressed genes in the DESeq2 analysis and 12,473 genes were input to the

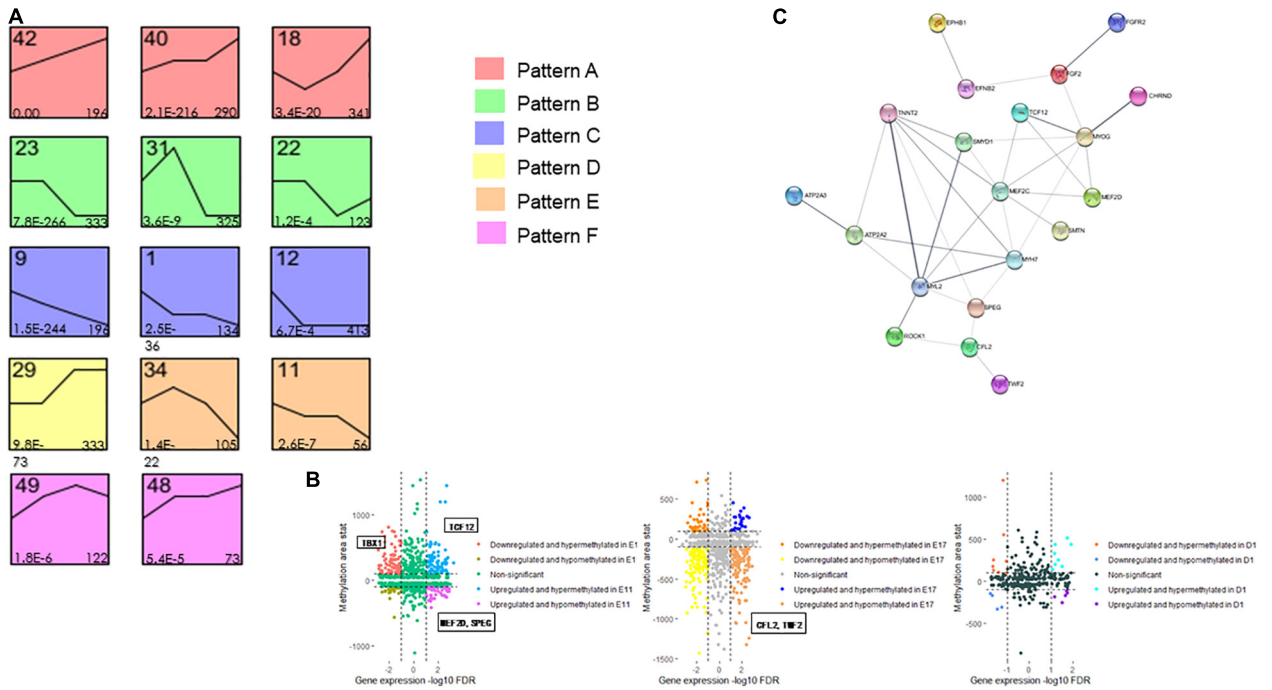

FIGURE 3 | Transcription of muscle development related genes is correlated with promoter DNA methylation. **(A)** Significant expression profiles ($p < 0.05$) of differentially expressed genes clustered via the STEM software during embryonic stages. The numbers in the top left corner of boxes are profile serial numbers, those in the bottom left corner are p values, and those in the bottom right corner are numbers of genes contained in profiles. Six general patterns were determined (patterns A–F) based on their similar expression features. **(B)** Quadrant plot showing promoter methylation and expression levels of the corresponding genes. The vertical dotted lines indicate a threshold of the adjusted p-value (FDR) equals 0.05, and parallel dotted lines show a threshold of the absolute methylation AreaStat equals 100. **(C)** The protein-protein interaction (PPI) network among both differentially methylated and expressed genes, and line thickness shows their strength of interaction.

STEM analysis. In total, 50 model profiles were detected and 14 expression profiles were specified with sufficient gene numbers and significant co-expression trends (**Figure 3A**). The significant expression patterns can be categorized into six feature patterns (**Figure 3A**) based on their continuous changes compared to the starting time point (E7). Intriguingly, we found that profile 48 always performed an obvious enrichment in muscle-related GO terms compared to other expression profiles (**Table 1**). Then, we integrated the methylation levels of genes corresponding to their expression profiles and found that their positive and negative relationships in genes are both differentially methylated and expressed (**Figure 3B**). Notably, genes *TBX1*, *TCF12*, *MEF2D*, *SPEG*, *CFL2*, and *TWF2* were strongly correlated with the methylation-caused expression switch and their functions in embryonic muscle formation should be investigated further. Moreover, to understand the protein interactions between the genes of interest, a protein-protein interaction (PPI) network was constructed and their strength of interaction, which was reflected through the line thickness, was showed with other actively interacted genes (**Figure 3C** and **Supplementary Table 1**).

TABLE 1 | Expression profile 48 enriched GO terms.

Category ID	Category_name	Cluster enrichment *p*-value	Gene included
GO:0071340	skeletal muscle acetylcholine-gated channel clustering	0.00041	*FZD9,RER1,FNTA*
GO:0060538	skeletal muscle organ development	0.04	*SMYD1,MEF2C, CHRND,FBXO22*
GO:0007519	skeletal muscle tissue development	0.03	*SMYD1,MEF2C, CHRND,FBXO22*
GO:0055001	muscle cell development	0.03	*MEF2C,ATP2A2, FBXO22*
GO:0042692	muscle cell differentiation	0.04	*SMYD1,MEF2C, ATP2A2,FBXO22*
GO:0042693	muscle cell fate commitment	0.02	*MEF2C*
GO:0042694	muscle cell fate specification	0.02	*MYL2*
GO:0014812	muscle cell migration	0.04	*MEF2C,ROCK1*

CFL2 Inhibits Chicken Skeletal Muscle Satellite Cells Proliferation

In order to reveal the function of *CFL2* in chicken skeletal muscle satellite cells, we transfected the *CFL2* siRNA into chicken SMSCs to assess its effect on cell proliferation and apoptosis. After the knockdown of *CFL2* with siRNA, the mRNA expression level of *CFL2* could be inhibited significantly (**Figure 4A**). The quantities of EdU staining-positive cells were

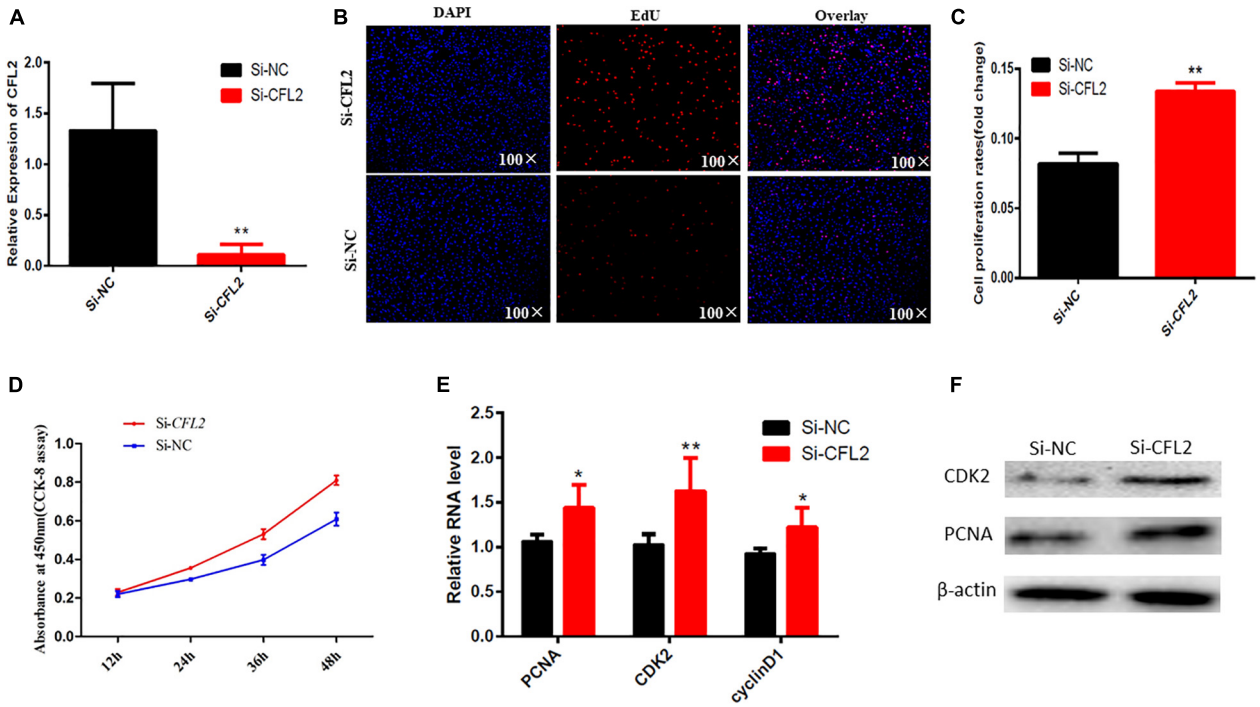

FIGURE 4 | *CFL2* regulates chicken skeletal muscle satellite cells proliferation. **(A)** Detection of *CFL2* mRNA expression after transfection of *CFL2* siRNA. **(B)** EdU staining-positive muscle cells were detected by the EdU kit after knockdown *CFL2*. **(C)** Cell proliferation rate after knockdown of *CFL2*. **(D)** Cell proliferation status was detected within 48 h at 450 nm with CCK-8 reagent after knockdown of *CFL2*. **(E)** Cell proliferation-related genes (*PCNA*, *CDK2*, and *cyclinD1*) mRNA expression level was detected by qRT-PCR after the knockdown of *CFL2*. **(F)** Cell proliferation-related genes (PCNA and CDK2) protein expression level was detected by Western blot. Data are presented as mean ± SEM; $^{*}p < 0.05$ and $^{**}p < 0.01$.

increased after the knockdown of *CFL2* (**Figures 4B,C**). CCK-8 assay can detect cell viability, and the results showed that SMSCs proliferation was significantly promoted following *CFL2* knockdown (**Figure 4D**). In parallel, the expression of cell proliferation marker genes *PCNA*, *CDK2*, and cyclinD1 were detected. qRT-PCR results showed that the knockdown of *CFL2* increased the mRNA expression levels of *PCNA*, *CDK2*, and *cyclinD1* (**Figure 4E**). Furthermore, the Western blot results showed that the expression of PCNA and CDK2 was promoted by transfection with *CFL2* siRNA (**Figure 4F**). Collectively, these results demonstrate that *CFL2* could inhibit chicken skeletal muscle satellite cells proliferation.

CFL2 Promotes Chicken Skeletal Muscle Satellite Cells Apoptosis

We also detected some cell survival genes *Bcl-2*, *caspase3*, and *caspase9* mRNA level by qRT-PCR. Compared with the control group, the expression levels of *caspase3* and *caspase9* in the *CFL2* SiRNA group were decreased, but the *Bcl-2* expression level was increased (**Figure 5A**). The corresponding protein levels of these genes also showed the same changes like their mRNA level (**Figure 5B**). Additionally, the number of apoptotic cells in the *CFL2* siRNA group was decreased compared with the control group (**Figure 5C**). We also found that the mitochondrial transmembrane potential ($\Delta\Psi m$) and reactive oxygen species (ROS) content decreased with the knockdown of *CFL2* (**Figures 5D,E**). All of these results indicate that *CFL2* promotes chicken skeletal muscle satellite cells apoptosis.

DISCUSSION

DNA methylation contributes substantially to phenotypic variations in aging (Bell et al., 2012), obesity (Wang et al., 2010), and body size (Relton et al., 2012). However, the regulatory mechanism of DNA methylation affecting chicken embryo skeletal muscle performance is still unclear. As a tissue of major economic importance in meat-producing animals, skeletal muscle plays important roles in initiating movements, supporting respiration, and maintaining homeostasis (Ge et al., 2014). In addition, chicken provides a unique model to perform embryological research due to the accessibility of its egg. Here, we use the Jiuyuan black chicken to explore the development of skeletal muscle in the embryonic period of chickens. We performed whole genome bisulfite sequencing and RNA-seq to systematically explore the prenatal DNA methylation landscape during chicken muscle development. We mainly focus on the systematic study of the four different embryonic stages of E7, E11, E17, and D1 to find the factors that affect the development of skeletal muscle.

Different CpG contexts (CG, CHG, and CHH) at the four developmental stages have similar DNA methylation levels and

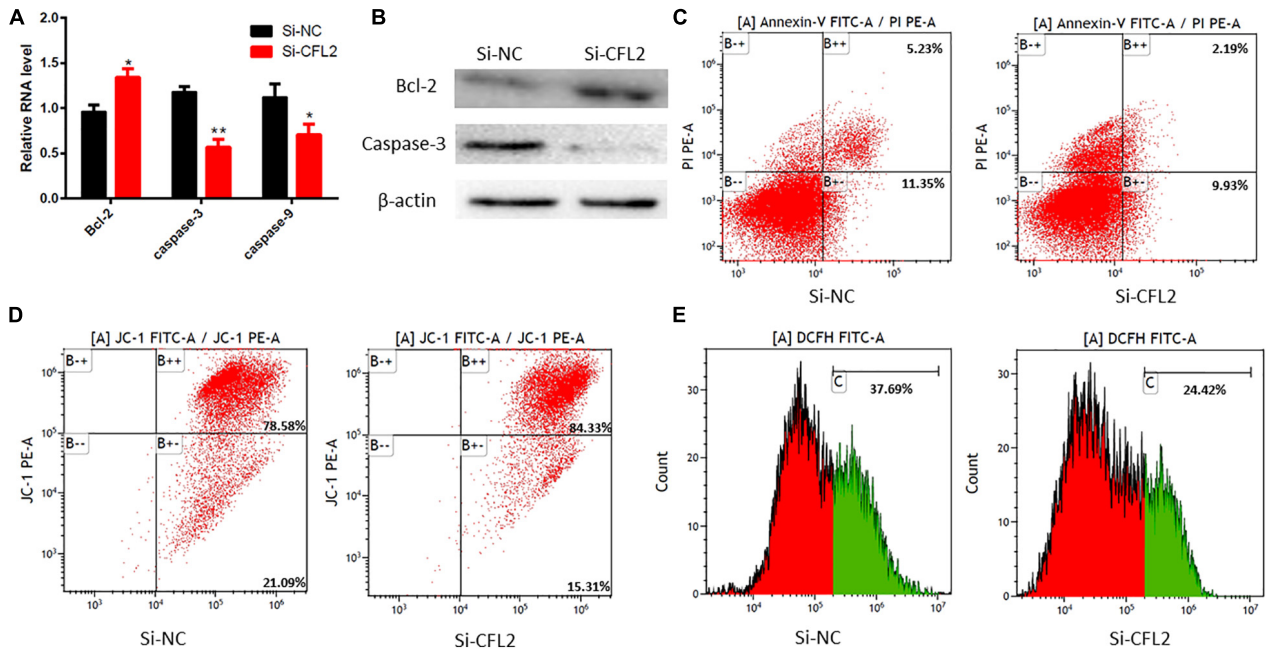

FIGURE 5 | *CFL2* regulates chicken skeletal muscle satellite cells apoptosis. **(A)** Cell apoptosis-related genes (*Bcl2*, *Caspase 3*, and *Caspase 9*) mRNA expression level was detected by qRT-PCR after the knockdown of *CFL2*. **(B)** Cell apoptosis-related genes (Bcl2 and Caspase 3) protein expression level was detected by Western blot. **(C)** Apoptotic muscle cells were detected by annexin V-FITC/PI-staining flow cytometry after the knockdown of *CFL2*. **(D)** Mitochondrial transmembrane potential ($\Delta\Psi$m) was detected by annexin V-FITC/PI-staining flow cytometry after knockdown of *CFL2*. **(E)** Reactive oxygen species (ROS) content was detected by annexin V-FITC/PI-staining flow cytometry after knockdown of *CFL2*. Data are presented as mean ± SEM; $^{*}p < 0.05$ and $^{**}p < 0.01$.

proportions, with the highest CG content and extremely low CHG and CHH content. These results were in accordance with findings in other species (Laurent et al., 2010; Sati et al., 2012). It has been well documented that gene-body exhibits higher methylation than the 5′ flanking regions and promoter methylation negatively correlates with gene expression (Law and Jacobsen, 2010; Zemach et al., 2010). For the gene body regions, we did not observe a higher methylation level in exons than in introns in chickens, which is in contrast to a previous research (Hu et al., 2013). Gene body methylation and expression levels apparently have a complex relationship, it has been demonstrated that CGIs could influence local chromatin structure (Deaton and Bird, 2011). In the present study, we found a large number of methylated CGIs in the intragenic and intergenic regions. These CGIs were proven to have the characteristics of functional promoters and the methylation of intragenic CGIs played a crucial role in regulating alternative promoters (Illingworth et al., 2010; Maunakea et al., 2010).

Next, we comprehensively compared the methylation levels of genes among four different developmental stages. There were more hypomethylated regions in E11 and E17 periods compared to E7 and D1, which may be responsible for their different speeds in muscle development. After assigning the annotation information to the DMRs, 5,660, 6,209, and 4,831 differentially methylated genes were obtained in E11 vs. E7, E17 vs. E11, and D1 vs. E17 groups, respectively. In chickens, Myofiber ontogenesis begins with the appearance of two successive waves of myoblasts, which are the primary fibers mainly formed in E3–E7 and the secondary fibers mainly formed in E8–E16 (Bandman and Rosser, 2000; Picard et al., 2002). Therefore, the number of DMRs was detected to rise dramatically at E17, suggesting that E17 may be a crucial period for chicken embryonic skeletal muscle development. Genes that overlapped with DMR at different times were regarded as DMGs and used for GO analysis. We found that DMGs at E11 was significantly enriched in muscle organ development (GO: 0007517) and regulation of skeletal muscle satellite cell proliferation (GO: 0014842), DMGs at E17 was significantly enriched in actin filament depolymerization (GO: 0030042). These terms are closely related to muscle development, thus, the DMGs at E11 and E17 may have an important role in the fetal phase of muscle development in chicken (Stockdale and Miller, 1987).

In addition, we also found that the methylation levels of the promoter regions of these GO term-related genes exhibited an opposite trend to their expression levels. Many of them are widely reported genes closely related to the growth and development of skeletal muscle, including those that regulates the muscle-specific genes expression, *MYOG* (Yin et al., 2011), promotes the proliferation of muscle precursor cells, *FGF2* (Velleman, 2007), and stimulates muscle cell differentiation, *MEF2D* (Wang et al., 2015), etc. These lower promoter methylation levels may be closely related to the rapid development of skeletal muscles in the middle and late stages of the embryo.

To characterize the correlation between gene methylation and expression levels, we further focused on identifying differentially

methylated (DMR-associated) and differentially expressed genes through DNA methylation profile and RNA-seq data. We have obtained 50 model profiles after the STEM analysis of 12,473 differential genes. Among them, we found that profile 48 always showed an obvious enrichment in muscle-related GO terms, such as skeletal muscle tissue development (GO:0007519), muscle cell development (GO:0055001), muscle cell differentiation (GO:0042692), etc. By integrating the methylation levels of genes corresponding to their expression profiles, it is found that their positive and negative relationship in genes were both differentially methylated and expressed. In particular, there are several genes which are strongly correlated with the methylation-caused expression switch.

We chose to study the function of the *CFL2* gene in embryonic skeletal muscle development further. The role of *CFL2* has been studied in cardiac muscle (Vafiadaki et al., 2020) and many types of congenital myopathies (Rosen et al., 2020), but not in chicken skeletal muscle development. Qian et al. (2017) found significant differences in the *CFL2* gene in chicken leg muscle transcriptomes of different ages. In the present study, we proved that *CFL2* acts as a negative regulator of chicken skeletal muscle satellite cell proliferation and can induce cell apoptosis. Furthermore, *CLF2* has been reported to be an essential mediator for myogenic differentiation in C2C12 myoblasts (Mai et al., 2020). These results suggest that *CFL2* is regulated by DNA methylation and participates in muscle development during embryonic stages. Subsequent knockdown and Western blot assay verified the results of our analysis, indicating the reliability of our analysis and the role of *CFL2* in muscle cells proliferation and apoptosis.

In conclusion, we revealed a comprehensive DNA methylome and transcriptome landscape during the embryonic developmental stages in chickens, and identified that *CFL2* gene plays a significant role in regulating SMSCs proliferation and apoptosis. Moreover, these results provide valuable data for future genome and epigenome studies of chicken skeletal muscle and may help reveal the molecular mechanisms of potential economic traits.

DATA AVAILABILITY STATEMENT

The data in this study has been deposited into BioProject (accession: PRJNA723059, https://www.ncbi.nlm.nih.gov/bioproject/PRJNA723059).

ETHICS STATEMENT

The animal study was reviewed and approved by the Animal Ethics Committee of Sichuan Agricultural University, Chengdu, China.

AUTHOR CONTRIBUTIONS

JR performed the experiments, analyzed the data, designed the study, and wrote and reviewed the manuscript. LY and DZ collected the samples. YL and CWY performed the project administration. CLY and JL performed the experiments. HD and XJ analyzed the data. All authors read and approved the final manuscript.

FUNDING

This research was financially supported by the Sichuan Province Science and Technology Project (2021ZHFP0163), the Key Projects of Breeding in Sichuan Province (2021YFYZ0031), and the Broiler Breeding Project in Qinba Mountain Area (2017NFP0098).

ACKNOWLEDGMENTS

We thank Wanyuan Hengkang Agricultural Development Co., Ltd. for providing the experimental fertilized eggs and chickens.

SUPPLEMENTARY MATERIAL

The Supplementary Material for this article can be found online at: https://www.frontiersin.org/articles/10.3389/fphys.2021.697121/full#supplementary-material

Supplementary Figure 1 | Classification of methylated cytosines at four different developmental stages.

Supplementary Figure 2 | Distribution of methylation levels in functional regions.

Supplementary Figure 3 | Distribution of DMR gene regions obtained by pairwise comparison of four different developmental stages.

Supplementary Figure 4 | Distribution of DMR gene length obtained by pairwise comparison of four different developmental stages.

Supplementary Table 1 | Gene Ontology (GO) analysis of PPI network proteins.

REFERENCES

Bandman, E., and Rosser, B. W. (2000). Evolutionary significance of myosin heavy chain heterogeneity in birds. *Microsc Res Tech*. 50, 473–491. doi: 10.1002/1097-0029(20000915)50:6<473::aid-jemt5>3.0.co;2-r

Bell, J. T., Tsai, P. C., Yang, T. P., Pidsley, R., and Nisbet, J. (2012). Epigenome-wide scans identify differentially methylated regions for age and age-related phenotypes in a healthy ageing population. *PLoS Genetics*. 8:e1002629. doi: 10.1371/journal.pgen.1002629

Chiappinelli, K., Strissel, P., Desrichard, A., Li, H., Henke, C., Akman, B., et al. (2015). Inhibiting DNA methylation causes an interferon response in cancer via dsrna including endogenous retroviruses. *Cell*. 162, 974–986. doi: 10.1016/j.cell.2015.07.011

Damian, S., Morris, J. H., Helen, C., Michael, K., Stefan, W., Milan, S., et al. (2017). The string database in 2017: quality-controlled protein–protein association networks, made broadly accessible. *Nucleic Acids Research* 45(D1), D362–D368.

Deaton, A. M., and Bird, A. (2011). CpG islands and the regulation of transcription. *Genes, Development*. 25, 1010–1022. doi: 10.1101/gad.2037511

Ge, X., Zhang, Y., Sungwon, P., Cong, X., Gerrard, D. E., and Jiang, H. (2014). Stac3 inhibits myoblast differentiation into myotubes. *Plos One*. 9:e95926. doi: 10.1371/journal.pone.0095926

Goldberg, A. D., Allis, C. D., and Bernstein, E. (2007). Epigenetics: a landscape takes shape. *Cell*. 128, 635–638. doi: 10.1016/j.cell.2007.02.006

Hu, Y., Xu, H., Li, Z., Zheng, X., Jia, X., Nie, Q., et al. (2013). Comparison of the genome-wide DNA methylation profiles between fast-growing and slow-growing broilers. *Plos One*. 8:e56411. doi: 10.1371/journal.pone.0056411

Huszar, G. (1972). Developmental changes of the primary structure and histidine methylation in rabbit skeletal muscle myosin. *Nature New Biology*. 240, 260–264. doi: 10.1038/newbio240260a0

Illingworth, R. S., Gruenewald-Schneider, U., Webb, S., Kerr, A. R., James, K. D., Turner, D. J., et al. (2010). Orphan cpg islands identify numerous conserved promoters in the mammalian genome. *PLoS Genetics*. 6:e1001134. doi: 10.1371/journal.pgen.1001134

Jones, P. A. (2012). Functions of DNA methylation: islands, start sites, gene bodies and beyond. *Nature Reviews Genetics*. 13, 484–492. doi: 10.1038/nrg3230

Kuleshov, M. V., Jones, M. R., Rouillard, A. D., Fernandez, N. F., Duan, Q., Wang, Z., et al. (2016). Enrichr: a comprehensive gene set enrichment analysis web server 2016 update. *Nucleic Acids Research* 44(W1), W90–W97.

Laurent, L., Wong, E., Li, G., Huynh, T., Tsirigos, A., Ong, C. T., et al. (2010). Dynamic changes in the human methylome during differentiation. *Genome Research*. 20, 320–331. doi: 10.1101/gr.101907.109

Law, J. A., and Jacobsen, S. E. (2010). Establishing, maintaining and modifying DNA methylation patterns in plants and animals. *Nature Reviews Genetics*. 11, 204–220. doi: 10.1038/nrg2719

Li, H., Yang, J., Wei, X., Song, C., Dong, D., Huang, Y., et al. (2018). Circfut10 reduces proliferation and facilitates differentiation of myoblasts by sponging mir-133a. *Journal of Cellular Physiology*. 233, 4643–4651. doi: 10.1002/jcp.26230

Lister, R., Mukamel, E. A., Nery, J. R., Urich, M., Puddifoot, C. A., Johnson, N. D., et al. (2013). Global epigenomic reconfiguration during mammalian brain development. *Science* 341(6146), 1237905. doi: 10.1126/science.1237905

Liu, Z., Han, S., Shen, X., Wang, Y., He, H., Cui, C., et al. (2019). The landscape of DNA methylation associated with the transcriptomic network in layers and broilers generates insight into embryonic muscle development in chicken. *Int J Biol Sci*. 15, 1404–1418. doi: 10.7150/ijbs.35073

Love, M. I., Huber, W., and Anders, S. (2014). Moderated estimation of fold change and dispersion for RNA-seq data with deseq2. *Genome Biology*. 15, 550.

Mai, T., Khm, A., Dk, A., Syp, A., and Wan, L. (2020). CFL2 is an essential mediator for myogenic differentiation in C2C12 myoblasts. *Biochemical and Biophysical Research Communications*. 533, 710–716. doi: 10.1016/j.bbrc.2020.11.016

Maunakea, A. K., Nagarajan, R. P., Bilenky, M., Ballinger, T. J., D'Souza, C., Fouse, S. D., et al. (2010). Conserved role of intragenic DNA methylation in regulating alternative promoters. *Nature* 466(7303), 253–257. doi: 10.1038/nature09165

Miyata, K., Miyata, T., Nakabayashi, K., Okamura, K., Naito, M., Kawai, T., et al. (2015). DNA methylation analysis of human myoblasts during in vitro myogenic differentiation: de novo methylation of promoters of muscle-related genes and its involvement in transcriptional down-regulation. *Human Molecular Genetics*. 24, 410–423. doi: 10.1093/hmg/ddu457

Moss, F. P., and Leblond, C. P. (1971). Satellite cells as the source of nuclei in muscles of growing rats. *Anatomical Record-advances in Integrative Anatomy & Evolutionary Biology* 170, 421–435. doi: 10.1002/ar.1091700405

Park, Y., and Wu, H. (2016). Differential methylation analysis for BS-seq data under general experimental design. *Bioinformatics*. 32, 1446–1453. doi: 10.1093/bioinformatics/btw026

Pertea, M., Kim, D., Pertea, G. M., Leek, J. T., and Salzberg, S. L. (2016). Transcript-level expression analysis of rna-seq experiments with hisat, stringtie and ballgown. *Nature Protocols*. 11, 1650–1667. doi: 10.1038/nprot.2016.095

Picard, B., Lefaucheur, L., Berri, C., and Duclos, M. J. (2002). Muscle fibre ontogenesis in farm animal species. *Reproduction Nutrition Development*. 42, 415–431. doi: 10.1051/rnd:2002035

Qian, X., Zhang, G., Li, T., Ling, J., and Wang, J. (2017). Transcriptomic profile of leg muscle during early growth in chicken. *PLoS ONE*. 12:e0173824. doi: 10.1371/journal.pone.0173824

Relton, C. L., Groom, A., Pourcain, B. S., Sayers, A. E., Swan, D. C., Embleton, N. D., et al. (2012). DNA methylation patterns in cord blood DNA and body size in childhood. *PLoS ONE*. 7:e31821. doi: 10.1371/journal.pone.0031821

Rosen, S. M., Mugdha, J., Talia, H., Beggs, A. H., and Agrawal, P. B. (2020). Knockin mouse model of the human cfl2 p.a35t mutation results in a unique splicing defect and severe myopathy phenotype. *Human Molecular Genetics* 29(12), 1996–2003. doi: 10.1093/hmg/ddaa035

Sati, S., Singh, T. V., Anand, K. K., Ashok, P., Vaibhav, J., Sourav, G., et al. (2012). High resolution methylome map of rat indicates role of intragenic dna methylation in identification of coding region. *PLoS ONE*. 7:e31621. doi: 10.1371/journal.pone.0031621

Stockdale, F. E., and Miller, J. B. (1987). The cellular basis of myosin heavy chain isoform expression during development of avian skeletal muscles. *Developmental Biology*. 123, 1–9. doi: 10.1016/0012-1606(87)90420-9

Vafiadaki, E., Arvanitis, D. A., Eliopoulos, A. G., Kranias, E. G., and Sanoudou, D. (2020). The cardioprotective pka-mediated hsp20 phosphorylation modulates protein associations regulating cytoskeletal dynamics. *International Journal of Molecular Sciences*. 21, 9572. doi: 10.3390/ijms21249572

Velleman, S. G. (2007). Muscle development in the embryo and hatchling. *Poult. Sci*. 86, 1050–1054. doi: 10.1093/ps/86.5.1050

Wang, H., Zhang, L., Cao, J., Wu, M., Ma, X., Liu, Z., et al. (2015). Genome-wide specific selection in three domestic sheep breeds. *PLoS ONE*. 10:e0128688. doi: 10.1371/journal.pone.0128688

Wang, X., Zhu, H., Snieder, H., Su, S., Munn, D., Harshfield, G., et al. (2010). Obesity related methylation changes in DNA of peripheral blood leukocytes. *BMC Medicine*. 8:87. doi: 10.1186/1741-7015-8-87

Yang, X., Han, H., Decarvalho, D., Lay, F., and Liang, G. (2014). Gene body methylation can alter gene expression and is a therapeutic target in cancer. *Cancer Cell*. 26(4), 577–590. doi: 10.1016/j.ccr.2014.07.028

Yang, Y., Liang, G., Niu, G., Zhang, Y., Zhou, R., Wang, Y., et al. (2017). Comparative analysis of DNA methylome and transcriptome of skeletal muscle in lean-, obese-, and mini-type pigs. *Scientific Reports*. 7, 39883.

Yin, H., Zhang, S., Gilbert, E. R., Siegel, P. B., Zhu, Q., and Wong, E. A. (2014). Expression profiles of muscle genes in postnatal skeletal muscle in lines of chickens divergently selected for high and low body weight. *Poult. Sci*. 93, 147–154. doi: 10.3382/ps.2013-03612

Yin, H., Zhang, Z., Xi, L., Zhao, X., and Zhu, Q. (2011). Association of myf5, myf6 and myog gene polymorphisms with carcass traits in Chinese meat type quality chicken populations. *Journal of Animal and Veterinary Advances*. 10, 704–708. doi: 10.3923/javaa.2011.704.708

Zemach, A., Mcdaniel, I. E., Silva, P., and Zilberman, D. (2010). Genome-wide evolutionary analysis of eukaryotic DNA methylation. *Science* 328, 916–919. doi: 10.1126/science.1186366

Zhang, M., Yan, F. B., Li, F., Jiang, K. R., Li, D. H., Han, R. L., et al. (2017). Genome-wide DNA methylation profiles reveal novel candidate genes associated with meat quality at different age stages in hens. *Scientific Reports*. 7, 45564.

Conflict of Interest: The authors declare that the research was conducted in the absence of any commercial or financial relationships that could be construed as a potential conflict of interest.

frontiers in Physiology

ORIGINAL RESEARCH
published: 06 July 2021
doi: 10.3389/fphys.2021.682441

FOSL2 Is Involved in the Regulation of Glycogen Content in Chicken Breast Muscle Tissue

Xiaojing Liu[1†], Lu Liu[2†], Jie Wang[1†], Huanxian Cui[1], Guiping Zhao[1] and Jie Wen[1]*

[1] State Key Laboratory of Animal Nutrition, Institute of Animal Sciences, Chinese Academy of Agricultural Sciences, Beijing, China, [2] College of Animal Science and Technology, College of Veterinary Medicine of Zhejiang A&F University, Hangzhou, China

The glycogen content in muscle of livestock and poultry animals affects the homeostasis of their body, growth performance, and meat quality after slaughter. FOS-like 2, AP-1 transcription factor subunit (FOSL2) was identified as a candidate gene related to muscle glycogen (MG) content in chicken in our previous study, but the role of FOSL2 in the regulation of MG content remains to be elucidated. Differential gene expression analysis and weighted gene coexpression network analysis (WGCNA) were performed on differentially expressed genes (DEGs) in breast muscle tissues from the high-MG-content (HMG) group and low-MG-content (LMG) group of Jingxing yellow chickens. Analysis of the 1,171 DEGs (LMG vs. HMG) identified, besides *FOSL2*, some additional genes related to MG metabolism pathway, namely *PRKAG3*, *CEBPB*, *FOXO1*, *AMPK*, and *PIK3CB*. Additionally, WGCNA revealed that *FOSL2*, *CEBPB*, *MAP3K14*, *SLC2A14*, *PPP2CA*, *SLC38A2*, *PPP2R5E*, and other genes related to the classical glycogen metabolism in the same coexpressed module are associated with MG content. Also, besides finding that *FOSL2* expression is negatively correlated with MG content, a possible interaction between *FOSL2* and *CEBPB* was predicted using the STRING (Search Tool for the Retrieval of Interacting Genes) database. Furthermore, we investigated the effects of lentiviral overexpression of FOSL2 on the regulation of the glycogen content *in vitro*, and the result indicated that FOSL2 decreases the glycogen content in DF1 cells. Collectively, our results confirm that FOSL2 has a key role in the regulation of the MG content in chicken. This finding is helpful to understand the mechanism of MG metabolism regulation in chicken and provides a new perspective for the production of high-quality broiler and the development of a comprehensive nutritional control strategy.

Keywords: chicken, muscle glycogen, FOSL2, CEBPB, gene network

OPEN ACCESS

Edited by:
Sandra G. Velleman, The Ohio State University, United States

Reviewed by:
Elizabeth Ruth Gilbert, Virginia Tech, United States
Yuwares Malila, National Center for Genetic Engineering and Biotechnology (BIOTEC), Thailand

***Correspondence:**
Jie Wen
wenjie@caas.cn

† These authors have contributed equally to this work

Specialty section:
This article was submitted to Avian Physiology, a section of the journal Frontiers in Physiology

Received: *18 March 2021*
Accepted: *03 May 2021*
Published: *06 July 2021*

Citation:
Liu X, Liu L, Wang J, Cui H, Zhao G and Wen J (2021) FOSL2 Is Involved in the Regulation of Glycogen Content in Chicken Breast Muscle Tissue. Front. Physiol. 12:682441. doi: 10.3389/fphys.2021.682441

INTRODUCTION

Muscle glycogen (MG), as the main source of glucose for muscle glycolysis (Godfrey and Quinlivan, 2016), can supply adenosine triphosphate to muscles through its own degradation, which is closely related to muscle growth and development (Puolanne and Immonen, 2014).Under special physiological conditions (such as intense exercise), it can maintain the stability of blood sugar

and regulate the balance of glucose metabolism. In addition, MG content affects various meat quality indicators, such as meat color, tenderness, and pH of livestock and poultry meat (Henckel, 1996; Berri et al., 2007; Le Bihan-Duval et al., 2008). The degradation of MG to lactic acid changes the pH, which affects meat quality; thus, pH is an important indicator of meat quality (Alnahhas et al., 2015).

A previous genome-wide association study (GWAS) analysis of the MG phenotype conducted using the whole-genome resequencing data of 474 chickens identified FOS-like 2, AP-1 transcription factor subunit (*FOSL2*) transcription factor subunit as a candidate gene whose product affects MG content (Liu et al., 2020). *FOSL2* belongs to the activator protein 1 (AP1) transcription factor family, which is expressed in various tissues and is involved in fat metabolism, bone development, and the pathogenesis of various diseases, such as cancer (Foletta et al., 1994; Chinenov and Kerppola, 2001; Eferl and Wagner, 2003). A study on the involvement of FOSL2 in type 2 diabetes found that the epigenetic downregulation of FOSL2 mRNA and protein expression levels by DNA hypermethylation may induce the occurrence of type 2 diabetes in patients (Li et al., 2016). FOSL2 plays a key role not only in human physiology and disease (Eferl et al., 2008), but also in the differentiation of chondrocytes by controlling osteoclast-specific transcription (Karreth et al., 2004). Additionally, FOSL2 regulates bone formation by osteoblasts in mouse and human mainly by regulating the expression of collagen isoforms collagen, type I, alpha 2 chain (COL1A2) and bone gamma-carboxyglutamate protein (BGLAP) (Bozec et al., 2010). Previous studies have reported that the *FOSL2* gene protein product activates *CEBPB* transcription in prostaglandin E_2 (PGE_2)–activated osteoblasts. Although the regulatory effect of transcription factor CEBPB on chicken MG content has also been reported (Sibut et al., 2011), the role of *FOSL2* expression in tissues other that bone tissue, such as its role in MG metabolism, has not been described to date. An interesting experiment conducted in mice found that osteoblasts specifically express *FOSL2* to regulate Adipoq and Bglap levels, which in turn influences systemic glucose and insulin metabolism (Bozec et al., 2013). Although the study did not clearly reveal that FOSL2 affects the content of MG, it suggested that FOSL2 is closely related to glucose metabolism. MG is synthesized from monomers of uridine diphosphate glucose and serves as a storage form of energy in the body. Thus, MG and glucose are inseparably related.

In this study, breast muscle tissues from the high-MG-content (HMG) group and the low-MG-content (LMG) group of Jingxing yellow (JX-Y) chickens were subjected to transcriptome sequencing. Combined with the weighted gene coexpression network analysis (WGCNA), the protein products of the identified candidate genes were further analyzed to study the effect of gene transcription on chicken MG content from the perspective of gene expression and its relationship with phenotype. Considering the complex function of FOSL2 in chickens of different breeds and sex, we studied the effects of the *FOSL2* expression level in breast muscle of Beijing You (BJY) chicken. Furthermore, we also investigated the effects of *FOSL2* expression on the MG content in chicken fibroblast DF1 cells. This study found that FOSL2 reduces MG content likely by downregulating the activity of *CEBPB*.

MATERIALS AND METHODS

Ethics Statement and Animals

All animals and experimental protocols used in this study were approved by the Beijing Institute of Animal Science, Chinese Academy of Agricultural Sciences (the scientific research department responsible for animal welfare issues) (no.: IAS2019-21).

In this study, the experimental samples were derived from 474 female 98-day-old JX-Y chickens, a synthetic breed by the Institute of Animal Science of Chinese Academy of Agricultural Sciences, with high fat content and unique flavor, which is a better material for meat quality research. Additionally, 30 male and 30 female 98-day old BJY chickens, a unique Chinese local breed, with high flavor characteristics, were selected to evaluate the influence of the breed and sex.

All experimental birds were raised in an environmentally controlled room, in three-story step cages. Basal diets were formulated based on the National Resource Council (1994) requirements and the Feeding Standards of Chickens established by the Ministry of Agriculture, Beijing, China (2004).x1 All birds were provided *ad libitum* access to feed and water up to 98 days of age. All chickens were individually euthanized using carbon dioxide anesthesia and exsanguination by severing the carotid artery at 98 days of age after 12-h fasting (no additional feed was supplied, and the feed trough was not emptied). After slaughtering, the skin was cut open, and internal tissue samples were collected along the direction of muscle fibers. The pectoralis major muscle samples were weighed, snap-frozen in liquid nitrogen, and stored at −80°C for determination of MG, RNA sequencing, and fluorescence quantitative real-time polymerase chain reaction (qRT-PCR).

Measurement of MG Content

Muscle Glycogen Assay Kit from Nanjing JianCheng Bioengineering Institute (Nanjing, China) was selected. Tissue samples of approximately 100 mg were first cut, with a fluctuation of no more than 0.5 mg among samples. Then, the breast muscle tissue samples were hydrolyzed with 300 μL of lye in a boiling water bath for 20 min and cooled afterward with running water. Subsequently, 0.1 mL of a 5% MG detection solution and 0.9 mL distilled water were added to the hydrolyzed samples and boiled for 5 min. Then, 2 mL of color reagent was added, and the optical density (OD) value was measured at a wavelength of 620 nm using a spectrophotometer. Finally, the MG content of the tested sample was calculated.

Samples Collection for RNA Sequencing and qRT-PCR Analysis

The MG content of the JX-Y chicken female population ranged from 0.2 to 9.0 mg/g (**Supplementary Material 1**). We included individuals with an MG content of less than 1 mg/g in the LMG

group and individuals with MG content of more than 4 mg/g in the HMG group. Transcriptome sequencing was performed on samples from 16 chickens (including three individuals in the HMG group, three individuals in the LMG group, and 10 individuals with random phenotypes). A total of six chickens in the HMG and LMG groups were analyzed by differential gene expression analysis to identify the differentially expressed genes (DEGs) between the two groups. In order to exclude the differences in FOSL2 gene expression caused by extreme phenotypes, we included 10 individuals with random phenotypes on the basis of six individuals for WGCNA. The MG content of BJY chicken was measured in 30 male and 30 female individuals. The MG content in male BJY chickens ranged from 0.8 to 5.1 mg/g, and in female BJY chickens, it ranged from 0.8 to 4.2 mg/g (**Supplementary Material 1**). We considered male and female individuals with MG content of less than 1 mg/g as the LMG group, and individuals with MG content of more than 2 mg/g as the HMG group. Fluorescence qRT-PCR analysis was performed on six male individuals and six female individuals (three individuals in the HMG group and three individuals in the LMG group).

RNA Extraction and Sequencing

Total RNA was extracted from the breast muscle tissue samples using TRIzol reagent (Invitrogen, Carlsbad, CA, United States). The quality of the RNA was assessed after separation by electrophoresis on a 1% agarose gel, and RNA concentration was determined by spectrophotometry using a NanoDrop 2000 spectrophotometer (Thermo Fisher Scientific Inc., Waltham, MA, United States). The OD 260/280 values of all samples were within the range of 1.8 to 2.0 for RNA sequencing and qRT-PCR analysis.

We used a cDNA library construction method previously described by Chen et al. (2019). The mRNA was enriched by binding of the mRNA poly-A tail to oligo (dT)–coated magnetic beads and fragmented into small pieces. Single- and double-stranded cDNAs were synthesized using mRNA as a template. The double-stranded cDNA was purified using the QIAQuick PCR purification kit (QIAGEN, Valencia, CA, United States). After purification, end repair, and ligation to sequencing adapters, agarose gel electrophoresis was used for fragment separation and fragment size selection. Finally, PCR enrichment was performed to obtain the final cDNA library. RNA sequencing was performed on an Illumina NovaSeq 6000 platform (Illumina Inc., San Diego, CA, United States) by Frasergen (Wuhan, China), and 150-bp paired-end reads were generated (**Supplementary Material 2**).

After quality control, the HISAT2 software (Kim et al., 2015) was used to align the second-generation sequence of each sample to the reference genome sequence galGal6.0. The number of reads compared to the transcript of the sample was counted by the comparison result of bowtie2 called by RSEM (Li and Dewey, 2011) and converted by the FPKM (fragments per kilobase of transcript per million bases) method (Trapnell et al., 2010).

For biological duplication, we used the DEseq2 software to analyze the significance of differences in gene and transcript expression (Love et al., 2014) and used the edgeR software for differential expression analysis without biological duplication. The standard for screening the total DEGs is $|\log2FC| > 1$.

qRT-PCR Analysis

All PCR primers were designed at or just outside exon/exon junctions to avoid the amplification of residual genomic DNA using the Primer-BLAST on the National Center for Biotechnology Information (Bethesda, MD, United States) website, and specificity was determined using BLASTN (**Supplementary Material 3**). First-strand cDNA was synthesized using 2 μg of total RNA, random primers, and oligo(dT) primers, with the Transcriptor First Strand cDNA synthesis Kit (Takara, Dalian, China) following the manufacturer instructions. Target mRNAs were quantified by qRT-PCR analysis using SYBR Green Master Mix (Takara). The qRT-PCR reaction of each sample was performed on the QuantStudio 7 Flex system (Applied Biosystems, Shanghai, China) using 40 cycles (95°C for 3 min, 95°C for 3 s, and 60°C for 34 s). The amplification reaction for each sample was performed in triplicate. The collected data were analyzed using the $2^{-\Delta\Delta CT}$ method (Livak and Schmittgen, 2001), and all the results were normalized to the β-actin rRNA gene (Livak and Schmittgen, 2001; Liu et al., 2019).

WGCNA

Network analysis was performed using WGCNA R package version 1.66 (Langfelder and Horvath, 2008). The WGCNA methods have been successfully applied to gene expression data from microarrays (Kadarmideen et al., 2011) and RNA sequencing platforms in animal studies (Kogelman et al., 2014). Before performing WGCNA analysis, the genes obtained through transcriptome sequencing were filtered to remove genes whose average expression level was less than 1. Next, we used the WGCNA program package to construct a weighted gene coexpression network. We first calculated the Pearson correlation between paired genes and constructed a Pearson correlation matrix based on all paired genes. Subsequently, the optimal β value (the β value of JX-Y chicken population = 14) that makes the gene distribution conform to the scale-free network was selected, and the weighted adjacency matrix was constructed. Then, based on the correlation expression value, the adjacency relationship matrix was converted into a topological overlap matrix, and each topological overlap matrix was used as a hierarchical clustering analysis (Zhang and Horvath, 2005). Finally, based on the topological overlap matrix, we used the dissimilarity between genes to cluster the genes and used the dynamic shearing method to cut the tree into different gene modules (i.e., gene clusters with high topological overlap).

After constructing the modules, we calculated the module eigengene (ME) (Zhao et al., 2010), which is defined as the first principal component of the standardized expression profiles. Module–trait relationships (Kogelman et al., 2014), assessed by Pearson correlation between the ME and phenotypic values, were used to select potential modules related to phenotypes. In addition, to assess the relationship between genes and traits, Pearson correlation between gene expression and phenotypic values was calculated and used as gene significance (GS)

(Liu et al., 2016), and the average of the absolute GS values within each module was used to determine the module GS (MS).

Comprehensive Analysis of PPI Network

We used the Search Tool for the Retrieval of Interacting Genes (STRING) database[1] to assess protein–protein interaction (PPI) data (Szklarczyk et al., 2015). In addition, in order to determine the relationship between FOSL2 and CEBPB, we used the STRING database and converted the results visually by using the Cytoscape software.

DF1 Cell Culture, Transfection, and Glycogen Detection

The chicken fibroblast DF1 cells were obtained from the cell bank of the Chinese Academy of Sciences. The DF1 cells were cultured in Dulbecco modified Eagle medium supplemented with 10% fetal bovine serum (Gibco, Grand Island, NY, United States) and 1% penicillin-streptomycin (Gibco). The cell lines were cultured at 37°C in a humidified incubator with 5% CO_2 (Li et al., 2020).

The FOSL2 (Gene ID: 421416) overexpressing lentivirus and empty vectors were constructed by Ubigene (Guangzhou, China) and denoted as YOE-LV001-FOSL2 and YOE-LV001-Ctrl, respectively. Cells were plated in six-well plates at a density of 1×10^6 cells per well, and YOE-LV001-FOSL2 and YOE-LV001-Ctrl were transfected into DF1 cells by the Polybrene, a transfection-promoting reagent provided by Ubigene. The formula for virus dosage is V (μL) = 1,000 × MOI × N/T, where MOI is multiplicity of infection, N is number of cells, and T is lentiviral infectious titer.

The transfected cells were selected with 2 μg/mL puromycin for 2 days. Using an inverted microscope, the imaging system is Olympus BX41, and the images are taken at a 100× field of view. Then cells were collected and tested for glycogen content. The amount of glycogen in DF1 cells was quantified using a glycogen content assay kit (Solarbio, BC0340, China) according to the manufacturer's instructions (Zhao et al., 2017). The cell experiment was repeated three times with samples in triplicate.

Statistical Analyses

The significance of the differences between groups was tested by the Student t test using the SPSS software version 22.0 (IBM Corp., Armonk, NY, United States). Confidence limits were set at 95% and $p < 0.05$ (*) or $p < 0.01$ (**) was considered significant. Data are presented as the mean ± standard error of the mean (SEM).

The GLM (general linear model) procedure in the SAS 9.4 software was used to analyze the differential expression of target genes of the HMG and LMG groups in BJY chickens, and the model was as follows:

$$y_{ij} = u + P_j + G_i + e_{ij}$$

where $y_{ij}$is gene expression quantity, u is population mean gene expression,$P_j$is sex effect, $G_i$is MG group effect, and $e_{ij}$is random error.

[1]https://www.string-db.org/

RESULTS

Comparison of MG Content in the HMG and LMG Chicken Groups

To study MG metabolism in breast muscle tissue from HMG and LMG groups of chickens, the MG content in breast muscle tissue samples was measured. The results revealed significant differences in the MG content between chickens from the HMG and LMG groups, as shown in **Figure 1A**. The MG content in the HMG group chickens was significantly ($p < 0.01$) higher than that in the LMG group chickens.

Differential Expression Analysis of Gene Expression Data From HMG and LMG Chicken Samples

The hierarchical clustering analysis showed that only individuals within the same group clustered more closely (**Figure 1B**). The comparison of the results of the transcriptome sequencing analysis of individuals from the LMG group and HMG group identified a total of 1,171 DEGs, of which 376 were upregulated and 795 were downregulated (**Figure 1C** and **Supplementary Material 4**).

The expression of classic glucose metabolism genes in the HMG and LMG groups is shown in **Figure 1D**. In the HMG group, *AMPK* and *PRKAG* expression is higher than that in the LMG group ($p < 0.01$). The expression of other genes, such as *FOSL2* and *CEBPB*, was higher in the LMG group than that in the HMG group ($p < 0.01$).

Construction of Weighted Gene Coexpression Network and Module Identification

A total of 15,934 genes were used to construct a weighted gene coexpression network. The gene modules shown in **Supplementary Figure 1A** were obtained based on the difference in hierarchical clustering. Based on the height value that quantifies the coexpressed similarity between modules, the modules with a value of less than 0.35 are merged. After merging, a total of 16 modules were identified. These coexpression modules are all represented in different colors in **Supplementary Figure 1B**, and the modules are named by the colors.

FOSL2 Modules Related to MG Traits

We searched for the gene modules most related to MG traits by correlating 16 ME and MG traits (**Figure 2A**). The ME midnight blue module shows the most significant negative correlation with MG traits in breast muscle tissue ($r = -0.68$; $P = 0.004$), which suggests that the genes in this module may play a critical role in MG metabolism.

In the midnight blue module, 621 genes that are highly correlated with the corresponding modules and traits were clustered together (**Figure 2B**). Besides the candidate genes *FOSL2* and *CEBPB*, some genes related to the classical sugar metabolism pathway, such as *MAP3K14*, *SLC2A14*, *SLC12A4*, *PPP2CA*, *SLC38A2*, *PPP2R5E*, and *IGBP1*, were also found

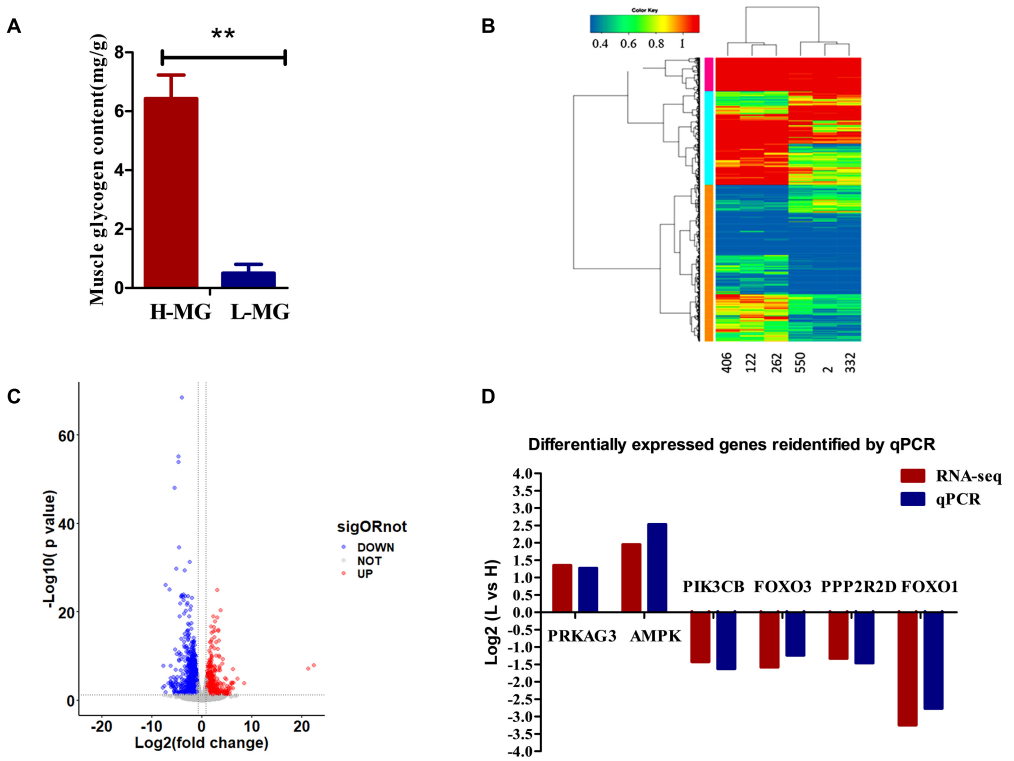

FIGURE 1 | The phenotypic analysis and the RNA sequencing analysis results. **(A)** The MG content in chickens from the HMG and LMG groups ($P = 0.0003$). **(B)** Hierarchical clustering analysis. The hierarchical clustering analysis was performed based on DEGs; the heatmaps of all six samples revealed that the gene expression profiles in the same group were very similar. **(C)** Changes in gene expression profiles of Jingxing yellow (JX-Y) chicken from the HMG and LMG groups. Red dots represent upregulated genes, blue dots represent downregulated genes, and black dots (No) represent insignificantly DEGs. **(D)** Expression levels (fold change) of representative genes involved in MG metabolism pathways according to transcriptome analysis data of chickens from the HMG and LMG.

in the midnight blue module. This indicates that the protein products of the *FOSL2* and *CEBPB* genes and those of the sugar metabolism pathway-related genes may coparticipate in similar biological pathways and coregulate MG metabolism. The data in **Supplementary Material 5** show the correlation between the aforementioned classic glucose metabolism–related genes and MG traits. The results reveal that the expression of the *FOSL2* and *CEBPB* genes is negatively correlated with MG content. The network analysis of all the genes of the midnight blue module in the JX-Y chicken WGCNA using the STRING software to predict the structure of the protein network revealed that there is an interaction between FOSL2 and CEBPB (**Figure 2C**).

In vivo Validation of FOSL2 Gene Expression in Different Populations

In order to verify whether *FOSL2* and *CEBPB* can play the same role in the regulation of the MG content in different breeds and different sex groups, BJY chicken from the HMG and LMG groups were used for quantification of their expression.

The HMG and LMG groups included six chickens (three males and three females). The transcript abundance of *FOSL2* and *CEBPB* was verified by qRT-PCR analysis. The data in **Table 1** show that the transcript abundance of the *FOSL2* and *CEBPB* was significantly upregulated in the LMG group ($p < 0.01$). These results were consistent with the results of the transcriptome analysis of JX-Y chicken muscle tissue, indicating that *FOSL2* and *CEBPB* also play a role in reducing MG content in BJY chicken.

TABLE 1 | The relative quantification (RQ) of mRNA levels of *FOSL2* and *CEBPB* in BJY chicken HMG and LMG groups.

	Group	RQF	RQC	MG
MG	High ($n = 6$)	0.82	0.82	3.06
	Low ($n = 6$)	1.30	1.33	0.89
Gender	M ($n = 6$)	1.15	1.15	2.23
	F ($n = 6$)	0.96	0.99	1.71
P value	SEM	0.09	0.06	0.53
	MG	0.03	0.01	0.00
	Gender	0.31	0.30	0.25
	MG × gender	0.06	0.01	0.28

M, male; F, female; RQF, relative quantification (RQ) of mRNA levels of FOSL2; RQC, relative quantification (RQ) of mRNA levels of CEBPB.

In vitro Validation of FOSL2 Gene

We generated chicken fibroblast DF1 cells overexpressing *FOSL2* after lentiviral transfection, and the efficiency of *FOSL2* overexpression in DF1 cells was confirmed by fluorescence

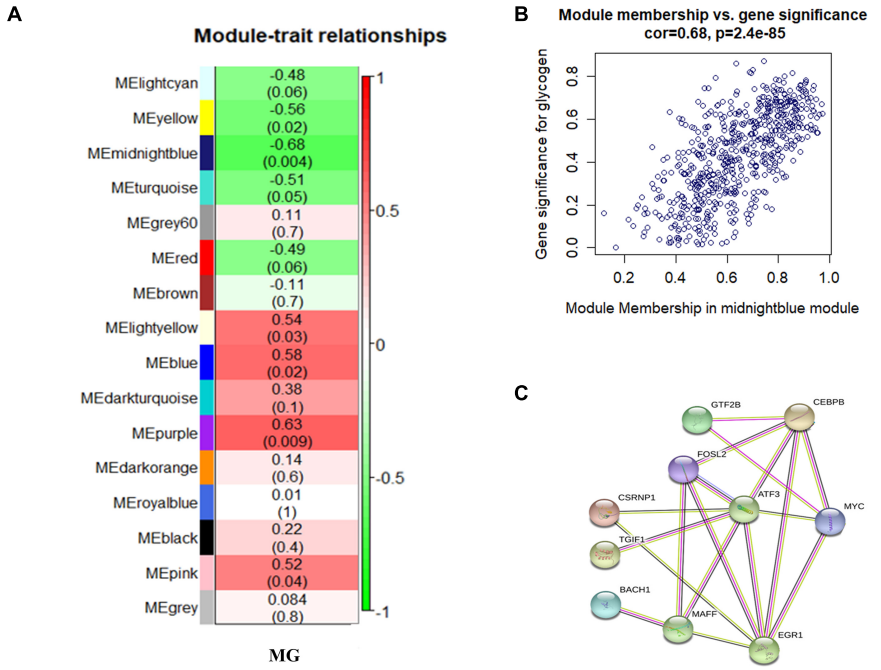

FIGURE 2 | (A) Relationship between gene modules and MG traits in chicken breast muscle tissue. Each row in the table corresponds to a module, and each column to a trait. Each cell contains the corresponding correlation and *P* value. The module name is shown on the left side of the heatmap. The correlation is shown on the right side of the heatmap, in accordance with the color legend (red means positive correlation, and green means negative correlation). **(B)** Scatterplots of gene significance versus module membership for MG modules, along with the indicated correlation coefficients and *P* values. There is a highly significant correlation between GS and MM in the midnight blue module (cor. = 0.82, *P* = 5.9e-56). **(C)** Protein–protein interaction network. Each node represents a kind of protein, and the line between the nodes indicates that the pair of proteins has an interaction relationship.

microscopy of transfected cells (**Figures 3A,C**). Enhanced green fluorescent protein (EGFP) is a mutant of green fluorescent protein (GFP), which emits more than six times of fluorescence intensity than GFP. EGFP plays a role only after gene expression. In addition, *FOSL2*-overexpressing DF1 cells had lower glycogen content compared with control group cells (**Figure 3B**). This is consistent with the results of our previous transcriptome analysis and WGCNA data analysis to mine FOSL2, which predicted their reduced MG content.

DISCUSSION

In the past few decades, livestock and poultry genetic breeding programs have focused on economically important traits, and significant progress has been made in genetic improvement. As an important intermediate in the process of sugar metabolism, MG interacts closely with blood sugar through glycogen synthesis. MG is not only involved in maintaining normal life activities of animals, but also affects the production performance and meat quality of livestock and poultry (Le Bihan-Duval et al., 2001; Berri et al., 2007; Alnahhas et al., 2014). However, the key genes that regulate the metabolism of MG in poultry have not yet been identified.

Numerous DEGs were identified in the HMG and LMG chicken groups. Among them, genes coding for proteins involved in the classical glycogen metabolism pathway, such as 5′-AMP–activated protein kinase (AMPK), which is a heterotrimeric protein that is involved in important signaling cascades to regulate cellular energy metabolism (Gowans and Hardie, 2014; Hardie and Ashford, 2014), Although this role of AMPK in glycogen metabolism has been widely established, increasing evidence suggests that the chronic activation of AMPK leads to glycogen accumulation instead of glycogen degradation (Hunter et al., 2011). For instance, it has been shown that the constitutive activation of AMPK via mutations in the γ2 and γ3 subunits leads to the accumulation of glycogen in the skeletal and cardiac muscles of pigs and mice (Milan et al., 2000; Ahmad et al., 2005; Luptak et al., 2007). According to the GeneCards[2] database, the AMPK gamma subunit (*PRKAG3*), phosphatidylinositol-4,5-bisphosphate 3-kinase catalytic subunit beta (*PIK3CB*), protein phosphatase 2 regulatory subunit Bdelta (*PPP2R2D*), forkhead box O1 (*FOXO1*), and forkhead box O3 (*FOXO3*) are involved in the AMPK signaling pathway, thereby regulating MG content.

As expected, it was found that the expression of *FOSL2* and *CEBPB* genes in the breast muscle tissue of the HMG group is different from that of the LMG breast muscle tissue. The information in GeneCards (see text footnote 2) shows that FOSL2 activates CEBPB transcription in PGE_2-activated osteoblasts. In addition, studies in the abdominal fat line broiler breeds bred by the French Ministry of Agriculture have shown

[2]https://www.genecards.org/

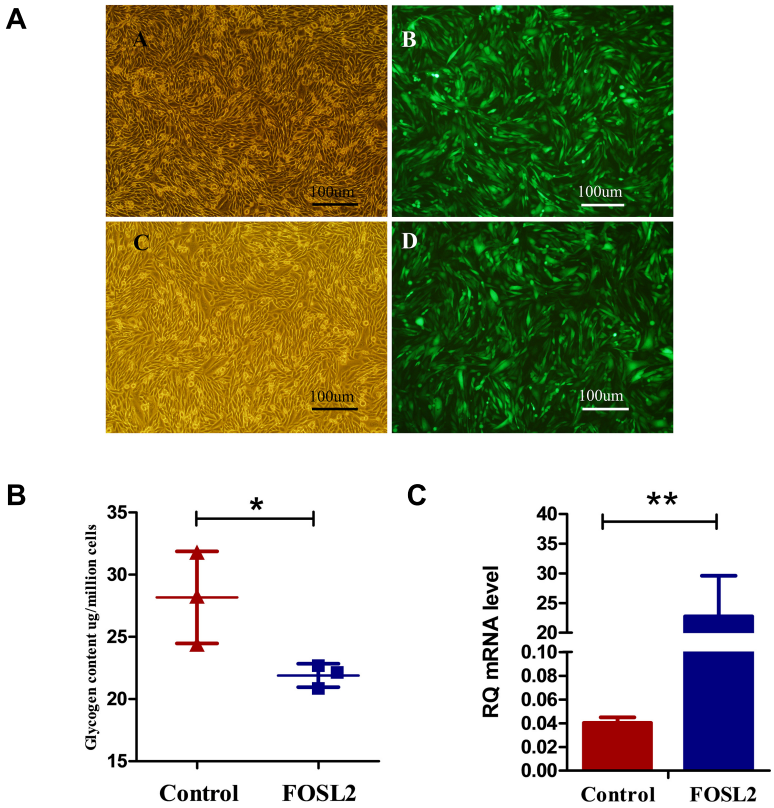

FIGURE 3 | (A,B) Bright-field images and fluorescence microscopy images of transfected cells of chickens from the control group, respectively. Bright-field images and fluorescence microscopy images of cells from the FOSL2-transfected group, respectively. More than 80% of DF1 cells expressed green fluorescent protein. Scale bar = 100 μm. **(B)** The glycogen of control and FOSL2 overexpressing DF1 cells ($P = 0.046$). Control refers to the control group, and FOSL2 refers to the overexpression group of FOSL2. **(C)** Expression level of *FOSL2* gene by qRT-PCR in the control group and FOSL2 overexpression group ($P < 0.001$). Data are presented as the mean ± SEM. Control refers to the control group, and FOSL2 refers to the overexpression group of FOSL2.RQ: relative quantification.

that the downregulation of CEBPB affects MG production through a cAMP-dependent signaling pathway (Sibut et al., 2011). Although there is no relevant literature on the involvement of FOSL2 in the regulation of MG content through activation of CEBPB, the DEGs identified by transcriptome analysis of breast muscle tissue from HMG and LMG groups and the existing research results on MG indicate that FOSL2 may regulate the activation of CEBPB and thereby lead to changes in the MG content.

Some studies have reported that the traditional transcriptome sequencing statistical analysis methods have the drawback of not being able to distinguish confounding factors (Barabási and Oltvai, 2004; Ghaemi et al., 2019), but WGCNA can solve some of the analysis issues caused by confounding factors (Camacho et al., 2018; Emilsson et al., 2018; Mangul et al., 2019). Because of the aforementioned problems in transcriptome analysis, 10 individual chickens were randomly added on the basis of the original six individual chickens for transcriptome sequencing and WGCNA. In the WGCNA of JX-Y chickens, the *FOSL2* and *CEBPB* genes present in the ME midnight blue module are highly negatively correlated with MG traits. Besides the candidate genes *FOSL2* and *CEBPB*, this module also comprises many classic genes related to MG and sugar metabolism. For example, *MAP3K14*, *PPP2CA*, *SLC38A2*, *PPP2R5E*, *IGBP1*, etc. The above results indicate that the *FOSL2* and *CEBPB* genes are coexpressed and their protein products may have a coregulatory role. Furthermore, network analysis of the MG-related genes in the ME midnight blue module performed using the STRING software to predict the possible relationship between their proteins revealed a regulatory network between FOSL2 and CEBPB. Based on the above findings, we hypothesize that low expression of FOSL2 will inhibit the transcription of CEBPB, thereby decreasing MG production.

Differences in the selection process and selection intensity will lead to differences in traits of different breeds. We selected BJY chickens of different sex to quantitatively analyze the expression of the *FOSL2* and *CEBPB* genes. The results showed that FOSL2 and CEBPB are also differentially expressed in the HMG and LMG chicken groups. These results not only showed that sex did not affect the effect of FOSL2 and CEBPB on the reduction of MG content, but also that both proteins had an effect in reducing MG content in BJY chickens. Currently, there is no report on whether sex differences affect MG content in poultry, but studies in cattle suggest that sex differences do not affect MG content (Komatsu et al., 2015).

Members of the Fos gene family are attracting increasing attention as they may have multifunctional roles in a variety of physiological processes, including fat metabolism, bone development, and the pathogenesis of diseases, such as cancer. In this study, transcriptome analysis and WGCNA revealed that FOSL2 was related to MG content. Overexpression of FOSL2 in chicken fibroblast DF1 cells also confirmed its important role in decreasing the MG content.

At present, there are only a few studies on the key genes involved in MG content regulation in chicken, but more studies have been performed in pigs, cattle, and other animals. For instance, a major MG-related gene, namely, *PHKG1*, has been discovered in pigs (Ma et al., 2014). In the JX-Y chicken transcriptome analysis in this study, the *PHKG1* gene was not found to be differentially expressed. This may be due to the small sample size and differences between species. Although our study has certain limitations, it still advances the existing knowledge of chicken MG traits and provides a theoretical basis for subsequent research.

Conventional transcriptome sequencing analysis has been widely used in the study of various traits of poultry (Luo et al., 2019; Yang et al., 2020). In this study, we used basic differential expression analysis and gene coexpression network analysis to identify molecular network pathways that are involved in the regulation of glycogen content in chicken breast muscle. Furthermore, combined with the results of the whole-genome association analysis in the previous period, a key gene that affects MG content, namely, FOSL2, was identified. The results of the quantitative analysis of FOSL2 expression in BJY chickens showed that its regulatory effect on the MG content is not affected by breed or sex. The results of the analysis in DF1 cells further confirmed the negative regulatory effect of FOSL2 on MG content.

CONCLUSION

Based on results from previous GWAS and WGCNA, we identified a key gene, namely, *FOSL2*, which negatively regulates MG content. Our data suggest that FOSL2 may decrease MG content by regulating its downstream gene *CEBPB*, as both genes exhibit the same pattern of expression. *In vivo* experiments showed that the effect of FOSL2 on MG was not affected by breed or sex. These results provide new insights and reference for the study of the regulation of MG metabolism.

DATA AVAILABILITY STATEMENT

The raw whole genome sequencing data reported in this paper have been deposited in the Genome Sequence Archive (Wang et al., 2017) in BIG National Genomics Data Center Members and Partners (2020) under accession number CRA004003 that can be publicly accessed at https://bigd.big.ac.cn/gsa.

ETHICS STATEMENT

All animals and experimental protocols used in this study were approved by the Beijing Institute of Animal Science, Chinese Academy of Agricultural Sciences (the scientific research department responsible for animal welfare issues) (No. IAS2019-21).

AUTHOR CONTRIBUTIONS

XL performed the study, analyzed the data, and drafted the manuscript. LL performed the study and drafted the manuscript. JWa analyzed the data and modified the manuscript. JWe, GZ, and HC contributed to the design of the study. All authors have read and agreed to the published version of the manuscript.

FUNDING

This research was funded by grants from the National Natural Science Foundation of China (31872340), the Agricultural Science and Technology Innovation Program (CAAS-ZDRW202005), the Basic Research from Chinese Academy of Agricultural Sciences (Y2019XK06), Basic Research from Institute of Animal Sciences of Chinese Academy of Agricultural Sciences (2019-YWF-YB-07), the Agricultural Science and Technology Innovation Program (ASTIP-IAS04), the Earmarked Fund for Modern Agro-Industry Technology Research System (CARS-41).

SUPPLEMENTARY MATERIAL

The Supplementary Material for this article can be found online at: https://www.frontiersin.org/articles/10.3389/fphys.2021.682441/full#supplementary-material

REFERENCES

Ahmad, F., Arad, M., Musi, N., He, H., Wolf, C., Branco, D., et al. (2005). Increased alpha2 subunit-associated AMPK activity and PRKAG2 cardiomyopathy. *Circulation* 112, 3140–3148. doi: 10.1161/circulationaha.105.550806

Alnahhas, N., Berri, C., Boulay, M., Baéza, E., Jégo, Y., Baumard, Y., et al. (2014). Selecting broiler chickens for ultimate pH of breast muscle: analysis of divergent selection experiment and phenotypic consequences on meat quality, growth, and body composition traits. *J. Anim. Sci.* 92, 3816–3824. doi: 10.2527/jas.2014-7597

Alnahhas, N., Le Bihan-Duval, E., Baéza, E., Chabault, M., Chartrin, P., Bordeau, T., et al. (2015). Impact of divergent selection for ultimate pH of pectoralis major muscle on biochemical, histological, and sensorial attributes of broiler meat. *J. Anim. Sci.* 93, 4524–4531. doi: 10.2527/jas.2015-9100

Barabási, A. L., and Oltvai, Z. N. (2004). Network biology: understanding the cell's functional organization. *Nat. Rev. Genet.* 5, 101–113. doi: 10.1038/nrg1272

Berri, C., Le Bihan-Duval, E., Debut, M., Santé-Lhoutellier, V., Baéza, E., Gigaud, V., et al. (2007). Consequence of muscle hypertrophy on characteristics of Pectoralis major muscle and breast meat quality of broiler chickens. *J. Anim. Sci.* 85, 2005–2011. doi: 10.2527/jas.2006-398

Bozec, A., Bakiri, L., Jimenez, M., Rosen, E. D., Catalalehnen, P., Schinke, T., et al. (2013). Osteoblast-specific expression of Fra-2/AP-1 controls adiponectin and osteocalcin expression and affects metabolism. *J. Cell Sci.* 126, 5432–5440.

Bozec, A., Bakiri, L., Jimenez, M., Schinke, T., Amling, M., and Wagner, E. F. (2010). Fra-2/AP-1 controls bone formation by regulating osteoblast differentiation and collagen production. *J. Cell Biol.* 190, 1093–1106. doi: 10.1083/jcb.201002111

Camacho, D. M., Collins, K. M., Powers, R. K., Costello, J. C., and Collins, J. J. (2018). Next-generation machine learning for biological networks. *Cell* 173, 1581–1592. doi: 10.1016/j.cell.2018.05.015

Chen, F., Wu, P., Shen, M., He, M., Chen, L., Qiu, C., et al. (2019). Transcriptome analysis of differentially expressed genes related to the growth and development of the jinghai yellow chicken. *Genes (Basel)* 10:539. doi: 10.3390/genes10070539

Chinenov, Y., and Kerppola, T. K. J. O. (2001). Close encounters of many kinds: fos-jun interactions that mediate transcription regulatory specificity. *Oncogene* 20, 2438–2452. doi: 10.1038/sj.onc.1204385

Eferl, R., Hasselblatt, P., Rath, M., Popper, H. H., Zenz, R., Komnenovic, V., et al. (2008). Development of pulmonary fibrosis through a pathway involving the transcription factor Fra-2/AP-1. *Proc. Natl. Acad. Sci. U.S.A.* 105, 10525–10530. doi: 10.1073/pnas.0801414105

Eferl, R., and Wagner, E. F. (2003). AP-1: a double-edged sword in tumorigenesis. *Nat. Rev. Cancer* 3, 859–868. doi: 10.1038/nrc1209

Emilsson, V., Ilkov, M., Lamb, J. R., Finkel, N., Gudmundsson, E. F., Pitts, R., et al. (2018). Co-regulatory networks of human serum proteins link genetics to disease. *Science* 361, 769–773. doi: 10.1126/science.aaq1327

Foletta, V. C., Sonobe, M. H., Suzuki, T., Endo, T., Iba, H., and Cohen, D. R. (1994). Cloning and characterisation of the mouse fra-2 gene. *Oncogene* 9, 3305–3311.

Ghaemi, M. S., DiGiulio, D. B., Contrepois, K., Callahan, B., Ngo, T. T. M., Lee-McMullen, B., et al. (2019). Multiomics modeling of the immunome, transcriptome, microbiome, proteome and metabolome adaptations during human pregnancy. *Bioinformatics* 35, 95–103. doi: 10.1093/bioinformatics/bty537

Godfrey, R., and Quinlivan, R. (2016). Skeletal muscle disorders of glycogenolysis and glycolysis. *Nat. Rev. Neurol.* 12, 393–402. doi: 10.1038/NRNEUROL.2016.75

Gowans, G. J., and Hardie, D. G. (2014). AMPK: a cellular energy sensor primarily regulated by AMP. *Biochem. Soc. Trans.* 42, 71–75. doi: 10.1042/bst20130244

Hardie, D. G., and Ashford, M. L. J. P. (2014). AMPK: regulating energy balance at the cellular and whole body levels. *Physiology (Bethesda)* 29, 99–107. doi: 10.1152/physiol.00050.2013

Henckel, P. (1996). "Physiology and biochemistry of muscle fibres in poultry," in *Proceedings from 2nd European Poultry Breeders Roundtable 6-8 September 1995*, Foulum.

Hunter, R. W., Treebak, J. T., Wojtaszewski, J. F., and Sakamoto, K. (2011). Molecular mechanism by which AMP-activated protein kinase activation promotes glycogen accumulation in muscle. *Diabetes* 60, 766–774. doi: 10.2337/db10-1148

Kadarmideen, H. N., Watson-Haigh, N. S., and Andronicos, N. M. (2011). Systems biology of ovine intestinal parasite resistance: disease gene modules and biomarkers. *Mol. Biosyst.* 7, 235–246. doi: 10.1039/c0mb00190b

Karreth, F. A., Hoebertz, A., Scheuch, H., Eferl, R., and Wagner, E. F. (2004). The AP1 transcription factor Fra2 is required for efficient cartilage development. *Development* 131, 5717–5725. doi: 10.1242/dev.01414

Kim, D., Langmead, B., and Salzberg, S. L. (2015). HISAT: a fast spliced aligner with low memory requirements. *Nat. Methods* 12, 357–360. doi: 10.1038/nmeth.3317

Kogelman, L. J., Cirera, S., Zhernakova, D. V., Fredholm, M., Franke, L., and Kadarmideen, H. N. (2014). Identification of co-expression gene networks, regulatory genes and pathways for obesity based on adipose tissue RNA Sequencing in a porcine model. *BMC Med. Genomics* 7:57. doi: 10.1186/1755-8794-7-57

Komatsu, T., Shoji, N., Saito, K., and Suzuki, K. (2015). Effects of genetic and environmental factors on muscle glycogen content in Japanese Black cattle. *Anim. Sci. J.* 85, 793–798. doi: 10.1111/asj.12201

Langfelder, P., and Horvath, S. (2008). WGCNA: an R package for weighted correlation network analysis. *BMC Bioinformatics* 9:559. doi: 10.1186/1471-2105-9-559

Le Bihan-Duval, E., Berri, C., Baeza, E., Millet, N., and Beaumont, C. (2001). Estimation of the genetic parameters of meat characteristics and of their genetic correlations with growth and body composition in an experimental broiler line. *Poult. Sci.* 80, 839–843. doi: 10.1093/ps/80.7.839

Le Bihan-Duval, E., Debut, M., Berri, C. M., Sellier, N., Santé-Lhoutellier, V., Jégo, Y., et al. (2008). Chicken meat quality: genetic variability and relationship with growth and muscle characteristics. *BMC Genet.* 9:53. doi: 10.1186/1471-2156-9-53

Li, B., and Dewey, C. N. (2011). RSEM: accurate transcript quantification from RNA-Seq data with or without a reference genome. *BMC Bioinformatics* 12:323. doi: 10.1186/1471-2105-12-323

Li, J., Li, S., Hu, Y., Cao, G., Wang, S., Rai, P., et al. (2016). The expression level of mRNA, Protein, and DNA methylation status of FOSL2 of Uyghur in XinJiang in Type 2 diabetes. *J. Diabetes Res.* 2016:5957404.

Li, Q., Wang, F., Wang, Q., Zhang, N., Zheng, J., Zheng, M., et al. (2020). SPOP promotes ubiquitination and degradation of MyD88 to suppress the innate immune response. *PLoS Pathog.* 16:e1008188. doi: 10.1371/journal.ppat.1008188

Liu, J., Jing, L., and Tu, X. (2016). Weighted gene co-expression network analysis identifies specific modules and hub genes related to coronary artery disease. *BMC Cardiovasc. Disord.* 16:54. doi: 10.1186/s12872-016-0217-3

Liu, L., Liu, X., Cui, H., Liu, R., Zhao, G., and Wen, J. (2019). Transcriptional insights into key genes and pathways controlling muscle lipid metabolism in broiler chickens. *BMC Genomics* 20:863. doi: 10.1186/s12864-019-6221-0

Liu, X., Liu, L., Wang, J., Cui, H., Chu, H., Bi, H., et al. (2020). Genome-Wide Association Study of Muscle Glycogen in Jingxing Yellow Chicken. *Genes* 11:497. doi: 10.3390/GENES11050497

Livak, K. J., and Schmittgen, T. D. (2001). Analysis of relative gene expression data using real-time quantitative PCR and the 2(-Delta Delta C(T)) Method. *Methods* 25, 402–408. doi: 10.1006/meth.2001.1262

Love, M. I., Huber, W., and Anders, S. (2014). Moderated estimation of fold change and dispersion for RNA-seq data with DESeq2. *Genome Biol.* 15, 550–550. doi: 10.1186/S13059-014-0550-8

Luo, J. J., Zhang, Y., Sun, H., Wei, J. T., Khalil, M. M., Wang, Y. W., et al. (2019). The response of glandular gastric transcriptome to T-2 toxin in chicks. *Food Chem. Toxicol.* 132:110658. doi: 10.1016/j.fct.2019.110658

Luptak, I., Shen, M., He, H., Hirshman, M. F., Musi, N., Goodyear, L. J., et al. (2007). Aberrant activation of AMP-activated protein kinase remodels metabolic network in favor of cardiac glycogen storage. *J. Clin. Invest.* 117, 1432–1439. doi: 10.1172/jci30658

Ma, J., Yang, J., Zhou, L., Ren, J., Liu, X., Zhang, H., et al. (2014). A splice mutation in the PHKG1 gene causes high glycogen content and low meat quality in pig skeletal muscle. *PLoS Genet.* 10:e1004710. doi: 10.1371/journal.pgen.1004710

Mangul, S., Martin, L. S., Hill, B. L., Lam, A. K., Distler, M. G., Zelikovsky, A., et al. (2019). Systematic benchmarking of omics computational tools. *Nat. Commun.* 10:1393. doi: 10.1038/s41467-019-09406-4

Milan, D., Jeon, J. T., Looft, C., Amarger, V., Robic, A., Thelander, M., et al. (2000). A mutation in PRKAG3 associated with excess glycogen content in pig skeletal muscle. *Science* 288, 1248–1251. doi: 10.1126/science.288.5469.1248

National Genomics Data Center Members and Partners (2020). Database resources of the national genomics data center in 2020. *Nucleic Acids Res.* 48, D24–D33. doi: 10.1093/nar/gkz913

Puolanne, E., and Immonen, K. (2014). *CONVERSION of Muscle to Meat. Glycogen*. Oxford: Academic Press.

Sibut, V., Hennequet-Antier, C., Bihan-Duval, E. L., Marthey, S., Duclos, M. J., and Berri, C. (2011). Identification of differentially expressed genes in chickens differing in muscle glycogen content and meat quality. *BMC Genom.* 12:112. doi: 10.1186/1471-2164-12-112

Szklarczyk, D., Franceschini, A., Wyder, S., Forslund, K., Heller, D., Huerta-Cepas, J., et al. (2015). STRING v10: protein-protein interaction networks, integrated over the tree of life. *Nucleic Acids Res.* 43, D447–D452. doi: 10.1093/nar/gku1003

Trapnell, C., Williams, B. A., Pertea, G., Mortazavi, A., Kwan, G., Baren, M. J., et al. (2010). Transcript assembly and quantification by RNA-Seq reveals unannotated transcripts and isoform switching during cell differentiation. *Nat. Biotechnol.* 28, 511–515. doi: 10.1038/nbt.1621

Wang, Y., Song, F., Zhu, J., Zhang, S., Yang, Y., Chen, T., et al. (2017). GSA: genome sequence archive. *Genom. Proteom. Bioinform.* 15, 14–18. doi: 10.1016/j.gpb.2017.01.001

Yang, L., Zheng, X., Mo, C., Li, S., Liu, Z., Yang, G., et al. (2020). Transcriptome analysis and identification of genes associated with chicken sperm storage duration. *Poult. Sci.* 99, 1199–1208. doi: 10.1016/j.psj.2019.10.021

Zhang, B., and Horvath, S. (2005). A general framework for weighted gene co-expression network analysis. *Stat. Appl. Genet. Mol. Biol.* 4:17. doi: 10.2202/1544-6115.1128

Zhao, W., Langfelder, P., Fuller, T., Dong, J., and Hovarth, S. (2010). Weighted gene coexpression network analysis: state of the art. *J. Biopharm. Stat.* 20, 281–300. doi: 10.1080/10543400903572753

Zhao, X., Sun, K., Lan, Z., Song, W., Cheng, L., Chi, W., et al. (2017). Tenofovir and adefovir down-regulate mitochondrial chaperone TRAP1 and succinate dehydrogenase subunit B to metabolically reprogram glucose metabolism and induce nephrotoxicity. *Sci. Rep.* 7:46344. doi: 10.1038/srep46344

Conflict of Interest: The authors declare that the research was conducted in the absence of any commercial or financial relationships that could be construed as a potential conflict of interest.

frontiers in Physiology

ORIGINAL RESEARCH
published: 22 July 2021
doi: 10.3389/fphys.2021.712694

Blood Plasma Biomarkers for Woody Breast Disease in Commercial Broilers

Byungwhi Kong[1], Bhuwan Khatri[1†], Seong Kang[1], Stephanie Shouse[1], Hakeem Kadhim[1,2], Michael Kidd Jr.[1], Kentu Lassiter[1], Joseph Hiltz[1], Barbara Mallmann[1†], Sara Orlowski[1], Nicholas Anthony[1†], Walter Bottje[1], Wayne Kuenzel[1] and Casey Owens[1]*

[1] Department of Poultry Science, Center of Excellence for Poultry Science, University of Arkansas, Fayetteville, AR, United States, [2] Veterinary Medicine College, University of Thi-Qar, Nasiriyah, Iraq

Woody breast (WB) myopathy results in poor muscle quality. The increasing incidence of WB over the last several years indicates a need for improved prediction or early diagnosis. We hypothesized that the use of body fluids, including blood, may be more suitable than breast muscle tissue in developing a minimally invasive diagnostic tool for WB detection. To identify potential early-age-biomarkers that may represent the potential onset of WB, blood samples were collected from 100, 4 wks old commercial male broilers. At 8 wks of age, WB conditions were scored by manual palpation. A total of 32 blood plasma samples (eight for each group of WB and non-WB control birds at two time points, 4 wks and 8 wks) were subjected to shotgun proteomics and untargeted metabolomics to identify differentially abundant plasma proteins and metabolites in WB broilers compared to non-WB control (Con) broilers. From the proteomics assay, 25 and 16 plasma proteins were differentially abundant ($p < 0.05$) in the 4 and 8 wks old samples, respectively, in WB compared with Con broilers. Of those, FRA10A associated CGG repeat 1 (FRAG10AC1) showed >2-fold higher abundance in WB compared with controls. In the 8 wks old broilers, 4 and 12 plasma proteins displayed higher and lower abundances, respectively, in WB compared with controls. Myosin heavy chain 9 (MYH9) and lipopolysaccharide binding protein (LBP) showed more than 2-fold higher abundances in WB compared with controls, while transferrin (TF) and complement C1s (C1S) showed more than 2-fold lower abundances compared with controls. From the untargeted metabolomics assay, 33 and 19 plasma metabolites were differentially abundant in birds at 4 and 8 wks of age, respectively, in WB compared with controls. In 4 wks old broilers, plasma 3-hydroxybutyric acid (3-HB) and raffinose concentrations showed the highest and lowest fold changes, respectively, in WB compared with controls. The blood plasma 3-HB and raffinose concentrations were confirmed with targeted biochemical assays. Blood biomarkers, such as 3-HB and raffinose, may be suitable candidate targets in the prediction of WB onset at early ages.

Keywords: woody breast, blood plasma, biomarker, proteomics, metabolomics

OPEN ACCESS

Edited by:
Sandra G. Velleman, The Ohio State University, United States

Reviewed by:
Yuwares Malila, National Center for Genetic Engineering and Biotechnology (BIOTEC), Thailand
Kent M. Reed, University of Minnesota Twin Cities, United States

***Correspondence:**
Byungwhi Kong
bkong@uark.edu

†Present address:
Bhuwan Khatri, Oklahoma Medical Research Foundation, Oklahoma, OK, United States
Barbara Mallmann, Adisseo Inc., Anthony, France
Nicholas Anthony, Cobb Vantress, Siloam Springs, AR, United States

Specialty section:
This article was submitted to Avian Physiology, a section of the journal Frontiers in Physiology

Received: *21 May 2021*
Accepted: *29 June 2021*
Published: *22 July 2021*

Citation:
Kong B, Khatri B, Kang S, Shouse S, Kadhim H, Kidd M Jr, Lassiter K, Hiltz J, Mallmann B, Orlowski S, Anthony N, Bottje W, Kuenzel W and Owens C (2021) Blood Plasma Biomarkers for Woody Breast Disease in Commercial Broilers. Front. Physiol. 12:712694. doi: 10.3389/fphys.2021.712694

INTRODUCTION

The incidence of woody breast (WB) myopathy has increased in the last several years, possibly in response to genetic selection for growth performance and a shift to heavier market weight birds (Velleman, 2015; Kuttappan et al., 2017; Lake and Abasht, 2020). Extensive investigations on WB myopathy characterized etiopathogenic mechanisms in breast muscle during the disease progression (Velleman and Clark, 2015; Abasht et al., 2016; Papah et al., 2017; Sihvo et al., 2017; Brothers et al., 2019; Greene et al., 2019; Maharjan et al., 2019; Petracci et al., 2019; Lake and Abasht, 2020). Those muscular mechanisms include phlebitis and inflammation, oxidative stress and metabolic dysfunction, myofiber degeneration, lipid deposition and development of hard pectoral muscle, resulting in poor muscle quality. The exact cause of WB myopathy is still unclear and most genetic, nutritional, and physiological studies have been conducted with breast muscle tissues. For early diagnosis or prediction for later onset of WB myopathy, less invasive body fluids including blood may become more suitable than breast muscle tissues in developing a diagnostic tool. A recent study using targeted metabolomics reported differentially abundant blood metabolites including homocysteine, cyclic GMP, trimethylamine N-oxide, tyramine, carnitine, and acetylcarnitine, which are mainly connected to the cardiovascular system (Maharjan et al., 2019). Less invasive biomarkers contained in blood samples, such as plasma proteins and metabolites, can be effective for pre-diagnosis of WB during the normal growth phase of broilers. The purpose of this study was to identify differentially abundant blood plasma proteins and metabolite biomarkers in efforts to explore identifying early-age-biomarkers that can represent the potential onset of WB using shotgun proteomics and untargeted metabolomics methods, respectively.

MATERIALS AND METHODS

Ethics Statement

The care and experimental use of animal protocols were accepted by the University of Arkansas Institutional Animal Care and Use Committee. Animals were maintained according to a standard management program at the Poultry Farm, University of Arkansas.

Animals and Sample Preparation

Commercial broiler chickens were raised in an environmentally controlled room. A standard commercial diet was fed *ad libitum*. At 4 and 8 wks old, blood from male birds was collected consistently and gently by the same person from the wing vein (brachial vein) to minimize human presence and handling stress. At 8 wks of age, live birds were clinically inspected by physical palpation and visual examination of the breast muscle (pectoralis major). The correlations between WB palpation and filet WB scores are known to be increased with increasing bird age (Mallmann, 2019), indicating that the physical palpation at 8 wks of age is suitable to determine WB scores. The palpation scores for WB ranged from 0 (no WB) to 3 (severe WB), with a score of 1 being mild WB and a score of two being moderate WB (Mallmann, 2019; Kang et al., 2020). Post palpation, the samples were grouped into control (Con, $n = 8$; WB score $= 0$) and WB ($n = 8$; WB score ≥ 2) birds. Blood samples were centrifuged and plasma was stored at -20°C until examined for metabolomics and proteomics.

Shotgun Proteomics

Plasma collected from Con and WB broilers at 4 and 8 wks of age (32 plasma samples in total) were subjected to shotgun proteomics analysis by trypsin digestion and tandem mass spectrometry (MS/MS) at the University of Arkansas Medical Science (UAMS) Proteomics Core Facility (Little Rock, AR). Raw mass spectrometric data were analyzed by database searching using the Mascot (Matrix Science, Boston, MA) search engine and the UniProtKB (http://www.uniprot.org/help/uniprotkb) database. Search results were compiled using Scaffold program (Proteome Software, Portland, OR). The mass spectrometry proteomics data have been deposited to the ProteomeXchange Consortium via the PRIDE (Perez-Riverol et al., 2019) partner repository with the dataset identifier PXD026896 and 10.6019/PXD026896. Normalization and statistical analyses are described in the "Statistical Analyses" section.

Untargeted Metabolomics

Plasma samples used for proteomics analysis were also subjected to primary metabolism analysis by GC-TOF MS at the UC Davis West Coast Metabolomics Center (Davis, CA). Normalization and statistical analyses are described below in the "Statistical Analyses" section.

Plasma Raffinose Assay

Plasma raffinose concentration was determined using raffinose/D-galactose assay kit (Megazyme, Ireland) following manufacturer's instructions with modifications for use in a microplate. Briefly, 20 μl plasma samples were mixed with either 10 μl α-galactosidase (pH 4.6) or 10 μl distilled water for determining concentration of raffinose + free D-galactose or free D-galactose only, respectively, and mixtures were incubated at 25°C for 20 min. Distilled water was used as blank control. Next, 20 μl buffer containing sodium azide, 200 μl distilled water, and 10 μl NAD^+ solution, were added, mixed, and absorbances read at 340 nm (A1 read) after 3 min. Then, 2 μl D-galactose dehydrogenase plus galactose mutarotase suspension was added, mixed, incubated at 40°C for 20 min, and absorbances read at 340 nm at the end of the reaction (A2 read). Raffinose concentration was calculated by:

$$C_{raffinose}(g/L) = (V \times MW \times \Delta A_{raffinose})/(\varepsilon \times d \times v)$$

V = final volume [ml]
MW = molecular weight of the substance (504.5 for raffinose) assayed [g/mol]

$$\Delta A_{raffinose} = \Delta A_{raffinose+freeD-galactose} - \Delta A_{free\ D-galactose}$$
$$\Delta A = A2 - A1$$

ε = extinction coefficient of NADH at 340 nm = 6300 [l × mol^{-1} × cm^{-1}]
d = light path [cm] = 1
v = sample volume [ml] = 0.02
The 96 well plate was read twice with a Synergy HT multimode microplate reader (BioTek, Winooski, VT). Average concentration of individual samples was used with standard error of mean (SE).

Plasma 3-Hydroxybutyric Acid Assay

Plasma 3-hydroxybutyric acid (3-HB) concentration was determined using D-3-hydroxybutyric acid assay kit (Megazyme, Ireland) following manufacturer's instructions for use in a microplate. Briefly, 10 μl plasma samples were mixed with 200 μl distilled water, 50 μl buffer mix containing sodium azide, 20 μl NAD^+ plus iodonitrotetrazolium chloride, and 2 μl diaphorase suspension, mixed, and absorbances read at 492 nm after 3 min (A1 read). Distilled water (210 μl), and 10 μl standard solution (0.06 mg/ml; provided by manufacturer) were used as blank control and internal standard concentration, respectively. Next, 2 μl 3-Hydroxybutyrate dehydrogenase suspension (3-HBDH) was added, mixed, and incubated at 25°C for ∼6 min, and absorbances read at 492 nm at the end of the reaction (A2 read). D-3-hygroxybutyric acid concentration was calculated by:

$$C_{D-3-hydroxybutyricacid}(g/L) = (\Delta A_{sample} \times g/L\ standard)/\Delta A_{standard}$$
$$\Delta A = A2 - A1$$

The 96 well plate was read twice with a Synergy HT multimode microplate reader (BioTek, Winooski, VT). Average concentration of individual samples was used with SE.

Statistical Analyses

Raw spectral counts of either proteomics or metabolomics were transformed to $\log_2$ values and normalized by Loess method using JMP Genomics (SAS Institute, Cary, NC). Differential abundances between WB and Con were calculated using $\log_2$fold change (FC), indicating $|\log_2 FC\ of\ 1.0| = |FC\ of\ 2.0|$ in numeric value. The Student's *t*-test was used separately for proteomics or metabolomics in comparing Con and WB samples. Proteins or metabolites showing $p < 0.05$ in the comparison between Con and WB were considered differential abundance. The *p*-value correction (FDR calculation) by multiple tests was not applied in this study since we used a less stringent approach on a molecule by molecule basis, and this allowed us to import more informative lists. For biochemical assays for raffinose and 3-HB, the Student's *t*-test comparing Con and WB was used and $p < 0.05$ was considered as significant differences.

RESULTS AND DISCUSSION

Body Weight

Body weights (average ± standard deviation; SD) at 8 wks for Con and WB broilers were 3334 ± 231 g and 3462 ± 261 g, respectively, indicating WB group broilers were slightly heavier (3.8%) than non-WB controls ($p > 0.05$).

TABLE 1 | Plasma protein biomarkers in WB at 4 wks of age compared to Con.

Symbol	Entrez gene name	Log_2FC	*P*-value
FRA10AC1	FRA10A associated CGG repeat 1	1.2	0.0402
GAL9	Gallinacin 9	0.9	0.0456
TALDO1	Transaldolase 1	0.6	0.0022
APOA5	Apolipoprotein A5	0.5	0.0163
ACAT2	Acetyl-CoA acetyltransferase 2	0.5	0.0008
CR1L	Complement C3b/C4b Receptor 1 Like	0.4	0.0246
CKB	Creatine kinase B	0.3	0.0486
FETUB	Fetuin B	0.2	0.0392
LDHB	Lactate dehydrogenase B	0.2	0.0145
GOT1	Glutamic-oxaloacetic transaminase 1	0.2	0.0363
HSPA5	Heat shock protein family A (Hsp70) member 5	0.1	0.0215
GLB1L	Galactosidase beta 1 like	−0.2	0.0160
TIMP2	TIMP metallopeptidase inhibitor 2	−0.2	0.0244
COL5A1	Collagen type V alpha 1 chain	−0.2	0.0451
SERPINF1	Serpin family F member 1	−0.2	0.0153
DKK3	Dickkopf WNT signaling pathway inhibitor 3	−0.3	0.0466
CHL1	Cell adhesion molecule L1 like	−0.4	0.0383
SERPINA1	Serpin family A member 1	−0.4	0.0466
MMP9	Matrix metallopeptidase 9	−0.4	0.0452
TXNDC5	Thioredoxin domain containing 5	−0.5	0.0184
COL1A2	Collagen type I alpha 2 chain	−0.5	0.0373
CCL26	Chemokine ligand 26	−0.6	0.0325
EPYC	Epiphycan	−0.6	0.0214
COL1A1	Collagen type 1 alpha 1 chain	−0.7	0.0259
CRTAC1	Cartilage acidic protein 1	−0.7	0.0183

Plasma Protein Biomarkers

Plasma samples (8 broilers × 2 groups × 2 time points) collected from commercial broilers, 4 and 8 wks of age, were subjected to both shotgun proteomics and primary metabolomics. From the proteomics assay, 25 and 16 plasma proteins were differentially abundant ($p < 0.05$) at 4 (**Table 1**) and 8 wks of age (**Table 2**), respectively, in WB compared with controls. In 4 wks old broilers, 11 and 14 plasma proteins showed higher and lower abundances, respectively, in WB compared with controls. Assuming greater differences in abundance of markers, their greater effects on physiology as well as improvements in their diagnostic method, has resulted in markers showing greater differences between WB and controls. Therefore, the value of $\log_2FC > 1.0$ were considered first in this analysis. Of differentially abundant blood proteins, FRA10AC1 ($\log_2FC = 1.2$) showed $\log_2FC$ higher than 1.0 abundance in WB broilers compared with controls, while none of the proteins showed $\log_2FC < -1.0$ abundance compared with controls. In 8 wk old broilers, 4 and 12 plasma proteins in WB showed higher and lower abundance, respectively, compared with controls. MYH9 ($\log_2FC = 2.9$) and LBP ($\log_2FC =$

TABLE 2 | Plasma protein biomarkers in WB at 8 wks of age compared to Con.

Symbol	Entrez gene name	Log_2FC	*P*-value
MYH9	Myosin heavy chain 9	2.9	0.0340
LBP	Lipopolysaccharide binding protein	1.4	0.0077
TKT	Transketolase	0.9	0.0018
F13A1	Coagulation factor XIII A chain	0.6	0.0458
MINPP1	Multiple inositol-polyphosphate phosphatase 1	−0.4	0.0359
CCL26	C-C motif chemokine ligand 26	−0.4	0.0491
SPP2	Secreted phosphoprotein 2	−0.5	0.0293
CDH11	Cadherin 11	−0.5	0.0393
COL1A1	Collagen type I alpha 1 chain	−0.6	0.0118
PPIC	Peptidylprolyl isomerase C	−0.6	0.0120
COL1A2	Collagen type I alpha 2 chain	−0.6	0.0165
GC	GC, vitamin D binding protein	−0.7	0.0202
A2M	Alpha-2-macroglobulin	−0.7	0.0417
CDH5	Cadherin 5	−0.8	0.0060
C1S	Complement C1s	−1.0	0.0396
TF	Transferrin	−1.9	0.0365

TABLE 3 | Plasma metabolite biomarkers in WB at 4- and 8 wks of age compared to Con.

Metabolite name	4 wks		8 wks	
	Log_2FC	*P*-value	Log_2FC	*P*-value
3-hydroxybutyric acid	1.6	0.0152	0.7	0.1042
Lysine	1.4	0.0263	−0.3	0.6155
Uridine	1.3	0.0228	0.2	0.4926
2-aminobutyric acid	1.0	0.0362	0.4	0.0949
Mucic acid	−1.1	0.0369	−0.6	0.0319
Asparagine	−1.1	0.0364	−0.1	0.7950
Orotic acid	−1.2	0.007	−0.7	0.0819
Pentitol	−1.2	0.0356	−0.4	0.0655
Xanthine	−1.3	0.0105	−0.3	0.4404
Xylonic acid	−1.3	0.0273	−0.5	0.0258
Butane-2,3-diol	−1.4	0.0406	0.4	0.3412
Pinitol	−1.6	0.0450	−0.5	0.0328
Beta-gentiobiose	−2.7	0.0345	−0.8	0.0326
Raffinose	−3.3	0.0441	−1.1	0.0491

1.4) showed log_2FC higher than 1.0 abundance in WB broilers compared with controls, while TF ($log_2FC = -1.9$) and C1S ($log_2FC = -1.0$) showed log_2FC <-1.0 abundance compared with controls. Interestingly, COL1A1, COL1A2, and CCL26 in plasma samples in both 4 and 8 wk old WB broilers were lower compared to controls, indicating consistently lower concentrations in WB plasma. However, the fold change values were marginal ($-1 < log_2FC < 1.0$) for all three plasma proteins.

FRA10A associated CGG repeat 1 (FRA10AC1; $log_2FC = 1.2$ higher in WB broilers), which is ubiquitously expressed and mainly localized in nucleoplasm (Sarafidou et al., 2004), has not been determined in blood plasma. Instead, circulating FRA10AC1 mRNA was identified as one of the RNA biomarkers for melanoma (Sole et al., 2019), suggesting that FRA10AC1 mRNA and protein can be circulating biomarkers for WB myopathy, though their functional role in blood is unknown. A subtype (COL1A1), of collagens which showed marginal differences in WB plasma in both 4 and 8 wks of age, was reported as a potential biomarker for heart failure progression (Hua et al., 2020). Likewise, C-C motif chemokine ligand 26 (CCL26) in blood is known to be significantly correlated with the disease activity of atopic dermatitis (Kagami et al., 2003). To use these blood biomarkers for early diagnostic purpose, highly specific (for FRA10AC1 as chicken specific antibody is not available), and sensitive assay methods need to be developed to discern the marginal differences in blood plasma.

Higher differential abundances of MYH ($log_2FC = 2.9$), LBP ($log_2FC = 1.4$), TF ($log_2FC = -1.9$), and C1S ($log_2FC = -1.0$) were detected in WB broilers in the late growth phase only (8 wks of age), thus these markers may not be suitable for early diagnosis for WB. Regarding plasma myosin species, it has been reported that red blood cells (RBCs) contain non-muscle myosins (Hammer, 2018). The function of non-muscle myosins in RBCs is different from its original function in normal cells reflecting the RBC's unusual actin organization. Thus, the inclusion of myosin subtype in blood plasma may be derived from breakdown of RBCs. Circulating lipoprotein binding protein (LBP) concentration is known to be significantly increased with type 2 diabetes and dramatically increased with obesity (Moreno-Navarrete et al., 2012). Lake et al. (2019) reported the relationship between dysregulation of lipid metabolism in WB muscle and human diabetes and further discussion will be followed elsewhere. Transferrin (TF) showed relatively large difference ($log_2FC = -1.9$) in WB broilers compared with controls, indicating the late phase of WB broilers may undergo hypoxic conditions, which were previously reported as a possible cause of WB incidence (Sihvo et al., 2018). Complement C1s (C1S) is a protease enzyme that functions in immunological host defense against microbial infection (Lu and Kishore, 2017), reflecting increased inflammatory responses in WB broilers in the late growth phase.

Plasma Metabolite Biomarkers

Untargeted metabolomics assay for primary metabolism analysis was conducted to identify differentially abundant plasma metabolites in WB broilers compared with controls. The same plasma samples used in the proteomics assays were used for metabolomics analysis. Overall, 33 and 19 plasma metabolites were differentially abundant ($p < 0.05$) at 4 (**Table 3**) and 8 wks old (**Supplementary Material**), respectively, in WB broilers compared with controls. In 4 wks old broilers, 4 and 10 metabolites showed log_2FC higher than 1.0 and lower than −1.0 abundances, respectively, in WB broilers compared with controls. In 8 wks old broilers, plasma metabolites displayed lowered differential abundance in WB compared with controls (**Supplementary Material**). **Table 3** shows log_2FC more than 1.0 or <-1.0 differentially abundant metabolites in 4 wks old WB broilers in addition to the corresponding log_2FC and *p*-values in plasma samples taken at 8 wks of age. Plasma raffinose contents showed the lowest FC values in WB broilers compared with

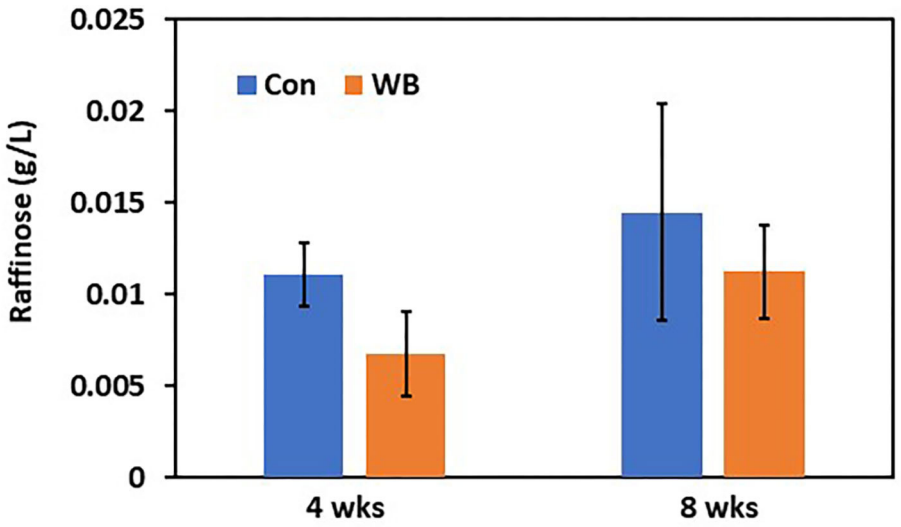

FIGURE 1 | Plasma raffinose concentration in WB and controls. Raffinose concentrations were determined at 4- and 8 wks of age. Bars indicate mean ± SE.

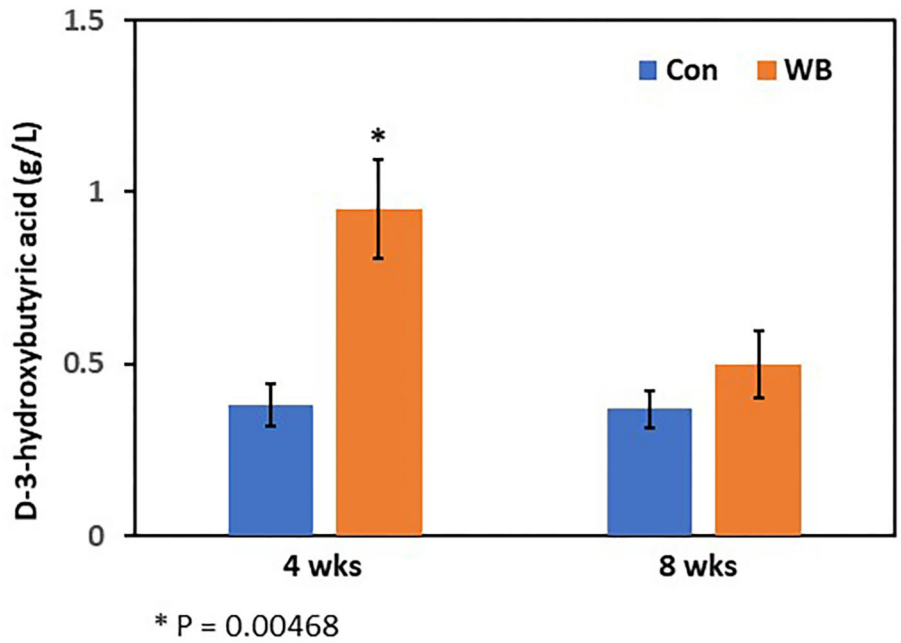

FIGURE 2 | Plasma 3-hydroxybutyric acid concentration in WB and controls. The 3-HB concentrations were determined at 4- and 8 wks of age. Bars indicate mean ± SE.

controls at 4 wks of age. Furthermore, raffinose contents were significantly lower in plasma samples at 8 wks of age. Results suggest that raffinose may be an effective plasma biomarker to diagnose WB in broilers during their early growth phase.

Plasma Concentration for Raffinose and 3-Hydroxybutyric Acid

To verify differential abundance of plasma raffinose as the lowest FC metabolite and 3-HB as the highest FC metabolite in WB broilers, concentrations for raffinose and 3-HB were determined using raffinose/D-galactose assay (**Figure 1**) and D-3-hydroxybutyric acid assay methods (**Figure 2**), respectively. Raffinose plasma concentrations in WB broilers at 4 wks of age was lower (0.006 ± 0.0023 g/L) than those of controls (0.01 ± 0.0017 g/L) consistent with the result of differential abundance in the metabolomics assay. At 8 wks of age, plasma raffinose concentrations in both Con and WB were higher than 4 wk old samples and those in the WB group were slightly lower

than controls ($p > 0.05$) consistent with the metabolomics data (**Figure 1**). However, the concentration of plasma raffinose showed very low levels (0.006–0.012 g/L), suggesting that a more sensitive measuring tool is needed to detect plasma raffinose.

Concentrations of plasma 3-HB in WB broilers at 4 wks of age (0.95 ± 0.15 g/L) were higher ($p = 0.005$) than those of controls (0.38 ± 0.06 g/L), which is also consistent with the result of the metabolomics analysis (**Figure 2**). In 8 wk old broilers, plasma 3-HB concentrations were slightly higher than in the Con group ($p > 0.05$) consistent with the metabolomics data.

Raffinose, a trisaccharide composed of galactose, glucose, and fructose, is mainly derived from soybean meal and is not digested in chicken gut due to lack of enzymes digesting raffinose (Valentine et al., 2017). The presence of plasma raffinose implicated two possible causes including leaky gut syndrome and/or differential microbial communities. Leaky gut syndrome, which is frequently observed in broiler production, may be associated with the incidence of WB. Differential microbial communities with variable abilities to digest raffinose may influence the incidence of WB. In fact, an earlier report (Zhang et al., 2019) characterized differential proportions of microbial species within the microbiome in WB compared with non-WB broilers, showing that *Selenomonas bovis* and *Bacteroids plebeius* were higher in caeca of WB broilers. Interestingly, *S. bovis* can breakdown raffinose (Zhang and Dong, 2009). Collectively, WB broilers may digest more raffinose by *S. bovis* in the gut, resulting in a higher incidence of WB.

The 3-hydroxybutyric acid (3-HB, also known as β-hydroxybutyric acid), together with acetone, and acetoacetic acid, is one of the ketone bodies that are a group of organic compounds of intermediary fat metabolism. High concentrations of ketone bodies decrease the rate of β-oxidation of fatty acids (Cadorniga-Valino et al., 1997). In human, circulating 3-HB levels > 3 mmol/L in children or >3.8 mmol/L in adults are considered the clinically significant level in diabetic ketoacidosis (DKA), whereas below 0.5 mmol/L is considered as normal. With starvation, levels can rise up to 6 mmol/L (Depczynski et al., 2019). Dogs with a blood ketone concentration >3.5 mmol/L are at higher risk for developing DKA (Di Tommaso et al., 2009). In this study, when examined at 4 wks of age, WB broilers showed 0.95 g/L (∼9.12 mmol/L in average; MW of 3-HB = 104.1) while non-disease controls showed 0.38 g/L (∼3.65 mmol/L in average). This is a striking result as higher 3-HB concentrations (∼9.12 mmol/L) at this early age of WB broilers is comparable to a severe clinical condition of DKA in humans (>3.8 mmol/L) and dogs (3.5 mmol/L). Moreover, non-WB broilers still showed the sub-clinical level of circulating 3-HB concentration (∼3.65 mmol/L). This may be correlated with the rapid growth in early life and altered muscular structures including decreased capillary blood supply, reduced connective tissue spacing between myofibers and muscle fiber bundles, and increased degeneration of myofibers, that occurred from intense growth-related selection resulting in modern broilers becoming more susceptible to the incidence of WB myopathy. Elevated levels of basal 3-HB in blood may be evidence of higher susceptibility of WB in modern broilers.

3-hydroxybutyric acid inhibits lipolysis via the PUMA-G receptor (Kimura et al., 2011) and reduces total energy expenditure by inhibiting short-chain fatty acid signaling through GPR41 (Taggart et al., 2005). A higher concentration of 3-HB in the blood of cows is considered an indicator of subclinical ketosis (Puppel and Kuczynska, 2016), and thus can be used as a biomarker for early diagnosis of ketosis (Puppel et al., 2019). In chicken, 3-HB concentration in blood after hatching is dramatically decreased to <20% of the concentration at 3 days and maintained at a steady level (Ohtsu et al., 2003). Therefore, higher concentrations of 3-HB in WB chicken plasma may indicate high ketoacidosis, suggesting that dysregulation of fat metabolism is a potential cause of WB. Increased concentration of 3-HB is a biomarker of increased ketosis showing subclinical or clinical conditions of metabolic diseases, such as diabetes in human (Depczynski et al., 2019). Lake et al. (2019) suggested that the altered physiological pathways, including dysregulation of lipid metabolism followed by lipid accumulation identified as early as 2 wks of age found in WB muscle were similar to those found in human diabetes (Lake and Abasht, 2020). Additional evidence of altered lipid metabolism in WB muscle associated with feed efficiency was revealed as metabolic signatures of susceptibility to muscle disorders in modern broilers (Abasht et al., 2019). Moreover, this result supports a previous report showing higher 3-HB concentration in WB muscle compared to non-WB muscle (Abasht et al., 2016). Taken together, these observations of higher concentrations of blood 3-HB in WB broilers suggests it is a potential less-invasive biomarker for early diagnosis of WB incidence.

CONCLUSION

Woody breast is a myopathy that exhibits greatest severity in the late growth phase of broilers with an etiology that may commence early in development (Lake and Abasht, 2020). Early diagnosis, when cases are mild, can be difficult to detect via palpation and thus, plasma biomarkers could be used to develop a less invasive diagnostic tool for early detection of WB, as reported in this study. Blood biomarkers, such as 3-HB and raffinose, are candidate targets to predict WB susceptibility. Further research evaluating a larger number of broilers and different broiler populations is needed to validate the candidate biomarkers. In this study, only two metabolites were confirmed by biochemical assays and other differentially abundant proteins (e.g., FRA10AC1) and metabolites will be examined with targeted biochemical assays in future studies.

DATA AVAILABILITY STATEMENT

The proteomics datasets presented in this study can be found in online repositories. The names of the repository/repositories

and accession number(s) can be found at: ProteomeXchange with identifier PXD026896 (Project DOI 10.6019/PXD026896).

ETHICS STATEMENT

The animal study was reviewed and approved by University of Arkansas Institutional Animal Care and Use Committee.

AUTHOR CONTRIBUTIONS

BKo, BKh, SK, WB, WK, and CO designed the experiments. BKo, BKh, SK, SS, HK, MK, KL, SO, JH, NA, WB, and WK performed the chicken experiments and analyzed the data. BM and CO conducted chicken processing and woody breast scoring. BKo wrote the draft of this manuscript. All authors have read, edited, and approved the final manuscript.

FUNDING

This work was supported by Arkansas Biosciences Institute (Little Rock, AR) and the Agricultural Experiment Station (Univ. of Arkansas, Fayetteville).

ACKNOWLEDGMENTS

We thank the technical and management support from staff members of Poultry Research Facility in University of Arkansas, Fayetteville, AR.

SUPPLEMENTARY MATERIAL

The Supplementary Material for this article can be found online at: https://www.frontiersin.org/articles/10.3389/fphys.2021.712694/full#supplementary-material

REFERENCES

Abasht, B., Mutryn, M. F., Michalek, R. D., and Lee, W. R. (2016). Oxidative stress and metabolic perturbations in wooden breast disorder in chickens. *PLoS ONE* 11:e0153750. doi: 10.1371/journal.pone.0153750

Abasht, B., Zhou, N., Lee, W. R., Zhuo, Z., and Peripolli, E. (2019). The metabolic characteristics of susceptibility to wooden breast disease in chickens with high feed efficiency. *Poult. Sci.* 98, 3246–3256. doi: 10.3382/ps/pez183

Brothers, B., Zhuo, Z., Papah, M. B., and Abasht, B. (2019). RNA-seq analysis reveals spatial and sex differences in pectoralis major muscle of broiler chickens contributing to difference in susceptibility to wooden breast disease. *Front. Physiol.* 10:764. doi: 10.3389/fphys.2019.00764

Cadorniga-Valino, C., Grummer, R. R., Armentano, L. E., Donkin, S. S., and Bertics, S. J. (1997). Effects of fatty acids and hormones on fatty acid metabolism and gluconeogenesis in bovine hepatocytes. *J. Dairy Sci.* 80, 646–656. doi: 10.3168/jds.S0022-0302(97)75983-6

Depczynski, B. A., Lee, T. K., Varndell, W., and Chiew, A. L. (2019). The significance of an increased beta-hydroxybutyrate at presentation to the emergency department in patients with diabetes in the absence of a hyperglycemic emergency. *J. Diabetes Res.* 2019:7387128. doi: 10.1155/2019/7387128

Di Tommaso, M., Aste, G., Rocconi, F., Guglielmini, C., and Boari, A. (2009). Evaluation of a portable meter to measure ketonemia and comparison with ketonuria for the diagnosis of canine diabetic ketoacidosis. *J. Vet. Intern. Med.* 23, 466–471. doi: 10.1111/j.1939-1676.2009.0302.x

Greene, E., Flees, J., Dadgar, S., Mallmann, B., Orlowski, S., Dhamad, A., et al. (2019). Quantum blue reduces the severity of woody breast myopathy via modulation of oxygen homeostasis-related genes in broiler chickens. *Front. Physiol.* 10:1251. doi: 10.3389/fphys.2019.01251

Hammer, J. A. (2018). Myosin goes for blood. *Proc. Natl. Acad Sci. U.S.A.* 115, 4813–4815. doi: 10.1073/pnas.1805253115

Hua, X., Wang, Y. Y., Jia, P., Xiong, Q., Hu, Y., Chang, Y., et al. (2020). Multi-level transcriptome sequencing identifies COL1A1 as a candidate marker in human heart failure progression. *BMC Med.* 18:2. doi: 10.1186/s12916-019-1469-4

Kagami, S., Kakinuma, T., Saeki, H., Tsunemi, Y., Fujita, H., Nakamura, K., et al. (2003). Significant elevation of serum levels of eotaxin-3/CCL26, but not of eotaxin-2/CCL24, in patients with atopic dermatitis: serum eotaxin-3/CCL26 levels reflect the disease activity of atopic dermatitis. *Clin. Exp. Immunol.* 134, 309–313. doi: 10.1046/j.1365-2249.2003.02273.x

Kang, S. W., Kidd, M. T. Jr., Kadhim, H. J., Shouse, S., Orlowski, S. K., Hiltz, J., et al. (2020). Characterization of stress response involved in chicken myopathy. *Gen. Comp. Endocrinol.* 295:113526. doi: 10.1016/j.ygcen.2020.113526

Kimura, I., Inoue, D., Maeda, T., Hara, T., Ichimura, A., Miyauchi, S., et al. (2011). Short-chain fatty acids and ketones directly regulate sympathetic nervous system via G protein-coupled receptor 41 (GPR41). *Proc. Natl. Acad. Sci. U.S.A.* 108, 8030–8035. doi: 10.1073/pnas.1016088108

Kuttappan, V. A., Bottje, W., Ramnathan, R., Hartson, S. D., Coon, C. N., Kong, B. W., et al. (2017). Proteomic analysis reveals changes in carbohydrate and protein metabolism associated with broiler breast myopathy. *Poult. Sci.* 96, 2992–2999. doi: 10.3382/ps/pex069

Lake, J. A., and Abasht, B. (2020). Glucolipotoxicity: a proposed etiology for wooden breast and related myopathies in commercial broiler chickens. *Front. Physiol.* 11:169. doi: 10.3389/fphys.2020.00169

Lake, J. A., Papah, M. B., and Abasht, B. (2019). Increased expression of lipid metabolism genes in early stages of wooden breast links myopathy of broilers to metabolic syndrome in humans. *Genes (Basel)* 10:746. doi: 10.3390/genes10100746

Lu, J., and Kishore, U. (2017). C1 complex: an adaptable proteolytic module for complement and non-complement functions. *Front. Immunol.* 8:592. doi: 10.3389/fimmu.2017.00592

Maharjan, P., Hilton, K., Weil, J., Suesuttajit, N., Beitia, A., Owens, C. M., et al. (2019). Characterizing woody breast myopathy in a meat broiler line by heat production, microbiota, and plasma metabolites. *Front. Vet. Sci.* 6:497. doi: 10.3389/fvets.2019.00497

Mallmann, B. A. (2019). *Prediction and Evaluation of Breast Myopathy, Poultry Science, University of Arkansas*. Available online at: https://core.ac.uk/download/pdf/250604484.pdf (accessed July 7, 2021).

Moreno-Navarrete, J. M., Ortega, F., Serino, M., Luche, E., Waget, A., Pardo, G., et al. (2012). Circulating lipopolysaccharide-binding protein (LBP) as a marker of obesity-related insulin resistance. *Int. J. Obes. (Lond.)* 36, 1442–1449. doi: 10.1038/ijo.2011.256

Ohtsu, H., Sato, K., Nishida, H., and Akiba, Y. (2003). High beta-hydroxybutyrate concentration in liver and skeletal muscle of newly hatched chicks. *Comp. Biochem. Physiol. A Mol. Integr. Physiol.* 134, 625–629. doi: 10.1016/S1095-6433(02)00353-7

Papah, M. B., Brannick, E. M., Schmidt, C. J., and Abasht, B. (2017). Evidence and role of phlebitis and lipid infiltration in the onset and pathogenesis of wooden breast disease in modern broiler chickens. *Avian Pathol.* 46, 623–643. doi: 10.1080/03079457.2017.1339346

Perez-Riverol, Y., Csordas, A., Bai, J., Bernal-Llinares, M., Hewapathirana, S., Kundu, D. J., et al. (2019). The PRIDE database and related tools and resources in 2019: improving support for quantification data. *Nucleic Acids Res.* 47, D442–D450. doi: 10.1093/nar/gky1106

Petracci, M., Soglia, F., Madruga, M., Carvalho, L., Ida, E., and Estevez, M. (2019). Wooden-breast, white striping, and spaghetti meat: causes, consequences and

consumer perception of emerging broiler meat abnormalities. *Compr. Rev. Food Sci. Food Saf.* 18, 565–583. doi: 10.1111/1541-4337.12431

Puppel, K., Golebiewski, M., Solarczyk, P., Grodkowski, G., Slosarz, J., Kunowska-Slosarz, M., et al. (2019). The relationship between plasma beta-hydroxybutyric acid and conjugated linoleic acid in milk as a biomarker for early diagnosis of ketosis in postpartum polish holstein-friesian cows. *BMC Vet. Res.* 15:367. doi: 10.1186/s12917-019-2131-2

Puppel, K., and Kuczynska, B. (2016). Metabolic profiles of cow's blood; a review. *J. Sci. Food Agric.* 96, 4321–4328. doi: 10.1002/jsfa.7779

Sarafidou, T., Kahl, C., Martinez-Garay, I., Mangelsdorf, M., Gesk, S., Baker, E., et al. (2004). Folate-sensitive fragile site FRA10A is due to an expansion of a CGG repeat in a novel gene, FRA10AC1, encoding a nuclear protein. *Genomics* 84, 69–81. doi: 10.1016/j.ygeno.2003.12.017

Sihvo, H. K., Airas, N., Linden, J., and Puolanne, E. (2018). Pectoral vessel density and early ultrastructural changes in broiler chicken wooden breast myopathy. *J. Comp. Pathol.* 161, 1–10. doi: 10.1016/j.jcpa.2018.04.002

Sihvo, H. K., Linden, J., Airas, N., Immonen, K., Valaja, J., and Puolanne, E. (2017). Wooden breast myodegeneration of pectoralis major muscle over the growth period in broilers. *Vet. Pathol.* 54, 119–128. doi: 10.1177/0300985816658099

Sole, C., Tramonti, D., Schramm, M., Goicoechea, I., Armesto, M., Hernandez, L. I., et al. (2019). The circulating transcriptome as a source of biomarkers for melanoma. *Cancers (Basel)* 11:70. doi: 10.3390/cancers11010070

Taggart, A. K., Kero, J., Gan, X., Cai, T. Q., Cheng, K., Ippolito, M., et al. (2005). (D)-beta-Hydroxybutyrate inhibits adipocyte lipolysis via the nicotinic acid receptor PUMA-G. *J. Biol. Chem.* 280, 26649–26652. doi: 10.1074/jbc.C500213200

Valentine, M. F., De Tar, J. R., Mookkan, M., Firman, J. D., and Zhang, Z. J. (2017). Silencing of soybean raffinose synthase gene reduced raffinose family oligosaccharides and increased true metabolizable energy of poultry feed. *Front. Plant Sci.* 8:692. doi: 10.3389/fpls.2017.00692

Velleman, S. G. (2015). Relationship of skeletal muscle development and growth to breast muscle myopathies: a review. *Avian Dis.* 59, 525–531. doi: 10.1637/11223-063015-Review.1

Velleman, S. G., and Clark, D. L. (2015). Histopathologic and myogenic gene expression changes associated with wooden breast in broiler breast muscles. *Avian Dis.* 59, 410–418. doi: 10.1637/11097-042015-Reg.1

Zhang, K., and Dong, X. (2009). *Selenomonas bovis* sp. nov., isolated from Yak Rumen contents. *Int. J. Syst. Evol. Microbiol.* 59, 2080–2083. doi: 10.1099/ijs.0.007641-0

Zhang, X., Zhang, L., Hendrix, J., Zhai, W., and Schilling, W. (2019). Characterization of ceacal microbiota in broilers that differ in genetic strain, nutrition, and development of woody breast. *Meat Muscle Biol.* 3:72. doi: 10.22175/mmb2019.0072

Conflict of Interest: The authors declare that the research was conducted in the absence of any commercial or financial relationships that could be construed as a potential conflict of interest.

frontiers in Physiology

ORIGINAL RESEARCH
published: 26 July 2021
doi: 10.3389/fphys.2021.712464

Differential Expression of Myogenic and Calcium Signaling-Related Genes in Broilers Affected With White Striping

*Caroline Michele Marinho Marciano[1], Adriana Mércia Guaratini Ibelli[2,3], Jorge Augusto Petroli Marchesi[4], Jane de Oliveira Peixoto[2,3], Lana Teixeira Fernandes[2], Igor Ricardo Savoldi[1], Kamilla Bleil do Carmo[5] and Mônica Corrêa Ledur[1,2]**

[1]Programa de Pós-Graduação em Zootecnia, Universidade do Estado de Santa Catarina (UDESC-Oeste), Chapecó, Brazil, [2]Embrapa Suínos e Aves, Concórdia, Brazil, [3]Programa de Pós-Graduação em Ciências Veterinárias, Universidade Estadual do Centro-Oeste, Guarapuava, Brazil, [4]Departamento de Genética, Universidade de São Paulo – Faculdade de Medicina de Ribeirão Preto, Ribeirão Preto, Brazil, [5]Universidade do Contestado, Concórdia, Brazil

OPEN ACCESS

Edited by:
Sandra G. Velleman,
The Ohio State University,
United States

Reviewed by:
Mahmoud Madkour,
National Research Center, Egypt
Shaaban Saad Elnesr,
Fayoum University, Egypt

***Correspondence:**
Mônica Corrêa Ledur
monica.ledur@embrapa.br

Specialty section:
This article was submitted to Avian Physiology, a section of the journal Frontiers in Physiology

Received: 20 May 2021
Accepted: 05 July 2021
Published: 26 July 2021

Citation:
Marciano CMM, Ibelli AMG, Marchesi JAP, Oliveira Peixoto J, Fernandes LT, Savoldi IR, Carmo KB and Ledur MC (2021) Differential Expression of Myogenic and Calcium Signaling-Related Genes in Broilers Affected With White Striping. Front. Physiol. 12:712464. doi: 10.3389/fphys.2021.712464

White Striping (WS) has been one of the main issues in poultry production in the last years since it affects meat quality. Studies have been conducted to understand WS and other myopathies in chickens, and some biological pathways have been associated to the prevalence of these conditions, such as extracellular calcium level, oxidative stress, localized hypoxia, possible fiber-type switching, and cellular repairing. Therefore, to understand the genetic mechanisms involved in WS, 15 functional candidate genes were chosen to be analyzed by quantitative PCR (qPCR) in breast muscle of normal and WS-affected chickens. To this, the pectoral major muscle (PMM) of 16 normal and 16 WS-affected broilers were collected at 42 days of age and submitted to qRT-PCR analysis. Out of the 15 genes studied, six were differentially expressed between groups. The *CA2*, *CSRP3*, and *PLIN1* were upregulated, while *CALM2*, *DNASE1L3*, and *MYLK2* genes were downregulated in the WS-affected when compared to the normal broilers. These findings highlight that the disruption on muscle and calcium signaling pathways can possibly be triggering WS in chickens. Improving our understanding on the genetic basis involved with this myopathy might contribute for reducing WS in poultry production.

Keywords: gene expression, glycogen metabolism, pectoral myopathy, chickens, quantitative PCR

INTRODUCTION

The White Striping (WS) is one of the most prevalent myopathies occurring in modern commercial broilers nowadays, which is characterized macroscopically by parallel white fatty striations across the muscle fibers on the surface of breast fillets and thighs (Kuttappan et al., 2013). The most prominent histological features associated to this condition are myodegeneration with regeneration, perivascular necrosis, interstitial inflammation, lipidosis, and infiltration of connective tissue (Kuttappan et al., 2013; Sihvo et al., 2014; Russo et al., 2015; Vanhatalo et al., 2021). From a meat quality standpoint, the WS disorder represents a huge economic impact on the chicken industry, since it affects the most valuable part of the broiler carcass,

increasing the downgrading percentages and condemnation of breast fillets. Moreover, the abnormal appearance of the meat negatively affects the consumer acceptance and increases concerns about animal welfare (Kuttappan et al., 2012; Petracci et al., 2015; Ayansola et al., 2021). In 2019, the world poultry meat production reached 120 million tons with an average consumption of 50.7 and 20.8 Kg per capita in the United States (USA) and European Union (EU), respectively (Avec, 2020). Breast muscle disorders in the USA poultry industry have been estimated to cause economic losses ranging from $200 million to more than $1 billion dollars per year (Kuttappan et al., 2016; Barbut, 2019).

It has been hypothesized that genetic selection of commercial broilers for fast growth increases the incidence of myopathies, and a number of factors have been associated with the onset and severity of WS, such as genotype (high breast yield), gender (males), fast growth rate, heavy weight of the *Pectoralis major*, and diets with high energy (Petracci et al., 2013; Mutryn et al., 2015; Trocino et al., 2015; Cruz et al., 2017; Griffin et al., 2018; Vanhatalo et al., 2021). Different causative mechanisms for WS occurrence have been suggested to date: hypoxia, oxidative stress, fiber-type switching, disruption in satellite cells proliferation and differentiation, metabolic disorders, and nutritional deficiencies, but no conclusive evidence was found regarding the etiology of this disorder (Russo et al., 2015; Daughtry et al., 2017; Boerboom et al., 2018; Marchesi et al., 2019; Soglia et al., 2019; Abasht et al., 2021; Lake et al., 2021). Swatland (1990) suggested that selection for rapid growth has created muscle that outgrow their life support systems and cause muscle damage. Therefore, the formation of large intercellular spaces leads to loss of muscle fiber fluids, compromising the muscular integrity of chickens. Thus, the selected modern hybrids have differences in muscle histology and metabolism, with higher density of fast twitch fiber, which is characterized by a higher diameter and a lower rate of protein degradation, compared to unselected broilers (Picard et al., 2010).

Genetic studies have shown heritability estimates ranging from 0.18 to 0.65 for WS (Bailey et al., 2015, 2020; Alnahhas et al., 2016; Lake et al., 2021) indicating an important genetic component influence on the occurrence of WS in broilers. Furthermore, positive genetic correlations between WS and body weight (0.23) and breast yield (0.31) traits, as well as with other myopathies, such as wooden breast (0.74) and deep pectoral myopathy (0.34) have also been found (Bailey et al., 2020). Recently, many genes have been associated with the occurrence of myopathies in chickens (Zambonelli et al., 2016; Beauclercq et al., 2017; Zampiga et al., 2018; Marchesi et al., 2019; Lake et al., 2021), and the identification of specific biomarkers can help to accurately assess the effect of genetics, environment, or management conditions in improving or aggravating the WS myopathy in broilers (Beauclercq et al., 2017). Some candidate genes involved with the development of WS in fast-growing broilers suggest that these genes play important role in molecular mechanisms, such as muscle differentiation, oxidative stress, calcium signaling, hypoxia, and muscle fiber type replacement (Mutryn et al., 2015; Marchesi et al., 2019). Despite the studies searching for the causes of the WS development, efforts are still needed to understand and, consequently, reduce this problem. In a recent review by Soglia et al. (2021), the importance of gene expression studies to unravel the molecular mechanisms underlying the findings obtained by different techniques and approaches to understand myopathic disorders in a global manner was highlighted. Thus, gene expression studies evaluating normal and WS-affected tissues would provide additional support to find the triggering pathways of this myopathy. Therefore, the aim of the present study was to evaluate the expression profile of 15 functional candidate genes by quantitative PCR (qPCR) in the breast muscle of normal and WS-affected chickens to provide more insights on the molecular events underlying the occurrence of moderate levels of WS.

MATERIALS AND METHODS

Experimental Animals and Tissue Collection

A total of 168 male broilers from the commercial line Cobb500 were raised at the Embrapa Swine and Poultry National Research Center farm, located in Concórdia, Santa Catarina State, Brazil. Chicks were vaccinated in the hatchery against fowl pox and Marek disease. The management conditions followed the guidelines of the line, with water and feed provided *ad libitum*. At 42 days of age, all broilers were weighed and slaughtered by cervical dislocation following the procedures of the Ethics Committee for Animal Use (CEUA) from the Embrapa Swine and Poultry National Research Center, under protocol No. 012/12.

Immediately after slaughter, a subsequent necropsy was performed, and breasts of all animals were visually evaluated for the presence and severity of WS and classified based on the 3 degrees of lesions established by Kuttappan et al. (2013). A total of 16 broilers with normal breasts and 16 with moderate degree of WS (fillets with white striations generally less than 1 mm thick on the surface of the breast) were chosen for this experiment. Samples from the cranial region of the pectoral major muscle (PMM) were collected by removing approximately 1 g of the breast muscle of each animal, which was immediately frozen in liquid nitrogen and stored at −80°C for further molecular analysis.

RNA Extraction and cDNA Synthesis

Frozen samples were ground in liquid nitrogen, and 100 mg of the PMM was submitted to RNA extraction using Trizol (Invitrogen, United States) following the manufacturer's protocol. Briefly, 1 ml of Trizol was added to the PMM, homogenized at room temperature (RT) for 5 min, and then 200 µl of chloroform was added and the samples were shaken vigorously. The tubes were centrifuged at 10,000 × *g* at 4°C for 15 min, and the aqueous phase was transferred to a microtube containing 500 µl of 100% isopropyl alcohol. Another RT incubation for 10 min was performed, followed by a 12,000 × *g* centrifugation for 10 min. The RNA pellet was washed with 75% ethanol and centrifuged at 7,500 × *g*

for 5 min at 4°C. Pellets were dried for 15 min at RT and resuspended in DEPC-treated water. The total RNA was quantified in BioDrop spectrophotometer (Biodrop, United Kingdom). Samples with 260:280 nm ratio higher than 1.8 were considered pure. The integrity of the RNAs were confirmed in 1.5% agarose gel after electrophorese for 90 min. The first strand cDNA was synthesized using 4 μg of total RNA and SuperScript III First-Strand Kit SuperMix Synthesis (Thermo Fischer Scientific, EUA), using oligo dT primer, following the manufacturer's recommendations.

Real Time RT-PCR

A total of 15 functional candidate genes (**Table 1**) previously reported as potentialy involved with WS development in chickens were chosen from the literature to be evaluated for gene expression analysis (Mutryn et al., 2015; Marchesi et al., 2019). These genes participate in several biological processes important for muscle development and homeostasis, such as regulation of actin cytoskeleton, focal adhesion, nitrogen metabolism, hypoxia, calcium signaling pathway, and insulin signaling pathway. The gene sequences were obtained in the Genbank[1] and Ensembl[2] databases. Primers for each gene (**Table 1**) were designed in exon-exon junctions to avoid DNA amplification using the Primer-Blast online tool (Ye et al., 2012), and primer's quality was evaluated in the Netprimer online tool.[3]

The qPCR reactions were amplified on an QuantStudio 6 (Applied Biosystems, Foster City, CA, United States), in a final volume of 15 μl containing 1x Maxima SYBR Green (Fermentas, United States), 0.13 μM of each primer, and 2 μl of 1:10 diluted cDNA. The reactions for all primers followed the cycling condition: 95°C for 10 min, 40 cycles of 15 s at 95 and 60°C. A melting curve stage of 70–95°C was added in all qPCR reactions to verify their specificity. Primer specificity was also confirmed by 1% agarose gel. The reactions were analyzed in duplicates, and negative controls were included to detect contamination. Primers efficiency were obtained by linear regression [efficiency = $10^{(-1/\text{slope})}$], according to Livak and Schmittgen (2001), and primers with efficiency between 95 and 105% were considered for gene expression analysis.

Differential Gene Expression Analysis

The average of cycle thresholds (Ct) values was collected, and the $2^{-\Delta\Delta CT}$ was calculated for each sample to obtain the fold-change (Livak and Schmittgen, 2001). The *RPL30* (*Ribosomal protein 30*) and *RPL5* (*Ribosomal protein L5*) reference genes were used for normalization (**Table 1**). These reference genes were chosen based on their stability values previously evaluated in the PMM of normal and WS-affected broilers (Marciano et al., 2020). The comparison of the relative gene expression between normal and WS-affected groups was performed using Mann-Whitney test. Genes with values of $p < 0.05$ were considered differentially expressed (DE).

[1]https://www.ncbi.nlm.nih.gov/genbank/
[2]https://www.ensembl.org
[3]http://www.premierbiosoft.com/netprimer

Gene Interaction Analysis

The STRING online software[4] was used to evaluate the interactions among the DE genes. This software predicts the evidence of gene interactions based on co-expression and co-localization. The gene network was constructed using both *Gallus gallus* and *Homo sapiens* databases, in order to improve the information about the interaction among genes.

RESULTS

From the total of 168 broilers evaluated in this experiment, 146 birds (87%) presented different degrees of macroscopic lesions associated with WS and 22 chickens (13%) showed normal breast muscle. The average body weight of the WS-affected and the normal groups were 2.89 kg and 2.85 kg, respectively.

The relative expression of all 15 genes studied was obtained from the breast muscle tissue of normal and WS-affected 42 days-old broilers (**Table 2**). The *CSRP3* gene had the highest fold-change (14.56) and the others had a magnitude ranging from 1 to 2.11 (**Table 2**; **Figure 1**).

Regarding the differentially expressed genes ($p < 0.05$), the *CALM2*, *DNASE1L3*, and *MYLK2* were downregulated in the WS-affected broilers when compared to the normal group (**Figure 1**). The expression levels of these three genes were, respectively, 1.79, 1.85, and 2.08 lower in WS-affected than in the normal broilers. The *CA2*, *CSRP3*, and *PLIN1* genes were 1.58, 14.56, and 2.11 more expressed in WS-affected broilers when compared to the normal group (**Table 2**; **Figure 1**). For the eight remaining evaluated genes, no differential expression was observed between groups (**Figure 1**).

In the gene network analysis performed with the six DE genes, the *CALM2* and *MYLK2* genes, which were downregulated in the WS-affected group (**Table 2**), were the main interactors of two gene clusters constructed from both chicken (**Figure 2A**) and human database (**Figure 2B**). One of the clusters was related to myogenesis and included the *CSRP3*, *MYOZ2*, *MYPBC3*, *MYL2*, and *MYL9* genes (**Figure 2A**), and the other was composed by phosphorylase kinase genic family (*PHKB*, *PHKA1*, *PHKA2*, *PHKG1*, and *PYGL*; **Figure 2A**), which play an important role in providing cell energy for muscle and liver tissue. The *CA2*, *DNASE1L3*, and *PLIN1* were not clustered with other genes according to the information available for *Gallus gallus* (**Figure 2A**). However, when the human database was used, the *PLIN1* gene was clustered with genes related to adipocyte differentiation, fatty acids, and glucose homeostasis (**Figure 2B**).

DISCUSSION

White Striping has been one of the main issues in poultry production in the last years. A number of studies have been conducted to understand the onset and development of WS, and other myopathies in chickens and some biological pathways

[4]https://string-db.org/

TABLE 1 | Primers for the 15 candidate genes and reference genes used for the quantitative PCR (qPCR) analysis in the breast muscle of normal and White Striping (WS)-affected broilers.

Gene	Ensembl ID	Primer (5'–3')	Size (bp)
ACTG1 Actin, gamma 1	ENSGALG00000028749	F: 5'-CTCTGTTCCAACCCTCTTTCCT-3' R: 3'-GTGTTGGCGTACAGATCCTTC-5'	112
CA2 Carbonic anhydrase 2	ENSGALG00000030781	F: 5'-GCTCTGAGCAGATGTGCAAAC-3' R: 3'-CTCATCGCTGAGGTTACTGGAAG-5'	144
*CALM2** Calmodulin 2	ENSGALG00000010023	F: 5´-CCACCATGGCTGATCAACTG-3' R: 5´-GCCATTGCCATCAGCGTCTA-3´	191
PLIN1 Perilipin 1	ENSGALG00000023395	F: 5'-GGCTATGGAGACGGTGGATG-3' R: 5'-CTGGCTTGCTCTCCTCTTCC-3'	173
CHST1 Carbohydrate sulfotransferase 1	ENSGALG00000008440	F: 5'-CGCCCCTCTTTCTCGTCTTC-3' R: 5'-CTCATCGCTGAGGTTACTGGAAG-3'	133
CSRP3 Cysteine and glycine rich protein 3	ENSGALG00000004044	F: 5'-GCTCTGAGCAGATGTGCAAAC-3' R: 3'-GCTTGGAGAGACCCGATTCC-5'	202
CTGF Connective tissue growth factor	ENSGALG00000037402	F: 5'-TCACCAACGATAATGCTTTCTG-3' R: 3'-GAATGCACTTTTTGCCTTTCTT-5'	111
DNASE1L3 Deoxyribonuclease I-like 3	ENSGALG00000005688	F: 5'-GAGTTTGCGTGGCTCATCG-3' R: 3'-CACGATCCTGTCATAGGGGC-5'	78
HDAC1 Histone deacetylase 1	ENSGALG00000003297	F: 5'-GGGGCGGGTTGCGTT-3' R: 3'-ACATCACCGTCGTAGTAGTAGC-5'	115
HIF1A Hypoxia inducible factor 1 alpha subunit	ENSGALG00000011870	F: 5'-CGTCACCGACAAGAAGAGGATT-3' R: 5'-GTCAGCCTCATAATGGATGCCT-3'	171
MAPK13 Mitogen-activated protein kinase 13	ENSGALG00000030966	F: 5'-TCTGCTCCGCCATAGACAAG-3' R: 5'-CAAGCAGCCCAATGACATTCTC-3'	150
MYLK2 Myosin light chain kinase 2	ENSGALG00000006273	F: 5'-ACCCTTTTGAGATATTGGACGA-3' R: 5'-TCCTTGGAGCTGAGGTTGTACT-3'	112
RYR2 Ryanodine receptor 2	ENSGALG00000010812	F: 5'-ATACAAGGGACCTGCTGGGT-3' R: 5'-GGGAGGCAAAACAATCTGGC-3'	92
SMAD3 SMAD family member 3	ENSGALG00000035701	F: 5'-CCCCATGTCATCTACTGCCG-3' R: 5'-GGTAACACTGGGGTCTCCAC-3'	158
TNNC2 Troponin C2, fast skeletal type	ENSGALG00000006835	F: 5'-GTCAATGACGGACCAGCAG-3' R: 5'-CGTCCGCATCAAACATGTCA-3'	95
*RPL5*** Ribosomal protein L5	ENSGALG00000005922	F: 5'-AATATAACGCCTGATGGGATGG-3' R:5'-CTTGACTTCTCTCTTGGGTTTCT-3'	99
RPL30 Ribosomal protein 30	ENSGALG00000029897	F: 5'-ATGATTCGGCAAGGCAAAGC-3' R: 5'-GTCAGAGTCACCTGGGTCAA	273

F, forward (5'-3'); R, reverse (3'-5').
**Paludo et al. (2017).*
***De Oliveira et al. (2017).*

have been associated to the occurrence of these conditions, such as extracellular calcium level, oxidative stress, localized hypoxia, possible fiber-type switching, and cellular repairing (Mutryn et al., 2015; Beauclercq et al., 2017; Kuttappan et al., 2017; Boerboom et al., 2018; Lake et al., 2019; Marchesi et al., 2019; Abasht et al., 2021; Bordini et al., 2021). In the present study, 15 functional candidate genes important for tissue development were investigated in normal and WS-affected broilers, and six of them (*CA2*, *CSRP3*, *PLIN1*, *CALM2*, *DNASE1L3*, and *MYLK2*) were differentially expressed.

The *CA2*, which was upregulated in WS-affected broilers in this study, is mainly involved in oxidative stress (Zimmerman et al., 2004). The *CA2* encodes zinc metalloenzymes and participates in a variety of biological processes, including calcification, acid-base balance, and bone resorption (Zimmerman et al., 2004). Genes of carbonic anhydrase (CA) family have regulatory and repair functions with the ability to act as an oxidant agent in both physiological and physiopathological conditions in skeletal muscle. This gene family is important to efficiently transport and eliminate carbon dioxide (CO^2) from tissues (Chegwidden and Carter, 2000). Some genes of this family were reported as DE in muscle myopathies in broilers. Among them, *CA3* could be highlighted since it was approximately 25 times more expressed in chickens affected with Wooden Breast myopathy than in normal broilers (Mutryn et al., 2015). Nishita et al. (2012) also found that *CA3* was upregulated in the pectoral muscle of broilers with muscular dystrophy compared to normal chickens. The *CA4* gene is involved in the regulation of extracellular pH, reducing the muscular contraction and possibly increasing the intracellular

acidosis (Peralta and Huidobro-Toro, 2016). The specific function of *CA2* associated to muscle development or myopathies, such as WS, has not yet been described, but it is also known that CAs are involved with lipid metabolism and obesity, and with the increase of mitochondrial oxidative stress (Supuran, 2012). Therefore, the upregulation of *CA2* in WS-affected broilers could be related to the adipose tissue deposition between muscle fibers. Nevertheless, the function of this gene should be further explored, since our results (**Figure 1**) differ from the expression pattern obtained by Marchesi et al. (2019), in which the *CA2* gene was downregulated in WS-affected broilers. Although both studies used 42 days-old broilers, we chose to analyze breast tissue with moderate levels of WS, whereas Marchesi et al. (2019) studied severe levels of the disorder. This discrepancy indicates that the expression of this gene could be modulated by the degree of WS lesions.

TABLE 2 | Relative expression (fold-change) between normal and WS-affected broilers, respective *p* values, and expression levels calculated for each group.

Genes	Relative expression	*p* value	Fold-change by group (Mean ± SD)	
			Normal	WS-affected
ACTG1	−1	0.717	1.12 ± 0.49	1.12 ± 0.56
CA2	1.58*	0.006	1.07 ± 0.38	1.68 ± 0.75
CALM2	−1,79*	0.007	1.11 ± 0.55	0.62 ± 0.62
CHST1	1.18	0.945	1.57 ± 1.61	1.84 ± 2.92
CSRP3	14.56*	0.0001	0.84 ± 0.56	12.38 ± 12.21
DNASE1L3	−1.85*	0.005	1.11 ± 0.50	0.60 ± 0.34
HDAC1	−1.01	0.508	1.11 ± 0.48	1.02 ± 0.44
HIF1A	−1.12	0.151	1.12 ± 0.58	0.99 ± 0.85
MAPK13	−1.03	0.703	1.21 ± 0.83	1.17 ± 0.58
MYLK2	−0.8*	0.001	1.16 ± 0.91	0.36 ± 0.4
PLIN1	2.11*	0.009	1.47 ± 1.11	3.10 ± 1.97
RYR2	−1.45	0.773	1.57 ± 1.47	1.08 ± 0.67
SMAD3	1.14	0.816	1.37 ± 0.86	1.51 ± 1.26
TNNC2	−1.17	0.386	1.14 ± 0.71	0.97 ± 0.66

SD, standard deviation.
*$p < 0.05$.

Oxidative stress is defined as the presence of metabolic and radical substances or so-called reactive (oxygen, nitrogen, or chlorine) species (Elnesr et al., 2019; Elwan et al., 2019). Regarding the oxidative stress in the skeletal muscle, the increase in reactive oxygen species (ROS) causes changes in the cell signaling pathways, affecting the release of calcium from the sarcoplasmic reticulum, resulting in damage to the contractile capacity of muscle cells (Allen et al., 2008). The increase in ROS is cytotoxic and can alter cell integrity, inducing severe stress and leading to the production of carbonic anhydrases signaling to the non-recoverable muscle damage (Zimmerman et al., 2004). In our study, the upregulation of the gene *CA2* in WS-affected broilers may have an oxidative action in the cell, which could lead to a hypoxic state in the tissue. This pattern has also been described in WB (Mutryn et al., 2015).

The *CSRP3* gene was upregulated in WS-affected broilers in our study. This gene encodes the LIM protein, which regulates important processes for the development and differentiation of satellite cells. In a very recent study of Wooden Breast in

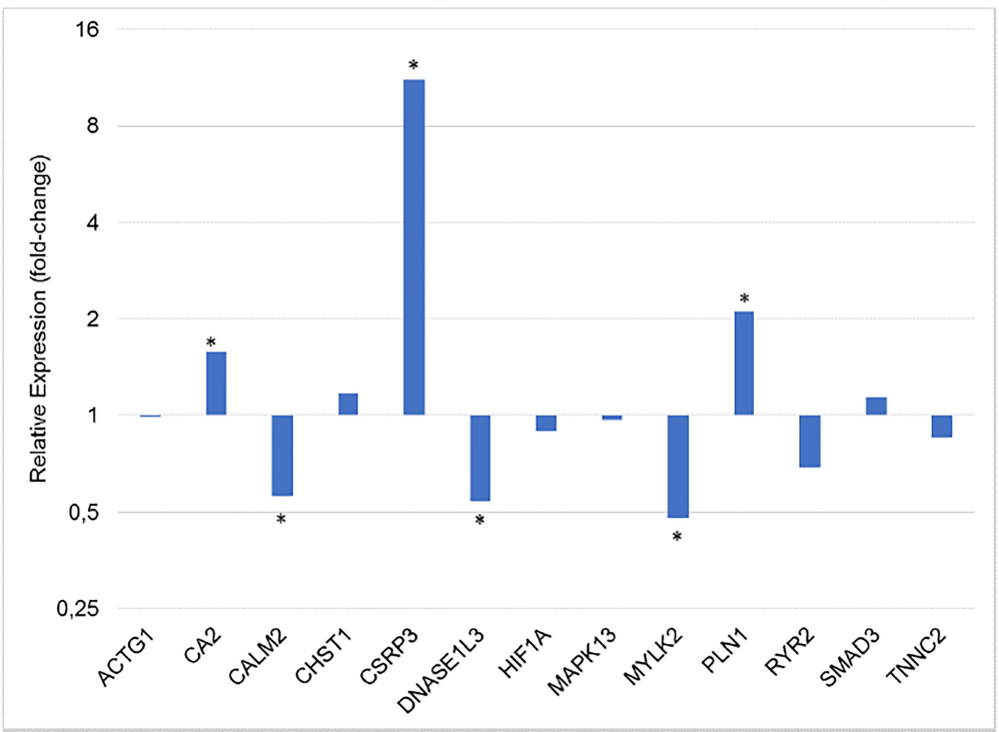

FIGURE 1 | Gene expression ratio between normal and WS-affected broilers at 42 days of age, normalized for *RPL30* and *RPL5* reference genes. *$p < 0.05$.

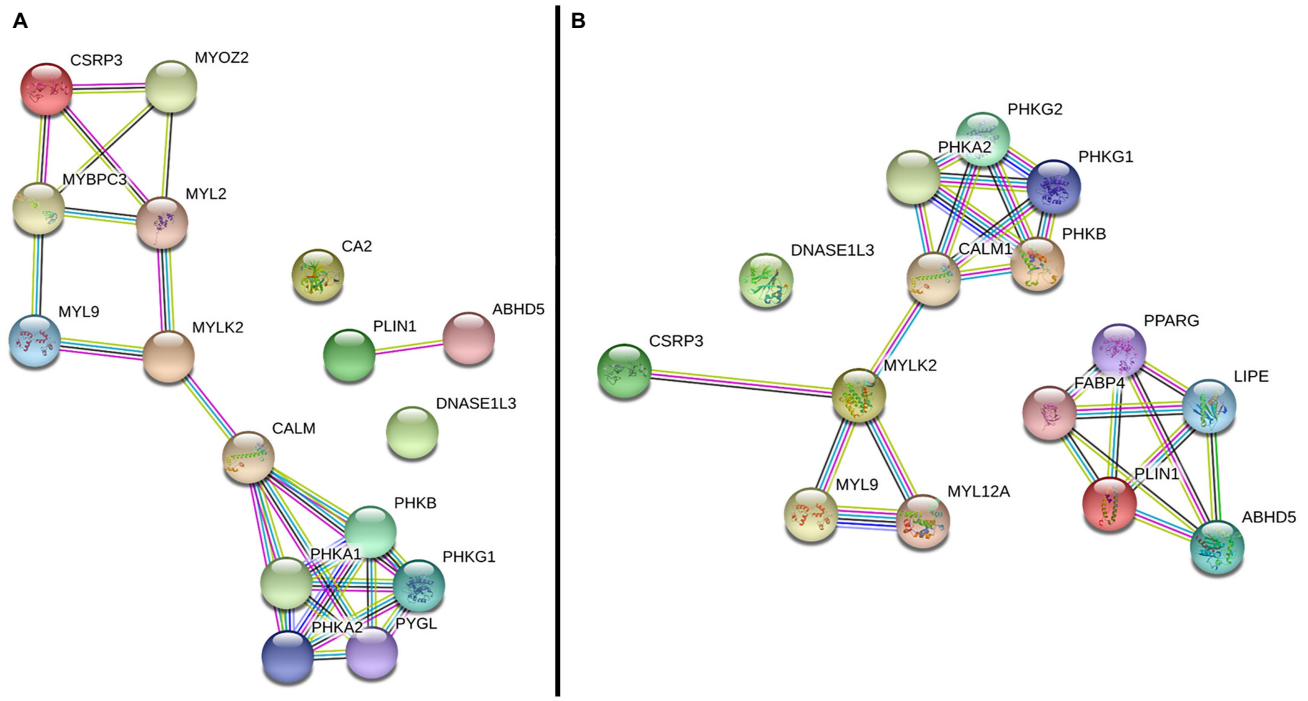

FIGURE 2 | Gene network performed with differentially expressed (DE) genes between normal and WS-affected broilers, obtained with the String database using *Gallus gallus* **(A)** and *Homo sapiens* **(B)** protein information. Circles represent the genes. Lines represent the interaction among the DE and other related genes based on the prediction methods: known interaction in curated databases (light blue) and experimentally determined (magenta), predicted co-occurrence (blue), gene fusion (red) or neighborhood (green), homology (purple), text mining information (yellow), and co-expression (black).

broilers, the upregulation of *CSRP3* reduced late proliferation of cultured satellite cells from birds before the WB appearance (Velleman et al., 2021). In the muscle, LIM interacts with various proteins, such as titin, participating on intracellular signaling cascades and in the maintenance of sarcomere integrity (Hershberger et al., 2008). Moreover, the LIM protein seems to be involved with stress response through compensatory signaling pathway. This protein appears to be essential to the structure and maintenance of the sarcomere (Shah et al., 2005) and its expression occurs mainly in slow skeletal muscle (Geier et al., 2008), helping the formation and growth of myotubes, which are key features for muscle repair (Schneider et al., 1999). Alterations in *CSRP3* expression profile changed the type of fibers from fast to slow in a study using rats as animal model (Geier et al., 2008). The upregulation of this gene has already been reported in PMM of chickens affected with myopathies, such as Wooden Breast (Mutryn et al., 2015) and WS (Marchesi et al., 2019).

According to Arber et al. (1994), the *CSRP3* promotes muscle differentiation, acting on regeneration, structural repair, and genetic regulation of the skeletal muscle. In WS-affected chickens, there is an increase in extracellular space because the muscle differentiation gradually leaves gaps between neighboring fibers and bundle fibers. In these gaps, the infiltration of mononuclear, adipose, and fibrous cells occurs and may be involved as a secondary response to myopathy (Barash et al., 2005). Offer and Cousins (1992) suggested that the upregulation of the *CSRP3* gene in chickens with myopathy is a repair mechanism of myofibers trying to regenerate the affected muscle. They also suggest that the positive regulation of *CSRP3* affects meat quality, since this gene is involved in the development of myofibers acting on the interchange of muscle fiber type. This gene has already been associated with different meat quality traits in bovine (Pierzchala et al., 2014) and porcine (Offer and Cousins, 1992; Xu et al., 2010), but no information is available in broilers. Moreover, *CSRP3* regulates the autophagy in muscle cells (He et al., 2014) and has already been associated with myopathies in humans (Rashid et al., 2015) and chickens (Picard et al., 2010), which make this gene a possible molecular marker for myopathies occurrence.

In the gene network (**Figure 2**), the *CSRP3* was grouped with several myogenic genes, including *MYLK2*, *MYL2*, and *MYOZ2*, which were DE in a previous chicken WS study (Marchesi et al., 2019). The *MYLK2*, a myosin light chain kinase gene, was downregulated in our study and it is essential for muscle contraction (**Figure 1**), composing the main myofibrillar proteins in muscle cells (Janin et al., 2018). This gene is a calcium/calmodulin dependent and it is responsible for light chain phosphorylation, facilitating its interaction with actin filaments and then inducing a contractile activity (Smith, 2010). *MYLK2* is expressed predominantly in fast skeletal muscle fibers, and studies with *MYLK2* knockout mice showed a decrease in the phosphorylation of the myosin regulatory light chain in the skeletal muscle (Park et al., 2011). Reduced levels of *MYLK2* in turkeys *pectoralis* muscle with PSE meat favored a low integrity of myofibrillar proteins reducing the skeletal muscle contraction

(Zhi et al., 2005). In broilers, it has been observed that breast muscle with severe WS myopathy has low integrity of myofibrillar proteins, resulting in reduced water retention capacity compared to normal breasts (Malila et al., 2019) and, consequently, affecting meat quality (Alnahhas et al., 2016). The hypothesis is that the structural alteration of myosin facilitates water loss (Offer et al., 1989; Russo et al., 2015). Therefore, the presence of myopathies impairs the water holding capacity during the meat processing and storage (Barbut et al., 2005, 2008; Petracci et al., 2009). Furthermore, the reduced *MYLK2* mRNA levels in WS-affected chickens could lead to a decrease of the light chain phosphorylation, changing the myosin formation and muscle contraction. A similar pattern of *MYLK2* expression was observed in a study evaluating broilers affected with deep pectoral myopathies (Yalcin et al., 2018), showing a similar expression profile of this gene across different myopathies.

It is interesting to note that besides the *MYLK2*, the *CALM2* gene was also downregulated (−1.8) in WS-affected when compared to normal broilers (**Table 2**). *MYLK2* and *CALM2* were the two genes linking the main branches of the gene network, one composed by muscle development and the other by gluconeogenesis related genes, respectively (**Figure 2**). Calmodulin binds Ca^{2+} with high affinity and it is the most important Ca^{2+} signal transducer in the cells, regulating the activity of a plethora of proteins, such as kinases, transcription factors, and ion channels in most of the eukaryotes (Yalcin et al., 2018). The lack of Ca^{2+} transport to muscle fibers could increase the calcium concentration in the sarcoplasmic reticulum (Marchesi et al., 2019; Urrutia et al., 2019) affecting several biological processes, such as muscle contraction, oxidative stress, inflammation, and glycogen metabolism (Soike and Bergmann, 1998; Gronski et al., 2009; Choi et al., 2016; Yalcin et al., 2018). The disruption of calcium signaling pathway has been associated with different myopathies in humans (Sanmartín et al., 2017) and in chickens (Mutryn et al., 2015; Marchesi et al., 2019). In our study, low levels of *CALM2* could affect myogenesis, since the intracellular calcium concentration is essential for myosin light chain phosphorylation (Zhu et al., 2012). Moreover, reduced levels of *CALM2* could lead to insufficient intracellular calcium transportation and, consequently, to a defective muscle contraction ratio (Yalcin et al., 2018).

In the current study, the *CALM2* gene was also grouped with several genes from phosphorylase kinase family (PHKs; **Figure 2**). This family is responsible for the phosphorylation of certain muscle substrates, such as troponin I (Zhou et al., 2013) and it is involved in the glycogen metabolism/catabolism. The carbohydrate metabolism is an essential part of the skeletal muscle physiology. In humans, several metabolic myopathies have been associated with the impairment of carbohydrates and lipid metabolism (DiMauro and Spiegel, 2011). Some of them are characterized as disturbances in the glycogenolysis, affecting the glycogen metabolism (Zhou et al., 2013; Gaspar et al., 2019; Kishnani et al., 2019). Reduced levels of calmodulin could be involved with deficiency of PHKs, which could prevent the catalysis of glycogen in G-6-phosphate. Some *PHK* genes have already been associated with myopathies in chickens (Zambonelli et al., 2016; Marchesi et al., 2019), which reinforces the hypothesis that calcium signaling and carbohydrate metabolism genes are possibly involved with the onset of chicken myopathies.

In our study, the expression of the *DNASE1L3* gene was also reduced (**Figure 1**) in the WS-affected group. This gene is a member of the *DNASE1* family, which acts on the DNA catabolic processes, regulating inflammatory response, cytotoxicity, and hypoxia and presenting key functions related to tissue structure and development (Haller and Vissing, 2002; Napirei et al., 2005; Shi et al., 2017). The *DNASE1L3* is also known as DNASE gamma, being part of an endonuclease gene family that depends on Ca^{+2} and Mg^{+2} ions to be activated, usually participating in DNA cleavage and apoptosis (Shiokawa et al., 2002; Wu et al., 2018). It is known that apoptosis is an important process involved in skeletal muscle development in vertebrates, since it is necessary during the myogenic differentiation (Wu et al., 2018). The activation of *DNASE1L3* is considered to be responsible for DNA fragmentation needed to myoblasts differentiation (Wu et al., 2018). Therefore, the downregulation of this gene in the WS-affected broilers could prevent the occurrence of the correct myogenesis and consequently the cell hyperplasia. Another gene of this family, the *DNASE1L1*, was related to Pompe's disease in humans, which is a glycogen storage disease characterized by muscle weakness (Perry and Rudnick, 2000). In chickens, there are few studies involving *DNASE1L3* gene function, especially considering its involvement with WS. Therefore, the association of this gene with WS development should be further investigated, since it is involved in important pathways associated to this condition. Furthermore, its calcium ion dependency could indicate some relationship between the downregulation of *CALM2* and *DNASE1L3*, narrowing the hypothesis that the dysregulation of calcium signaling is one of the most important pathways contributing to WS myopathy.

The *PLIN1* gene was twice upregulated in broilers affected with WS compared with the normal broilers (**Figure 1**) and, in the gene network analysis; this gene was not grouped with the main network in chickens neither in humans (**Figure 2**). The PLIN1 is one of the main proteins found in adipocytes, being required for the maintenance of the lipid metabolism, and normally inhibits the lipolysis of the cell (Haller and Vissing, 2002; Napirei et al., 2005; Kozusko et al., 2015). *PLIN1* has already been associated with intramuscular fat in pigs (Tansey et al., 2001) and lipodystrophy in humans (Kozusko et al., 2015). In chickens, it was previously described that retinoid X receptor α (*RXRα*) can promote adipogenesis by upregulating *PLIN1* expression (Sun et al., 2020). Furthermore, a RNA sequencing analysis was performed on pectoralis muscle samples of chickens with high and low triglyceride content and the *PLIN1* gene was differentially expressed between groups, suggesting that a high lipid deposition occurs in animals with high levels of triglycerides (Liu et al., 2019). Therefore, the upregulation of *PLIN1* in WS-affected broilers could explain the adipocyte differentiation and fat deposition between muscle fibers.

Finally, the other genes evaluated in this study were not differentially expressed between groups, although they participate in biological functions associated with myopathies, such as hypoxia, oxidative stress, immune response, and cellular repair.

Nevertheless, previous studies have shown that some of those genes were related to chicken myopathies (Zambonelli et al., 2016; Marchesi et al., 2019). The discrepancy in these results could be due to several factors, such as high variation within the studied groups, the low magnitude of fold-changes, difference in the methodology used, the study of a single myopathy at a time and, more importantly, to differences in the severity of the myopathies, as shown by Malila et al. (2020). Furthermore, reporting expression profiles in different genetic groups, age and levels of white striping contribute to increasing the data on chicken myopathies and, consequently, mapping the main mechanisms involved in these conditions.

CONCLUSION

The genes *CA2*, *CSRP3*, *MYLK2*, *CALM2*, *PLIN1*, and *DNASE1L3* were differentially expressed between normal broilers and those affected with moderate levels of WS at 42 days of age. These findings highlight that the disruption of muscle and calcium signaling pathways are involved in the development of WS in chickens. These results might be a reflection of the transition from moderate to severe levels of lesions or even the contrary, toward recovery of the muscle. Time course studies using broilers affected uniquely by white striping are needed to unravel the evolution of this disorder over time. Improving our understanding on the genetic basis involved with this myopathy may help finding alternatives to reduce White Striping in poultry production.

DATA AVAILABILITY STATEMENT

The original contributions presented in the study are included in the article/supplementary material; further inquiries can be directed to the corresponding author.

ETHICS STATEMENT

The animal study was reviewed and approved by the Ethics Committee on Animal Utilization of the Embrapa Swine and Poultry National Research Center, under protocol number # 12/2012.

AUTHOR CONTRIBUTIONS

JO, ML, and AI conceived and designed the experiment. JO and ML were responsible for the data collection. AI, CM, JM, KC, and IS performed the laboratory experiment. AI, CM, KC, and IS performed the data analysis. AI, CM, JO, LF, and ML interpreted the results and wrote the manuscript. All authors reviewed, edited, and approved the final manuscript.

FUNDING

This study was supported by project number 01.11.07.002.04.03 from the Brazilian Agricultural Research Corporation (EMBRAPA).

ACKNOWLEDGMENTS

The authors are grateful to A. L. Tessmann for technical assistance. CM received a Scholarship from CAPES/FAPESC, Brazil and JM received a Scholarship from the National Council of Scientific and Technological Development (CNPq). IS and KC were sponsored by a PIBIC Scholarship from CNPq at the Embrapa Swine and Poultry, Brazil, and lately, IS received a PROMOP/Udesc scholarship. LF is an Embrapa/CNPq fellow (380282/2021-6).

REFERENCES

Abasht, B., Papah, M. B., and Qiu, J. (2021). Evidence of vascular endothelial dysfunction in wooden breast disorder in chickens: insights through gene expression analysis, ultra-structural evaluation and supervised machine learning methods. *PLoS One* 16:e0243983. doi: 10.1371/journal.pone.0243983

Allen, D. G., Lamb, G. D., and Westerblad, H. (2008). Impaired calcium release during fatigue. *J. Appl. Physiol.* 104, 296–305. doi: 10.1152/japplphysiol.00908.2007

Alnahhas, N., Berri, C., Chabault, M., Chartrin, P., Boulay, M., Bourin, M. C., et al. (2016). Genetic parameters of white striping in relation to body weight, carcass composition, and meat quality traits in two broiler lines divergently selected for the ultimate pH of the pectoralis major muscle. *BMC Genet.* 17:61. doi: 10.1186/s12863-016-0369-2

Arber, S., Halder, G., and Caroni, P. (1994). Muscle LIM protein, a novel essential regulator of myogenesis, promotes myogenic differentiation. *Cell* 79, 221–231. doi: 10.1016/0092-8674(94)90192-9

Avec (2020). Avec Annual Report. Brussels. Available at: https://www.avec-poultry.eu/wp-content/uploads/2020/09/05691-AVEC-annual-report-2020.pdf (Accessed June 28, 2021).

Ayansola, H., Liao, C., Dong, Y., Yu, X., Zhang, B., and Wang, B. (2021). Prospect of early vascular tone and satellite cell modulations on white striping muscle myopathy. *Poult. Sci.* 100:100945. doi: 10.1016/j.psj.2020.12.042

Bailey, R. A., Souza, E., and Avendano, S. (2020). Characterising the influence of genetics on breast muscle myopathies in broiler chickens. *Front. Physiol.* 11:1041. doi: 10.3389/fphys.2020.01041

Bailey, R. A., Watson, K. A., Bilgili, S. F., and Avendano, S. (2015). The genetic basis of pectoralis major myopathies in modern broiler chicken lines. *Poult. Sci.* 94, 2870–2879. doi: 10.3382/ps/pev304

Barash, I. A., Mathew, L., Lahey, M., Greaser, M. L., and Lieber, R. L. (2005). Muscle LIM protein plays both structural and functional roles in skeletal muscle. *Am. J. Physiol. Physiol.* 289, C1312–C1320. doi: 10.1152/ajpcell.00117.2005

Barbut, S. (2019). Recent myopathies in broiler's breast meat fillets. *Worlds Poult. Sci. J.* 75, 559–582. doi: 10.1017/S0043933919000436

Barbut, S., Sosnicki, A. A., Lonergan, S. M., Knapp, T., Ciobanu, D. C., Gatcliffe, L. J., et al. (2008). Progress in reducing the pale, soft and exudative (PSE) problem in pork and poultry meat. *Meat Sci.* 79, 46–63. doi: 10.1016/j.meatsci.2007.07.031

Barbut, S., Zhang, L., and Marcone, M. (2005). Effects of pale, normal, and dark chicken breast meat on microstructure, extractable proteins, and cooking of marinated fillets. *Poult. Sci.* 84, 797–802. doi: 10.1093/ps/84.5.797

Beauclercq, S., Hennequet-Antier, C., Praud, C., Godet, E., Collin, A., Tesseraud, S., et al. (2017). Muscle transcriptome analysis reveals molecular pathways and biomarkers involved in extreme ultimate pH and meat defect occurrence in chicken. *Sci. Rep.* 7:6447. doi: 10.1038/s41598-017-06511-6

Boerboom, G., Van Kempen, T., Navarro-Villa, A., and Pérez-Bonilla, A. (2018). Unraveling the cause of white striping in broilers using metabolomics. *Poult. Sci.* 97, 3977–3986. doi: 10.3382/ps/pey266

Bordini, M., Zappaterra, M., Soglia, F., Petracci, M., and Davoli, R. (2021). Weighted gene co-expression network analysis identifies molecular pathways and hub genes involved in broiler white striping and wooden breast myopathies. *Sci. Rep.* 11:1776. doi: 10.1038/s41598-021-81303-7

Chegwidden, W. R., and Carter, N. D. (2000). "Introduction to the carbonic anhydrases," in *The Carbonic Anhydrases.* eds. W. R. Chegwidden, N. D. Carter and Y. H. Edwards (Birkhäuser Basel), 13–28.

Choi, R., Park, H. D., Kang, B., Choi, S. Y., Ki, C. S., Lee, S. Y., et al. (2016). PHKA2 mutation spectrum in Korean patients with glycogen storage disease type IX: prevalence of deletion mutations. *BMC Med. Genet.* 17:33. doi: 10.1186/s12881-016-0295-1

Cruz, R. F. A., Vieira, S. L., Kindlein, L., Kipper, M., Cemin, H. S., and Rauber, S. M. (2017). Occurrence of white striping and wooden breast in broilers fed grower and finisher diets with increasing lysine levels. *Poult. Sci.* 96, 501–510. doi: 10.3382/ps/pew310

Daughtry, M. R., Berio, E., Shen, Z., Suess, E. J. R., Shah, N., Geiger, A. E., et al. (2017). Satellite cell-mediated breast muscle regeneration decreases with broiler size. *Poult. Sci.* 96, 3457–3464. doi: 10.3382/ps/pex068

De Oliveira, H. C., Garcia, A. A. P., Gromboni, J. G. G., Filho, R. V. F., Do Nascimento, C. S., and Wenceslau, A. A. (2017). Influence of heat stress, sex and genetic groups on reference genes stability in muscle tissue of chicken. *PLoS One* 12:e0176402. doi: 10.1371/journal.pone.0176402

DiMauro, S., and Spiegel, R. (2011). Progress and problems in muscle glycogenoses. *Acta Myol.* 30, 96–102.

Elnesr, S. S., Elwan, H. A. M., Xu, Q. Q., Xie, C., Dong, X. Y., and Zou, X. T. (2019). Effects of in ovo injection of sulfur-containing amino acids on heat shock protein 70, corticosterone hormone, antioxidant indices, and lipid profile of newly hatched broiler chicks exposed to heat stress during incubation. *Poult. Sci.* 98, 2290–2298. doi: 10.3382/ps/pey609

Elwan, H. A. M., Elnesr, S. S., Xu, Q., Xie, C., Dong, X., and Zou, X. (2019). Effects of in ovo methionine-cysteine injection on embryonic development, antioxidant status, IGF-I and TLR4 gene expression, and jejunum histomorphometry in newly hatched broiler chicks exposed to heat stress during incubation. *Animals* 9:25. doi: 10.3390/ani9010025

Gaspar, B. L., Vasishta, R. K., Radotra, B. D., Gaspar, B. L., Vasishta, R. K., and Radotra, B. D. (2019). "Metabolic myopathies and related diseases," in *Myopathology.* Singapore: Springer, 217–240.

Geier, C., Gehmlich, K., Ehler, E., Hassfeld, S., Perrot, A., Hayess, K., et al. (2008). Beyond the sarcomere: CSRP3 mutations cause hypertrophic cardiomyopathy. *Hum. Mol. Genet.* 17, 2753–2765. doi: 10.1093/hmg/ddn160

Griffin, J. R., Moraes, L., Wick, M., and Lilburn, M. S. (2018). Onset of white striping and progression into wooden breast as defined by myopathic changes underlying Pectoralis major growth. Estimation of growth parameters as predictors for stage of myopathy progression. *Avian Pathol.* 47, 2–13. doi: 10.1080/03079457.2017.1356908

Gronski, M. A., Kinchen, J. M., Juncadella, I. J., Franc, N. C., and Ravichandran, K. S. (2009). An essential role for calcium flux in phagocytes for apoptotic cell engulfment and the anti-inflammatory response. *Cell Death Differ.* 16, 1323–1331. doi: 10.1038/cdd.2009.55

Haller, R. G., and Vissing, J. (2002). Spontaneous "second wind" and glucose-induced second "second wind" in McArdle disease oxidative mechanisms. *Arch. Neurol.* 59, 1395–1402. doi: 10.1001/archneur.59.9.1395

He, H., Zhang, H. L., Li, Z.-X., Liu, Y., and Liu, X. L. (2014). Expression, SNV identification, linkage disequilibrium, and combined genotype association analysis of the muscle-specific gene CSRP3 in Chinese cattle. *Gene* 535, 17–23. doi: 10.1016/j.gene.2013.11.014

Hershberger, R. E., Parks, S. B., Kushner, J. D., Li, D., Ludwigsen, S., Jakobs, P., et al. (2008). Coding sequence mutations identified in MYH7, TNNT2, SCN5A, CSRP3, LBD3, and TCAP from 313 patients with familial or idiopathic dilated cardiomyopathy. *Clin. Transl. Sci.* 1, 21–26. doi: 10.1111/j.1752-8062.2008.00017.x

Janin, A., Bessière, F., Chauveau, S., Chevalier, P., and Millat, G. (2018). First identification of homozygous truncating CSRP3 variants in two unrelated cases with hypertrophic cardiomyopathy. *Gene* 676, 110–116. doi: 10.1016/j.gene.2018.07.036

Kishnani, P. S., Goldstein, J., Austin, S. L., Arn, P., Bachrach, B., Bali, D. S., et al. (2019). Diagnosis and management of glycogen storage diseases type VI and IX: a clinical practice resource of the American College of Medical Genetics and Genomics (ACMG). *Genet. Med.* 21, 772–789. doi: 10.1038/s41436-018-0364-2

Kozusko, K., Tsang, V. H. M., Bottomley, W., Cho, Y. H., Gandotra, S., Mimmack, M., et al. (2015). Clinical and molecular characterization of a novel PLIN1 frameshift mutation identified in patients with familial partial lipodystrophy. *Diabetes* 64, 299–310. doi: 10.2337/db14-0104

Kuttappan, V. A., Bottje, W., Ramnathan, R., Hartson, S. D., Coon, C. N., Kong, B. W., et al. (2017). Proteomic analysis reveals changes in carbohydrate and protein metabolism associated with broiler breast myopathy. *Poult. Sci.* 96, 2992–2999. doi: 10.3382/ps/pex069

Kuttappan, V. A., Hargis, B. M., and Owens, C. M. (2016). White striping and woody breast myopathies in the modern poultry industry: a review. *Poult. Sci.* 95, 2724–2733. doi: 10.3382/ps/pew216

Kuttappan, V. A., Lee, Y. S., Erf, G. F., Meullenet, J. F. C., Mckee, S. R., and Owens, C. M. (2012). Consumer acceptance of visual appearance of broiler breast meat with varying degrees of white striping. *Poult. Sci.* 91, 1240–1247. doi: 10.3382/ps.2011-01947

Kuttappan, V. A., Shivaprasad, H. l., Shaw, D. P., Valentine, B. A., Hargis, B. M., Clark, F. D., et al. (2013). Pathological changes associated with white striping in broiler breast muscles. *Poult. Sci.* 92, 331–338. doi: 10.3382/ps.2012-02646

Lake, J. A., Dekkers, J. C. M., and Abasht, B. (2021). Genetic basis and identification of candidate genes for wooden breast and white striping in commercial broiler chickens. *Sci. Rep.* 11:6785. doi: 10.1038/s41598-021-86176-4

Lake, J. A., Papah, M. B., and Abasht, B. (2019). Increased expression of lipid metabolism genes in early stages of wooden breast links myopathy of broilers to metabolic syndrome in humans. *Gene* 10:746. doi: 10.3390/genes10100746

Liu, L., Liu, X., Cui, H., Liu, R., Zhao, G., and Wen, J. (2019). Transcriptional insights into key genes and pathways controlling muscle lipid metabolism in broiler chickens. *BMC Genomics* 20:863. doi: 10.1186/s12864-019-6221-0

Livak, K. J., and Schmittgen, T. D. (2001). Analysis of relative gene expression data using real-time quantitative PCR and the 2 C T method. *Methods* 25, 402–408. doi: 10.1006/meth.2001.1262

Malila, Y., Thanatsang, K., Arayamethakorn, S., Uengwetwanit, T., Srimarut, Y., Petracci, M., et al. (2019). Absolute expressions of hypoxia-inducible factor-1 alpha (HIF1A) transcript and the associated genes in chicken skeletal muscle with white striping and wooden breast myopathies. *PLoS One* 14:e0220904. doi: 10.1371/journal.pone.0220904

Malila, Y., Uengwetwanit, T., Arayamethakorn, S., Srimarut, Y., Thanatsang, K. V., Soglia, F., et al. (2020). Transcriptional profiles of skeletal muscle associated with increasing severity of white striping in commercial broilers. *Front. Physiol.* 11:580. doi: 10.3389/fphys.2020.00580

Marchesi, J. A. P., Ibelli, A. M. G., Peixoto, J. O., Cantão, M. E., Pandolfi, J. R. C., Marciano, C. M. M., et al. (2019). Whole transcriptome analysis of the pectoralis major muscle reveals molecular mechanisms involved with white striping in broiler chickens. *Poult. Sci.* 98, 590–601. doi: 10.3382/ps/pey429

Marciano, C. M. M., Ibelli, A. M. G., Peixoto, J. O., Savoldi, I. R., do Carmo, K. B., Fernandes, L. T., et al. (2020). Stable reference genes for expression studies in breast muscle of normal and white striping-affected chickens. *Mol. Biol. Rep.* 47, 45–53. doi: 10.1007/s11033-019-05103-z

Mutryn, M. F., Brannick, E. M., Fu, W., Lee, W. R., and Abasht, B. (2015). Characterization of a novel chicken muscle disorder through differential gene expression and pathway analysis using RNA-sequencing. *BMC Genomics* 16:399. doi: 10.1186/s12864-015-1623-0

Napirei, M., Wulf, S., Eulitz, D., Mannherz, H. G., and Kloeckl, T. (2005). Comparative characterization of rat deoxyribonuclease 1 (Dnase1) and murine deoxyribonuclease 1-like 3 (Dnase1l3). *Biochem. J.* 389, 355–364. doi: 10.1042/BJ20042124

Nishita, T., Yorifuji, D., Orito, K., Ichihara, N., and Arishima, K. (2012). Muscle carbonic anhydrase III levels in normal and muscular dystrophia afflicted chickens. *Acta Vet. Scand.* 54:34. doi: 10.1186/1751-0147-54-34

Offer, G., and Cousins, T. (1992). The mechanism of drip production: formation of two compartments of extracellular space in musclePost mortem. *J. Sci. Food Agric.* 58, 107–116. doi: 10.1002/jsfa.2740580118

Offer, G., Knight, P., Jeacocke, R., Almond, R., Cousins, T., Offer, G., et al. (1989). The structural basis of the water-holding, appearance and toughness of meat and meat products. Available at: http://digitalcommons.usu.edu/foodmicrostructurehttp://digitalcommons.usu.edu/foodmicrostructure/vol8/iss1/17 (Accessed April 23, 2020).

Paludo, E., Ibelli, A. M. G., Peixoto, J. O., Tavernari, F. C., Lima-Rosa, C. A. V., Pandolfi, J. R. C., et al. (2017). The involvement of RUNX2 and SPARC

genes in the bacterial chondronecrosis with osteomyelitis in broilers. *Animal* 11, 1063–1070. doi: 10.1017/S1751731116002433

Park, I., Han, C., Jin, S., Lee, B., Choi, H., Kwon, J. T., et al. (2011). Myosin regulatory light chains are required to maintain the stability of myosin II and cellular integrity. *Biochem. J.* 434, 171–180. doi: 10.1042/BJ20101473

Peralta, F., and Huidobro-Toro, J. (2016). Zinc as allosteric ion channel modulator: ionotropic receptors as metalloproteins. *Int. J. Mol. Sci.* 17:1059. doi: 10.3390/ijms17071059

Perry, R. L., and Rudnick, M. A. (2000). Molecular mechanisms regulating myogenic determination and differentiation. *Front. Biosci.* 5, D750–D767.

Petracci, M., Bianchi, M., and Cavani, C. (2009). The European perspective on pale, soft, exudative conditions in poultry. *Poult. Sci.* 88, 1518–1523. doi: 10.3382/ps.2008-00508

Petracci, M., Mudalal, S., Soglia, F., and Cavani, C. (2015). Meat quality in fast-growing broiler chickens. *Worlds Poult. Sci. J.* 71, 363–374. doi: 10.1017/S0043933915000367

Petracci, M., Sirri, F., Mazzoni, M., and Meluzzi, A. (2013). Comparison of breast muscle traits and meat quality characteristics in 2 commercial chicken hybrids. *Poult. Sci.* 92, 2438–2447. doi: 10.3382/ps.2013-03087

Picard, B., Berri, C., Lefaucheur, L., Molette, C., Sayd, T., and Terlouw, C. (2010). Skeletal muscle proteomics in livestock production. *Brief. Funct. Genomics* 9, 259–278. doi: 10.1093/bfgp/elq005

Pierzchala, M., Hoekman, A. J. W., Urbanski, P., Kruijt, L., Kristensen, L., Young, J. F., et al. (2014). Validation of biomarkers for loin meat quality (*M. longissimus*) of pigs. *J. Anim. Breed. Genet.* 131, 258–270. doi: 10.1111/jbg.12081

Rashid, M. M., Runci, A., Polletta, L., Carnevale, I., Morgante, E., Foglio, E., et al. (2015). Muscle LIM protein/CSRP3: a mechanosensor with a role in autophagy. *Cell Death Dis.* 1:15014. doi: 10.1038/cddiscovery.2015.14

Russo, E., Drigo, M., Longoni, C., Pezzotti, R., Fasoli, P., and Recordati, C. (2015). Evaluation of white striping prevalence and predisposing factors in broilers at slaughter. *Poult. Sci.* 94, 1843–1848. doi: 10.3382/ps/pev172

Sanmartín, C. D., Veloso, P., Adasme, T., Lobos, P., Bruna, B., Galaz, J., et al. (2017). RyR2-mediated Ca2+ release and mitochondrial ROS generation partake in the synaptic dysfunction caused by amyloid β peptide oligomers. *Front. Mol. Neurosci.* 10:115. doi: 10.3389/fnmol.2017.00115

Schneider, A. G., Sultan, K. R., and Pette, D. (1999). Muscle LIM protein: expressed in slow muscle and induced in fast muscle by enhanced contractile activity. *Am. J. Phys.* 276, C900–C906. doi: 10.1152/ajpcell.1999.276.4.C900

Shah, J. P., Phillips, T. M., Danoff, J. V., and Gerber, L. H. (2005). An in vivo microanalytical technique for measuring the local biochemical milieu of human skeletal muscle. *J. Appl. Physiol.* 99, 1977–1984. doi: 10.1152/japplphysiol.00419.2005

Shi, G., Abbott, K. N., Wu, W., Salter, R. D., and Keyel, P. A. (2017). Dnase1L3 regulates inflammasome-dependent cytokine secretion. *Front. Immunol.* 8:522. doi: 10.3389/fimmu.2017.00522

Shiokawa, D., Kobayashi, T., and Tanuma, S. I. (2002). Involvement of DNase $γ$ in apoptosis associated with myogenic differentiation of C2C12 cells. *J. Biol. Chem.* 277, 31031–31037. doi: 10.1074/jbc.M204038200

Sihvo, H. K., Immonen, K., and Puolanne, E. (2014). Myodegeneration with fibrosis and regeneration in the pectoralis major muscle of broilers. *Vet. Pathol.* 51, 619–623. doi: 10.1177/0300985813497488

Smith, D. M. (2010). "Functional properties of muscle proteins in processed poultry products," in *Poultry Meat Processing*. ed. C. M. Owens. Boca Raton: CRC Press), 231–244.

Soglia, F., Mazzoni, M., and Petracci, M. (2019). Spotlight on avian pathology: current growth-related breast meat abnormalities in broilers. *Avian Pathol.* 48, 1–3. doi: 10.1080/03079457.2018.1508821

Soglia, F., Petracci, M., Davoli, R., and Zappaterra, M. (2021). A critical review of the mechanisms involved in the occurrence of growth-related abnormalities affecting broiler chicken breast muscles. *Poult. Sci.* 100:101180. doi: 10.1016/j.psj.2021.101180

Soike, D., and Bergmann, V. (1998). Comparison of skeletal muscle characteristics in chicken bred for meat or egg production: II. Histochemical and morphometric examination. *J. Vet. Med. Ser. A Physiol. Pathol. Clin. Med.* 45, 169–174. doi: 10.1111/j.1439-0442.1998.tb00813.x

Sun, Y., Zhai, G., Li, R., Zhou, W., Li, Y., Cao, Z., et al. (2020). RXRα positively regulates expression of the chicken PLIN1 gene in a PPARγ-independent manner and promotes adipogenesis. *Front. Cell Dev. Biol.* 8:349. doi: 10.3389/fcell.2020.00349

Supuran, C. T. (2012). Structure-based drug discovery of carbonic anhydrase inhibitors. *J. Enzyme Inhib. Med. Chem.* 27, 759–772. doi: 10.3109/14756366.2012.672983

Swatland, H. J. (1990). A note on the growth of connective tissues binding Turkey muscle fibers together. *Can. Inst. Food Sci. Technol. J.* 23, 239–241.

Tansey, J. T., Sztalryd, C., Gruia-Gray, J., Roush, D. L., Zee, J. V., Gavrilova, O., et al. (2001). Perilipin ablation results in a lean mouse with aberrant adipocyte lipolysis, enhanced leptin production, and resistance to diet-induced obesity. *Proc. Natl. Acad. Sci. U. S. A.* 98, 6494–6499. doi: 10.1073/pnas.101042998

Trocino, A., Piccirillo, A., Birolo, M., Radaelli, G., Bertotto, D., Filiou, E., et al. (2015). Effect of genotype, gender and feed restriction on growth, meat quality and the occurrence of white striping and wooden breast in broiler chickens. *Poult. Sci.* 94, 2996–3004. doi: 10.3382/ps/pev296

Urrutia, J., Aguado, A., Muguruza-Montero, A., Núñez, E., Malo, C., Casis, O., et al. (2019). The crossroad of ion channels and Calmodulin in disease. *Int. J. Mol. Sci.* 20:400. doi: 10.3390/ijms20020400

Vanhatalo, O. E., Henderson, J. D., De La Torre, U., Garrity, C. R., Pechanec, M. Y., Mienaltowski, A., et al. (2021). Research note: evaluation of the incidence of white striping and underlying myopathic abnormalities affected by fast weight gain in commercially fed broiler chickens. *Poult. Sci.* 100:101020. doi: 10.1016/j.psj.2021.101020

Velleman, S. G., Coy, C. S., and Abasht, B. (2021). Effect of growth selection of broilers on breast muscle satellite cell function: response of satellite cells to NOV, COMP, MYBP-C1, and CSRP3. *Comp. Biochem. Physiol. Part A Mol. Integr. Physiol.* 255:110917. doi: 10.1016/j.cbpa.2021.110917

Wu, T. W., Liu, C. C., Hung, C. L., Yen, C. H., Wu, Y. J., Wang, L. Y., et al. (2018). Genetic profiling of young and aged endothelial progenitor cells in hypoxia. *PLoS One* 13:e0196572. doi: 10.1371/journal.pone.0196572

Xu, X., Qiu, H., Du, Z. Q., Fan, B., Rothschild, M. F., Yuan, F., et al. (2010). Porcine CSRP3: polymorphism and association analyses with meat quality traits and comparative analyses with CSRP1 and CSRP2. *Mol. Biol. Rep.* 37, 451–459. doi: 10.1007/s11033-009-9632-1

Yalcin, S., Şahin, K., Tuzcu, M., Bilgen, G., Özkan, S., Izzetoğlu, G. T., et al. (2018). Muscle structure and gene expression in pectoralis major muscle in response to deep pectoral myopathy induction in fast- and slow-growing commercial broilers. *Br. Poult. Sci.* 60, 195–201. doi: 10.1080/00071668.2018.1430351

Ye, J., Coulouris, G., Zaretskaya, I., Cutcutache, I., Rozen, S., and Madden, T. L. (2012). Primer-BLAST: a tool to design target-specific primers for polymerase chain reaction. *BMC Bioinformatics* 13:134. doi: 10.1186/1471-2105-13-134

Zambonelli, P., Zappaterra, M., Soglia, F., Petracci, M., Sirri, F., Cavani, C., et al. (2016). Detection of differentially expressed genes in broiler pectoralis major muscle affected by white striping—wooden breast myopathies. *Poult. Sci.* 95, 2771–2785. doi: 10.3382/ps/pew268

Zampiga, M., Flees, J., Meluzzi, A., Dridi, S., and Sirri, F. (2018). Application of omics technologies for a deeper insight into quali-quantitative production traits in broiler chickens: a review. *J. Anim. Sci. Biotechnol.* 9:61. doi: 10.1186/s40104-018-0278-5

Zhi, G., Ryder, J. W., Huang, J., Ding, P., Chen, Y., Zhao, Y., et al. (2005). Myosin light chain kinase and myosin phosphorylation effect frequency-dependent potentiation of skeletal muscle contraction. *Proc. Natl. Acad. Sci. U. S. A.* 102, 17519–17524. doi: 10.1073/pnas.0506846102

Zhou, H., Rokach, O., Feng, L., Munteanu, I., Mamchaoui, K., Wilmshurst, J. M., et al. (2013). RyR1 deficiency in congenital myopathies disrupts excitation-contraction coupling. *Hum. Mutat.* 34, 986–996. doi: 10.1002/humu.22326

Zhu, X. S., Xu, X. L., Min, H. H., and Zhou, G. H. (2012). Occurrence and characterization of pale, soft, exudative-like broiler muscle commercially produced in China. *J. Integr. Agric.* 11, 1384–1390. doi: 10.1016/S2095-3119(12)60137-3

Zimmerman, U. J. P., Wang, P., Zhang, X., Bogdanovich, S., and Forster, R. E. (2004). Anti-oxidative response of carbonic anhydrase III in skeletal muscle. *IUBMB Life* 56, 343–347. doi: 10.1080/1521-6540400000850

Conflict of Interest: The authors declare that the research was conducted in the absence of any commercial or financial relationships that could be construed as a potential conflict of interest.

frontiers in Physiology

ORIGINAL RESEARCH
published: 09 August 2021
doi: 10.3389/fphys.2021.711711

Serum Creatine Kinase as a Biomarker to Predict Wooden Breast *in vivo* for Chicken Breeding

Fuli Kong[1,2], Guiping Zhao[1,2], Zhengxiao He[1,2], Jiahong Sun[1,2], Xicai Wang[1,2], Dawei Liu[3], Dan Zhu[3], Ranran Liu[1,2] and Jie Wen[1,2]**

[1] Institute of Animal Sciences, Chinese Academy of Agricultural Sciences, Beijing, China, [2] State Key Laboratory of Animal Nutrition, Key Laboratory of Animal (Poultry), Genetics Breeding and Reproduction, Ministry of Agriculture, Beijing, China, [3] Foshan Gaoming Xinguang Agricultural and Animal Industrials Corporation, Foshan, China

The present study aimed to find a blood marker for the prediction of wooden breast (WB) in live broiler to assist the genetic selection of fast-growing chickens. The experiments were carried out with two chicken flocks: 250 male broilers in flock 1 and 100 male and female broilers in flock 2. Both flocks were slaughtered and measured. The breast filets were assessed by combining subjective scoring and compression force at 28 (flock 1 only) and 42 days of age. The enzyme activity in serum and breast tissue (flock 1 only) of normal and affected groups was tested. The results showed that the compression force was significantly different between the normal and affected groups at 28 and 42 days of age ($P < 0.001$), and it increased significantly with rising WB and WS scores. The serum creatine kinase (CK) value increased significantly with rising compression force at 42 days of age ($P < 0.001$). The serum CK positively correlated with compression force ($r = 0.608$; $P < 0.001$) and the linear regression equation (serum CK = 0.9960*compression force + 1.884) was established for the line studied. The association between serum CK and compression force is consistent between flocks 1 and 2. In conclusion, our study confirmed that compression force could be the quantitative indicator to differentiate breast filets and found that serum CK could be a candidate biomarker to predict WB in live broilers and assist genetic selection in broiler breeding.

Keywords: creatine kinase, biomarker, predict, wooden breast, *in vivo*, chicken breeding

OPEN ACCESS

Edited by:
Sandra G. Velleman, The Ohio State University, United States

Reviewed by:
Francesca Soglia, University of Bologna, Italy
Eero Puolanne, University of Helsinki, Finland

****Correspondence:***
Ranran Liu
liuranran112@126.com
Jie Wen
wenjie@caas.cn

Specialty section:
This article was submitted to Avian Physiology, a section of the journal Frontiers in Physiology

Received: *19 May 2021*
Accepted: *14 July 2021*
Published: *09 August 2021*

Citation:
Kong F, Zhao G, He Z, Sun J, Wang X, Liu D, Zhu D, Liu R and Wen J (2021) Serum Creatine Kinase as a Biomarker to Predict Wooden Breast in vivo for Chicken Breeding. Front. Physiol. 12:711711. doi: 10.3389/fphys.2021.711711

INTRODUCTION

The past five decades have witnessed an increase in consumer preference for chicken meat. To satisfy the still-growing demand for poultry meat, poultry industry experts have implemented different methods to increase the growth rate, feed efficiency, and muscle yield of broilers. However, artificial selection for the traits above in meat-type chickens has been associated with certain drawbacks, such as muscle fibers and meat quality alterations (Petracci et al., 2013; Velleman and Clark, 2015). To be specific, wooden breast (WB) features out-bulging and pale areas of hardened consistency and the distinctive traits of white striping (WS) is the presence of white striations parallel to the direction of muscle fibers (Kuttappan et al., 2012a, 2013b; Sihvo et al., 2014). WB and WS can appear together or individually and they are emerging globally in recent years. These abnormal breast filets can be visually detected at processing sites and lead to downgrades, as well as during packaging and marketing, and could contribute to consumer rejection. The problem

is worsening and could hinder the advancement of the poultry industry (Zuidhof et al., 2014; Tallentire et al., 2018).

Researchers and breeding companies have studied and explored the contribution of genetic, nutrition, environmental, and management factors associated with the occurrence of WS and WB myopathies. Different dietary restriction schemes or some feed additives have only mild efficacy in decreasing the incidence of WS or WB (Bodle et al., 2018; Meloche et al., 2018a,b; Petracci et al., 2019a,b). The environmental enrichment does not appear to be a risk factor for WB (Pedersen et al., 2020). Furthermore, genetic selection has been found to have a significant effect on breast quality (Kuttappan et al., 2013a). In this regard, it was also reported that the heritability of WB was $h^2 < 0.1$, WS was $h^2 \leq 0.338$ (Bailey et al., 2015), and in the pHu + line WS was $h^2 = 0.65$ (Alnahhas et al., 2016). Moreover, Pampouille et al. (2018) explained that there is no major gene responsible for the occurrence of WS, but rather a polygenic inheritance exists. Lake et al. identified candidate genes for WB and WS in commercial broiler chickens, such as *KCNQ1* and *LSP1* (Lake et al., 2021). According to previous research, poultry breeding could be an important part of eliminating broiler meat abnormalities in the future. Before key genes and mutations that control WS and WB are resolved, live broiler breeder selection may be an effective way to reduce the occurrence of abnormal breast filets.

Kawasaki et al. (2016) reported the ability of wing lifting as a diagnostic method for WB broilers. Nevertheless, screening broilers only by appearance may neglect some less severe individuals. It is also reported breast echogenicity can be an additional tool to early detect alterations related to WB, and the correlation between WB and echogenicity was 0.430 at 42 days (Simoes et al., 2020). There is still need for quantitative and convenient methods to assess breast meat defects in live broilers. It is known that the damage that occurs in muscle tissue could be reflected in plasma or serum biochemical profiles. It was reported that the damage of muscle tissue could disrupt the integrity of the sarcolemma resulting in the leaking of various enzymes, such as creatine kinase (CK) and lactate dehydrogenase (LDH), into the plasma or serum (Hoffman and Solter, 2008). Moreover, in turkeys, it was also demonstrated that individuals with plasma CK levels above 1,000 units/ml could be considered susceptible to deep pectoral myopathy (Siller, 1985). We could not find a report that focuses on serum enzyme activity and the degree of WB. The purpose of this study is to assess whether different degrees of WB can be reflected in serum enzyme levels and try to find the boundary value to screen live broilers with breast meat defects in broiler breeding.

MATERIALS AND METHODS

Broilers Husbandry and Sample Collection

All the chickens in this study were obtained from a 9th generation (G9) fast-growing white-feathered line B chickens and produced by the Xinguang Agricultural and Animal Industrials Co., Ltd. (Mile, China). The broilers of flock 1 were raised by the company farm. Chickens in flock 2 were raised by IAS in the CAAS Experimental Base. All Broilers were raised in stair-step cages with individual pens under the same recommended environmental and nutritional conditions (Feeding Standard of Chickens, China, NY 33-2004). Broilers were free access to feed and water and the composition of ingredients used in the diets is shown in **Table 1**.

Broilers of flock 1 were fasted for 12 h and individually weighed at 28 and 42 days of age. The average weights of the 100 broilers at 28 and 150 broilers 42 days of age were determined, respectively, in the flock 1. The blood samples were collected from the wing vein and centrifuged (2,500 RPM for 10 min) to obtain serum and stored at −80°C until analyses of enzyme activity. All the broilers were electrically stunned, bled for 3 min, and scalded at 60°C for 45 s to de-feather. The right breasts were snap-frozen immediately in liquid nitrogen then stored at −80°C for subsequent analyses. The left breasts were deboned by a small group of trained personnel (6–8 people) to avoid any filet weight difference and stored in 4°C for 3 h before scoring. Broilers of flock 2 were also collected blood and left breast samples at 42 days, and the procedure was the same as for flock 1.

Wooden Breast and White Striping Scores

All the deboned left filets were submitted to trained personnel (2–3 people) to provide WB and WS scores. The WB scores were as described by Tijare et al. (2016) and included the absence of WB (normal breast score 0), mild hardening in the upper part of the filet (score 1), moderate hardening in the upper and/or lower part of the filet (score 2), severe hardening (score 3) and severe hardening with hemorrhagic lesions, increased volume and presence of yellow fluid (score > 3). The WS scores included no distinct white line (normal breast score 0), moderate WS (small white lines, generally <1 mm thick, but visible on the filet surface score 1), severe WS (white lines 1–2 mm thick, very visible on the filet surface, score 2), and extreme severe WS (thick white bands > 2 mm thickness, covering almost the entire surface of filet, score 3; Kuttappan et al., 2012b).

Compression Force Measurement

The left filets were used for compression force analysis according to the method reported by the Sun et al. (2018). Filets were compressed to 20% on different cranial regions using a 6-mm flat probe on a TA.XT Plus Texture Analyzer (Stable Micro Systems Ltd., Godalming, United Kingdom). The trigger force was set at 5 g, probe height was set at 55 mm (higher than the thickest filet sample); pre- and post-probe speeds were both 10 mm/s and the test speed of the probe was 5 mm/s. All the breast filets were measured three times at different positions of the filet cranial region, and the average compression force values were used for statistical analysis.

Enzyme Activity in Serum and Breast Tissue

The serum stored at −80°C were used to estimate the activities of CK, LDH, aspartate transaminase (AST), and alanine

TABLE 1 | Ingredient composition of diets fed to Line B broilers from 1 to 42 days of age.

Item	Pre-Starter 1–7 days	Starter 8–20 days	Grower 21–34 days	Finisher 35–42 days
Ingredients, %				
Corn	54.8	57.5	58.5	62
Soybean meal	38.22	35	32.33	28.53
Soybean oil	4.5	5	5.2	5.5
Limestone	0	0	1.95	1.95
Dicalcium phosphate	1.72	1.74	1.35	1.35
Salt	0.3	0.3	0.3	0.3
DL-Met	0.26	0.26	0.16	0.16
Premix compound	0.2	0.2	0.2	0.2
Nutrient composition, %				
ME, MJ/kg	12.78	12.99	12.94	13.13
CP	22.1	20.9	19	18
Ca	0.5	0.5	0.57	0.55
Nonphytate P	0.4	0.4	0.31	0.3
Lys	1.1	1.1	1	1
Met	0.6	0.6	0.42	0.42

For starter diet, premix compound provided per kilogram of diet: vitamin A 12,500 IU; vitamin D 3,750 IU; vitamin E 33 IU; vitamin K 2.5 mg; thiamin 2.5 mg; riboflavin, 10.0 mg; vitamin B6, 2.5 mg; vitamin B12, 0.015 mg; calcium pantothenate, 15 mg; niacin 32.5 mg; folic acid 1.25 mg; biotin 0.125 mg; choline 700 mg; Cu 8 mg; Mn 100 mg; Fe 80 mg; Zn 60 mg; I 0.35 mg; Se 0.15 mg. For grower diet, premix compound provided per kilogram of diet: vitamin A 10,000 IU; vitamin D3,300 IU; vitamin E 20 IU; vitamin K 2.0 mg; thiamin 2.0 mg; riboflavin 8.0 mg; vitamin B6 2.0 mg; vitamin B12 0.01 mg; calcium pantothenate 12.5 mg; niacin 26.0 mg; folic acid 1.0 mg; biotin 0.10 mg; choline 500 mg; Cu 8 mg; Mn 80 mg; Zn 40 mg; Fe 80 mg; I 0.35 mg; Se 0.15 mg. For finish diet, premix compound provided per kilogram of diet: vitamin A 9,500 IU; vitamin D 3,000 IU; vitamin E 16 IU; vitamin K 2.0 mg; thiamin 1.8 mg; riboflavin 6.4 mg; vitamin B6 2.0 mg; vitamin B12 0.01 mg; calcium pantothenate 10 mg; niacin 26.0 mg; folic acid 1.0 mg; biotin 0.10 mg; choline 500 mg; Cu 6 mg; Mn 60 mg; Zn 30 mg; Fe 80 mg; I 0.35 mg; Se 0.15 mg.

TABLE 2 | Bodyweight, filet weight, and wooden breast and white striping scores at 28 and 42 days of age in flock 1.

Group	Score	Body weight (g) (mean ± SD)	Filet weight (g) (mean ± SD)	*N*
28 days				
NORM	WS + WB = 0	1,288 ± 6	120 ± 3[a]	10
MILD	WB = 1	1,274 ± 29	134 ± 3[b]	10
P-value		ns	<0.01	
42 days				
WB score				
NORM	WB = 0	2,530 ± 138[b]	241 ± 19[b]	67
MILD	WB = 1	2,528 ± 121[b]	242 ± 45[b]	37
MOD	WB = 2	2,603 ± 175[c]	259 ± 25[c]	31
P-value		<0.05	<0.05	
WS score				
NORM	WS = 0	2,531 ± 151	241 ± 22	73
MOD	WS = 1	2,565 ± 137	250 ± 38	62
P-value		ns	ns	
WS and WB				
NORM	WS + WB = 0	2,520 ± 127[a]	236 ± 17[a]	39
MILD	WS + WB ≥ 1	2,536 ± 151[a]	245 ± 35[a]	77
MOD	WS + WB = 3	2,639 ± 123[b]	268 ± 15[b]	19
P-value		<0.01	<0.01	

[a,b] *Different letters indicate a significant difference ($P < 0.01$).*
[b,c] *Different letters indicate a significant difference ($P < 0.05$).*

transaminase (ALT) and the right breast tissues were used to estimate the activities of CK and LDH. The brief procedures are as below: 100 mg breast tissue and 0.9 ml 0.9% NaCl solution was put in the tube and smashed for 1–2 min with tissue grinder, then centrifuged at 2,500 *g* for 10 min at 4°C to obtain the supernatant. Total protein concentrations in the supernatant were measured using a BCA protein assay kit (Nanjing Jiancheng Bioengineering Institute, Nanjing, China). The enzyme

TABLE 3 | Spearman's correlation coefficients between WB and WS scores, bodyweight, filet weight and compression force in flock 1.

Category	WB	WS	WB + WS	Body weight	Filet weight	Compression force
WB	1					
WS	0.138	1				
WB + WS	0.872**	0.606**	1			
Body weight	0.179*	0.119	0.203*	1		
Filet weight	0.224**	0.146	0.253**	0.500**	1	
Compression force	0.718**	0.336**	0.693**	0.094	0.228**	1

WB, wooden breast score; WS, white striping score; WS + WB, wooden breast score plus white striping score.
***Significantly different ($P < 0.01$).*
**Significantly different ($P < 0.05$).*

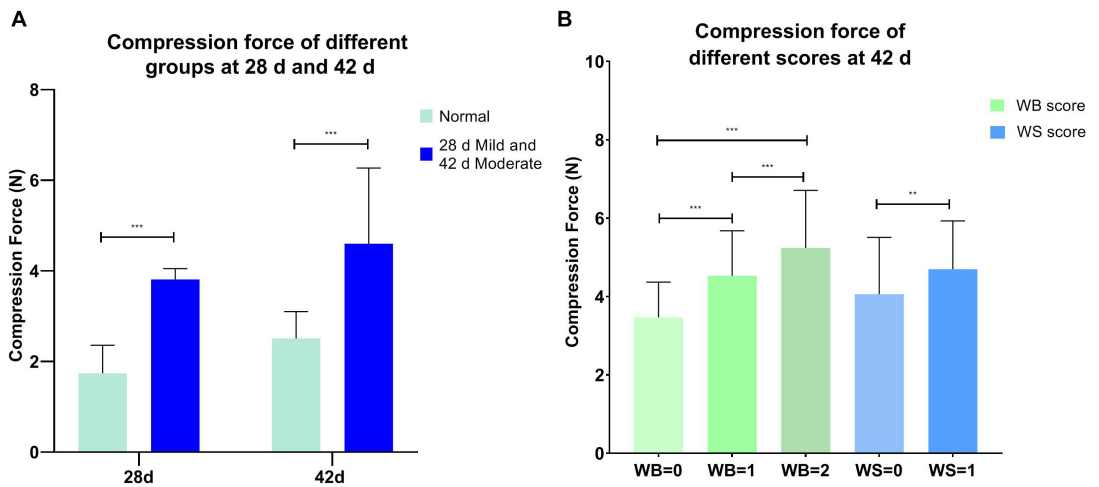

FIGURE 1 | (A) Compression force in the normal and mild/moderate groups at 28 (n = 20 in total) and 42 days of age (n = 49 in total); **(B)** compression force of different wooden breast and white striping scores at 42 days of age (n = 135 in total). ***$P < 0.001$; **$P < 0.01$.

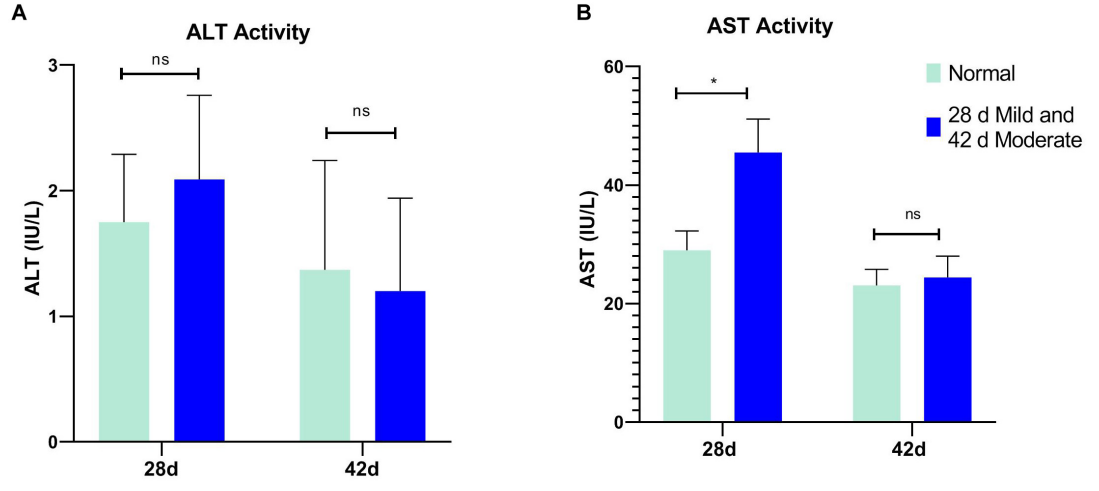

FIGURE 2 | Serum alanine transaminase (ALT) and aspartate transaminase (AST) activity at 28 (n = 20 in total) and 42 days of age (n = 49 in total). **(A)** ALT activity; **(B)** AST activity. *$P < 0.05$; ns, $P > 0.05$.

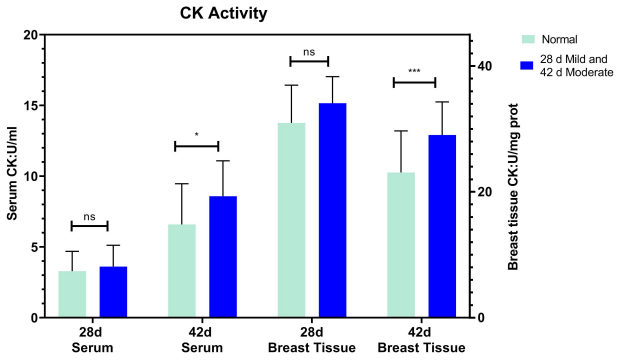

FIGURE 3 | Creatine kinase (CK) activity in serum and breast tissue at 28 (n = 20 in total) and 42 days of age (n = 49 in total). ***$P < 0.001$; *$P < 0.05$; ns, $P > 0.05$.

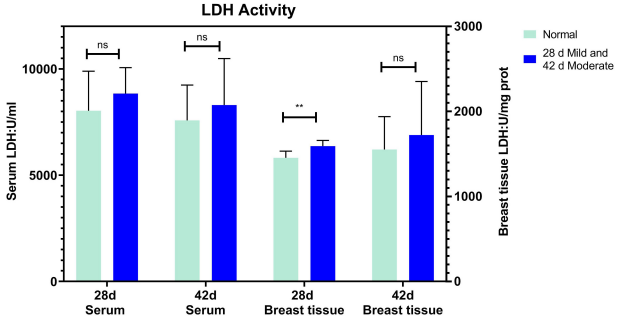

FIGURE 4 | Lactate dehydrogenase activity in serum and breast tissue at 28 (n = 20 in total) and 42 days of age (n = 49 in total). **$P < 0.01$; ns, $P > 0.05$.

activity in breast supernatant and serum were determined using the detection kit (Nanjing Jiancheng Bioengineering Institute, Nanjing, China). All the procedures were carried out according to the manufacturers' instructions. Enzyme activity in breast tissue and serum were expressed as units per milligram of protein and units per milliliter, respectively.

Statistical Analyses

In this study, the dietary treatment and all management factors were the same to avoid any confounding effects. Each chicken was an individual experimental unit. All results were presented as mean and standard deviation and analyzed by GraphPad Prism 8 software (GraphPad Software, Inc. San Diego, CA, United States). One-way analysis of variance was used to compare the mean differences among the different groups. $P < 0.05$ or 0.01 was assigned as a significance level.

RESULTS

Assessment of Breast Filet and Identification of Candidate Biomarkers

Bodyweight, filet weight and the scores of the WB and WS at 28 and 42 days of age are shown in **Table 2**. Despite the similar bodyweight of the two groups, the filet weight of the mild group was significantly higher than the normal group at 28 days of age ($P < 0.01$). There were no severe WS and WB filets in this study and more than half of the affected breast filets appeared as WS and WB together at 42 days of age. The bodyweight and filet weight of the moderate WB group were significantly higher than the other two groups ($P < 0.05$), and there was no significant difference according to the WS score ($P > 0.05$). Spearman's correlation coefficients between the WB and WS scores, bodyweight, and filet weights are presented in **Table 3**.

The compression force was significantly different between the normal and affected group at 28 and 42 days ($P < 0.001$, **Figure 1A**), and it increased significantly with the rising WB and WS scores ($P < 0.01$, **Figure 1B**) at 42 days. WB = 0 (normal group), WB = 1 (mild group), and WB = 2 (moderate group) corresponded to compression forces 3.18 ± 0.55 N, 4.62 ± 0.34 N, and 6.42 ± 0.95 N, respectively. WS = 0 (normal group) and WS = 1(moderate group) could be represented by compression force 4.06 ± 1.45 N and 4.70 ± 1.20 N. As shown in **Table 3**, compression force had a positive strong correlation ($P < 0.001$) with WB score ($r = 0.718$) and WB + WS score ($r = 0.693$). All the observations demonstrated that compression force could be the quantitative indicator to differentiate WB affected breast filets.

The serum ALT of the normal and affected group had no significant differences at 28 and 42 days ($P > 0.05$, **Figure 2A**). The serum AST of the mild group was significantly higher than the normal group ($P = 0.031$) at 28 days but not at 42 days ($P > 0.05$, **Figure 2B**). CK activity in serum and breast tissue of the moderate group was remarkably higher than in the normal group at 42 days of age ($P < 0.05$, $P < 0.001$, **Figure 3**). The tendency of the two groups at 28 days was the same as at 42 days but did not show a significant difference ($P > 0.05$, **Figure 3**). The LDH activity of the mild and moderate group in serum was higher than in the normal group at 28 and 42 days, but there were no significant differences ($P > 0.05$, **Figure 4**). These results

TABLE 4 | Serum creatine kinase (CK) level of different groups at 42 days of age in flock 1.

Group	Compression force range (N)	Compression force (N)	Creatine kinase (U/ml)	*N*
Normal	<4	3.2 ± 0.6^{a}	4.8 ± 1.5^{a}	39
Mild	4–5.5	4.6 ± 0.3^{b}	6.3 ± 1.6^{b}	36
Moderate	≥5.5	6.4 ± 1.0^{c}	8.7 ± 1.6^{c}	17
P-value		<0.001	<0.001	

^{a,b,c}*Different letters indicate significant difference ($P < 0.001$).*

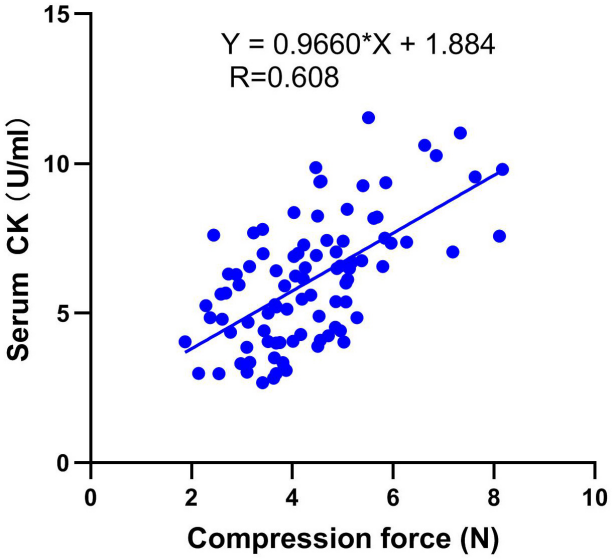

FIGURE 5 | Correlation analysis between serum CK level and compression force (r = 0.608, P < 0.001). n = 92.

indicated that CK could be a potential blood marker to predict defects in the breast filet.

Validation of Serum Creatine Kinase as a Biomarker

The above results demonstrate that compression force could be the quantitative indicator to differentiate breast filets. To verify the biomarker, serum was grouped by compression force as shown in **Table 4**. The results showed that the CK value increased significantly with compression force increasing at 42 days of age (P < 0.001). Correlation analysis between serum CK level and compression force is described in **Figure 5**. It shows that the serum CK level positively correlated with compression force (r = 0.608, P < 0.001). The equation of linear regression was described as serum CK = 0.9960*compression force + 1.884.

To verify the results, the flock 2 serum was divided into three groups according to the criteria set by flock 1. The results showed that serum CK value increased significantly with rising compression force (P < 0.05, **Table 5**).

DISCUSSION

Over the past decade, the increasing occurrence of WS and WB in commercial broilers has triggered considerable concern in the poultry industry. Previous studies suggested that the main reason for the myopathies might be linked to the intensive broiler selection scheme for massive breast yield (Kuttappan et al., 2012a, 2013a; Petracci et al., 2013; Malila et al., 2018). The bodyweight and breast filet weight of the WB affected broilers were significantly higher than that of normal broilers in the studied line (P < 0.05). Published data, as well as data from the present study, corroborate that the growth rate, especially the breast filet yield may be the origin of the myopathies. The rapid growth and inadequate vascularization in breast induced the hypoxic conditions, then kinds of response mechanisms such as energetic metabolism, inflammation, degeneration, and regeneration were modified or triggered. All these alterations were strictly related to the progression of myopathic disorders (Soglia et al., 2021). In addition, significant accumulation of lipofuscin was associated with the development of WB (Hasegawa et al., 2021). Fibrosis was also one of the main features of WB and this may be related to the activation of transforming growth factor-beta signaling and the dysregulation of the matrix metalloproteinases and tissue inhibitor of metalloproteinases system (Xing et al., 2021). Besides, Praud et al. (2020) suggested that a balance between *TGFB1* and *PPARG* would be essential for fibrosis or adiposis induction during the development of WB and WS. All the results suggested that there are several biological pathways, as well as response mechanisms involved in the development of WB.

Generally, breast meat defects are subjectively judged by prominent characteristics. WB was identified by assessing the filet hardness and WS was divided by the thickness of white stripes (Sihvo et al., 2014; Tijare et al., 2016). Dalgaard et al. (2018) reported a classification method of WB affected breast including the moisture content, resistance to compression, mobile water fraction, drip loss and cooking loss, as well as intramuscular and surface pH. This method removed the subjectiveness of the previous method, but need many laboratory tests. Thus, there is still need for an objective and fast method to quantify the meat defects. Previous research found that the compression test can be an objective and effective tool to identify and determine the severity of WB (Mudalal et al., 2015; Soglia et al., 2017; Sun et al., 2018; Campo et al., 2020). In this study, despite no severe WB and WS, compression force increased significantly with the increase in WB and WS scores. Different compression

TABLE 5 | Serum CK level of different group at 42 days of age in flock 2.

Group	Compression force range (N)	Compression force (N)	Creatine kinase (U/ml)	*N*
Normal	<4	2.4 ± 0.9^{a}	4.6 ± 1.3^{d}	49
Mild	4–5.5	4.3 ± 0.2^{b}	5.1 ± 1.5^{e}	13
Moderate	≥5.5	6.2 ± 0.8^{c}	6.4 ± 1.5^{f}	8
P-value		<0.001	<0.05	

^{a,b,c}*Different letters indicate significant difference (P < 0.001),* ^{d,e,f}*different letters indicate significant difference (P < 0.05).*

force ranges could present normal, mild, and moderate WB and WS groups. Moreover, compression force had a strong positive correlation ($P < 0.001$) with WB score ($r = 0.718$) and WB + WS score ($r = 0.693$). These results suggest that compression force could be an objective and quantitative index to differentiate the affected breast filets, especially for WB and when WB and WS appear together in breast meat.

It was reported that increasing levels of ALT, AST, CK, and LDH were associated with liver or muscle damage; and that a CK assay with blood samples was mainly a major marker of skeletal muscle injury (Hoffman and Solter, 2008; Lumeij, 2008). Kuttappan et al. (2013b) showed that broilers with severe WS ($P < 0.05$) had elevated serum levels of CK, ALT, AST, and LDH. Kawasaki et al. (2018) demonstrated that serum CK and AST values in most WB affected broilers were higher than those in normal broilers at 20 days of age. In addition, research by Meloche et al. (2018a,b)) demonstrated that plasma CK and LDH increased ($P < 0.05$) with increasing WB and WS scores. However, they believed that LDH may have more value as a predictor of myopathy. Serum CK was selected as an indicator to assess the effects of different feed schemes in reducing the occurrence of WS and WB (Simoes et al., 2020) and can be used as an independent factor for predicting amyotrophic lateral sclerosis in patients (Chen et al., 2021).

In this study, the liver damage was slight because there was no significant difference in ALT and AST at 42 d of age. This result indicated that most of the serum enzyme activity variation was derived from muscles or other organs but not the liver at 42 days. The AST level of the mild group was significantly higher than the normal group at 28 days. This alteration may relate to myocardial injury and functional compensation due to rapid weight gain with a high metabolic rate and more oxygen demand at 28 days of age. This result was in step with Takeshi Kawasaki et al. (2018). Changes in LDH serum levels did not respond to the degree of WB and WS which were not wholly consistent with previous reports (Meloche et al., 2018a,b). Different broiler lines and different degrees of WB and WS may contribute to the variations. Also, the LDH level in serum was higher than that of breast tissue and indicated that it may be inappropriate to take LDH as a predictor of WB and WS.

The serum CK value was about 10–25% of that in breast tissue, suggesting that the breast defects may make a great contribution to the serum CK. However, all the serum CK values increased with age but the moderate group was significantly higher than the normal group at 42 days ($P < 0.05$) and the tendency was the same at 28 days ($P > 0.05$). These indicated that despite serum CK value increasing with age, it mirrored the damage of the breast issue well and could be a candidate blood marker to predict filet defects at 42 days of age. Besides, the correlation between serum CK and compression force at 35 d or earlier deserves to study to screen the affected broilers as early as possible. Moreover, the results of the confirmatory experiment showed that the serum CK value increased significantly with compression force increasing in the two chicken flocks ($P < 0.001$). However, the compression force and CK value of flock 2 were lower than that of flock 1, which could be explained by different gender because the occurrence of WB and WS in male broilers was higher than that of female broilers (Trocino et al., 2015).

Most importantly, the serum CK positively correlated with compression force ($r = 0.608$, $P < 0.001$) and the equation of the linear regression was described as serum CK = 0.9960*compression force + 1.884. Because different compression force ranges could present normal, mild, and moderate WB groups for specific line, the breast compression force of live broilers can be predicted and the WB broilers could be screened by serum CK detection. However, the incidence of WB and the production performance of their offspring should be analyzed when discarding broilers by this method, because keeping a good balance between high-quality breast and high yield is a great challenge for broiler breeding. Furthermore, to avoid adverse effects on breast yield, the genetic correlation between serum CK level and filet weight should be studied further in the next generation.

CONCLUSION

In conclusion, this study confirmed that compression force could be the quantitative indicator to differentiate breast filets and found that serum CK could be an objective testing method for the prediction of compression force through the linear regression equation in broiler breeding. Different compression force ranges could represent normal or affected groups for specific line, so the WB affected broilers could be screened by serum CK detection.

DATA AVAILABILITY STATEMENT

The original contributions presented in the study are included in the article/supplementary material, further inquiries can be directed to the corresponding authors.

ETHICS STATEMENT

Broiler experiments were conducted under the guidelines for experimental animals established by the Ministry of Science and Technology (Beijing, China). Ethical approval on animal survival was given by the animal welfare and ethics committee of Institute Animal Sciences (IAS, Beijing, China) and the Chinese Academy of Agricultural Sciences (CAAS, Beijing, China) with the following reference number: IAS2019-44.

AUTHOR CONTRIBUTIONS

FK collected all the data, performed the analyses, and drafted the first manuscript. GZ, ZH, and JS contributed to the data interpretation and manuscript revision. XW, DL, and DZ contributed to the chicken raising, sample and data collection. JW and RL designed the research and contributed to data collection, data analysis and interpretation, and revise the manuscript. All authors submitted comments on the draft and approved the final manuscript.

FUNDING

This study was funded by the National Key Research and Development Program of China (No. 2018YFD0500401); the Agricultural Science and Technology Innovation Program (CAAS-ZDRW202005); the National Nonprofit Institute Research Grant (Y2020PT02); and the China Agriculture Research System of MOF and MARA (CARS-41).

REFERENCES

Alnahhas, N., Berri, C., Chabault, M., Chartrin, P., Boulay, M., Bourin, M. C., et al. (2016). Genetic parameters of white striping in relation to body weight, carcass composition, and meat quality traits in two broiler lines divergently selected for the ultimate pH of the pectoralis major muscle. *BMC Genet.* 17:61. doi: 10.1186/s12863-016-0369-2

Bailey, R. A., Watson, K. A., Bilgili, S. F., and Avendano, S. (2015). The genetic basis of pectoralis major myopathies in modern broiler chicken lines. *Poult. Sci.* 94, 2870–2879. doi: 10.3382/ps/pev304

Bodle, B. C., Alvarado, C., Shirley, R. B., Mercier, Y., and Lee, J. T. (2018). Evaluation of different dietary alterations in their ability to mitigate the incidence and severity of woody breast and white striping in commercial male broilers. *Poult. Sci.* 97, 3298–3310. doi: 10.3382/ps/pey166

Campo, M. D., Mur, M. L., Guerrero, A., Barahona, M., Resconi, V. C., Magalhaes, D. R., et al. (2020). Differentiating breast myopathies through color and texture analyses in broiler. *Foods* 9:824. doi: 10.3390/foods9060824

Chen, X. P., Wei, Q. Q., Ou, R. W., Hou, Y. B., Zhang, L. Y., Yuan, X. Q., et al. (2021). Creatine kinase in the diagnosis and prognostic prediction of amyotrophic lateral sclerosis: a retrospective case-control study. *Neural Regen. Res.* 16, 591–595. doi: 10.4103/1673-5374.293159

Dalgaard, L. B., Rasmussen, M. K., Bertram, H. C., Jensen, J. A., Møller, H. S., and Aaslyng, M. D. (2018). Classification of wooden breast myopathy in chicken pectoralis major by a standardised method and association with conventional quality assessments. *Int. J. Food Sci. Technol.* 53, 1744–1752. doi: 10.1111/ijfs.13759

Hasegawa, Y., Kawasaki, T., Maeda, N., Yamada, M., Takahashi, N., Watanabe, T., et al. (2021). Accumulation of lipofuscin in broiler chicken with wooden breast. *Anim. Sci. J.* 92:e13517. doi: 10.1111/asj.13517

Hoffman, W. E., and Solter, P. F. (2008). "Diagnostic enzymology of domestic animals," in *Clinical Biochemistry of Domestic Animals*, 6th Edn, eds J. J. Kaneko, J. W. Harvey, and M. L. Bruss (Burlington, MA: Academic Press), 351–378.

Kawasaki, T., Iwasaki, T., Yamada, M., Yoshida, T., and Watanabe, T. (2018). Rapid growth rate results in remarkably hardened breast in broilers during the middle stage of rearing: a biochemical and histopathological study. *PLoS One* 13:e0193307. doi: 10.1371/journal.pone.0193307

Kawasaki, T., Yoshida, T., and Watanabe, T. (2016). Simple method for screening the affected birds with remarkably hardened pectoralis major muscles among broiler chickens. *J. Poult. Sci.* 53, 291–297.

Kuttappan, V. A., Brewer, V. B., Apple, J. K., Waldroup, P. W., and Owens, C. M. (2012a). Influence of growth rate on the occurrence of white striping in broiler breast fillets. *Poult. Sci.* 91, 2677–2685. doi: 10.3382/ps.2012-02259

Kuttappan, V. A., Brewer, V. B., Mauromoustakos, A., McKee, S. R., Emmert, J. L., Meullenet, J. F., et al. (2013a). Estimation of factors associated with the occurrence of white striping in broiler breast fillets. *Poult. Sci.* 92, 811–819. doi: 10.3382/ps.2012-02506

Kuttappan, V. A., Huff, G. R., Huff, W. E., Hargis, B. M., Apple, J. K., Owens, C. M., et al. (2013b). Comparison of hematologic and serologic profiles of broiler birds with normal and severe degrees of white striping in breast fillets. *Poult. Sci.* 92, 339–345. doi: 10.3382/ps.2012-02647

Kuttappan, V. A., Lee, Y. S., Erf, G. F., Meullenet, J. F., McKee, S. R., and Owens, C. M. (2012b). Consumer acceptance of visual appearance of broiler breast meat with varying degrees of white striping. *Poult. Sci.* 91, 1240–1247. doi: 10.3382/ps.2011-01947

Lake, J. A., Dekkers, J. C. M., and Abasht, B. (2021). Genetic basis and identification of candidate genes for wooden breast and white striping in commercial broiler chickens. *Sci. Rep.* 11:6785. doi: 10.1038/s41598-021-86176-4

Lumeij, J. T. (2008). "Avian clinical biochemistry," in *Clinical Biochemistry of Domestic Animals*, 6th Edn, eds J. J. Kaneko, J. W. Harvey, and M. L. Bruss (Burlington, MA: Academic Press), 839–872.

Malila, Y., Srimarut, Y., Chaiwiwattrakul, P., Uengwetwanit, T., Arayamethakorn, S., Visessanguan, W., et al. (2018). Monitoring of white striping and wooden breast cases and impacts on quality of breast meat collected from commercial broilers (*Gallus gallus*). *Asian Australas. J. Anim. Sci.* 31, 1807–1817. doi: 10.5713/ajas.18.0355

Meloche, K. J., Fancher, B. I., Emmerson, D. A., Bilgili, S. F., and Dozier, W. A. (2018a). Effects of reduced digestible lysine density on myopathies of the pectoralis major muscles in broiler chickens at 48 and 62 days of age. *Poult. Sci.* 97, 3311–3324. doi: 10.3382/ps/pey171

Meloche, K. J., Fancher, B. I., Emmerson, D. A., Bilgili, S. F., and Dozier, W. A. (2018b). Effects of reduced dietary energy and amino acid density on pectoralis major myopathies in broiler chickens at 36 and 49 days of age1. *Poult. Sci.* 97, 1794–1807. doi: 10.3382/ps/pex454

Mudalal, S., Lorenzi, M., Soglia, F., Cavani, C., and Petracci, M. (2015). Implications of white striping and wooden breast abnormalities on quality traits of raw and marinated chicken meat. *Animal* 9, 728–734. doi: 10.1017/S175173111400295X

Pampouille, E., Berri, C., Boitard, S., Hennequet-Antier, C., Beauclercq, S. A., Godet, E., et al. (2018). Mapping QTL for white striping in relation to breast muscle yield and meat quality traits in broiler chickens. *BMC Genomics* 19:202. doi: 10.1186/s12864-018-4598-9

Pedersen, I. J., Tahamtani, F. M., Forkman, B., Young, J. F., Poulsen, H. D., and Riber, A. B. (2020). Effects of environmental enrichment on health and bone characteristics of fast growing broiler chickens. *Poult. Sci.* 99, 1946–1955. doi: 10.1016/j.psj.2019.11.061

Petracci, M., Mudalal, S., Bonfiglio, A., and Cavani, C. (2013). Occurrence of white striping under commercial conditions and its impact on breast meat quality in broiler chickens. *Poult. Sci.* 92, 1670–1675. doi: 10.3382/ps.2012-03001

Petracci, M., Mudalal, S., Soglia, F., and Cavani, C. (2019a). Meat quality in fast-growing broiler chickens. *Worlds Poult. Sci. J.* 71, 363–374. doi: 10.1017/s0043933915000367

Petracci, M., Soglia, F., Madruga, M., Carvalho, L., Ida, E., and Estévez, M. (2019b). Wooden-breast, white striping, and spaghetti meat: causes, consequences and consumer perception of emerging broiler meat abnormalities. *Compr. Rev. Food Sci. Food Saf.* 18, 565–583. doi: 10.1111/1541-4337.12431

Praud, C., Jimenez, J., Pampouille, E., Courousse, N., Godet, E., Le Bihan-Duval, E., et al. (2020). Molecular phenotyping of white striping and wooden breast myopathies in chicken. *Front. Physiol.* 11:633. doi: 10.3389/fphys.2020.00633

Sihvo, H. K., Immonen, K., and Puolanne, E. (2014). Myodegeneration with fibrosis and regeneration in the pectoralis major muscle of broilers. *Vet. Pathol.* 51, 619–623. doi: 10.1177/0300985813497488

Siller, W. G. (1985). Deep pectoral myopathy: a penalty of successful selection for muscle growth. *Poult. Sci.* 64, 1591–1595.

Simoes, C. T., Vieira, S. L., Stefanello, C., Kindlein, L., Ferreira, T., and Xavier, B. (2020). An in vivo evaluation of the effects of feed restriction regimens on wooden breast using ultrasound images as a predictive tool. *Br. Poult. Sci.* 61, 583–589. doi: 10.1080/00071668.2020.1764909

Soglia, F., Gao, J., Mazzoni, M., Puolanne, E., Cavani, C., Ertbjerg, P., et al. (2017). Superficial and deep changes of histology, texture and particle size distribution in broiler wooden breast muscle during refrigerated storage. *Poult. Sci.* 96, 3465–3472. doi: 10.3382/ps/pex115

Soglia, F., Petracci, M., Davoli, R., and Zappaterra, M. (2021). A critical review of the mechanisms involved in the occurrence of growth-related abnormalities affecting broiler chicken breast muscles. *Poult. Sci.* 100:101180. doi: 10.1016/j.psj.2021.101180

Sun, X., Koltes, D. A., Coon, C. N., Chen, K., and Owens, C. M. (2018). Instrumental compression force and meat attribute changes in woody broiler breast fillets during short-term storage. *Poult. Sci.* 97, 2600–2606. doi: 10.3382/ps/pey107

Tallentire, C. W., Leinonen, I., and Kyriazakis, I. (2018). Artificial selection for improved energy efficiency is reaching its limits in broiler chickens. *Sci. Rep.* 8:1168. doi: 10.1038/s41598-018-19231-2

Tijare, V. V., Yang, F. L., Kuttappan, V. A., Alvarado, C. Z., Coon, C. N., and Owens, C. M. (2016). Meat quality of broiler breast fillets with white striping and woody breast muscle myopathies. *Poult. Sci.* 95, 2167–2173. doi: 10.3382/ps/pew129

Trocino, A., Piccirillo, A., Birolo, M., Radaelli, G., Bertotto, D., and Xiccato, G. (2015). Effect of genotype, gender and feed restriction on growth, meat quality and the occurrence of white striping and wooden breast in broiler chickens. *Poult. Sci.* 94, 2996–3004. doi: 10.3382/ps/pev296

Velleman, S. G., and Clark, D. L. (2015). Histopathologic and myogenic gene expression changes associated with wooden breast in broiler breast muscles. *Avian Dis.* 59, 410–418. doi: 10.1637/11097-042015-Reg.1

Xing, T., Zhao, Z. R., Zhao, X., Xu, X. L., Zhang, L., and Gao, F. (2021). Enhanced transforming growth factor-beta signaling and fibrosis in the pectoralis major muscle of broiler chickens affected by wooden breast myopathy. *Poult. Sci.* 100:100804. doi: 10.1016/j.psj.2020.10.058

Zuidhof, M. J., Schneider, B. L., Carney, V. L., Korver, D. R., and Robinson, F. E. (2014). Growth, efficiency, and yield of commercial broilers from 1957, 1978, and 2005. *Poult. Sci.* 93, 2970–2982. doi: 10.3382/ps.2014-04291

Conflict of Interest: The authors declare that the research was conducted in the absence of any commercial or financial relationships that could be construed as a potential conflict of interest.

frontiers in Physiology

ORIGINAL RESEARCH
published: 25 August 2021
doi: 10.3389/fphys.2021.712095

Histological Analysis and Gene Expression of Satellite Cell Markers in the Pectoralis Major Muscle in Broiler Lines Divergently Selected for Percent 4-Day Breast Yield

Sara K. Orlowski[1], Sami Dridi[1], Elizabeth S. Greene[1], Cynthia S. Coy[2], Sandra G. Velleman[2] and Nicholas B. Anthony[1]*

[1]Department of Poultry Science, University of Arkansas, Fayetteville, AR, United States, [2]Department of Animal Sciences, The Ohio State University, Wooster, OH, United States

OPEN ACCESS

Edited by:
Xiquan Zhang, South China Agricultural University, China

Reviewed by:
Tomohide Takaya, Shinshu University, Japan
Francesca Soglia, University of Bologna, Italy

***Correspondence:**
Sara K. Orlowski
orlowski@uark.edu

Specialty section:
This article was submitted to Avian Physiology, a section of the journal Frontiers in Physiology

Received: *19 May 2021*
Accepted: *15 July 2021*
Published: *25 August 2021*

Citation:
Orlowski SK, Dridi S, Greene ES, Coy CS, Velleman SG and Anthony NB (2021) Histological Analysis and Gene Expression of Satellite Cell Markers in the Pectoralis Major Muscle in Broiler Lines Divergently Selected for Percent 4-Day Breast Yield. Front. Physiol. 12:712095. doi: 10.3389/fphys.2021.712095

Muscle development during embryonic and early post-hatch growth is primarily through hyperplastic growth and accumulation of nuclei through satellite cell contribution. Post-hatch, muscle development transitions from hyperplasia to hypertrophic growth of muscle fibers. Commercial selection for breast yield traditionally occurs at ages targeting hypertrophic rather than hyperplastic growth. This has resulted in the production of giant fibers and concomitant challenges with regard to muscle myopathies. The current study investigates the impact of selection during the period of hyperplastic growth. It is hypothesized that selection for percentage breast yield during hyperplasia will result in an increased number of muscle cells at hatch and potentially impact muscle fiber characteristics at processing. This study characterizes the breast muscle histology of three broiler lines at various ages in the growth period. The lines include a random bred control (RAN) as well as lines which have been selected from RAN for high (HBY4) and low (LBY4) percentage 4-day breast yield. Post-rigor pectoralis major samples from six males of each line and age were collected and stored in formalin. The sample ages included embryonic day 18 (E18), post-hatch day 4 (d4), and day 56 (d56). The samples were processed using a Leica tissue processor, embedded in paraffin wax, sectioned, and placed on slides. Slides were stained using hematoxylin and eosin. E18 and d4 post-hatch analysis showed advanced muscle fiber formation for HBY4 and immature muscle development for LBY4 as compared to RAN. Post-hatch d56 samples were analyzed for fiber number, fiber diameter, endomysium, and perimysium spacing. Line HBY4 had the largest muscle fiber diameter (54.2 ± 0.96 μm) when compared to LBY4 (45.4 ± 0.96 μm). There was no line difference in endomysium spacing while perimysium spacing was higher for HBY4 males. Selection for percentage 4-day breast yield has impacted the rate and extent of muscle fiber formation in both the LBY4 and HBY4 lines with no negative impact on fiber spacing. The shift in processing age to later ages has exposed issues associated with muscle fiber viability. Selection during the period of muscle hyperplasia may impact growth rate; however, the potential benefits of additional satellite cells are still unclear.

Keywords: hyperplasia, broiler-chicken, histology, gene expression, selection

INTRODUCTION

Broiler production in the United States has increased drastically over the past 50 years as demand for poultry meat by consumers has risen. Broiler genetic progress has resulted in a bird that is faster growing, high yielding, and more efficient than the broiler from the 1950s. This has allowed for the poultry industry to meet the growing demand in a cost-effective way (Barbut et al., 2008). Unfortunately, genetic progress and changes in management and environment have resulted in concomitant challenges in the areas of meat quality, with woody breast and white striping being two myopathies that have developed in recent years (Barbut, 1996, 1997, 1998; Anthony, 1998). Woody breast is characterized as a hardening of the breast muscle at varying levels and the deposition of collagen in place of muscle fibers (Petracci et al., 2014; Sihvo et al., 2014; Tijare et al., 2016). White striping is superficial striated fat deposition that runs parallel to the muscle fibers and creates a visually unappealing filet to consumers (Kuttappan et al., 2013). Changes in management and environment, specifically changes in nutrition have been hypothesized and shown to decrease the incidence and severity of these two myopathies but at the cost of a decrease in yield (Bodle et al., 2018; Livingston et al., 2018; Meloche et al., 2018). Heritabilities have been shown to be relatively low (Bailey et al., 2015) with a majority of the variation seen in woody breast associated with non-genetic factors (Trocino et al., 2015). Novel selection methods, however, are being evaluated for their effectiveness in controlling the development of both woody breast and white striping in the industry to avoid further economic losses from the muscle myopathies. Advancements in methods of characterization may also help increase the heritability of this trait by focusing on quantitative measures instead of subjective scoring systems.

One novel selection method being evaluated at the University of Arkansas focuses on an earlier form of breast muscle development. Muscle development in a broiler occurs primarily through two different processes. The first stage of muscle development occurs during the embryonic growth period of a broiler and is called hyperplasia (Stockdale and Miller, 1987). Hyperplasia is the increase in cell, fiber, and number with cell number typically being set by hatch (Smith, 1963). Post-hatch, muscle development transitions from hyperplasia to hypertrophy, or the enlargement of tissue due to an increase in cell size (Moss, 1968; Mozdziak et al., 1997). Current commercial selection practices in broilers typically focus on ages targeting hypertrophy typically between 6 and 8 weeks of age. Therefore, an emphasis is put on an increase in fiber size and not necessarily on fiber number. While great improvements have been made in the areas of growth rate, yield, feed conversion, and disease resistance (Havenstein et al., 2003), genetic selection for hypertrophy or fiber size may be reaching a physiological limit (Mahon, 1999) as indicated by the recent development of muscle myopathies, such as white striping, and woody breast.

A majority of the breast yield at 4 days of age is going to be a result of fiber number as cells are just starting to enter into the hypertrophic growth period. Selection for 4-day percentage breast yield in broilers was hypothesized to focus not on fiber size but on fiber number. It has been shown in porcine breeds that additional fiber numbers have exhibited a positive correlation with improved meat quality (Lengerken et al., 1994; Karlsson et al., 1999; Fiedler et al., 2003; Suzuki et al., 2003). Additionally, selection at a young age may have the ability to impact the number of satellite cells, also known as adult myoblasts. Satellite cells are important in post-hatch growth and repair (Velleman et al., 2010). Satellite cells are reactivated to re-enter the cell cycle, fuse to damaged muscle fibers, and contribute their nuclei to support post-hatch growth and repair of damaged muscle fibers. The additional nuclei allow for increased protein accretion, or growth and repair of potentially damaged fibers (Fu et al., 2015). A study by Daughtry et al. (2017) found that satellite cell functionality decreased with age as they only have a certain number of divisions due to telomeric shortening. With a decrease in functionality at older ages where protein accretion is still occurring, it is possible that the satellite cells can no longer aid in repair of damaged muscle fibers resulting in the development of both woody breast and white striping. By selecting for additional satellite cells, it is possible to alleviate some of the concerns about aging satellite cells as there are more available to aid in repair.

The goal of this study was to evaluate divergently selected broiler type lines after five generations of selection for 4-day percentage breast yield. Histological changes as well as any differences in gene expression markers associated with satellite cells will be documented. These factors will be used to determine if selection at 4 days post-hatch has altered hyperplastic growth and cell number.

MATERIALS AND METHODS

Broiler Lines

The University of Arkansas, Division of Agriculture Institutional Animal Care and Use Committee approved all live animal care and sampling utilized in this study (AUP #18083). Three broiler lines maintained and housed at the University of Arkansas were used. The first line of birds has been maintained as a random bred population that originated by mating of seven male and six female lines commercially available in the 1990s (RAN; Harford et al., 2014). From this RAN line, divergent selection was utilized to create the high (HBY4) and low (LBY4) percentage breast yield lines (Mason et al., 2020). These lines have been selected through the use of sibling selection for 4 day percentage breast yield [(Breast Wt)/(Body Wt−YolkSac)*100] for five generations. Since their creation, these lines have been maintained as closed populations and a randomly mated breeding structure is used with the avoidance of full and half siblings to decrease the rate of inbreeding accumulation.

Sample Collection

For this study, one non-pedigreed hatch from the RAN, HBY4, and LBY4 lines was set and incubated at 37.5°C and 56%

relative humidity from embryonic day 0 (E0) to embryonic day 18 (E18). At E18, they were transferred to a hatcher and hatched chicks were banded by line. Post-hatch, chicks were randomly placed by line into wood shavings litter floor pens with feed and water provided ad libitum throughout the study. Feed was formulated to meet or exceed the National Research Council (NRC) requirements with a commercial starter feed being fed from 0 to 21 days and a commercial finisher feed being feed from 22 to 56 days (NRC, 1994). At the processing age of d56, feed was removed from the birds 12 h prior to processing with access to water remaining constant.

Samples were collected at various ages throughout the embryonic and post-hatch growth period including embryonic age E18 and post-hatch d4 (selection age) and d56. These ages were selected to evaluate three periods where muscle growth and development are known to differ. At E18 and d4, samples were collected for all lines in a similar fashion. For histology, the left breast and keel were excised and stored in formalin solution until processing. At d56 post-hatch, birds were euthanized using CO_2 gas. The birds were placed in a cooler overnight to allow for the breast muscle to complete the process of rigor mortis to avoid contraction of the collected muscle sample. After 24 h in the cooler, a small rectangular segment running parallel to the muscle fibers was cut and stored in formalin solution. At E18 and d4, samples from six males and six females were collected from each of the three lines. At d56, samples from six males and six females were collected from the HBY4 and LBY4 lines. For gene expression at E18, d4, and d56, birds were euthanized and a small section of breast muscle was immediately flash frozen in liquid nitrogen and stored at −80°C until further processing. At E18 and d4, samples were collected from six males per line. At d56, samples were collected from six males and six females from the HBY4 and LBY4 lines.

Histology

Samples for histology at all ages were processed in a similar way. Small rectangular sections running parallel to the muscle fibers of each sample were cut and placed in plastic tissue processing cassettes in a 10% buffered formalin fixative solution (pH 7.0) at 4°C for a minimum of 17 h. Following storage in the fixative solution, muscle samples were dehydrated through a graded alcohol series previously described by Jarrold et al. (1999). Samples were then cleared in Pro-Par Clearent (Anatechm Battle Creek, MI) for 1 h with one change at 30 min. They were then infiltrated with paraffin wax at 55°C for 4 h with a single change at 1 h using a Leica TP1020 tissue processor (Leica, Nusslock, Germany). Following tissue processing, samples were then embedded in paraffin wax blocks and sectioned using a Leica microtome at a cross section of 5 μm. Four sections of each sample were adhered to Starfrost polarized slides (Mercedes Medical, Sarasota, FL) and stained using hematoxylin and Eosin Y (H&E) according to Velleman and Nestor (2004). Four images per sample were taken using an Olympus BX50 microscope (Olympus America, Center Valley, PA). At E18 and d4, 40X magnification was used and samples were compared for their stage of development. At d56, images were taken at 10X magnification and samples were evaluated for average fiber number per sample image (1,200 μm × 1,200 μm), fiber diameter, endomysium (spacing between muscle fibers), and perimysium (spacing between muscle fiber bundles) using the ImagePro® software (Media Cybernetics, Bethesda, MD). For fiber number, a 200 × 200 μm grid was overlaid over each image and the number of fibers within four randomly selected squares was counted and averaged. A fiber was counted in the square if over 50% of the fiber was located within the boundaries. For fiber diameter, 30 fibers were randomly selected, measured (in μm), and averaged per sample. Thirty random distances between fibers were measured and averaged for endomysium spacing and 10 random distances between fiber bundles were measured and averaged for perimysium spacing.

Gene Expression

Extraction of total RNA from the right breast muscle was done using Trizol reagent (Life Technologies, Grand Island, NY) using only the male samples from each line. Total RNA concentrations were determined for each sample by Take 3 Micro-Volume Plate using Synergy HT multimode microplate reader (BioTek, Winooski, VT) after DNAse treatment and purification. RNA integrity and quality were assessed by both OD260/OD280 nm absorption ratio (>1.9). For cDNA synthesis, total RNA (1 μg) was reverse transcribed using qScript cDNA Synthesis Kit (Quanta Biosciences, Gaithersburg, MD) in a 20 μl total reaction. Real-time quantitative (Applied Biosystems 7500 Real-Time PCR system) was performed using 5 μl of 10×−diluted cDNA, 0.5 μM of each forward and reverse specific primers for each gene, and SYBR Green Master Mix (Thermo Fisher Scientific, Rockford, IL) in a total 20 μl reaction (Lassiter et al., 2015; Flees et al., 2017). Oligonucleotide primers specific for paired box protein 7 (Pax-7), paired box protein 3 (Pax-3), myogenic factor 5 (Myf5), and r18S as a housekeeping gene were utilized (**Table 1**). The housekeeping gene was chosen as results have been constant and repeatable in several studies completed in the laboratory. Relative expressions of target genes were determined by the $2^{-\Delta\Delta Ct}$ method (Schmittgen and Livak, 2008). At the end of the amplification, melting curve analysis was applied using the dissociation protocol from the Sequence Detection system to exclude contamination with unspecific PCR products. The PCR products were also confirmed by agarose gel and showed only one specific band of the predicted size. Samples extracted from the E18 age, RAN line were used as a calibrator in this study.

Statistical Analysis

The d56 image analysis was analyzed using a two-way ANOVA in JMP Pro 14 (SAS Institute Inc., 2010). Images were analyzed for average fiber number, fiber diameter, endomysium spacing, and perimysium spacing. The main effects analyzed were line and sex as well as the interaction between line and sex. Means were considered statistically different at a $p < 0.05$ with means being separated using the Tukey's HSD. For each trait, gene

TABLE 1 | Oligonucleotide PCR/qPCR primers.

Gene	Accession number[1]	Primer sequence	Orientation	Product size, bp
PAX7	NM-205065	AGGCTCCGATGTCGAATCAG	For	55
		GCGGCGCTGCTTCCT	Rev	
PAX3	NM_204269	GCCTCACCAGCCCCAAA	For	57
		GGCTCCAGACCTCCAGTCAA	Rev	
Myf5	NM_001030363	CCTCATGTGGGCTTGCAAA	For	59
		CCTTCCGCCGGTCCAT	Rev	
r18S	AF173612	TCCCCTCCCGTTACTTGGAT	For	60
		GCGCTCGTCGGCATGTA	Rev	

Myf5, myogenic factor 5; PAX, paired box.[1]Accession number refers to Genbank (NCBI).

expression results were analyzed using a two-way ANOVA using GraphPad Prism version 7.00 (GraphPad Software, La Jolla California, United States). Main effects analyzed included Line and Age as well as their interaction with means separated by Tukey's HSD. The E18, RAN line was used as a calibrator in this study.

RESULTS

Quantitative image analysis was not possible for ages E18 and d4 as a result of lines being in different stages of muscle fiber formation. Images from E18 males for each line are shown in **Figure 1**. At this age, lines appeared to be in different stages of development with the HBY4 line showing advanced muscle fiber development by 1 to 2 days and the LBY4 line lagging behind a day when compared to the RAN line. Of the six samples taken from the HBY4 line, five of the six showed advanced muscle fiber formation when compared to the RAN while only two of the six from the LBY4 line appeared to be lagging behind in development. At d4 (selection age), it is still apparent that the HBY4 line is slightly more advanced in muscle development and growth with all of the images showing advanced muscle fiber formation. Images for the three lines at d4 are shown in **Figure 2**. For the LBY4 line, only three of the six samples appear similar to the RAN line in terms of fiber growth and development.

At d56, images were analyzed for fiber diameter, fiber number, endomysium spacing, and perimysium spacing. Since a line*sex interaction was not present for fiber number, fiber diameter, or endomysium only main effects are presented. Line effects were present for fiber diameter with the HBY4 line having a larger fiber than the LBY4 line. No differences were observed for the number of fibers of endomysium (fiber spacing; **Table 2**). A sex effect was present for fiber number in which the males had a higher fiber number than the females. No differences were observed between males and females for fiber diameter or endomysium (**Table 3**). A line*sex interaction was present for perimysium (muscle fiber bundle spacing). For perimysium, the HBY4 males had the greatest perimysium spacing with no difference between the LBY4 males and females from either line (**Table 4**).

At E18, d4, and d56, gene expression was analyzed for Pax7, Pax3, and Myf5, all markers associated with satellite cell presence and functionality (**Figure 3**). For Pax7, an interaction was present for Line and Age. All lines at E18 and the RAN line at d4 had higher expression of Pax7 than the remaining groups. No differences were observed for the expression levels of Pax3 in any of the groups evaluated. For Myf5, the RAN line at d4 had the highest expression level of Myf5, while all lines at d56 had the lowest level of expression.

DISCUSSION

The objective of this study was to evaluate the HBY4 and LBY4 lines for differences in histological development and satellite cell associated gene expression after five generations of divergent selection for 4-day percentage breast yield. Research done in the previous generations has shown that the HBY4 line and LBY4 line do not differ in body weights throughout a 56 day grow-out period; however, their percent breast yield differs at all ages measured (Mason et al., 2020). It has remained unclear from the previous research what is driving the difference in percentage breast meat yield, whether it be from an increase in fiber number, an increase in satellite cells, or a combination of the two traits.

To better evaluate the effect of genetic selection, histology sections of the breast muscle from the LBY4, HBY4, and RAN lines were evaluated for both sexes at three different ages. The first age evaluated was E18. At E18, hyperplasia is nearly complete as the breast muscle development is in its final stage of proliferation, the satellite cell proliferation wave (Stockdale and Miller, 1987). Around this time, the number of fibers in a broiler will be at its highest (Hartley et al., 1992). Evaluation of the lines at this age showed changes in the rate of development between the lines. The HBY4 line at this age appeared to be slightly more advanced than the RAN line in its muscle fiber development. Distinct spacing between the fibers, known as the endomysium, (Aberle et al., 2012) was visible in the HBY4 line. However, in the LBY4 line, muscle fiber spacing lagged behind with a majority of the images taken at this age showing little fiber formation and only an organized mass of muscle cells. The RAN line appeared to be in between the HBY4 line and LBY4 line in terms of fiber development. It appeared that selection for a high percent breast yield at d4 has increased the rate of muscle fiber development embryonically

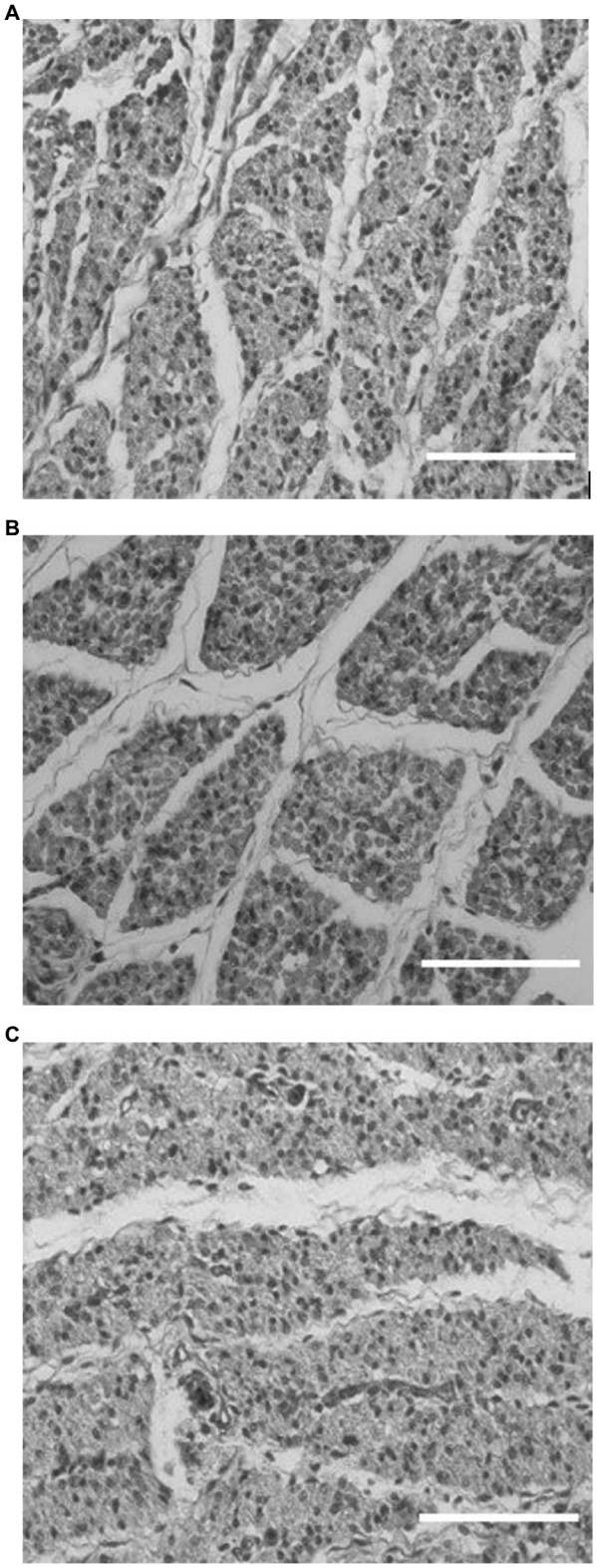

FIGURE 1 | Histology images from the RAN **(A)**, HBY4 **(B)**, and LBY4 **(C)** lines at embryonic day 18 under 40X magnification (Bar = 50 μm). RAN-random bred control, BY4-high percent breast yield at 4 days post-hatch, and LBY4-low percent breast yield at 4 days post-hatch.

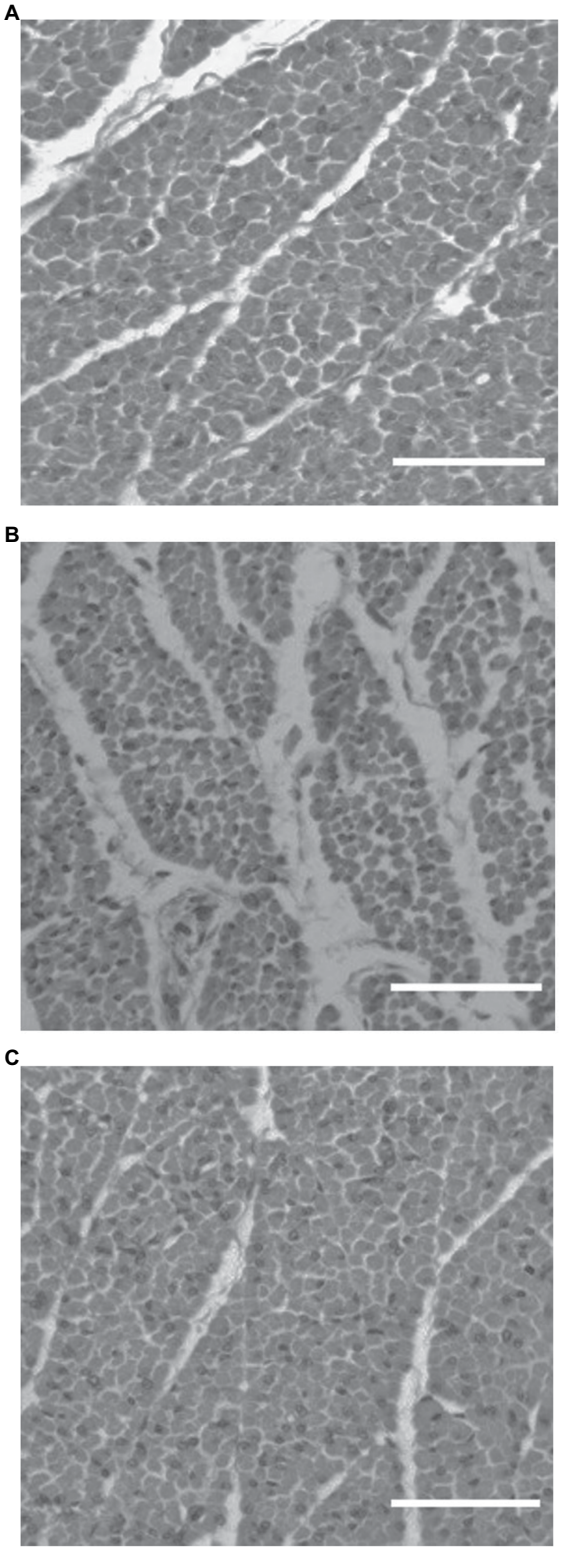

FIGURE 2 | Histology images from the RAN **(A)**, HBY4 **(B)**, and LBY4 **(C)** lines at post-hatch day 4 (selection age) under 40X magnification (Bar = 50 μm). Different letters indicate significant differences at $p < 0.05$. RAN-random bred control, HBY4-high percent breast yield at 4 days post-hatch, and LBY4-low percent breast yield at 4 days post-hatch.

TABLE 2 | Line effects at d56 between the HBY4 and LBY4 lines[1] for histological analysis (Mean ± SEM).

Trait	HBY4	Significance[2]	LBY4
Fiber number	17.53 ± 0.39	NS	18.02 ± 0.40
Fiber diameter	54.29 ± 1.13	***	45.39 ± 0.92
Endomysium	12.11 ± 0.42	NS	13.04 ± 0.33

*[1]HBY4-high percent breast yield at 4 days post-hatch and LBY4-low percent breast yield at 4 days post-hatch. [2]Significance: ***, highly significant ($p < 0.001$); NS, no significance.*

TABLE 3 | Sex effects at day 56 between males and females for histological analysis (Mean ± SE).

Trait	Males	Significance[1]	Females
Fiber number	18.38 ± 0.43	*	17.18 ± 0.34
Fiber diameter	47.28 ± 1.31	***	52.40 ± 0.98
Endomysium	12.33 ± 0.39	NS	13.04 ± 0.39

*[1]Significance: ***, highly significant ($p < 0.001$); *, significant ($p < 0.05$); and NS, no significance.*

TABLE 4 | Line*Sex[1] interaction for perimysium measurement (μm) at d56 (Mean ± SE)[2].

	HBY4 – M	LBY4 – M	HBY4 – F	LBY4 – F
Perimysium	44.01 ± 2.84[a]	33.05 ± 1.60[b]	29.57 ± 1.30[b]	29.77 ± 1.35[b]

[1]HBY4-M-high 4-day breast yield males, LBY4-M-low percent breast yield males, HBY4-F-high 4-day breast yield females, and LBY4-F-low percent breast yield females. [2a–b]For each trait, groups with no common letter within a row are different at $p \leq 0.05$.

while selection for a low percent breast yield resulted in a decrease in the rate of muscle fiber development.

The next age evaluated was the selection age of post-hatch d4. At d4, muscle development is transitioning from hyperplastic growth that occurred embryonically to hypertrophy in which cells are growing through the accumulation of protein (Moss, 1968; Mozdziak et al., 1997) from the fusion and incorporation of nuclei from the satellite cells. Satellite cells are located between the sarcolemma and basement membrane on the muscle fibers (Mauro, 1961). At this age, using H&E staining, it appeared that the HBY4 line was at a more advanced stage of development than the LBY4 and RAN lines. Images from the HBY4 line showed nuclei moving to the periphery of the muscle fiber where they will remain. The LBY4 line still showed nuclei spread throughout the fiber and was lagging slightly in the rate of development. Because the lines appeared to be at different stages of development, no numerical differences in fiber number or number of nuclei could be evaluated. It did appear that the HBY4 line entered hypertrophic growth at an earlier age than the RAN and LBY4 lines.

The final age evaluated histologically was a typical processing age of commercial broilers, post-hatch d56. At d56, only samples from the HBY4 and LBY4 lines were evaluated. Muscle sections from both lines showed healthy muscle fibers with only slight degradation of the fibers as a result of age (images not shown). Because these lines were developed from a population that was commercially available in the 1990s, they did not exhibit current muscle myopathies, such as woody breast or white striping. Typical histology samples of breast filets affected by woody breast at older ages exhibit severe fiber degeneration, fibrosis, and lipidosis (Soglia et al., 2016). Muscle sections appeared healthier, with less degeneration and fat infiltration than a modern commercial broiler breast filet that typically exhibit one or both myopathies described.

For the analysis, muscle fiber number, muscle fiber diameter, muscle fiber spacing (endomysium), and muscle fiber bundle spacing (perimysium) were evaluated. For muscle fiber number, no differences were present for fiber number between the HBY4 and LBY4 lines. As muscles grow, muscle fibers can fuse together to form larger fibers (Aberle et al., 2012). It is still possible that at a younger age, muscle fiber number differs between the HBY4 and LBY4 lines. While fiber number did not differ, fiber size was larger in the HBY4 line than the LBY4 line supporting the theory that the HBY4 line may still have a higher fiber number but those fibers have fused together resulting in a larger fiber diameter. This larger fiber diameter was also responsible for the higher yields observed in the HBY4 line. No differences were present for the endomysium, meaning the spacing of muscle fibers was similar between the lines. Visual analysis showed healthy spacing between the fibers for both lines.

A sex effect was present for both fiber number and fiber diameter. Males had a higher fiber number and a smaller fiber diameter when compared to females. In broilers, females have been shown to have a higher percentage breast meat yield, which could be a result of the larger fiber diameter and an increase in the amount of protein accretion. No difference was seen for endomysium with both males and females showing healthy fiber spacing regardless of line. An interaction was present for perimysium or the spacing between muscle fiber bundles. The HBY4 males had the largest perimysium spacing than the LBY4 males or either line of females. Results were inconsistent with a study done by An et al. (2010) in which a sex effect was present for the endomysial spacing with no effect on perimysium.

A continuing theory with the HBY4 and LBY4 lines is that selection for breast yield at an early age has the potential to impact satellite cell quantity. To evaluate this, three genes associated with satellite cells were analyzed for gene expression. Quiescent satellite cells exhibit the paired box protein 7 (Pax7) transcription factor (Seale et al., 2000). Upon activation, Pax7 was co-expressed with MyoD which is a member of the myogenic regulatory factor (MRF) family of proteins in addition to MRF 5 (Myf5). The interplay between paired box proteins and MRFs is important in the indication of self-renewal of satellite cells. Pax7 expression decreases during activation and differentiation of satellite cells (Asakura et al., 2007). MRF family proteins are the main regulators in skeletal myogenesis with Myf5 being the earliest to be expressed. The expression of the paired box protein Pax3 and Pax7 along with the expression of Myf5 is key regulators in the myogenesis process and satellite cell proliferation and activation (Francetic and Li, 2011). All three genes in combination are good indicators not only of the presence of satellite cells but also their activity as well.

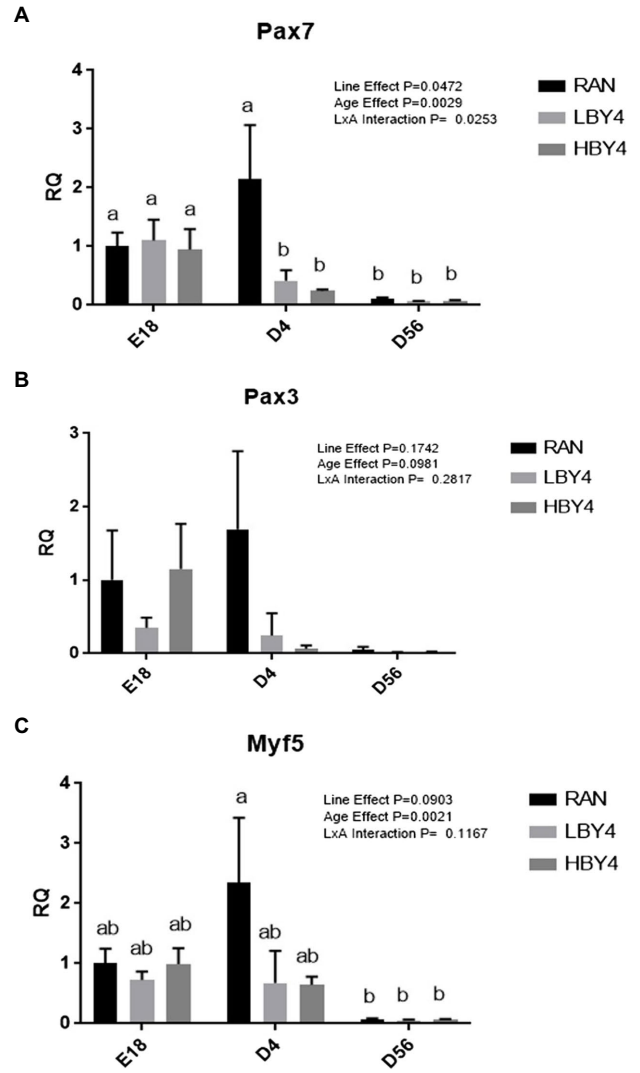

FIGURE 3 | Relative gene expression (Mean ± SE) of Pax7 **(A)**, Pax3 **(B)**, and Myf5 **(C)** at embryonic day 18, d4 and d56 post-hatch for the HBY4, RAN, and LBY4 lines. Different letters indicate significant differences at $p < 0.05$. Pax7-paired box protein 7, Pax3-Paired box protein 3, Myf5-myogenic regulatory factor 5, RAN-random bred control, HBY4-high percent breast yield at 4 days post-hatch, and LBY4-low percent breast yield at 4 days post-hatch.

This study aimed to determine what has been altered during genetic selection for 4-day relative breast yield in broilers. The gene expression levels of three key genes were the first step in determining any differences that may exist between the lines after five generations of selection. A line by age interaction was present for Pax7. The RAN line at d4 had the highest mRNA expression of PAX7 compared to the two selected lines. As selection typically occurs on the divergent lines at this age, it is possible that the expression of genes associated with satellite cells has been altered from the selection process. Looking solely at each age evaluated, no differences were observed in any of the genes measured at E18. At this age, satellite cells are still proliferating, and all three populations showed high expression levels of Pax7, Pax3, and Myf5. However, at d4, Pax7 and Pax3 appeared to be downregulated in both lines. It is possible though that for the HBY4 line, satellite cells were already active in contributing their nuclei to the fibers aiding in growth resulting in the differences in percentage breast yield when compared to the RAN line at this age. Concurrently, the LBY4 line may not have had as many satellite cells present because of selection resulting in a similarly low expression of both Pax7 and Pax3. At d56, there was no difference in expression levels between the lines. At this age period, growth is slowing and satellite cells are typically becoming mitotically quiescent, resulting in lower expression levels of genes associated with them. Evaluation of protein levels within these lines will result in a clearer understanding of the results of the selection program in relation to gene expression and will be evaluated in a future study.

CONCLUSION

A divergent selection program for 4-day percentage breast yield in broilers had been implemented for five generations. After five generations of selection, it appears that the embryonic and early post-hatch development of the two broiler lines has been altered compared to their random bred control. The HBY4 line has exhibited an increased rate of muscle fiber formation while the LBY4 appeared to be lagging. At processing ages, no differences existed between the lines for fiber number while the HBY4 line exhibited a larger fiber diameter. Differences between lines for satellite cell markers were not consistent at the three ages evaluated for satellite cell markers after five generations of selection for 4-day percentage breast yield. It still remains unclear if selection for 4-day percentage breast yield has altered the number of muscle fibers or satellite cells in these populations, however is does appear that selection in the upward direction has increased both the post-hatch transition to and rate of hypertrophic growth. Future selection programs utilizing a more modern base population for line development may give better insight into the effect of selection during a period of hyperplastic on muscle myopathies, such as WB and WS.

DATA AVAILABILITY STATEMENT

The raw data supporting the conclusions of this article will be made available by the authors, without undue reservation.

ETHICS STATEMENT

The animal study was reviewed and approved by International Animal Care and Use Committee, Protocol #18083.

AUTHOR CONTRIBUTIONS

SO and NA conceived and designed the study and collected the samples. SO, CC, and SV conducted the histology work.

SO, EG, and SD determined gene and protein expression and analyzed the data. SO wrote the paper. All authors contributed to the article and approved the submitted version

FUNDING

This study was supported by the Anthony and Velleman laboratories.

REFERENCES

Aberle, E. D., Forrest, J. C., Gerrard, D. E., and Mills, E. W. (2012). *Principles of Meat Science. 5th Edn*. Dubuque, IA: Kendall Hunt Publishing Company.

An, J. Y., Zheng, J. X., Li, J. Y., Zeng, D., Qu, J. L., Xu, G. Y., et al. (2010). Effect of myofibrillar characteristics and thickness of perimysium on meat tenderness in chickens. *Poult. Sci.* 89, 1750–1754. doi: 10.3382/ps.2009-00583

Anthony, N. B. (1998). A review of genetic practices in poultry. Efforts to improve meat quality. *J. Muscle Foods* 9, 25–33. doi: 10.1111/j.1745-4573.1998.tb00641.x

Asakura, A., Hirai, H., Kablar, B., Morita, S., Ishibashi, J., Piras, B. A., et al. (2007). Increased survival of muscle stem cells lacking the MyoD gene after transplantation into regenerating skeletal muscle. *PNAS* 104, 16552–16557. doi: 10.1073/pnas.0708145104

Bailey, R. A., Watson, K. A., Bilgili, S. F., and Avendano, S. (2015). The genetic basis of pectoralis major myopathies in modern broiler chicken lines. *Poult. Sci.* 94, 2870–2879. doi: 10.3382/ps/pev304

Barbut, S. (1996). Estimates and detection of the PSE problem in young Turkey breast. *Can. J. Anim. Sci.* 76, 455–457. doi: 10.4141/cjas96-066

Barbut, S. (1997). Problem of pale soft exudative meat in broiler chickens. *Br. Poult. Sci.* 38, 355–358. doi: 10.1080/00071669708418002

Barbut, S. (1998). Estimating the magnitude of the PSE problem in poultry. J. *Muscle Foods* 9, 35–49. doi: 10.1111/j.1745-4573.1998.tb00642.x

Barbut, S., Sosnicki, A. A., Lonergan, S. M., Knapp, T., Ciobanu, D. C., Gatcliffe, L. J., et al. (2008). Progress in reducing the pale soft and exudative (PSE) problem in pork and poultry meat. *Meat Sci.* 79, 46–63. doi: 10.1016/j.meatsci.2007.07.031

Bodle, B. C., Alvarado, C., Shirley, R. B., Mercier, Y., and Lee, J. T. (2018). Evaluation of different dietary alterations in their ability to mitigate the incidence and severity of woody breast and white striping in commercial male broilers. *Poult. Sci.* 97, 3298–3310. doi: 10.3382/ps/pey166

Daughtry, M. R., Berio, E., Shen, Z., Suess, E. J. R., Shah, N., Geiger, A. E., et al. (2017). Satellite cell-mediated breast muscle regeneration decreases with broiler size. *Poult. Sci.* 96, 3457–3464. doi: 10.3382/ps/pex068

Fiedler, I., Nürnberg, K., Harge, T., Nürnberg, G., and Ender, K. (2003). Phenotypic variations of muscle fiber and intramuscular traits in longissimus muscle of F2 population Duroc x Berlin miniature pig and relationships to meat quality. *Meat Sci.* 63, 131–139. doi: 10.1016/S0309-1740(02)00075-X

Flees, J., Rajaei-Sharifabadi, H., Greene, E., Beer, L., Hargis, B. M., Ellestad, L., et al. (2017). Effect of *Morinda citrifolia* (noni)-enriched diet on hepatic heat shock protein and lipid metabolism-related genes in heat stressed broiler chickens. *Front. Physiol.* 8, 919–936. doi: 10.3389/fphys.2017.00919

Francetic, T., and Li, Q. (2011). Skeletal myogenesis and Myf5 activation. *Transcription* 2, 109–114. doi: 10.4161/trns.2.3.15829

Fu, X., Wang, H., and Hu, P. (2015). Stem cell activation in skeletal muscle regeneration. *Cell. Mol. Life Sci.* 72, 1663–1677. doi: 10.1007/s00018-014-1819-5

Harford, I. D., Pavlidis, H. O., and Anthony, N. B. (2014). Divergent selection for muscle color in broilers. *Poult. Sci.* 93, 1059–1066. doi: 10.3382/ps.2013-03446

Hartley, R. S., Bandman, E., and Yablonka-Reuveni, Z. (1992). Skeletal muscle satellite cells appear during late chicken embryogenesis. *Dev. Biol.* 153, 206–216. doi: 10.1016/0012-1606(92)90106-Q

Havenstein, G. B., Ferket, P. R., and Qureshi, M. A. (2003). Carcass composition and yield of 1957 versus 2001 broilers when fed representative 1957 and 2001 broiler diets. *Poult. Sci.* 82, 1509–1518. doi: 10.1093/ps/82.10.1509

Jarrold, B. B., Bacon, W. L., and Velleman, S. G. (1999). Expression and localization of the proteoglycan decorin during the progression of cholesterol induced atherosclerosis in Japanese quail: implication for interaction with collagen type I and lipoproteins. *Atherosclerosis* 146, 299–308. doi: 10.1016/S0021-9150(99)00154-9

Karlsson, A. H., Klont, R. E., and Fernandez, X. (1999). Skeletal muscle fibres as factors for pork quality. *Livest. Prod. Sci.* 60, 255–270. doi: 10.1016/S0301-6226(99)00098-6

Kuttappan, V. A., Brewer, V. B., Mauromoustakos, A., McKee, S. R., Emmert, J. L., Meullenet, J. F., et al. (2013). Estimation of factors associated with the occurrence of white striping in broiler breast fillets. *Poult. Sci.* 92, 811–819. doi: 10.3382/ps.2012-02506

Lassiter, K., Greene, E., Piekarski, A., Faulkner, O. B., Hargis, B. M., Bottje, W., et al. (2015). Orexin system is expressed in avian muscle cells and regulates mitochondrial dynamics. *Am. J. Phys. Regul. Integr. Comp. Phys.* 308, R173–R187. doi: 10.1152/ajpregu.00394.2014

Lengerken, G. V., Maak, S., Wicke, M., Fiedler, I., and Ender, K. (1994). Suitability of structural and functional traits of skeletal muscle for genetic improvement of meat quality in pigs. *Arch. Tierz.* 37, 133–143.

Livingston, M. L., Landon, C., Barnes, H. J., and Brake, J. (2018). White striping and wooden breast myopathies of broiler breast muscle is affected by time-limited feeding, genetic background, and egg storage. *Poult. Sci.* 98, 217–226.

Mahon, M. (1999). "Muscle abnormalities-morphological aspects," in *Poultry Meat Science. Poultry Science Symposium Series*. eds. R. I. Richardson and G. C. Mead (Manchester, UK: Wallingford, CAB INTL), 19–64. doi: 10.3382/ps/pey333

Mason, J. G., Gilley, A. D., Orlowski, S. K., and Anthony, N. B. (2020). Divergent selection for relative breast yield at 4-D posthatch and the effect on embryonic and early posthatch development. *Poult. Sci.* 99, 2888–2894. doi: 10.1016/j.psj.2020.01.025

Mauro, A. (1961). Satellite cell of skeletal muscle fibers. *J. Biophys. Biochem. Cytol.* 9, 493–495. doi: 10.1083/jcb.9.2.493

Meloche, K. J., Fancher, B. I., Emmerson, D. A., Bilgili, S. F., and Dozier, W. A. III (2018). Effects of reduced dietary energy and amino acid density on *pectoralis major* myopathies in broiler chickens at 36 and 49 days of age. *Poult. Sci.* 97, 1794–1807. doi: 10.3382/ps/pex454

Moss, F. P. (1968). The relationship between the dimensions of the fibres and the number of nuclei during normal growth of skeletal muscle in the domestic fowl. *Am. J. Anat.* 122, 555–563.

Mozdziak, P. E., Schultz, E., and Cassens, R. G. (1997). Myonuclear accretion is a major determinant of avian skeletal muscle growth. *Am. J. Phys.* 272, 565–571.

NRC (1994). *Nutrient Requirements of Poultry. 9th Edn*. Washington, DC: National Academy Press.

Petracci, M., Mudalal, S., Babini, E., and Cavani, C. (2014). Effect of white striping on chemical composition and nutritional value of chicken breast meat. *Ital. J. Anim. Sci.* 13, 179–183. doi: 10.4081/ijas.2014.3138

SAS Institute Inc (2010). *SAS/STAT® User's Guide*. Cary, NC: 2010 Edition of SAS Institute Inc.

Schmittgen, T. D., and Livak, K. J. (2008). Analyzing real-time PCR data by the comparative C(T) method. *Nat. Protoc.* 3, 1101–1108. doi: 10.1038/nprot.2008.73

Seale, P., Sabourin, L. A., Girgis-Gabardo, A., Mansouri, A., Gruss, P., and Rudnicki, M. A. (2000). Pax7 is required for the specification of myogenic satellite cells. *Cell* 102, 777–778. doi: 10.1016/S0092-8674(00)00066-0

Sihvo, H. K., Immonen, K., and Puolanne, E. (2014). Myodegeneration with fibrosis and regeneration in the pectoralis major muscle of broiler. *Vet. Pathol.* 51, 619–623. doi: 10.1177/0300985813497488

Smith, J. H. (1963). Relation of body size to muscle cell size in the chicken. *Poult. Sci.* 42, 283–290. doi: 10.3382/ps.0420283

Soglia, F., Mudalal, S., Babini, E., Di Nunzio, M., Mazzoni, M., Sirri, F., et al. (2016). Histology, composition and quality traits of chicken pectoralis major muscle affected by wooden breast abnormality. *Poult. Sci.* 95, 651–659. doi: 10.3382/ps/pev353

Stockdale, F. A., and Miller, J. B. (1987). The cellular basis of heavy chain isoform expression during development of avian skeletal muscles. *Dev. Biol.* 123, 1–9. doi: 10.1016/0012-1606(87)90420-9

Suzuki, K., Shibata, T., Kadowaki, H., and Toyoshima, T. (2003). Meat quality comparison of Berkshire, Duroc and crossbred pigs sired by Berkshire and Duroc. *Meat Sci.* 64, 35–42. doi: 10.1016/s0309-1740(02)00134-1

Tijare, V. V., Yang, F. L., Kuttappan, V. A., Alvarado, C. Z., Coon, C. N., and Owens, C. M. (2016). Meat quality of broiler breast fillets with white striping and woody breast muscle myopathies. *Poult. Sci.* 95, 2167–2173. doi: 10.3382/ps/pew129

Trocino, A., Piccirillo, A., Birolo, M., Radaelli, G., Bertotto, D., Filiou, E., et al. (2015). Effect of the genotype, gender and feed restriction on growth, meat quality, and the occurrence of white striping and wooden breast in broiler chickens. *Poult. Sci.* 94, 2996–3004. doi: 10.3382/ps/pev296

Velleman, S. G., and Nestor, K. E. (2004). Inheritance of breast muscle morphology in turkeys at sixteen weeks of age. *Poult. Sci.* 83, 1060–1066. doi: 10.1093/ps/83.7.1060

Velleman, S. G., Zhang, X., Coy, C. S., Song, Y., and McFarland, D. C. (2010). Changes in satellite cell proliferation and differentiation during Turkey muscle development. *Poult. Sci.* 89, 709–715. doi: 10.3382/ps.2009-00467

Conflict of Interest: The authors declare that the research was conducted in the absence of any commercial or financial relationships that could be construed as a potential conflict of interest.

Publisher's Note: All claims expressed in this article are solely those of the authors and do not necessarily represent those of their affiliated organizations, or those of the publisher, the editors and the reviewers. Any product that may be evaluated in this article, or claim that may be made by its manufacturer, is not guaranteed or endorsed by the publisher.

frontiers in Physiology

ORIGINAL RESEARCH
published: 22 September 2021
doi: 10.3389/fphys.2021.712649

Acceptability of Artificial Intelligence in Poultry Processing and Classification Efficiencies of Different Classification Models in the Categorisation of Breast Fillet Myopathies

*Aftab Siddique[1], Samira Shirzaei[2], Alice E. Smith[2], Jaroslav Valenta[3], Laura J. Garner[1] and Amit Morey[1]**

[1] Department of Poultry Science, Auburn University, Auburn, AL, United States, [2] Department of Industrial and Systems Engineering and Department of Computer Science and Software Engineering, Auburn University, Auburn, AL, United States, [3] Department of Animal Science, Czech University of Life Sciences, Prague, Czechia

OPEN ACCESS

Edited by:
Sandra G. Velleman,
The Ohio State University,
United States

Reviewed by:
Hong Zhuang,
US National Poultry Research Centre (USDA-ARS), United States
Guillermo Tellez,
University of Arkansas, United States

***Correspondence:**
Amit Morey
azm0011@auburn.edu

Specialty section:
This article was submitted to Avian Physiology, a section of the journal Frontiers in Physiology

Received: 20 May 2021
Accepted: 16 August 2021
Published: 22 September 2021

Citation:
Siddique A, Shirzaei S, Smith AE, Valenta J, Garner LJ and Morey A (2021) Acceptability of Artificial Intelligence in Poultry Processing and Classification Efficiencies of Different Classification Models in the Categorisation of Breast Fillet Myopathies. Front. Physiol. 12:712649. doi: 10.3389/fphys.2021.712649

Breast meat from modern fast-growing big birds is affected with myopathies such as woody breast (WB), white striping, and spaghetti meat (SM). The detection and separation of the myopathy-affected meat can be carried out at processing plants using technologies such as bioelectrical impedance analysis (BIA). However, BIA raw data from myopathy-affected breast meat are extremely complicated, especially because of the overlap of these myopathies in individual breast fillets and the human error associated with the assignment of fillet categories. Previous research has shown that traditional statistical techniques such as ANOVA and regression, among others, are insufficient in categorising fillets affected with myopathies by BIA. Therefore, more complex data analysis tools can be used, such as support vector machines (SVMs) and backpropagation neural networks (BPNNs), to classify raw poultry breast myopathies using their BIA patterns, such that the technology can be beneficial for the poultry industry in detecting myopathies. Freshly deboned (3–3.5 h post slaughter) breast fillets ($n = 100 \times 3$ flocks) were analysed by hand palpation for WB (0-normal; 1-mild; 2-moderate; 3-Severe) and SM (presence and absence) categorisation. BIA data (resistance and reactance) were collected on each breast fillet; the algorithm of the equipment calculated protein and fat index. The data were analysed by linear discriminant analysis (LDA), and with SVM and BPNN with 70::30: training::test data set. Compared with the LDA analysis, SVM separated WB with a higher accuracy of 71.04% for normal (data for normal and mild merged), 59.99% for moderate, and 81.48% for severe WB. Compared with SVM, the BPNN training model accurately (100%) separated normal WB fillets with and without SM, demonstrating the ability of BIA to detect SM. Supervised learning algorithms, such as SVM and BPNN, can be combined with BIA and successfully implemented in poultry processing to detect breast fillet myopathies.

Keywords: support vector machines, backpropagation neural networking, woody breast, meat myopathies, spaghetti meat, bioelectrical impedance analysis, machine learning, artificial intelligence

INTRODUCTION

Globally, consumers are choosing meat and meat products for their higher nutritional value, especially protein (Heinz and Hautzinger, 2009). There has been a drastic increase in the consumption of these products worldwide in the last couple of decades. In developing countries, the per capita consumption of poultry has increased from 1.2 in the 1960s to 10.5 kg in the 2000s and will reach up to 14 kg by 2030 (FAO, 2003). In the United States, more than nine billion broilers were raised in 2018, with a total live weight of 27.1 billion kilogrammes; and in 2020, the per capita consumption of chicken was 44.23 kg (National Chicken Council, 2020). Chicken is a popular consumer choice because of various physicochemical and sensorial attributes such as texture, colour, and flavour (Petracci et al., 2013). To supply the increasing demand for breast meat, breeders have increased the growth rate of the birds through genetics, in turn increasing total carcass yield (Petracci and Cavani, 2012). Markets are continuously changing because of the preference and demands of consumers, which are presently driving the market toward cut-up chicken parts and further processed products. Fast-growing chickens with increased breast meat yield have developed breast muscle myopathies, leading to meat quality defects, such as woody breast (WB). In the past 10 years, WB has been more prominently found in heavier birds (Zampiga et al., 2020). Woody breast-affected fillets are characterised by an intricate and dull appearance (Sihvo et al., 2014; Kuttappan et al., 2017), and tough texture due to collagen deposition (Soglia et al., 2016). These breast myopathies also affect meat quality parameters such as pH, colour, water holding capacity (WHC), proximate composition, cook loss, and texture, which ultimately influence the quality of further processed products (Kuttappan et al., 2012). Because of lower meat quality, WB meat is sorted out in processing plants by manual hand-palpation (**Figure 1**) and different grading scales based on the level of severity (**Table 1**). However, this method is unreliable and subjective, leading to potential misclassification of the breast meat (Morey et al., 2020). By setting specific standards to accurately separate WB fillets, poultry processors will be able to reduce fillet misclassification and, ultimately, losses related to it.

We investigated bioelectrical impedance analysis as a potential objective method to detect woody breast-affected fillets. Under ideal conditions, the resistance of a conducting material is directly proportional to its length ($R \alpha L$) and inversely proportional to its cross-sectional area ($R \alpha 1/A$) but can be affected by the shape, size, thickness, and composition of different matrixes (Kyle et al., 2004). The electrical conductivity of a conductor depends on cell physiological and biochemical composition (the amount of water with dissolved electrolytes, intracellular fluid, extra-cellular fluid, moisture, and protein content) and on the applied signal frequency (Bera, 2014). BIA technology has been used in many species to measure physical composition and properties such as body water content and fat content. Nyboer et al. (1950) and Hoffer et al. (1969) introduced the four-electrode, whole body, and bioelectrical impedance methods in clinical studies for the measurement of bodily fluid from hand to foot. Since its inception, the use of BIA has expanded beyond clinical studies. In the food sector, BIA parameters can be calibrated to specific species and have been used in fish for the rapid detection of proximate composition and the pre-harvest condition of fish (Cox et al., 2011). The ability of meat to conduct electricity can be potentially used to detect meat myopathies such as WB and SM. WB presents itself with increased proliferation of collagen (non-conducting material), affecting resistance, while changes in intra- and extra-cellular water (conducting material) in the meat matrix alter the reactance (Kyle et al., 2004; Sihvo et al., 2014; Velleman, 2015; Soglia et al., 2016; Morey et al., 2020). Morey et al. (2020) successfully demonstrated the ability of bioelectric impedance analysis to differentiate between varying levels of WB as well as SM. The researchers attributed the differences in the electrical properties to the accumulation of collagen and increase in extra-myofibrillar water (Kennedy-Smith et al., 2017; Tasoniero et al., 2017). Contrary to WB, Morey et al. (2020) reported that loose muscle fibres acted as insulators and increased resistance readings. Morey et al. (2020) have successfully demonstrated the ability of BIA to differentiate WB and SM at different severity levels as an alternative to hand palpation to reduce human error. However, various classification algorithms should be used to further increase the accuracy of the BIA technology.

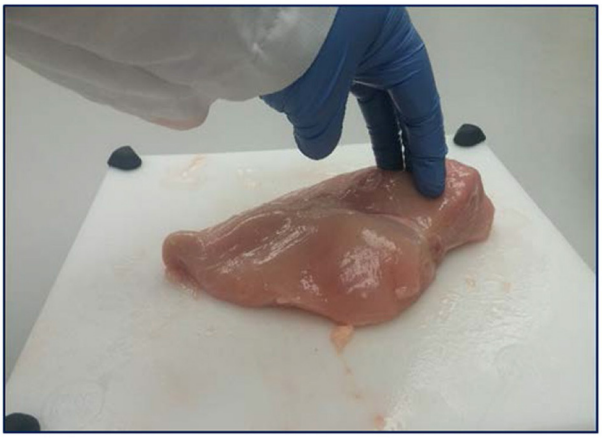

FIGURE 1 | Hand-palpation method for identifying the severity of woody breast myopathy in breast fillets.

Classification accuracies of bioelectrical impedance analysis data can be improved through the use of modern data analytics techniques such as machine learning (ML), which includes data mining, artificial neural networks (ANNs), deep learning (DL), and artificial intelligence (AI) (Tufféry, 2011). ML is a complex field with a wide range of frameworks, concepts, approaches, or a combination of these methods; it is commonly used in the manufacturing sector for process optimization, tracking, and management applications in production and predictive maintenance (Wiendahl and Scholtissek, 1994; Gardner and Bicker, 2000; Alpaydin, 2010). These techniques have been widely applied to enhance quality control in production processes (Apte et al., 1993), particularly in complex production processes where

TABLE 1 | Different subjective scales used for the classification of woody breast meat.

Woody breast subjective classification scale[a]	Condition	Description
2 point scale	Normal	No toughness or hardness
	Severe	Tough fillets
3 point scale	Normal	No toughness or hardness
	Moderate	Medium toughness up to 50%
	Severe	More than 50% toughness
4 point scale	Normal	No toughness or hardness
	Mild	Hardness at cranial region
	Moderate	Fillets extremely hard and rigid through from cranial region of caudal tip fillets that were hard throughout but flexible in mid-to caudal region
	Severe	More than 50% of fillet area is woody

[a] *2-point scale (Sihvo et al., 2014), 3-point scale (Sihvo et al., 2014), and 4-point scale (Tijare et al., 2016).*

predicting causes of problems is challenging (Kusiak, 2006). Over the last few decades, automated product inspection systems incorporating ML have been used in a wide variety of food industries such as potato and apple (Tao et al., 1995), oil palm fruit (Abdullah et al., 2002), rice and grains (Carter et al., 2005), beef fat (Chen et al., 2010), and colour in bakery applications (Nashat et al., 2011).

The use of machine learning models has increased in recent years because of circumstances such as the availability of complex data with little accountability (Smola and Vishwanathan, 2008) and will become more critical in the future. Although several ML algorithms are available, such as ANNs, support vector machines (SVMs), and distributed hierarchical decision trees, their ability to deal with large data sets varies significantly (Monostori, 2003; Bar-Or et al., 2005; Do et al., 2010). In the production sector, only specific ML algorithms are capable of handling high-dimensional datasets, and having the ability to deal with high dimensionality is considered a benefit of using ML in the processing industry. One of the main benefits of ML algorithms is finding previously unknown (hidden) information and recognising its associations in large datasets. The available information criteria can depend mainly on the characteristics of an ML algorithm (supervised/unsupervised or reinforcement learning, RL). Nevertheless, the general process of the ML method for producing outcomes in a production environment has been proven conclusively (Filipič and Junkar, 2000; Guo et al., 2008; Alpaydin, 2010; Kala, 2012). The use of the BIA method in poultry processing provides complex data with high dimensionality, which can be used to train SVM algorithms for the classification of WB (based on severity) and SM fillets. Support vector machines (SVMs), with a kernel-based procedure, has emerged in machine learning as one strategy for sample classification (Pardo and Sberveglieri, 2005). The implication of SVMs in machine learning as a supervised learning technique provides good generalisation ability and more minor overfitting tendencies. Using kernel functions in SVMs makes original input values linearly separable in a higher dimensional space. Moreover, SVMs can simultaneously reduce estimation errors and model dimensions (Singh et al., 2011). The main objective of this research was to determine the accuracy of linear discriminant analysis (LDA), SVMs, and backpropagation neural networks (BPNNs) to classify WB and SM using multi-dimensional BIA data. The LDA, SVM, and BPNN methods are discussed in detail, their accuracies were compared, and reasons for the differences in the classification accuracies are discussed.

Poultry researchers and the industry collect enormous amounts of data on a regular basis but use simpler statistical methods to derive meaning from the data. Through the presented research, we envision to introduce the poultry research community to several data analytics techniques to analyze complex datasets.

MATERIALS AND METHODS

Data Collection

Freshly deboned breast fillets from 56-day old broilers (Ross 708) were analysed in a federally inspected commercial poultry processing facility after deboning. The breast fillets ($n = 300$, 3 replications or flocks) were randomly selected from the processing line 3 to 3.5 h post slaughter. The deboned breast fillets were analysed for WB incidence through hand palpation by an experienced team member (**Figure 1**). The breast fillets were classified into normal, mild (for data analysis mild was grouped with normal), moderate, and severe WB fillets (Tijare et al., 2016), and SM presence was evaluated by observing the turgor in the cranial-ventral portion of the breast fillets, with a decrease in turgor indicating the presence of SM and increase in turgor representing the absence of SM. The collected chicken breast fillets from the processing line were subjected to BIA by utilising a hand-held CQ Reader (**Figure 2**; Seafood Analytics, Clinton Town, MI, United States) (Morey et al., 2020), equipped with four spring-loaded electrodes (RJL Systems, Detroit, MI, United States). All the four electrodes were placed to make contact with the ventral surface of the breast fillets. Once the electrodes were in contact with the breast fillets, the circuit was complete and linked. Then, the device measured the data for resistance, reactance, fat index, and protein index, and the stored data were downloaded for analysis later (Seafood Analytics Certified Quality Reader, Version 3.0.0.3; Seafood Analytics, MI, United States). Individual weights of the fillets were also

FIGURE 2 | Hand-held bioelectrical impedance device to measure the severity level of fillets.

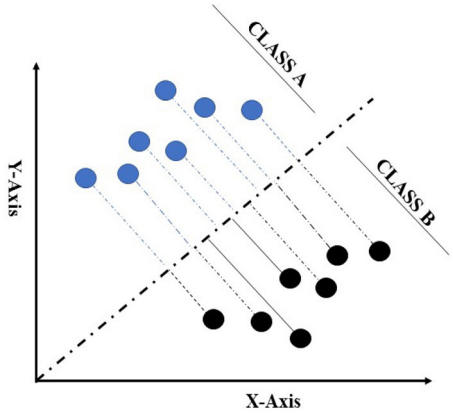

FIGURE 3 | Representation of two-class data in dimensional space for linear discriminant analysis (LDA) to maximise the classifiable data on the hyper-plane. This Figure adapted from Fisher (1936).

determined using a weighing balance (Ohaus Corporation, Pine Brook, NJ, United States) for the analysis and used to train the SVM and BPNN models.

Linear Discriminant Analysis

Linear discriminant analysis is one of the conventional data mining algorithms used in supervised and unsupervised learning contemplated by Fisher (1936) for resolving the issue related to flower classification (Xanthopoulos et al., 2013). The LDA model is used to project an imaginary hyper-plane that minimises the interclass variance and maximises the distance between class means. Additionally, it produces a transformation in the data that is discriminative in some data cases (Fukunaga, 2013). LDA is more appropriate for data where unequal within-class frequencies are given, and its classification performances have been randomly examined on generated test data. This approach maximises the ratio of between-class variance to within-class variance with maximum separability. Data sets used in LDA analysis can be transformed, and related test vectors can be classified in the imaginary hyper-plane by class-dependent transformation and class independent transformation (Balakrishnama and Ganapathiraju, 1998). The class-dependent transformation approach maximises the ratio of between-class variance to within-class variance. This kind of class transformation helps in maximising class separability (Tharwat et al., 2017). The main objective for implementing LDA is to create a subspace of lower-dimensional data points compared with the sample data set, in which the original data points from the data set can be easily separable (**Figure 3**; Fisher, 1936). The use of LDA provides a solution that can be implemented in a generalised eigenvalue system, which provides huge and fast data optimization. The original LDA algorithm was used to solve binary classification taxonomic problems; however, Rao (1948) had also proposed multi-class generalisations. In this study, both class classification and multi-class case classification derivation were provided to better understand the concept from the simple two-class case (Xanthopoulos et al., 2013).

Let "a1,..., $a_p \in R^m$" be a set of "q" data sets related to the two separate classes, A and B. For each class defined, sample means are

$$a_A = \mathrm{IN_A} \sum \mathrm{a} \in \mathrm{A_{a,}},\ \bar{\mathrm{a}}\mathrm{B} = 1\mathrm{N_B} \sum \mathrm{a} \in \mathrm{B_{a.}} \tag{1.1}$$

N_A, N_B is the total number of samples in data sets A and B. Scatter matrices for the data set by the equation

$$\begin{aligned} \mathrm{S_A} &= \sum \mathrm{a} \in \mathrm{A}\,(\mathrm{a} - \bar{\mathrm{a}}_\mathrm{A})\,(\mathrm{a} - \bar{\mathrm{a}}_\mathrm{A})^\mathrm{T}, \\ \mathrm{S_B} &= \sum \mathrm{a}\epsilon\mathrm{B}\,(\mathrm{a} - \bar{\mathrm{a}}_\mathrm{B})\,(\mathrm{a} - \bar{\mathrm{a}}_\mathrm{B})^\mathrm{T} \end{aligned} \tag{1.2}$$

Each of the matrices mentioned above is used for the imaginary hyper-plane, which is defined by the vector (φ), and the variance for the calculation is minimal and can be explained by the equation

$$\begin{aligned} Min\ \varphi \left(\varphi^T s_A \varphi + \varphi^T s_B \varphi\right) &= min\ \varphi\varphi^T\,(s_A + s_B) \\ \varphi &= min\varphi\varphi^T s_\phi \end{aligned} \tag{1.3}$$

where $S = S_A + S_B$ by definition and from equations 1.2, the scatter matrix for supposed two matrixes for the two classes are

$$s_{AB} = (\bar{a}_A - \bar{a}_B)\,(\bar{a}_A - \bar{a}_B)^T. \tag{1.4}$$

LDA is based on Fisher's projection hyper-plane, i.e., maximizing the distance between the means and minimizing the variance of each considered class that can be mathematically described by Fisher's criterion equation as:

$$Max\varphi J\,(\varphi) = max\ \varphi\varphi^T s_{AB\varphi}\varphi^T S_\varphi. \tag{1.5}$$

There could be several solutions for the optimization-related problem with the same function value. For a solution ϕ,∗ all the vectors c·φ∗ will give the same value, and considering no loss in generality, we select only one best possible solution by substituting the denominator with an equality constraint. Then, the problem becomes

$$Max\ \varphi\varphi^T S_{AB}\varphi \tag{1.6a}$$
$$s.t \cdot \varphi^T s_\varphi = 1 \tag{1.6b}$$

The Lagrangian mechanism associated with this problem is

$$LLDA\left(a,\lambda\right) = \varphi^T S_{AB}\varphi - \lambda\left(\varphi T S_\varphi - 1\right) \tag{1.7}$$

where λ is the LaGrange multiplier associated with the equation 1.6b. Since S_{AB} is positive and the nature of the problem is convex, the global minimum will be at the point for which

$$\partial LLDA\left(x,\lambda\right)/\partial x = 0 \Leftrightarrow S_{AB}\varphi - \lambda S_\varphi = 0. \tag{1.8}$$

The optimal φ obtained as the eigenvector that corresponds to the smallest value for the generalised eigensystem:

$$S_{AB}\varphi = \lambda S_\varphi. \tag{1.9}$$

Multi-class LDA is only the extension of the two-class classification problem. Given x classes, the matrices will be redefined, and the intra-class matrix becomes

$$S = S_1 + S_2 + \ldots . S_n, \tag{1.10}$$

while the inter-class scatter matrix is annotated by

$$S_{1,\ldots}n = n\sum i = 1pi\left(\overline{a}_i - \overline{a}\right)\left(\overline{a}_i - \overline{a}\right)^T, \tag{1.11}$$

where the number of samples (p_i) in the ith class, a_i is the mean, and a is mean vector given in equation

$$\overline{a} = 1pn\sum i = 1pi\bar{}ai.$$

The linear transformation φ can be achieved by solving the above equation:

$$S1, \ldots, n\,\varphi\ = \lambda S\varphi$$

to achieve a better classification by projection of the hyper-plane. Once the transformation ϕ is achieved, the class of a new point "y" is determined by

$$class\left(y\right) = arg\ minn\left\{d\left(y\varphi, \bar{}an\varphi\right)\right\} \tag{1.12}$$

where a_n is the centroid of nth class. The calculation reflects that all the centroids of the classes were defined first and that the unknown points on the subspace were defined by φ and the closest class concerning D.

Support Vector Machines

Vapnik (2013) first contemplated the support vector machine method in 1995, and recently it has enticed an enormous level of endeavour in the machine learning applications community. Several studies have mentioned that the SVM method has immense performance in classification accuracy compared with other data classification algorithm methods (Maji et al., 2008; Shao and Lunetta, 2012; Vijayarani et al., 2015). SVM generates a line between two or more classes known as hyper-planes for data set classification. Input data Q that can fall on either side of the hyper-plane (QT•W–b) > 0 are labelled as +1, and those that fall on the other side, (QT•W–b) < 0, are labelled as −1 (**Figure 4A**; Lee and To, 2010); let {Qi, yi} ∈ R^n be training data set, y_i ∈{1, −1}, i = 1, 2,. . . ,n.

There exits hyper-plane,

$$P\ =\ \left\{Q \in\ Rn/QT \bullet W +\ b\ =\ 0\right\} \tag{2}$$

The equation for the training data set can be written as

$$QiT\ W\ +\ b\ \geq 1,\ yi\ = 1$$
$$QiT\ W\ +\ b\ \geq -1,\ yi\ = -1 \tag{2.1}$$

The above-mentioned equations can be written as

$$yi\ \left(QiT\ W\ +\ b\ -1\ \right)\ \geq\ 0$$

Another definition for the hyper-plane considering P^- and P^+, let {Qi, yi} ∈ R^n be training data set, y iÎ {1, −1}, i = 1,2,. . . ,n,

$$P+ = \{Q\ \in\ Rn\ /QTi\ W\ +\ b\ = 1\}$$
$$P- = \{Q\ \in\ Rn\ /QTi\ W\ +\ b\ = -1\} \tag{2.2}$$

The optimization mentioned above is a form non-convex optimization problem that relies on the absolute value of |W| and is difficult to solve than convex optimization problems. The equation for the absolute value W can be replaced using 1/ 2 | |W| |^2 without having any change in the final solution; so, the representation of the SVM-related problem in quadratic programming (QP) form is as follows (Osuna et al., 1997):

$$Min\ 1/\ 2\ |\ |W|\ |2,$$
$$s\,t.\ yi\left(Q_i^T\ \mathrm{W} + b\right) - 1 \geq 0, 1 \leq i \leq n \tag{2.3}$$

After solving the SVM optimization problem using Lagrange multipliers (a_i), the Wolfe dual of the optimization problem was achieved (Craven, 1989):

$$L\left(w,b\right) = \frac{1}{2}\left\|w\right\|^2 - \sum\nolimits_{i=1}^{n} aiyi\left[\left(Q_i^T W + b\right) - 1\right]. \tag{2.4}$$

After solving for the value for W and b,

$$\frac{\partial L\left(w,b\right)}{\partial w} = 0,\ \frac{\partial L\left(w,b\right)}{\partial b} = 0 \tag{2.5}$$

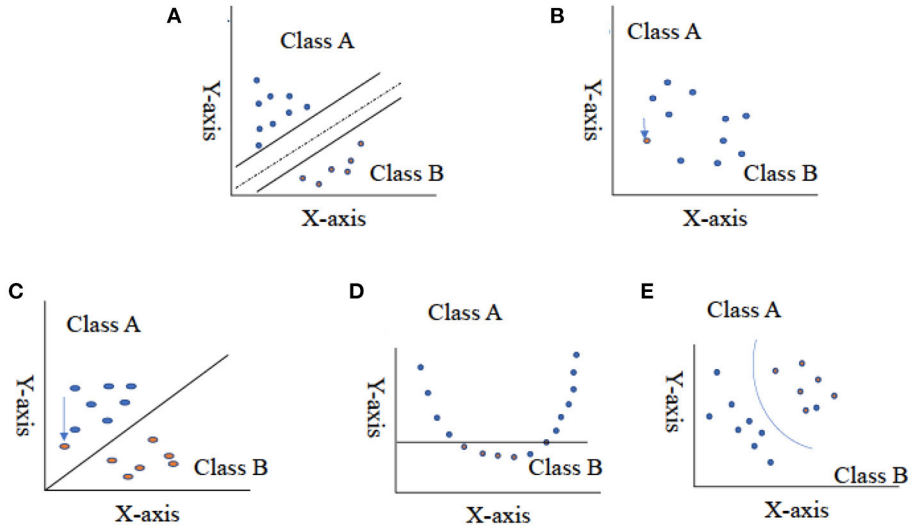

FIGURE 4 | Representation of two-class data using hyper-plane for support vector machine. **(A)** Represents split data set in half, **(B)** represents the two-close value, **(C)** represents the outlier value as the solution for the figure **(B)**, **(D)** represents non-linear data set, and **(E)** represents the use of kernel function and change in dimensionality of data. This Figure adapted from Noble (2006).

the solution in Equation (2.5) is the following condition:

$$w = \sum_{i=1}^{n} \alpha_i yiQi$$
$$\sum_{i=1}^{n} \alpha_i yi = 0 \quad (2.6)$$

putting the value of 2.6 into equation 2.4, we get the dual form of SVM,

$$W(a) = \sum_{i=1} \alpha_i - \left(\sum_{i=1}^{n} \alpha_i \alpha_j y_i y_j \left(Q_i \cdot Q_j\right)\right)/2,$$
$$s\,t. \sum_{i=1}^{n} \alpha_i y_i \left(Q_i \cdot Q_j\right) = 0$$
$$0 \leq ai \leq c,\ i = 1, 2, \ldots . n \quad (2.7)$$

The number of variables in the Equation derived is equivalent to the total number of data cases (n). The training set data with $a_i > 0$ represents the position of support vectors for the classification, and *Qi p+ or* $Q_i p-$.

The equation for hyper-plane decision can be written as Pontil and Verri (1998)

$$f(x) = \pm\left(\sum_{i=1}^{n} \alpha_i^* yi \left(q \cdot q_i\right) - b^*\right) \quad (2.8)$$

where q is the unknown input data that need to be classified. The SVM method has been employed in a considerable range of real-world problems associated with different fields of automation, forensics, biotechnology, agriculture statistics, and is now being used in food sciences for the classification of bakery products, fresh produce, and meat product classifications (Liu et al., 2013; Chen and Zhang, 2014; Asmara et al., 2017; Chen et al., 2017; Arsalane et al., 2018). It has been proven that SVMs are persistently most appropriate for diverse supervised learning methods. Despite this, the performance of SVMs is very receptive to the cost parameter, and kernel frameworks are set. As a result, research industries want to conduct ample cross-validation to determine the most influential parameter setting (Durgesh and Lekha, 2010).

Backpropagation Neural Networking

According to Lippmann (1987), there were no practical algorithms available for interconnecting weight values to achieve an overall minimum training error in multilayer networks. Rumelhart et al. (1986) proposed a generalised rule for backpropagation neural networking, an iterative, gradient descent training procedure. The input data, in the form of vector, are a pattern to be learned, and the desired output is in the form of a vector produced by the network upon recall of the input training pattern (Paola and Schowengerdt, 1995). The main goal of the training is to minimise the overall error between the test set data and training set data outputs of the network (Paola and Schowengerdt, 1995). BPNN is also recognized as multilayer perceptrons, one of the multiple layers forward neural networks. A BPNN comprises one input layer, one or more hidden layers, and one output layer (Bharathi and Subashini, 2011; Liu et al., 2013). Consideration of distinct factors plays a fundamental role when developing a BPNN that consists of the structure of network, initialisation, and switch functions in each hidden and output layer, the training way and algorithm, the learning rate, the error-goal (ε), and preprocessed input data. BPNN has some advantages, such as easy architecture, ease of assembling the mannequin, and fast calculation speed. However, BPNNs have some issues, such as (i) possible to contain in local extremum, (ii) poor generalisation ability, (iii) lack of strict format packages with a theoretical foundation, and (iv) challenging to manage the learning and training method (Yao, 1999).

In spite of these problems, backpropagation neural networks have been successfully implemented in a range of fields. Users

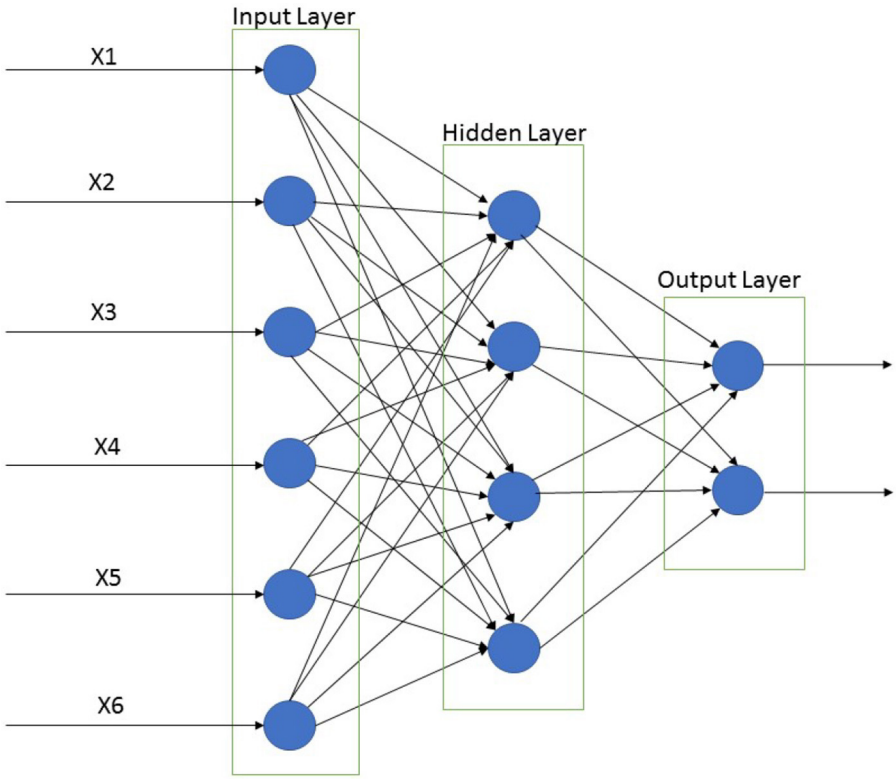

FIGURE 5 | Back propagation neural network classification for input, hidden, and output layer. This Figure was adapted from Rumelhart et al. (1986).

have applied their experiences and prior knowledge during the design of a BPNN to overcome these problems (Liu et al., 2013). A supervised BPNN learning algorithm consists of an input layer, one or more hidden layers, an output layer, and the nodes of the hidden layers primarily affect the classification efficiency of the neural network (**Figure 5**). Parameters that are required to be defined by the users are learning rate ($0 < \eta < 1$) and momentum ($0 < \eta < 1$).

BPNN program training procedure (Lee and To, 2010; Yang et al., 2011):

1. Design and input for network.
2. Normalise the initial input weights W and threshold values (θ).
3. Define the training and testing data set and input the training matrix X and output matrix Y.
4. Estimate the output vector of each neural synaptic unit.

(a). Evaluate the output vector (Z) for the hidden layer:

$$net_k = \Sigma w_{ik} x_i - \theta_{k,} \tag{3.1}$$

$$Zk = f\left(net\ k\right) \tag{3.2}$$

$$net_j = \Sigma w_{kj} Z_i - \theta_{j,} \tag{3.3}$$

$$Y_j = f(\text{net}_j)(3.4) \tag{3.4}$$

(b). The root of the mean square:

$$RMS = \sqrt{\frac{\sum \left(y_j - T_j\right)^2}{n}} \tag{3.5}$$

5. Estimate distance δ for the output layer and hidden layer from Equations (3.6, 3.7):

$$\delta_j = \left(T_j - y_i\right) - f\left(net_j\right) \tag{3.6}$$

$$\delta_k = \left(\sum\nolimits_j \delta_j w_{kj}\right) - f^{'(net_j)} \tag{3.7}$$

6. Evaluate modifications for initial weights (W) and distance (δ) (η is the learning rate, α is the momentum) for both output layer (Equations 3.8, 3.9) and hidden layer (Equations 3.10, 3.11):

$$\Delta w_{kj(n)} = \eta \delta_j z_k + \alpha \Delta w_{Kj}\left(n - 1\right) \tag{3.8}$$

$$\Delta \theta_j\left(n\right) = -\eta \delta_j + \alpha \Delta \theta_j\left(n - 1\right) \tag{3.9}$$

$$\Delta w_{ik(n)} = \eta \delta_j X_i + \alpha \Delta w_{ik} (n-1) \quad (3.10)$$

$$\Delta \theta_k (n) = -\eta \delta_k + \alpha \Delta \theta_k (n-1) \quad (3.11)$$

7. Redefine initial weight (W) and the threshold value (θ), redefine W and θ of the output and hidden layer:

$$w_{kj}(p) = w_{kj}(P-1) + \Delta w_{k_j} \quad (3.12)$$

$$\theta_j(p) = \theta_j(p-1) + \Delta \theta_j \quad (3.13)$$

$$w_{ik}(p) = w_{ik}(P-1) + \Delta w_{ik} \quad (3.14)$$

$$\theta_k(p) = \theta_k(p-1) + \Delta \theta_k \quad (3.15)$$

After modifying output and hidden layer, the steps will be renewed, and steps 3–7 will be repeated until converge.

BPNN program-testing process (Lee and To, 2010; Yang et al., 2011):

1. Input parameters related to the network.
2. Input the initial weights (W) and the threshold value (θ).
3. Unknown data entry for data matrix X.
4. Evaluate output vector (Z) for the output and hidden layer:

$$net_k = \Sigma W_{ik} x_i - \theta_k \quad (3.16)$$

$$z_k = f(nt_k) \quad (3.17)$$

$$nt_j = \Sigma w_{kj} z_i - \theta_j \quad (3.18)$$

$$Y_j = f(nt_j) \quad (3.19)$$

Statistical Analysis

All the parameters (resistance, reactance, fat index, protein index, and fillet weights) were analysed by one-way analysis of variance with Tukey's honestly significant difference (HSD) ($p < 0.05$) to determine significant differences among the levels of myopathy severity. The data were further analysed using three classification methods, linear discriminant analysis (LDA) (SAS, Version 9.4), support vector machines (SVMs), and backpropagation neural networking (BPNN). For each method, the data were analysed using three different scenarios: (1) all data (WB scores, fillet weight, resistance, reactance, protein index, and fat index); (2) without fillet weights (WB scores, resistance, reactance, protein index, and fat index); and (3) without fat and protein index (WB scores, fillet weight, resistance and reactance). For the SVM and BPNN analysis of collected data, R software (Version 4.0.0, Arbour Day) was used by using the caret package in the analysis to classify various chicken breast fillet myopathies. The data sets collected for the different conditions were divided into 70::30 training set and testing set. The caret package algorithm calculated the best-suited tuning parameter or value of cost (C) for both the training and testing data sets. A seed value was set for 3,000 for the SVM analysis. For BPNN the classification of fillets, the Neural net and BBmisc packages were used to classify the collected data sets (WB and SM), and the data sets were divided into 70::30 training and testing data sets. Low learning rate (0.01), the threshold value (0.01), number of maximum steps (10,000), and four hidden layers were used in the BPNN classification algorithm for the analysis.

RESULTS

The differences in various parameters among the levels of woody breast and spaghetti meat severity are shown in **Tables 2**, **3**, respectively. As shown in **Table 2**, there are significant differences ($p < 0.05$) in the resistance, reactance, and fillet weights among the WB categories. There were no significant differences ($p > 0.05$) in the fat and protein index between WB severity levels (**Table 2**). On the contrary, there are no significant differences in the parameters between breast fillets with and without SM (**Table 3**). Classification efficiencies of the fillets are greatly affected by the analysis of all the data, without fillet weights and without fat and protein index, indicating the significance of variables in classification accuracy (**Table 2**). The LDA, SVM, and BPNN analyses showed that when the fillet weights were removed from the dataset, classification accuracy (testing %) was reduced by as high as 20% (**Table 2**). The LDA analysis without fillet weight data set showed less classification efficiency in the testing data set (normal = 43.8%, moderate = 17.2%, and severe = 50.0%) compared with the training data set (normal= 62.1%, moderate = 32.2%, and severe = 64%), indicating that the training model was not efficient in classification at the testing stage. Similarly, the SVM analysis showed low classification efficiency for the testing set (normal = 56.52%, moderate = 49.77%, and severe = 64.63%). The removal of fat and protein index data from the analysis showed that the LDA analysis for normal (training::testing = 61.7::75.6) and moderate fillets (training::testing = 31.3::33.33) improved as compared with the analysis without the fillet weight data set and all the data sets (including resistance, reactance, protein index, fat index, and fillet weights). The lower efficiency may be due to the misclassification of fillets due to fat and protein index value overlapping. The SVM analysis showed a higher classification pattern for normal (training::testing = 65.75::73.28) and severe breast fillets (training::testing = 72.49::81.48), similar to the overall data set. For the classification of SM fillets from the normal fillets, the SVM analysis performed better in the classification of normal fillets (training::testing = 57.06::60.00) from spaghetti meat-conditioned fillets (training::testing = 45.5::22.2) (**Table 2**). On the other hand, the SVM analysis for the resistance, reactance, and weight data set showed slightly

TABLE 2 | Comparison of bioelectrical impedance parameters and fillet weights among woody breast fillets with varying myopathy severity levels.

Condition	No. of fillets	Resistance	Reactance	Fat index	Protein index	Weight of fillets
Normal	148	71.89 ± 0.52^{a}	36.93 ± 0.44^{a}	13.27 ± 0.21^{a}	37.71 ± 0.27^{a}	455.80 ± 3.85^{c}
Moderate	82	68.78 ± 0.55^{b}	32.21 ± 0.49^{b}	13.32 ± 0.21^{a}	37.56 ± 0.27^{a}	485.66 ± 3.80^{b}
Severe	70	67.90 ± 0.55^{b}	30.72 ± 0.50^{c}	14.09 ± 0.21^{a}	37.11 ± 0.27^{a}	514.86 ± 3.75^{a}

Means with different superscript are significantly different from each other.

TABLE 3 | Comparison of bioelectrical impedance parameters and fillet weights among normal breast fillets with and without spaghetti meat conditions.

Parameters	Spaghetti meat (Yes)	Spaghetti meat (No)
Resistance	69.88 ± 0.52^{a}	70.19 ± 0.52^{a}
Reactance	35.63 ± 0.44^{a}	34.08 ± 0.44^{a}
Fat index	13.73 ± 0.21^{a}	13.39 ± 0.21^{a}
Protein index	37.36 ± 0.27^{a}	38.05 ± 0.27^{a}
Weight of fillets	473.26 ± 3.75^{a}	479.24 ± 3.75^{a}

Spaghetti meat (Yes = 75; No = 225). [a]means with same letter superscript are not significantly different.

improved classification efficiency for fillets with SM condition (training::testing = 50.00::52.35). BPNN did not perform well in any of the given conditions for the classification of fillets based on WB severity and SM fillets conditions.

DISCUSSION

Using only visual and hand palpation characteristics to identify woody breast and spaghetti meat muscle myopathies poses various challenges, such as misclassifications, processing inefficiencies, and increase in labour costs, when classification is performed on a processing line. WB is found primarily in the superficial area of breast fillets and, many times, includes the visual presence of surface haemorrhages, appearance of light-yellow surface, rigid bulged fillet, and by mechanical palpability of the muscle (**Figure 6**; Mazzoni et al., 2015; Mudalal et al., 2015). Additionally, normal breast fillets have smaller cross-sectional areas as compared with woody breast fillets (Huang and Ahn, 2018), with higher collagen content and elevated post processing pH (Petracci et al., 2015; Chatterjee et al., 2016; Clark and Velleman, 2016; Soglia et al., 2016). SM, on the other hand, is related to immature intramuscular connective tissues in the breast meat, and it has lower muscular cohesion than the breast meat from unaffected fillets (**Figure 7**; Bowker and Zhuang, 2016; Radaelli et al., 2017; Sihvo et al., 2017). The thickness of connective tissues in the breast fillets showing SM decreases gradually in the endomysium and perimysium, causing different muscle fibres to deteriorate or have a mushy texture (Baldi et al., 2018). Therefore, using an assortment of already available complex data, we were able to make improvements to the classification of fillets among the WB and SM myopathies.

Significant differences were observed in the resistance and reactance among the normal, moderate, and severe woody breast fillets (**Table 2**), indicating changes in the muscle architecture and the intra- and extra-cellular water contents of the meat (Morey et al., 2020). It was expected to find significant differences in the fillet weights among the levels of WB severity, with severe WB fillets weighing significantly heavier than the normal fillets ($p < 0.05$). However, contrary to Morey et al. (2020), this research reports an inverse trend in resistance and reactance of normal and severe woody breast. Morey et al. (2020) reported that resistance and reactance were lower in normal meat (72.18 and 28.04 Ω, respectively), and higher in severe WB meat (78.27 and 37.54 Ω). In this study, resistance and reactance were higher in normal meat (71.89 and 36.93 Ω) and lower in severe WB meat (67.9 and 30.72 Ω). As for the normal meat with and without SM (**Table 3**), the observations were contrary to Morey et al. (2020). This study (**Table 3**) did not find significant differences in the resistance, reactance, fat index, protein index and weight of the normal fillets with and without SM.

FIGURE 6 | Spaghetti meat condition in chicken breast fillets.

In this study, the breast fillets were taken from water-chilled birds, which were immediately deboned on a deboning line and analysed in a plant, while in the study by Morey et al. (2020),

FIGURE 7 | Severe woody breast fillet in the collected samples.

the fillets were transported to a lab and analysed within 6 h of procurement. It would be of interest to investigate if the differences in bioelectrical properties are (1) water-retention in the normal breast fillets due to immersion chilling and (2) post deboning holding time. The findings emphasise the fact that the bioelectrical parameters were standardised by the processors prior to use.

The results obtained with training accuracy for linear discriminant analysis (70::30) classification were 72.31, 43.75, and 75% for the normal, moderate, and severe woody breast (**Table 4**) fillet classifications, respectively, using the bioelectrical impedance analysis and fillet weight data set ($n = 300$). The testing set was lower in accuracy than the training set, with only 52.63% normal classified, 29.41% moderate classified, and 59.09% severe WB classified ($n = 300$; **Table 4**). The testing data set was lower in accuracy compared with the training set data, possibly because of the low sample size and non-linearity of the data set. The non-linear data set is likely due to human error during the manual hand-palpation of the breast fillets; however, in future studies, larger data sets could be implemented to increase the accuracy of the BIA method combined with conventional algorithms. Morey et al. (2020) also performed LDA (60::40) with a BIA data set ($n = 120$) and reported 68.69–70.55% accuracy for the classification of normal fillets and 54.42–57.75% accuracy for severe WB fillets in the testing set. Wold et al. (2019) analysed a near infrared spectroscopy (NIR) data set ($n = 102$) using an LDA (50::50) classification algorithm with 100% accuracy for fillet classification in the training set and 96% accuracy in the testing set, for a rapid on-line detection method for WB myopathy in processing plants. LDA is a well-recognised technique for reducing the dimensionality of data in a dataset. However, LDA can only be used for single-label multi-class categorizations and cannot explicitly be extended to multi-label multi-class classification systems. The LDA technique is used to convert high-dimensional data into a low-dimensional data space, maximising the ratio of between-class variation to within-class variance, thereby ensuring optimal class separation (Pan et al., 2014). The LDA technique works by projecting the initial data matrix onto a lower-dimensional region. For the reduction of dimensionality, three steps are required: (i) the inter-class difference or between-class matrix is used to measure the separability across multiple categories (i.e., the distance between the means of different classes), (ii) the within-class variance, also known as the within-class matrix, is calculated as the difference between the mean and the class samples, and (iii) the creation of a lower-dimensional space that maximises between-class variance while minimising within-class variance (Mandal et al., 2009). In this research and that of Morey et al. (2020), the low performance of data collected and analysed by LDA compared with the data collected may have two key factors: small sample size and data linearity issues. Su et al. (2017) also found low performance in data sets with small sample size and non-linear data.

The linear discriminant analysis technique is used to find a linear transformation that discriminates between various groups. However, LDA cannot find a lower-dimensional space if the groups are non-linearly separable. In other words, where discriminatory knowledge is not in the means of classes, LDA fails to locate the LDA space. One of the significant issues with the LDA methodology is singularity, also known as small sample size or under-sampling. This issue arises because of high-dimensional trend classification problems or a low number of training samples available for each class compared with the dimensionality of the sample space (Huang et al., 2002; Lu et al., 2005; Zhuang and Dai, 2005; Su et al., 2017; Tharwat et al., 2017).

The machine learning theory lays the groundwork for support vector machine, and this algorithm has gained widespread attention because of its unique performance efficiency, and ability to accomplish pinpoint accuracy and manage high-dimensional, multi-variate data sources. Cortes and Vapnik (1995) implemented SVMs as a new ML technique for two-group classification problems. Researchers have reported that SVMs are an economical, sensitive, and easy to use classifier that can be implemented in organised evaluation assignments (Vapnik, 1995). The inspection of large collected data sets during production is a significant application of SVM (Burbidge et al., 2001; Chinnam, 2002). SVM is frequently used in various food production environments, including product monitoring systems, mechanical fault detection, and dimensional accuracy (Ribeiro, 2005; Salahshoor et al., 2011; Çaydaş and Ekici, 2012; Azadeh et al., 2013). SVMs are used in different processing areas, such as drug designing and discovery, surgery, and cancer treatment, in addition to the food product processing industry (Vapnik, 2013). Product quality control (Borin et al., 2006), polymer recognition, and other applications are also possible (Li et al., 2009) areas in which SVM can be incorporated. These examples from different industries demonstrate that SVM algorithms have a broad range of applicability and

TABLE 4 | Percentage classification efficiency for various supervised machine-learning algorithms (linear discriminant analysis, support vector machines, and back propagation neural networking) for breast fillets with woody breast[a] and spaghetti meat[b] in three different scenarios (all data, without fillet weights, and without fat and protein index value).

Classification method	Subjective classification	Accuracy (all data)[c]		Accuracy (without fillet weights)[d]		Accuracy (without fat and protein index)[e]	
		Training (%)	Testing (%)	Training (%)	Testing (%)	Training (%)	Testing (%)
Woody breast meat							
Linear discriminant analysis	Normal	72.31	52.63	62.10	43.80	61.70	75.60
	Moderate	43.75	29.41	32.20	17.20	31.30	33.33
	Severe	75.00	59.09	64.00	50.00	68.50	56.30
Support vector machines	Normal	63.86	71.04	60.11	56.52	65.74	73.28
	Moderate	49.88	59.99	50.09	49.77	49.88	50.00
	Severe	71.78	81.48	59.94	64.63	72.49	81.48
Back propagation neural networking	Normal	50.00	47.77	32.85	40.00	42.38	42.22
	Moderate	29.04	23.33	6.67	2.22	7.14	1.12
	Severe	20.95	28.88	14.76	11.12	16.19	14.44
Spaghetti meat							
Support vector machines	Normal fillet without spaghetti	69.38	50.00	57.06	60.00	52.15	52.22
	Normal fillet with spaghetti	53.33	50.00	45.5	22.2	50.00	52.35
Back propagation neural networking	Normal fillet without spaghetti	100.00	52.95	65.51	42.30	58.62	50.00
	Normal fillet with spaghetti	100.00	75.00	29.31	19.23	29.31	11.50

Woody breast [a]n = 300 (normal = 148, moderate = 82, severe = 70); spaghetti meat [b]n = 84; All data[c]-WB scores, fillet weight, resistance, reactance, protein index, and fat index; without fillet weights[d]-woody breast (WB) scores, resistance, reactance, protein index, and fat index; and Data without fat and protein index[e]-WB scores, fillet weight, resistance, and reactance.

versatility (Kotsiantis et al., 2007). This research demonstrates the ability for the implementation of SVM and BPNN in combination with BIA and fillet weight data to classify WB and SM fillets.

Statistical learning theory (SLT) is a robust and appropriate supervised learning algorithm for production research problems. Under SLT, algorithmic learning allows it to use an achieving function, representing the relationship between different components without being directly connected (Evgeniou et al., 2000). The algorithm enquires about the problem concerning how well the selected method resolves the problem, and accuracy prediction performance for previously unknown inputs is the subject of SLT (Evgeniou et al., 2000). A few more realistic techniques, such as autoencoders, SVM, and Bayesian optimization, are based on the theories of SLT (Battiti et al., 2002). SVM is considered a mathematical expression in its most basic form, a method (or algorithm) for optimising alphanumeric equations, with a given set of data (Noble, 2006).

The fundamental idea of support vector machine algorithmic expression can be easily understood by four fundamental concepts: (i) the imaginary hyper-plane, (ii) the margin of hyper-plane, (iii) the soft margin, and (iv) the kernel function (Tharwat, 2019). A solid line splits the region in half in two dimensions (**Figure 4A**), but we require a hypothetical plane to split the area into three dimensions. A hyper-plane is a collective term for a straight line in a high-dimensional region, and the dividing hyper-plane is the line that separates the pieces of data (Kecman, 2001; Tharwat, 2019). SVM, on the other hand, differs from other hyper-plane-based classifiers based on how the hyper-plane is chosen. Consider the grouping shown in **Figure 4**. By implementing SLT, it is easier to find the best possible plane to create the hyper-plane that will be used in the classification of data (Vapnik, 1963). The capability of SVM to classify the correct data points between given classes can be improved by using an imaginary hyper-plane in the space. The SLT theorem implies that the data used to train SVM originates from the same dataset as the data used to test it. For example, if an SVM algorithm is trained on the sensory property of a product, it cannot be used to train the data collected for the subjective response of consumers. Furthermore, we cannot expect SVM to work well if training is conducted with an SM breast fillet data set, so a WB data set is used for testing. At the same time, the SLT principle does not assume that two data sets come from the same class of distributions. For example, an SVM algorithm does not assume that training data values follow a normal distribution.

For a better understanding of support vector machine and its function, we have concluded an imaginary data set for classes A and B, which can be divided using a straight line. When the values in a data set are closer together or intersected (**Figure 4B**), SVM will manage this overlapping of data by inserting a soft margin. In essence, this causes specific data points to pass across the margin of the dividing hyper-plane, without influencing the outcome. The use of the soft margin provides the solution to the problem of misclassification (shown in **Figure 4B**) by considering the data point as an outlier (shown in **Figure 4C**). Another essential function for SVM classification is the kernel function (shown in **Figures 4D,E**), a mathematical trick that allows SVM to perform a two-dimensional classification of a one-dimensional data set. In

general, a kernel function projects data from a low-dimensional space to a space of higher dimension.

Support vector machine classification efficiency (**Table 4**) for the separation of high dimensionality data showed better classification efficiency for normal (training efficiency 63.86%, testing efficiency 71.04%), moderate (training efficiency 49.88%, testing efficiency 59.99%), and severe WB (training efficiency 71.78%, testing efficiency 81.48%) compared with the LDA algorithm used by Morey et al. (2020). The BIA and fillet weight data set used in training the SVM performed well because of the higher dimensionality of the data set. When data are highly dimensional and the sample sets are relatively small, SVM analysis is more accurate to classify data, and has been used by other authors to help classify multi-dimensional data. Barbon et al. (2018) used a relatively small data set ($n = 158$) of NIR results combined with SVM (75::25) to classify normal and pale meat, as it relates to pale, soft, and exudative poultry breast meat. They demonstrated the use of SVM as a classification tool for breast fillets with muscle myopathies where the classification accuracy for normal fillets was 53.4 and 72. % for pale fillets. Geronimo et al. (2019), using an NIR system equipped with an image acquisition system, found 91.83% classification efficiencies (fillet images) using SVM to analyze a WB fillet sample set (sample size is unclear) with a 70::30 model. These researchers also used multilayer perceptron (a feed-forward network differing from the backpropagation network in BPNN) to classify the data set, and classification accuracy was 90.67% for WB. Yang et al. (2021) analysed images derived from the expressible fluid of breast meat to classify WB using SVM (training and testing ratio is unreported) and DL (training to testing is 2 to 1). These researchers found fewer classification efficiencies for SVM algorithms in the testing set (38.25–63.89%), compared with the training set (40.41–81.94%) in three out of the four SVM classification methods used. In their DL classification (a type of ANN) to classify WB, they reported 100% accuracy in the training set and 93.3% accuracy in the testing set.

Connexions of random different nodes or units in a computing system to solve problems that are impossible to solve by conventional statistical methods are known as artificial neural networks and are based on the circuitry of the human brain. When applied to a processor framework, the subconscious network can execute unique functions (perception, speech synthesis, image recognition), which have proven to be useful in industrial applications (Alpaydin, 2010). Neural networks allow an automated artificial skill to operate unsupervised reinforcement and classification algorithm functions (neural networks) by simulating the decentralised "data analysis" capabilities of the central nervous platform through neural networks (Pham and Afify, 2005; Corne et al., 2012). Decentralisation employs many necessary interconnected neurons or nodes and the capacity to process data through the complex response of these endpoints and their links to exogenous variables (Akay, 2011). These algorithms are crucial in the modern machine learning development of today (Nilsson, 2005) and can be classified into two categories: interpretation and algorithm. Neural networks are used in a variety of industrial sectors for a range of problems (Wang et al., 2005) e.g., process control, emphasising their key benefit and overall predictive validity (Pham and Afify, 2005). However, ANN (similar to SVM) requires a large sample size to attain maximum precision (Kotsiantis et al., 2007). Overfitting, which is linked to high-variance implementations, is universally acknowledged as a disadvantage of the ANN algorithm (Kotsiantis et al., 2007). Other difficulties with using neural networks include the sophistication of generated models, aversion for missing values, and, often, lengthy dataset training method (Pham and Afify, 2005; Kotsiantis et al., 2007).

For backpropagation neural networks, the data were pre-processed and consisted of just two dimensions with a lower level of classification complexity (Panchal et al., 2011). Classification efficiencies for the WB fillets using BPNN (**Table 4**) show that the testing data set for the normal (47.77%) and moderate fillets (23.33%) did not perform well, compared with the classification efficiency for the severe WB fillets (28.88%). The BPNN classification algorithm for the WB fillets did not perform well-because of the complexity of the data after pre-processing, and overfitting of the learning model due to the uneven distribution of weight on the input neuron layer. The BPNN classification algorithm for the SM data set (**Table 4)** performed well for the training data set for normal (training 100%, testing 52.95%) and SM fillets (training 100%, testing 75%). However, due to the complexity of pre-processed data, overfitting of BPNN and small data set, the classification efficiency of the testing set was lower than that of the training set. These studies all use SVM and ANN algorithms to classify small sample data sets, where the results always show that the accuracy in the training set data was higher than that in the testing set data, indicating that the training of the model is not performing well. Collection of larger data set for the supervised learning methods of classification provides the chances for getting lower error rates and better learning ability for the machine learning algorithms.

In a backpropagation neural network, the input data vector represents the pattern to be trained, and the output data vector represents the optimal set of output values that the network can generate when the training pattern is recalled. The aim of BPNN training is to reduce the total error between the expected and real outputs of the network (Panchal et al., 2011). To generate a reduction in error, the residual differences in the weights at each iteration must be unmeasurable. A learning rate metric, which reflects the rate of the move taken toward minimal error, must be defined to accomplish a reasonable training period. Learning will take too much time if this amount is too small, and if it is too high, the loss function will degenerate and errors will rise (Ganatra et al., 2011). When using neural networks to analyze WB data, overlearning or overfitting happens when the algorithm takes too long to run, and the network is too complicated for the problem or the amount of data available, whereas, to classify SM in a group of fillets, BPNN was used, and data are processed differently.

Additional analysis of the data was conducted to determine if the parameters used in data classification would make a difference in classification accuracies using the three methods (linear discriminant analysis, support vector machine, and backpropagation neural network) for both woody breast and spaghetti meat. Irrespective of the methodologies used, removing

fillet weight reduced the classification accuracies of WB classification by up to 20%, indicating the importance of using fillet weights (for classification), which were significantly different among the WB categories ($p < 0.05$; **Table 2**). Removing the fat and protein indexes, which were not significantly different among the WB categories ($p > 0.05$; **Table 3**) increased the classification accuracy (Testing %) of the LDA models, while it was similar for the SVM and BPNN models. The finding indicates the significance of using fillet weight in the models and that the SVM and BPNN models analyze the significance of each parameter in the classification models.

It was interesting to note that the bioelectrical impedance analysis parameters, such as weight, were not significantly different between normal meat with and without spaghetti meat (**Table 3**). However, those parameters could be used collectively to develop classification models using LDA, SVM and BPNN models. Most importantly, removing weights did make a difference in the classification accuracies, but retaining the fillet weights and removing the fat and protein indexes did not necessarily increase the accuracy of the model. In the case of SM, more data are needed to build more accurate and stronger models.

CONCLUSION

This project demonstrates the application of machine learning in poultry production processes to categorise chicken breast fillets into groups based on the severity of myopathy. The use of SVM and BPNN can be combined with BIA and fillet weight data to more accurately classify breast fillet myopathies, such as WB and SM, from normal breast fillets in real-time online, compared with the subjective hand palpation method. With the implementation of other meat quality parameters, such as water content, the classification accuracy of SVM and BPNN could be improved. To obtain a well-trained model for classification efficiency and to reduce overfitting and underfitting problems related to classification, future research should include larger data sets for breast fillet myopathies to avoid the overlapping of conditions caused by human error in the sorting of fillets. The innovative combination of these tools has the potential to improve poultry processing efficiencies and downgrades of breast fillets affected by undesirable myopathies while reducing customer complaints.

DATA AVAILABILITY STATEMENT

The raw data supporting the conclusions of this article will be made available by the authors, without undue reservation.

ETHICS STATEMENT

Ethics approval was not required for this study in line with national/local guidelines.

AUTHOR CONTRIBUTIONS

AM is the lead investigator who conceptualised the idea, secured funding, and conducted the research. AM, AS, and JV conducted the bioelectrical impedance analysis data collection. AS performed the SVM, BPNN analysis, and manuscript preparation. AES and SS have helped in the cross-validation of analysis results and review of the manuscript. AM and LG assisted in writing—review and editing. All authors contributed to the article and approved the submitted version.

REFERENCES

Abdullah, M. Z., Guan, L. C., Mohamed, A. M. D., and Noor, M. A. M. (2002). Color vision system for ripeness inspection of oil palm Elaeisguineensis. *J. Food Process. Preserv*. 26, 213–223. doi: 10.1111/j.1745-4549.2002.tb00481.x

Akay, D. (2011). Grey relational analysis based on instance-based learning approach for classification of risks of occupational low back disorders. *Saf. Sci*. 49, 1277–1282. doi: 10.1016/j.ssci.2011.04.018

Alpaydin, E. (2010). *Introduction to Machine Learning*. Cambridge, MA: MIT Press.

Apte, C., Weiss, S., and Grout, G. (1993). "Predicting defects in disk drive manufacturing: A case study in high-dimensional classification. Artificial intelligence for applications," in *Proceedings of 9th IEEE Conference* (Orlando, FL). doi: 10.1109/CAIA.1993.366608

Arsalane, A., El Barbri, N., Tabyaoui, A., Klilou, A., Rhofir, K., and Halimi, A. (2018). Anembedded system based on DSP platform and PCA-SVM algorithms for rapid beef meatfreshness prediction and identification. *Comput. Electron. Agric*. 152,385–392. doi: 10.1016/j.compag.2018.07.031

Asmara, R. A., Rahutomo, F., Hasanah, Q., and Rahmad, C. (2017). "Chicken meatfreshness identification using the histogram color feature," in *Sustainable Information Engineering and Technology (SIET)* (Malang: IEEE). doi: 10.1109/SIET.2017.8304109

Azadeh, A., Saberi, M., Kazem, A., Ebrahimipour, V., Nourmohammadzadeh, A., and Saberi, Z. (2013). A flexible algorithm for fault diagnosis in a centrifugal pump with corrupted dataand noise based on ANN and support vector machine with hyper-parametersoptimization. *Appl. Soft. Comput*. 13, 1478–1485. doi: 10.1016/j.asoc.2012.06.020

Balakrishnama, S., and Ganapathiraju, A. (1998). "Linear discriminant analysis-a brief tutorial," in *Institute for Signal and Information Processing* (Piscataway, NJ: IEEE), 1–8.

Baldi, G., Soglia, F., Mazzoni, M., Sirri, F., Canonico, L., Babini, E., et al. (2018). Implications of white striping and spaghetti meat abnormalities on meat quality and histological features in broilers. *Animal* 12, 164–173. doi: 10.1017/S1751731117001069

Barbon, S., Costa Barbon, A. P. A. D., Mantovani, R. G., and Barbin, D. F. (2018). Machinelearning applied to near-infrared spectra for chicken meat classification. *J. Spectrosc*. 2018:894971. doi: 10.1155/2018/8949741

Bar-Or, A., Schuster, A., Wolff, R., and Keren, D. (2005). "Decision tree induction in highdimensional, hierarchically distributed databases. Society for Industrial and Applied Mathematics," in *Proceedings SIAM International* (Newport, CA). doi: 10.1137/1.9781611972757.42

Battiti, R., Brunato, M., and Villani, A. (2002). *Statistical Learning Theory for Location Fingerprinting in Wireless LANs*. Available online at: http://eprints.biblio.unitn.it/238/ (accessed April 15, 2021).

Bera, T. K. (2014). Bioelectrical impedance methods for noninvasive health monitoring: a review. *J. Med. Eng*. 2014, 1–28. doi: 10.1155/2014/381251

Bharathi, P. T., and Subashini, P. (2011). Optimization of image processing techniques usingneural networks: a review. *WSEAS Trans. Inf. Sci. Appli.* 8, 300–328.

Borin, A., Ferrao, M. F., Mello, C., Maretto, D. A., and Poppi, R. J. (2006). Least-squares supportvector machines and near infrared spectroscopy for quantification of common adulterantsin powdered milk. *Anal. Chim. Acta* 579, 25–32. doi: 10.1016/j.aca.2006.07.008

Bowker, B., and Zhuang, H. (2016). Impact of white striping on functionality attributes of broiler breast meat. *Poult. Sci.* 95, 1957–1965. doi: 10.3382/ps/pew115

Burbidge, R., Trotter, M., Buxton, B., and Holden, S. (2001). Drug design by machine learning: support vector machines for pharmaceutical data analysis. *Comput. Chem.* 26, 5–14. doi: 10.1016/S0097-8485(01)00094-8

Carter, R. M., Yan, Y., and Tomlins, K. (2005). Digital imaging-based classification andauthentication of granular food products. *Meas. Sci. Technol.* 17:235. doi: 10.1088/0957-0233/17/2/002

Çaydaş, U., and Ekici, S. (2012). Support vector machines models for surface roughness prediction in CNC turning of AISI 304 austenitic stainless steel. *J. Intell. Manuf.* 23, 639–650. doi: 10.1007/s10845-010-0415-2

Chatterjee, D., Zhuang, H., Bowker, B. C., Rincon, A. M., and Sanchez-Brambila, G. (2016). Instrumental texture characteristics of broiler *Pectoralis major* with the wooden breast condition. *Poult. Sci.* 95, 2449–2454. doi: 10.3382/ps/pew204

Chen, C. P., and Zhang, C. Y. (2014). Data-intensive applications, challenges, techniques andtechnologies: a survey on big data. *Inf. Sci.* 275, 314–347. doi: 10.1016/j.ins.2014.01.015

Chen, K., Sun, X., Qin, C., and Tang, X. (2010). Color grading of beef fat by using computervision and support vector machine. *Comput. Electron. Agr.* 70, 27–32. doi: 10.1016/j.compag.2009.08.006

Chen, Z., Cao, S., and Mao, Z. (2017). Remaining useful life estimation of aircraft engines using amodified similarity and supporting vector machine (SVM) approach. *Energies* 11, 1–14. doi: 10.3390/en11010028

Chinnam, R. B. (2002). Support vector machines for recognizing shifts in correlated and othermanufacturing processes. *Int. J. Prod. Res.* 40, 4449–4466. doi: 10.1080/00207540210152920

Clark, D. L., and Velleman, S. G. (2016). Spatial influence on breast muscle morphological structure, myofiber size, and gene expression associated with the wooden breast myopathy in broilers. *Poult. Sci.* 95, 2930–2945. doi: 10.3382/ps/pew243

Corne, D., Dhaenens, C., and Jourdan, L. (2012). Synergies between operations research and datamining: the emerging use of multi-objective approaches. *Eur. J. Oper. Res.* 221, 469–479. doi: 10.1016/j.ejor.2012.03.039

Cortes, C., and Vapnik, V. (1995). Support-vector networks. *Mach. Learn.* 20, 273–297. doi: 10.1007/BF00994018

Cox, M. K., Heintz, R., and Hartman, K. (2011). Measurements of resistance and reactance in fish with the use of bioelectrical impedance analysis: sources of error. *Fishery Bull.* 109, 34–47.

Craven, B. D. (1989). A modified Wolfe dual for weak vector minimization. *Numer. Funct. Anal. Optim.* 10, 899–907. doi: 10.1080/01630568908816337

Do, T. N., Lenca, P., Lallich, S., and Pham, N. K. (2010). "Classifying very-high-dimensional data with random forests of oblique decision trees," in *Advances in Knowledge Discovery and Management,* eds F. Guillet, G. Ritschard, D. A. Zighed, and H. Briand (Berlin: Springer). doi: 10.1007/978-3-642-00580-0_3

Durgesh, K. S., and Lekha, B. (2010). Data classification using support vector machine. *J. Theor. Appl.* 12, 1–7.

Evgeniou, T., Pontil, M., and Poggio, T. (2000). Statistical learning theory: A primer. *Int. J. Comput. Vis.* 38, 9–13. doi: 10.1023/A:1008110632619

FAO (2003). *Livestock Commodities.* Available online at: http://www.fao.org/3/y4252e/y4252e00.htm#TopOfPage (accessed April 17, 2021).

Filipič, B., and Junkar, M. (2000). Using inductive machine learning to support decision making inmachining processes. *Comput. Ind.* 43, 31–41. doi: 10.1016/S0166-3615(00)00056-7

Fisher, R. A. (1936). The use of multiple measurements in taxonomic problems. *Ann. Eugen.* 7, 179–188. doi: 10.1111/j.1469-1809.1936.tb02137.x

Fukunaga, K. (2013). *Introduction to Statistical Pattern Recognition*. San Diego, CA: Academic Press, INC.

Ganatra, A., Kosta, Y. P., Panchal, G., and Gajjar, C. (2011). Initial classification through back propagation in a neural network following optimization through GA to evaluate the fitness of an algorithm. *Int. J. Comput. Sci. Appl.* 3, 98–116. doi: 10.5121/ijcsit.2011.3108

Gardner, R., and Bicker, J. (2000). Using machine learning to solve tough manufacturingproblems. *Int. J. Ind. Eng. Theory Appl. Pract.* 7, 359–364.

Geronimo, B. C., Mastelini, S. M., Carvalho, R. H., Júnior, S. B., Barbin, D. F., Shimokomaki, M., et al. (2019). Computer vision system and near-infrared spectroscopy foridentification and classification of chicken with wooden breast, and physicochemical andtechnological characterization. *Infrared Phys. Technol.* 96, 303–310. doi: 10.1016/j.infrared.2018.11.036

Guo, X., Sun, L., Li, G., and Wang, S. (2008). A hybrid wavelet analysis and support vectormachines in forecasting development of manufacturing. *Expert Syst. Appl.* 35, 415–422. doi: 10.1016/j.eswa.2007.07.052

Heinz, G., and Hautzinger, P. (2009). Meat Processing Technology for Small to Medium Scale Producers. FAO. Available online at: https://agris.fao.org/agris-search/search.do?recordID=XF2016077667 (accessed March 3, 2021).

Hoffer, E. C., Meador, C. K., and Simpson, D. C. (1969). Correlation of whole-body impedancewith total body water volume. *J. Appl. Physiol.* 27, 531–534. doi: 10.1152/jappl.1969.27.4.531

Huang, R., Liu, Q., Lu, H., and Ma, S. (2002). "Solving the small sample size problem of LDA," in *Object Recognition Supported by User Interaction for Service Robots* (Quebec City, QC: IEEE), 29–32. doi: 10.1109/ICPR.2002.1047787

Huang, X., and Ahn, D. U. (2018). The incidence of muscle abnormalities in broiler breast meat–A review. *Korean J. Food Sci. Anim. Resour.* 38:835. doi: 10.5851/kosfa.2018.e2

Kala, R. (2012). Multi-robot path planning using co-evolutionary genetic programming. *Expert Syst. Appl.* 39, 3817–3831. doi: 10.1016/j.eswa.2011.09.090

Kecman, V. (2001). *Learning and Soft Computing: Support Vector Machines, Neural Networks, and Fuzzy Logic Models*. Cambridge, MA: MIT Press.

Kennedy-Smith, A., Johnson, M. L., Bauermeister, L. J., Cox, M. K., and Morey, A. (2017). Evaluating a novel bioelectric impedance analysis technology for the rapid detection of wooden breast myopathy in broiler breast filets. *Int. Poultry Sci.* 96:252.

Kotsiantis, S. B., Zaharakis, I., and Pintelas, P. (2007). "Supervised machine learning: a review of classification techniques" in *Emerging Artificial Intelligence Applications in Computer Engineering* (Amsterdam: IOS Press), 3–24. doi: 10.1007/s10462-007-9052-3

Kusiak, A. (2006). Data mining in manufacturing: a review. *J. Manuf. Sci. Eng.* 128, 969doi: 10.1115/1.2194554

Kuttappan, V., Lee, Y., Erf, G., Meullenet, J., McKee, S., and Owens, C. (2012). Consumer acceptance of visual appearance of broiler breast meat with varying degrees of white striping. *Poul. Sci. J.* 91, 1240–1247. doi: 10.3382/ps.2011-01947

Kuttappan, V. A., Owens, C. M., Coon, C., Hargis, B. M., and Vazquez-Anon, M. (2017). Incidence of broiler breast myopathies at 2 different ages and its impact on selected raw meat quality parameters. *Poult. Sci. J.* 96, 3005–3009. doi: 10.3382/ps/pex072

Kyle, U. G., Bosaeus, I., De Lorenzo, A. D., Deurenberg, P., Elia, M., Gómez, J. M., and Composition of the ESPEN and Working Group. (2004). Bioelectrical impedance analysispart I: review of principles and methods. *Clin. Nutr.* 23, 1226–1243. doi: 10.1016/j.clnu.2004.06.004

Lee, M. C., and To, C. (2010). Comparison of support vector machine and back propagation neural network in evaluating the enterprise financial distress. *IJAIA* 1, 31–43. doi: 10.5121/ijaia.2010.1303

Li, H., Liang, Y., and Xu, Q. (2009). Support vector machines and its applications in chemistry. *Chemom. Intell. Lab. Syst.* 95, 188–198. doi: 10.1016/j.chemolab.2008.10.007

Lippmann, R. (1987). "An introduction to computing with neural nets" in *IEEE Assp Magazine* (New York, NY:IEEE), 4–22. doi: 10.1109/MASSP.1987.1165576

Liu, M., Wang, M., Wang, J., and Li, D. (2013). Comparison of random forest, support vector machine and back propagation neural network for electronic tongue data classification: Application to the recognition of orange beverage and Chinese vinegar. *Sens. Actuat. B Chem.* 177, 970–980. doi: 10.1016/j.snb.2012.11.071

Lu, J., Plataniotis, K. N., and Venetsanopoulos, A. N. (2005). Regularization studies of linear discriminant analysis in small sample size scenarios with application to face recognition. *Patt. Recogn. Lett.* 26, 181–191. doi: 10.1016/j.patrec.2004.09.014

Maji, S., Berg, A. C., and Malik, J. (2008). "Classification using intersection kernel support vector machines is efficient," in *Computer Vision and Pattern Recognition* (Anchorage, AK: IEEE). doi: 10.1109/CVPR.2008.4587630

Mandal, T., Wu, Q. J., and Yuan, Y. (2009). Curvelet based face recognition via dimension reduction. *Sig. Proc.* 89, 2345–2353. doi: 10.1016/j.sigpro.2009.03.007

Mazzoni, M., Petracci, M., Meluzzi, A., Cavani, C., Clavenzani, P., and Sirri, F. (2015).Relationship between *Pectoralis major* muscle histology and quality traits of chicken meat. *Poult. Sci.* 94, 123–130. doi: 10.3382/ps/peu043

Monostori, L. (2003). AI and machine learning techniques for managing complexity, changes and uncertainties in manufacturing. *Eng. Appl. Artif. Intell.* 16, 277–291. doi: 10.1016/S0952-1976(03)00078-2

Morey, A., Smith, A. E., Garner, L. J., and Cox, M. K. (2020). Application of bioelectrical impedance analysis to detect broiler breast filets affected with woody breast myopathy. *Front. Physiol.* 11:808. doi: 10.3389/fphys.2020.00808

Mudalal, S., Lorenzi, M., Soglia, F., Cavani, C., and Petracci, M. (2015). Implications of white striping and wooden breast abnormalities on quality traits of raw and marinated chicken meat. *Animals* 9, 728–734. doi: 10.1017/S175173111400295X

Nashat, S., Abdullah, A., Aramvith, S., and Abdullah, M. Z. (2011). Support vector machineapproach to real-time inspection of biscuits on moving conveyor belt. *Comput. Electron. Agr.* 75, 147–158. doi: 10.1016/j.compag.2010.10.010

National Chicken Council (2020). *Per Capita Consumption of Poultry and Livestock, 1965 to Estimated 2021.* Available online at: https://www.nationalchickencouncil.org/about-the-industry/statistics/per-capita-consumption-of-poultry-and-livestock-1965-to-estimated-2021-in-pounds/ (accessed March 30, 2021).

Nilsson, N. J. (2005). *Introduction to Machine Learning.* Stanford, CA: Standford University Press.

Noble, W. S. (2006). What is a support vector machine? *Nat. Biotechnol.* 24, 1565–1567. doi: 10.1038/nbt1206-1565

Nyboer, J., Kreider, M. M., and Hannapel, L. (1950). Electrical impedance plethysmography: a physical and physiologic approach to peripheral vascular study. *Circulation* 2, 811–821. doi: 10.1161/01.CIR.2.6.811

Osuna, E., Freund, R., and Girosi, F. (1997). "An improved training algorithm for support vector machines". in *Neural Networks for Signal Processing VII* (New York, NY:IEEE), 276–285. doi: 10.1109/NNSP.1997.622408

Pan, F., Song, G., Gan, X., and Gu, Q. (2014). Consistent feature selection and its application to face recognition. *J. Intell. Inf. Syst.* 43, 307–321. doi: 10.1007/s10844-014-0324-5

Panchal, G., Ganatra, A., Shah, P., and Panchal, D. (2011). Determination of over-learning and over-fitting problem in back propagation neural network. *Int. J. Soft. Comput.* 2, 40–51. doi: 10.5121/ijsc.2011.2204

Paola, J. D., and Schowengerdt, R. A. (1995). A review and analysis of backpropagation neuralnetworks for classification of remotely-sensed multi-spectral imagery. *Int. J. Remote Sens.* 16, 3033–3058. doi: 10.1080/01431169508954607

Pardo, M., and Sberveglieri, G. (2005). Classification of electronic nose data with support vectormachines. *Sens. Actuat. B Chem.* 107, 730–737. doi: 10.1016/j.snb.2004.12.005

Petracci, M., Bianchi, M., Mudalal, S., and Cavani, C. (2013). Functional ingredients for poultrymeat products. *Trends Food Sci. Technol.* 33, 27–39. doi: 10.1016/j.tifs.2013.06.004

Petracci, M., and Cavani, C. (2012). Muscle growth and poultry meat quality issues. *Nutrients* 4, 1–12. doi: 10.3390/nu4010001

Petracci, M., Mudalal, S., Soglia, F., and Cavani, C. (2015). Meat quality in fast-growing broiler chickens. *Worlds Poult. Sci. J.* 71, 363–374. doi: 10.1017/S0043933915000367

Pham, D. T., and Afify, A. A. (2005). Machine-learning techniques and their applications inmanufacturing. *Proc. Inst. Mech. Eng. B J. Eng. Manuf.* 219, 395–412. doi: 10.1243/095440505X32274

Pontil, M., and Verri, A. (1998). Properties of support vector machines. *Neural Comput.* 10, 955–974. doi: 10.1162/089976698300017575

Radaelli, G., Piccirillo, A., Birolo, M., Bertotto, D., Gratta, F., Ballarin, C., et al. (2017). Effect of age on the occurrence of muscle fiber degeneration associated with myopathies in broiler chickens submitted to feed restriction. *Poult. Sci.* 96, 309–319. doi: 10.3382/ps/pew270

Rao, C. R. (1948). The utilization of multiple measurements in problems of biological classification. *J. R. Stat. Soc. Ser. B Stat. Methodol.* 10, 159–193. doi: 10.1111/j.2517-6161.1948.tb00008.x

Ribeiro, B. (2005). Support vector machines for quality monitoring in a plastic injection moldingprocess. *IEEE T. Syst. Man. Cyber. C* 35, 401–410. doi: 10.1109/TSMCC.2004.843228

Rumelhart, D. E., Hinton, G. E., and Williams, R. J. (1986). "Learning internal representations by error propagation" in *Parallel Distributed Processing: Explorations in the Microstructures of Cognition* (Cambridge, MA: MIT Press), 318–362. doi: 10.21236/ADA164453

Salahshoor, K., Khoshro, M. S., and Kordestani, M. (2011). Fault detection and diagnosis of anindustrial steam turbine using a distributed configuration of adaptive neuro-fuzzyinference systems. *Simul. Model Pract. Theory* 19, 1280–1293. doi: 10.1016/j.simpat.2011.01.005

Shao, Y., and Lunetta, R. S. (2012). Comparison of support vector machine, neural network, and CART algorithms for the land-cover classification using limited training data points. *ISPRSJ. Photogramm. Remote Sens.* 70, 78–87. doi: 10.1016/j.isprsjprs.2012.04.001

Sihvo, H., Immonen, K., and Puolanne, E. (2014). Myodegeneration with fibrosis and regeneration in thepectoralis major muscle of broilers. *Vet. Pathol.* 51, 619–623. doi: 10.1177/0300985813497488

Sihvo, H. K., Lindén, J., Airas, N., Immonen, K., Valaja, J., and Puolanne, E. (2017). Wooden breast myodegeneration of *Pectoralis major* muscle over the growth period in broilers. *Vet. Pathol.* 54, 119–128. doi: 10.1177/0300985816658099

Singh, K. P., Basant, N., and Gupta, S. (2011). Support vector machines in water qualitymanagement. *Anal. Chim. Acta* 703, 152–162. doi: 10.1016/j.aca.2011.07.027

Smola, A., and Vishwanathan, S. V. N. (2008). *Introduction to Machine Learning.* Cambridge: Cambridge University Press.

Soglia, F., Mudalal, S., Babini, E., Di Nunzio, M., Mazzoni, M., Sirri, F., and Petracci, M. (2016).Histology, composition, and quality traits of chicken Pectoralis major muscle affected bywooden breast abnormality. *Poult. Sci. J.* 95, 651–659. doi: 10.3382/ps/pev353

Su, B., Ding, X., Wang, H., and Wu, Y. (2017). Discriminative dimensionality reduction for multi-dimensional sequences. *IEEE PAMI* 40, 77–91. doi: 10.1109/TPAMI.2017.2665545

Tao, Y., Heinemann, P. H., Varghese, Z., Morrow, C. T., and Sommer, III., H. J. (1995). Machinevision for color inspection of potatoes and apples. *Trans. ASAE* 38, 1555–1561. doi: 10.13031/2013.27982

Tasoniero, G., Bertram, H. C., Young, J. F., Dalle Zotte, A., and Puolanne, E. (2017). Relationship between hardness and myowater properties in wooden breast affected chicken meat: a nuclear magnetic resonance study. *LWT* 86, 20–24. doi: 10.1016/j.lwt.2017.07.032

Tharwat, A. (2019). Parameter investigation of support vector machine classifier with kernel functions. *Knowl. Inf. Syst.* 61, 1269–1302. doi: 10.1007/s10115-019-01335-4

Tharwat, A., Gaber, T., Ibrahim, A., and Hassanien, A. E. (2017). Linear discriminant analysis: a detailed tutorial. *AI Commun.* 30, 169–190. doi: 10.3233/AIC-170729

Tijare, V. V., Yang, F. L., Kuttappan, V. A., Alvarado, C. Z., Coon, C. N., and Owens, C. M. (2016). Meat quality of broiler breast fillets with white striping and woody breast musclemyopathies. *Poult. Sci. J.* 95, 2167–2173. doi: 10.3382/ps/pew129

Tufféry, S. (2011). *Data Mining and Statistics for Decision Making.* Hoboken, NJ: John Wiley & Sons. doi: 10.1002/9780470979174

Vapnik, V. (1963). Pattern recognition using generalized portrait method. *Autom. Remote Control* 24, 774–780.

Vapnik, V. (1995). *The Nature of Statistical Learning Theory*. New York, NY: Springer-Verlag. doi: 10.1007/978-1-4757-2440-0

Vapnik, V. (2013). *The Nature of Statistical Learning Theory*. Berlin: Springer Science & Business Media.

Velleman, S. G. (2015). Relationship of skeletal muscle development and growth to breast muscle myopathies: a review. *Avian Dis.* 59, 525–531. doi: 10.1637/11223-063015-Review.1

Vijayarani, S., Dhayanand, S., and Phil, M. (2015). Kidney disease prediction using SVM and ANN algorithms. *Int. J. Comput. Mark. Res.* 6, 1–12.

Wang, K. J., Chen, J. C., and Lin, Y. S. (2005). A hybrid knowledge discovery model usingdecision tree and neural network for selecting dispatching rules

of a semiconductor finaltesting factory. *Prod. Plan. Control*. 16, 665–680. doi: 10.1080/09537280500213757

Wiendahl, H. P., and Scholtissek, P. (1994). Management and control of complexity inmanufacturing. *Cirp. Ann. Manuf. Techn*. 43, 533–540. doi: 10.1016/S0007-8506(07)60499-5

Wold, J. P., Måge, I., Løvland, A., Sanden, K. W., and Ofstad, R. (2019). Near-infraredspectroscopy detects woody breast syndrome in chicken fillets by the markers proteincontent and degree of water binding. *Poult. Sci. J*. 98, 480–490. doi: 10.3382/ps/pey351

Xanthopoulos, P., Pardalos, P. M., and Trafalis, T. B. (2013). "Linear discriminant analysis", in *Robust Data Mining* (New York, NY: Springer), 27–33. doi: 10.1007/978-1-4419-9878-1_4

Yang, Y., Wang, W., Zhuang, H., Yoon, S. C., Bowker, B., Jiang, H., et al. (2021). Evaluation of broiler breast fillets with the woody breast condition using expressible fluid measurement combined with deep learning algorithm. *J. Food Eng*. 288:110133. doi: 10.1016/j.jfoodeng.2020.110133

Yang, Y., Zhu, J., Zhao, C., Liu, S., and Tong, X. (2011). The spatial continuity study of NDVI based on kriging and BPNN algorithm. *Math. Comput. Model* 54, 1138–1144. doi: 10.1016/j.mcm.2010.11.046

Yao, X. (1999). Evolving artificial neural networks. *Proc. IEEE* 87, 1423–1447. doi: 10.1109/5.784219

Zampiga, M., Soglia, F., Baldi, G., Petracci, M., Strasburg, G. M., and Sirri, F. (2020). Muscle abnormalities and meat quality consequences in modern turkey hybrids. *Front. Physiol*. 11:554. doi: 10.3389/fphys.2020.00554

Zhuang, X. S., and Dai, D. Q. (2005). Inverse Fisher discriminate criteria for small sample size problem and its application to face recognition. *Patt. Recog*. 38, 2192–2194 doi: 10.1016/j.patcog.2005.02.011

Conflict of Interest: The authors declare that the research was conducted in the absence of any commercial or financial relationships that could be construed as a potential conflict of interest.

Publisher's Note: All claims expressed in this article are solely those of the authors and do not necessarily represent those of their affiliated organizations, or those of the publisher, the editors and the reviewers. Any product that may be evaluated in this article, or claim that may be made by its manufacturer, is not guaranteed or endorsed by the publisher.

Advantages of publishing in Frontiers

OPEN ACCESS
Articles are free to read for greatest visibility and readership

FAST PUBLICATION
Around 90 days from submission to decision

HIGH QUALITY PEER-REVIEW
Rigorous, collaborative, and constructive peer-review

TRANSPARENT PEER-REVIEW
Editors and reviewers acknowledged by name on published articles

Frontiers
Avenue du Tribunal-Fédéral 34
1005 Lausanne | Switzerland

Visit us: www.frontiersin.org
Contact us: frontiersin.org/about/contact

REPRODUCIBILITY OF RESEARCH
Support open data and methods to enhance research reproducibility

DIGITAL PUBLISHING
Articles designed for optimal readership across devices

FOLLOW US
@frontiersin

IMPACT METRICS
Advanced article metrics track visibility across digital media

EXTENSIVE PROMOTION
Marketing and promotion of impactful research

LOOP RESEARCH NETWORK
Our network increases your article's readership